frontiers | Research Topics

Cellular contributors and consequences of protein misfolding and aggregation

Edited by
Anoop Arunagiri, Emily Sontag and Verena Kohler

Coordinated by
Arunkumar Venkatesan

Published in
Frontiers in Molecular Biosciences
Frontiers in Cell and Developmental Biology

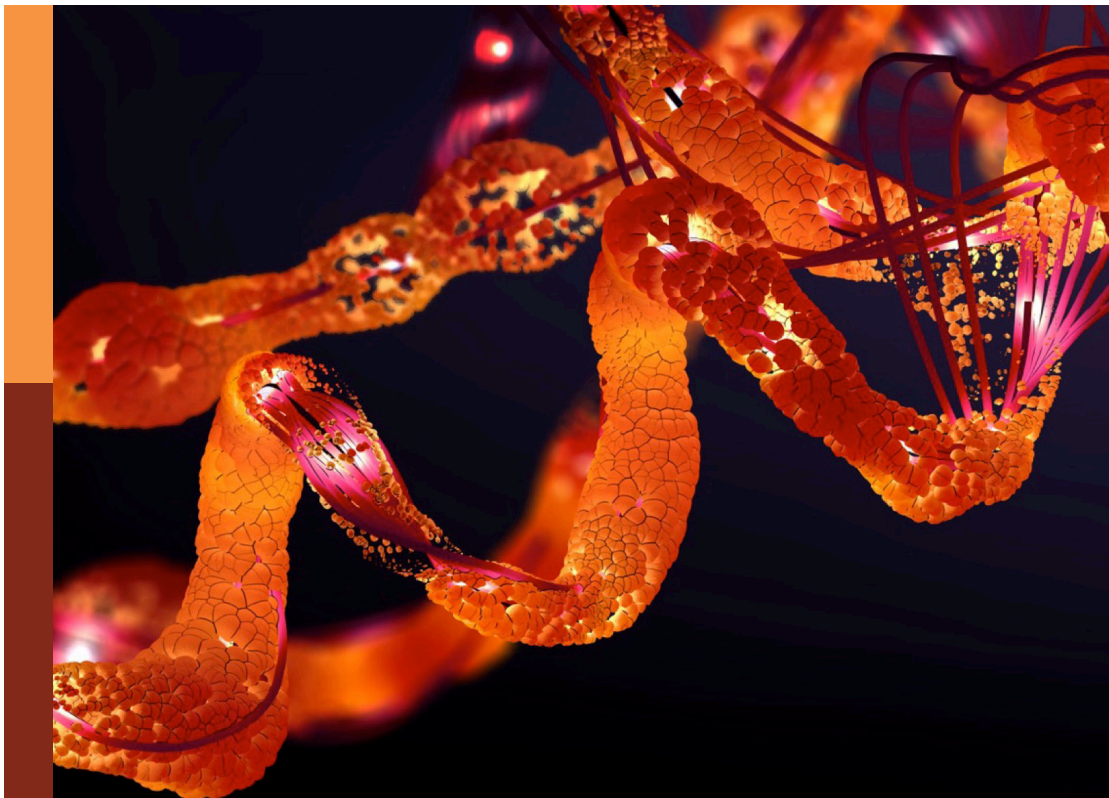

ISSN 1664-8714
ISBN 978-2-8325-7365-5
DOI 10.3389/978-2-8325-7365-5

Generative AI statement
Any alternative text (Alt text) provided alongside figures in the articles in this ebook has been generated by Frontiers with the support of artificial intelligence and reasonable efforts have been made to ensure accuracy, including review by the authors wherever possible. If you identify any issues, please contact us.

About Frontiers

Frontiers is more than just an open access publisher of scholarly articles: it is a pioneering approach to the world of academia, radically improving the way scholarly research is managed. The grand vision of Frontiers is a world where all people have an equal opportunity to seek, share and generate knowledge. Frontiers provides immediate and permanent online open access to all its publications, but this alone is not enough to realize our grand goals.

Frontiers journal series

The Frontiers journal series is a multi-tier and interdisciplinary set of open-access, online journals, promising a paradigm shift from the current review, selection and dissemination processes in academic publishing. All Frontiers journals are driven by researchers for researchers; therefore, they constitute a service to the scholarly community. At the same time, the *Frontiers journal series* operates on a revolutionary invention, the tiered publishing system, initially addressing specific communities of scholars, and gradually climbing up to broader public understanding, thus serving the interests of the lay society, too.

Dedication to quality

Each Frontiers article is a landmark of the highest quality, thanks to genuinely collaborative interactions between authors and review editors, who include some of the world's best academicians. Research must be certified by peers before entering a stream of knowledge that may eventually reach the public - and shape society; therefore, Frontiers only applies the most rigorous and unbiased reviews. Frontiers revolutionizes research publishing by freely delivering the most outstanding research, evaluated with no bias from both the academic and social point of view. By applying the most advanced information technologies, Frontiers is catapulting scholarly publishing into a new generation.

What are Frontiers Research Topics?

Frontiers Research Topics are very popular trademarks of the *Frontiers journals series*: they are collections of at least ten articles, all centered on a particular subject. With their unique mix of varied contributions from Original Research to Review Articles, Frontiers Research Topics unify the most influential researchers, the latest key findings and historical advances in a hot research area.

Find out more on how to host your own Frontiers Research Topic or contribute to one as an author by contacting the Frontiers editorial office: frontiersin.org/about/contact

Cellular contributors and consequences of protein misfolding and aggregation

Topic editors

Anoop Arunagiri — East Tennessee State University, United States

Emily Sontag — Marquette University, United States

Verena Kohler — Umeå University, Sweden

Topic coordinator

Arunkumar Venkatesan — Upstate Medical University, United States

Citation

Arunagiri, A., Sontag, E., Kohler, V., Venkatesan, A., eds. (2026). *Cellular contributors and consequences of protein misfolding and aggregation*. Lausanne: Frontiers Media SA. doi: 10.3389/978-2-8325-7365-5

Table of contents

frontiers | Frontiers in Molecular Biosciences

TYPE Editorial
PUBLISHED 05 January 2026
DOI 10.3389/fmolb.2025.1759495

OPEN ACCESS

EDITED AND REVIEWED BY
Graça Soveral,
University of Lisbon, Portugal

*CORRESPONDENCE
Anoop Arunagiri,
arunagiri@etsu.edu
Emily Sontag,
emily.sontag@marquette.edu
Verena Kohler,
verena.kohler@umu.se
Arunkumar Venkatesan,
venkatea@upstate.edu

RECEIVED 03 December 2025
ACCEPTED 08 December 2025
PUBLISHED 05 January 2026

CITATION
Arunagiri A, Sontag E, Kohler V and Venkatesan A (2026) Editorial: Cellular contributors and consequences of protein misfolding and aggregation.
Front. Mol. Biosci. 12:1759495.
doi: 10.3389/fmolb.2025.1759495

Editorial: Cellular contributors and consequences of protein misfolding and aggregation

Anoop Arunagiri[1]*, Emily Sontag[2]*, Verena Kohler[3]* and Arunkumar Venkatesan[4]*

[1]Department of Biological Sciences, East Tennessee State University, Johnson City, TN, United States, [2]Department of Biological Sciences, Marquette University, Milwaukee, WI, United States, [3]Department of Molecular Biology, Faculty of Medicine, Umeå University, Umeå, Sweden, [4]Department of Ophthalmology and Visual Sciences, SUNY Upstate Medical University, Syracuse, NY, United States

KEYWORDS

endoplasmic reticulum–mitochondria association, liquid–liquid phase separation, neurodegeneration, protein aggregation, proteostasis

Editorial on the Research Topic
Cellular contributors and consequences of protein misfolding and aggregation

Protein function is dictated by its structure, which governs its propensity for self-assembly whether it exists as a folded globular protein or as an intrinsically disordered polypeptide. The material properties of these assemblies range from dynamic liquid-like condensates to solid aggregates. Condensates serve fundamental biological roles, but when regulatory mechanisms fail, it leads to disease. This research explores how proteostasis collapses, driving various proteinopathies, moving beyond fibril formation to uncover complex cellular failures and delineate novel therapeutic strategies.

The core challenge in many neurodegenerative diseases, reviewed by Tsekrekou et al., is the toxicity of soluble oligomers of proteins like TDP-43 and SOD1 in amyotrophic lateral sclerosis (ALS). This underscores the urgent need for mechanism-based inhibitors (e.g., ebselen and QBP1) that stabilize the native protein state or block toxic assembly. This challenge is mirrored in diabetes, as Zavarzadeh et al. reviewed how proinsulin misfolding due to insulin gene mutations (as in mutant INS-gene-induced diabetes of youth, MIDY) or metabolic stress (as in type 2 diabetes) triggers toxic endoplasmic reticulum (ER) stress and the unfolded protein response (UPR). This failure was also identified by Venkatesan and Bernstein as central to glaucoma pathology, where misfolded MYOC and OPTN drive chronic ER stress and mitochondrial dysfunction. However, potential solutions exist. Simha et al. demonstrated that the herb *Sida cordifolia* effectively mitigated Huntington's disease (HD) pathology in models by specifically reducing mutant huntingtin (mHtt) aggregates and, critically, by suppressing the toxic ER–UPR pathways (PERK, IRE1α, and ATF6).

Beyond genetic and folding defects, the cellular environment plays a crucial role. Da Costa et al. established that mitochondrial inorganic polyphosphate (polyP) is essential for mitochondrial proteostasis, acting as a non-transcriptional regulator that prevents stress-induced protein aggregation (TUFM). Similarly, Suzuki and Itoh highlighted that the synergistic effect of missense mutations and resulting glycosylation defects

drives pathology in inherited diseases like CADASIL (NOTCH3) and FH (LDLR), where altered structure near a glycosylation site accelerates misfolding and aggregation. This environmental influence extends to membranes. Schepers et al. reviewed how lipid dysregulation, driven by factors like GBA1 and APOE ε4, is fundamentally linked to the pathology of synucleinopathies (PD and DLB) and dictates the specific alpha-synuclein strains (e.g., Lewy fold vs. MSA filaments) that explain clinical heterogeneity.

Finally, the most unifying concept is the dynamic nature of assembly, which requires new tools for study. Oldam et al. developed a simple thioflavin T in-gel staining method for the quick characterization and quantification of both fibrils and toxic pre-amyloid oligomers (PAOs). Applying this mechanistic understanding, Navalkar et al. synthesized the evidence that the core pathological defect is the failure to maintain the dynamic, liquid material state of protein assemblies, arguing that initially functional liquid–liquid phase separation (LLPS) condensates (like TDP-43 in stress granules or CgB in secretory granules) transition into immobile, microreactor aggregates (like Tau or IAPP) under stress. Ultimately, preserving the liquid-like state of these assemblies emerges as the central therapeutic goal.

Author contributions

AA: Writing – original draft. ES: Writing – review and editing. VK: Writing – review and editing. AV: Writing – review and editing.

Funding

The author(s) declared that financial support was not received for this work and/or its publication.

Acknowledgements

The authors thank all contributors to this Research Topic.

Conflict of interest

The author(s) declared that this work was conducted in the absence of any commercial or financial relationships that could be construed as a potential conflict of interest.

The author AA declared that they were an editorial board member of Frontiers at the time of submission. This had no impact on the peer review process and the final decision.

Generative AI statement

The author(s) declared that generative AI was not used in the creation of this manuscript.

Any alternative text (alt text) provided alongside figures in this article has been generated by Frontiers with the support of artificial intelligence and reasonable efforts have been made to ensure accuracy, including review by the authors wherever possible. If you identify any issues, please contact us.

Publisher's note

frontiers | Frontiers in Molecular Biosciences

TYPE Review
PUBLISHED 24 May 2024
DOI 10.3389/fmolb.2024.1383453

OPEN ACCESS

EDITED BY
Emily Sontag,
Marquette University, United States

REVIEWED BY
Valentina Bonetto,
Mario Negri Institute for Pharmacological Research (IRCCS), Italy
Eunice Domínguez-Martín,
National Institute of Neurological Disorders and Stroke (NIH), United States

*CORRESPONDENCE
Georgios Skretas,
skretas@fleming.gr

RECEIVED 07 February 2024
ACCEPTED 02 May 2024
PUBLISHED 24 May 2024

CITATION
Tsekrekou M, Giannakou M, Papanikolopoulou K and Skretas G (2024), Protein aggregation and therapeutic strategies in SOD1- and TDP-43- linked ALS. *Front. Mol. Biosci.* 11:1383453. doi: 10.3389/fmolb.2024.1383453

Protein aggregation and therapeutic strategies in SOD1- and TDP-43- linked ALS

Maria Tsekrekou[1], Maria Giannakou[1,2], Katerina Papanikolopoulou[3,4] and Georgios Skretas[1,4,5]*

[1]Institute of Chemical Biology, National Hellenic Research Foundation, Athens, Greece, [2]Department of Biology, National and Kapodistrian University of Athens, Athens, Greece, [3]Institute for Fundamental Biomedical Research, Biomedical Sciences Research Centre "Alexander Fleming", Vari, Greece, [4]ResQ Biotech, Patras Science Park, Rio, Greece, [5]Institute for Bio-innovation, Biomedical Sciences Research Centre "Alexander Fleming", Vari, Greece

Amyotrophic lateral sclerosis (ALS) is a fatal neurodegenerative disease with severe socio-economic impact. A hallmark of ALS pathology is the presence of aberrant cytoplasmic inclusions composed of misfolded and aggregated proteins, including both wild-type and mutant forms. This review highlights the critical role of misfolded protein species in ALS pathogenesis, particularly focusing on Cu/Zn superoxide dismutase (SOD1) and TAR DNA-binding protein 43 (TDP-43), and emphasizes the urgent need for innovative therapeutic strategies targeting these misfolded proteins directly. Despite significant advancements in understanding ALS mechanisms, the disease remains incurable, with current treatments offering limited clinical benefits. Through a comprehensive analysis, the review focuses on the direct modulation of the misfolded proteins and presents recent discoveries in small molecules and peptides that inhibit SOD1 and TDP-43 aggregation, underscoring their potential as effective treatments to modify disease progression and improve clinical outcomes.

KEYWORDS

amyotrophic lateral sclerosis, SOD1, TDP-43, protein misfolding, protein aggregation, neurotoxicity, therapeutics

Introduction

Precise activity of cellular protein networks is essential for the proper function and fitness of cells and organisms. Protein function highly depends on its three-dimensional structure, i.e., its folding state (Yadav et al., 2019). To ensure functionality, biological systems have evolved protein quality control mechanisms comprising molecular chaperones, proteases and regulatory factors, which supervise protein folding and direct protein species which fail to meet cellular quality control criteria for degradation. Despite the existence of highly specialized protein folding surveillance mechanisms, protein misfolding and aggregation are hallmarks of numerous human diseases (Chiti and Dobson, 2006; Chiti and Dobson, 2017). These diseases range from systemic amyloidoses, where amyloid fibrils accumulate throughout the human body, to neurodegenerative disorders such as Alzheimer's disease (AD), Parkinson's disease (PD) and ALS, where protein aggregates are mainly deposited either extracellularly (AD) or intracellularly (PD, ALS) within the central nervous system (CNS).

ALS is a neurodegenerative disease (Hardiman et al., 2017) characterized by the selective degeneration of both upper motor neurons in the motor cortex and lower motor neurons in the brainstem and spinal cord (Tandan and Bradley, 1985; Hardiman et al., 2017; van Es et al., 2017). It is the most common form of motor neuron disease with adult onset and the third most common neurodegenerative disease (Hou et al., 2019). The survival rate is highly variable, with a median rate of about 3–5 years after symptom onset; however, up to 10% of ALS patients survive for more than 10 years (Chio et al., 2009; van Es et al., 2017; Longinetti and Fang, 2019). ALS affects approximately two to four people per 100,000 individuals per year in Caucasian populations and about one person or less per 100,000 individuals annually in Asian and Hispanic populations (Cronin et al., 2007; Al-Chalabi and Hardiman, 2013; Hardiman et al., 2017; Longinetti and Fang, 2019), with the exception of Japan where the incidence rate is closer to the that of Western countries (Doi et al., 2014). Recent studies indicate a trend of rising incidence rates for ALS (Collaborators, 2019; Longinetti and Fang, 2019; Ryan et al., 2019).

ALS has traditionally been classified as either sporadic (sALS), representing approximately 90%–95% of cases, or familial (fALS), typically characterized by Mendelian autosomal dominant inheritance (van Es et al., 2017; Ranganathan et al., 2020; Kirola et al., 2022). The term "sporadic" is applied to cases which are unrelated to family incidence, even when gene mutations associated with or causing ALS are present (Mejzini et al., 2019). Comprehensive analyses from large-scale genome-wide association studies (GWAS) on sALS patients have revealed that the genetic landscape of ALS predominantly comprises rare variants (van Rheenen et al., 2016; van Rheenen et al., 2021). Consequently, the field is progressing toward a more precise genetic classification, emphasizing the identification of risk genes (Cooper-Knock et al., 2021; Brenner and Freischmidt, 2022). Regardless of the subclassification criteria, both forms of ALS are clinically indistinguishable (Couratier et al., 2021), differing only in the age of onset, with fALS occurring about a decade earlier than sALS (Wijesekera and Leigh, 2009).

Familial cases of ALS have facilitated the identification of the involvement of the genetic background in disease pathogenesis (Gros-louis et al., 2006). Currently more than 40 genes have been associated with fALS (van Rheenen et al., 2021; Brenner and Freischmidt, 2022; Suzuki et al., 2023), enabling the generation of animal models carrying ALS-related gene mutations (Bonifacino et al., 2021; Zhu et al., 2023). *In vivo* modelling of ALS has provided a valuable tool to elucidate the pathogenic mechanisms contributing to disease onset and progression, and allowing for targeted drug development (Hardiman et al., 2017; Bonifacino et al., 2021; Zhu et al., 2023). Importantly, research of ALS animal models has revealed an intertwining network of molecular (e.g., aberrant RNA metabolism, impaired protein homeostasis, oxidative stress, mitochondrial dysfunction, impaired DNA repair and dysregulated vesicle transport) and cellular disruptions (such as hyperexcitability, glial dysfunction and axonopathy) that build up to systemic aberrations, ultimately leading to the disease (Hardiman et al., 2017).

ALS is a complex disease, characterized by significant clinical heterogeneity. This heterogeneity is evident in the variability of the site and age of disease onset, the rate of progression, and the degree of cognitive impairment (Chio et al., 2011; Ferrari et al., 2011; Statland et al., 2015). Despite this clinical variability, a cellular hallmark of ALS is the presence of ubiquitinated skein-like or dense and round cytoplasmic inclusions of certain proteins, such as SOD1, TDP-43, and fused in sarcoma (FUS) in motor neurons (Leigh et al., 1988; Lowe et al., 1988). Approximately 97% of ALS cases exhibit TDP-43-positive inclusions (Mackenzie et al., 2007). Notably, TDP-43 cytoplasmic inclusions are also found in other neurodegenerative disorders including Frontotemporal lobar degeneration (FTLD), combined ALS-FTLD, AD and atypical Parkinsonism (de Boer et al., 2020). TDP-43 inclusions are absent in ALS cases caused by mutations in *SOD1* and *FUS*; in these instances, protein deposits consist of the respective mutated gene products (Neumann et al., 2009; Vance et al., 2009).

Considering that aberrant cytoplasmic inclusions are a ubiquitous finding in ALS patients, numerous research efforts have been directed toward inhibiting the aggregation of ALS-related proteins. In this review, we focus on two extensively studied ALS-related proteins associated with protein misfolding and aggregation, SOD1 and TDP-43. We examine the contribution of their accumulation to disease phenotypes and review the recent progress in identifying inhibitors of their aggregation, which could serve as lead molecules for the development of effective anti-ALS treatments.

Misfolding- and aggregation-mediated toxicity in ALS

Aggregation-prone proteins in ALS

SOD1 plays a major role in regulating redox potential by catalyzing the conversion of the superoxide anion O_2^- into hydrogen peroxide, which is further processed by other enzymes (Bunton-Stasyshyn et al., 2015; Huai and Zhang, 2019). In its functional form, SOD1 forms a homodimer, with each subunit containing a copper and a zinc ion at its [Cu/Zn] site and an intra-subunit C57-C146 disulfide bond (Valentine et al., 2005; Huai and Zhang, 2019). The discovery of *SOD1* mutations causing fALS in 1993 was a milestone for ALS research (Rosen et al., 1993). To date, more than 200 mutations in human *SOD1* have been associated with ALS (van der Spek et al., 2019). Mutations in *SOD1*, lead to classical dominantly inherited ALS, accounting for about 10%–15% of fALS cases and approximately 1.5% of sALS cases (Gros-louis et al., 2006). Although SOD1 misfolding and aggregation are considered hallmarks of SOD1-fALS (Saccon et al., 2013), SOD1-immunoreactive inclusions have also been detected in a significant percentage of sALS cases (Bosco et al., 2010; Forsberg et al., 2019). As the longest-studied ALS-related protein, SOD1 has been associated with a large number of pathophysiological mechanisms causing neurotoxicity, including protein misfolding, excitotoxicity, oxidative stress, impaired axonal transport, inflammation and mitochondrial dysfunction (Ferraiuolo et al., 2011).

Wild-type SOD1 is an unusually stable protein, which remains active even under denaturing conditions (Arnesano et al., 2004). It is able to maintain its disulfide status inside the reducing cytosolic environment and is highly resistant to proteolysis (Arnesano et al.,

2004; Valentine et al., 2005). This remarkable stability is regulated by the disulfide bond and the metalation status, which mutually affect each other (Arnesano et al., 2004; Tiwari et al., 2005; Nordlund et al., 2009). Disruption of the disulfide bond or loss of the metal co-factors can lead to pathogenic misfolding. Specific post-translational modifications (PTMs), including phosphorylation, acetylation, and succinylation, play crucial roles in regulating the structure and functions of SOD1, such as ROS scavenging, cytoskeletal organization, and transcriptional activity (Banks and Andersen, 2019), while others like sumoylation and oxidation can lead to misfolding and aggregation (Fei et al., 2006; Xu et al., 2018; Trist et al., 2022).

Interestingly, mutations associated with ALS have been identified across all five exons of human SOD1. These mutations impact the structure of SOD1 in different ways, often leading to varying degrees of misfolding, aggregation and consequent variable toxicities (Brasil et al., 2018). Initially, it was proposed that ALS-causing mutations in SOD1 were linked to a loss of enzymatic function (Rosen et al., 1993; Saccon et al., 2013); however, subsequent studies in SOD1 mice contradicted this notion (Gurney et al., 1994; Reaume et al., 1996). Mutant SOD1 retaining partial or complete enzymic function was found to induce ALS-like phenotypes (Gurney et al., 1994), and *Sod1* knockout mice did not develop ALS (Reaume et al., 1996). In contrast, ALS-related SOD1 variants are associated with decreased metal binding, reduced formation of a stabilizing intramolecular disulfide bond, diminished structural stability and an increased tendency to monomerize and aggregate (Ray et al., 2004). Importantly, the aggregation propensity of several SOD1 variants has been linked to life expectancy after the onset of ALS symptoms in both humans and transgenic mouse models (Wang et al., 2008; Prudencio et al., 2009; Pratt et al., 2014; Lang et al., 2015; McAlary et al., 2020).

TDP-43, encoded by the *TARDBP* gene, was identified in 2006 as a major component of cytoplasmic protein inclusions accompanied by nuclear clearance of the protein, as observed in motor neurons of ALS cases (Arai et al., 2006; Neumann et al., 2006; Mackenzie et al., 2007). TDP-43 pathology is present in nearly all ALS cases except for those caused by mutations in *SOD1* or *FUS*. *TARDBP* mutations account for approximately 5% of familial and almost 1% of sporadic ALS cases. It is an RNA-binding protein (RBP) involved in the regulation of gene expression at multiple levels by playing an active role in alternative splicing of pre-mRNAs (Bhardwaj et al., 2013; Lukavsky et al., 2013; Kuo et al., 2014), splicing of non-coding RNAs (Tollervey et al., 2011) and mRNA stability (Fukushima et al., 2019), thus affecting diverse cell processes, including mitochondrial homeostasis (Izumikawa et al., 2017), DNA damage response (Konopka et al., 2020; Riancho et al., 2020; Wood et al., 2020) and axonal transport (Fallini et al., 2012; Tripathi et al., 2014). While TDP-43 primarily localizes in the nucleus, upon cellular stress, it translocates to the cytoplasm to form stress granules together with other RBPs and stalled ribosomes (Colombrita et al., 2009). Interestingly, single cell proteomic analysis of somatic motor neurons (MNs) derived from *postmortem* spinal cords of ALS donors with TDP-43 pathology, not only facilitated the differentiation of disease states in individual MNs but also uncovered significant reduction in the abundance of proteins with critical roles in cell energetics, protein translation, proteostasis, and trafficking mechanisms such as Golgi-lysosome trafficking (Guise et al., 2024). Furthermore, *C9orf72* mutations lead to the formation of RNA foci which sequester a range of RBPs including TDP-43, resulting in its aberrant accumulation in the cytoplasm (Lee et al., 2013; Chew et al., 2019).

TDP-43 consists of four domains that mediate distinct activities: (a) a globular N-terminal domain (NTD) with a nuclear localization signal (NLS). The NTD is crucial for the formation of the TDP-43 functional dimer/oligomer (Qin et al., 2014; Mompean et al., 2016; Afroz et al., 2017; Jiang et al., 2017; Mompean et al., 2017) and recruits RNA for splicing (Jiang et al., 2017); (b) two tandem RNA recognition motifs (RRM1 and RRM2) (Lukavsky et al., 2013) with a nuclear export signal (NES) in RRM2 (Winton et al., 2008), although the NES functionality has been questioned (Archbold et al., 2018; Pinarbasi et al., 2018), and (c) a prion-like domain (PrLD) at the C-terminus encompassing two subdomains, a glutamine/asparagine-rich and a glycine-rich region, which is disordered and essential for protein-protein interactions (Buratti, 2020; Jiang et al., 2013). Six cysteine residues are present in TDP-43, with four located in the two RRM domains (Cys173, Cys175, Cys198, and Cys244), while the other two (Cys39 and Cys50) in the N-terminal domain (Valle and Carri, 2017). The oxidation of cysteines within the two RRMs decreases protein solubility and induces the formation of intra- and inter-molecular disulfide linkages (Cohen et al., 2012; Chang et al., 2013). The PrLD mediates TDP-43 intrinsic aggregation propensity (Johnson et al., 2009) and its incorporation into stress granules via its ability to undergo liquid-liquid phase separation (LLPS) (Conicella et al., 2016; Wang et al., 2018). Interestingly, the majority (~95%) of the ALS-linked *TARDBP* mutations are localized at the C-terminal domain (Prasad et al., 2019); these TDP-43 variants show increased stress granule formation upon oxidative stress (Liu-Yesucevitz et al., 2010) and higher aggregation propensity (Conicella et al., 2016). Moreover, certain *TARDBP*-linked mutations enhance cytoplasmic mislocalization of TDP-43 (Barmada et al., 2010; Mutihac et al., 2015; Mitsuzawa et al., 2018). Finally, in addition to cysteine oxidation, also other PTMs such as phosphorylation, acetylation, ubiquitination and the proteolytic processing of TDP-43 that leads to the formation of C-terminal fragments are closely associated with the misfolding and aggregation of the protein (Buratti, 2018; Farina et al., 2021).

Cell culture and animal models have provided compelling evidence indicating a significant involvement of TDP-43 in the initiation and progression of motor neuron degeneration (Bonifacino et al., 2021). Transgenic mice overexpressing TDP-43 with familial fALS mutations, develop aggregates and manifest a full spectrum of ALS-like phenotypes at the molecular, cellular and behavioral levels (Ke et al., 2015; Huang et al., 2020). Similarly, the overexpression of a TDP-43 variant lacking the nuclear localization signal (dNLS), leads to the accumulation of insoluble, phosphorylated cytoplasmic TDP-43 in the brain and spinal cord. This is accompanied by brain atrophy, muscle denervation, significant motor neuron loss, and the development of progressive motor impairment (Walker et al., 2015). Notably, suppression of TDP-43 overexpression leads to a rapid clearance of TDP-43 pathology and rescues motor deficits in inducible mouse models (Ke et al., 2015; Walker et al., 2015). These collective findings strongly suggest that TDP-43 is a key protein implicated in neurodegenerative processes in motor neurons.

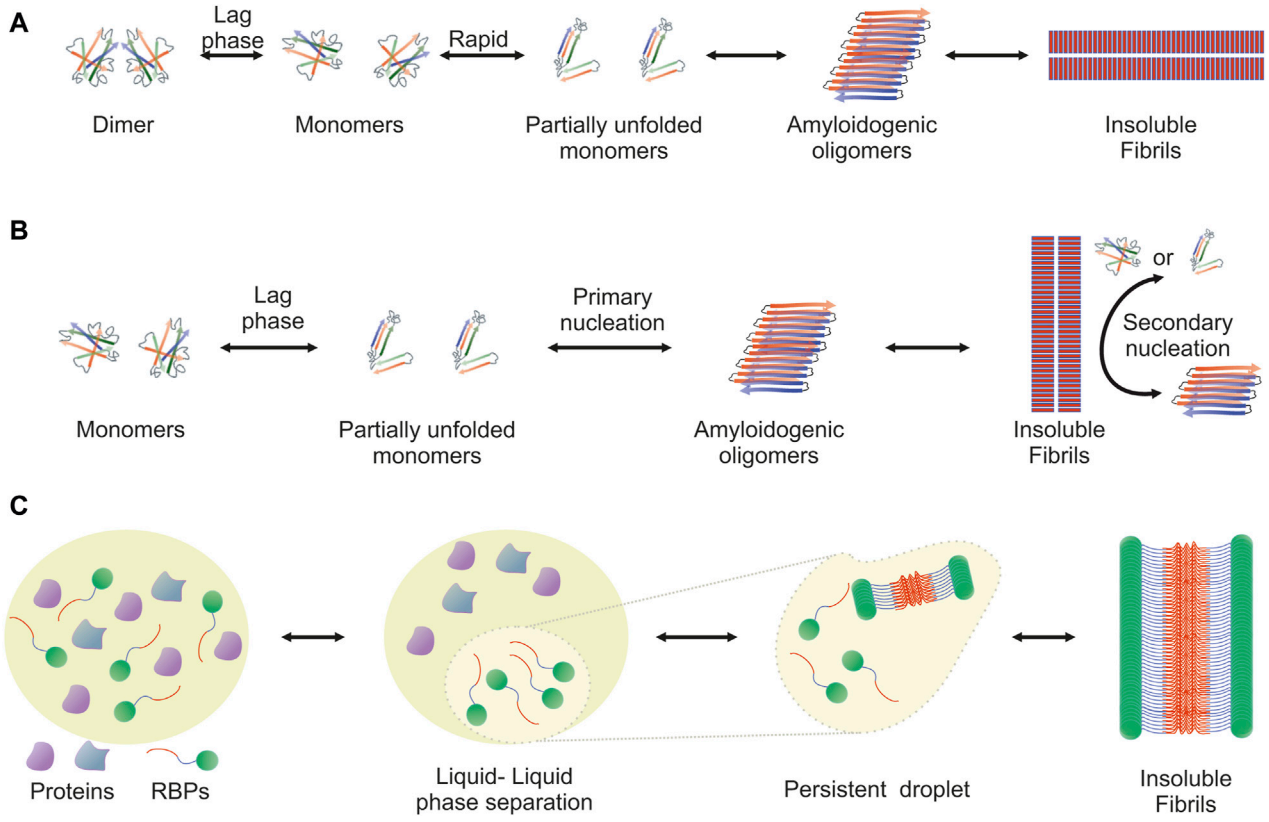

FIGURE 1
Visualization of the amyloidogenic pathway featuring three distinct models. Detailed overview of the diverse mechanisms through which amyloid fibrils can form, each highlighting different aspects and stages of the amyloidogenic process. **(A)** Downhill Polymerization Model: The protein first dissociates into native monomers, which is the rate-limiting step in the formation of fibrils. Subsequently, the monomeric species partially unfold to form the aggregation intermediates. Once such intermediates are formed, the following self-assembly process is a downhill polymerization. **(B)** Nucleation-Growth Model: Amyloid aggregation is kinetically dependent on nucleation events, which include primary and secondary nucleation. Primary nucleation refers to initial events where protein monomers associate into nucleation "seeds." This is a rate-limiting, kinetically unfavorable process, but once the nuclei are formed, addition of further monomers is more favorable through an elongation process. Primary nucleation causes elongation into fibrils, which eventually leads to the formation of a critical mass of fibrils capable of catalyzing a secondary nucleation phase in which nucleus formation from monomers is catalyzed by existing aggregates. This creates a positive feedback loop of aggregation, where small and large oligomers are constantly formed. **(C)** Liquid-Liquid Phase Separation (LLPS) Model: It proposes that amyloidogenic proteins first undergo liquid-liquid phase separation, forming protein-rich droplets. Within these droplets, the concentration of proteins reaches a threshold that facilitates the transition from a disordered liquid state to a more ordered solid state, leading to amyloid fibril formation. This model provides insight into the spatial and temporal regulation of amyloidogenesis within cellular environments.

The aggregation process

The term protein aggregation describes the transition of a protein from its native biologically functional state to the formation of oligomers and medium- or higher-order aggregates through self-association. Protein aggregation is usually caused by the presence of unfolded or misfolded species of the protein. Misfolded conformations typically expose hydrophobic segments within a hydrophilic- either intracellular or extracellular- environment, which subsequently tend to self-associate into soluble oligomers and eventually to larger insoluble aggregates. Most often, the building block of oligomeric and aggregated species is the protein's unfolded/misfolded/partially folded monomer. The structure of such aggregates highly depends on the conformation of the monomeric state: disordered amorphous aggregates are usually formed by unfolded or native monomers while well-defined fibrils with cross-β structure (amyloid fibrils) can originate from partially folded monomers (Almeida and Brito, 2020). Amyloid deposits have been extensively implicated in disease pathogenesis, while there are few disorders associated with amorphous aggregates, such as cataracts caused by γD-crystallin disordered deposition (Moreau and King, 2012).

The amyloidogenic pathway has been extensively studied and two distinct mechanisms, the downhill polymerization and the nucleation-growth model, have been described. Both are characterized by sigmoidal kinetics and differ in the factor that determines the rate-limiting step. In each case, the mechanism of aggregation employed depends on the protein. Downhill polymerization (Figure 1A) is typically observed in proteins with oligomeric native conformation, such as transthyretin (TTR) (Hammarstrom et al., 2003; Eisele et al., 2015). The rate-limiting step is the disassembly of the native oligomer into unstable monomers, which then rapidly form aggregates (Lai et al., 1996; Hurshman et al., 2004; Eisele et al., 2015). Importantly, the lag phase is governed by the slow dissociation of native oligomeric state and seeding does not accelerate the aggregation process. The

nucleation-growth model (Figure 1B), characteristic of the aggregation of amyloid-β peptide (Knowles et al., 2014), resembles the crystallization process (Teplow, 1998; Scherzinger et al., 1999; Wood et al., 1999; Knowles et al., 2014). The rate-limiting step for amyloid fibril development is the formation of protein oligomers (nuclei or seeds), which subsequently drive the rapid elongation of the fibrils by further monomeric or oligomeric species binding to the nuclei. The slow lag phase can be eliminated by adding pre-formed nuclei.

Another mechanism that leads to the formation of ordered aggregates is mediated by LLPS, typically observed in RBPs (Figure 1C). Approximately 30% of the genes associated with ALS encode RBPs, such as TDP-43, FUS, TATA-box binding protein associated factor 15 (TAF15) and proteins from the heterogeneous nuclear ribonucleoprotein (hnRNP) family, including hnRNPA1 and hnRNPA2B1 (Wroe et al., 2008). These proteins form cytoplasmic inclusions in motor neurons of ALS patients and their aggregation propensity is linked to the PrLDs they harbor (Molliex et al., 2015; Patel et al., 2015). PrLDs are a subset of intrinsic disordered regions (IDRs), characterized by low sequence complexity, comprising only a subset of the 20 amino acids; in particular, PrLDs are enriched in uncharged polar amino acids and glycine (Alberti et al., 2009). Intriguingly, about 30% of the 240 human proteins containing predicted PrLDs are involved in RNA processing (March et al., 2016; Verdile et al., 2019). LLPS describes liquid-liquid de-mixing: a high local concentration of IDRs promotes LLPS through transient and weak interactions among the IDRs of RBPs. Importantly, association of RBPs into "droplets" which are separated from the nucleoplasm or the cytoplasm is dynamic and transient. However, persistent association of RBPs with the separated liquid state results in the formation of stable hydrogels and eventually fibrils (Kato et al., 2012; Lin Y. et al., 2015; Guo and Shorter, 2015; Molliex et al., 2015; Murakami et al., 2015; Patel et al., 2015; Kato and McKnight, 2017; Shin and Brangwynne, 2017).

Until recently, there was intense debate over whether the protein aggregates detected in ALS patients are typical amyloids, primarily due to controversial findings. Initially, reports indicated that the TDP-43 positive filamentous aggregates found in ALS-affected motor neurons (Hasegawa et al., 2008; Lin and Dickson, 2008) did not stain with the amyloid-specific dyes Congo red and Thioflavin S (ThS) (Kerman et al., 2010). This finding was further supported by *in vitro* experiments, where recombinant TDP-43 formed Thioflavin T (ThT)-negative granulo-filamentous aggregates similar to those observed in ALS patients (Johnson et al., 2009) or amorphous aggregates (Capitini et al., 2014). On the other hand, it has been shown that peptide fragments from the C-terminal domain and certain TDP-43 variants form ThT-positive aggregates *in vitro*, acquiring a β-sheet-enriched structure (Chen et al., 2010; Guo et al., 2011; Zhu et al., 2014; Jiang et al., 2016). These conflicting findings can now be explained based on the structure of TDP-43 aggregates from ALS with FTLD (Arseni et al., 2022), revealing the formation of filaments which are structurally distinct from cross-β amyloid fibrils and a novel fold that bears no similarity to TDP-43 filaments formed *in vitro* (Cao et al., 2019; Li et al., 2021).

The Falcon group employed cryogenic electron microscopy to determine the structures of aggregated TDP-43 in the frontal and motor cortices of an individual who succumbed to ALS with FTLD, as well as in the frontal cortex of another individual with the same diagnosis (Arseni et al., 2022). Remarkably, they identified an identical amyloid-like filament structure consisting of a single protofilament in both brain regions and individuals. The ordered filament core, spanning residues 282 to 360 in the TDP-43 low-complexity domain, adopts a unique double-spiral-shaped fold. The filament structure lacks the typical β-sheet stacking associated with cross-β amyloid formation due to an abundance of glycine and neutral polar residues, facilitating numerous turns and restricting β-strand length. The uneven distribution of residues results in structurally and chemically distinct surfaces, suggesting potential ligand binding sites on external densities.

This study also revealed that the brain-derived TDP-43 filaments are structurally distinct compared to filaments assembled *in vitro* from its LCD under mildly acidic conditions (pH 4), or related fragments (Li et al., 2021). These differences include opposite chirality and variations in both protein fold and secondary structure. For the LCD, the structure revealed single protofilament fibrils featuring a large core comprised of 139 residues out of the 148 present in the LCD, tightly packed together. The C-terminal segment of this core exhibits mainly planar characteristics and is marked by a small proportion of hydrophobic amino acids. In contrast, the N-terminal region includes numerous hydrophobic residues and adopts a non-planar backbone conformation, leading to the rugged surfaces observed at the ends of the fibrils.

Cryo-electron microscopy was also employed to elucidate the structures of two segments identified as the pathogenic cores in human TDP-43 aggregation (Cao et al., 2019). The first segment, SegA (residues 311–360), exhibits three polymorphs, each characterized by a dagger-shaped fold, spanning residues 312–346. Tight hydrophobic interactions are formed by hydrophobic residues ranging from Phe313 to Ala341 whereas the dagger tip is created by a sharp 160° kink at Gln327. The variations among the three SegA polymorphs primarily arise from differences in protofilament numbers and symmetry. In contrast to the polymorphic nature of SegA, the second segment, SegB A315E (residues 286–331, containing the ALS hereditary mutation A315E), forms fibrils with a consistent morphology. These fibrils adopt an R-shaped fold spanning residues 288–319, which, overall, displays a more pronounced kink compared to the dagger-shaped fold, likely attributable to the higher prevalence of glycine residues. Each fibril is composed of four protofilaments, and notably, all four R-folds are characterized by the presence of a salt-bridge between Arg293 and Glu315, facilitated by the pathogenic A315E mutation. This salt-bridge may impact the kinetics of fibril growth and nucleation, providing a mechanistic explanation for A315E's propensity to promote TDP-43 aggregation through electrostatic attraction with Arg293.

Along the same lines, SOD1-positive inclusions from ALS cases display a fibrillary morphology (Kato et al., 2000) but do not react with ThS (Kerman et al., 2010). In contrast, SOD1 cytoplasmic aggregates from a transgenic SOD1-fALS mouse model could be stained with ThS (Furukawa et al., 2008). Importantly, the aggregation kinetics of SOD1 are typically monitored by ThT staining (Rakhit et al., 2002; Furukawa et al., 2008; Iwakawa et al., 2017; Shvil et al., 2018) and pre-formed SOD1 aggregates exhibit seeding activity both *in vitro* and intracellularly (Furukawa

et al., 2008; Furukawa et al., 2013). Moreover, ALS-related SOD1 mutant proteins crystallize in forms comprising higher-order assemblies of aligned β-sheets (Elam et al., 2003). On the other hand, *in vitro* monitoring of SOD1 aggregation has demonstrated that a competition between amorphous and amyloid aggregation occurs (Abdolvahabi et al., 2016), proposing a possible factor for the wide variability in kinetic results among publications (Crown et al., 2019).

In a recent study, cytotoxic amyloid fibrils were generated from full-length human apo-SOD1 under reducing conditions, and their atomic structure was elucidated using cryo-EM (Wang LQ. et al., 2022). The SOD1 fibril is composed of a singular protofilament featuring a left-handed helix. Within the fibril core, a serpentine fold is formed, incorporating six β-strands of the N-terminal segment (residues 3–55) and seven β-strands of the C-terminal segment (residues 86–153), with an unstructured region in between. This novel amyloid fibril structure displays a very compact fold, and the connection of the two segments is stabilized by three pairs of salt bridges, effectively "zipping up" the structure.

Characteristics of oligomeric species

A multitude of pathogenic mechanisms have been described for ALS, including protein misfolding and aggregation, glutamate excitotoxicity, oxidative stress, mitochondrial dysfunction, declined autophagy, neuroinflammation and DNA damage. However, the drive behind ALS onset and progression, as well as the degree to which each mechanism contributes to disease phenotypes and heterogeneity, remains unclear. Current evidence supports that protein misfolding and aggregation exert toxic effects on cellular fitness, eventually compromising organismal health. Regarding the toxic agent in ALS and other conformational neurodegenerative diseases, the debate continuous on whether soluble misfolded species (monomeric or oligomeric) or insoluble aggregates confer toxicity (Gelpi and Colom-Cadena, 2019).

Recent work has highlighted SOD1 oligomers, particularly the trimeric variants, as the neurotoxic entities (Proctor et al., 2016). The study revealed that SOD1 mutants promoting trimerization led to increased neuronal cell death and established a direct association between misfolded oligomers and neuron death by linking cytotoxicity to trimer stability. Additional studies showed that large aggregates are non-toxic and actually play a neuroprotective role (Zhu et al., 2018; Gill et al., 2019). Interestingly, SOD1 mutants designed to promote the formation of large aggregates and destabilize toxic trimers did not impact cell viability (Zhu et al., 2018). The mechanism leading to the formation of non-native trimers remains unclear, however, in order to occur, SOD1 must undergo dissociation into monomers (Khare et al., 2004). External factors, such as oxidative stress (Wilcox et al., 2009) or exposure to the toxin β-methylamino-L-alanine (BMMA) (Proctor et al., 2019), may play a role in the transition of SOD1 dimers into monomers. At present, there are two hypotheses regarding trimer formation (Choi and Dokholyan, 2021). The first suggests that trimers occur on the pathway from monomers to native dimers (dissociating into monomers), then to trimers and finally to larger aggregates. The second posits that trimer formation is an off-pathway phenomenon, meaning it does not lead to the generation of large aggregates, and current experimental evidence favors this scenario (Hnath and Dokholyan, 2022). Indicatively, the abundance of soluble misfolded SOD1 subfractions, in the range from monomeric to trimeric in size, has been associated with a reduced lifespan in SOD1-ALS mouse models (Zetterstrom et al., 2007).

Despite the association of TDP-43 aggregation with disease (Neumann et al., 2006; Hasegawa et al., 2008), several studies have highlighted the functional oligomerization of TDP-43 in physiological contexts. The NTD residues 1–105 and 1–265 induce the formation of homo-oligomeric species in a concentration-dependent manner, initiated by the formation of intermolecular disulfide bonds ultimately leading to its tetramerization (Chang et al., 2012; Jiang et al., 2017). Oligomerization of TDP-43 is crucial for its nuclear RNA splicing activity and, interestingly, serves to prevent the aggregation of the C-terminal TDP-43 within the nucleus of neuronal cells (Afroz et al., 2017; Jiang et al., 2017). The crystal structure of a purified recombinant human TDP-43 fragment (residues 1–80) was determined at a resolution of 2.1 Å, revealing a unique pattern of head-to-tail interactions between monomers, resulting in the formation of solenoid-like polymers (Afroz et al., 2017). In contrast to physiological oligomers, pathological TDP-43 oligomers exhibit distinct characteristics. Detectable in the early stages of aggregation, their formation is accelerated in the presence of disease-associated TDP-43 mutations (Johnson et al., 2009; French et al., 2019). Using a polyclonal TDP-43 oligomer-specific antibody (Fang et al., 2014), pathological TDP-43 oligomers were identified in FTLD patients (Kao et al., 2015).

The TDP-43 oligomers manifest as a diverse spectrum of molecules, ranging from low-molecular-weight species like dimers, trimers, and tetramers, to a variety of high-molecular-weight species (Johnson et al., 2009; Guo et al., 2011; Choksi et al., 2014; Fang et al., 2014; French et al., 2019). Described as heterogeneous structures at the intermediate stage of aggregate formation, the oligomerization process may involve cysteine oxidation, particularly in the initial stages (Bozzo et al., 2016). Extracellular exposure to TDP-43 oligomers demonstrated cytotoxicity in neuroblastome cells (Choksi et al., 2014), and intrahippocampal injection of these oligomers caused damage to hippocampal neurons in wild-type mice (Fang et al., 2014), further substantiating their neurotoxicity. Interestingly, in an animal model expressing the ALS-related TDP-43 (M377V) variant at nearly endogenous levels, there was complete absence of mature insoluble aggregates (Gordon et al., 2019). However, these mice progressively developed motor function deficits concomitant with the loss of neuromuscular junction integrity, thus recapitulating ALS phenotypes (Gordon et al., 2019). Taken together, current evidence is not sufficient to argue towards one or the other direction, though it seems possible that both oligomeric soluble species and insoluble aggregates contribute differentially to ALS pathogenesis (Arnold et al., 2013; Gordon et al., 2019).

The ability to isolate, cultivate, and reprogram cells obtained from patients, such as fibroblasts, into central nervous system (CNS) cells, has introduced a novel approach that complements traditional preclinical *in vitro* and *in vivo* models (Ferraiuolo and Maragakis, 2021; Du et al., 2023). There are two primary approaches to this method. Several laboratories have investigated the use of induced pluripotent stem cells (iPSCs), focusing on generating motor

neurons from patients with mutations in *TARDBP*, *FUS*, *SOD1*, and *C9orf72*, or those with sporadic disease (Ferraiuolo and Maragakis, 2021). For instance, motor neurons derived from ALS patients with mutated TDP-43, developed cytosolic aggregates resembling those observed in *postmortem* tissues and displayed shorter neurites (Egawa et al., 2012). Importantly, the accumulation of insoluble protein inclusions has been observed in numerous studies using iPSC-derived motor neurons (Dimos et al., 2008; Burkhardt et al., 2013; Chen et al., 2014; Seminary et al., 2018), although neuronal cell death is not observed, supporting the non-cell-autonomous hypothesis of ALS neurodegeneration (Ilieva et al., 2009; Wachter et al., 2015).

Limiting the screening approach to monocultured motor neurons restricts the influence of non-neuronal cells on observed phenotypes. In ALS, neighboring cells like astrocytes and microglia significantly impact neurodegenerative phenotypes and neuronal survival (Boillee et al., 2006). Additionally, iPSC technology often results in the loss of the cellular aging signature (Lapasset et al., 2011; Patterson et al., 2012). An alternative method involves trans-differentiating patient fibroblasts into neural progenitors, which can then be further differentiated into neurons or astrocytes (Meyer et al., 2014; Mertens et al., 2016; Tang et al., 2017). These astrocytes exhibit expected toxicity toward co-cultured motor neurons and seem to maintain the associated aging phenotype (Gatto et al., 2021). Interestingly, a study using iPSC-derived motor neurons and astrocytes revealed that recombinant TDP-43 oligomers, can induce neuronal toxicity, leading to increased caspase-3 activity and to apoptosis of neurons but not astrocytes (Smethurst et al., 2020).

Mechanisms of aggregation-mediated toxicity

Concerning the mechanisms underlying aggregation-mediated toxicity in ALS and other protein misfolding diseases, two major models have been proposed: the loss-of-function hypothesis and the gain-of-toxic activity hypothesis. While both terms are borrowed from genetics, mutations are not always relevant within the context of misfolding and aggregation. In the majority of ALS cases, misfolded species originate from a wild-type protein devoid of inherited mutations. Thus, in this section we focus on how the aggregation process itself, rather than the genetic background (as reviewed in Kim et al., 2020), can lead to phenotypes resembling loss and gain of activity. Importantly, these mechanisms are not mutually exclusive; in fact, some alterations observed in ALS-related cellular physiology can be better explained by a combination of loss and gain of activity.

The loss-of-function hypothesis

In genetics, the term "loss-of-function" is used to describe a mutation that partially or completely disrupts the activity of a gene product. Accordingly, during the aggregation process, sequestration and often mislocalization of a protein within aggregates, reduce its abundance, thereby leading to impaired activity. Indicatively, most ALS-affected motor neurons exhibit wild-type TDP-43 cytoplasmic inclusions concomitant with TDP-43 clearance from the nucleus, indicating that a loss of TDP-43 splicing activity could contribute to disease phenotypes (Polymenidou et al., 2011; Tollervey et al., 2011). In support of this, *Tardbp* knockout mice display early embryonic lethality (Kraemer et al., 2010); moreover, TDP-43 is essential for normal motor neuron function in flies (Feiguin et al., 2009) and mice (Yang et al., 2014), as evidenced by motor dysfunction and deficits in the neuromuscular junction after TDP-43 depletion. Conditional *Tardbp* knockout mice, when crossed with various tissue-specific Cre lines, exhibit diverse cellular and behavioral phenotypes, ranging from electrophysiological abnormalities to deficits in motor movement (Iguchi et al., 2013; Wu et al., 2019). TDP-43 has been demonstrated to interact with RNA transcripts of over 6,000 genes in mice. Accordingly, the reduction of TDP-43 levels in adult mouse brains using antisense oligonucleotides (ASOs) led to the differential regulation of approximately 600 genes, mostly involved in synaptic activity and neuronal development, and to the alteration of 1,000 splicing events (Polymenidou et al., 2011).

Loss of function, at least partially, can also be attributed to SOD1-linked ALS. Although *Sod1* knockout mice ($Sod1^{-/-}$) develop normally and do not display evident ALS-like phenotypes (Reaume et al., 1996), they do exhibit- together with other pathologies- progressive motor neuropathy characterized by peripheral motor axon degeneration (Flood et al., 1999; Fischer et al., 2011; Larkin et al., 2011; Fischer et al., 2012; Shi et al., 2014; Ivannikov and Van Remmen, 2015). Furthermore, recent human genetics studies indicate that SOD1 homozygous loss-of-function can lead to debilitating phenotypes, including progressive loss of motor abilities, tetraspasticity, and hyperreflexia, but not ALS. In contrast, heterozygous carriers remained unaffected (Andersen et al., 2019; Park et al., 2019).

The gain-of-toxic activity hypothesis

The accumulation of insoluble proteins is a prominent feature in ALS pathology, suggesting an interconnection between protein aggregation and disease development. The hypothesis posits that protein aggregates may initiate the disease process by acquiring toxic properties, which are mainly exerted through the sequestration of crucial components of physiological processes, such as RNA metabolism, DNA damage response, synaptic signaling and axonal trafficking, thereby disrupting these cellular functions and contributing to disease progression (Ilieva et al., 2009). For instance, TDP-43 aggregates have been found to contain proteins like the RNA-processing factor Matrin 3 (MATR3) (Tada et al., 2018), the ubiquitin-proteasome system factor Ubiquilin 2 (UBQLN2) (Deng et al., 2011; Williams et al., 2012), the Golgi complex and membrane trafficking factor Optineurin (OPN) (Hortobagyi et al., 2011) and the Rho guanine nucleotide exchange factor 28 (RGNEF) (Keller et al., 2012) involved in synapse formation and dendritic morphogenesis. Other potential mechanisms for the induction of cell toxicity by protein aggregation in ALS include disruption of the proteostasis network, leading to impairment of crucial protein degradation pathways like the ubiquitin proteasome system and autophagy (Medinas et al., 2017; Ramesh and Pandey, 2017; Montibeller et al., 2020). Compelling evidence also connects aggregated SOD1 and TDP-43 to mitochondrial dysfunction and degeneration (Jankovic et al., 2021). TDP-43 aggregates sequester specific microRNAs and mitochondrial proteins encoded by the nuclear genome, with dysregulation of their expression levels leading to mitochondrial dysfunction and oxidative stress (Zuo et al., 2021).

Aggregates of mutant SOD1 in the intermembrane space of mitochondria diminish the activity of the electron transport chain (ETC) complexes in rats (Pickles et al., 2013) and affect mitophagy by disabling recruitment of autophagy receptors on damaged mitochondria in N2a cells (Tak et al., 2020).

Alternatively, aberrant protein aggregates can induce a chronic inflammatory response in the brain contributing to disease progression (Appel et al., 2021). In a recent study, Yu et al. demonstrated that TDP-43 induces inflammation in ALS by initiating the release of mitochondrial DNA into the cytoplasm. This, in turn, activates the cytoplasmic DNA-sensing cyclic GMP-AMP synthase (cGAS)/stimulator of interferon genes (STING) pathway (Yu et al., 2020). Separately, the nuclear factor-kappa β (NF-κB) protein has been reported as a master regulator of inflammation in ALS (Haidet-Phillips et al., 2011); in mutant SOD1 mice, NF-κB signaling becomes activated within glia as the disease progresses (Frakes et al., 2014). In support of these findings, extensive astrocytosis (Kushner et al., 1991; Nagy et al., 1994; Reischauer et al., 2018; Schiffer et al., 1996), microglial activation (Henkel et al., 2004; Turner et al., 2004; Zurcher et al., 2015), as well as increased levels of inflammatory cytokines (Moreau et al., 2005; Liu et al., 2015; Lu et al., 2016) and elevated levels of chitotriosidase (Chit-1) and chitinase-3-like protein 1 (CHI3L1) in cerebrospinal fluid (CSF) correlated to disease progression (Vu et al., 2020), have been detected in ALS patients.

Therapeutic targeting of misfolding and aggregation

Among neurodegenerative diseases, ALS stands out as one of the few for which disease-modifying therapies have gained approval. The current standard of care for ALS patients involves multidisciplinary symptom management, both pharmacological and non-pharmacological, such as nutritional and respiratory support (Hardiman et al., 2017; Mejzini et al., 2019). Clinical trials in ALS have assessed over 60 compounds (Petrov et al., 2017), each with distinct mechanisms of action; however, only four- riluzole, edaravone, AMX0035 and tofersen- have been granted regulatory clearance for clinical use. Riluzole, the first FDA-approved ALS therapy in 1995 (Lacomblez et al., 1996a; Lacomblez et al., 1996b), is not a cure for ALS. Instead, it is a neuroprotective drug that decreases glutamate release into the synaptic cleft by blocking voltage-gated sodium channels on presynaptic neurons, thereby mitigating excitotoxicity (Wang et al., 2004; Bissaro and Moro, 2019). While Riluzole does not modify the course of the disease (Fang et al., 2018), it prolongs the patient's survival from 6 to 19 months (Andrews et al., 2020). Edaravone is a potent anti-oxidant and a free-radical scavenger, preventing oxidative stress-induced motor neuron death (Jami et al., 2015; Soejima-Kusunoki et al., 2022). A randomized controlled trial conducted in Japan demonstrated the effectiveness of Edaravone in slowing the rate of motor function deterioration, particularly in selected patients with early disease onset and rapid progression (Writing Group and Edaravone MCI-186 ALS 19 Study Group, 2017). Its impact on survival is yet to be determined. Apart from Japan and other Asian countries, its use has been approved by the FDA and Health Canada, but not yet from the EMA. A recently developed oral formulation in the United States is expected to replace the intravenous version (Pattee et al., 2023). AMX0035 was approved in 2022 for the treatment of ALS in the United States and Canada, and it is currently being evaluated in the PHOENIX phase III clinical trial (Nikitin et al., 2023). It is a coformulation of sodium phenylbutyrate, a chemical chaperone that improves endoplasmic reticulum (ER) folding capacity by upregulating heat-shock proteins (Suaud et al., 2011), and taurursodiol (tauroursodeoxycholic acid), an inhibitor of mitochondrial-associated apoptosis (Rodrigues et al., 2003). This therapeutic approach is designed to address various ALS-associated pathophysiological mechanisms such as mitochondrial dysfunction and ER stress that ultimately lead to motor neuron injury and cell death.

Tofersen is an antisense oligonucleotide (ASO) that obtained its initial approval in the United States on April 25, 2023, and in Europe on February 22, 2024, for the treatment of ALS in patients with a confirmed *SOD1* mutation. It has been designed to mediate RNase H–dependent degradation of *SOD1* mRNA to reduce the synthesis of SOD1 protein (McCampbell et al., 2018; Rinaldi and Wood, 2018). The preclinical rationale supporting the ASO knockdown of SOD1 was very robust, stemming from several years of systematic analysis showing increased survival and enhanced motor performance in SOD1 (G93A) rats and mice and decreased SOD1 protein levels in nonhuman primates (Iannitti et al., 2018; McCampbell et al., 2018). Its intrathecal administration in clinical trials demonstrated a deceleration in the decline of participants with rapidly progressing disease and apparent clinical stabilization in those with slower progressing disease (Miller et al., 2022). During the intervention period, concentrations of phosphorylated neurofilament heavy and neurofilament light (NFL) in plasma and CSF, biomarkers indicative of axonal injury and neurodegeneration, were found to be decreased (Miller et al., 2022). Tofersen is currently being evaluated in the phase III ATLAS study for its ability to delay the clinical onset of ALS in pre-symptomatic individuals with a confirmed SOD1 mutation (Benatar et al., 2022).

The complex nature of ALS genetics, coupled with the disease's high heterogeneity, presents a great challenge in developing treatment strategies that universally benefit every patient. Consequently, there has been a shift in focus towards identifying converging paths and common pathologies that contribute to motor neuron vulnerability and degeneration in ALS. Among these factors, protein aggregation emerges as a prevalent underlying cause not only in ALS but also in various other neurodegenerative diseases. Despite the diversity of mutations in different genes, leading to potential variations in the aggregated proteins, the shared problem of protein aggregation spans a wide spectrum of patients, encompassing familial ALS (fALS), sporadic ALS (sALS), and ALS with frontotemporal dementia (ALS/FTLD) (Blokhuis et al., 2013). As a result, the pursuit of therapies targeting protein aggregation holds significant promise and represents a crucial step forward in addressing ALS and related disorders (Elliott et al., 2020).

Several approaches have been applied to reduce the levels of toxic variants; these include proteolysis targeting chimeras (PROTACs) inducing protein degradation (Tseng et al., 2023), antibodies (Maier et al., 2018; Pozzi et al., 2019; Afroz et al.,

2023; Audrain et al., 2023; Bakavayev et al., 2023), vaccines (Zhao et al., 2019), antisense oligonucleotides (Iannitti et al., 2018; Mead et al., 2023), RNA interference (RNAi) with small RNAs (shRNA and miRNA) (Bravo-Hernandez et al., 2020; Mueller et al., 2020), and CRISPR/Cas9 gene editing (Duan et al., 2020). Another way of reducing the accumulation of toxic aggregates is to restore dysfunctional proteostasis by upregulating chaperones (Kalmar and Greensmith, 2017; Kinger et al., 2023), inducing autophagy (Chen et al., 2020) and activating the proteasome (Webster et al., 2017). Currently, many compounds targeting proteostasis, such as trehalose (Seelos Therapeutics) and Trametinib (GENUV) are being explored in clinical trials. Moreover, PMN-267 (ProMIS Neurosciences), an antibody that targets the formation of misfolded TDP-43, is under preclinical development (Mead et al., 2023). Despite the success of Tofersen, a similar strategy utilizing intrathecally delivered ASOs for C9orf72-associated ALS did not show clinical benefits, leading to the termination of the clinical trial in 2022 (Mead et al., 2023).

In this review, we focus on molecules that directly target the misfolded species (monomers, oligomers or mature aggregates) to (a) **stabilize** the native protein conformation, (b) **restore** the native conformation of misfolded species and (c) inhibit protein **oligomerization**. Such molecules fall into two categories depending on the specificity to bind to their target, namely, chemical and pharmacological chaperones.

The term "chaperone" is borrowed from the name of a class of cellular proteins that assist polypeptide chains in acquiring their native, functionally active, conformation. They participate in (a) the folding of nascent polypeptides (*de novo* folding) or the refolding of stress-mediated misfolding, (b) the disaggregation of protein aggregates and (c) proteostatic pathways that direct denatured and misfolded/unfolded proteins for degradation (Wentink and Rosenzweig, 2023). However, pharmacological chaperones, unlike proteins, are low molecular weight chemical molecules that exert their action by specifically binding to their target proteins. They typically stabilize an already folded or partially folded protein, protect it from thermal denaturation, prevent proteolytic degradation and also inhibit aggregation, restoring proper steady-state levels (Convertino et al., 2016; Bose and Cho, 2017). Pharmacological chaperones have successfully been used experimentally *in vitro* and *in vivo* (Leidenheimer and Ryder, 2014; Hou et al., 2018), and they have entered clinical trials, to restore the function of specific misfolded proteins (Liguori et al., 2020; Tran et al., 2020). For example, Tafamidis has been approved for the treatment of transthyretin amyloidosis (ATTR) (Bulawa et al., 2012; Maurer et al., 2018) and Migalastat has been licensed for the treatment of Fabry disease (FD) in patients carrying specific lysosomal enzyme α-galactosidase A (GLA) variants (Germain et al., 2016).

Chemical chaperones are also low-molecular-weight compounds that lack specificity since they can bind to and stabilize virtually any protein without having a designated binding site (Cortez and Sim, 2014). They can be divided into two groups: osmolytes and hydrophobic compounds. Osmolytes, such as glycerol, produce a hydrophobic environment around proteins by removing water molecules, thereby increasing the free energy of the unfolded state and eventually shifting the equilibrium towards the folded state (Wang and Bolen, 1997; Street et al., 2006). Hydrophobic chaperones facilitate proper folding by directly interacting with the exposed hydrophobic regions of unfolded proteins, resembling the action of molecular chaperones (Kuzuhara et al., 2008). For example, the green tea catechin, (−)-epigallocatechin gallate (EGCG), seems to exert its general anti-amyloidogenic properties by directly binding to unfolded/misfolded proteins (Debnath et al., 2016). As mentioned above, the best-known example of chemical chaperone for ALS treatment is sodium phenylbutyrate (Suaud et al., 2011).

Discovering inhibitors of protein misfolding and aggregation

Developing a new drug is a complex and challenging process that yields significant benefits for both society and the scientific community. High-throughput screening (HTS) is crucial in the early stages of small-molecule drug development, particularly when insufficient information limits structure-based approaches (Blay et al., 2020). For targets such as oligomeric species and aggregates, which lack well-defined structures and exist in dynamically varying mixtures, HTS requires innovative strategies to discover effective treatments. The utilized methods must be biologically relevant, sensitive, robust, and cost-effective, targeting diseases of significant relevance. HTS integrates biochemical and cell-based assays with computational strategies to identify potential drug candidates. *In silico* screening employs computational methods to predict interactions between molecules and targets, a critical step given the extensive chemical space. Unlike traditional HTS, which assesses thousands of compounds, virtual screening has the capacity to evaluate billions (Bohacek et al., 1996; Gorgulla et al., 2022), showcasing the expansive scope of modern drug discovery efforts.

In 2005, Ray et al. employed an *in silico* screening strategy of approximately 1.5 million compounds from commercial libraries (Ray et al., 2005). The objective was to identify molecules capable of stabilizing the SOD1 (A4V) dimer. The screening process yielded 100 hits, and subsequent mutagenesis studies using various *in vitro* aggregation assay protocols helped narrow down the selection to the 15 most effective compounds. Notably, three of the top five compounds shared pyrimidine-like structures. However, subsequent co-crystal structures of SOD1 with various small molecules and pyrimidine-like compounds challenged the initial assumption that the observed protection was solely due to binding to the hydrophobic cavity formed at the dimer interface. Instead, these structures suggested that the ligands interacted with Trp32, offering new insights into the mechanism of action (Antonyuk et al., 2010; Wright et al., 2013).

Nowak et al. developed (Nowak et al., 2011) an algorithm for the *in silico* screening of an extensive library comprising 2.2 million small molecules sourced from 11 commercially available databases. The primary objective was to discern compounds exhibiting selective binding affinity for mutant SOD1 over plasma proteins. Their investigation revealed a substantial subset of compounds displaying robust binding capabilities to SOD1, particularly within a hydrophobic cavity encompassing Val7–Gly147–Val148 at the dimerization interface. Notably, *in vitro* experimentation demonstrated the pronounced inhibitory effects of both isoproterenol and 5-fluorouridine on the aggregation process of mutant SOD1.

In another computational screen involving 4,400 drugs and compounds, three flavonoids, quercitrin, quercetin-3-β-D-glucoside (Q3BDG) and EGCG, were predicted to bind around the dimer interface and stabilize SOD1, potentially inhibiting its aggregation, predictions which were confirmed experimentally (Ip et al., 2017). Interestingly, quercitrin and Q3BDG outperformed EGCG both *in silico* and *in vitro*. The tripeptide CGH (Srinivasan and Rajasekaran, 2019), hesperidin and 2,3,5,4′-tetrahydroxystilbene-2-O-β-D-glucoside retrieved from the traditional Chinese medicine database (Huang et al., 2014), and the natural polyphenols, kaempferol, and kaempferide (Srinivasan and Rajasekaran, 2018) have all been predicted to bind SOD1 and inhibit its aggregation, necessitating experimental verification.

Biochemical screens

This type of screens involves the use of a purified target protein of interest to assess the aggregation-inhibitory activity of test compounds. To quantify the outcomes of these assays, various optical methods such as absorbance, fluorescence, or luminescence are employed as readouts (Fang, 2012). For example, a screening assay of 640 FDA-approved drugs, aiming to evaluate their impact on the abnormal oligomerization of SOD1 (G37R) has been conducted *in vitro*. The primary objective was to identify molecules capable of inhibiting the formation of insoluble disulfide-linked oligomers. Among the extensive drug repertoire, six compounds - simvastatin, lovastatin, mevastatin, miltefosine, alfacalcidol and calcitriol-exhibited remarkable efficacy in almost completely suppressing the increase in solution turbidity (Anzai et al., 2016).

Cellular screens

Cell-based assays play a crucial role at every stage of the drug discovery process, serving various purposes from target identification and validation to lead optimization and safety screening (Macarron and Hertzberg, 2009; McGown and Stopford, 2018). For ALS, cell models employed in these assays include the NSC-34 cell line (Barber et al., 2009), created by fusing MN from the spinal cords of mouse embryos with mouse neuroblastoma cells, human astrocyte-derived H4 cells (Murakami et al., 2011), and PC12 cells from the rat adrenal gland (Benmohamed et al., 2011; Xia et al., 2011; Zhang W. et al., 2012; Wright et al., 2012; Boyd et al., 2014). Emphasis has also been given to the use of primary rat MN cultures (Vincent et al., 2005) or mouse embryonic stem cell-derived MNs in small molecule screening studies (Yang et al., 2013; Thams et al., 2019). Finally, the use of iPSC technology has significantly contributed to the development of current ALS drug-screening platforms (Burkhardt et al., 2013; Imamura et al., 2017).

In the following section, we describe molecules that have emerged from drug-screens based on the above platforms and target misfolded species of SOD1 and TDP-43 (Figure 2).

Molecules targeting SOD1 misfolding and aggregation

Stabilization of the dimer

Upon translation, SOD1 undergoes spontaneous folding, primarily initiated around hydrophobic residues, culminating in the formation of a monomeric Greek-key β-barrel structure. For SOD1 to achieve activity and stability, three essential PTMs are required. The binding of zinc and the formation of an intra-subunit disulphide bond establish the SOD1 homodimer interface in conjunction with the N- and C-termini and four inter-subunit hydrogen bonds are formed. The introduction of copper to the SOD1 active site enhances thermal stability and activates enzymatic functionality (Hornberg et al., 2007). In the absence of these PTMs and the subsequent homodimer formation, SOD1 exhibits diminished thermal stability, populates unfolded conformations, and is susceptible to self-association (Culik et al., 2018). Interestingly, the engineering of an inter-subunit disulfide bond in the SOD1 (A4V) variant alleviated aggregation and restored enzymic activity (Ray et al., 2004), suggesting that stabilizing the dimer is a promising therapeutic strategy (McAlary and Yerbury, 2019; Yerbury and Cashman, 2020).

Targeting the Cys111 residue

The covalent attachment of small molecules to Cys111 has been a frequently employed strategy in the discovery of pharmacological chaperones for SOD1. This is attributed to their accessibility, reactivity, and potential for linking or stabilizing the SOD1 homodimer, as opposing Cys111 residues are separated by a short distance across the dimer interface and possess a highly reactive sulfhydryl group. Tethering Cys111 residues with maleimide linkers to bridge the 9 Å gap across the SOD1 dimer interface substantially increases the thermal stability of the SOD1 (G93A) and SOD1 (G85R) ALS-linked variants, restoring the enzymatic activity and metal-binding ability of the otherwise inactive G85R variant (Auclair et al., 2010). However, maleimide compounds do not exhibit favorable drug-like properties (Gavrin et al., 2012), while maleimide crosslinking inhibits SOD1 complex formation with the human copper chaperone for SOD1 (CCS), an interaction essential for SOD1 activation (Wright et al., 2016). Similarly, cyclic disulfides have demonstrated the ability to link opposing Cys111 residues and exhibited cell penetrability (Wright, 2020). For example, mono-S-oxo derivatives were able to bind and tether 95% of SOD1 monomers as dimers within cells (Donnelly et al., 2018). Taking a different approach, cisplatin enhances the thermal stability of metal-free SOD1 and can effectively prevent or reverse SOD1 aggregation within cells without the need for subunit tethering (Banci et al., 2012) but hinders complex formation between SOD1 and hCCS (Wright et al., 2016).

Synthetic organo-selenium pharmaceutical compounds, such as ebselen and ebsulphur, function as bifunctional small molecule chaperones for various mutant forms of SOD1 by forming covalent bonds with Cys111 (Capper et al., 2018). The SOD1 dimer interface groove can accommodate two ebselen molecules, binding to opposing Cys111 residues and expanding the hydrophobic SOD1 homodimer interface through aromatic π–π stacking of adjacent ligands. As a result, the affinity between monomers significantly increases, particularly for the SOD1 (A4V) mutant, shifting the monomer-dimer equilibrium towards the dimer (Capper et al., 2018). Ebsulphur exhibits similar binding properties. Importantly, ebselen does not interfere with the SOD1-CCS interaction (Capper et al., 2018), giving it a significant advantage over other Cys111-binding compounds, such as cisplatin. Ebselen is also known for its anti-inflammatory,

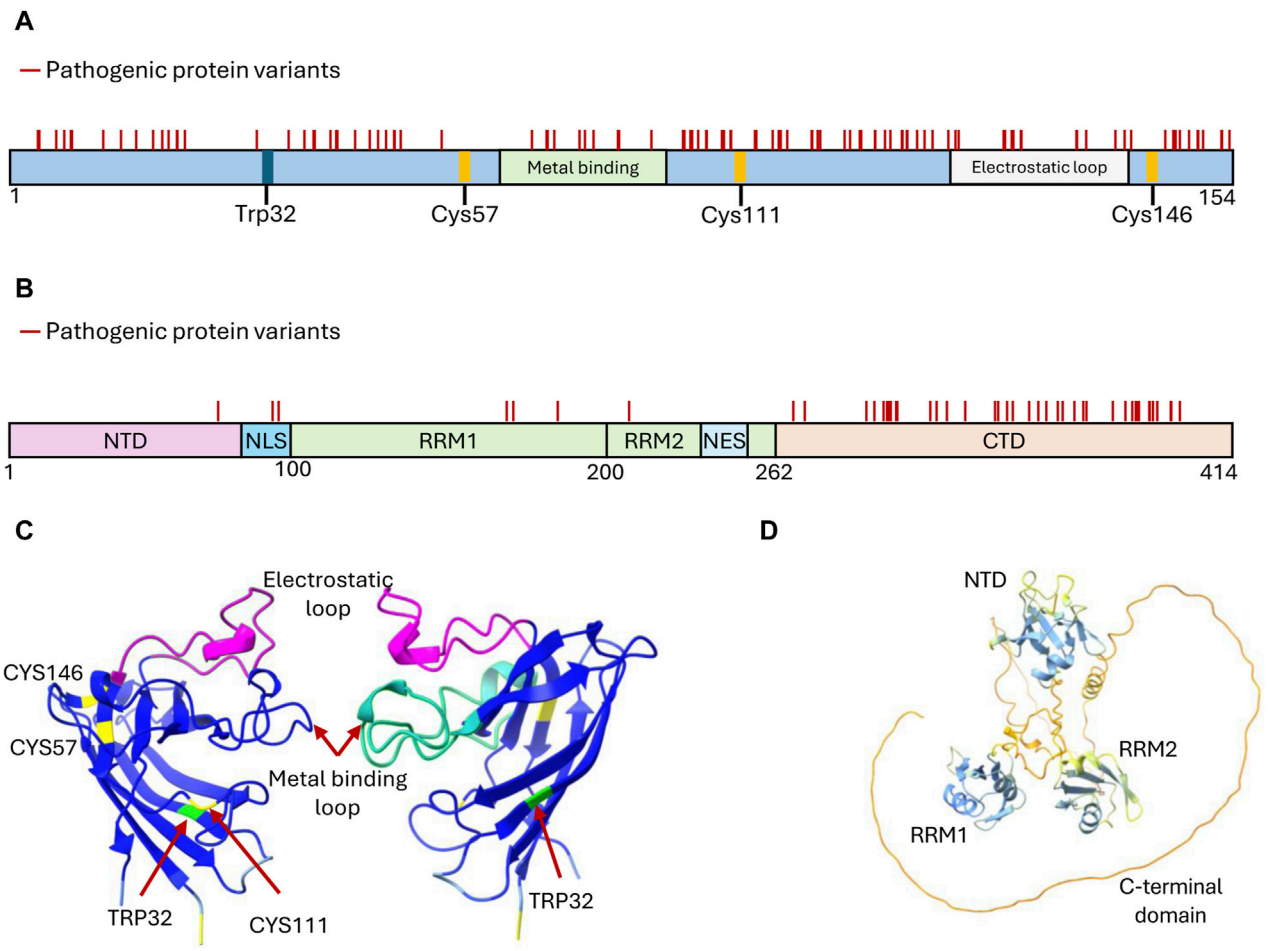

FIGURE 2
Structural features of SOD1 and TDP-43 proteins targeted by developed aggregation inhibitors. **(A)** Domain organization of SOD1 depicting structural features critical for its function, i.e., the cysteine residues participating in disulfide bond formation (Cys57 and Cys146), the metal-binding domain, and the electrostatic loop. These sites, along with Trp32 and Cys111, have been explored for drug discovery targeting SOD1 inhibition of aggregate formation. Mutations that generate amino acid substitutions in SOD1 are depicted with solid lines. **(B)** Domain organization of TDP-43 depicting the features that mediate functional oligomerization (N terminal domain-NTD), RNA binding (RNA Recognition motifs RRM1 and RRM2), protein interactions and liquid-liquid phase separation (C terminal domain-CTD), and nucleo-cytoplasmic shuffling (Nuclear Localization Signal-NLS and Nuclear Export Signal-NES). Mutations leading to amino acid substitutions in TDP-43 are represented by solid lines. **(C)** Structure of two SOD1 subunits rotated 180° to showcase the arrangement of key residues and domains (Uniprot P00441). Reconstituted using Chimera X (AlphaFold). **(D)** Structure of TDP-43 (Uniprot Q13148) highlighting the arrangement of its domains. Predicted AlphaFold structure reconstituted using Chimera X (Pettersen et al., 2021).

antioxidant, and cytoprotective properties (Schewe, 1995; Saito et al., 1998; Yamaguchi et al., 1998; Wood-Allum et al., 2006). However, achieving target engagement and specificity remains challenging due to the abundance of free thiols and the large number of ebselen-binding proteins within cells (Chen et al., 2018). Thus, a medium-throughput screen using a differential scanning fluorescence assay to investigate the stabilization of SOD1 (A4V) mutants by ebselen derivatives was developed, aiming for improved SOD1 dimer stabilization and drug-like properties (Amporndanai et al., 2020; Chantadul et al., 2020). Potent candidates exhibited remarkable neuroprotective activities without observable toxicity in cells, while *in vivo* experiments with a selected compound demonstrated a significant delay in ALS disease onset in SOD1(G93A) mice, showcasing its potential therapeutic effect (Amporndanai et al., 2020).

Targeting the Trp32 residue

The sole tryptophan residue within SOD1 has been identified as a key factor in the misfolding of both mutant and wild-type proteins, through oxidative and prion-like aggregation mechanisms (Coelho et al., 2014; Pokrishevsky et al., 2018; Duval et al., 2019; Gill et al., 2019; Manjula et al., 2019; Crown et al., 2020). Trp32, residing on the solvent-exposed external layer of the protein, distanced from the Zn/Cu active site and the homodimer interface, is subject to oxidative post-translational modifications *in vivo* (Medinas et al., 2010; Figueroa et al., 2020). The bicarbonate-dependent peroxidase activity of SOD1 further enhances the oxidation rate of Trp32 *in vitro* (Coelho et al., 2014), while upon chronic ER stress conditions Trp32 oxidation is increased in cytosolic and mitochondrial extracts from transgenic WT SOD1 mice (Medinas et al., 2018). Site-directed mutagenesis studies have emphasized the

pivotal role of Trp32 in aggregate formation as substitution of this residue in SOD1 (G93A) cultured motor neurons (Taylor et al., 2007) and in HEK cells expressing SOD1 (G127X) and SOD1 (G85R) (Grad et al., 2011) considerably reduced mutant cytotoxicity and aggregation propensity.

Prion-like propagation and *in vivo* conversion of WT SOD1 to a misfolded state linked to Trp32, has been identified following exposure to misfolded SOD1 mutant seed species. SOD1 (G127X) can convert WT SOD1 to the misfolded state in various cell lines (Grad et al., 2011) while SOD1 (G93A) induces WT SOD1 aggregation accelerating disease progression in mice (Bruijn et al., 1998; Deng et al., 2006; Wang et al., 2009; Ayers et al., 2016). Notably, human SOD1 mutants did not induce misfolding of murine SOD1 protein both *in vivo* (Wang et al., 2009; Audet et al., 2010) and in cells (Grad et al., 2011), due to a different codon for the residue at position 32 between humans and mice. This differentiation, from a tryptophan to a serine, has been associated with the observed aggregation resistance in mice. Intriguingly, the SOD1(W32F) variant significantly reduced the formation of high-molecular weight and disulfide-dependent SOD1 aggregates in NSC-34 cells (Medinas et al., 2018). Moreover, zebrafish embryos injected with SOD1(W32S) showed mitigated motor deficiency and motor neuron axonopathy compared to embryos injected with WT or ALS-related SOD1 variants (Duval et al., 2019), supporting the notion that reducing SOD1 self-interactions at Trp32 might be of therapeutic interest.

Recognizing the role of Trp32 oxidation in potentiating protein aggregation and cytotoxicity has spurred the development of small molecules targeting Trp32 in SOD1 (Ray et al., 2005; Antonyuk et al., 2010; Wright et al., 2013; Manjula et al., 2019). Pyrimidine-like molecules, such as 5-Fluorouridine (5-FUrd), 5-Fluorouracil (5-FU) and Telbivudine (a synthetic thymine analogue), have all demonstrated the ability to decrease SOD1 aggregation in cellular and animal models of ALS (Pokrishevsky et al., 2018; Duval et al., 2019; Rando et al., 2019). In particular, 5-FU administration in SOD1 (G93A) transgenic mice delayed disease onset, increased survival and ameliorated motor performance deficits (Rando et al., 2019). Additionally, telbivudine improved motor performance and reduced SOD1 toxicity in a SOD1-ALS zebrafish model (Duval et al., 2019). Both 5-FU and telbivudine are licensed in the United States and EU as chemotherapeutic and antiviral agents, respectively, and importantly, both compounds can also penetrate the BBB (Formica et al., 2006; Ahrens and Manno, 2014).

Targeting the electrostatic loop

The structure and activity of SOD1 depend on two important loops, the Zn-binding (residues 49-82) and the electrostatic loop (E-loop or loop VII, residues 121-142). A highly conserved cluster of charged residues situated on the surface of the electrostatic loop forms an active site channel, facilitating effective interaction with superoxide (Getzoff et al., 1992; Polticelli et al., 1995). NMR analysis of SOD1 folding and misfolding pathways identified thermal fluctuations within the electrostatic loop that mediate the formation of aberrant intermolecular interactions and the development of abnormal oligomers (Sekhar et al., 2015). Furthermore, structural and dynamic changes affecting this loop have been previously identified as a shared property of 13 familial ALS-related SOD1 variants (Molnar et al., 2009), while mutations dispersed throughout the SOD1 sequence that destabilize the electrostatic loop aberrantly expose the metal site of the protein to water (Souza et al., 2019). Thus, the binding of small molecules to the loop could alleviate the impact of mutations on the structure. Interestingly, the cyclic peptide HGG^{4F}FQ (^{4F}F = 4-fluorophenylalanine), selected by an epitope-specific high-throughput screen for binding to the peptide sequence of the electrostatic loop, can bind to both mature and metal-free SOD1 at the electrostatic loop, stabilize the native state and accelerate the WT and SOD1 (G93A) folding rates (Bunck et al., 2018).

Targeting intramolecular disulfide cross-linking

Short segments of SOD1 have a tendency to aggregate into oligomers and fibrils through the establishment of intramolecular hydrogen bonds and hydrophobic interactions (Ivanova et al., 2014; Sangwan et al., 2017). Additionally, SOD1 can create non-native oligomers in which monomers are connected through intermolecular disulfide bonds (Furukawa et al., 2006; Toichi et al., 2013). Several symptomatic transgenic ALS mouse models exhibit disulfide cross-linked SOD1 multimers detected in insoluble fractions derived from the animals' spinal cords (Furukawa et al., 2006; Anzai et al., 2017). Importantly, such multimers are absent from transgenic mice expressing a C-terminally truncated SOD1 lacking Cys146, suggesting that this residue has a significant role in disulfide-linked multimerization *in vivo* (Furukawa et al., 2006). A screening of 640 FDA-approved drugs was conducted to evaluate their impact on abnormally cross-linked SOD1 oligomers derived from metal deficient apo-SOD1 (G37R)$^{S-S}$ in an *in vitro* assay. The goal was to identify compounds that could inhibit the formation of insoluble S-S oligomers. Six compounds, namely, simvastatin, lovastatin, mevastatin, miltefosine, alfacalcidol and calcitriol were discovered to significantly suppress solution turbidity (Anzai et al., 2016). Despite this finding, treatment of an ALS mouse model expressing human SOD1 (G93A) with simvastatin resulted in accelerated disease progression and shortened survival (Su et al., 2016).

Inhibiting self-assembly and the aggregation process

Apart from stabilizing the SOD1 dimer and promoting proper folding to prevent SOD1 aggregation, molecules which can interfere with the self-assembly, the nucleation, or the fibrillation process are of high therapeutic interest. A prime example is Methylene Blue (MB), a phenothiazine dye, which has shown considerable potential in modulating the aggregation of various amyloidogenic proteins (Gureev et al., 2022). The ability of MB to readily cross the blood-brain barrier has significantly increased interest in its use as a therapeutic agent for central nervous system disorders (Rojas et al., 2012). *In vitro* assays have demonstrated that MB inhibits both the spontaneous amyloid aggregation of SOD1 and the elongation of pre-existing fibrils (Malik et al., 2020; Musteikyte et al., 2020). However, MB treatment of SOD1 (G93A) mice had no effect on motor neuron loss, or on the aggregation or misfolding of SOD1 (Audet et al., 2012).

Natural products

Flavonoids are the most common phytochemicals, exerting pharmacological effects and possessing antioxidant properties (Nday et al., 2015), metal chelator abilities (Nday et al., 2015), anti-inflammatory effects (Lin L. et al., 2015) and neuroprotective properties (Prakash and Sudhandiran, 2015). Importantly, some flavonoids can cross the BBB, rendering them attractive drug candidates for CNS diseases, including AD, PD and ALS (de Andrade Teles et al., 2018; Maher, 2019). Certain flavonoids such as myricetin, lacmoid, EGCG and curcumin (Zhao et al., 2018) have demonstrated the ability to reduce apo-SOD1 aggregation in an *in vitro* assay by restraining the nucleation step and inhibiting fibril elongation (Malik et al., 2020). Despite evidence of a direct inhibitory role in SOD1 aggregation (Malik et al., 2020), myricetin may exert its beneficial effects through additional cellular mechanisms. For example, the observed decrease in intracellular accumulation of ubiquitin-positive SOD1 inclusions in myricetin-treated cells expressing SOD1 (G37R) may also be mediated by modulation of the endogenous levels of Hsp70 and the quality control E3 ubiquitin ligase E6-AP (Joshi et al., 2019). EGCG is another flavonoid that has shown beneficial effects on onset delay, motor function, neuroprotection and extension of the lifespan of SOD1 (G93A) mice (Koh et al., 2006; Xu et al., 2006), combined with the suppression of microglial activation and inflammation (Xu et al., 2006). Finally, curcumin in an *in vitro* assay, reduced the fibril formation propensity of DTT-treated SOD1, favoring the formation of small amorphous aggregates which are not cytotoxic (Bhatia et al., 2015).

Molecular tweezers

Molecular tweezers are small, horseshoe-shaped artificial receptors that can form complexes with guest molecules, such as a nucleic acids, carbohydrates, amino acids or proteins, via non-covalent interactions (Mbarek et al., 2019). The molecular tweezer CLR01 selectively binds to positively charged lysine and arginine residues, interfering with the self-assembly process by disrupting hydrophobic and electrostatic interactions, thereby preventing the aggregation process in various amyloidogenic proteins (Sinha et al., 2011; Attar et al., 2012; Acharya et al., 2014; Ferreira et al., 2014; Herzog et al., 2015; Lopes et al., 2015; Zheng et al., 2015; Vopel et al., 2017; Mittal et al., 2018; Malishev et al., 2021). CLR01 also inhibits mutant SOD1 aggregation, as measured by ThT fluorescence assays, but leads to a marginal reduction in disease duration in the SOD1 (G93A) ALS mouse model despite reduced levels of misfolded SOD1 in the spinal cord (Malik et al., 2019). Recently, Lys61 and Lys92 have been identified as the preferential binding sites of CLR01 to SOD1, with the authors providing further evidence of CLR01's ability to stabilize the monomer (Samanta et al., 2022).

Peptides

Peptides constitute a promising class of therapeutic molecules (Wang L. et al., 2022). Synthetic peptides from structure-based designs possess the ability to function as beta-sheet breakers of amyloid forming proteins (Sievers et al., 2011; Young et al., 2017), and their use in preventing aggregate formation has demonstrated promising outcomes in various disorders, including Alzheimer's, prion, and polyglutamic diseases (Truex and Nowick, 2016; Alam et al., 2017; Goyal et al., 2017; Mukundan et al., 2017; Ryan et al., 2018). Peptide inhibitors, as potential drug candidates, combine several advantages such as high specificity, low toxicity and good tolerance (Hard and Lendel, 2012; Goyal et al., 2017). The peptide SE-12 (LSGDHCIIGRTLVVHEKADD) has been shown to bind SOD1 variants and to direct the aggregation of ALS-related SOD1 mutants from the typical amyloid to an amorphous aggregation pathway, which is presumably less toxic (Banerjee et al., 2016). Further studies were based on this peptide for the *in silico* design of tripeptides with inhibitory activity against SOD1 (A4V) aggregation, identifying CGH as the one with the greatest binding affinity among the tested sequences (Srinivasan and Rajasekaran, 2019). However, none of these peptides have been evaluated in cells or *in vivo*. In another approach, a peptide library comprising engineered variants of the hyperthermophilic variant of protein G (HTB1) was constructed and subsequently evaluated for specificity and affinity by a yeast display platform, identifying HTB1M as a selective inhibitor of SOD1 (G93A) and SOD1 (G85R) aggregation (Banerjee et al., 2017). Moreover, HTB1M prevented the accumulation of misfolded proteins in living cells and reduced the cytotoxicity of SOD1 (G93A) expressed in NSC-34 motor neuron–like cells. Importantly, the peptide library was designed using a computational algorithm for mapping protein surfaces predisposed to HTB1 intermolecular interactions. This conversion of an IgG-binding domain into a targeted SOD1 inhibitor showcases the potential usefulness of rational design for discovering peptide drug candidates. Finally, a bacterial platform was used to screen a combinatorial library of cyclic tetra-, penta- and hexapeptides for discovering rescuers of the misfolding and aggregation of the ALS-associated variant SOD1 (A4V). Among other hits, this high-throughput screen revealed that cyclic pentapeptides with the consensus cyclo-T (Φ1, S)SΦ2W motif, where Φ1 is one of the hydrophobic (Φ) amino acids A, W or F, while Φ2 is V, W or F, are efficient rescuers of SOD1 (A4V) aggregation (Matis et al., 2017).

Molecules targeting TDP-43 misfolding and aggregation

Despite its central role in cellular health and disease, most strategies for removing pathological TDP-43 primarily focus on cellular clearance pathways (i.e., ubiquitin/proteasome system, autophagy) (Babazadeh et al., 2023) rather than directly targeting TDP-43 to inhibit its aggregation (Buratti et al., 2005), possibly due to the lack of typical druggable pockets in its structure (Francois-Moutal et al., 2019). Additionally, TDP-43 demonstrates a significant tendency to aggregate either during or shortly after the purification process (Wright et al., 2020; Yang et al., 2023), constraining the development of high-throughput assays for screening molecules inhibiting TDP-43 misfolding and aggregation. Notably, the design of stable monomeric TDP-43 variants (i.e., double mutant S333D/S342D) with the ability to be purified as stable monomers enabled the identification of small molecules capable of stabilizing the protein's native state and preventing aggregation (Yang et al., 2023). Compounds with the ability to modulate the aggregation pathways and toxicity of amyloidogenic proteins such as MB and curcumin (Lo Cascio et al., 2021; Gureev et al., 2022) also prevent TDP-43

aggregation. MB reduces cytoplasmic TDP-43 inclusions in cells (Yamashita et al., 2009) and suppresses mutant TDP-43-mediated toxicity in *C. elegans* and zebrafish ALS (Vaccaro et al., 2012; Vaccaro et al., 2013) but was ineffective in reducing disease symptoms and cytoplasmic accumulation of TDP-43 in transgenic TDP-43 (G348C) mice (Audet et al., 2012). Similarly, the improved curcumin analogue monocarbonyl dimethoxy-curcumin C has been shown to inhibit the aggregation of mutant TDP-43 and to diminish oxidative stress in cells (Duan et al., 2014).

Targeting the C-terminal domain and LLPS

The extended C-terminal disordered region includes a hydrophobic α-helix (residues 320–340) and dispersed aromatic residues that facilitate the LLPS of TDP-43, allowing its incorporation to stress granules (Li et al., 2018). A substantial body of evidence indicates the Q/N-rich segment (residues 341–366) as the pivotal region for amyloid formation (Johnson et al., 2009; Budini et al., 2012; Kametani et al., 2016), further supported by the recently determined cryo-EM structure of aggregated TDP-43 (Arseni et al., 2022). Inhibitors that block the aggregation of TDP-43 mediated by the Q/N-rich segment without interfering with the hydrophobic segment's ability to drive association with stress granules could be an effective therapeutic approach. Polyglutamine binding peptide 1 (QBP1) is an octapeptide, designed to prevent polyglutamine amyloid formation (Nagai et al., 2000; Nagai et al., 2003; Takeuchi and Nagai, 2017). QBP1 exhibits a relatively broad specificity, capable of hindering amyloid formation by various amyloid-prone polypeptides, including huntingtin, the yeast Sup35 prion domain, α-synuclein, and the functional amyloid CPEB3. However, it does not affect certain amyloids like Aβ (Bauer et al., 2010; Hervas et al., 2012; Popiel et al., 2013; Hervas et al., 2016). Biochemical *in vitro* assays showed that QBP1 binds to the Q/N rich region of TDP-43 C-terminal domain and inhibits its aggregation (Mompean et al., 2019).

The small planar molecule AIM4 [4,5-bis acridine] is an acridine derivative, which has been predicted to bind amino acids 288-319 in the C-terminal domain of TDP-43 (Girdhar et al., 2020). AIM4 exhibited pronounced inhibitory effects on TDP-43 aggregation in both a yeast model expressing TDP-43-YFP and *in vitro*, using a recombinantly purified C-terminal fragment spanning amino acids 193 to 414 (Prasad et al., 2016). Recently, the amyloid fiber-detecting molecules, 4′-dianilino-1,1′-binaphthyl-5,5′-disulfonic acid (bis-ANS) and Congo Red, have been shown to modulate LLPS of TDP-43 (Babinchak et al., 2020). Importantly, these molecules allow TDP-43 LLPS at low concentrations while decondensing the liquid droplets at higher concentrations, indicating that they do not interfere with physiological phase transitions. Although bis-ANS and Congo red are toxic and therefore not suitable for drugs, their use as lead compounds could assist in the development of optimized molecules.

In an effort to design aggregation blockers, Liu and coworkers developed peptides based on sequence motifs of TDP-43. Through this approach, they discovered that two synthetic peptides from the C-terminal region effectively hindered the formation of TDP-43 protein aggregates in a concentration-dependent manner within HeLa cells overexpressing a mutant TDP-43. However, it's noteworthy that despite their ability to reduce aggregation, these peptides did not mitigate or prevent cell death (Liu et al., 2013). In another attempt, TDP-43-derived peptides based on two core aggregation-prone motifs of TDP-43 (Saini and Chauhan, 2011), 246-EDLIIKGISV-255 and 311-MNFGAFSINP-320, have been functionalized to enhance desired properties (Gao et al., 2019). These multi-functional peptides comprise three moieties: (a) a hydrophobic motif consisting of adamantane, (b) a TDP-43-derived peptide and (c) a Tat (RRRQRRKKRG) or Poly-D-Arginine (D-Arg) tag, each one conferring to the functionality of the compound. Adamantane mimics the unfolded state of proteins, and consequently, adamantane-tagged proteins are directed to the degradation machineries of the cell (Coll-Martinez et al., 2020). Moreover, adamantane increases the BBB permeability of conjugated molecules (Tsuzuki et al., 1994). Tat or $(D\text{-}Arg)_8$ tags are used to increase cell-permeability of conjugated molecules (Szabo et al., 2022). While the peptide M311/P320 was not further examined due to low solubility, the peptide E246/V255 exhibited a potent capacity to trigger TDP-43 degradation within cells and to diminish TDP-43-induced cytotoxicity. Additionally, it was effective in lowering TDP-43 levels in a transgenic *Drosophila* model. Importantly, peptides lacking the adamantane moiety had no effect.

Targeting the RRMs

TDP-43 localization to stress granules (SGs) is mediated by both its RRM1 and the C-terminal domain (Colombrita et al., 2009; Dewey et al., 2011). To discover small-molecule modulators influencing SG formation and decrease TDP-43 accumulation in induced pluripotent stem cell-derived motor neurons (iPSC-MN) from ALS patients, a cellular screen was conducted using a 50,000-member small molecule library (Fang et al., 2019). The screen involved HEK293T and neural precursor cells treated with $NaAsO_2$ to induce SG formation. Approximately 100 hits were identified, and among them, mitoxantrone, quinacrine and pyrvinium planar compounds which act as nucleic acid intercalating molecules, showed reduced recruitment of TDP-43 to SGs. More recently, it has been reported that small molecules inhibiting the binding of TDP-43 to RNA could reduce neuronal toxicity (Francois-Moutal et al., 2019). Using an amplified luminescent proximity assay, the investigators observed that compound rTRD01 displaced (G4C2)4 RNA of the disease-linked *c9orf72* gene from TDP-43 and improved larval neuromuscular coordination of *Drosophila* overexpressing mutant TDP-43 (Francois-Moutal et al., 2019). Despite being targeted to an aggregation-mediating domain of the protein, it has not been examined whether rTRD01 reduces TDP-43 aggregation propensity.

In another study, through *in silico* docking of 50,000 compounds to the N-terminal domain of TDP-43, a small molecule (nTRD22) that binds specifically to the NTD domain has been identified. Notably, nTRD22 induced allosteric modulation of the RRM of TDP-43, leading to reduced RNA binding *in vitro* (Mollasalehi et al., 2020). Furthermore, exposure of primary motor neurons to nTRD22 resulted in a decrease in TDP-43 protein levels, akin to the effect observed with TDP-43 RNA binding-deficient mutants (Zacco et al., 2018; Flores et al., 2019), supporting the idea that

TABLE 1 A summary of compounds identified by their ability to inhibit aggregation of TDP-43 or SOD1.

Compound	Target protein	Mechanism of action	Stage of development (level of evidence)[a]	References
Auranofin	TDP-43	N/A	Preclinical (cell assays)	Madeira et al. (2013), Oberstadt et al. (2018)
PolyQ binding peptide 1	TDP-43	N/A	Preclinical (*in vitro*)	Mompean et al. (2019)
AIM4	TDP-43	N/A	Preclinical (*in vitro*)	Girdhar et al. (2020)
TDP-43-derived peptides	TDP-43	Trigger TDP-43 degradation	Preclinical (*in vivo- Drosophila*)	Gao et al. (2019)
nTRD22	TDP-43	Allosteric modulation of the RRM	Preclinical (*in vivo- Drosophila*)	Mollasalehi et al. (2020)
Curcumin	TDP-43	Modulator of aggregation	Preclinical (cell assays)	Duan et al. (2014)
	SOD1		Preclinical (*in vitro*)	Bhatia et al. (2015)
Methylene Blue	TDP-43	Modulator of aggregation	Preclinical (*in vitro*; no effect *in vivo*)	Yamashita et al. (2009)
	SOD1		Preclinical (*in vitro*; no effect *in vivo*)	Musteikyte et al. (2020)
Maleimide	SOD1	Crosslinking at Cys111	Preclinical (*in vitro*)	Auclair et al. (2010), Gavrin et al. (2012)
1,2-dithiane-1-oxide (Cyclic disulphides)	SOD1	Crosslinking at Cys111	Preclinical (cell assays)	Donnelly et al. (2018)
Cisplatin	SOD1	Binding at Cys111	Licensed[b] (*in vitro*)	Banci et al. (2012)
Ebselen	SOD1	Binding at Cys111	Licensed[b] (*in vivo*)	Capper et al. (2018)
Ebsulphur			Preclinical (*in vitro*)	
5-Fluorouridine	SOD1	Attenuation of solvent-exposed hydrophobic Trp32	Preclinical (*in vivo*- Zebrafish)	Pokrishevsky et al. (2018), Rando et al. (2019)
5-Fluorouracil			Licensed[b] (*in vivo*)	
Telbivudine	SOD1	Attenuation of solvent-exposed hydrophobic Trp32	Licensed[b] (*in vivo*- Zebrafish)	Duval et al. (2019)
HGGF$^{4-\text{fluorophenylalanine}}$Q	SOD1	Binding to the electrostatic loop	Preclinical (*in vitro*)	Bunck et al. (2018)
Myricetin	SOD1	Modulator of aggregation	Preclinical (cell assays)	Malik et al. (2020)
EGCG	SOD1	Modulator of aggregation	Preclinical (*in vivo*)	Malik et al. (2020)
Molecular tweezer CLR01	SOD1	Inhibits self-interactions	Preclinical (*in vitro*; no effect *in vivo*)	Malik et al. (2019), Samanta et al. (2022)
Arylsulfanyl pyrazolone (ASP) & derivatives	SOD1	Modulator of aggregation	Preclinical (cell assays)	Benmohamed et al. (2011), Chen et al. (2011), Limpert et al. (2013)
Cyclo- hexane-1,3-dione (CHD) & derivatives	SOD1	N/A	Preclinical (cell assays)	Benmohamed et al. (2011), Zhang et al. (2012b), Gavrin et al. (2012), Limpert et al. (2013)
Pyrimidine-2,4,6-trione (PYT) & derivatives	SOD1	N/A	Preclinical (cell assays)	Benmohamed et al. (2011), Limpert et al. (2013), Xia et al. (2014)
Simvastatin	SOD1	Target intramolecular disulfide cross-linking	Licensed[b] (*in vitro*; no effect *in vivo*)	Anzai et al. (2016)
Alfacalcidol	SOD1	Target intramolecular disulfide cross-linking	Licensed[b] (*in vitro*)	Anzai et al. (2016)
Miltefosine	SOD1	Target intramolecular disulfide cross-linking	Licensed[b] (*in vitro*)	Anzai et al. (2016)
LSGDHCIIGRTLVVHEKADD	SOD1	Inhibits self-interaction	Preclinical (*in vitro*)	Banerjee et al. (2016)
HTB1M	SOD1	Inhibits self-interaction	Preclinical (cell assays)	Banerjee et al. (2017)
Cyclo-T (Φ1,S)SΦ2W motif, where Φ1 is one of the hydrophobic (Φ) amino acids A, W or F, while Φ2 is V, W or F	SOD1	N/A	Preclinical (*in vitro*)	Matis et al. (2017)

[a]This column specifies the current stage of drug development and the type of evidence supporting each molecule's ability to inhibit the aggregation of the target protein.
[b]"Licensed" denotes drugs that are already authorized for indications other than ALS.

nTRD22 disrupts the binding of TDP-43 to RNA. Interestingly, in a *Drosophila* ALS model, nTRD22 alleviated motor impairment (Mollasalehi et al., 2020). Additionally, several studies have demonstrated that nucleotides rich in UG/TG sequences can impede the aggregation of TDP-43 using *in vitro* biochemical assays (Huang et al., 2013; Sun et al., 2014; Rengifo-Gonzalez et al., 2021) but also in cells (Yang et al., 2023).

Auranofin [gold (1+)-3,4,5- triacetyloxy- 6- (acetyloxymethyl) oxane-2 - thiolate-triethyl-phosphanium] is an organic gold thiol compound currently used to treat rheumatoid arthritis due to its anti-inflammatory properties (Madeira et al., 2013; Madeira et al., 2014; Madeira et al., 2015). Auranofin has been shown to inhibit TDP-43 self-interaction in mouse N2a neuroblastoma cells without affecting endogenous levels of the protein and without conferring cellular toxicity (Oberstadt et al., 2018). This effect of auranofin was discovered in a cell-based screen of 1280 pharmacologically active compounds where TDP-43 self-interaction was monitored by establishing a NanoBit luciferase complementation assay in which the presence of auranofin enhances the protein's partitioning in the soluble fraction (Oberstadt et al., 2018). Although its mechanism of action is not known, it has been proposed that auranofin modulates the cysteine residues of TDP-43 located in the RRMs, thus affecting its self-interaction and eventually aggregation (Oberstadt et al., 2018). Importantly, auranofin holds desirable pharmacokinetic properties as it is able to reach the CNS of mice and rats after oral administration (Madeira et al., 2013), rendering it an attractive drug candidate.

Concluding remarks

The role of protein aggregation in the pathogenesis of ALS is critical, owing to its adverse effects on neuronal function and survival. Proteins such as SOD1 and TDP-43, when aggregated, can disrupt cellular processes, impair protein quality control mechanisms, and trigger toxicity, ultimately resulting in the degeneration of motor neurons, a hallmark of ALS. Present therapeutic strategies aim to mitigate these effects through various approaches, including the degradation of mRNA or the inhibition of its translation, the clearance of protein aggregates *via* antibodies, the disruption of protein-protein interactions that facilitate aggregation, the prevention of aggregate formation through vaccines, and the activation of protein clearance pathways. Nonetheless, an approach focused on directly targeting misfolded proteins might offer a more precise method for altering the course of the disease. Such specific interventions could provide greater accuracy in mitigating the detrimental impacts of certain protein aggregates. A better understanding of the aggregation mechanisms could lead to the development of molecules or screening techniques aimed at particular stages of the fibrillation process. For instance, targeting the dimerization of SOD1 at late folding stages may not yield effective *in vivo* results. Instead, compounds that facilitate metal binding or disulfide bond formation at earlier stages of SOD1 maturation could prove more beneficial therapeutically. Information on how misfolded and aggregated species confer toxicity *via* gains and losses of activity may also guide candidate drug decisions.

Despite the authorization of Tofersen, an antisense oligonucleotide targeting SOD1, there remains a critical need for additional therapeutic interventions to manage SOD1 aggregation. The specificity of Tofersen for SOD1-linked familial ALS, which accounts for only a fraction of ALS cases, underscores the necessity for a broader range of therapeutic strategies that can effectively reduce SOD1 aggregation. In this context, a strategy aiming at restoring SOD1's conformation and eventually its function could be invaluable, serving as either a standalone or complementary therapeutic intervention. Furthermore, the ubiquity of TDP-43 in ALS pathology across the majority of cases positions it as a primary focus of ALS research. Efforts to mitigate TDP-43 aggregation are promising and could benefit a broad spectrum of ALS patients. However, challenges such as differentiating between the protein's physiological and pathological states within cells, and the obstacles in crossing the blood-brain barrier with therapeutic agents, must be addressed. Significantly, evidence from cellular and animal studies has shown that identifying compounds capable of inhibiting misfolding and/or aggregation or promoting disaggregation may lead to disease-modifying effects (both *in vitro* and *in vivo*, as summarized in Table 1), yet none has proceeded to clinical trials. This situation highlights the urgent need for continued research and development in this area.

The high rate of failure in ALS clinical trials can be attributed to multiple pivotal factors. Historically, ALS has been treated as a uniform condition, overlooking its inherent heterogeneity. Future research must categorize ALS patients by specific genetic determinants and disease progression rates. Enhancing the use of biomarkers, refining preclinical models, improving trial design, and facilitating early intervention are crucial strategies to advance the development of ALS therapies. A holistic approach that integrates target-specific *in vitro* screening, validation using patient-derived iPSC neurons and glia, and mechanistic studies in model organisms such as zebrafish, fruit flies, and mice, can enhance the prediction of therapeutic effectiveness and its translation to clinical settings.

Author contributions

MT: Data curation, Investigation, Methodology, Writing–original draft, Writing–review and editing. MG: Data curation, Investigation, Methodology, Writing–original draft. KP: Data curation, Investigation, Writing–original draft, Writing–review and editing. GS: Conceptualization, Funding acquisition, Supervision, Writing–review and editing.

Funding

The authors declare that financial support was received for the research, authorship, and/or publication of this article. This work was financed for research and authorship by: (i) the European Research Council (ERC) under the European Union's Horizon 2020 research and innovation program (Project "ProMiDis"; grant agreement no. 819934; support for GS and MT); (ii) Greece and the European Union

(European Social Fund- ESF) through the Operational Programme "Human Resources Development, Education and Lifelong Learning" in the context of the project "Strengthening Human Resources Research Potential via Doctorate Research–2nd Cycle" (MIS 5000432), implemented by the State Scholarships Foundation (IKY) (support for MG); (iii) the Horizon Europe Programme under the "Widening Participation and Spreading Excellence" component (call Twinning "HORIZON-WIDERA-2021-ACCESS-03-1"); Project "Twin4Promis"; Grant Agreement No. 101079363 (support for GS); (v) the Horizon Europe Programme under the "Widening Participation & Spreading Excellence" component (call Twinning "HORIZON-WIDERA-2022- TALENTS-01-01–ERA Chairs"); Project "Boost4Bio"; Grant Agreement No. 101087471 (support for GS and KP). Financial support for the publication of this article was provided by the Horizon Europe Programme under the "Widening Participation and Spreading Excellence" component (call Twinning "HORIZON-WIDERA-2021-ACCESS- 03-1"); Project "Twin4Promis"; Grant Agreement No. 101079363.

Conflict of interest

Author GS is co-founder and shareholder of the company ResQ Biotech and author KP was employed by the company ResQ Biotech.

The remaining authors declare that the research was conducted in the absence of any commercial or financial relationships that could be construed as a potential conflict of interest.

Publisher's note

References

Abdolvahabi, A., Shi, Y., Chuprin, A., Rasouli, S., and Shaw, B. F. (2016). Stochastic Formation of fibrillar and amorphous superoxide dismutase oligomers linked to amyotrophic lateral sclerosis. *ACS Chem. Neurosci.* 7 (6), 799–810. doi:10.1021/acschemneuro.6b00048

Acharya, S., Safaie, B. M., Wongkongkathep, P., Ivanova, M. I., Attar, A., Klarner, F. G., et al. (2014). Molecular basis for preventing α-synuclein aggregation by a molecular tweezer. *J. Biol. Chem.* 289 (15), 10727–10737. doi:10.1074/jbc.M113.524520

Afroz, T., Chevalier, E., Audrain, M., Dumayne, C., Ziehm, T., Moser, R., et al. (2023). Immunotherapy targeting the C-terminal domain of TDP-43 decreases neuropathology and confers neuroprotection in mouse models of ALS/FTD. *Neurobiol. Dis.* 179, 106050. doi:10.1016/j.nbd.2023.106050

Afroz, T., Hock, E. M., Ernst, P., Foglieni, C., Jambeau, M., Gilhespy, L. A. B., et al. (2017). Functional and dynamic polymerization of the ALS-linked protein TDP-43 antagonizes its pathologic aggregation. *Nat. Commun.* 8 (1), 45. doi:10.1038/s41467-017-00062-0

Ahrens, C. L., and Manno, E. M. (2014). Neurotoxicity of commonly used hepatic drugs. *Handb. Clin. Neurol.* 120, 675–682. doi:10.1016/B978-0-7020-4087-0.00046-2

Alam, P., Siddiqi, K., Chturvedi, S. K., and Khan, R. H. (2017). Protein aggregation: from background to inhibition strategies. *Int. J. Biol. Macromol.* 103, 208–219. doi:10.1016/j.ijbiomac.2017.05.048

Alberti, S., Halfmann, R., King, O., Kapila, A., and Lindquist, S. (2009). A systematic survey identifies prions and illuminates sequence features of prionogenic proteins. *Cell* 137 (1), 146–158. doi:10.1016/j.cell.2009.02.044

Al-Chalabi, A., and Hardiman, O. (2013). The epidemiology of ALS: a conspiracy of genes, environment and time. *Nat. Rev. Neurol.* 9 (11), 617–628. doi:10.1038/nrneurol.2013.203

Almeida, Z. L., and Brito, R. M. M. (2020). Structure and aggregation mechanisms in amyloids. *Molecules* 25 (5), 1195. doi:10.3390/molecules25051195

Amporndanai, K., Rogers, M., Watanabe, S., Yamanaka, K., Neill, P. M. O., and Hasnain, S. S. (2020). Novel Selenium-based compounds with therapeutic potential for SOD1-linked amyotrophic lateral sclerosis. *EBioMedicine* 59, 102980. doi:10.1016/j.ebiom.2020.102980

Andersen, P. M., Nordstrom, U., Tsiakas, K., Johannsen, J., Volk, A. E., Bierhals, T., et al. (2019). Phenotype in an infant with SOD1 homozygous truncating mutation. *N. Engl. J. Med.* 381 (5), 486–488. doi:10.1056/NEJMc1905039

Andrews, J. A., Jackson, C. E., Heiman-Patterson, T. D., Bettica, P., Brooks, B. R., and Pioro, E. P. (2020). Real-world evidence of riluzole effectiveness in treating amyotrophic lateral sclerosis. *Amyotroph. Lateral Scler. Front. Degener.* 21 (7-8), 509–518. doi:10.1080/21678421.2020.1771734

Antonyuk, S., Strange, R. W., and Hasnain, S. S. (2010). Structural discovery of small molecule binding sites in Cu-Zn human superoxide dismutase familial amyotrophic lateral sclerosis mutants provides insights for lead optimization. *J. Med. Chem.* 53 (3), 1402–1406. doi:10.1021/jm9017948

Anzai, I., Toic, Hi K., Tokuda, E., Mukaiyama, A., Akiyama, S., and Furukawa, Y. (2016). Screening of drugs inhibiting *in vitro* oligomerization of Cu/Zn-superoxide dismutase with a mutation causing amyotrophic lateral sclerosis. *Front. Mol. Biosci.* 3, 1–11. doi:10.3389/fmolb.2016.00040

Anzai, I., Tokuda, E., Mukaiyama, A., Akiyama, S., Endo, F., Yamanaka, K., et al. (2017). A misfolded dimer of Cu/Zn-superoxide dismutase leading to pathological oligomerization in amyotrophic lateral sclerosis. *Protein Sci. a Publ. Protein Soc.* 26 (3), 484–496. doi:10.1002/pro.3094

Appel, S. H., Beers, D. R., and Zhao, W. (2021). Amyotrophic lateral sclerosis is a systemic disease: peripheral contributions to inflammation-mediated neurodegeneration. *Curr. Opin. Neurol.* 34 (5), 765–772. doi:10.1097/WCO.0000000000000983

Arai, T., Hasegawa, M., Akiyama, H., Ikeda, K., Nonaka, T., Mori, H., et al. (2006). TDP-43 is a component of ubiquitin-positive tau-negative inclusions in frontotemporal lobar degeneration and amyotrophic lateral sclerosis. *Biochem. Biophys. Res. Commun.* 351 (3), 602–611. doi:10.1016/j.bbrc.2006.10.093

Archbold, H. C., Jackson, K. L., Arora, A., Weskamp, K., Tank, E. M., Li, X., et al. (2018). TDP43 nuclear export and neurodegeneration in models of amyotrophic lateral sclerosis and frontotemporal dementia. *Sci. Rep.* 8 (1), 4606. doi:10.1038/s41598-018-22858-w

Arnesano, F., Banci, L., Bertini, I., Martinelli, M., Furukawa, Y., and O'Halloran, T. V. (2004). The unusually stable quaternary structure of human Cu,Zn-superoxide dismutase 1 is controlled by both metal occupancy and disulfide status. *J. Biol. Chem.* 279 (46), 47998–48003. doi:10.1074/jbc.M406021200

Arnold, E. S., Ling, S. C., Huelga, S. C., Lagier-Tourenne, C., Polymenidou, M., Ditsworth, D., et al. (2013). ALS-linked TDP-43 mutations produce aberrant RNA splicing and adult-onset motor neuron disease without aggregation or loss of nuclear TDP-43. *Proc. Natl. Acad. Sci. U. S. A.* 110 (8), E736–E745. doi:10.1073/pnas.1222809110

Arseni, D., Hasegawa, M., Murzin, A. G., Kametani, F., Arai, M., Yoshida, M., et al. (2022). Structure of pathological TDP-43 filaments from ALS with FTLD. *Nature* 601 (7891), 139–143. doi:10.1038/s41586-021-04199-3

Attar, A., Ripoli, C., Riccardi, E., Maiti, P., Li Puma, D. D., Liu, T., et al. (2012). Protection of primary neurons and mouse brain from Alzheimer's pathology by molecular tweezers. *Brain* 135 (Pt 12), 3735–3748. doi:10.1093/brain/aws289

Auclair, J. R., Boggio, K. J., Petsko, G. A., Ringe, D., and Agar, J. N. (2010). Strategies for stabilizing superoxide dismutase (SOD1), the protein destabilized in the most common form of familial amyotrophic lateral sclerosis. *Proc. Natl. Acad. Sci. U. S. A.* 107, 21394–21399. doi:10.1073/pnas.1015463107

Audet, J. N., Gowing, G., and Julien, J. P. (2010). Wild-type human SOD1 overexpression does not accelerate motor neuron disease in mice expressing murine Sod1 G86R. *Neurobiol. Dis.* 40 (1), 245–250. doi:10.1016/j.nbd.2010.05.031

Audet, J. N., Soucy, G., and Julien, J. P. (2012). Methylene blue administration fails to confer neuroprotection in two amyotrophic lateral sclerosis mouse models. *Neuroscience* 209, 136–143. doi:10.1016/j.neuroscience.2011.12.047

Audrain, M., Egesipe, A. L., Tentillier, N., Font, L., Ratnam, M., Mottier, L., et al. (2023). Targeting amyotrophic lateral sclerosis by neutralizing seeding-competent TDP-43 in CSF. *Brain Commun.* 5 (6), fcad306. doi:10.1093/braincomms/fcad306

Ayers, J. I., Fromholt, S. E., O'Neal, V. M., Diamond, J. H., and Borchelt, D. R. (2016). Prion-like propagation of mutant SOD1 misfolding and motor neuron disease spread along neuroanatomical pathways. *Acta Neuropathol.* 131 (1), 103–114. doi:10.1007/s00401-015-1514-0

Babazadeh, A., Rayner, S. L., Lee, A., and Chung, R. S. (2023). TDP-43 as a therapeutic target in neurodegenerative diseases: focusing on motor neuron disease and frontotemporal dementia. *Ageing Res. Rev.* 92, 102085. doi:10.1016/j.arr.2023.102085

Babinchak, W. M., Dumm, B. K., Venus, S., Boyko, S., Putnam, A. A., Jankowsky, E., et al. (2020). Small molecules as potent biphasic modulators of protein liquid-liquid phase separation. *Nat. Commun.* 11 (1), 5574. doi:10.1038/s41467-020-19211-z

Bakavayev, S., Stavsky, A., Argueti-Ostrovsky, S., Yehezkel, G., Fridmann-Sirkis, Y., Barak, Z., et al. (2023). Blocking an epitope of misfolded SOD1 ameliorates disease phenotype in a model of amyotrophic lateral sclerosis. *Brain* 146 (11), 4594–4607. doi:10.1093/brain/awad222

Banci, L., Bertini, I., Blaz, O., Calderone, V., Cantini, F., Mao, J., et al. (2012). Interaction of cisplatin with human superoxide dismutase. *JACS* 134, 7009–7014. doi:10.1021/ja211591n

Banerjee, V., Oren, O., Ben-Zeev, E., Taube, R., Engel, S., and Papo, N. (2017). A computational combinatorial approach identifies a protein inhibitor of superoxide dismutase 1 misfolding, aggregation, and cytotoxicity. *J. Biol. Chem.* 292 (38), 15777–15788. doi:10.1074/jbc.M117.789610

Banerjee, V., Shani, T., Katzman, B., Vyazmensky, M., Papo, N., Israelson, A., et al. (2016). Superoxide dismutase 1 (SOD1)-Derived peptide inhibits amyloid aggregation of familial amyotrophic lateral sclerosis SOD1 mutants. *ACS Chem. Neurosci.* 7, 1595–1606. doi:10.1021/acschemneuro.6b00227

Banks, C. J., and Andersen, J. L. (2019). Mechanisms of SOD1 regulation by post-translational modifications. *Redox Biol.* 26, 101270. doi:10.1016/j.redox.2019.101270

Barber, S. C., Higginbottom, A., Mead, R. J., Barber, S., and Shaw, P. J. (2009). An *in vitro* screening cascade to identify neuroprotective antioxidants in ALS. *Free Radic. Biol. Med.* 46 (8), 1127–1138. doi:10.1016/j.freeradbiomed.2009.01.019

Barmada, S. J., Skibinski, G., Korb, E., Rao, E. J., Wu, J. Y., and Finkbeiner, S. (2010). Cytoplasmic mislocalization of TDP-43 is toxic to neurons and enhanced by a mutation associated with familial amyotrophic lateral sclerosis. *J. Neurosci.* 30 (2), 639–649. doi:10.1523/JNEUROSCI.4988-09.2010

Bauer, P. O., Goswami, A., Wong, H. K., Okuno, M., Kurosawa, M., Yamada, M., et al. (2010). Harnessing chaperone-mediated autophagy for the selective degradation of mutant huntingtin protein. *Nat. Biotechnol.* 28 (3), 256–263. doi:10.1038/nbt.1608

Benatar, M., Wuu, J., Andersen, P. M., Bucelli, R. C., Andrews, J. A., Otto, M., et al. (2022). Design of a randomized, placebo-controlled, phase 3 trial of tofersen initiated in clinically presymptomatic SOD1 variant carriers: the ATLAS study. *Neurotherapeutics* 19 (4), 1248–1258. doi:10.1007/s13311-022-01237-4

Benmohamed, R., Arvanites, A. C., Kim, J., Ferrante, R. J., Silverman, R. B., Morimoto, R. I., et al. (2011). Identification of compounds protective against G93A-SOD1 toxicity for the treatment of amyotrophic lateral sclerosis. *Amyotroph. Lateral Scler.* 12 (2), 87–96. doi:10.3109/17482968.2010.522586

Bhardwaj, A., Myers, M. P., Buratti, E., and Baralle, F. E. (2013). Characterizing TDP-43 interaction with its RNA targets. *Nucleic Acids Res.* 41 (9), 5062–5074. doi:10.1093/nar/gkt189

Bhatia, N. K., Srivastava, A., Katyal, N., Jain, N., Khan, M. A., Kundu, B., et al. (2015). Curcumin binds to the pre-fibrillar aggregates of Cu/Zn superoxide dismutase (SOD1) and alters its amyloidogenic pathway resulting in reduced cytotoxicity. *Biochim. Biophys. Acta* 1854 (5), 426–436. doi:10.1016/j.bbapap.2015.01.014

Bissaro, M., and Moro, S. (2019). Rethinking to riluzole mechanism of action: the molecular link among protein kinase CK1δ activity, TDP-43 phosphorylation, and amyotrophic lateral sclerosis pharmacological treatment. *Neural Regen. Res.* 14 (12), 2083–2085. doi:10.4103/1673-5374.262578

Blay, V., Tolani, B., Ho, S. P., and Arkin, M. R. (2020). High-Throughput Screening: today's biochemical and cell-based approaches. *Drug Discov. Today* 25 (10), 1807–1821. doi:10.1016/j.drudis.2020.07.024

Blokhuis, A. M., Groen, E. J., Koppers, M., van den Berg, L. H., and Pasterkamp, R. J. (2013). Protein aggregation in amyotrophic lateral sclerosis. *Acta Neuropathol.* 125 (6), 777–794. doi:10.1007/s00401-013-1125-6

Bohacek, R. S., McMartin, C., and Guida, W. C. (1996). The art and practice of structure-based drug design: a molecular modeling perspective. *Med. Res. Rev.* 16 (1), 3–50. doi:10.1002/(SICI)1098-1128(199601)16:1<3::AID-MED1>3.0.CO;2-6

Boillee, S., Vande Velde, C., and Cleveland, D. W. (2006). ALS: a disease of motor neurons and their nonneuronal neighbors. *Neuron* 52 (1), 39–59. doi:10.1016/j.neuron.2006.09.018

Bonifacino, T., Zerbo, R. A., Balbi, M., Torazza, C., Frumento, G., Fedele, E., et al. (2021). Nearly 30 Years of animal models to study amyotrophic lateral sclerosis: a historical overview and future perspectives. *Int. J. Mol. Sci.* 22 (22), 12236. doi:10.3390/ijms222212236

Bosco, D. A., Morfini, G., Karabacak, N. M., Song, Y., Gros-Louis, F., Pasinelli, P., et al. (2010). Wild-type and mutant SOD1 share an aberrant conformation and a common pathogenic pathway in ALS. *Nat. Neurosci.* 13 (11), 1396–1403. doi:10.1038/nn.2660

Bose, S., and Cho, J. (2017). Targeting chaperones, heat shock factor-1, and unfolded protein response: promising therapeutic approaches for neurodegenerative disorders. *Ageing Res. Rev.* 35, 155–175. doi:10.1016/j.arr.2016.09.004

Boyd, J. D., Lee, P., Feiler, M. S., Zauur, N., Liu, M., Concannon, J., et al. (2014). A high-content screen identifies novel compounds that inhibit stress-induced TDP-43 cellular aggregation and associated cytotoxicity. *J. Biomol. Screen* 19 (1), 44–56. doi:10.1177/1087057113501553

Bozzo, F., Salvatori, I., Iacovelli, F., Mirra, A., Rossi, S., Cozzolino, M., et al. (2016). Structural insights into the multi-determinant aggregation of TDP-43 in motor neuron-like cells. *Neurobiol. Dis.* 94, 63–72. doi:10.1016/j.nbd.2016.06.006

Brasil, A. A., Magalhaes, R. S. S., De Carvalho, M. D. C., Paiva, I., Gerhardt, E., Pereira, M. D., et al. (2018). Implications of fALS mutations on Sod1 function and oligomerization in cell models. *Mol. Neurobiol.* 55 (6), 5269–5281. doi:10.1007/s12035-017-0755-4

Bravo-Hernandez, M., Tadokoro, T., Navarro, M. R., Platoshyn, O., Kobayashi, Y., Marsala, S., et al. (2020). Spinal subpial delivery of AAV9 enables widespread gene silencing and blocks motoneuron degeneration in ALS. *Nat. Med.* 26 (1), 118–130. doi:10.1038/s41591-019-0674-1

Brenner, D., and Freischmidt, A. (2022). Update on genetics of amyotrophic lateral sclerosis. *Curr. Opin. Neurol.* 35 (5), 672–677. doi:10.1097/WCO.0000000000001093

Bruijn, L. I., Houseweart, M. K., Kato, S., Anderson, K. L., Anderson, S. D., Ohama, E., et al. (1998). Aggregation and motor neuron toxicity of an ALS-linked SOD1 mutant independent from wild-type SOD1. *Science* 281 (5384), 1851–1854. doi:10.1126/science.281.5384.1851

Budini, M., Buratti, E., Stuani, C., Guarnaccia, C., Romano, V., De Conti, L., et al. (2012). Cellular model of TAR DNA-binding protein 43 (TDP-43) aggregation based on its C-terminal Gln/Asn-rich region. *J. Biol. Chem.* 287 (10), 7512–7525. doi:10.1074/jbc.M111.288720

Bulawa, C. E., Connelly, S., Devit, M., Wang, L., Weigel, C., Fleming, J. A., et al. (2012). Tafamidis, a potent and selective transthyretin kinetic stabilizer that inhibits the amyloid cascade. *Proc. Natl. Acad. Sci. U. S. A.* 109 (24), 9629–9634. doi:10.1073/pnas.1121005109

Bunck, D., Atsavapranee, B., Museth, A., VanderVelde, D., and Heath, J. (2018). Modulating the folding landscape of superoxide dismutase 1 with targeted molecular binders. *Angew. Chem. Int. Ed.* 57, 6212–6215. doi:10.1002/anie.201802269

Bunton-Stasyshyn, R. K., Saccon, R. A., Fratta, P., and Fisher, E. M. (2015). SOD1 function and its implications for amyotrophic lateral sclerosis pathology: new and renascent themes. *Neuroscientist* 21 (5), 519–529. doi:10.1177/1073858414561795

Buratti, E. (2018). TDP-43 post-translational modifications in health and disease. *Expert Opin. Ther. targets* 22 (3), 279–293. doi:10.1080/14728222.2018.1439923

Buratti, E. (2020). Targeting TDP-43 proteinopathy with drugs and drug-like small molecules. *Br. J. Pharmacol.* 178, 1298–1315. doi:10.1111/bph.15148

Buratti, E., Brindisi, A., Giombi, M., Tisminetzky, S., Ayala, Y. M., and Baralle, F. E. (2005). TDP-43 binds heterogeneous nuclear ribonucleoprotein A/B through its C-terminal tail: an important region for the inhibition of cystic fibrosis transmembrane conductance regulator exon 9 splicing. *J. Biol. Chem.* 280 (45), 37572–84. doi:10.1074/jbc.M505557200

Burkhardt, M. F., Martinez, F. J., Wright, S., Ramos, C., Volfson, D., Mason, M., et al. (2013). A cellular model for sporadic ALS using patient-derived induced pluripotent stem cells. *Mol. Cell Neurosci.* 56, 355–364. doi:10.1016/j.mcn.2013.07.007

Cao, Q., Boyer, D. R., Sawaya, M. R., Ge, P., and Eisenberg, D. S. (2019). Cryo-EM structures of four polymorphic TDP-43 amyloid cores. *Nat. Struct. Mol. Biol.* 26 (7), 619–627. doi:10.1038/s41594-019-0248-4

Capitini, C., Conti, S., Perni, M., Guidi, F., Cascella, R., De Poli, A., et al. (2014). TDP-43 inclusion bodies formed in bacteria are structurally amorphous, non-amyloid and inherently toxic to neuroblastoma cells. *PLoS One* 9 (1), e86720. doi:10.1371/journal.pone.0086720

Capper, M. J., Wright, G. S. A., Barbieri, L., Luchinat, E., Mercatelli, E., Mcalary, L., et al. (2018). The cysteine-reactive small molecule ebselen facilitates effective SOD1 maturation. *Nat. Commun.* 9, 1693–1699. doi:10.1038/s41467-018-04114-x

Chang, C. K., Chiang, M. H., Toh, E. K., Chang, C. F., and Huang, T. H. (2013). Molecular mechanism of oxidation-induced TDP-43 RRM1 aggregation and loss of function. *FEBS Lett.* 587 (6), 575–582. doi:10.1016/j.febslet.2013.01.038

Chang, C. K., Wu, T. H., Wu, C. Y., Chiang, M. H., Toh, E. K., Hsu, Y. C., et al. (2012). The N-terminus of TDP-43 promotes its oligomerization and enhances DNA binding affinity. *Biochem. Biophys. Res. Commun.* 425 (2), 219–224. doi:10.1016/j.bbrc.2012.07.071

Chantadul, V., Wright, G. S. A., Amporndanai, K., Shahid, M., Antonyuk, S. V., Washbourn, G., et al. (2020). Ebselen as template for stabilization of A4V mutant dimer for motor neuron disease therapy. *Commun. Biol.* 3 (1), 97. doi:10.1038/s42003-020-0826-3

Chen, A. K., Lin, R. Y., Hsieh, E. Z., Tu, P. H., Chen, R. P., Liao, T. Y., et al. (2010). Induction of amyloid fibrils by the C-terminal fragments of TDP-43 in amyotrophic lateral sclerosis. *J. Am. Chem. Soc.* 132 (4), 1186–1187. doi:10.1021/ja9066207

Chen, H., Qian, K., Du, Z., Cao, J., Petersen, A., Liu, H., et al. (2014). Modeling ALS with iPSCs reveals that mutant SOD1 misregulates neurofilament balance in motor neurons. *Cell Stem Cell* 14 (6), 796–809. doi:10.1016/j.stem.2014.02.004

Chen, T., Benmohamed, R., Arvanites, A. C., Ralay, H., Morimoto, R. I., Ferrante, R. J., et al. (2011). Arylsulfanyl pyrazolones block mutant SOD1-G93A aggregation. Potential

application for the treatment of amyotrophic lateral sclerosis. *Bioorg. Med. Chem.* 19, 613–622. doi:10.1016/j.bmc.2010.10.052

Chen, Y., Wang, H., Ying, Z., and Gao, Q. (2020). Ibudilast enhances the clearance of SOD1 and TDP-43 aggregates through TFEB-mediated autophagy and lysosomal biogenesis: the new molecular mechanism of ibudilast and its implication for neuroprotective therapy. *Biochem. Biophys. Res. Commun.* 526 (1), 231–238. doi:10.1016/j.bbrc.2020.03.051

Chen, Z., Jiang, Z., Chen, N., Shi, Q., Tong, L., Kong, F., et al. (2018). Target discovery of ebselen with a biotinylated probe. *Chem. Commun.* 54 (68), 9506–9509. doi:10.1039/c8cc04258f

Chew, J., Cook, C., Gendron, T. F., Jansen-West, K., Del Rosso, G., Daughrity, L. M., et al. (2019). Aberrant deposition of stress granule-resident proteins linked to C9orf72-associated TDP-43 proteinopathy. *Mol. Neurodegener.* 14 (1), 9. doi:10.1186/s13024-019-0310-z

Chio, A., Calvo, A., Moglia, C., Mazzini, L., Mora, G., and group, P. (2011). Phenotypic heterogeneity of amyotrophic lateral sclerosis: a population based study. *J. Neurol. Neurosurg. Psychiatry* 82 (7), 740–746. doi:10.1136/jnnp.2010.235952

Chio, A., Logroscino, G., Hardiman, O., Swingler, R., Mitchell, D., Beghi, E., et al. (2009). Prognostic factors in ALS: a critical review. *Amyotroph. Lateral Scler.* 10 (5-6), 310–323. doi:10.3109/17482960802566824

Chiti, F., and Dobson, C. M. (2006). Protein misfolding, functional amyloid, and human disease. *Annu. Rev. Biochem.* 75, 333–366. doi:10.1146/annurev.biochem.75.101304.123901

Chiti, F., and Dobson, C. M. (2017). Protein misfolding, amyloid formation, and human disease: a summary of progress over the last decade. *Annu. Rev. Biochem.* 86, 27–68. doi:10.1146/annurev-biochem-061516-045115

Choi, E. S., and Dokholyan, N. V. (2021). SOD1 oligomers in amyotrophic lateral sclerosis. *Curr. Opin. Struct. Biol.* 66, 225–230. doi:10.1016/j.sbi.2020.12.002

Choksi, D. K., Roy, B., Chatterjee, S., Yusuff, T., Bakhoum, M. F., Sengupta, U., et al. (2014). TDP-43 Phosphorylation by casein kinase Iε promotes oligomerization and enhances toxicity *in vivo*. *Hum. Mol. Genet.* 23 (4), 1025–1035. doi:10.1093/hmg/ddt498

Coelho, F. R., Iqbal, A., Linares, E., Silva, D. F., Lima, F. S., Cuccovia, I. M., et al. (2014). Oxidation of the tryptophan 32 residue of human superoxide dismutase 1 caused by its bicarbonate-dependent peroxidase activity triggers the non-amyloid aggregation of the enzyme. *J. Biol. Chem.* 289 (44), 30690–30701. doi:10.1074/jbc.M114.586370

Cohen, T. J., Hwang, A. W., Unger, T., Trojanowski, J. Q., and Lee, V. M. (2012). Redox signalling directly regulates TDP-43 via cysteine oxidation and disulphide cross-linking. *EMBO J.* 31 (5), 1241–1252. doi:10.1038/emboj.2011.471

Collaborators, GBDN (2019). Global, regional, and national burden of neurological disorders, 1990-2016: a systematic analysis for the Global Burden of Disease Study 2016. *Lancet Neurology* 18 (5), 459–480. doi:10.1016/S1474-4422(18)30499-X

Coll-Martinez, B., Delgado, A., and Crosas, B. (2020). The potential of proteolytic chimeras as pharmacological tools and therapeutic agents. *Molecules* 25 (24), 5956. doi:10.3390/molecules25245956

Colombrita, C., Zennaro, E., Fallini, C., Weber, M., Sommacal, A., Buratti, E., et al. (2009). TDP-43 is recruited to stress granules in conditions of oxidative insult. *J. Neurochem.* 111 (4), 1051–1061. doi:10.1111/j.1471-4159.2009.06383.x

Conicella, A. E., Zerze, G. H., Mittal, J., and Fawzi, N. L. (2016). ALS mutations disrupt phase separation mediated by α-helical structure in the TDP-43 low-complexity C-terminal domain. *Structure* 24 (9), 1537–1549. doi:10.1016/j.str.2016.07.007

Convertino, M., Das, J., and Dokholyan, N. V. (2016). Pharmacological chaperones: design and development of new therapeutic strategies for the treatment of conformational diseases. *ACS Chem. Biol.* 11 (6), 1471–1489. doi:10.1021/acschembio.6b00195

Cooper-Knock, J., Harvey, C., Zhang, S., Moll, T., Timpanaro, I. S., Kenna, K. P., et al. (2021). Advances in the genetic classification of amyotrophic lateral sclerosis. *Curr. Opin. Neurol.* 34 (5), 756–764. doi:10.1097/WCO.0000000000000986

Cortez, L., and Sim, V. (2014). The therapeutic potential of chemical chaperones in protein folding diseases. *Prion* 8 (2), 197–202. doi:10.4161/pri.28938

Couratier, P., Lautrette, G., Luna, J. A., and Corcia, P. (2021). Phenotypic variability in amyotrophic lateral sclerosis. *Rev. Neurol.* 177 (5), 536–543. doi:10.1016/j.neurol.2021.03.001

Cronin, S., Hardiman, O., and Traynor, B. J. (2007). Ethnic variation in the incidence of ALS: a systematic review. *Neurology* 68 (13), 1002–1007. doi:10.1212/01.wnl.0000258551.96893.6f

Crown, A., Mcalary, L., Fagerli, E., Brown, H., Yerbury, J. J., Galaleldeen, A., et al. (2020). Tryptophan residue 32 in human Cu-Zn superoxide dismutase modulates prion-like propagation and strain selection. *PLoS ONE* 15, e0227655. doi:10.1371/journal.pone.0227655

Crown, A. M., Roberts, B. L., Crosby, K., Brown, H., Ayers, J. I., Hart, P. J., et al. (2019). Experimental mutations in superoxide dismutase 1 provide insight into potential mechanisms involved in aberrant aggregation in familial amyotrophic lateral sclerosis. *G3 (Bethesda)* 9 (3), 719–728. doi:10.1534/g3.118.200787

Culik, R. M., Sekhar, A., Nagesh, J., Deol, H., Rumfeldt, J. A. O., Meiering, E. M., et al. (2018). Effects of maturation on the conformational free-energy landscape of SOD1. *Proc. Natl. Acad. Sci. U. S. A.* 115 (11), E2546–E55. doi:10.1073/pnas.1721022115

de Andrade Teles, R. B., Diniz, T. C., Costa Pinto, T. C., de Oliveira Junior, R. G., Gama, E. S. M., de Lavor, E. M., et al. (2018). Flavonoids as therapeutic agents in Alzheimer's and Parkinson's diseases: a systematic review of preclinical evidences. *Oxid. Med. Cell Longev.* 2018, 7043213. doi:10.1155/2018/7043213

Debnath, K., Shekhar, S., Kumar, V., Jana, N. R., and Jana, N. R. (2016). Efficient inhibition of protein aggregation, disintegration of aggregates, and lowering of cytotoxicity by green tea polyphenol-based self-assembled polymer nanoparticles. *ACS Appl. Mater Interfaces* 8 (31), 20309–20318. doi:10.1021/acsami.6b06853

de Boer, E. M. J., Orie, V. K., Williams, T., Baker, M. R., De Oliveira, H. M., Polvikoski, T., et al. (2020). TDP-43 proteinopathies: a new wave of neurodegenerative diseases. *J. Neurol. Neurosurg. Psychiatry* 92, 86–95. doi:10.1136/jnnp-2020-322983

Deng, H. X., Chen, W., Hong, S. T., Boycott, K. M., Gorrie, G. H., Siddique, N., et al. (2011). Mutations in UBQLN2 cause dominant X-linked juvenile and adult-onset ALS and ALS/dementia. *Nature* 477 (7363), 211–215. doi:10.1038/nature10353

Deng, H. X., Shi, Y., Furukawa, Y., Zhai, H., Fu, R., Liu, E., et al. (2006). Conversion to the amyotrophic lateral sclerosis phenotype is associated with intermolecular linked insoluble aggregates of SOD1 in mitochondria. *Proc. Natl. Acad. Sci. U. S. A.* 103 (18), 7142–7147. doi:10.1073/pnas.0602046103

Dewey, C. M., Cenik, B., Sephton, C. F., Dries, D. R., Mayer, P., Good, S. K., et al. (2011). TDP-43 is directed to stress granules by sorbitol, a novel physiological osmotic and oxidative stressor. *Mol. Cell. Biol.* 31 (5), 1098–1108. doi:10.1128/MCB.01279-10

Dimos, J. T., Rodolfa, K. T., Niakan, K. K., Weisenthal, L. M., Mitsumoto, H., Chung, W., et al. (2008). Induced pluripotent stem cells generated from patients with ALS can be differentiated into motor neurons. *Science* 321 (5893), 1218–1221. doi:10.1126/science.1158799

Doi, Y., Atsuta, N., Sobue, G., Morita, M., and Nakano, I. (2014). Prevalence and incidence of amyotrophic lateral sclerosis in Japan. *J. Epidemiol.* 24 (6), 494–499. doi:10.2188/jea.JE20140059

Donnelly, D. P., Dowgiallo, M. G., Salisbury, J. P., Krishna, C., Iyengar, S., Chaudhari, M., et al. (2018). Cyclic thiosulfinates and cyclic disulfides selectively crosslink thiols while avoiding modification of lone thiols. *JACS* 140, 7377–7380. doi:10.1021/jacs.8b01136

Du, H., Huo, Z., Chen, Y., Zhao, Z., Meng, F., Wang, X., et al. (2023). Induced pluripotent stem cells and their applications in amyotrophic lateral sclerosis. *Cells* 12 (6), 971. doi:10.3390/cells12060971

Duan, W., Guo, M., Yi, L., Liu, Y., Li, Z., Ma, Y., et al. (2020). The deletion of mutant SOD1 via CRISPR/Cas9/sgRNA prolongs survival in an amyotrophic lateral sclerosis mouse model. *Gene Ther.* 27 (3-4), 157–169. doi:10.1038/s41434-019-0116-1

Duan, W., Guo, Y., Xiao, J., Chen, X., Li, Z., Han, H., et al. (2014). Neuroprotection by monocarbonyl dimethoxycurcumin C: ameliorating the toxicity of mutant TDP-43 via HO-1. *Mol. Neurobiol.* 49 (1), 368–379. doi:10.1007/s12035-013-8525-4

Duval, M. G., Hinge, V. K., Snyder, N., Kanyo, R., Bratvold, J., Pokrishevsky, E., et al. (2019). Tryptophan 32 mediates SOD1 toxicity in a *in vivo* motor neuron model of ALS and is a promising target for small molecule therapeutics. *Neurobiol. Dis.* 124, 297–310. doi:10.1016/j.nbd.2018.11.025

Egawa, N., Kitaoka, S., Tsukita, K., Naitoh, M., Takahashi, K., Yamamoto, T., et al. (2012). Drug screening for ALS using patient-specific induced pluripotent stem cells. *Sci. Transl. Med.* 4 (145), 145ra104. doi:10.1126/scitranslmed.3004052

Eisele, Y. S., Monteiro, C., Fearns, C., Encalada, S. E., Wiseman, R. L., Powers, E. T., et al. (2015). Targeting protein aggregation for the treatment of degenerative diseases. *Nat. Rev. Drug Discov.* 14 (11), 759–780. doi:10.1038/nrd4593

Elam, J. S., Taylor, A. B., Strange, R., Antonyuk, S., Doucette, P. A., Rodriguez, J. A., et al. (2003). Amyloid-like filaments and water-filled nanotubes formed by SOD1 mutant proteins linked to familial ALS. *Nat. Struct. Biol.* 10 (6), 461–467. doi:10.1038/nsb935

Elliott, E., Bailey, O., Waldron, F. M., Hardingham, G. E., Chandran, S., and Gregory, J. M. (2020). Therapeutic targeting of proteostasis in amyotrophic lateral sclerosis-a systematic review and meta-analysis of preclinical research. *Front. Neurosci.* 14, 511. doi:10.3389/fnins.2020.00511

Fallini, C., Bassell, G. J., and Rossoll, W. (2012). The ALS disease protein TDP-43 is actively transported in motor neuron axons and regulates axon outgrowth. *Hum. Mol. Genet.* 21 (16), 3703–3718. doi:10.1093/hmg/dds205

Fang, M. Y., Markmiller, S., Vu, A. Q., Javaherian, A., Dowdle, W. E., Jolivet, P., et al. (2019). Small-molecule modulation of TDP-43 recruitment to stress granules prevents persistent TDP-43 accumulation in ALS/FTD. *Neuron* 103 (5), 802–819. doi:10.1016/j.neuron.2019.05.048

Fang, T., Al Khleifat, A., Meurgey, J. H., Jones, A., Leigh, P. N., Bensimon, G., et al. (2018). Stage at which riluzole treatment prolongs survival in patients with amyotrophic lateral sclerosis: a retrospective analysis of data from a dose-ranging study. *Lancet Neurology* 17 (5), 416–422. doi:10.1016/S1474-4422(18)30054-1

Fang, Y. (2012). Ligand-receptor interaction platforms and their applications for drug discovery. *Expert Opin. Drug Discov.* 7 (10), 969–988. doi:10.1517/17460441.2012.715631

Fang, Y. S., Tsai, K. J., Chang, Y. J., Kao, P., Woods, R., Kuo, P. H., et al. (2014). Full-length TDP-43 forms toxic amyloid oligomers that are present in frontotemporal lobar dementia-TDP patients. *Nat. Commun.* 5, 4824. doi:10.1038/ncomms5824

Farina, S., Esposito, F., Battistoni, M., Biamonti, G., and Francia, S. (2021). Post-translational modifications modulate proteinopathies of TDP-43, FUS and hnRNP-A/B in amyotrophic lateral sclerosis. *Front. Mol. Biosci.* 8, 693325. doi:10.3389/fmolb.2021.693325

Fei, E., Jia, N., Yan, M., Ying, Z., Sun, Q., Wang, H., et al. (2006). SUMO-1 modification increases human SOD1 stability and aggregation. *Biochem. Biophys. Res. Commun.* 347 (2), 406–412. doi:10.1016/j.bbrc.2006.06.092

Feiguin, F., Godena, V. K., Romano, G., D'Ambrogio, A., Klima, R., and Baralle, F. E. (2009). Depletion of TDP-43 affects Drosophila motoneurons terminal synapsis and locomotive behavior. *FEBS Lett.* 583 (10), 1586–1592. doi:10.1016/j.febslet.2009.04.019

Ferraiuolo, L., Kirby, J., Grierson, A. J., Sendtner, M., and Shaw, P. J. (2011). Molecular pathways of motor neuron injury in amyotrophic lateral sclerosis. *Nat. Rev. Neurol.* 7 (11), 616–630. doi:10.1038/nrneurol.2011.152

Ferraiuolo, L., and Maragakis, N. J. (2021). Mini-Review: induced pluripotent stem cells and the search for new cell-specific ALS therapeutic targets. *Neurosci. Lett.* 755, 135911. doi:10.1016/j.neulet.2021.135911

Ferrari, R., Kapogiannis, D., Huey, E. D., and Momeni, P. (2011). FTD and ALS: a tale of two diseases. *Curr. Alzheimer Res.* 8 (3), 273–294. doi:10.2174/156720511795563700

Ferreira, N., Pereira-Henriques, A., Attar, A., Klarner, F. G., Schrader, T., Bitan, G., et al. (2014). Molecular tweezers targeting transthyretin amyloidosis. *Neurotherapeutics* 11 (2), 450–461. doi:10.1007/s13311-013-0256-8

Figueroa, J. D., Zarate, A. M., Fuentes-Lemus, E., Davies, M. J., and Lopez-Alarcon, C. (2020). Formation and characterization of crosslinks, including Tyr-Trp species, on one electron oxidation of free Tyr and Trp residues by carbonate radical anion. *RSC Adv.* 10 (43), 25786–25800. doi:10.1039/d0ra04051g

Fischer, L. R., Igoudjil, A., Magrane, J., Li, Y., Hansen, J. M., Manfredi, G., et al. (2011). SOD1 targeted to the mitochondrial intermembrane space prevents motor neuropathy in the Sod1 knockout mouse. *Brain* 134 (Pt 1), 196–209. doi:10.1093/brain/awq314

Fischer, L. R., Li, Y., Asress, S. A., Jones, D. P., and Glass, J. D. (2012). Absence of SOD1 leads to oxidative stress in peripheral nerve and causes a progressive distal motor axonopathy. *Exp. Neurol.* 233 (1), 163–171. doi:10.1016/j.expneurol.2011.09.020

Flood, D. G., Reaume, A. G., Gruner, J. A., Hoffman, E. K., Hirsch, J. D., Lin, Y. G., et al. (1999). Hindlimb motor neurons require Cu/Zn superoxide dismutase for maintenance of neuromuscular junctions. *Am. J. Pathol.* 155 (2), 663–672. doi:10.1016/S0002-9440(10)65162-0

Flores, B. N., Li, X., Malik, A. M., Martinez, J., Beg, A. A., and Barmada, S. J. (2019). An intramolecular salt bridge linking TDP43 RNA binding, protein stability, and TDP43-dependent neurodegeneration. *Cell Rep.* 27 (4), 1133–1150. doi:10.1016/j.celrep.2019.03.093

Formica, V., Leary, A., Cunningham, D., and Chua, Y. J. (2006). 5-Fluorouracil can cross brain-blood barrier and cause encephalopathy: should we expect the same from capecitabine? A case report on capecitabine-induced central neurotoxicity progressing to coma. *Cancer Chemother. Pharmacol.* 58 (2), 276–278. doi:10.1007/s00280-005-0159-4

Forsberg, K., Graffmo, K., Pakkenberg, B., Weber, M., Nielsen, M., Marklund, S., et al. (2019). Misfolded SOD1 inclusions in patients with mutations in C9orf72 and other ALS/FTD-associated genes. *J. Neurol. Neurosurg. Psychiatry* 0, 861–869. doi:10.1136/jnnp-2018-319386

Frakes, A. E., Ferraiuolo, L., Haidet-Phillips, A. M., Schmelzer, L., Braun, L., Miranda, C. J., et al. (2014). Microglia induce motor neuron death via the classical NF-κB pathway in amyotrophic lateral sclerosis. *Neuron* 81 (5), 1009–1023. doi:10.1016/j.neuron.2014.01.013

Francois-Moutal, L., Felemban, R., Scott, D. D., Sayegh, M. R., Miranda, V. G., Perez-Miller, S., et al. (2019). Small molecule targeting TDP-43's RNA recognition motifs reduces locomotor defects in a Drosophila model of amyotrophic lateral sclerosis (ALS). *ACS Chem. Biol.* 14 (9), 2006–2013. doi:10.1021/acschembio.9b00481

French, R. L., Grese, Z. R., Aligireddy, H., Dhavale, D. D., Reeb, A. N., Kedia, N., et al. (2019). Detection of TAR DNA-binding protein 43 (TDP-43) oligomers as initial intermediate species during aggregate formation. *J. Biol. Chem.* 294 (17), 6696–6709. doi:10.1074/jbc.RA118.005889

Fukushima, M., Hosoda, N., Chifu, K., and Hoshino, S. I. (2019). TDP-43 accelerates deadenylation of target mRNAs by recruiting Caf1 deadenylase. *FEBS Lett.* 593 (3), 277–287. doi:10.1002/1873-3468.13310

Furukawa, Y., Fu, R., Deng, H. X., Siddique, T., and O'Halloran, T. V. (2006). Disulfide cross-linked protein represents a significant fraction of ALS-associated Cu, Zn-superoxide dismutase aggregates in spinal cords of model mice. *Proc. Natl. Acad. Sci. U. S. A.* 103 (18), 7148–7153. doi:10.1073/pnas.0602048103

Furukawa, Y., Kaneko, K., Watanabe, S., Yamanaka, K., and Nukina, N. (2013). Intracellular seeded aggregation of mutant Cu,Zn-superoxide dismutase associated with amyotrophic lateral sclerosis. *FEBS Lett.* 587 (16), 2500–2505. doi:10.1016/j.febslet.2013.06.046

Furukawa, Y., Kaneko, K., Yamanaka, K., O'Halloran, T. V., and Nukina, N. (2008). Complete loss of post-translational modifications triggers fibrillar aggregation of SOD1 in the familial form of amyotrophic lateral sclerosis. *J. Biol. Chem.* 283 (35), 24167–24176. doi:10.1074/jbc.M802083200

Gao, N., Huang, Y. P., Chu, T. T., Li, Q. Q., Zhou, B., Chen, Y. X., et al. (2019). TDP-43 specific reduction induced by Di-hydrophobic tags conjugated peptides. *Bioorg. Chem.* 84, 254–259. doi:10.1016/j.bioorg.2018.11.042

Gatto, N., Dos Santos Souza, C., Shaw, A. C., Bell, S. M., Myszczynska, M. A., Powers, S., et al. (2021). Directly converted astrocytes retain the ageing features of the donor fibroblasts and elucidate the astrocytic contribution to human CNS health and disease. *Aging Cell* 20 (1), e13281. doi:10.1111/acel.13281

Gavrin, L. K., Denny, R. A., and Saiah, E. (2012). Small molecules that target protein misfolding. *J. Med. Chem.* 55, 10823–10843. doi:10.1021/jm301182j

Gelpi, E., and Colom-Cadena, M. (2019). Oligomers: a hot topic for neurodegeneration and a note of caution for experimental models. *Brain* 142 (2), 228–230. doi:10.1093/brain/awy342

Germain, D. P., Hughes, D. A., Nicholls, K., Bichet, D. G., Giugliani, R., Wilcox, W. R., et al. (2016). Treatment of fabry's disease with the pharmacologic chaperone Migalastat. *N. Engl. J. Med.* 375 (6), 545–555. doi:10.1056/NEJMoa1510198

Getzoff, E. D., Cabelli, D. E., Fisher, C. L., Parge, H. E., Viezzoli, M. S., Banci, L., et al. (1992). Faster superoxide dismutase mutants designed by enhancing electrostatic guidance. *Nature* 358 (6384), 347–351. doi:10.1038/358347a0

Gill, C., Phelan, J. P., Hatzipetros, T., Kidd, J. D., Tassinari, V. R., Levine, B., et al. (2019). SOD1-positive aggregate accumulation in the CNS predicts slower disease progression and increased longevity in a mutant SOD1 mouse model of ALS. *Sci. Rep.* 9 (1), 6724. doi:10.1038/s41598-019-43164-z

Girdhar, A., Bharathi, V., Tiwari, V. R., Abhishek, S., Deeksha, W., Mahawar, U. S., et al. (2020). Computational insights into mechanism of AIM4-mediated inhibition of aggregation of TDP-43 protein implicated in ALS and evidence for *in vitro* inhibition of liquid-liquid phase separation (LLPS) of TDP-43(2C)-A315T by AIM4. *Int. J. Biol. Macromol.* 147, 117–130. doi:10.1016/j.ijbiomac.2020.01.032

Gordon, D., Dafinca, R., Scaber, J., Alegre-Abarrategui, J., Farrimond, L., Scott, C., et al. (2019). Single-copy expression of an amyotrophic lateral sclerosis-linked TDP-43 mutation (M337V) in BAC transgenic mice leads to altered stress granule dynamics and progressive motor dysfunction. *Neurobiol. Dis.* 121, 148–162. doi:10.1016/j.nbd.2018.09.024

Gorgulla, C., Jayaraj, A., Fackeldey, K., and Arthanari, H. (2022). Emerging frontiers in virtual drug discovery: from quantum mechanical methods to deep learning approaches. *Curr. Opin. Chem. Biol.* 69, 102156. doi:10.1016/j.cbpa.2022.102156

Goyal, D., Shuaib, S., Mann, S., and Goyal, B. (2017). Rationally designed peptides and peptidomimetics as inhibitors of amyloid-β (Aβ) aggregation: potential therapeutics of Alzheimer's disease. *ACS Comb. Sci.* 19 (2), 55–80. doi:10.1021/acscombsci.6b00116

Grad, L. I., Guest, W. C., Yanai, A., Pokrishevsky, E., O'Neill, M. A., Gibbs, E., et al. (2011). Intermolecular transmission of superoxide dismutase 1 misfolding in living cells. *Proc. Natl. Acad. Sci. U. S. A.* 108 (39), 16398–16403. doi:10.1073/pnas.1102645108

Gros-louis, F., Gaspar, C., and Rouleau, G. A. (2006). Genetics of familial and sporadic amyotrophic lateral sclerosis. *Biochim. Biophys. Acta* 1762, 956–972. doi:10.1016/j.bbadis.2006.01.004

Guise, A. J., Misal, S. A., Carson, R., Chu, J. H., Boekweg, H., Van Der Watt, D., et al. (2024). TDP-43-stratified single-cell proteomics of postmortem human spinal motor neurons reveals protein dynamics in amyotrophic lateral sclerosis. *Cell Rep.* 43 (1), 113636. doi:10.1016/j.celrep.2023.113636

Guo, L., and Shorter, J. (2015). It's raining liquids: RNA tunes viscoelasticity and dynamics of membraneless organelles. *Mol. Cell* 60 (2), 189–192. doi:10.1016/j.molcel.2015.10.006

Guo, W., Chen, Y., Zhou, X., Kar, A., Ray, P., Chen, X., et al. (2011). An ALS-associated mutation affecting TDP-43 enhances protein aggregation, fibril formation and neurotoxicity. *Nat. Struct. Mol. Biol.* 18 (7), 822–830. doi:10.1038/nsmb.2053

Gureev, A. P., Sadovnikova, I. S., and Popov, V. N. (2022). Molecular mechanisms of the neuroprotective effect of methylene blue. *Biochem. Biokhimiia* 87 (9), 940–956. doi:10.1134/S0006297922090073

Gurney, M. E., Pu, H., Chiu, A. Y., Dal Canto, M. C., Polchow, C. Y., Alexander, D. D., et al. (1994). Motor neuron degeneration in mice that express a human Cu,Zn superoxide dismutase mutation. *Science* 264 (5166), 1772–1775. doi:10.1126/science.8209258

Haidet-Phillips, A. M., Hester, M. E., Miranda, C. J., Meyer, K., Braun, L., Frakes, A., et al. (2011). Astrocytes from familial and sporadic ALS patients are toxic to motor neurons. *Nat. Biotechnol.* 29 (9), 824–828. doi:10.1038/nbt.1957

Hammarstrom, P., Wiseman, R. L., Powers, E. T., and Kelly, J. W. (2003). Prevention of transthyretin amyloid disease by changing protein misfolding energetics. *Science* 299 (5607), 713–716. doi:10.1126/science.1079589

Hard, T., and Lendel, C. (2012). Inhibition of amyloid formation. *J. Mol. Biol.* 421 (4-5), 441–465. doi:10.1016/j.jmb.2011.12.062

Hardiman, O., Al-Chalabi, A., Chio, A., Corr, E. M., Logroscino, G., Robberecht, W., et al. (2017). Amyotrophic lateral sclerosis. *Nat. Rev. Dis. Prim.* 3, 17071. doi:10.1038/nrdp.2017.71

Hasegawa, M., Arai, T., Nonaka, T., Kametani, F., Yoshida, M., Hashizume, Y., et al. (2008). Phosphorylated TDP-43 in frontotemporal lobar degeneration and amyotrophic lateral sclerosis. *Ann. Neurol.* 64 (1), 60–70. doi:10.1002/ana.21425

Henkel, J. S., Engelhardt, J. I., Siklos, L., Simpson, E. P., Kim, S. H., Pan, T., et al. (2004). Presence of dendritic cells, MCP-1, and activated microglia/macrophages in amyotrophic lateral sclerosis spinal cord tissue. *Ann. Neurol.* 55 (2), 221–235. doi:10.1002/ana.10805

Hervas, R., Li, L., Majumdar, A., Fernandez-Ramirez Mdel, C., Unruh, J. R., Slaughter, B. D., et al. (2016). Molecular basis of Orb2 amyloidogenesis and blockade of memory consolidation. *PLoS Biol.* 14 (1), e1002361. doi:10.1371/journal.pbio.1002361

Hervas, R., Oroz, J., Galera-Prat, A., Goni, O., Valbuena, A., Vera, A. M., et al. (2012). Common features at the start of the neurodegeneration cascade. *PLoS Biol.* 10 (5), e1001335. doi:10.1371/journal.pbio.1001335

Herzog, G., Shmueli, M. D., Levy, L., Engel, L., Gazit, E., Klarner, F. G., et al. (2015). The lys-specific molecular tweezer, CLR01, modulates aggregation of the mutant p53 DNA binding domain and inhibits its toxicity. *Biochemistry* 54 (24), 3729–3738. doi:10.1021/bi501092p

Hnath, B., and Dokholyan, N. V. (2022). Toxic SOD1 trimers are off-pathway in the formation of amyloid-like fibrils in ALS. *Biophysical J.* 121 (11), 2084–2095. doi:10.1016/j.bpj.2022.04.037

Hornberg, A., Logan, D. T., Marklund, S. L., and Oliveberg, M. (2007). The coupling between disulphide status, metallation and dimer interface strength in Cu/Zn superoxide dismutase. *J. Mol. Biol.* 365 (2), 333–342. doi:10.1016/j.jmb.2006.09.048

Hortobagyi, T., Troakes, C., Nishimura, A. L., Vance, C., van Swieten, J. C., Seelaar, H., et al. (2011). Optineurin inclusions occur in a minority of TDP-43 positive ALS and FTLD-TDP cases and are rarely observed in other neurodegenerative disorders. *Acta Neuropathol.* 121 (4), 519–527. doi:10.1007/s00401-011-0813-3

Hou, Y., Dan, X., Babbar, M., Wei, Y., Hasselbalch, S. G., Croteau, D. L., et al. (2019). Ageing as a risk factor for neurodegenerative disease. *Nat. Rev. Neurol.* 15 (10), 565–581. doi:10.1038/s41582-019-0244-7

Hou, Z. S., Ulloa-Aguirre, A., and Tao, Y. X. (2018). Pharmacoperone drugs: targeting misfolded proteins causing lysosomal storage-ion channels-and G protein-coupled receptors-associated conformational disorders. *Expert Rev. Clin. Pharmacol.* 11 (6), 611–624. doi:10.1080/17512433.2018.1480367

Huai, J., and Zhang, Z. (2019). Structural properties and interaction partners of familial ALS-associated SOD1 mutants. *Front. Neurol.* 10, 527. doi:10.3389/fneur.2019.00527

Huang, H. J., Chang, T. T., Chen, H. Y., and Chen, C. Y. (2014). Finding inhibitors of mutant superoxide dismutase-1 for amyotrophic lateral sclerosis therapy from traditional Chinese medicine. *Evidence-based complementary Altern. Med. eCAM.* 2014, 156276. doi:10.1155/2014/156276

Huang, S. L., Wu, L. S., Lee, M., Chang, C. W., Cheng, W. C., Fang, Y. S., et al. (2020). A robust TDP-43 knock-in mouse model of ALS. *Acta Neuropathol. Commun.* 8 (1), 3. doi:10.1186/s40478-020-0881-5

Huang, Y. C., Lin, K. F., He, R. Y., Tu, P. H., Koubek, J., Hsu, Y. C., et al. (2013). Inhibition of TDP-43 aggregation by nucleic acid binding. *PLoS One* 8 (5), e64002. doi:10.1371/journal.pone.0064002

Hurshman, A. R., White, J. T., Powers, E. T., and Kelly, J. W. (2004). Transthyretin aggregation under partially denaturing conditions is a downhill polymerization. *Biochemistry* 43 (23), 7365–7381. doi:10.1021/bi049621l

Iannitti, T., Scarrott, J. M., Likhite, S., Coldicott, I. R. P., Lewis, K. E., Heath, P. R., et al. (2018). Translating SOD1 gene silencing toward the clinic: a highly efficacious, off-target-free, and biomarker-supported strategy for fALS. *Mol. Ther. Nucleic acids* 12, 75–88. doi:10.1016/j.omtn.2018.04.015

Iguchi, Y., Katsuno, M., Niwa, J., Takagi, S., Ishigaki, S., Ikenaka, K., et al. (2013). Loss of TDP-43 causes age-dependent progressive motor neuron degeneration. *Brain* 136 (Pt 5), 1371–1382. doi:10.1093/brain/awt029

Ilieva, H., Polymenidou, M., and Cleveland, D. W. (2009). Non-cell autonomous toxicity in neurodegenerative disorders: ALS and beyond. *J. Cell Biol.* 187 (6), 761–772. doi:10.1083/jcb.200908164

Imamura, K., Izumi, Y., Watanabe, A., Tsukita, K., Woltjen, K., Yamamoto, T., et al. (2017). The Src/c-Abl pathway is a potential therapeutic target in amyotrophic lateral sclerosis. *Sci. Transl. Med.* 9 (391), eaaf3962. doi:10.1126/scitranslmed.aaf3962

Ip, P., Sharda, P. R., Cunningham, A., Chakrabartty, S., Pande, V., and Chakrabartty, A. (2017). Quercitrin and quercetin 3-β-d-glucoside as chemical chaperones for the A4V SOD1 ALS-causing mutant. *Protein Eng. Des. Sel.* 30, 431–440. doi:10.1093/protein/gzx025

Ivannikov, M. V., and Van Remmen, H. (2015). Sod1 gene ablation in adult mice leads to physiological changes at the neuromuscular junction similar to changes that occur in old wild-type mice. *Free Radic. Biol. Med.* 84, 254–262. doi:10.1016/j.freeradbiomed.2015.03.021

Ivanova, M. I., Sievers, S. A., Guenther, E. L., Johnson, L. M., Winkler, D. D., Galaleldeen, A., et al. (2014). Aggregation-triggering segments of SOD1 fibril formation support a common pathway for familial and sporadic ALS. *PNAS* 111, 197–201. doi:10.1073/pnas.1320786110

Iwakawa, N., Morimoto, D., Walinda, E., Kawata, Y., Shirakawa, M., and Sugase, K. (2017). Real-Time observation of the interaction between Thioflavin T and an amyloid protein by using high-sensitivity rheo-NMR. *Int. J. Mol. Sci.* 18 (11), 2271. doi:10.3390/ijms18112271

Izumikawa, K., Nobe, Y., Yoshikawa, H., Ishikawa, H., Miura, Y., Nakayama, H., et al. (2017). TDP-43 stabilises the processing intermediates of mitochondrial transcripts. *Sci. Rep.* 7 (1), 7709. doi:10.1038/s41598-017-06953-y

Jami, M. S., Salehi-Najafabadi, Z., Ahmadinejad, F., Hoedt, E., Chaleshtori, M. H., Ghatrehsamani, M., et al. (2015). Edaravone leads to proteome changes indicative of neuronal cell protection in response to oxidative stress. *Neurochem. Int.* 90, 134–141. doi:10.1016/j.neuint.2015.07.024

Jankovic, M., Novakovic, I., Gamil, A. D. P., Gamil, A. D. A., Drinic, A., Abdel, M. F. I., et al. (2021). Current concepts on genetic aspects of mitochondrial dysfunction in amyotrophic lateral sclerosis. *Int. J. Mol. Sci.* 22 (18), 9832. doi:10.3390/ijms22189832

Jiang, L. L., Che, M. X., Zhao, J., Zhou, C. J., Xie, M. Y., Li, H. Y., et al. (2013). Structural transformation of the amyloidogenic core region of TDP-43 protein initiates its aggregation and cytoplasmic inclusion. *J. Biol. Chem.* 288 (27), 19614–19624. doi:10.1074/jbc.M113.463828

Jiang, L. L., Xue, W., Hong, J. Y., Zhang, J. T., Li, M. J., Yu, S. N., et al. (2017). The N-terminal dimerization is required for TDP-43 splicing activity. *Sci. Rep.* 7 (1), 6196. doi:10.1038/s41598-017-06263-3

Jiang, L. L., Zhao, J., Yin, X. F., He, W. T., Yang, H., Che, M. X., et al. (2016). Two mutations G335D and Q343R within the amyloidogenic core region of TDP-43 influence its aggregation and inclusion formation. *Sci. Rep.* 6, 23928. doi:10.1038/srep23928

Johnson, B. S., Snead, D., Lee, J. J., McCaffery, J. M., Shorter, J., and Gitler, A. D. (2009). TDP-43 is intrinsically aggregation-prone, and amyotrophic lateral sclerosis-linked mutations accelerate aggregation and increase toxicity. *J. Biol. Chem.* 284 (30), 20329–20339. doi:10.1074/jbc.M109.010264

Joshi, V., Poluri, K. M., Upadhyay, A., Amanullah, A., Singh, S., Kumar, A., et al. (2019). Polyphenolic flavonoid (Myricetin) upregulated proteasomal degradation mechanisms: eliminates neurodegenerative proteins aggregation. *J. Cell. Physiology* 234 (2), 20900–20914. doi:10.1002/jcp.28695

Kalmar, B., and Greensmith, L. (2017). Cellular chaperones as therapeutic targets in ALS to restore protein homeostasis and improve cellular function. *Front. Mol. Neurosci.* 10, 251. doi:10.3389/fnmol.2017.00251

Kametani, F., Obi, T., Shishido, T., Akatsu, H., Murayama, S., Saito, Y., et al. (2016). Mass spectrometric analysis of accumulated TDP-43 in amyotrophic lateral sclerosis brains. *Sci. Rep.* 6, 23281. doi:10.1038/srep23281

Kao, P. F., Chen, Y. R., Liu, X. B., DeCarli, C., Seeley, W. W., and Jin, L. W. (2015). Detection of TDP-43 oligomers in frontotemporal lobar degeneration-TDP. *Ann. Neurol.* 78 (2), 211–221. doi:10.1002/ana.24431

Kato, M., Han, T. W., Xie, S., Shi, K., Du, X., Wu, L. C., et al. (2012). Cell-free formation of RNA granules: low complexity sequence domains form dynamic fibers within hydrogels. *Cell* 149 (4), 753–767. doi:10.1016/j.cell.2012.04.017

Kato, M., and McKnight, S. L. (2017). Cross-β polymerization of low complexity sequence domains. *Cold Spring Harb. Perspect. Biol.* 9 (3), a023598. doi:10.1101/cshperspect.a023598

Kato, S., Takikawa, M., Nakashima, K., Hirano, A., Cleveland, D. W., Kusaka, H., et al. (2000). New consensus research on neuropathological aspects of familial amyotrophic lateral sclerosis with superoxide dismutase 1 (SOD1) gene mutations: inclusions containing SOD1 in neurons and astrocytes. *Amyotroph. Lateral Scler. Other Mot. Neuron Disord.* 1 (3), 163–184. doi:10.1080/14660820050515160

Ke, Y. D., van Hummel, A., Stevens, C. H., Gladbach, A., Ippati, S., Bi, M., et al. (2015). Short-term suppression of A315T mutant human TDP-43 expression improves functional deficits in a novel inducible transgenic mouse model of FTLD-TDP and ALS. *Acta Neuropathol.* 130 (5), 661–678. doi:10.1007/s00401-015-1486-0

Keller, B. A., Volkening, K., Droppelmann, C. A., Ang, L. C., Rademakers, R., and Strong, M. J. (2012). Co-aggregation of RNA binding proteins in ALS spinal motor neurons: evidence of a common pathogenic mechanism. *Acta Neuropathol.* 124 (5), 733–747. doi:10.1007/s00401-012-1035-z

Kerman, A., Liu, H. N., Croul, S., Bilbao, J., Rogaeva, E., Zinman, L., et al. (2010). Amyotrophic lateral sclerosis is a non-amyloid disease in which extensive misfolding of SOD1 is unique to the familial form. *Acta Neuropathol.* 119, 335–344. doi:10.1007/s00401-010-0646-5

Khare, S. D., Caplow, M., Dokholyan, N. V., and O, M. (2004). The rate and equilibrium constants for a multistep reaction sequence for the aggregation of superoxide dismutase in amyotrophic lateral sclerosis. *PNAS* 101, 15094–15099. doi:10.1073/pnas.0406650101

Kim, G., Gautier, O., Tassoni-Tsuchida, E., Ma, X. R., and Gitler, A. D. (2020). ALS genetics: gains, losses, and implications for future therapies. *Neuron* 108, 822–842. doi:10.1016/j.neuron.2020.08.022

Kinger, S., Dubey, A. R., Kumar, P., Jagtap, Y. A., Choudhary, A., Kumar, A., et al. (2023). Molecular chaperones' potential against defective proteostasis of amyotrophic lateral sclerosis. *Cells* 12 (9), 1302. doi:10.3390/cells12091302

Kirola, L., Mukherjee, A., and Mutsuddi, M. (2022). Recent updates on the genetics of amyotrophic lateral sclerosis and frontotemporal dementia. *Mol. Neurobiol.* 59 (9), 5673–5694. doi:10.1007/s12035-022-02934-z

Knowles, T. P., Vendruscolo, M., and Dobson, C. M. (2014). The amyloid state and its association with protein misfolding diseases. *Nat. Rev. Mol. Cell Biol.* 15 (6), 384–396. doi:10.1038/nrm3810

Koh, S. H., Lee, S. M., Kim, H. Y., Lee, K. Y., Lee, Y. J., Kim, H. T., et al. (2006). The effect of epigallocatechin gallate on suppressing disease progression of ALS model mice. *Neurosci. Lett.* 395 (2), 103–107. doi:10.1016/j.neulet.2005.10.056

Konopka, A., Whelan, D. R., Jamali, M. S., Perri, E., Shahheydari, H., Toth, R. P., et al. (2020). Impaired NHEJ repair in amyotrophic lateral sclerosis is associated with TDP-43 mutations. *Mol. Neurodegener.* 15 (1), 51. doi:10.1186/s13024-020-00386-4

Kraemer, B. C., Schuck, T., Wheeler, J. M., Robinson, L. C., Trojanowski, J. Q., Lee, V. M., et al. (2010). Loss of murine TDP-43 disrupts motor function and plays an essential role in embryogenesis. *Acta Neuropathol.* 119 (4), 409–419. doi:10.1007/s00401-010-0659-0

Kuo, P. H., Chiang, C. H., Wang, Y. T., Doudeva, L. G., and Yuan, H. S. (2014). The crystal structure of TDP-43 RRM1-DNA complex reveals the specific recognition for UG- and TG-rich nucleic acids. *Nucleic Acids Res.* 42 (7), 4712–4722. doi:10.1093/nar/gkt1407

Kushner, P. D., Stephenson, D. T., and Wright, S. (1991). Reactive astrogliosis is widespread in the subcortical white matter of amyotrophic lateral sclerosis brain. *J. neuropathology Exp. neurology* 50 (3), 263–277. doi:10.1097/00005072-199105000-00008

Kuzuhara, T., Suganuma, M., and Fujiki, H. (2008). Green tea catechin as a chemical chaperone in cancer prevention. *Cancer Lett.* 261 (1), 12–20. doi:10.1016/j.canlet.2007.10.037

Lacomblez, L., Bensimon, G., Leigh, P. N., Guillet, P., and Meininger, V. (1996a). Dose-ranging study of riluzole in amyotrophic lateral sclerosis. Amyotrophic Lateral Sclerosis/Riluzole Study Group II. *Lancet* 347 (9013), 1425–1431. doi:10.1016/s0140-6736(96)91680-3

Lacomblez, L., Bensimon, G., Leigh, P. N., Guillet, P., Powe, L., Durrleman, S., et al. (1996b). A confirmatory dose-ranging study of riluzole in ALS. ALS/Riluzole Study Group-II. *Neurology* 47 (6 Suppl. 4), S242–S250. doi:10.1212/wnl.47.6_suppl_4.242s

Lai, Z., Colon, W., and Kelly, J. W. (1996). The acid-mediated denaturation pathway of transthyretin yields a conformational intermediate that can self-assemble into amyloid. *Biochemistry* 35 (20), 6470–6482. doi:10.1021/bi952501g

Lang, L., Zetterstrom, P., Brannstrom, T., Marklund, S. L., Danielsson, J., and Oliveberg, M. (2015). SOD1 aggregation in ALS mice shows simplistic test tube behavior. *Proc. Natl. Acad. Sci. U. S. A.* 112 (32), 9878–9883. doi:10.1073/pnas.1503328112

Lapasset, L., Milhavet, O., Prieur, A., Besnard, E., Babled, A., Ait-Hamou, N., et al. (2011). Rejuvenating senescent and centenarian human cells by reprogramming through the pluripotent state. *Genes Dev.* 25 (21), 2248–2253. doi:10.1101/gad.173922.111

Larkin, L. M., Davis, C. S., Sims-Robinson, C., Kostrominova, T. Y., Van Remmen, H., Richardson, A., et al. (2011). Skeletal muscle weakness due to deficiency of CuZn-superoxide dismutase is associated with loss of functional innervation. *Am. J. Physiol. Regul. Integr. Comp. Physiol.* 301 (5), R1400–R1407. doi:10.1152/ajpregu.00093.2011

Lee, Y. B., Chen, H. J., Peres, J. N., Gomez-Deza, J., Attig, J., Stalekar, M., et al. (2013). Hexanucleotide repeats in ALS/FTD form length-dependent RNA foci, sequester RNA binding proteins, and are neurotoxic. *Cell Rep.* 5 (5), 1178–1186. doi:10.1016/j.celrep.2013.10.049

Leidenheimer, N. J., and Ryder, K. G. (2014). Pharmacological chaperoning: a primer on mechanism and pharmacology. *Pharmacol. Res.* 83, 10–19. doi:10.1016/j.phrs.2014.01.005

Leigh, P. N., Anderton, B. H., Dodson, A., Gallo, J. M., Swash, M., and Power, D. M. (1988). Ubiquitin deposits in anterior horn cells in motor neurone disease. *Neurosci. Lett.* 93 (2-3), 197–203. doi:10.1016/0304-3940(88)90081-x

Li, H. R., Chiang, W. C., Chou, P. C., Wang, W. J., and Huang, J. R. (2018). TAR DNA-binding protein 43 (TDP-43) liquid-liquid phase separation is mediated by just a few aromatic residues. *J. Biol. Chem.* 293 (16), 6090–6098. doi:10.1074/jbc.AC117.001037

Li, Q., Babinchak, W. M., and Surewicz, W. K. (2021). Cryo-EM structure of amyloid fibrils formed by the entire low complexity domain of TDP-43. *Nat. Commun.* 12 (1), 1620. doi:10.1038/s41467-021-21912-y

Liguori, L., Monticelli, M., Allocca, M., Hay Mele, B., Lukas, J., Cubellis, M. V., et al. (2020). Pharmacological chaperones: a therapeutic approach for diseases caused by destabilizing missense mutations. *Int. J. Mol. Sci.* 21 (2), 489. doi:10.3390/ijms21020489

Limpert, A. S., Mattmann, M. E., and Cosford, N. D. P. (2013). Recent progress in the discovery of small molecules for the treatment of amyotrophic lateral sclerosis (ALS). *Beilstein J. Org. Chem.* 9, 717–732. doi:10.3762/bjoc.9.82

Lin, L., Ni, B., Lin, H., Zhang, M., Li, X., Yin, X., et al. (2015b). Traditional usages, botany, phytochemistry, pharmacology and toxicology of Polygonum multiflorum Thunb.: a review. *J. Ethnopharmacol.* 159, 158–183. doi:10.1016/j.jep.2014.11.009

Lin, W. L., and Dickson, D. W. (2008). Ultrastructural localization of TDP-43 in filamentous neuronal inclusions in various neurodegenerative diseases. *Acta Neuropathol.* 116 (2), 205–213. doi:10.1007/s00401-008-0408-9

Lin, Y., Protter, D. S., Rosen, M. K., and Parker, R. (2015a). Formation and maturation of phase-separated liquid droplets by RNA-binding proteins. *Mol. Cell* 60 (2), 208–219. doi:10.1016/j.molcel.2015.08.018

Liu, J., Gao, L., and Zang, D. (2015). Elevated levels of IFN-gamma in CSF and serum of patients with amyotrophic lateral sclerosis. *PLoS One* 10 (9), e0136937. doi:10.1371/journal.pone.0136937

Liu, R., Yang, G., Nonaka, T., Arai, T., Jia, W., and Cynader, M. S. (2013). Reducing TDP-43 aggregation does not prevent its cytotoxicity. *Acta Neuropathol. Commun.* 1, 49. doi:10.1186/2051-5960-1-49

Liu-Yesucevitz, L., Bilgutay, A., Zhang, Y. J., Vanderweyde, T., Citro, A., Mehta, T., et al. (2010). Tar DNA binding protein-43 (TDP-43) associates with stress granules: analysis of cultured cells and pathological brain tissue. *PLoS One* 5 (10), e13250. doi:10.1371/journal.pone.0013250

Lo Cascio, F., Marzullo, P., Kayed, R., and Palumbo Piccionello, A. (2021). Curcumin as scaffold for drug discovery against neurodegenerative diseases. *Biomedicines* 9 (2), 173. doi:10.3390/biomedicines9020173

Longinetti, E., and Fang, F. (2019). Epidemiology of amyotrophic lateral sclerosis: an update of recent literature. *Curr. Opin. Neurol.* 32 (5), 771–776. doi:10.1097/WCO.0000000000000730

Lopes, D. H., Attar, A., Nair, G., Hayden, E. Y., Du, Z., McDaniel, K., et al. (2015). Molecular tweezers inhibit islet amyloid polypeptide assembly and toxicity by a new mechanism. *ACS Chem. Biol.* 10 (6), 1555–1569. doi:10.1021/acschembio.5b00146

Lowe, J., Lennox, G., Jefferson, D., Morrell, K., McQuire, D., Gray, T., et al. (1988). A filamentous inclusion body within anterior horn neurones in motor neurone disease defined by immunocytochemical localisation of ubiquitin. *Neurosci. Lett.* 94 (1-2), 203–210. doi:10.1016/0304-3940(88)90296-0

Lu, C. H., Allen, K., Oei, F., Leoni, E., Kuhle, J., Tree, T., et al. (2016). Systemic inflammatory response and neuromuscular involvement in amyotrophic lateral sclerosis. *Neurology(R) Neuroimmunol. neuroinflammation* 3 (4), e244. doi:10.1212/NXI.0000000000000244

Lukavsky, P. J., Daujotyte, D., Tollervey, J. R., Ule, J., Stuani, C., Buratti, E., et al. (2013). Molecular basis of UG-rich RNA recognition by the human splicing factor TDP-43. *Nat. Struct. Mol. Biol.* 20 (12), 1443–1449. doi:10.1038/nsmb.2698

Macarron, R., and Hertzberg, R. P. (2009). Design and implementation of high-throughput screening assays. *Methods Mol. Biol.* 565, 1–29. doi:10.1385/1-59259-180-9:001

Mackenzie, I. R., Bigio, E. H., Ince, P. G., Geser, F., Neumann, M., Cairns, N. J., et al. (2007). Pathological TDP-43 distinguishes sporadic amyotrophic lateral sclerosis from amyotrophic lateral sclerosis with SOD1 mutations. *Ann. Neurol.* 61 (5), 427–434. doi:10.1002/ana.21147

Madeira, J. M., Bajwa, E., Stuart, M. J., Hashioka, S., and Klegeris, A. (2014). Gold drug auranofin could reduce neuroinflammation by inhibiting microglia cytotoxic secretions and primed respiratory burst. *J. Neuroimmunol.* 276 (1-2), 71–79. doi:10.1016/j.jneuroim.2014.08.615

Madeira, J. M., Renschler, C. J., Mueller, B., Hashioka, S., Gibson, D. L., and Klegeris, A. (2013). Novel protective properties of auranofin: inhibition of human astrocyte cytotoxic secretions and direct neuroprotection. *Life Sci.* 92 (22), 1072–1080. doi:10.1016/j.lfs.2013.04.005

Madeira, J. M., Schindler, S. M., and Klegeris, A. (2015). A new look at auranofin, dextromethorphan and rosiglitazone for reduction of glia-mediated inflammation in neurodegenerative diseases. *Neural Regen. Res.* 10 (3), 391–393. doi:10.4103/1673-5374.153686

Maher, P. (2019). The potential of flavonoids for the treatment of neurodegenerative diseases. *Int. J. Mol. Sci.* 20, 3056. doi:10.3390/ijms20123056

Maier, M., Welt, T., Wirth, F., Montrasio, F., Preisig, D., McAfoose, J., et al. (2018). A human-derived antibody targets misfolded SOD1 and ameliorates motor symptoms in mouse models of amyotrophic lateral sclerosis. *Sci. Transl. Med.* 10 (470), eaah3924. doi:10.1126/scitranslmed.aah3924

Malik, R., Corrales, C., Sepanj, N., and Bitan, G. (2020). Examination of SOD1 aggregation modulators and their effect on SOD1 enzymatic activity as a proxy for potential toxicity. *FASEB J.* 34 (9), 1–12. doi:10.1096/fj.202000948R

Malik, R., Meng, H., Wongkongkathep, P., Corrales, C. I., Sepanj, N., Atlasi, R. S., et al. (2019). The molecular tweezer CLR01 inhibits aberrant superoxide dismutase 1 (SOD1) self-assembly *in vitro* and in the G93A-SOD1 mouse model of ALS. *J. Biol. Chem.* 294, 3501–3513. doi:10.1074/jbc.RA118.005940

Malishev, R., Salinas, N., Gibson, J., Eden, A. B., Mieres-Perez, J., Ruiz-Blanco, Y. B., et al. (2021). Inhibition of *Staphylococcus aureus* biofilm-forming functional amyloid by molecular tweezers. *Cell Chem. Biol.* 28 (9), 1310–1320.e5. doi:10.1016/j.chembiol.2021.03.013

Manjula, R., Unni, S., Wright, G. S. A., Bharath, M. M. S., and Padmanabhan, B. (2019). Rational discovery of a SOD1 tryptophan oxidation inhibitor with therapeutic potential for amyotrophic lateral sclerosis. *J. Biomol. Struct. Dyn.* 37 (15), 3936–3946. doi:10.1080/07391102.2018.1531787

March, Z. M., King, O. D., and Shorter, J. (2016). Prion-like domains as epigenetic regulators, scaffolds for subcellular organization, and drivers of neurodegenerative disease. *Brain Res.* 1647, 9–18. doi:10.1016/j.brainres.2016.02.037

Matis, I., Delivoria, D. C., Mavroidi, B., Papaevgeniou, N., Panoutsou, S., Bellou, S., et al. (2017). An integrated bacterial system for the discovery of chemical rescuers of

disease-associated protein misfolding. *Nat. Biomed. Eng.* 1 (10), 838–852. doi:10.1038/s41551-017-0144-3

Maurer, M. S., Schwartz, J. H., Gundapaneni, B., Elliott, P. M., Merlini, G., Waddington-Cruz, M., et al. (2018). Tafamidis treatment for patients with transthyretin amyloid cardiomyopathy. *N. Engl. J. Med.* 379 (11), 1007–1016. doi:10.1056/NEJMoa1805689

Mbarek, A., Moussa, G., and Chain, J. L. (2019). Pharmaceutical applications of molecular tweezers, clefts and clips. *Molecules* 24 (9), 1803. doi:10.3390/molecules24091803

McAlary, L., Chew, Y. L., Lum, J. S., Geraghty, N. J., Yerbury, J. J., and Cashman, N. R. (2020). Amyotrophic lateral sclerosis: proteins, proteostasis, prions, and promises. *Front. Cell. Neurosci.* 14, 581907. doi:10.3389/fncel.2020.581907

McAlary, L., and Yerbury, J. J. (2019). Strategies to promote the maturation of ALS-associated SOD1 mutants: small molecules return to the fold. *Neural Regen Res* 9, 1511–1512. doi:10.4103/1673-5374.255962

McCampbell, A., Cole, T., Wegener, A. J., Tomassy, G. S., Setnicka, A., Farley, B. J., et al. (2018). Antisense oligonucleotides extend survival and reverse decrement in muscle response in ALS models. *J. Clin. investigation* 128 (8), 3558–3567. doi:10.1172/JCI99081

McGown, A., and Stopford, M. J. (2018). High-throughput drug screens for amyotrophic lateral sclerosis drug discovery. *Expert Opin. Drug Discov.* 13 (11), 1015–1025. doi:10.1080/17460441.2018.1533953

Mead, R. J., Shan, N., Reiser, H. J., Marshall, F., and Shaw, P. J. (2023). Amyotrophic lateral sclerosis: a neurodegenerative disorder poised for successful therapeutic translation. *Nat. Rev. Drug Discov.* 22 (3), 185–212. doi:10.1038/s41573-022-00612-2

Medinas, D. B., Gozzo, F. C., Santos, L. F., Iglesias, A. H., and Augusto, O. (2010). A ditryptophan cross-link is responsible for the covalent dimerization of human superoxide dismutase 1 during its bicarbonate-dependent peroxidase activity. *Free Radic. Biol. Med.* 49 (6), 1046–1053. doi:10.1016/j.freeradbiomed.2010.06.018

Medinas, D. B., Rozas, P., Martínez, F., Woehlbier, U., Brown, R. H., Bosco, D. A., et al. (2018). Endoplasmic reticulum stress leads to accumulation of wild-type SOD1 aggregates associated with sporadic amyotrophic lateral sclerosis. *PNAS* 115, 8209–8214. doi:10.1073/pnas.1801109115

Medinas, D. B., Valenzuela, V., and Hetz, C. (2017). Proteostasis disturbance in amyotrophic lateral sclerosis. *Hum. Mol. Genet.* 26 (R2), R91–R104. doi:10.1093/hmg/ddx274

Mejzini, R., Flynn, L. L., Pitout, I. L., Fletcher, S., Wilton, S. D., and Akkari, P. A. (2019). ALS genetics, mechanisms, and therapeutics: where are we now?. *Front. Neurosci.* 13, 1–27. doi:10.3389/fnins.2019.01310

Mertens, J., Marchetto, M. C., Bardy, C., and Gage, F. H. (2016). Evaluating cell reprogramming, differentiation and conversion technologies in neuroscience. *Nat. Rev. Neurosci.* 17 (7), 424–437. doi:10.1038/nrn.2016.46

Meyer, K., Ferraiuolo, L., Miranda, C. J., Likhite, S., McElroy, S., Renusch, S., et al. (2014). Direct conversion of patient fibroblasts demonstrates non-cell autonomous toxicity of astrocytes to motor neurons in familial and sporadic ALS. *Proc. Natl. Acad. Sci. U. S. A.* 111 (2), 829–832. doi:10.1073/pnas.1314085111

Miller, T. M., Cudkowicz, M. E., Genge, A., Shaw, P. J., Sobue, G., Bucelli, R. C., et al. (2022). Trial of antisense oligonucleotide tofersen for SOD1 ALS. *N. Engl. J. Med.* 387 (12), 1099–1110. doi:10.1056/NEJMoa2204705

Mitsuzawa, S., Akiyama, T., Nishiyama, A., Suzuki, N., Kato, M., Warita, H., et al. (2018). TARDBP p.G376D mutation, found in rapid progressive familial ALS, induces mislocalization of TDP-43. *eNeurologicalSci* 11, 20–22. doi:10.1016/j.ensci.2018.04.001

Mittal, S., Bravo-Rodriguez, K., and Sanchez-Garcia, E. (2018). Mechanism of inhibition of beta amyloid toxicity by supramolecular tweezers. *J. Phys. Chem. B* 122 (15), 4196–4205. doi:10.1021/acs.jpcb.7b10530

Mollasalehi, N., Francois-Moutal, L., Scott, D. D., Tello, J. A., Williams, H., Mahoney, B., et al. (2020). An allosteric modulator of RNA binding targeting the N-terminal domain of TDP-43 yields neuroprotective properties. *ACS Chem. Biol.* 15 (11), 2854–2859. doi:10.1021/acschembio.0c00494

Molliex, A., Temirov, J., Lee, J., Coughlin, M., Kanagaraj, A. P., Kim, H. J., et al. (2015). Phase separation by low complexity domains promotes stress granule assembly and drives pathological fibrillization. *Cell* 163 (1), 123–133. doi:10.1016/j.cell.2015.09.015

Molnar, K. S., Karabacak, N. M., Johnson, J. L., Wang, Q., Tiwari, A., Hayward, L. J., et al. (2009). A common property of amyotrophic lateral sclerosis-associated variants: destabilization of the copper/zinc superoxide dismutase electrostatic loop. *J. Biol. Chem.* 284 (45), 30965–30973. doi:10.1074/jbc.M109.023945

Mompean, M., Ramirez de Mingo, D., Hervas, R., Fernandez-Ramirez, M. D. C., Carrion-Vazquez, M., and Laurents, D. V. (2019). Molecular mechanism of the inhibition of TDP-43 amyloidogenesis by QBP1. *Arch. Biochem. Biophys.* 675, 108113. doi:10.1016/j.abb.2019.108113

Mompean, M., Romano, V., Pantoja-Uceda, D., Stuani, C., Baralle, F. E., Buratti, E., et al. (2016). The TDP-43 N-terminal domain structure at high resolution. *FEBS J.* 283 (7), 1242–1260. doi:10.1111/febs.13651

Mompean, M., Romano, V., Pantoja-Uceda, D., Stuani, C., Baralle, F. E., Buratti, E., et al. (2017). Point mutations in the N-terminal domain of transactive response DNA-binding protein 43 kDa (TDP-43) compromise its stability, dimerization, and functions. *J. Biol. Chem.* 292 (28), 11992–12006. doi:10.1074/jbc.M117.775965

Montibeller, L., Tan, L. Y., Kim, J. K., Paul, P., and de Belleroche, J. (2020). Tissue-selective regulation of protein homeostasis and unfolded protein response signalling in sporadic ALS. *J. Cell. Mol. Med.* 24 (11), 6055–6069. doi:10.1111/jcmm.15170

Moreau, C., Devos, D., Brunaud-Danel, V., Defebvre, L., Perez, T., Destee, A., et al. (2005). Elevated IL-6 and TNF-alpha levels in patients with ALS: inflammation or hypoxia? *Neurology* 65 (12), 1958–1960. doi:10.1212/01.wnl.0000188907.97339.76

Moreau, K. L., and King, J. A. (2012). Protein misfolding and aggregation in cataract disease and prospects for prevention. *Trends Mol. Med.* 18 (5), 273–282. doi:10.1016/j.molmed.2012.03.005

Mueller, C., Berry, J. D., McKenna-Yasek, D. M., Gernoux, G., Owegi, M. A., Pothier, L. M., et al. (2020). SOD1 suppression with adeno-associated virus and MicroRNA in familial ALS. *N. Engl. J. Med.* 383 (2), 151–158. doi:10.1056/NEJMoa2005056

Mukundan, V., Maksoudian, C., Vogel, M. C., Chehade, I., Katsiotis, M. S., Alhassan, S. M., et al. (2017). Cytotoxicity of prion protein-derived cell-penetrating peptides is modulated by pH but independent of amyloid formation. *Arch. Biochem. Biophys.* 613, 31–42. doi:10.1016/j.abb.2016.11.001

Murakami, G., Inoue, H., Tsukita, K., Asai, Y., Amagai, Y., Aiba, K., et al. (2011). Chemical library screening identifies a small molecule that downregulates SOD1 transcription for drugs to treat amyotrophic lateral sclerosis. *J. Biomol. Screen.* 16, 405–414. doi:10.1177/1087057110397888

Murakami, T., Qamar, S., Lin, J. Q., Schierle, G. S., Rees, E., Miyashita, A., et al. (2015). ALS/FTD mutation-induced phase transition of FUS liquid droplets and reversible hydrogels into irreversible hydrogels impairs RNP granule function. *Neuron* 88 (4), 678–690. doi:10.1016/j.neuron.2015.10.030

Musteikyte, G., Ziaunys, M., and Smirnovas, V. (2020). Methylene blue inhibits nucleation and elongation of SOD1 amyloid fibrils. *PeerJ* 8, e9719. doi:10.7717/peerj.9719

Mutihac, R., Alegre-Abarrategui, J., Gordon, D., Farrimond, L., Yamasaki-Mann, M., Talbot, K., et al. (2015). TARDBP pathogenic mutations increase cytoplasmic translocation of TDP-43 and cause reduction of endoplasmic reticulum Ca^{2+} signaling in motor neurons. *Neurobiol. Dis.* 75, 64–77. doi:10.1016/j.nbd.2014.12.010

Nagai, Y., Fujikake, N., Ohno, K., Higashiyama, H., Popiel, H. A., Rahadian, J., et al. (2003). Prevention of polyglutamine oligomerization and neurodegeneration by the peptide inhibitor QBP1 in Drosophila. *Hum. Mol. Genet.* 12 (11), 1253–1259. doi:10.1093/hmg/ddg144

Nagai, Y., Tucker, T., Ren, H., Kenan, D. J., Henderson, B. S., Keene, J. D., et al. (2000). Inhibition of polyglutamine protein aggregation and cell death by novel peptides identified by phage display screening. *J. Biol. Chem.* 275 (14), 10437–10442. doi:10.1074/jbc.275.14.10437

Nagy, D., Kato, T., and Kushner, P. D. (1994). Reactive astrocytes are widespread in the cortical gray matter of amyotrophic lateral sclerosis. *J. Neurosci. Res.* 38 (3), 336–347. doi:10.1002/jnr.490380312

Nday, C. M., Halevas, E., Jackson, G. E., and Salifoglou, A. (2015). Quercetin encapsulation in modified silica nanoparticles: potential use against Cu(II)-induced oxidative stress in neurodegeneration. *J. Inorg. Biochem.* 145, 51–64. doi:10.1016/j.jinorgbio.2015.01.001

Neumann, M., Roeber, S., Kretzschmar, H. A., Rademakers, R., Baker, M., and Mackenzie, I. R. (2009). Abundant FUS-immunoreactive pathology in neuronal intermediate filament inclusion disease. *Acta Neuropathol.* 118 (5), 605–616. doi:10.1007/s00401-009-0581-5

Neumann, M., Sampathu, D. M., Kwong, L. K., Truax, A. C., Micsenyi, M. C., Chou, T. T., et al. (2006). Ubiquitinated TDP-43 in frontotemporal lobar degeneration and amyotrophic lateral sclerosis. *Science* 314 (5796), 130–133. doi:10.1126/science.1134108

Nikitin, D., Makam, A. N., Suh, K., McKenna, A., Carlson, J. J., Richardson, M., et al. (2023). The effectiveness and value of AMX0035 and oral edaravone for amyotrophic lateral sclerosis: a summary from the Institute for clinical and economic review's midwest comparative effectiveness public advisory Council. *J. Manag. care & specialty Pharm.* 29 (2), 216–221. doi:10.18553/jmcp.2023.29.2.216

Nordlund, A., Leinartaite, L., Saraboji, K., Aisenbrey, C., Grobner, G., Zetterstrom, P., et al. (2009). Functional features cause misfolding of the ALS-provoking enzyme SOD1. *Proc. Natl. Acad. Sci. U. S. A.* 106 (24), 9667–9672. doi:10.1073/pnas.0812046106

Nowak, R. J., Cuny, G. D., Choi, S., Lansbury, P. T., and Ray, S. S. (2011). Improving binding specificity of pharmacological chaperones that target mutant superoxide dismutase-1 linked to familial amyotrophic lateral sclerosis using computational methods. *J. Med. Chem.* 53, 2709–2718. doi:10.1021/jm901062p

Oberstadt, M., Stieler, J., Simpong, D. L., Romuss, U., Urban, N., Schaefer, M., et al. (2018). TDP-43 self-interaction is modulated by redox-active compounds Auranofin, Chelerythrine and Riluzole. *Sci. Rep.* 8 (1), 2248. doi:10.1038/s41598-018-20565-0

Park, J. H., Elpers, C., Reunert, J., McCormick, M. L., Mohr, J., Biskup, S., et al. (2019). SOD1 deficiency: a novel syndrome distinct from amyotrophic lateral sclerosis. *Brain* 142, 2230–2237. doi:10.1093/brain/awz182

Patel, A., Lee, H. O., Jawerth, L., Maharana, S., Jahnel, M., Hein, M. Y., et al. (2015). A liquid-to-solid phase transition of the ALS protein FUS accelerated by disease mutation. *Cell* 162 (5), 1066–1077. doi:10.1016/j.cell.2015.07.047

Pattee, G. L., Genge, A., Couratier, P., Lunetta, C., Sobue, G., Aoki, M., et al. (2023). Oral edaravone - introducing a flexible treatment option for amyotrophic lateral sclerosis. *Expert Rev. Neurother.* 23 (10), 859–866. doi:10.1080/14737175.2023.2251687

Patterson, M., Chan, D. N., Ha, I., Case, D., Cui, Y., Van Handel, B., et al. (2012). Defining the nature of human pluripotent stem cell progeny. *Cell Res.* 22 (1), 178–193. doi:10.1038/cr.2011.133

Petrov, D., Mansfield, C., Moussy, A., and Hermine, O. (2017). ALS clinical trials review: 20 Years of failure. *Are We Any Closer Registering a New Treat. ?* 9, 1–11. doi:10.3389/fnagi.2017.00068

Pettersen, E. F., Goddard, T. D., Huang, C. C., Meng, E. C., Couch, G. S., Croll, T. I., et al. (2021). UCSF ChimeraX: structure visualization for researchers, educators, and developers. *Protein science a publication of the Protein Society* 30 (1), 70–82. doi:10.1002/pro.3943

Pickles, S., Destroismaisons, L., Peyrard, S. L., Cadot, S., Rouleau, G. A., Brown, R. H., Jr., et al. (2013). Mitochondrial damage revealed by immunoselection for ALS-linked misfolded SOD1. *Human molecular genetics* 22 (19), 3947–3959. doi:10.1093/hmg/ddt249

Pinarbasi, E. S., Cagatay, T., Fung, H. Y. J., Li, Y. C., Chook, Y. M., and Thomas, P. J. (2018). Active nuclear import and passive nuclear export are the primary determinants of TDP-43 localization. *Sci Rep* 8 (1), 7083. doi:10.1038/s41598-018-25008-4

Pokrishevsky, E., Mcalary, L., Farrawell, N. E., Zhao, B., Sher, M., Yerbury, J. J., et al. (2018). Tryptophan 32-mediated SOD1 aggregation is attenuated by pyrimidine-like compounds in living cells. *Scientific Reports* 8, 15590. doi:10.1038/s41598-018-32835-y

Polticelli, F., Bottaro, G., Battistoni, A., Carri, M. T., Djinovic-Carugo, K., Bolognesi, M., et al. (1995). Modulation of the catalytic rate of Cu,Zn superoxide dismutase in single and double mutants of conserved positively and negatively charged residues. *Biochemistry* 34 (18), 6043–6049. doi:10.1021/bi00018a006

Polymenidou, M., Lagier-Tourenne, C., Hutt, K. R., Huelga, S. C., Moran, J., Liang, T. Y., et al. (2011). Long pre-mRNA depletion and RNA missplicing contribute to neuronal vulnerability from loss of TDP-43. *Nat Neurosci* 14 (4), 459–468. doi:10.1038/nn.2779

Popiel, H. A., Takeuchi, T., Burke, J. R., Strittmatter, W. J., Toda, T., Wada, K., et al. (2013). Inhibition of protein misfolding/aggregation using polyglutamine binding peptide QBP1 as a therapy for the polyglutamine diseases. *Neurotherapeutics* 10 (3), 440–446. doi:10.1007/s13311-013-0184-7

Pozzi, S., Thammisetty, S. S., Codron, P., Rahimian, R., Plourde, K. V., Soucy, G., et al. (2019). Virus-mediated delivery of antibody targeting TAR DNA-binding protein-43 mitigates associated neuropathology. *The Journal of clinical investigation* 129 (4), 1581–1595. doi:10.1172/JCI123931

Prakash, D., and Sudhandiran, G. (2015). Dietary flavonoid fisetin regulates aluminium chloride-induced neuronal apoptosis in cortex and hippocampus of mice brain. *J Nutr Biochem.* 26 (12), 1527–1539. doi:10.1016/j.jnutbio.2015.07.017

Prasad, A., Bharathi, V., Sivalingam, V., Girdhar, A., and Patel, B. K. (2019). Molecular mechanisms of TDP-43 misfolding and pathology in amyotrophic lateral sclerosis. *Front Mol Neurosci* 12, 25. doi:10.3389/fnmol.2019.00025

Prasad, A., Raju, G., Sivalingam, V., Girdhar, A., Verma, M., Vats, A., et al. (2016). An acridine derivative, [4,5-bis{(N-carboxy methyl imidazolium)methyl}acridine] dibromide, shows anti-TDP-43 aggregation effect in ALS disease models. *Sci Rep* 6, 39490. doi:10.1038/srep39490

Pratt, A. J., Shin, D. S., Merz, G. E., Rambo, R. P., Lancaster, W. A., Dyer, K. N., et al. (2014). Aggregation propensities of superoxide dismutase G93 hotspot mutants mirror ALS clinical phenotypes. *Proceedings of the National Academy of Sciences of the U. S. A.* 111 (43), E4568–E4576. doi:10.1073/pnas.1308531111

Proctor, E. A., Fee, L., Tao, Y., Redler, R. L., Fay, J. M., Zhang, Y., et al. (2016). Nonnative SOD1 trimer is toxic to motor neurons in a model of amyotrophic lateral sclerosis. *Proceedings of the National Academy of Sciences of the U. S. A.* 113 (3), 614–619. doi:10.1073/pnas.1516725113

Proctor, E. A., Mowrey, D. D., and Dokholyan, N. V. (2019). β-Methylamino-L-alanine substitution of serine in SOD1 suggests a direct role in ALS etiology. *PLoS computational biology* 15 (7), e1007225. doi:10.1371/journal.pcbi.1007225

Prudencio, M., Hart, P. J., Borchelt, D. R., and Andersen, P. M. (2009). Variation in aggregation propensities among ALS-associated variants of SOD1: correlation to human disease. *Human molecular genetics* 18 (17), 3217–3226. doi:10.1093/hmg/ddp260

Qin, H., Lim, L. Z., Wei, Y., and Song, J. (2014). TDP-43 N terminus encodes a novel ubiquitin-like fold and its unfolded form in equilibrium that can be shifted by binding to ssDNA. *Proceedings of the National Academy of Sciences of the U. S. A.* 111 (52), 18619–18624. doi:10.1073/pnas.1413994112

Rakhit, R., Cunningham, P., Furtos-Matei, A., Dahan, S., Qi, X. F., Crow, J. P., et al. (2002). Oxidation-induced misfolding and aggregation of superoxide dismutase and its implications for amyotrophic lateral sclerosis. *J Biol Chem* 277 (49), 47551–47556. doi:10.1074/jbc.M207356200

Ramesh, N., and Pandey, U. B. (2017). Autophagy dysregulation in ALS: when protein aggregates get out of hand. *Front Mol Neurosci* 10, 263. doi:10.3389/fnmol.2017.00263

Rando, A., de la Torre, M., Martinez-Muriana, A., Zaragoza, P., Musaro, A., Hernandez, S., et al. (2019). Chemotherapeutic agent 5-fluorouracil increases survival of SOD1 mouse model of ALS. *PLoS One* 14 (1), e0210752. doi:10.1371/journal.pone.0210752

Ranganathan, R., Haque, S., Coley, K., Shepheard, S., Cooper-Knock, J., and Kirby, J. (2020). Multifaceted genes in amyotrophic lateral sclerosis-frontotemporal dementia. *Frontiers in neuroscience* 14, 684. doi:10.3389/fnins.2020.00684

Ray, S. S., Nowak, R. J., Brown, R. H., and Lansbury, P. T. (2005). Small-molecule-mediated stabilization of familial amyotrophic lateral sclerosis-linked superoxide dismutase mutants against unfolding and aggregation. *PNAS* 102, 3639–3644. doi:10.1073/pnas.0408277102

Ray, S. S., Nowak, R. J., Strokovich, K., Brown, R. H., Walz, T., and Lansbury, P. T. (2004). An intersubunit disulfide bond prevents *in vitro* aggregation of a superoxide dismutase-1 mutant linked to familial amytrophic lateral sclerosis. *Biochemistry* 43 (17), 4899–4905. doi:10.1021/bi030246r

Reaume, A. G., Elliott, J. L., Hoffman, E. K., Kowall, N. W., Ferrante, R. J., Siwek, D. F., et al. (1996). Motor neurons in Cu/Zn superoxide dismutase-deficient mice develop normally but exhibit enhanced cell death after axonal injury. *Nat Genet* 13 (1), 43–47. doi:10.1038/ng0596-43

Reischauer, C., Gutzeit, A., Neuwirth, C., Fuchs, A., Sartoretti-Schefer, S., Weber, M., et al. (2018). *In-vivo* evaluation of neuronal and glial changes in amyotrophic lateral sclerosis with diffusion tensor spectroscopy. *Neuroimage Clin.* 20, 993–1000.

Rengifo-Gonzalez, J. C., El Hage, K., Clement, M. J., Steiner, E., Joshi, V., Craveur, P., et al. (2021). The cooperative binding of TDP-43 to GU-rich RNA repeats antagonizes TDP-43 aggregation. *Elife* 10, e67605. doi:10.7554/eLife.67605

Riancho, J., Castanedo-Vazquez, D., Gil-Bea, F., Tapia, O., Arozamena, J., Duran-Vian, C., et al. (2020). ALS-derived fibroblasts exhibit reduced proliferation rate, cytoplasmic TDP-43 aggregation and a higher susceptibility to DNA damage. *J Neurol* 267 (5), 1291–1299. doi:10.1007/s00415-020-09704-8

Rinaldi, C., and Wood, M. J. A. (2018). Antisense oligonucleotides: the next frontier for treatment of neurological disorders. *Nat Rev Neurol* 14 (1), 9–21. doi:10.1038/nrneurol.2017.148

Rodrigues, C. M., Sola, S., Sharpe, J. C., Moura, J. J., and Steer, C. J. (2003). Tauroursodeoxycholic acid prevents Bax-induced membrane perturbation and cytochrome C release in isolated mitochondria. *Biochemistry* 42 (10), 3070–3080. doi:10.1021/bi026979d

Rojas, J. C., Bruchey, A. K., and Gonzalez-Lima, F. (2012). Neurometabolic mechanisms for memory enhancement and neuroprotection of methylene blue. *Prog Neurobiol* 96 (1), 32–45. doi:10.1016/j.pneurobio.2011.10.007

Rosen, D. R., Siddiquet, T., Pattersont, D., Figlewicz, D. A., Ii, P. S., Hentatit, A., et al. (1993). Mutations in Cu/Zn superoxide dismutase gene are associated with familial amyotrophic lateral sclerosis. *Nature* 362, 59–62. doi:10.1038/362059a0

Ryan, M., Heverin, M., McLaughlin, R. L., and Hardiman, O. (2019). Lifetime risk and heritability of amyotrophic lateral sclerosis. *JAMA neurology* 76 (11), 1367–1374. doi:10.1001/jamaneurol.2019.2044

Ryan, P., Patel, B., Makwana, V., Jadhav, H. R., Kiefel, M., Davey, A., et al. (2018). Peptides, peptidomimetics, and carbohydrate-peptide conjugates as amyloidogenic aggregation inhibitors for Alzheimer's disease. *ACS Chem Neurosci* 9 (7), 1530–1551. doi:10.1021/acschemneuro.8b00185

Saccon, R. A., Bunton-Stasyshyn, R. K., Fisher, E. M., and Fratta, P. (2013). Is SOD1 loss of function involved in amyotrophic lateral sclerosis? *Brain* 136 (Pt 8), 2342–2358. doi:10.1093/brain/awt097

Saini, A., and Chauhan, V. S. (2011). Delineation of the core aggregation sequences of TDP-43 C-terminal fragment. *Chembiochem a European journal of chemical biology* 12 (16), 2495–2501. doi:10.1002/cbic.201100427

Saito, I., Asano, T., Sano, K., Takakura, K., Abe, H., Yoshimoto, T., et al. (1998). Neuroprotective effect of an antioxidant, ebselen, in patients with delayed neurological deficits after aneurysmal subarachnoid hemorrhage. *Neurosurgery* 42 (2), 269–277. doi:10.1097/00006123-199802000-00038

Samanta, N., Ruiz-Blanco, Y. B., Fetahaj, Z., Gnutt, D., Lantz, C., Loo, J. A., et al. (2022). Superoxide dismutase 1 folding stability as a target for molecular tweezers in SOD1-related amyotrophic lateral sclerosis. *Chembiochem a European journal of chemical biology* 23 (21), e202200396. doi:10.1002/cbic.202200396

Sangwan, S., Zhao, A., Adams, K. L., Jayson, C. K., Sawaya, M. R., Guenther, E. L., et al. (2017). Atomic structure of a toxic, oligomeric segment of SOD1 linked to amyotrophic lateral sclerosis (ALS). *Proceedings of the National Academy of Sciences of the U. S. A.* 114 (33), 8770–8775. doi:10.1073/pnas.1705091114

Scherzinger, E., Sittler, A., Schweiger, K., Heiser, V., Lurz, R., Hasenbank, R., et al. (1999). Self-assembly of polyglutamine-containing huntingtin fragments into amyloid-like fibrils: implications for Huntington's disease pathology. *Proceedings of the National Academy of Sciences of the U. S. A.* 96 (8), 4604–4609. doi:10.1073/pnas.96.8.4604

Schewe, T. (1995). Molecular actions of ebselen--an antiinflammatory antioxidant. *Gen Pharmacol* 26 (6), 1153–1169. doi:10.1016/0306-3623(95)00003-j

Schiffer, D., Cordera, S., Cavalla, P., and Migheli, A. (1996). Reactive astrogliosis of the spinal cord in amyotrophic lateral sclerosis. *J Neurol Sci* 139 (Suppl. l), 27–33. doi:10.1016/0022-510x(96)00073-1

Sekhar, A., Rumfeldt, J. A., Broom, H. R., Doyle, C. M., Bouvignies, G., Meiering, E. M., et al. (2015). Thermal fluctuations of immature SOD1 lead to separate folding and misfolding pathways. *Elife* 4, e07296. doi:10.7554/eLife.07296

Seminary, E. R., Sison, S. L., and Ebert, A. D. (2018). Modeling protein aggregation and the heat shock response in ALS iPSC-derived motor neurons. *Frontiers in neuroscience* 12, 86. doi:10.3389/fnins.2018.00086

Shi, Y., Ivannikov, M. V., Walsh, M. E., Liu, Y., Zhang, Y., Jaramillo, C. A., et al. (2014). The lack of CuZnSOD leads to impaired neurotransmitter release,

neuromuscular junction destabilization and reduced muscle strength in mice. *PLoS One* 9 (6), e100834. doi:10.1371/journal.pone.0100834

Shin, Y., and Brangwynne, C. P. (2017). Liquid phase condensation in cell physiology and disease. *Science*. 357 (6357), eaaf4382. doi:10.1126/science.aaf4382

Shvil, N., Banerjee, V., Zoltsman, G., Shani, T., Kahn, J., Abu-hamad, S., et al. (2018). MIF inhibits the formation and toxicity of misfolded SOD1 amyloid aggregates: implications for familial ALS. *Cell Death and Disease* 9, 107. doi:10.1038/s41419-017-0130-4

Sievers, S. A., Karanicolas, J., Chang, H. W., Zhao, A., Jiang, L., Zirafi, O., et al. (2011). Structure-based design of non-natural amino-acid inhibitors of amyloid fibril formation. *Nature* 475 (7354), 96–100. doi:10.1038/nature10154

Sinha, S., Lopes, D. H., Du, Z., Pang, E. S., Shanmugam, A., Lomakin, A., et al. (2011). Lysine-specific molecular tweezers are broad-spectrum inhibitors of assembly and toxicity of amyloid proteins. *J Am Chem Soc* 133 (42), 16958–16969. doi:10.1021/ja206279b

Smethurst, P., Risse, E., Tyzack, G. E., Mitchell, J. S., Taha, D. M., Chen, Y. R., et al. (2020). Distinct responses of neurons and astrocytes to TDP-43 proteinopathy in amyotrophic lateral sclerosis. *Brain* 143 (2), 430–440. doi:10.1093/brain/awz419

Soejima-Kusunoki, A., Okada, K., Saito, R., and Watabe, K. (2022). The protective effect of edaravone on TDP-43 Plus oxidative stress-induced neurotoxicity in neuronal cells: analysis of its neuroprotective mechanisms using RNA sequencing. *Pharmaceuticals* 15 (7), 842. doi:10.3390/ph15070842

Souza, P. C. T., Thallmair, S., Marrink, S. J., and Mera-Adasme, R. (2019). An allosteric pathway in copper, zinc superoxide dismutase unravels the molecular mechanism of the G93A amyotrophic lateral sclerosis-linked mutation. *J Phys Chem Lett* 10 (24), 7740–7744. doi:10.1021/acs.jpclett.9b02868

Srinivasan, E., and Rajasekaran, R. (2018). Comparative binding of kaempferol and kaempferide on inhibiting the aggregate formation of mutant (G85R) SOD1 protein in familial amyotrophic lateral sclerosis: a quantum chemical and molecular mechanics study. *BioFactors* 44, 431–442. doi:10.1002/biof.1441

Srinivasan, E., and Rajasekaran, R. (2019). Rational design of linear tripeptides against the aggregation of human mutant SOD1 protein causing amyotrophic lateral sclerosis. *J Neurol Sci* 405, 116425. doi:10.1016/j.jns.2019.116425

Statland, J. M., Barohn, R. J., McVey, A. L., Katz, J. S., and Dimachkie, M. M. (2015). Patterns of weakness, classification of motor neuron disease, and clinical diagnosis of sporadic amyotrophic lateral sclerosis. *Neurol Clin* 33 (4), 735–748. doi:10.1016/j.ncl.2015.07.006

Street, T. O., Bolen, D. W., and Rose, G. D. (2006). A molecular mechanism for osmolyte-induced protein stability. *Proceedings of the National Academy of Sciences of the U. S. A.* 103 (38), 13997–14002. doi:10.1073/pnas.0606236103

Su, X. W., Nandar, W., Neely, E. B., Simmons, Z., and Connor, J. R. (2016). Statins accelerate disease progression and shorten survival in SOD1(G93A) mice. *Muscle & nerve* 54 (2), 284–291. doi:10.1002/mus.25048

Suaud, L., Miller, K., Panichelli, A. E., Randell, R. L., Marando, C. M., and Rubenstein, R. C. (2011). 4-Phenylbutyrate stimulates Hsp70 expression through the Elp2 component of elongator and STAT-3 in cystic fibrosis epithelial cells. *J Biol Chem* 286 (52), 45083–45092. doi:10.1074/jbc.M111.293282

Sun, Y., Arslan, P. E., Won, A., Yip, C. M., and Chakrabartty, A. (2014). Binding of TDP-43 to the 3'UTR of its cognate mRNA enhances its solubility. *Biochemistry* 53 (37), 5885–5894. doi:10.1021/bi500617x

Suzuki, N., Nishiyama, A., Warita, H., and Aoki, M. (2023). Genetics of amyotrophic lateral sclerosis: seeking therapeutic targets in the era of gene therapy. *Journal of human genetics* 68 (3), 131–152. doi:10.1038/s10038-022-01055-8

Szabo, I., Yousef, M., Soltesz, D., Bato, C., Mezo, G., and Banoczi, Z. (2022). Redesigning of cell-penetrating peptides to improve their efficacy as a drug delivery system. *Pharmaceutics* 14 (5), 907. doi:10.3390/pharmaceutics14050907

Tada, M., Doi, H., Koyano, S., Kubota, S., Fukai, R., Hashiguchi, S., et al. (2018). Matrin 3 is a component of neuronal cytoplasmic inclusions of motor neurons in sporadic amyotrophic lateral sclerosis. *Am J Pathol* 188 (2), 507–514. doi:10.1016/j.ajpath.2017.10.007

Tak, Y. J., Park, J. H., Rhim, H., and Kang, S. (2020). ALS-related mutant SOD1 aggregates interfere with mitophagy by sequestering the autophagy receptor Optineurin. *Int J Mol Sci* 21 (20), 7525. doi:10.3390/ijms21207525

Takeuchi, T., and Nagai, Y. (2017). Protein misfolding and aggregation as a therapeutic target for polyglutamine diseases. *Brain Sci* 7 (10), 128. doi:10.3390/brainsci7100128

Tandan, R., and Bradley, W. G. (1985). Amyotrophic lateral sclerosis: Part 1. Clinical features, pathology, and ethical issues in management. *Ann Neurol* 18 (3), 271–280. doi:10.1002/ana.410180302

Tang, Y., Liu, M. L., Zang, T., and Zhang, C. L. (2017). Direct reprogramming rather than iPSC-based reprogramming maintains aging hallmarks in human motor neurons. *Front Mol Neurosci* 10, 359. doi:10.3389/fnmol.2017.00359

Taylor, D. M., Gibbs, B. F., Kabashi, E., Minotti, S., Durham, H. D., and Agar, J. N. (2007). Tryptophan 32 potentiates aggregation and cytotoxicity of a copper/zinc superoxide dismutase mutant associated with familial amyotrophic lateral sclerosis. *J Biol Chem* 282 (22), 16329–16335. doi:10.1074/jbc.M610119200

Teplow, D. B. (1998). Structural and kinetic features of amyloid beta-protein fibrillogenesis. *Amyloid* 5 (2), 121–142. doi:10.3109/13506129808995290

Thams, S., Lowry, E. R., Larraufie, M. H., Spiller, K. J., Li, H., Williams, D. J., et al. (2019). A stem cell-based screening platform identifies compounds that desensitize motor neurons to endoplasmic reticulum stress. *Molecular therapy the journal of the American Society of Gene Therapy* 27 (1), 87–101. doi:10.1016/j.ymthe.2018.10.010

Tiwari, A., Xu, Z., and Hayward, L. J. (2005). Aberrantly increased hydrophobicity shared by mutants of Cu,Zn-superoxide dismutase in familial amyotrophic lateral sclerosis. *J Biol Chem* 280 (33), 29771–29779. doi:10.1074/jbc.M504039200

Toichi, K., Yamanaka, K., and Furukawa, Y. (2013). Disulfide scrambling describes the oligomer formation of superoxide dismutase (SOD1) proteins in the familial form of amyotrophic lateral sclerosis. *J Biol Chem* 288, 4970–4980. doi:10.1074/jbc.M112.414235

Tollervey, J. R., Curk, T., Rogelj, B., Briese, M., Cereda, M., Kayikci, M., et al. (2011). Characterizing the RNA targets and position-dependent splicing regulation by TDP-43. *Nat Neurosci* 14 (4), 452–458. doi:10.1038/nn.2778

Tran, M. L., Genisson, Y., Ballereau, S., and Dehoux, C. (2020). Second-generation pharmacological chaperones: beyond inhibitors. *Molecules* 25 (14), 3145. doi:10.3390/molecules25143145

Tripathi, V. B., Baskaran, P., Shaw, C. E., and Guthrie, S. (2014). Tar DNA-binding protein-43 (TDP-43) regulates axon growth *in vitro* and *in vivo*. *Neurobiol Dis* 65, 25–34. doi:10.1016/j.nbd.2014.01.004

Trist, B. G., Genoud, S., Roudeau, S., Rookyard, A., Abdeen, A., Cottam, V., et al. (2022). Altered SOD1 maturation and post-translational modification in amyotrophic lateral sclerosis spinal cord. *Brain* 145 (9), 3108–3130. doi:10.1093/brain/awac165

Truex, N. L., and Nowick, J. S. (2016). Coassembly of peptides derived from β-sheet regions of β-amyloid. *J Am Chem Soc* 138 (42), 13891–13900. doi:10.1021/jacs.6b06001

Tseng, Y. L., Lu, P. C., Lee, C. C., He, R. Y., Huang, Y. A., Tseng, Y. C., et al. (2023). Degradation of neurodegenerative disease-associated TDP-43 aggregates and oligomers via a proteolysis-targeting chimera. *Journal of biomedical science* 30 (1), 27. doi:10.1186/s12929-023-00921-7

Tsuzuki, N., Hama, T., Kawada, M., Hasui, A., Konishi, R., Shiwa, S., et al. (1994). Adamantane as a brain-directed drug carrier for poorly absorbed drug. 2. AZT derivatives conjugated with the 1-adamantane moiety. *Journal of pharmaceutical sciences* 83 (4), 481–484. doi:10.1002/jps.2600830407

Turner, M. R., Cagnin, A., Turkheimer, F. E., Miller, C. C., Shaw, C. E., Brooks, D. J., et al. (2004). Evidence of widespread cerebral microglial activation in amyotrophic lateral sclerosis: an [11C](R)-PK11195 positron emission tomography study. *Neurobiol Dis* 15 (3), 601–609. doi:10.1016/j.nbd.2003.12.012

Vaccaro, A., Patten, S. A., Aggad, D., Julien, C., Maios, C., Kabashi, E., et al. (2013). Pharmacological reduction of ER stress protects against TDP-43 neuronal toxicity *in vivo*. *Neurobiol Dis* 55, 64–75. doi:10.1016/j.nbd.2013.03.015

Vaccaro, A., Patten, S. A., Ciura, S., Maios, C., Therrien, M., Drapeau, P., et al. (2012). Methylene blue protects against TDP-43 and FUS neuronal toxicity in *C. elegans* and *D. rerio*. *PLoS One* 7 (7), e42117. doi:10.1371/journal.pone.0042117

Valentine, J. S., Doucette, P. A., and Potter, S. Z. (2005). Copper-zinc superoxide dismutase and amyotrophic lateral sclerosis. *Annu. Rev Biochem.* 74, 563–593. doi:10.1146/annurev.biochem.72.121801.161647

Valle, C., and Carri, M. T. (2017). Cysteine modifications in the pathogenesis of ALS. *Front Mol Neurosci* 10, 5. doi:10.3389/fnmol.2017.00005

Vance, C., Rogelj, B., Hortobagyi, T., De Vos, K. J., Nishimura, A. L., Sreedharan, J., et al. (2009). Mutations in FUS, an RNA processing protein, cause familial amyotrophic lateral sclerosis type 6. *Science* 323 (5918), 1208–1211. doi:10.1126/science.1165942

van der Spek, R. A. A., van Rheenen, W., Pulit, S. L., Kenna, K. P., van den Berg, L. H., Veldink, J. H., et al. (2019). The project MinE databrowser: bringing large-scale whole-genome sequencing in ALS to researchers and the public. *Amyotroph Lateral Scler Frontotemporal Degener* 20 (5-6), 432–440. doi:10.1080/21678421.2019.1606244

van Es, M. A., Hardiman, O., Chio, A., Al-Chalabi, A., Pasterkamp, R. J., Veldink, J. H., et al. (2017). Amyotrophic lateral sclerosis. *The Lancet* 390, 2084–2098. doi:10.1016/S0140-6736(17)31287-4

van Rheenen, W., Shatunov, A., Dekker, A. M., McLaughlin, R. L., Diekstra, F. P., Pulit, S. L., et al. (2016). Genome-wide association analyses identify new risk variants and the genetic architecture of amyotrophic lateral sclerosis. *Nat Genet* 48 (9), 1043–1048. doi:10.1038/ng.3622

van Rheenen, W., van der Spek, R. A. A., Bakker, M. K., van Vugt, J., Hop, P. J., Zwamborn, R. A. J., et al. (2021). Common and rare variant association analyses in amyotrophic lateral sclerosis identify 15 risk loci with distinct genetic architectures and neuron-specific biology. *Nat Genet* 53 (12), 1636–1648. doi:10.1038/s41588-021-00973-1

Verdile, V., De Paola, E., and Paronetto, M. P. (2019). Aberrant phase transitions: side effects and novel therapeutic strategies in human disease. *Front Genet* 10, 173. doi:10.3389/fgene.2019.00173

Vincent, A. M., Backus, C., Taubman, A. A., and Feldman, E. L. (2005). Identification of candidate drugs for the treatment of ALS. *Amyotroph Lateral Scler Other Motor Neuron Disord* 6 (1), 29–36. doi:10.1080/14660820510026171

Vopel, T., Bravo-Rodriguez, K., Mittal, S., Vachharajani, S., Gnutt, D., Sharma, A., et al. (2017). Inhibition of huntingtin exon-1 aggregation by the molecular tweezer CLR01. *J Am Chem Soc.* 139 (16), 5640–5643. doi:10.1021/jacs.6b11039

Vu, L., An, J., Kovalik, T., Gendron, T., Petrucelli, L., and Bowser, R. (2020). Cross-sectional and longitudinal measures of chitinase proteins in amyotrophic lateral sclerosis and expression of CHI3L1 in activated astrocytes. *J Neurol Neurosurg Psychiatry* 91 (4), 350–358. doi:10.1136/jnnp-2019-321916

Wachter, N., Storch, A., and Hermann, A. (2015). Human TDP-43 and FUS selectively affect motor neuron maturation and survival in a murine cell model of ALS by non-cell-autonomous mechanisms. *Amyotroph Lateral Scler Frontotemporal Degener* 16 (7-8), 431–441. doi:10.3109/21678421.2015.1055275

Walker, A. K., Spiller, K. J., Ge, G., Zheng, A., Xu, Y., Zhou, M., et al. (2015). Functional recovery in new mouse models of ALS/FTLD after clearance of pathological cytoplasmic TDP-43. *Acta Neuropathol* 130 (5), 643–660. doi:10.1007/s00401-015-1460-x

Wang, A., and Bolen, D. W. (1997). A naturally occurring protective system in urea-rich cells: mechanism of osmolyte protection of proteins against urea denaturation. *Biochemistry* 36 (30), 9101–9108. doi:10.1021/bi970247h

Wang, A., Conicella, A. E., Schmidt, H. B., Martin, E. W., Rhoads, S. N., Reeb, A. N., et al. (2018). A single N-terminal phosphomimic disrupts TDP-43 polymerization, phase separation, and RNA splicing. *EMBO J.* 37 (5). doi:10.15252/embj.201797452

Wang, L., Deng, H. X., Grisotti, G., Zhai, H., Siddique, T., and Roos, R. P. (2009). Wild-type SOD1 overexpression accelerates disease onset of a G85R SOD1 mouse. *Human molecular genetics* 18 (9), 1642–1651. doi:10.1093/hmg/ddp085

Wang, L., Wang, N., Zhang, W., Cheng, X., Yan, Z., Shao, G., et al. (2022b). Therapeutic peptides: current applications and future directions. *Signal transduction and targeted therapy* 7 (1), 48. doi:10.1038/s41392-022-00904-4

Wang, Q., Johnson, J. L., Agar, N. Y., and Agar, J. N. (2008). Protein aggregation and protein instability govern familial amyotrophic lateral sclerosis patient survival. *PLoS Biol.* 6 (7), e170. doi:10.1371/journal.pbio.0060170

Wang, L. Q., Ma, Y., Yuan, H. Y., Zhao, K., Zhang, M. Y., Wang, Q., et al. (2022a). Cryo-EM structure of an amyloid fibril formed by full-length human SOD1 reveals its conformational conversion. *Nature communications* 13 (1), 3491. doi:10.1038/s41467-022-31240-4

Wang, S. J., Wang, K. Y., and Wang, W. C. (2004). Mechanisms underlying the riluzole inhibition of glutamate release from rat cerebral cortex nerve terminals (synaptosomes). *Neuroscience* 125 (1), 191–201. doi:10.1016/j.neuroscience.2004.01.019

Webster, C. P., Smith, E. F., Shaw, P. J., and De Vos, K. J. (2017). Protein homeostasis in amyotrophic lateral sclerosis: therapeutic opportunities? *Front Mol Neurosci* 10, 123. doi:10.3389/fnmol.2017.00123

Wentink, A., and Rosenzweig, R. (2023). Protein disaggregation machineries in the human cytosol. *Current opinion in structural biology* 83, 102735. doi:10.1016/j.sbi.2023.102735

Wijesekera, L. C., and Leigh, P. N. (2009). Amyotrophic lateral sclerosis. *Orphanet Journal of Rare Diseases* 4, 3–22. doi:10.1186/1750-1172-4-3

Wilcox, K. C., Zhou, L., Jordon, J. K., Huang, Y., Yu, Y., Redler, R. L., et al. (2009). Modifications of superoxide dismutase (SOD1) in human erythrocytes: a possible role in amyotrophic lateral sclerosis. *J Biol Chem* 284, 13940–13947. doi:10.1074/jbc.M809687200

Williams, K. L., Warraich, S. T., Yang, S., Solski, J. A., Fernando, R., Rouleau, G. A., et al. (2012). UBQLN2/ubiquilin 2 mutation and pathology in familial amyotrophic lateral sclerosis. *Neurobiol Aging* 33 (10), 2527 e3–e10. doi:10.1016/j.neurobiolaging.2012.05.008

Winton, M. J., Igaz, L. M., Wong, M. M., Kwong, L. K., Trojanowski, J. Q., and Lee, V. M. (2008). Disturbance of nuclear and cytoplasmic TAR DNA-binding protein (TDP-43) induces disease-like redistribution, sequestration, and aggregate formation. *J Biol Chem* 283 (19), 13302–13309. doi:10.1074/jbc.M800342200

Wood, M., Quinet, A., Lin, Y. L., Davis, A. A., Pasero, P., Ayala, Y. M., et al. (2020). TDP-43 dysfunction results in R-loop accumulation and DNA replication defects. *J Cell Sci* 133 (20), jcs244129. doi:10.1242/jcs.244129

Wood, S. J., Wypych, J., Steavenson, S., Louis, J. C., Citron, M., and Biere, A. L. (1999). alpha-synuclein fibrillogenesis is nucleation-dependent. Implications for the pathogenesis of Parkinson's disease. *J Biol Chem* 274 (28), 19509–19512. doi:10.1074/jbc.274.28.19509

Wood-Allum, C. A., Barber, S. C., Kirby, J., Heath, P., Holden, H., Mead, R., et al. (2006). Impairment of mitochondrial anti-oxidant defence in SOD1-related motor neuron injury and amelioration by ebselen. *Brain* 129 (Pt 7), 1693–1709. doi:10.1093/brain/awl118

Wright, G. S. A. (2020). Molecular and pharmacological chaperones for SOD1. *Biochem. Soc Trans.* 48, 1795–1806. doi:10.1042/BST20200318

Wright, G. S. A., Antonyuk, S. V., and Hasnain, S. S. (2016). A faulty interaction between SOD1 and hCCS in neurodegenerative disease. *Sci Rep* 6, 27691–27699. doi:10.1038/srep27691

Wright, G. S. A., Antonyuk, S. V., Kershaw, N. M., Strange, R. W., and Samar Hasnain, S. (2013). Ligand binding and aggregation of pathogenic SOD1. *Nat Commun* 4, 1758–58. doi:10.1038/ncomms2750

Wright, G. S. A., Watanabe, T. F., Amporndanai, K., Plotkin, S. S., Cashman, N. R., Antonyuk, S. V., et al. (2020). Purification and structural characterization of aggregation-prone human TDP-43 involved in neurodegenerative diseases. *iScience* 23 (6), 101159. doi:10.1016/j.isci.2020.101159

Wright, P. D., Wightman, N., Huang, M., Weiss, A., Sapp, P. C., Cuny, G. D., et al. (2012). A high-throughput screen to identify inhibitors of SOD1 transcription. *Frontiers in bioscience* 4 (8), 2701–2708. doi:10.2741/e584

Writing Group and Edaravone (MCI-186) ALS 19 Study Group (2017). Safety and efficacy of edaravone in well defined patients with amyotrophic lateral sclerosis: a randomised, double-blind, placebo-controlled trial. *The Lancet Neurology* 16 (7), 505–512. doi:10.1016/S1474-4422(17)30115-1

Wroe, R., Wai-Ling, B. A., Andersen, P. M., Powell, J. F., and Al-Chalabi, A. (2008). ALSOD: the amyotrophic lateral sclerosis online database. *Amyotroph Lateral Scler* 9 (4), 249–250. doi:10.1080/17482960802146106

Wu, L. S., Cheng, W. C., Chen, C. Y., Wu, M. C., Wang, Y. C., Tseng, Y. H., et al. (2019). Transcriptomopathies of pre- and post-symptomatic frontotemporal dementia-like mice with TDP-43 depletion in forebrain neurons. *Acta Neuropathol Commun* 7 (1), 50. doi:10.1186/s40478-019-0674-x

Xia, G., Benmohamed, R., Kim, J., Arvanites, A. C., Morimoto, R. I., Ferrante, R. J., et al. (2011). Pyrimidine-2, 4, 6-trione derivatives and their inhibition of mutant SOD1-dependent protein aggregation. Toward a treatment for amyotrophic lateral sclerosis. *J Med Chem* 54, 2409–2421. doi:10.1021/jm101549k

Xia, G., Benmohamed, R., Morimoto, R. I., Kirsch, D. R., and Silverman, R. B. (2014). Deuteration and fluorination of 1,3-bis(2-phenylethyl)pyrimidine-2,4,6(1H,3H,5H)-trione to improve its pharmacokinetic properties. *Bioorganic & Medicinal Chemistry Letters* 24, 5098–5101. doi:10.1016/j.bmcl.2014.08.066

Xu, W. C., Liang, J. Z., Li, C., He, Z. X., Yuan, H. Y., Huang, B. Y., et al. (2018). Pathological hydrogen peroxide triggers the fibrillization of wild-type SOD1 via sulfenic acid modification of Cys-111. *Cell death & disease* 9 (2), 67. doi:10.1038/s41419-017-0106-4

Xu, Z., Chen, S., Li, X., Luo, G., Li, L., and Le, W. (2006). Neuroprotective effects of (-)-epigallocatechin-3-gallate in a transgenic mouse model of amyotrophic lateral sclerosis. *Neurochem. Res* 31 (10), 1263–1269. doi:10.1007/s11064-006-9166-z

Yadav, K., Yadav, A., Vashistha, P., Pandey, V. P., and Dwivedi, U. N. (2019). Protein misfolding diseases and therapeutic approaches. *Curr Protein Pept Sci* 20 (12), 1226–1245. doi:10.2174/1389203720666190610092840

Yamaguchi, T., Sano, K., Takakura, K., Saito, I., Shinohara, Y., Asano, T., et al. (1998). Ebselen in acute ischemic stroke: a placebo-controlled, double-blind clinical trial. Ebselen Study Group. *Stroke* 29 (1), 12–17. doi:10.1161/01.str.29.1.12

Yamashita, M., Nonaka, T., Arai, T., Kametani, F., Buchman, V. L., Ninkina, N., et al. (2009). Methylene blue and dimebon inhibit aggregation of TDP-43 in cellular models. *FEBS Lett* 583 (14), 2419–2424. doi:10.1016/j.febslet.2009.06.042

Yang, C., Wang, H., Qiao, T., Yang, B., Aliaga, L., Qiu, L., et al. (2014). Partial loss of TDP-43 function causes phenotypes of amyotrophic lateral sclerosis. *Proceedings of the National Academy of Sciences of the U. S. A.* 111 (12), E1121–E1129. doi:10.1073/pnas.1322641111

Yang, L., Jasiqi, Y., Zettor, A., Vadas, O., Chiaravalli, J., Agou, F., et al. (2023). Effective inhibition of TDP-43 aggregation by native state stabilization. *Angewandte Chemie* 63, e202314587. doi:10.1002/anie.202314587

Yang, Y. M., Gupta, S. K., Kim, K. J., Powers, B. E., Cerqueira, A., Wainger, B. J., et al. (2013). A small molecule screen in stem-cell-derived motor neurons identifies a kinase inhibitor as a candidate therapeutic for ALS. *Cell Stem Cell* 12 (6), 713–726. doi:10.1016/j.stem.2013.04.003

Yerbury, J. J., and Cashman, N. R. (2020). Selenium-based compounds: emerging players in the ever-unfolding story of SOD1 in amyotrophic lateral sclerosis. *EBioMedicine* 59, 102997. doi:10.1016/j.ebiom.2020.102997

Young, L. M., Ashcroft, A. E., and Radford, S. E. (2017). Small molecule probes of protein aggregation. *Current opinion in chemical biology* 39, 90–99. doi:10.1016/j.cbpa.2017.06.008

Yu, C. H., Davidson, S., Harapas, C. R., Hilton, J. B., Mlodzianoski, M. J., Laohamonthonkul, P., et al. (2020). TDP-43 triggers mitochondrial DNA release via mPTP to activate cGAS/STING in ALS. *Cell* 183 (3), 636–649. doi:10.1016/j.cell.2020.09.020

Zacco, E., Martin, S. R., Thorogate, R., and Pastore, A. (2018). The RNA-recognition motifs of TAR DNA-binding protein 43 may play a role in the aberrant self-assembly of the protein. *Front Mol Neurosci* 11, 372. doi:10.3389/fnmol.2018.00372

Zetterstrom, P., Stewart, H. G., Bergemalm, D., Jonsson, P. A., Graffmo, K. S., Andersen, P. M., et al. (2007). Soluble misfolded subfractions of mutant superoxide dismutase-1s are enriched in spinal cords throughout life in murine ALS models. *Proceedings of the National Academy of Sciences of the U. S. A.* 104 (35), 14157–14162. doi:10.1073/pnas.0700477104

Zhang, W., Benmohamed, R., Arvanites, A. C., Morimoto, R. I., Ferrante, R. J., Kirsch, D. R., et al. (2012a). Cyclohexane 1, 3-diones and their inhibition of mutant SOD1-dependent protein aggregation and toxicity in PC12 cells. *Bioorg Med Chem* 20, 1029–1045. doi:10.1016/j.bmc.2011.11.039

Zhang, Y., Benmohamed, R., Zhang, W., Kim, J., Edgerly, C. K., Zhu, Y., et al. (2012b). Chiral cyclohexane 1,3-diones as inhibitors of mutant SOD1- dependent protein

aggregation for the treatment of ALS. *ACS Med Chem Lett* 3, 584–587. doi:10.1021/ml3000963

Zhao, B., Marciniuk, K., Gibbs, E., Yousefi, M., Napper, S., and Cashman, N. R. (2019). Therapeutic vaccines for amyotrophic lateral sclerosis directed against disease specific epitopes of superoxide dismutase 1. *Vaccine* 37 (35), 4920–4927. doi:10.1016/j.vaccine.2019.07.044

Zhao, B., Zhuang, X., Pi, Z., Liu, S., Liu, Z., and Song, F. (2018). Determining the effect of catechins on SOD1 conformation and aggregation by ion mobility mass spectrometry combined with optical spectroscopy. *J Am Soc Mass Spectrom* 29, 734–741. doi:10.1007/s13361-017-1864-z

Zheng, X., Liu, D., Klarner, F. G., Schrader, T., Bitan, G., and Bowers, M. T. (2015). Amyloid β-protein assembly: the effect of molecular tweezers CLR01 and CLR03. *The journal of physical chemistry B* 119 (14), 4831–4841. doi:10.1021/acs.jpcb.5b00692

Zhu, C., Beck, M. V., Griffith, J. D., Deshmukh, M., and Dokholyan, N. V. (2018). Large SOD1 aggregates, unlike trimeric SOD1, do not impact cell viability in a model of amyotrophic lateral sclerosis. *Proceedings of the National Academy of Sciences of the U. S. A.* 115 (18), 4661–4665. doi:10.1073/pnas.1800187115

Zhu, L., Li, S., Li, X. J., and Yin, P. (2023). Pathological insights from amyotrophic lateral sclerosis animal models: comparisons, limitations, and challenges. *Translational neurodegeneration* 12 (1), 46. doi:10.1186/s40035-023-00377-7

Zhu, L., Xu, M., Yang, M., Yang, Y., Li, Y., Deng, J., et al. (2014). An ALS-mutant TDP-43 neurotoxic peptide adopts an anti-parallel β-structure and induces TDP-43 redistribution. *Human molecular genetics* 23 (25), 6863–6877. doi:10.1093/hmg/ddu409

Zuo, X., Zhou, J., Li, Y., Wu, K., Chen, Z., Luo, Z., et al. (2021). TDP-43 aggregation induced by oxidative stress causes global mitochondrial imbalance in ALS. *Nature structural & molecular biology* 28 (2), 132–142. doi:10.1038/s41594-020-00537-7

Zurcher, N. R., Loggia, M. L., Lawson, R., Chonde, D. B., Izquierdo-Garcia, D., Yasek, J. E., et al. (2015). Increased *in vivo* glial activation in patients with amyotrophic lateral sclerosis: assessed with [(11)C]-PBR28. *NeuroImage Clinical* 7, 409–414. doi:10.1016/j.nicl.2015.01.009

frontiers | Frontiers in Cell and Developmental Biology

TYPE Original Research
PUBLISHED 10 July 2024
DOI 10.3389/fcell.2024.1423208

OPEN ACCESS

EDITED BY
Anoop Arunagiri,
University of Michigan, United States

REVIEWED BY
Surabhi Mehra,
University of Toronto, Canada
Verena Kohler,
Umeå University, Sweden

*CORRESPONDENCE
Maria E. Solesio,
m.solesio@rutgers.edu

†PRESENT ADDRESSES
Mariona Guitart-Mampel,
Centre de Recerca Biomèdica CELLEX, Institut d'Investigacions Biomèdiques August Pi i Sunyer (IDIBAPS), Faculty of Medicine and Health Sciences, University of Barcelona, Spain; Internal Medicine Department, Hospital Clinic of Barcelona, Barcelona, Spain; CIBERER—Spanish Biomedical Research Centre in Rare Diseases - ISCIII, Spain

‡These authors have contributed equally to this work

RECEIVED 25 April 2024
ACCEPTED 07 June 2024
PUBLISHED 10 July 2024

CITATION
Da Costa RT, Urquiza P, Perez MM, Du Y, Khong ML, Zheng H, Guitart-Mampel M, Elustondo PA, Scoma ER, Hambardikar V, Ueberheide B, Tanner JA, Cohen A, Pavlov EV, Haynes CM and Solesio ME (2024), Mitochondrial inorganic polyphosphate is required to maintain proteostasis within the organelle.
Front. Cell Dev. Biol. 12:1423208.
doi: 10.3389/fcell.2024.1423208

Mitochondrial inorganic polyphosphate is required to maintain proteostasis within the organelle

Renata T. Da Costa[1], Pedro Urquiza[1‡], Matheus M. Perez[1‡], YunGuang Du[2], Mei Li Khong[3,4], Haiyan Zheng[5], Mariona Guitart-Mampel[1†], Pia A. Elustondo[6], Ernest R. Scoma[1], Vedangi Hambardikar[1], Beatrix Ueberheide[7], Julian A. Tanner[4,8,9], Alejandro Cohen[6], Evgeny V. Pavlov[10], Cole M. Haynes[2] and Maria E. Solesio[1*]

[1]Department of Biology, College of Arts and Sciences, Rutgers University, Camden, NJ, United States, [2]Department of Molecular, Cell, and Cancer Biology, University of Massachusetts Chan Medical School, Amherst, MA, United States, [3]School of Clinical Medicine, LKS Faculty of Medicine, The University of Hong Kong, Pokfulam, Hong Kong SAR, China, [4]School of Biomedical Sciences, LKS Faculty of Medicine, The University of Hong Kong, Pokfulam, Hong Kong SAR, China, [5]Center for Advanced Biotechnology and Medicine, Rutgers University, New Brunswick, NJ, United States, [6]Biological Mass Spectrometry Core Facility, Faculty of Medicine, Dalhousie University, Halifax, NS, Canada, [7]Proteomics Laboratory, Division of Advanced Research Technologies, New York University-Grossman School of Medicine, New York City, NY, United States, [8]Materials Innovation Institute for Life Sciences and Energy (MILES), HKU-SIRI, Shenzhen, China, [9]Advanced Biomedical Instrumentation Centre, Hong Kong Science Park, Hong Kong SAR, China, [10]Department of Molecular Pathobiology, College of Dentistry, New York University, New York City, NY, United States

The existing literature points towards the presence of robust mitochondrial mechanisms aimed at mitigating protein dyshomeostasis within the organelle. However, the precise molecular composition of these mechanisms remains unclear. Our data show that inorganic polyphosphate (polyP), a polymer well-conserved throughout evolution, is a component of these mechanisms. In mammals, mitochondria exhibit a significant abundance of polyP, and both our research and that of others have already highlighted its potent regulatory effect on bioenergetics. Given the intimate connection between energy metabolism and protein homeostasis, the involvement of polyP in proteostasis has also been demonstrated in several organisms. For example, polyP is a bacterial primordial chaperone, and its role in amyloidogenesis has already been established. Here, using mammalian models, our study reveals that the depletion of mitochondrial polyP leads to increased protein aggregation within the organelle, following stress exposure. Furthermore, mitochondrial polyP is able to bind to proteins, and these proteins differ under control and stress conditions. The depletion of mitochondrial polyP significantly affects the proteome under both control and stress conditions, while also exerting regulatory control over gene expression. Our findings suggest that mitochondrial polyP is a previously unrecognized, and potent component of mitochondrial proteostasis.

KEYWORDS

mitochondria, mitochondrial inorganic polyphosphate, polyP, protein homeostasis, proteostasis

1 Introduction

Increased mitochondrial protein misfolding and aggregation is a well-known trigger of mitochondrial dysfunction, which ultimately leads to increased apoptotic cell death in many human pathologies (Nakamura et al., 2012). Despite the situation in other organelles, such as the endoplasmic reticulum (ER) (Araki and Nagata, 2012), the mechanism that governs mitochondrial mammalian proteostasis still remains largely unknown (Haynes and Ron, 2010; Pellegrino et al., 2013; Rainbolt et al., 2013; Schulz and Haynes, 2015). One of the main intracellular contributors to protein dyshomeostasis is the increased generation of reactive oxygen species (ROS). ROS are mostly generated in mitochondria during oxidative phosphorylation (OXPHOS); hence mitochondrial proteins are especially prone to be deleteriously affected by ROS. Moreover, it is known that misfolded proteins are imported from the cytosol into mitochondria, probably for degradation (Ruan et al., 2017). All this evidence suggests the presence of a potent mechanism that regulates protein homeostasis within the organelle. However, this mechanism is poorly understood.

Inorganic polyphosphate (polyP) is a well-conserved throughout evolution and ubiquitous polymer (Morrissey et al., 2012; Osorio et al., 2022). It is composed of multiple subunits of orthophosphates linked together by phosphoanhydride bonds, similar to those present in ATP (Kornberg et al., 1999; Muller et al., 2017; Desfougeres et al., 2020). While polyP shows a ubiquitous distribution among cells and organisms, a high presence of this polymer in mammalian mitochondria has already been demonstrated (Abramov et al., 2007; Solesio et al., 2016a). In fact, the regulatory effects of polyP on the maintenance of cellular bioenergetics are known in mammals and other organisms (Solesio et al., 2016a; Solesio et al., 2020; Borden et al., 2021; McIntyre and Solesio, 2021; Solesio et al., 2021; Scoma et al., 2023). Maintaining proper protein homeostasis is a highly energy-dependent process. Therefore, the close relationship between the status of OXPHOS and that of mitochondrial proteostasis has already been demonstrated (Nargund et al., 2015). Accordingly, the regulatory role of polyP on protein homeostasis has been proposed in different organisms. For example, polyP is a primordial chaperone in bacteria, and this effect is independent of any transcriptional factors (Gray et al., 2014). Furthermore, the important role played by polyP in the regulation of amyloidogenesis is also known (Cremers et al., 2016; Yoo et al., 2018; Lempart and Jakob, 2019; Xie and Jakob, 2019). This effect is induced by the ability of the polymer to accelerate fibril formation of amyloidogenic proteins, and it protects against amyloid-induced cytotoxicity (Lempart et al., 2019). Aging is one of the main trigger of protein dyshomeostasis, including amyloidogenesis, in mammals (Squier, 2001). Interestingly, polyP levels decrease with aging in these organisms (Lorenz et al., 1997).

The main goal of our study was to address the regulatory role of mitochondrial polyP in proteostasis within the organelle. To conduct our experiments, we used Wild-type (Wt) and MitoPPX HEK293 cells. MitoPPX cells have been enzymatically depleted of mitochondrial polyP. We previously thoroughly characterized them (Guitart-Mampel et al., 2022; Hambardikar et al., 2022), demonstrating that MitoPPX HEK293 cells have decreased endogenous levels of mitochondrial polyP. Using this model, our data show the protective role of mitochondrial polyP against heat shock (HS)-induced protein aggregation within the organelle. Moreover, ourpull-down data supports previous findings regarding the ability of polyP to bind to proteins in mammals (Labberton et al., 2018), and it show that the specific proteins bound to polyP are different under control and stress conditions. Lastly, our data demonstrate the strong regulatory effects exerted by mitochondrial polyP on the expression levels of some genes, and the levels of some proteins, involved in the maintenance of protein homeostasis within the organelle, in response to ROS-induced stress.

Our data indicate a potent regulatory role for mitochondrial polyP in the maintenance of proper protein homeostasis within the organelle, especially under stress conditions, and independently of the nature of the stress stimuli. While mitochondrial protein dyshomeostasis has been broadly described in human pathology, the molecular mechanisms involved in this process remain to be fully elucidated. Therefore, our findings could contribute to the understanding of the etiopathology of many of these diseases. These conditions, for example, include all the main neurodegenerative disorders (Irvine et al., 2008; Patro et al., 2021).

2 Materials and methods

2.1 Reagents

Dulbecco's Modified Eagle medium (DMEM), penicillin/streptomycin, geneticin (G418), trypsin, heat-inactivated fetal bovine serum (FBS), and MitoTracker Green were purchased from Gibco-Invitrogen (Carlsbad, CA, United States). Dimethyl Sulfoxide (DMSO), toluidine blue (TBO), rotenone, Triton X-100, sodium chloride (NaCl), methanol, phosphate-buffered saline (PBS), β-mercaptoethanol, tris(hydroxymethyl)-1,3-propanediol hydrochloride (TRIS-HCl), glycerol, phenylmethylsulfonyl fluoride (PMSF), Tween-20, potassium chloride (KCl), sucrose, mannitol, ethylenediaminetetraacetic acid (EDTA), ethylene glycol-bis(2-aminoethylether)-N,N,N′,N′-tetraacetic acid (EGTA), acetic acid, lodoacetamide, 1,4-dithiothreitol (DTT), formaldehyde, deuterated formaldehyde, triethylammonium bicarbonate buffer (TEAB), sodium cyanoborohydride, urea, calcium chloride, trifluoroacetic acid, acetonitrile, formic acid, ammonium formate, ammonium hydroxide, ammonium bicarbonate, LiCl, Ziptips, and acetone were purchased from Sigma-Aldrich (St. Louis, MO, United States). 1-ethyl-3-(3-dimethylaminopropyl) carbodiimide (EDAC), Pierce BCA protein assay kit, Pierce ECL Western blotting substrate, NuPAGE 4%–12% Bis-Tris Gel, P700-immobilised beads, Poros beads, GelCode Blue Strain, and Pierce halt protease and phosphatase inhibitor cocktails were purchased from Thermo Fisher Scientific (Waltham, MA, United States). Alexa Fluor 647 cadaverine was purchased from Life Technologies (Carlsbad, CA, United States).

2.2 Cell culture

Human Embryonic Kidney (HEK293) cells were acquired from the American Type Culture Collection (ATCC, Manassas,

VA, United States). MitoPPX HEK293 cells were created as previously described (Solesio et al., 2016b; Solesio et al., 2021). Briefly, MitoPPX cells were generated by the stable transfection of HEK293 cells with a DNA construct containing the sequence for mammalian expression of the *Saccharomyces cerevisiae* exopolyphosphatase (PPX) enzyme, a mitochondrial-targeted sequence, and the sequence for expression GFP. Cells were grown in DMEM supplemented with 10% (v/v) FBS, 0.1 mg/mL streptomycin and 100 units/mL penicillin at 37°C and 5% CO_2 in a humidified cell culture incubator. In the case of the MitoPPX cells, the medium was also supplemented with 40 μg/mL G418. The cells were maintained in a medium without G418 for at least 7 days prior to conducting the experiments. We have already broadly characterized MitoPPX HEK293 cells. For example, we have previously demonstrated that the mitochondrial expression of PPX is a valid method to decrease polyP levels in the organelle (Hambardikar et al., 2023). Moreover, our previous studies show that 48 h post seeding, cell viability of MitoPPX cells is not significantly different from that of Wt cells, under control conditions (Hambardikar et al., 2022). However, we have reported significant differences in the mitochondrial ultrastructure of MitoPPX cells; as well as in their ability to maintain proper bioenergetics, including the regulation of calcium homeostasis (Solesio et al., 2016a; Solesio et al., 2020; Solesio et al., 2021; Guitart-Mampel et al., 2022; Hambardikar et al., 2022; Hambardikar et al., 2023).

2.3 Rotenone treatment

Cells were plated on Petri dishes until they were at a 70%–80% confluence and treated with 4 or 6 μM rotenone for 3 h in fresh medium. After that, cells were harvested and the specific experiments were conducted.

2.4 LDH cell viability assay

Cells were seeded in 96-wells plates. After 48 h, they were treated with 4 or 6 μM rotenone. Triplicate wells were prepared for each experimental condition. LDH assay was then conducted following the instructions provided by the manufacturer (Roche, Indianapolis, IN, United States). Absorbance was measured at 492 and 620 nm using a microplate reader (CLARIOstart spectrophotometer, BMG Labtech, Ortenberg, Germany). Data was standardized vs. Wt control (0% cytotoxicity).

2.5 Immunoblotting assays

Immunoblotting assays were conducted as previously reported (Solesio et al., 2013a; Baltanas et al., 2013; Solesio et al., 2013b; Liu et al., 2019; Castro et al., 2020). Briefly, cell pellets were lysed for 15 min at 4°C with rotation in the presence of 50–100 μL of 1x RIPA buffer supplemented with protease inhibitor cocktail (Sigma-Aldrich, St. Louis, MO, United States). After centrifugate the samples at 14,000 xg for 5 min, the supernatant was transferred to a fresh 1.5 mL tube. Protein concentration of the cell lysates was determined by a BCA assay. 1× Laemmli Sample Buffer (BioRad, Hercules, CA, United States), which was completed with 2-Mercaptoetanol was added, and samples were incubated for 5 min at 95°C. Proteins were separated on 12% pre-cast acrylamide gels (BioRad, Hercules, CA, United States). Gels were then transferred into Polyvinylidene difluoride (PVDF) membranes (BioRad, Hercules, CA, United States) and blocked for 1 h in a solution containing 5% fat free milk and 0.05% Tween 20 in 1× PBS. Membranes were then incubated with the primary antibodies overnight at 4°C, followed by PBS washes and incubation with horseradish-peroxidase (HRP)-conjugated secondary antibodies for 1 h at room temperature. Chemiluminescent detection of bands was performed using ECL reagent (ThermoFisher Scientific, Waltham, MA, United States). Quantification of the bands was performed using ImageJ (NIH, Bethesda, MD, United States).

Primary antibodies were purchased from the following vendors: anti-βactin (Abcam, cat. ab8226); anti-CHOP (Cell Signaling, cat. 2895); anti-Sirt3 (Cell Signaling, cat. 2627); anti-SOD2 (Millipore, cat. 06-984); anti-Hsp60 (Santa Cruz, cat. sc-13115); anti-Hsp10 (Sigma-Aldrich, cat SAB4501465); anti-FoxO3a (Cell Signaling, cat. 2497); anti-Acetyl-FoxO3a (Affinity, cat. AF3771); anti-TOM20 (Cell Signaling, cat. 42406); anti-Parkin (Santa Cruz Technology, cat. sc-32282); and anti-LC3B (Abcam, cat. Ab192890); All the antibodies were used at a 1:1,000 dilution. The HRP-conjugated secondary antibodies used were anti-mouse; DαMo-HRP (Bio-Rad, cat. 170616), anti-Rabbit; DαRb-HRP (Bio-Rad, cat. 170615). In this case, both antibodies were used at a 1:5,000 dilution.

2.6 Mitochondrial isolation

Mitochondrial isolation was conducted as previously described (Fossati et al., 2016; Solesio et al., 2018; Solesio et al., 2021). Freshly isolated mitochondria were used for all the experiments.

2.7 HS experiments

HS was performed on isolated mitochondria. Specifically, mitochondria used for these experiments were placed for 30 min at 45°C. These conditions have been broadly used to induce HS in mammalian cells and to conduct protein biology studies (Duncan and Hershey, 1984; Mizzen and Welch, 1988; Abe et al., 1999; Kim et al., 2011). The control samples were maintained at 25°C for the same length of time. To maintain the desired temperatures, the tubes containing mitochondria were placed on a Mixer HC thermoblock (USA Scientific, Ocala, FL, United States).

2.8 Soluble and insoluble protein fractions preparation

After mitochondrial isolation and the corresponding treatments, protein content was quantified using the BSA assay. All the samples were then diluted to the lowest concentration found in each set of experiments, to ensure that equal amounts of protein were used to conduct the separation of the soluble and insoluble protein fractions.

This separation procedure was carried out according to the previously described method (Wilkening et al., 2018). After the isolation of soluble and insoluble protein fraction, these fractions were loaded in gels and samples were analyzed via immunoblotting assay. Please, note that no loading controls were included since different amounts of proteins were loaded in each of the fractions (soluble and insoluble), due to the nature of the experiment. As mentioned above, the amount of protein used before starting the cellular fractioning was exactly the same. The obtained results are therefore qualitative, rather than quantitative.

2.9 Transcript expression analysis (RT-qPCR assay)

RNA was isolated from Wt and MitoPPX cells using the RNeasy Mini Kit (Qiagen, Hilden, Germany), following the protocol provided by the manufacturer. RNA concentrations were determined by spectrophotometry (NanoDrop One, GE Health Care, Buckinghamshire, United Kingdom). cDNA was synthetized using the QuantiTect Reverse Transcription Kit (Qiagen, Hilden, Germany), with an input of 0.5 µg of total RNA. The RT-qPCR amplifications were conducted using a QuantStudio™ 6 Flex Real-Time PCR System (Applied Biosystems, Foster City, CA, United States), and Power SYBR™ Green PCR Master Mix (Qiagen, Hilden, Germany). Specifically, we used the following thermal conditions: 10 min at 95°C (hot start); 45 cycles of 15 s at 95°C, and 25 s at 60°C. The primers were designed with Primer3web 4.1.0 (available at https://primer3.ut.ee/), and their sequences are described below. GAPDH (glyceraldehyde 3-phosphate dehydrogenase) was used as the housekeeping gene. The fold change values for the differential gene expression were evaluated using the $2^{-\Delta\Delta Ct}$ formula (Livak and Schmittgen, 2001).

Primers used for the transcript expression analysis by RT-qPCR.

Gene	Forward and reverse sequences	Amplicon (bp)
GAPDH	TTGGCTACAGCAACAGGGTG	161
	GGGGAGATTCAGTGTGGTGG	
SOD2	TGGGGTTGGCTTGGTTTCAA	95
	GGAATAAGGCCTGTTGTTCCTTG	
SIRT3	CGGCTCTACACGCAGAACATC	225
	CAGCGGCTCCCCAAAGAACAC	
PRKN	GTGCCGTATTTGAAGCCTCA	123
	GACAGGGCTTGGTGGTTTTC	
TOMM20	CCCCAACTTCAAGAACAGGC	185
	GATGGTCTACGCCCTTCTCA	
DNM1L	AGAATATTCAAGACAGTGTGCCA	145
	TGTGCCATGTCCTCAGATTCT	
ATF5	CTGGGATGGCTCGTAGACTA	258
	CTTGAGGAGGGAGGCCATAG	
HSPD1	GGGTACTGGCTCCTCATCTC	140
	CACTGTTCTTCCCTTTGGCC	
HSPE1	CTTTGCGGCGCTACACTAG	118
	GCAGCACTCCTTTCAACCAA	
DDIT3	TTCCTTTTGTCTACTCCAAGCCTTC	274
	ATGAAAGGAAAGTGGCACAGCTA	

2.10 Liquid chromatography-tandem mass spectrometry (LC-MS/MS)

We conducted LC-MS/MS assays in two distinct sets of samples: 1) Soluble and insoluble mitochondrial fractions from Wt and MitoPPX cells, under control conditions and after HS, and 2) gel pull-down of proteins bound to polyP. In each case, the sample preparation and the LC-MS/MS assay were conducted using different methods. In the case of 1), after the statistical "analysis" predictions of the affected pathways and diseases were created using Ingenuity Pathway Analysis (IPA, Qiagen, Hilden, Germany).

2.10.1 Mitochondrial soluble and insoluble fractions

Cells were grown, scraped, and pelleted following the protocols described above. Mitochondria were isolated and HS was conducted. The protein content was quantified using the BCA assay, following the protocol described above. Subsequently, the soluble and insoluble fractions were separated as previously described, with equal amounts of protein used. The samples were then loaded onto SDS-PAGE gels and bands were excised as a single gel slice, following the previously published protocol (Sleat et al., 2008; Sleat et al., 2009). Subsequently, samples were treated as it follows:

2.10.1.1 In-gel digestion

Each gel band was subjected to reduction with 10 mM DTT for 30 min at 60°C, followed by alkylation with 20 mM iodoacetamide for 45 min at room temperature in the dark. The bands were then digestion with trypsin and incubated overnight at 37°C.

2.10.1.2 Peptide extraction

The peptides were extracted twice with a 5% formic acid and 60% acetonitrile. The resulting extract was then dried under vacuum.

2.10.1.3 LC-MS/MS

Samples were analyzed by nano LC-MS/MS using an Eclipse tribid mass spectrometer interfaced with an Ultimate 3000 RSLCnano chromatography system (Thermo Fisher Scientific, Waltham, MA, United States). The samples were loaded onto a fused silica trap column (Acclaim PepMap 100, 75 µm × 2 cm, Thermo Fisher Scientific, Waltham, MA, United States). After washing for 5 min at a flow rate of 5 µL/min with 0.1% trifluoroacetic acid, the trap column was brought in-line with an analytical column (Nanoease MZ peptide BEH C18, 130 A, 1.7 µm, 75 µm × 250 mm, Waters, Milford, MA, United States) for LC-MS/MS analysis. Peptides were chromatographed at 300 nL/min using a segmented linear gradient 4%–15% B in 30 min (A: 0.2% formic acid; B: 0.16% formic acid, 80% acetonitrile), 15%–25% B in 40 min, 25%–50% B in 44 min, and 50%–90% B in 11 min.

The scan sequence began with an MS1 spectrum (Orbitrap analysis, resolution 120,000, scan range from M/Z 375–1,500, automatic gain control (AGC) target 1E6, maximum injection time 100 m). The top S (3 s) duty cycle scheme was used for determining the number of MSMS performed for each cycle. Parent ions of charge 2–7 were selected for MSMS and dynamic exclusion of 60 s was used to avoid repeat sampling. Parent masses were isolated in the quadrupole with an isolation window of 1.2 m/z, automatic gain control (AGC) target 1E5, and fragmented with higher-energy collisional dissociation with a normalized collision energy of 30%. The fragments were scanned in Orbitrap with resolution of 15,000. The MSMS scan ranges were determined by the charge state of the parent ion but lower limit was set at 110 atomic mass units.

2.10.1.4 Database search

Peak lists (mgf files) were generated using Thermo Proteome Discoverer v. 2.1 (Thermo Fisher Scientific, Waltham, MA, United States) and searched against the Uniprot human database and a database composed of common contaminants (cRAP), using a local implementation of TANDEM (Craig and Beavis, 2004). The search parameters were as it follows: protein and peptide log10 expectation scores < −4 and −2, respectively; fragment mass error: 20 ppm, parent mass error: ± 7 ppm; static modification: Cys carboxymethylation; dynamic or variable modifications during the initial search: Gly-Gly tag on internal lysine for ubiquitination and monoxidation on methionine; dynamic or variable modifications during refinement: round 1, Met and Trp mono oxidation, Asn and Gln deamidation; round 2, Met and Trp dioxidation. The peptide false positive rates were 0.4%.

2.10.2 Pull-down of proteins bound to polyP

Mitochondria were isolated from mice liver following the protocol published in (PMID: 22509855). Mice liver were obtained from animals used for other experiments in the department. Subsequently, functional mitochondria were heat shocked also as stated above, or treated with 200 μM H_2O_2 for 30 min. Following this, incubation with P700-immobilized beads, pull-down, elution using LiCl, and SDS-PAGE were conducted according to the previously published protocol (Khong et al., 2020). P-700 beads were used for the pull-down procedure, as preliminary studies using P-100 beads resulted in a minimal number of proteins being pulled-down.

2.10.2.1 Gel digestion

Samples were reduced with 2 μL of 0.2 M DTT at 57°C for 1 h; alkylated with 2 μL of 0.5 M iodoacetic acid at room temperature in the dark for 45 min; and loaded onto a NuPAGE 4%–12% Bis-Tris Gel 1.0 mM. The gels were run for approximately 12 min at 200 V. Subsequently, the gel was then stained using GelCode Blue Stain Reagent and Coomassie-stained bands were excised from the gel for analysis.

The excised bands were first distained in a 1:1 v/v solution of methanol and 100 mM ammonium bicarbonate, and then partially dehydrated with acetonitrile and further dried using a SpeedVac for 20 min. Next, 200 ng of trypsin was added to each sample. After the enzyme was absorbed, 70–150 μL of 10 mM ammonium bicarbonate was added to cover the gel fragments. Finally, the gel fragments were digested overnight with agitation at room temperature.

2.10.2.2 Protein extraction

The following day, R2 20 μM Poros beads in a solution of 5% formic acid and 0.2% trifluoroacetic acid were added to each sample in a 1:1 v/v proportion to the amount of ammonium bicarbonate added the previous night. The samples were soaked for 3 h at 4°C. Afterwards, the beads were loaded onto equilibrated C18 Ziptips and a microcentrifuge was used to spin them for 30 s at 6,000 xg. Gel fragments were rinsed three times with 0.1% trifluoracetic acid, and each rinse was added to its corresponding Ziptip, followed by microcentrifugation. The extracted Poros beads were then washed with 0.5% acetic acid. To elute the peptides, 40% acetonitrile in 0.5% acetic acid was used, followed by 80% acetonitrile in 0.5% acetic acid. The organic solvents were subsequently removed using a Speed Vac. Finally, the samples were then reconstituted in 0.5% acetic acid.

2.10.2.3 Mass spectrometry

The samples were individually analyzed as previously described (Drummond et al., 2020). The spectra were searched against UniProt database using Byonic Search Engine within Proteome Discoverer.

2.11 Statistical analysis

All the experiments, including the samples for the proteomics assays, were performed at least in biological triplicates. The only exception to this is the experiment for the pull-down for proteins bound to polyP, which were conducted once, following the standard procedures in the field (Khong et al., 2020; Okpara et al., 2022). In the case of the IPA analysis, only pathways with –log (*p*-value) higher than 1.3 (that is, *p*-value ≤0.05) were included. Data is expressed as the mean ± SEM, unless otherwise stated. The relative units are expressed with respect to the control samples. Statistical analyses were carried out with GraphPad Prism (GraphPad, La Jolla, CA, United States). The comparison of the data was carried out using unpaired Student's t-tests, one-way ANOVAs with Tukey's *post hoc* analyses; and Brown-Forsythe and Welch ANOVA tests for data sets that the assumption of equal variances across groups was violated (stated in the figure legend). Values of $p \leq 0.05$ were considered significant ($^{*}p \leq 0.05$, $^{**}p \leq 0.01$, $^{***}p \leq 0.001$, $^{****}p \leq 0.0001$). Please, note that in the parts of the graphs where nothing is indicated, *p* is higher than 0.05. Images of the original uncropped gels are included at the end of the Supplementary Material.

3 Results

3.1 Mitochondrial polyP prevents aggregation of TUFM after HS

TUFM (mitochondrial translation elongation factor Tu) is the first among the mammalian mitochondrial proteins which aggregates in response to heat stress (Wilkening et al., 2018). Accordingly, we decided to assay the presence of TUFM in the soluble and the insoluble fractions of Wt and MitoPPX cells [cells enzymatically depleted of mitochondrial polyP (Solesio et al.,

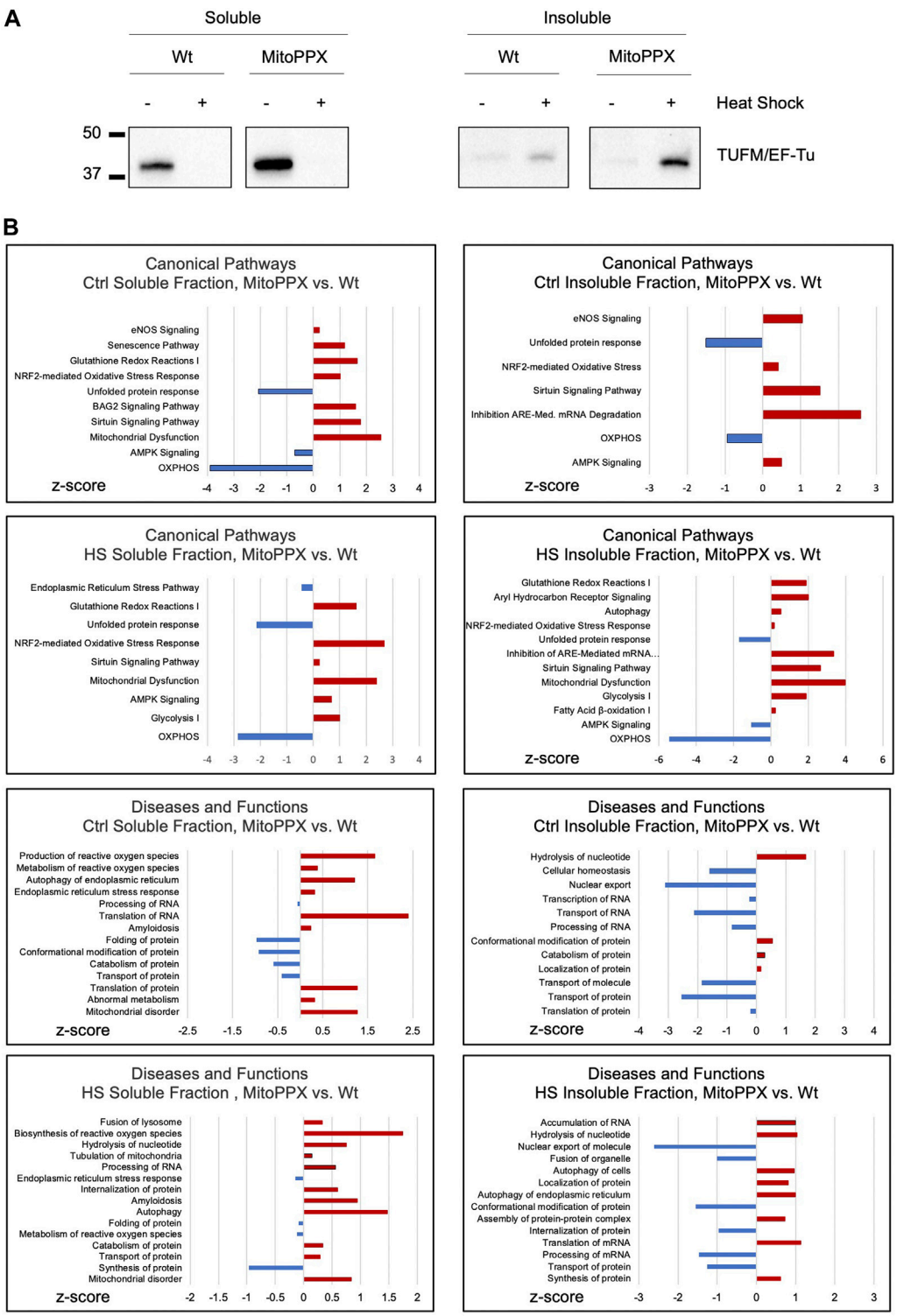

FIGURE 1
Lack of mitochondrial polyP deleteriously affects protein homeostasis within the organelle. **(A)**. Significant immunoblots showing the aggregation behavior of TUFM under control conditions (25°C) and after HS (30 min, 45°C). Protein content was normalized before separation of the soluble and insoluble mitochondrial fractions by centrifugation. Original uncropped membranes are presented in the Supplementary Material. At least three independent experiments were conducted. **(B).** IPA analysis of the proteomics data obtained from the soluble and insoluble mitochondrial protein fractions of the Wt and MitoPPX HEK293, both under control conditions and after HS. The main canonical pathways; and diseases and functions which are predicted to be affected based on the LC-MS/MS are represented in the graphs. Data is represented as the values obtained in MitoPPX vs. those obtained in Wt cells. Selection of the canonical pathways; and disease and functions were conducted among those with p-values ≤0.05, considering z-scores and relationship with mitochondrial physiology and protein homeostasis. Three independent sets of cells were used to obtained the proteomics data. Data sets obtained in the mass spectrometry experiments are included in Supplementary Table S1.

2016a; Solesio et al., 2020; Hambardikar et al., 2022)], after conducting HS in isolated mitochondria, since it is known that aggregated proteins tend to be insoluble (Hipp et al., 2014; Weids et al., 2016). To separate the soluble and insoluble fractions, equal amounts of mitochondrial protein were used, and samples were centrifugated at high speed. Subsequently, the presence of TUFM was determined in the pellets (insoluble fraction) and supernatants (soluble fraction). Our results show that HS increases the presence of TUFM in the insoluble fraction of MitoPPX cells, when compared with the Wt samples. However, we also detected a higher presence of TUFM in the soluble fraction of MitoPPX mitochondria, compared to Wt, in the absence of HS (Figure 1A).

We then analyzed the proteome of the soluble and insoluble mitochondrial fractions of the Wt and MitoPPX cells, obtained under control conditions and after HS. To do this, we used mass spectrometry (Figure 1B). The results were analyzed using IPA to generate predictions; and the main pathways which were relevant for our studies were selected and plotted based on their z-scores. Regarding the IPA analysis, only pathways with a p-value ≤ 0.05 ($-\log$ (p-value) higher than 1.3) were included in the analysis. Major differences regarding the affected pathways were found between Wt and MitoPPX cells, both in the soluble and insoluble fractions, and under control and HS conditions. For example, under control conditions, both soluble and insoluble fractions of MitoPPX cells are predicted to show upregulation of cellular stress response, as well as downregulation of OXPHOS and unfolded protein response (UPR), when compared to the Wt cells. Notably, after HS, mitochondrial dysfunction-related pathways are predicted to be upregulated in the soluble and insoluble fractions of the MitoPPX cells. Furthermore, the analysis of the insoluble fraction revealed that MitoPPX cells are predicted to exhibit impaired proteostasis; as evidenced by the upregulation of autophagy, and cellular stress response (canonical pathways); as well as of protein synthesis and transport (disease and functions pathways); and the downregulation of the UPR. The complete proteomics data sets are included in Supplementary Table S1.

3.2 Mitochondrial polyP can bind mammalian mitochondrial proteins. The number and the specific type of proteins bound are different under control and stress conditions

We performed a pull-down of proteins bound to polyP, using isolated mitochondria from mice liver. The pull-down experiments were conducted under both control and stress conditions, specifically increased ROS and HS (Figure 2A). Following the analysis of the proteins that were present in each condition using LC-MS/MS, we plotted the data using Venn diagrams (Figure 2B). Our analysis reveals that stress has a potent effect on protein binding to polyP. For example, under control conditions, a total of 199 proteins were pulled-down with polyP, out of which 76 were found to be bound to polyP in this condition. After HS, a decreased number of proteins bound to polyP was observed (165). Among these proteins, 66 were bound to polyP in this condition. Lastly, exposure of mitochondria to H_2O_2 resulted in a further decrease of the total number of proteins bound to polyP (97 proteins). In this condition, only 14 proteins were bound to polyP.

Additionally, we plotted the number of peptide spectral matches (PSMs) vs. % coverage data to provide further evidence of significant differences in the studied conditions (Figure 2C). The PSMs analysis complemented the initial findings by identifying and quantifying proteins binding to polyP under different conditions tested. Our findings revealed specific protein interactions with polyP under different stress conditions. Specifically, we observed that lactoferrin Ltf binds to polyP after HS, while protein staphylococcal nuclease-binding domain containing 1 (SND1) showed binding after oxidative stress. The complete mass spectrometry data set is included in Supplementary Table S2, and further experimental details from this assay are included in Supplementary Figure S1.

3.3 The enzymatic depletion of mitochondrial polyP affects the expression levels of some of the main genes and proteins which are involved in the maintenance of mammalian protein homeostasis

To further elucidate the mechanisms that explain the differences observed between Wt and MitoPPX cells in the levels of insolubility of TUFM, we assayed the effects of polyP in the regulation of some of the genes that encode proteins that are involved in mammalian protein homeostasis. In this case, to induce stress, we increased the levels of ROS, since the role of these increased levels on activating the stress response has been broadly demonstrated (Schieber and Chandel, 2014). To accomplish this, we used rotenone, a well-known inhibitor of complex I from the electron transfer chain (ETC) (Li et al., 2003). Short-term treatment and subtoxic treatment with rotenone were chosen to avoid any cellular and/or mitochondrial compensatory effects, as well as to decrease the chances of inhibition of protein import within the organelle. In fact, multiple studies show the need for increased length of treatment and/or concentration of rotenone to induce major effects on the ETC in mammalian cells, including HEK293 (Seo et al., 1999; Koopman et al., 2005; Chen et al., 2007; Teixeira et al., 2018). The use of different stressors also contributes to elucidate whether the observed effects in the case of treatment with rotenone are a consequence of differences in mitochondrial protein import. However, we recognize that we cannot completely rule out the possibility that some our observed effects could be a consequence of the inhibition of the ETC by rotenone. To determine the specific conditions of the pharmacological treatment with this drug, we conducted cell viability assays (Supplementary Figure S2).

Based on the bibliography, we decided to study the levels of gene expression levels of DDIT3 (DNA damage-inducible transcript 3) (Martinus et al., 1996; Zhao et al., 2002), ATF5 (activating transcription factor 5) (Fiorese et al., 2016; Melber and Haynes, 2018), SIRT3 (sirtuin 3) (Papa and Germain, 2014; Kenny et al., 2017), SOD2 (superoxide dismutase 2) (He et al., 2016; Kenny et al., 2017), HSPD1 (heat shock protein family D member 1) (Benedetti et al., 2006; Haynes et al., 2007; Lin et al., 2016), and HSPE1 (heat shock protein family E member 1) (Voos, 2013; Beck et al., 2016)

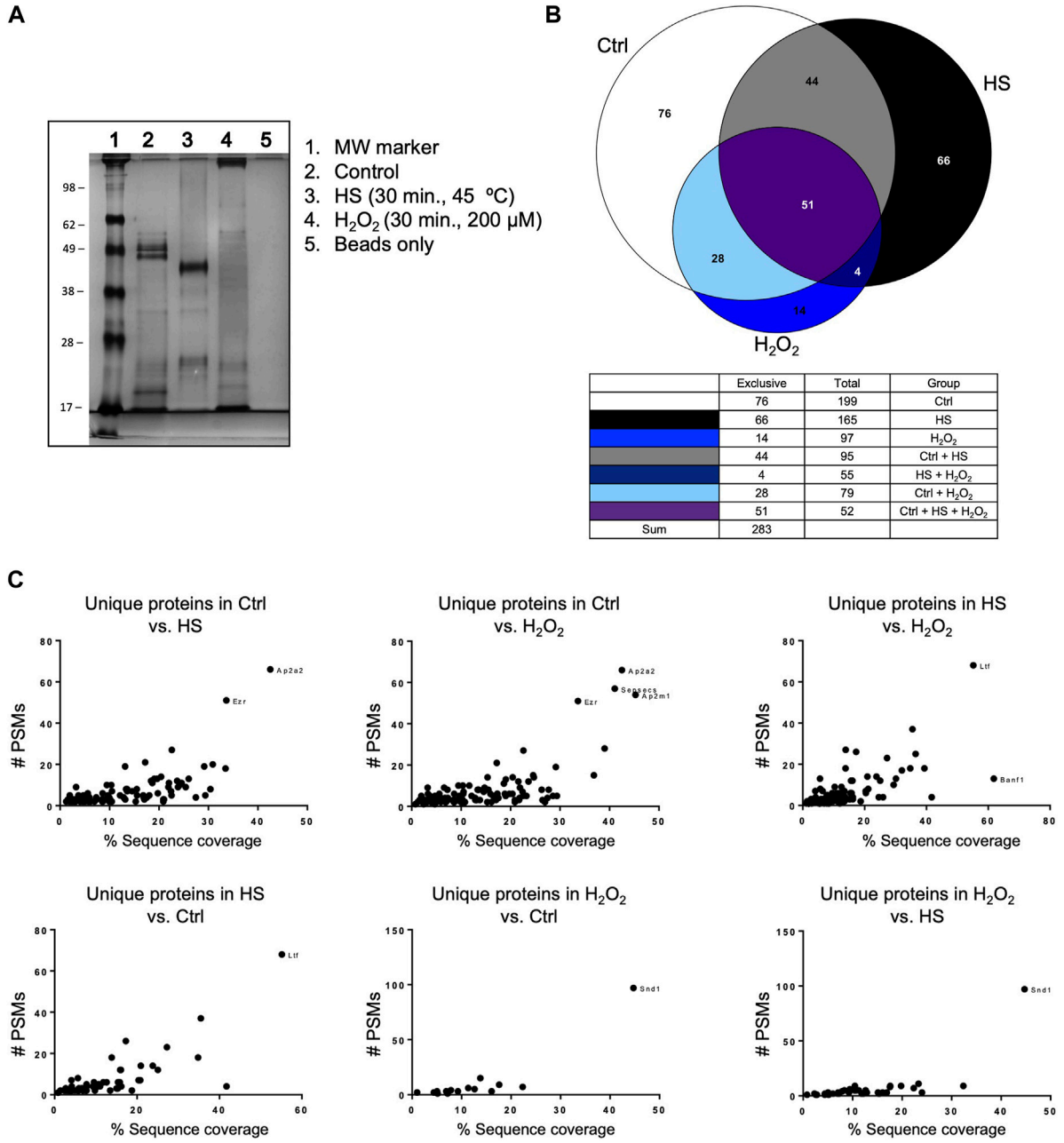

FIGURE 2
Mitochondrial polyP is able to bind proteins. This binding is affected by the presence of different stressors. **(A)** Coomassie-stained SDS-PAGE showing the crude extracts pulled-down with polyP (lanes 2, 3, and 4). The treatments (HS or H_2O_2) and the pull-down were conducted on isolated mitochondria from mice liver. HS was conducted for 30 min at 45°C, and the treatment with H_2O_2 was conducted for 30 min, using 200 µM. **(B)** Venn Diagrams showing the number of proteins that were present in each of the studied conditions and the overlapping areas. Proteins were detected by LC-MS/MS **(C)**. Scatter plots showing unique proteins that were present in the comparison between the different conditions. To show this comparison, the results were plotted as PSMs vs. % of sequence coverage. The outliers are the proteins that are more abundant in each of the comparisons, and each dot represents a different protein. Following the standards in the pull-down field, this experiment was conducted only once. The name of these proteins, the exact number of PSMs, and the complete LC-MS/MS results are included in Supplementary Table S2.

(Figure 3A). The regulation of these genes, and of the proteins encoded by them, have been proposed to be involved in the regulation of the mitochondrial UPR (UPR^{mt}) (Munch, 2018), which is a potent mechanism to counteract increased protein dyshomeostasis in the organelle, even if its exact regulation still remains unclear. For example, the interplay between DDIT3 and ATF5 is dynamically regulated during the activation of the UPR (Teske et al., 2013). Accordingly, the expression of DDIT3 and ATF5 were examined as an approach to investigate the early activation (regulated by ATF5 expression) and late activation (regulated by DDIT3 expression) of UPR. Moreover, SIRT3 and SOD2 encode for proteins which are crucial in the regulation of mitochondrial physiology and the antioxidant defense, respectively (Palma et al., 2020; Zhang et al., 2020). Interestingly, SIRT3 can also

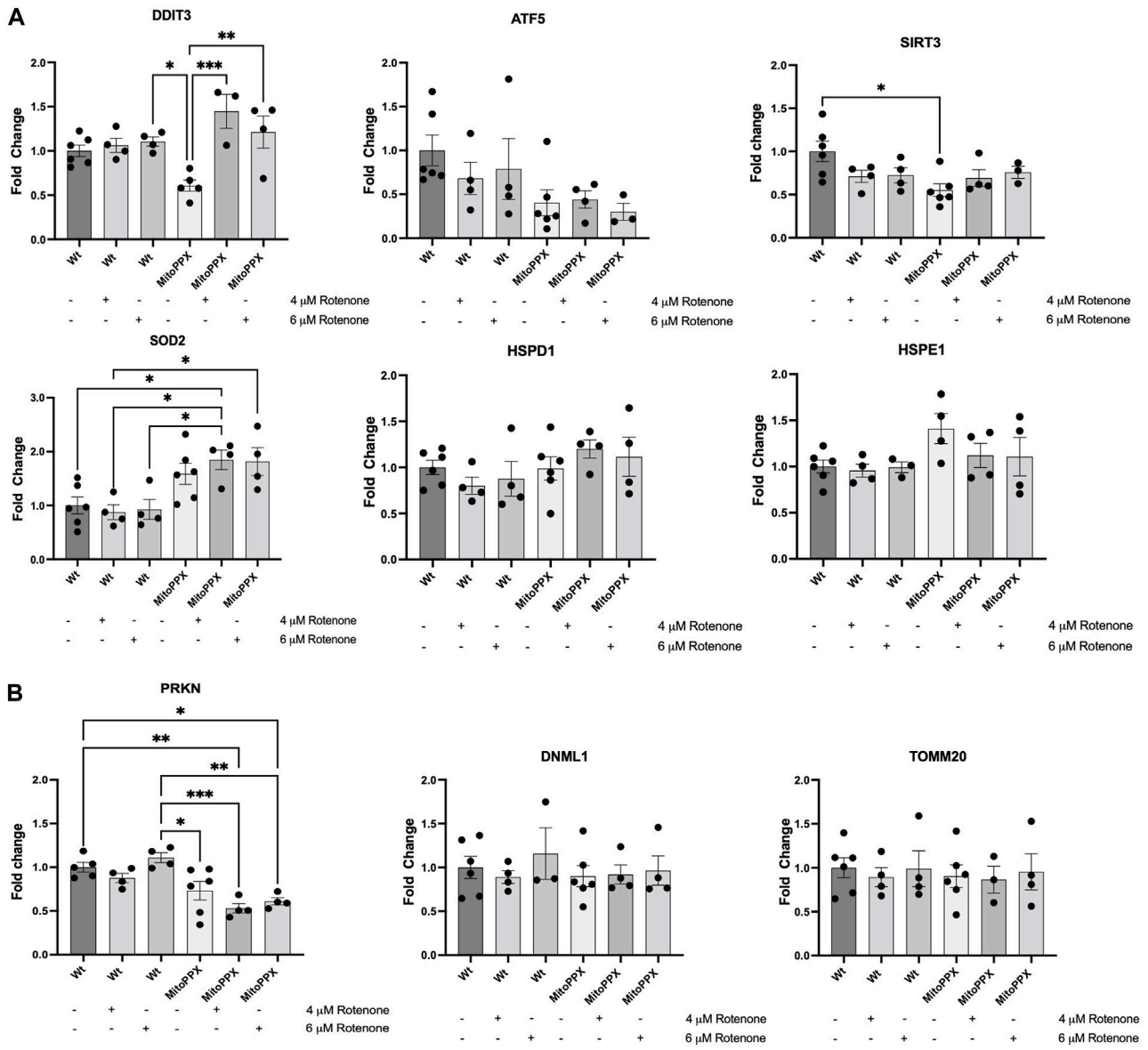

FIGURE 3
The enzymatic depletion of mitochondrial polyP is a potent regulator of mammalian gene expression. qRT-PCR assays were conducted on samples obtained from at least three independent experiments. Specifically, we assayed the expression levels of some key genes involved on the maintenance of **(A)** Mitochondrial proteostasis (DDIT3, ATF5, SIRT3, SOD2, HSPD1, and HSPE1), and **(B)**. Mitochondrial physiology, further than proteostasis (PRKN, DNML1, and TOMM20) in Wt and MitoPPX HEK293 cells. Experiments were conducted under control conditions and after treatment with rotenone (4 and 6 μM for 3 h). Values were standardized with those found in Wt control. The statistical analysis was carried out by one-way ANOVA with Tukey's post-test for multiple comparisons; with the exemption of HSPE1, whose statistical analysis was carried out with Brown-Forsythe and Welch ANOVA due to the unequal variances between groups compared. Data is expressed as mean ± SEM from at least three independent experiments. Unless otherwise indicated, the differences between the groups are not significant. *$p \leq 0.05$, **$p \leq 0.01$, and ***$p \leq 0.001$.

indirectly regulate the expression and activity of SOD2 (Ong and Logue, 2023). Additionally, HSPD1 and HSPE1 are mitochondrial chaperones that have been associated to transcription factors involved in the activation of the UPR^{mt} (Benedetti et al., 2006; Haynes et al., 2007; Voos, 2013; Beck et al., 2016; Lin et al., 2016). As a housekeeper gene, we used GAPDH (Barber et al., 2005). Our results show a significant increase in DDIT3 expression after treatment with rotenone (4 μM and 6 μM), in MitoPPX cells, compared to the same cells under control conditions. We also show a constitutive decreased expression of SIRT3, and upregulated SOD2 in MitoPPX after treatment with rotenone, in both cases when compared with the Wt samples. No significant differences in the expression of ATF5, HSPD1, and HSPE1 were detected.

Using the same methods, we also assayed the expression levels of some of the main genes involved in the regulation of mitochondrial physiology [PRKN, and DNML1; they are crucial regulators of mitochondrial proteostasis (Thorne and Tumbarello, 2022)]; as well as of TOMM20, to determine whether protein import was impacted by treatment with rotenone (Figure 3B). Our results show

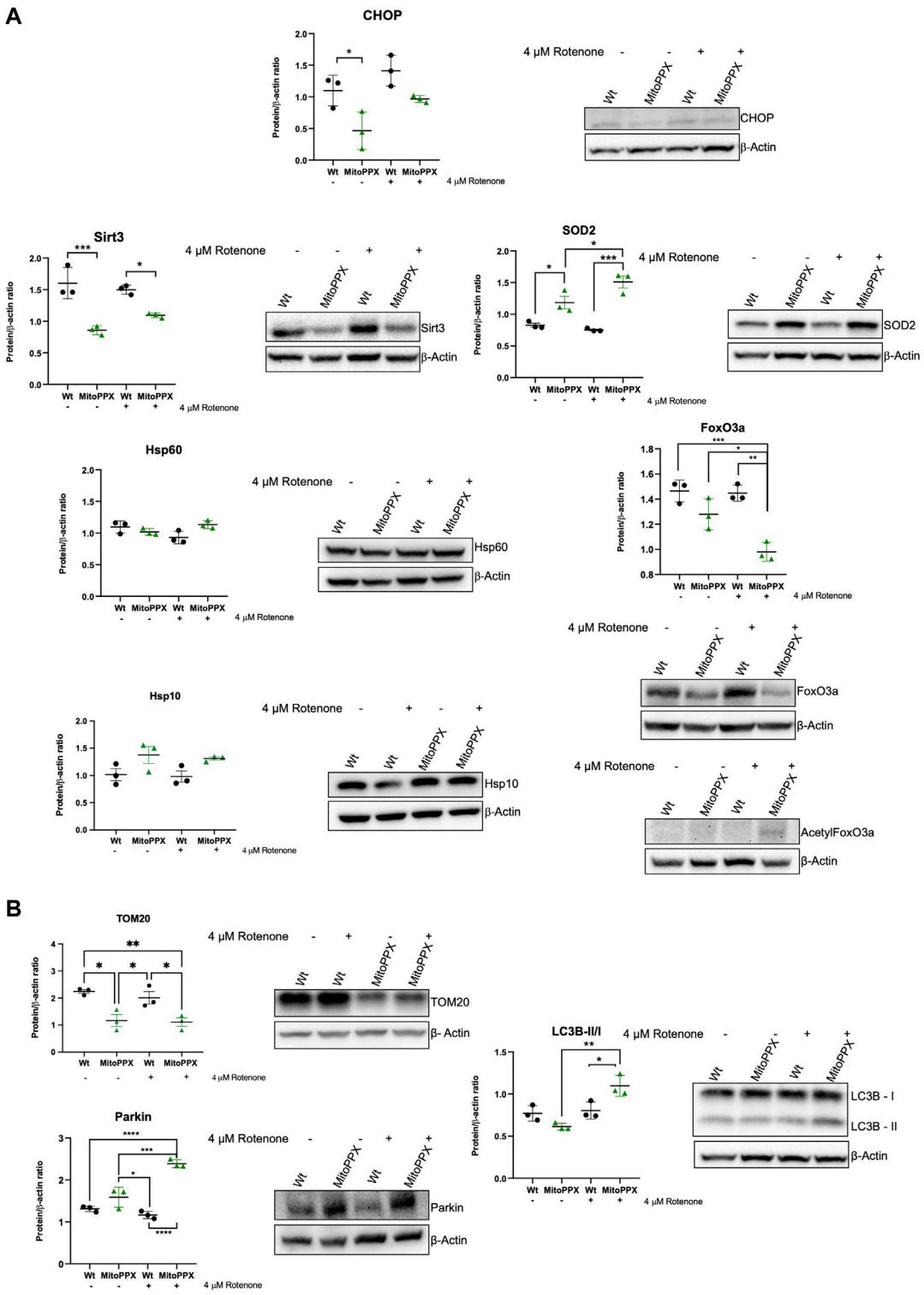

FIGURE 4
Proteins involved in the maintenance of mitochondrial proteostasis are affected by the depletion of mitochondrial polyP. Representative immunoblots analysis and quantification of protein levels obtained from cell lysates. In this case, we followed the same rationale as for the studies of gene expression, and we assayed some key proteins involved in the maintenance of **(A)**. Mitochondrial proteostasis (CHOP, Sirt3, SOD2, Hsp60, Hsp10, and FoxO3a), and **(B)**. Mitochondrial physiology, further than proteostasis (TOM20, Parkin, and LC3 I/II). To conduct these experiments, Wt and MitoPPX cells were used under control conditions and after treatment with rotenone 4 μM for 3 h to increase protein dyshomeostasis via a rise in the generation of mitochondrial ROS. Original uncropped membranes are included in the Supplementary Material. Data is expressed as mean ± SEM from at least three independent experiments. One-way ANOVA followed by Tukey's multiple comparisons test was performed to determine statistical significance. Otherwise indicated, the differences between the groups are not significant. *$p \leq 0.05$, **$p \leq 0.01$, ***$p \leq 0.001$, and ****$p \leq 0.0001$.

a clear decreased expression of PRKN in MitoPPX cells, specifically after the treatment with rotenone, when compared with the Wt samples, while no differences are present in the expression levels of TOMM20 and DNML1.

Subsequently, we assayed the levels of some of the main proteins which have been described to be involved in the maintenance of mammalian protein homeostasis. Following the same rationale as in our studies of gene expression, we assayed CHOP (DDIT3 gene), Sirt3, SOD2, Hsp60 (HSPD1), and Hsp10 (HSPE1). We also assayed the levels of FoxO3a (forkhead box O3a) and acetylated FoxO3a, which is another protein usually involved in the maintenance of mitochondrial proteostasis, whose effects are tightly controlled by post-translational modifications (Mouchiroud et al., 2013). In this case, we did not analyze ATF5 due to the lack of reliable commercial antibodies for this protein. Our immunoblots corroborate some of the data obtained by PCR (Figure 4A). For example, under control conditions, CHOP expression is decreased in MitoPPX compared to Wt cells. Additionally, decreased Sirt3 is observed in MitoPPX cells, even if this effect seems to be more drastic when we assayed protein presence over gene expression. There is also a clear increase in the levels of SOD2 in MitoPPX cells, compared to the Wt samples, especially after the treatment with rotenone. Finally, no significant changes in Hsp60 and Hsp10 were observed between Wt and MitoPPX cells, which corroborates our findings obtained by PCR analysis. In the case of FoxO3a, the levels of the protein are clearly decreased in MitoPPX cells after treatment with rotenone, when compared with the Wt samples. However, acetylation is of a higher magnitude in the case of the MitoPPX cells, especially after treatment with rotenone (Figure 4A).

Lastly, also here, we assayed the levels of some of the main proteins involved in the maintenance of mitochondrial physiology (Figure 4B). Our data show that the depletion of mitochondrial polyP affects the mitochondrial outer membrane import system, as demonstrated by changes in the levels of TOM20. Moreover, contrarily to what we describe in the PCR data, the protein levels of Parkin are increased in MitoPPX cells after treatment with rotenone. Furthermore, we assayed the LC3B-II/I ration, since mitochondrial and cellular proteostasis seem to be connected with autophagy (Aman et al., 2021); and LC3B is a well-described marker of autophagy (Tanida et al., 2008). LC3B is also one of the main components of the cellular UPR, which is mostly orchestrated by the ER (Luhr et al., 2019). Our data show an activation of this pathway in MitoPPX cells after treatment with rotenone.

4 Discussion

The pivotal regulatory role of polyP in mammalian bioenergetics has been extensively demonstrated by our research and others (Solesio et al., 2016a; Solesio et al., 2020; Borden et al., 2021; McIntyre and Solesio, 2021; Solesio et al., 2021; Scoma et al., 2023). Furthermore, the intricate interplay between bioenergetic status and proteostasis, along with the involvement of polyP in preserving bacterial proteostasis and regulating amyloidogenesis, are known (Gray et al., 2014; Nargund et al., 2015; Cremers et al., 2016; Yoo et al., 2018; Lempart et al., 2019; Lempart and Jakob, 2019; Xie and Jakob, 2019). However, little is known regarding the role of polyP on the maintenance of mitochondrial protein homeostasis. In this study, we delve into this role for the first time, shedding light on its significance. To disturb proteostasis in our samples, we used increased ROS and HS, which are well-known stressors in mammalian cells (Duncan and Hershey, 1984; Mizzen and Welch, 1988; Abe et al., 1999; Squier, 2001; Kim et al., 2011; Levy et al., 2019). We used both insults to show that our results are not dependent on the specific type of stimuli.

Our data show the chaperoning effect of polyP against the aggregation of mitochondrial proteins. Specifically, we studied the distribution of TUFM between the soluble and insoluble fractions of mitochondria to conduct these studies. We chose TUFM because it has been demonstrated that this is the first mitochondrial protein to aggregate under stress conditions (Wilkening et al., 2018). We found an increased presence of TUFM in the insoluble fraction of MitoPPX cells, when compared with Wt samples. However, the presence of TUFM was already increased in the soluble fraction of the MitoPPX cells under control conditions. One plausible explanation for these observed differences could be that the depletion of mitochondrial polyP in MitoPPX cells leads to unbalanced energy homeostasis, as we have already shown in our previous studies (Solesio et al., 2021; Hambardikar et al., 2023). Unbalanced bioenergetics could ultimately compromise the efficiency of protein folding and assembly within mitochondria. Furthermore, the overexpression of TUFM in the soluble fraction of MitoPPX cells could be a compensatory response to the mitochondrial stress induced by the depletion of mitochondrial polyP. Specifically, upregulated TUFM could be an attempt to enhance mitochondrial protein translation, ultimately mitigating impaired proteostasis. However, after HS, high levels of TUFM accumulates in the insoluble fraction. Moreover, MitoPPX HEK293 cells do not present impaired cell viability, or any major structural changes, as we have previously shown (Solesio et al., 2016a; Solesio et al., 2020; Solesio et al., 2021; Hambardikar et al., 2022). Additionally, the role of polyP as a bacterial chaperone is already known (Dahl et al., 2015; Cremers et al., 2016; Yoo et al., 2018), and this mechanism could be conserved in mammalian cells, especially considering how well polyP is conserved throughout evolution. Considering all this, the increased levels of TUFM in the soluble fraction of the MitoPPX cells could be interpreted as a protective mechanism to mitigate the deleterious effects caused by the depletion of polyP on the chaperoning ability of the organelle.

To further study whether the depletion of mitochondrial polyP affects protein homeostasis within the organelle, we analyzed the proteome of the soluble and insoluble mitochondrial fractions from Wt and MitoPPX cells, under control and HS conditions. Our IPA predictions show that HS induces significant changes in the proteins that are present in the different mitochondrial fractions of MitoPPX cells. For example, OXPHOS is clearly downregulated in MitoPPX cells when compared to Wt samples, even under control conditions and in both fractions. A considerable number of the protein complexes involved in OXPHOS are encoded in mitochondrial DNA. Therefore, increased proteotoxicity due to decreased levels of mitochondrial polyP could contribute to the dysfunction of OXPHOS, which could further contribute to increased

proteotoxicity (due to the high demands of energy of chaperones), creating add deleterious feedback. Our data also show upregulated UPR and mitochondrial dysfunction in both the soluble and insoluble fraction of MitoPPX cells, after HS. The upregulation of these pathways is already predicted in MitoPPX cells under control conditions. These findings suggest that the potent effects of polyP on mitochondrial protein homeostasis are already exerted under basal conditions, and they are more dramatic when proteotoxic stress is present. Additionally, upregulated autophagy is present in the insoluble fraction of MitoPPX cells after HS, which suggest that the activation of the stress response when polyP is depleted in mitochondria is of a bigger scope.

The pull-down of proteins bound to polyP revealed substantial changes in under control and stress (increased ROS and HS) conditions. For example, our findings show that HS induces a higher number of proteins to be pulled-down compared to increased ROS. This suggests that HS induces a more pronounced interaction between polyP and proteins. Moreover, we found that Ltf binds to polyP in HS but not under control conditions. Ltf is a glycoprotein with various effects in mammalian cells, including binding to organic iron to protect against oxidative stress (Kowalczyk et al., 2022). The finding that Ltf binds to polyP under HS conditions suggests that it may play a role in the response against protein dyshomeostasis, potentially contributing to the cellular defense mechanisms during stress. Furthermore, after treatment with H_2O_2, we found that SND1, also known as P100, is bound to polyP. This binding is not present under control conditions. SND1 is a well-conserved protein among eukaryotes. It is found in mitochondria, where it plays multifaceted roles. Recently, mitochondrial SND1 has been reported to increase under stress conditions. In fact, it has been demonstrated that SND1 is recruited to mitochondria in response to stress stimulus and that it promotes mitophagy through the PGAM5—Drp1^{S635} dephosphorylation pathway (Liang et al., 2022). Accordingly, our findings align with the existing literature, which shows that polyP can bind to mammalian proteins (Morrissey et al., 2012), and highlights the potent role of the polyP in maintaining protein homeostasis in bacteria and in mammalian amyloidogenesis (Gray et al., 2014; Dahl et al., 2015; Yoo et al., 2018; Lempart et al., 2019; Lempart and Jakob, 2019; Xie and Jakob, 2019). They also suggest a significant regulatory role for polyP in mammalian protein homeostasis and provide insights into the cellular mechanisms involved in the mammalian stress response and adaptation.

HS and oxidative stress are distinct cellular stressors that can elicit diverse responses in biological systems, including mitochondria (Slimen et al., 2014). This is further confirmed by our pull-down data. Therefore, we decided to address whether the protective effects of polyP on mitochondrial proteostasis are conserved independently of the specific stressor. Since the studies with TUFM were conducted using HS, we decided to address the status of gene expression and protein levels in response to sub-toxic concentrations of rotenone.

The enzymatic depletion of mitochondrial polyP induces a sharp effect in the expression of some of the main genes in charge of maintaining mitochondrial proteostasis, including some of those proposed to be involved in the UPR^{mt}, both under control conditions and in response to treatment with rotenone. For example, our data show increased expression of DDIT3 in MitoPPX cells in response to rotenone, which suggest the late activation of the UPR (Ong and Logue, 2023), especially considering the lack of differences in the expression of ATF5. In fact, previous studies have shown that the upregulation of DDIT3 mRNA is associated with a prolonged ER stress pathway (Tsai et al., 2017; Yu et al., 2022). The activation of the UPR and the UPR^{mt} are intimately related in mammalian physiology, and the number of publications showing a close relationship between the physiology of mitochondria and ER has increased in the last decade (Zhang et al., 2023). Therefore, by dysregulating mitochondrial proteostasis, the depletion of polyP within the organelle could have a global effect in the cell. As mentioned above, the expression of ATF5 do not show substantial changes between our different experimental conditions. While ATF5 has been described as one of the main regulators of the mammalian UPR^{mt}, current knowledge suggests that the effects of ATF5 in mitochondrial protein homeostasis are mediated by the mitochondrial levels of the protein, and not necessarily by its expression levels (Fiorese et al., 2016). Moreover, other regulatory mechanisms of the UPR^{mt}, independent of ATF5, may also be present in mammalian cells.

Our data also show that, under control conditions, the enzymatic depletion of mitochondrial polyP induces a constitutive downregulation in the expression of SIRT3, a protein involved in the maintenance of mitochondrial physiology, including protein homeostasis (Papa and Germain, 2014; Zhang et al., 2020). In fact, the downregulation of SIRT3 can disrupt the protein quality control mechanisms within mitochondria, including the UPR^{mt} (Meng et al., 2019), and potentially trigger cellular stress responses. However, when stress is present, the levels of SIRT3 are similar in Wt and MitoPPX cells, which suggest the existence of a compensatory mechanism. Our data also show increased expression of SOD2 in the MitoPPX cells. SOD2 is one of the main mitochondrial antioxidant enzymes in mammalian cells (Flynn and Melov, 2013). We have already demonstrated that even if MitoPPX HEK293 cells are viable and fully functional, they have increased levels of ROS, probably due to dysregulated OXPHOS (Solesio et al., 2021; Hambardikar et al., 2022). Probably as a compensatory effect, an increased presence of antioxidants in MitoPPX cells has been reported (Hambardikar et al., 2022). Therefore, the rise in the expression of SOD2 could be related to the dsyregulation of bioenergetics, instead of being directly linked to mitochondrial proteostasis. Furthermore, we did not find significant differences in the expression of HSPD1 and HSPE1 after rotenone treatment. These two genes encode for two of the main mammalian chaperones: Hsp60 and its co-chaperone Hsp10, respectively. The lack of regulatory effects of polyP in these genes corroborates the results obtained in the ATF5 assay, since ATF5 is a major regulator of mitochondrial chaperones, including Hsp60 and Hsp10 (Fiorese et al., 2016). Accordingly, our data suggests that the protective effects of polyP on proteostasis are not mediated by the regulation of the expression of the classical mitochondrial chaperones. Moreover, our results show that PRKN gene expression is decreased in MitoPPX cells, especially under treatment conditions. This effect is not observed when we assayed the protein levels. Lastly, no changes in the expression levels of DNM1L and TOMM20 were observed, which suggest that the effects of polyP on these cells are circumscribed to the regulation of protein homeostasis.

Immunoblots corroborate much of our previous regarding gene expression findings. However, we found two exceptions to this: TOM20 and Parkin. Increased Parkin-mediated mitophagy is

associated with degradation of mitochondrial membranes, and therefore it can lead decreased levels of TOM20, which are found in our studies (Yoshii et al., 2011). An increased presence of Parkin in the MitoPPX cells also suggests a rise in the activation of mitophagy. In this case, the differences between the gene expression levels and the protein presence could be explained by the multiple post-translational modifications that Parkin undergoes to be active, including phosphorylation (Durcan and Fon, 2015). Depletion of mitochondrial polyP could modify phosphate homeostasis in mitochondria. Moreover, polyP is able to polyphosphorylate proteins (Azevedo et al., 2015; Azevedo et al., 2018; Bentley-DeSousa et al., 2018). All this could affect the levels of active Parkin. Decreased levels of TOM20 could further affect mitochondrial protein homeostasis. TOM20 is a translocase of the outer mitochondrial membrane, which is part of the TOM (transporter outer membrane) protein import machinery. TOM has been demonstrated to be impaired in human disease, including neurodegeneration (Chai et al., 2018; Franco-Iborra et al., 2018). In fact, dysregulated mitochondrial protein import could trigger proteotoxic stress in both the organelle and the cytosol. Furthermore, deficits in mitochondrial protein import could affect the import of proteins required for proper mitochondrial functioning, including some of the components of the ETC. Therefore, decreased levels of polyP could also indirectly affect mitochondrial proteostasis.

To further understand the effects of polyP in cellular physiology, we addressed whether cellular autophagy, a process which is closely related to mitophagy (Glick et al., 2010; Youle and Narendra, 2011), is affected by the depletion of mitochondrial polyP. Specifically, we assayed variations in the LC3B-I/LC3B-II ratio, as this is one of the most common markers of autophagy (Tanida et al., 2008; Bjorkoy et al., 2009). Our results align with those found in Parkin, indicating a rise in the autophagic processes in MitoPPX cells, and corroborate previous findings from both our research group and others, highlighting the global impact of the depletion of mitochondrial polyP on cellular processes. (Bondy-Chorney et al., 2020; Solesio et al., 2021; Hambardikar et al., 2022). Using immunoblots, we were not able to assay the levels of ATF5 due to the lack of reliable antibodies. However, we included FoxO3a (and its acetylated form) in our study. FoxO3a is involved in the regulation of oxygen metabolism and mitochondrial gene expression (Ferber et al., 2012), two processes in which polyP is involved, and which are closely related to the status of mitochondrial proteostasis. While the levels of FoxO3a are decreased in MitoPPX cells when rotenone is present, its acetylation is clearly increased in the same samples. Interestingly, post-translational modifications of FoxO3a modulate the subcellular location of the protein, as well as its activity (Boccitto and Kalb, 2011). For example, in response to stress and after these post-translational modifications, FoxO3a migrates to nuclei and mitochondria, where it is active (Fasano et al., 2019). Moreover, increased acetylation of FoxO3a has been shown to regulate mitophagy besides the antioxidant response (Gupta et al., 2022). Previous studies have demonstrated the close relationship between FoxO3a and Sirt3. Specifically, in response to stress stimuli, Sirt3, which is primarily located in the mitochondria, can deacetylate FoxO3a, likely to protect the organelle against increased oxidative stress by activating the expression of antioxidant enzymes, such as SOD2 (Tseng et al., 2013). Furthermore, deacetylation of FoxO3a upregulates the expression of a set of genes that are involved in the maintenance of mitochondrial proteostasis (Tseng et al., 2013). MitoPPX cells exhibit decreased levels of Sirt3, which correlates with the increased levels of acetylated FoxO3a observed in the same samples. We recognize that the regulation of FoxO3a is complex, and other explanations (such as variations in the antioxidant system) could also underlie our findings.

Some of these findings may suggest that the regulatory influence of polyP on mitochondrial proteostasis operates through the modulation of the transcriptome, rather than directly impacting protein stability. This hypothesis finds support in the known regulatory function of long-chain polyP in the mammalian transcriptome (Bondy-Chorney et al., 2020). However, previous studies examining the protective effects of polyP on protein homeostasis, particularly those focused on elucidating its role in amyloidogenesis, indicate a direct impact of polyP on protein stability (Cremers et al., 2016; Yoo et al., 2018; Lempart et al., 2019). In fact, polyP has already been described as a "polyanionic protein scaffold" (Xie and Jakob, 2019; Guan and Jakob, 2024).

Altogether, our findings show for the first time the critical role played by polyP in the regulation of mitochondrial proteostasis, and they could pave the road for further studies using the metabolism of mitochondrial polyP as a potent pharmacological target in pathologies where mitochondrial protein dyshomeostasis has been demonstrated. These diseases range from neurodegeneration to cancer (Boland et al., 2013; Patro et al., 2021).

Data availability statement

The mass spectrometric data presented in this study are deposited at https://massive.ucsd.edu accession numbers Massive MSV000095168, and MSV000095178.

Author contributions

RC: Conceptualization, Data curation, Formal Analysis, Investigation, Methodology, Visualization, Writing–review and editing. PU: Conceptualization, Data curation, Formal Analysis, Investigation, Methodology, Visualization, Writing–review and editing. MP: Data curation, Formal Analysis, Methodology, Visualization, Writing–review and editing. YD: Data curation, Formal Analysis, Investigation, Validation, Writing–review and editing. MK: Data curation, Formal Analysis, Investigation, Validation, Writing–review and editing. HZ: Data curation, Formal Analysis, Investigation, Validation, Writing–review and editing. MG-M: Data curation, Formal Analysis, Investigation, Validation, Writing–review and editing. PE: Data curation, Formal Analysis, Investigation, Validation, Writing–review and editing. ES: Data curation, Formal Analysis, Investigation, Validation, Writing–review and editing. VH: Data curation, Formal Analysis, Investigation, Validation, Writing–review and editing. BU: Data curation, Formal Analysis, Investigation, Validation, Writing–review and editing. JT: Data curation, Formal Analysis, Investigation, Validation, Writing–review and editing. AC: Data curation, Formal Analysis, Investigation, Validation, Writing–review and editing. EP: Conceptualization, Resources, Supervision, Writing–review and editing. CH: Conceptualization, Resources, Supervision, Writing–review and

editing. MS: Conceptualization, Funding acquisition, Methodology, Project administration, Resources, Supervision, Writing–original draft, Writing–review and editing.

Funding

The author(s) declare that financial support was received for the research, authorship, and/or publication of this article. This study was supported by the National Institutes of Health (1K99AG055701-01A1 and 4R00AG055701-03 to MS) and by the Start Up funds from Rutgers University to MS. At her present institution, currently, MGM is funded by CD21/00019 (ISCIII – FSE+). This project was also partially funded thanks to the 5R35GM139615 from the National institutes of Health to EP.

Acknowledgments

We kindly thank Mitch Maleki, Esq., for editing this manuscript. We also kindly thank Guiseppe Federico Amodeo for isolating mitochondria from mice liver for us.

Conflict of interest

The authors declare that the research was conducted in the absence of any commercial or financial relationships that could be construed as a potential conflict of interest.

Publisher's note

Supplementary material

The Supplementary Material for this article can be found online at: https://www.frontiersin.org/articles/10.3389/fcell.2024.1423208/full#supplementary-material

References

Abe, T., Gotoh, S., and Higashi, K. (1999). Higher induction of heat shock protein 72 by heat stress in cisplatin-resistant than in cisplatin-sensitive cancer cells. *Biochim. Biophys. Acta* 1445, 123–133. doi:10.1016/s0167-4781(99)00036-6

Abramov, A. Y., Fraley, C., Diao, C. T., Winkfein, R., Colicos, M. A., Duchen, M. R., et al. (2007). Targeted polyphosphatase expression alters mitochondrial metabolism and inhibits calcium-dependent cell death. *Proc. Natl. Acad. Sci. U. S. A.* 104, 18091–18096. doi:10.1073/pnas.0708959104

Aman, Y., Schmauck-Medina, T., Hansen, M., Morimoto, R. I., Simon, A. K., Bjedov, I., et al. (2021). Autophagy in healthy aging and disease. *Nat. Aging* 1, 634–650. doi:10.1038/s43587-021-00098-4

Araki, K., and Nagata, K. (2012). Protein folding and quality control in the ER. *Cold Spring Harb. Perspect. Biol.* 4, a015438. doi:10.1101/cshperspect.a015438

Azevedo, C., Livermore, T., and Saiardi, A. (2015). Protein polyphosphorylation of lysine residues by inorganic polyphosphate. *Mol. Cell* 58, 71–82. doi:10.1016/j.molcel.2015.02.010

Azevedo, C., Singh, J., Steck, N., Hofer, A., Ruiz, F. A., Singh, T., et al. (2018). Screening a protein array with synthetic biotinylated inorganic polyphosphate to define the human PolyP-ome. *ACS Chem. Biol.* 13, 1958–1963. doi:10.1021/acschembio.8b00357

Baltanas, A., Solesio, M. E., Zalba, G., Galindo, M. F., Fortuño, A., and Jordán, J. (2013). The senescence-accelerated mouse prone-8 (SAM-P8) oxidative stress is associated with upregulation of renal NADPH oxidase system. *J. Physiol. Biochem.* 69, 927–935. doi:10.1007/s13105-013-0271-6

Barber, R. D., Harmer, D. W., Coleman, R. A., and Clark, B. J. (2005). GAPDH as a housekeeping gene: analysis of GAPDH mRNA expression in a panel of 72 human tissues. *Physiol. Genomics* 21, 389–395. doi:10.1152/physiolgenomics.00025.2005

Beck, J. S., Mufson, E. J., and Counts, S. E. (2016). Evidence for mitochondrial UPR gene activation in familial and sporadic alzheimer's disease. *Curr. Alzheimer Res.* 13, 610–614. doi:10.2174/1567205013666151221145445

Benedetti, C., Haynes, C. M., Yang, Y., Harding, H. P., and Ron, D. (2006). Ubiquitin-like protein 5 positively regulates chaperone gene expression in the mitochondrial unfolded protein response. *Genetics* 174, 229–239. doi:10.1534/genetics.106.061580

Bentley-DeSousa, A., Holinier, C., Moteshareie, H., Tseng, Y. C., Kajjo, S., Nwosu, C., et al. (2018). A screen for candidate targets of lysine polyphosphorylation uncovers a conserved network implicated in ribosome biogenesis. *Cell Rep.* 22, 3427–3439. doi:10.1016/j.celrep.2018.02.104

Bjorkoy, G., Lamark, T., Pankiv, S., Øvervatn, A., Brech, A., and Johansen, T. (2009). Monitoring autophagic degradation of p62/SQSTM1. *Methods Enzymol.* 452, 181–197. doi:10.1016/S0076-6879(08)03612-4

Boccitto, M., and Kalb, R. G. (2011). Regulation of Foxo-dependent transcription by post-translational modifications. *Curr. Drug Targets* 12, 1303–1310. doi:10.2174/138945011796150316

Boland, M. L., Chourasia, A. H., and Macleod, K. F. (2013). Mitochondrial dysfunction in cancer. *Front. Oncol.* 3, 292. doi:10.3389/fonc.2013.00292

Bondy-Chorney, E., Abramchuk, I., Nasser, R., Holinier, C., Denoncourt, A., Baijal, K., et al. (2020). A broad response to intracellular long-chain polyphosphate in human cells. *Cell Rep.* 33, 108318. doi:10.1016/j.celrep.2020.108318

Borden, E. A., Furey, M., Gattone, N. J., Hambardikar, V. D., Liang, X. H., Scoma, E. R., et al. (2021). Is there a link between inorganic polyphosphate (polyP), mitochondria, and neurodegeneration? *Pharmacol. Res.* 163, 105211. doi:10.1016/j.phrs.2020.105211

Castro, C. M., Corciulo, C., Solesio, M. E., Liang, F., Pavlov, E. V., and Cronstein, B. N. (2020). Adenosine A2A receptor (A2AR) stimulation enhances mitochondrial metabolism and mitigates reactive oxygen species-mediated mitochondrial injury. *FASEB J.* 34, 5027–5045. doi:10.1096/fj.201902459R

Chai, Y. L., Xing, H., Chong, J. R., Francis, P. T., Ballard, C. G., Chen, C. P., et al. (2018). Mitochondrial translocase of the outer membrane alterations may underlie dysfunctional oxidative phosphorylation in alzheimer's disease. *J. Alzheimer's Dis. JAD* 61, 793–801. doi:10.3233/JAD-170613

Chen, Y., McMillan-Ward, E., Kong, J., Israels, S. J., and Gibson, S. B. (2007). Mitochondrial electron-transport-chain inhibitors of complexes I and II induce autophagic cell death mediated by reactive oxygen species. *J. Cell Sci.* 120, 4155–4166. doi:10.1242/jcs.011163

Craig, R., and Beavis, R. C. (2004). TANDEM: matching proteins with tandem mass spectra. *Bioinformatics* 20, 1466–1467. doi:10.1093/bioinformatics/bth092

Cremers, C. M., Knoefler, D., Gates, S., Martin, N., Dahl, J. U., Lempart, J., et al. (2016). Polyphosphate: a conserved modifier of amyloidogenic processes. *Mol. Cell* 63, 768–780. doi:10.1016/j.molcel.2016.07.016

Dahl, J. U., Gray, M. J., and Jakob, U. (2015). Protein quality control under oxidative stress conditions. *J. Mol. Biol.* 427, 1549–1563. doi:10.1016/j.jmb.2015.02.014

Desfougeres, Y., Saiardi, A., and Azevedo, C. (2020). Inorganic polyphosphate in mammals: where's Wally? *Biochem. Soc. Trans.* 48, 95–101. doi:10.1042/BST20190328

Drummond, E., Pires, G., MacMurray, C., Askenazi, M., Nayak, S., Bourdon, M., et al. (2020). Phosphorylated tau interactome in the human Alzheimer's disease brain. *Brain* 143, 2803–2817. doi:10.1093/brain/awaa223

Duncan, R., and Hershey, J. W. (1984). Heat shock-induced translational alterations in HeLa cells. Initiation factor modifications and the inhibition of translation. *J. Biol. Chem.* 259, 11882–11889. doi:10.1016/s0021-9258(20)71294-9

Durcan, T. M., and Fon, E. A. (2015). The three 'P's of mitophagy: PARKIN, PINK1, and post-translational modifications. *Genes Dev.* 29, 989–999. doi:10.1101/gad.262758.115

Fasano, C., Disciglio, V., Bertora, S., Lepore Signorile, M., and Simone, C. (2019). FOXO3a from the nucleus to the mitochondria: a round trip in cellular stress response. *Cells* 8, 1110. doi:10.3390/cells8091110

Ferber, E. C., Peck, B., Delpuech, O., Bell, G. P., East, P., and Schulze, A. (2012). FOXO3a regulates reactive oxygen metabolism by inhibiting mitochondrial gene expression. *Cell Death Differ.* 19, 968–979. doi:10.1038/cdd.2011.179

Fiorese, C. J., Schulz, A. M., Lin, Y. F., Rosin, N., Pellegrino, M. W., and Haynes, C. M. (2016). The transcription factor ATF5 mediates a mammalian mitochondrial UPR. *Curr. Biol.* 26, 2037–2043. doi:10.1016/j.cub.2016.06.002

Flynn, J. M., and Melov, S. (2013). SOD2 in mitochondrial dysfunction and neurodegeneration. *Free Radic. Biol. Med.* 62, 4–12. doi:10.1016/j.freeradbiomed.2013.05.027

Fossati, S., Giannoni, P., Solesio, M. E., Cocklin, S. L., Cabrera, E., Ghiso, J., et al. (2016). The carbonic anhydrase inhibitor methazolamide prevents amyloid beta-induced mitochondrial dysfunction and caspase activation protecting neuronal and glial cells *in vitro* and in the mouse brain. *Neurobiol. Dis.* 86, 29–40. doi:10.1016/j.nbd.2015.11.006

Franco-Iborra, S., Cuadros, T., Parent, A., Romero-Gimenez, J., Vila, M., and Perier, C. (2018). Defective mitochondrial protein import contributes to complex I-induced mitochondrial dysfunction and neurodegeneration in Parkinson's disease. *Cell Death Dis.* 9, 1122. doi:10.1038/s41419-018-1154-0

Glick, D., Barth, S., and Macleod, K. F. (2010). Autophagy: cellular and molecular mechanisms. *J. Pathol.* 221, 3–12. doi:10.1002/path.2697

Gray, M. J., Wholey, W. Y., Wagner, N. O., Cremers, C. M., Mueller-Schickert, A., Hock, N. T., et al. (2014). Polyphosphate is a primordial chaperone. *Mol. Cell* 53, 689–699. doi:10.1016/j.molcel.2014.01.012

Guan, J., and Jakob, U. (2024). The protein scaffolding functions of polyphosphate. *J. Mol. Biol.* 168504, 168504. doi:10.1016/j.jmb.2024.168504

Guitart-Mampel, M., Urquiza, P., Carnevale Neto, F., Anderson, J. R., Hambardikar, V., Scoma, E. R., et al. (2022). Mitochondrial inorganic polyphosphate (polyP) is a potent regulator of mammalian bioenergetics in SH-SY5Y cells: a proteomics and metabolomics study. *Front. Cell Dev. Biol.* 10, 833127. doi:10.3389/fcell.2022.833127

Gupta, P., Sharma, G., Lahiri, A., and Barthwal, M. K. (2022). FOXO3a acetylation regulates PINK1, mitophagy, inflammasome activation in murine palmitate-conditioned and diabetic macrophages. *J. Leukoc. Biol.* 111, 611–627. doi:10.1002/JLB.3A0620-348RR

Hambardikar, V., Akosah, Y. A., Scoma, E. R., Guitart-Mampel, M., Urquiza, P., Da Costa, R. T., et al. (2023). Toolkit for cellular studies of mammalian mitochondrial inorganic polyphosphate. *Front. Cell Dev. Biol.* 11, 1302585. doi:10.3389/fcell.2023.1302585

Hambardikar, V., Guitart-Mampel, M., Scoma, E. R., Urquiza, P., Nagana, G. G. A., Raftery, D., et al. (2022). Enzymatic depletion of mitochondrial inorganic polyphosphate (polyP) increases the generation of reactive oxygen species (ROS) and the activity of the pentose phosphate pathway (PPP) in mammalian cells. *Antioxidants (Basel)* 11, 685. doi:10.3390/antiox11040685

Haynes, C. M., and Hekimi, S. (2022). Mitochondrial dysfunction, aging, and the mitochondrial unfolded protein response in *Caenorhabditis elegans*. *Genetics* 222, iyac160. doi:10.1093/genetics/iyac160

Haynes, C. M., Petrova, K., Benedetti, C., Yang, Y., and Ron, D. (2007). ClpP mediates activation of a mitochondrial unfolded protein response in *C. elegans*. *Dev. Cell* 13, 467–480. doi:10.1016/j.devcel.2007.07.016

Haynes, C. M., and Ron, D. (2010). The mitochondrial UPR - protecting organelle protein homeostasis. *J. Cell Sci.* 123, 3849–3855. doi:10.1242/jcs.075119

Haynes, C. M., Yang, Y., Blais, S. P., Neubert, T. A., and Ron, D. (2010). The matrix peptide exporter HAF-1 signals a mitochondrial UPR by activating the transcription factor ZC376.7 in *C. elegans*. *Mol. Cell* 37, 529–540. doi:10.1016/j.molcel.2010.01.015

He, C., Hart, P. C., Germain, D., and Bonini, M. G. (2016). SOD2 and the mitochondrial UPR: partners regulating cellular phenotypic transitions. *Trends Biochem. Sci.* 41, 568–577. doi:10.1016/j.tibs.2016.04.004

Hipp, M. S., Park, S. H., and Hartl, F. U. (2014). Proteostasis impairment in protein-misfolding and -aggregation diseases. *Trends Cell Biol.* 24, 506–514. doi:10.1016/j.tcb.2014.05.003

Irvine, G. B., El-Agnaf, O. M., Shankar, G. M., and Walsh, D. M. (2008). Protein aggregation in the brain: the molecular basis for Alzheimer's and Parkinson's diseases. *Mol. Med.* 14, 451–464. doi:10.2119/2007-00100.Irvine

Kenny, T. C., Hart, P., Ragazzi, M., Sersinghe, M., Chipuk, J., Sagar, M. A. K., et al. (2017). Selected mitochondrial DNA landscapes activate the SIRT3 axis of the UPR(mt) to promote metastasis. *Oncogene* 36, 4393–4404. doi:10.1038/onc.2017.52

Khong, M. L., Li, L., Solesio, M. E., Pavlov, E. V., and Tanner, J. A. (2020). Inorganic polyphosphate controls cyclophilin B-mediated collagen folding in osteoblast-like cells. *FEBS J.* 287, 4500–4524. doi:10.1111/febs.15249

Kim, H. J., Joo, H. J., Kim, Y. H., Ahn, S., Chang, J., Hwang, K. B., et al. (2011). Systemic analysis of heat shock response induced by heat shock and a proteasome inhibitor MG132. *PLoS One* 6, e20252. doi:10.1371/journal.pone.0020252

Koopman, W. J., Verkaart, S., Visch, H. J., van der Westhuizen, F. H., Murphy, M. P., van den Heuvel, L. W. P. J., et al. (2005). Inhibition of complex I of the electron transport chain causes O2-. -mediated mitochondrial outgrowth. *Am. J. Physiol. Cell Physiol.* 288, C1440–C1450. doi:10.1152/ajpcell.00607.2004

Kornberg, A., Rao, N. N., and Ault-Riche, D. (1999). Inorganic polyphosphate: a molecule of many functions. *Annu. Rev. Biochem.* 68, 89–125. doi:10.1146/annurev.biochem.68.1.89

Kowalczyk, P., Kaczyńska, K., Kleczkowska, P., Bukowska-Ośko, I., Kramkowski, K., and Sulejczak, D. (2022). The lactoferrin phenomenon-A miracle molecule. *Molecules* 27, 2941. doi:10.3390/molecules27092941

Labberton, L., Long, A. T., Gendler, S. J., Snozek, C. L., Stavrou, E. X., Nickel, K. F., et al. (2018). A flow cytometry-based assay for procoagulant platelet polyphosphate. *Cytom. B Clin. Cytom.* 94, 369–373. doi:10.1002/cyto.b.21492

Lempart, J., and Jakob, U. (2019). Role of polyphosphate in amyloidogenic processes. *Cold Spring Harb. Perspect. Biol.* 11, a034041. doi:10.1101/cshperspect.a034041

Lempart, J., Tse, E., Lauer, J. A., Ivanova, M. I., Sutter, A., Yoo, N., et al. (2019). Mechanistic insights into the protective roles of polyphosphate against amyloid cytotoxicity. *Life Sci. Alliance* 2, e201900486. doi:10.26508/lsa.201900486

Levy, E., El Banna, N., Baïlle, D., Heneman-Masurel, A., Truchet, S., Rezaei, H., et al. (2019). Causative links between protein aggregation and oxidative stress: a review. *Int. J. Mol. Sci.* 20, 3896. doi:10.3390/ijms20163896

Li, N., Ragheb, K., Lawler, G., Sturgis, J., Rajwa, B., Melendez, J. A., et al. (2003). Mitochondrial complex I inhibitor rotenone induces apoptosis through enhancing mitochondrial reactive oxygen species production. *J. Biol. Chem.* 278, 8516–8525. doi:10.1074/jbc.M210432200

Liang, S., Zhu, C., Suo, C., Wei, H., Yu, Y., Gu, X., et al. (2022). Mitochondrion-localized SND1 promotes mitophagy and liver cancer progression through PGAM5. *Front. Oncol.* 12, 857968. doi:10.3389/fonc.2022.857968

Lin, Y. F., Schulz, A. M., Pellegrino, M. W., Lu, Y., Shaham, S., and Haynes, C. M. (2016). Maintenance and propagation of a deleterious mitochondrial genome by the mitochondrial unfolded protein response. *Nature* 533, 416–419. doi:10.1038/nature17989

Liu, Z., Solesio, M. E., Schaffler, M. B., Frikha-Benayed, D., Rosen, C. J., Werner, H., et al. (2019). Mitochondrial function is compromised in cortical bone osteocytes of long-lived growth hormone receptor null mice. *J. Bone Min. Res.* 34, 106–122. doi:10.1002/jbmr.3573

Livak, K. J., and Schmittgen, T. D. (2001). Analysis of relative gene expression data using real-time quantitative PCR and the 2(-Delta Delta C(T)) Method. *Methods* 25, 402–408. doi:10.1006/meth.2001.1262

Lorenz, B., Münkner, J., Oliveira, M. P., Kuusksalu, A., Leitão, J. M., Müller, W. E., et al. (1997). Changes in metabolism of inorganic polyphosphate in rat tissues and human cells during development and apoptosis. *Biochim. Biophys. Acta* 1335, 51–60. doi:10.1016/s0304-4165(96)00121-3

Luhr, M., Torgersen, M. L., Szalai, P., Hashim, A., Brech, A., Staerk, J., et al. (2019). The kinase PERK and the transcription factor ATF4 play distinct and essential roles in autophagy resulting from tunicamycin-induced ER stress. *J. Biol. Chem.* 294, 8197–8217. doi:10.1074/jbc.RA118.002829

Martinus, R. D., Garth, G. P., Webster, T. L., Cartwright, P., Naylor, D. J., Høj, P. B., et al. (1996). Selective induction of mitochondrial chaperones in response to loss of the mitochondrial genome. *Eur. J. Biochem.* 240, 98–103. doi:10.1111/j.1432-1033.1996.0098h.x

McIntyre, B., and Solesio, M. E. (2021). Mitochondrial inorganic polyphosphate (polyP): the missing link of mammalian bioenergetics. *Neural Regen. Res.* 16, 2227–2228. doi:10.4103/1673-5374.310687

Melber, A., and Haynes, C. M. (2018). UPR(mt) regulation and output: a stress response mediated by mitochondrial-nuclear communication. *Cell Res.* 28, 281–295. doi:10.1038/cr.2018.16

Meng, H., Yan, W. Y., Lei, Y. H., Wan, Z., Hou, Y. Y., Sun, L. K., et al. (2019). SIRT3 regulation of mitochondrial quality control in neurodegenerative diseases. *Front. Aging Neurosci.* 11, 313. doi:10.3389/fnagi.2019.00313

Mizzen, L. A., and Welch, W. J. (1988). Characterization of the thermotolerant cell. I. Effects on protein synthesis activity and the regulation of heat-shock protein 70 expression. *J. Cell Biol.* 106, 1105–1116. doi:10.1083/jcb.106.4.1105

Morrissey, J. H., Choi, S. H., and Smith, S. A. (2012). Polyphosphate: an ancient molecule that links platelets, coagulation, and inflammation. *Blood* 119, 5972–5979. doi:10.1182/blood-2012-03-306605

Mouchiroud, L., Houtkooper, R. H., Moullan, N., Katsyuba, E., Ryu, D., Cantó, C., et al. (2013). The NAD(+)/Sirtuin pathway modulates longevity through activation of mitochondrial UPR and FOXO signaling. *Cell* 154, 430–441. doi:10.1016/j.cell.2013.06.016

Muller, W. E. G., Wang, S., Neufurth, M., Kokkinopoulou, M., Feng, Q., Schröder, H. C., et al. (2017). Polyphosphate as a donor of high-energy phosphate for the synthesis of ADP and ATP. *J. Cell Sci.* 130, 2747–2756. doi:10.1242/jcs.204941

Munch, C. (2018). The different axes of the mammalian mitochondrial unfolded protein response. *BMC Biol.* 16, 81. doi:10.1186/s12915-018-0548-x

Nakamura, T., Cho, D. H., and Lipton, S. A. (2012). Redox regulation of protein misfolding, mitochondrial dysfunction, synaptic damage, and cell death in neurodegenerative diseases. *Exp. Neurol.* 238, 12–21. doi:10.1016/j.expneurol.2012.06.032

Nargund, A. M., Fiorese, C. J., Pellegrino, M. W., Deng, P., and Haynes, C. M. (2015). Mitochondrial and nuclear accumulation of the transcription factor ATFS-1 promotes OXPHOS recovery during the UPR(mt). *Mol. Cell* 58, 123–133. doi:10.1016/j.molcel.2015.02.008

Okpara, M. O., Hermann, C., van der Watt, P. J., Garnett, S., Blackburn, J. M., and Leaner, V. D. (2022). A mass spectrometry-based approach for the identification of Kpnβ1 binding partners in cancer cells. *Sci. Rep.* 12, 20171. doi:10.1038/s41598-022-24194-6

Ong, G., and Logue, S. E. (2023). Unfolding the interactions between endoplasmic reticulum stress and oxidative stress. *Antioxidants (Basel)* 12, 981. doi:10.3390/antiox12050981

Osorio, T., Scoma, E. R., Shain, D. H., Melissaratos, D. S., Riggs, L. M., Hambardikar, V., et al. (2022). The Glacier ice worm, mesenchytraeus solifugus, elevates mitochondrial inorganic polyphosphate (PolyP) levels in response to stress. *Biol. (Basel)* 11, 1771. doi:10.3390/biology11121771

Palma, F. R., He, C., Danes, J. M., Paviani, V., Coelho, D. R., Gantner, B. N., et al. (2020). Mitochondrial superoxide dismutase: what the established, the intriguing, and the novel reveal about a key cellular redox switch. *Antioxid. Redox Signal* 32, 701–714. doi:10.1089/ars.2019.7962

Papa, L., and Germain, D. (2014). SirT3 regulates the mitochondrial unfolded protein response. *Mol. Cell Biol.* 34, 699–710. doi:10.1128/MCB.01337-13

Patro, S., Ratna, S., Yamamoto, H. A., Ebenezer, A. T., Ferguson, D. S., Kaur, A., et al. (2021). ATP synthase and mitochondrial bioenergetics dysfunction in alzheimer's disease. *Int. J. Mol. Sci.* 22, 11185. doi:10.3390/ijms222011185

Pellegrino, M. W., Nargund, A. M., and Haynes, C. M. (2013). Signaling the mitochondrial unfolded protein response. *Biochim. Biophys. Acta* 1833, 410–416. doi:10.1016/j.bbamcr.2012.02.019

Rainbolt, T. K., Atanassova, N., Genereux, J. C., and Wiseman, R. L. (2013). Stress-regulated translational attenuation adapts mitochondrial protein import through Tim17A degradation. *Cell Metab.* 18, 908–919. doi:10.1016/j.cmet.2013.11.006

Ruan, L., Zhou, C., Jin, E., Kucharavy, A., Zhang, Y., Wen, Z., et al. (2017). Cytosolic proteostasis through importing of misfolded proteins into mitochondria. *Nature* 543, 443–446. doi:10.1038/nature21695

Schieber, M., and Chandel, N. S. (2014). ROS function in redox signaling and oxidative stress. *Curr. Biol.* 24, R453–R462. doi:10.1016/j.cub.2014.03.034

Schulz, A. M., and Haynes, C. M. (2015). UPR(mt)-mediated cytoprotection and organismal aging. *Biochim. Biophys. Acta* 1847, 1448–1456. doi:10.1016/j.bbabio.2015.03.008

Scoma, E. R., Da Costa, R. T., Leung, H. H., Urquiza, P., Guitart-Mampel, M., Hambardikar, V., et al. (2023). Human prune regulates the metabolism of mammalian inorganic polyphosphate and bioenergetics. *Int. J. Mol. Sci.* 24, 13859. doi:10.3390/ijms241813859

Seo, B. B., Matsuno-Yagi, A., and Yagi, T. (1999). Modulation of oxidative phosphorylation of human kidney 293 cells by transfection with the internal rotenone-insensitive NADH-quinone oxidoreductase (NDI1) gene of *Saccharomyces cerevisiae*. *Biochim. Biophys. Acta* 1412, 56–65. doi:10.1016/s0005-2728(99)00051-1

Sleat, D. E., Della Valle, M. C., Zheng, H., Moore, D. F., and Lobel, P. (2008). The mannose 6-phosphate glycoprotein proteome. *J. Proteome Res.* 7, 3010–3021. doi:10.1021/pr800135v

Sleat, D. E., Ding, L., Wang, S., Zhao, C., Wang, Y., Xin, W., et al. (2009). Mass spectrometry-based protein profiling to determine the cause of lysosomal storage diseases of unknown etiology. *Mol. Cell Proteomics* 8, 1708–1718. doi:10.1074/mcp.M900122-MCP200

Slimen, I. B., Najar, T., Ghram, A., Dabbebi, H., Ben Mrad, M., and Abdrabbah, M. (2014). Reactive oxygen species, heat stress and oxidative-induced mitochondrial damage. A review. *Int. J. Hyperth.* 30, 513–523. doi:10.3109/02656736.2014.971446

Solesio, M. E., Demirkhanyan, L., Zakharian, E., and Pavlov, E. V. (2016a). Contribution of inorganic polyphosphate towards regulation of mitochondrial free calcium. *Biochim. Biophys. Acta* 1860, 1317–1325. doi:10.1016/j.bbagen.2016.03.020

Solesio, M. E., Elustondo, P. A., Zakharian, E., and Pavlov, E. V. (2016b). Inorganic polyphosphate (polyP) as an activator and structural component of the mitochondrial permeability transition pore. *Biochem. Soc. Trans.* 44, 7–12. doi:10.1042/BST20150206

Solesio, M. E., Garcia Del Molino, L. C., Elustondo, P. A., Diao, C., Chang, J. C., and Pavlov, E. V. (2020). Inorganic polyphosphate is required for sustained free mitochondrial calcium elevation, following calcium uptake. *Cell Calcium* 86, 102127. doi:10.1016/j.ceca.2019.102127

Solesio, M. E., Peixoto, P. M., Debure, L., Madamba, S. M., de Leon, M. J., Wisniewski, T., et al. (2018). Carbonic anhydrase inhibition selectively prevents amyloid β neurovascular mitochondrial toxicity. *Aging Cell* 17, e12787. doi:10.1111/acel.12787

Solesio, M. E., Prime, T. A., Logan, A., Murphy, M. P., Del Mar Arroyo-Jimenez, M., Jordán, J., et al. (2013a). The mitochondria-targeted anti-oxidant MitoQ reduces aspects of mitochondrial fission in the 6-OHDA cell model of Parkinson's disease. *Biochim. Biophys. Acta* 1832, 174–182. doi:10.1016/j.bbadis.2012.07.009

Solesio, M. E., Saez-Atienzar, S., Jordan, J., and Galindo, M. F. (2013b). 3-Nitropropionic acid induces autophagy by forming mitochondrial permeability transition pores rather than activating the mitochondrial fission pathway. *Br. J. Pharmacol.* 168, 63–75. doi:10.1111/j.1476-5381.2012.01994.x

Solesio, M. E., Xie, L., McIntyre, B., Ellenberger, M., Mitaishvili, E., Bhadra-Lobo, S., et al. (2021). Depletion of mitochondrial inorganic polyphosphate (polyP) in mammalian cells causes metabolic shift from oxidative phosphorylation to glycolysis. *Biochem. J.* 478, 1631–1646. doi:10.1042/BCJ20200975

Squier, T. C. (2001). Oxidative stress and protein aggregation during biological aging. *Exp. Gerontol.* 36, 1539–1550. doi:10.1016/s0531-5565(01)00139-5

Tanida, I., Ueno, T., and Kominami, E. (2008). LC3 and autophagy. *Methods Mol. Biol.* 445, 77–88. doi:10.1007/978-1-59745-157-4_4

Teixeira, J., Basit, F., Swarts, H. G., Forkink, M., Oliveira, P. J., Willems, P. H. G. M., et al. (2018). Extracellular acidification induces ROS- and mPTP-mediated death in HEK293 cells. *Redox Biol.* 15, 394–404. doi:10.1016/j.redox.2017.12.018

Teske, B. F., Fusakio, M. E., Zhou, D., Shan, J., McClintick, J. N., Kilberg, M. S., et al. (2013). CHOP induces activating transcription factor 5 (ATF5) to trigger apoptosis in response to perturbations in protein homeostasis. *Mol. Biol. Cell* 24, 2477–2490. doi:10.1091/mbc.E13-01-0067

Thorne, N. J., and Tumbarello, D. A. (2022). The relationship of alpha-synuclein to mitochondrial dynamics and quality control. *Front. Mol. Neurosci.* 15, 947191. doi:10.3389/fnmol.2022.947191

Tsai, S. F., Tao, M., Ho, L. I., Chiou, T. W., Lin, S. Z., Su, H. L., et al. (2017). Isochaihulactone-induced DDIT3 causes ER stress-PERK independent apoptosis in glioblastoma multiforme cells. *Oncotarget* 8, 4051–4061. doi:10.18632/oncotarget.13266

Tseng, A. H., Shieh, S. S., and Wang, D. L. (2013). SIRT3 deacetylates FOXO3 to protect mitochondria against oxidative damage. *Free Radic. Biol. Med.* 63, 222–234. doi:10.1016/j.freeradbiomed.2013.05.002

Voos, W. (2013). Chaperone-protease networks in mitochondrial protein homeostasis. *Biochim. Biophys. Acta* 1833, 388–399. doi:10.1016/j.bbamcr.2012.06.005

Weids, A. J., Ibstedt, S., Tamas, M. J., and Grant, C. M. (2016). Distinct stress conditions result in aggregation of proteins with similar properties. *Sci. Rep.* 6, 24554. doi:10.1038/srep24554

Wilkening, A., Rub, C., Sylvester, M., and Voos, W. (2018). Analysis of heat-induced protein aggregation in human mitochondria. *J. Biol. Chem.* 293, 11537–11552. doi:10.1074/jbc.RA118.002122

Wu, Y., Williams, E. G., Dubuis, S., Mottis, A., Jovaisaite, V., Houten, S. M., et al. (2014). Multilayered genetic and omics dissection of mitochondrial activity in a mouse reference population. *Cell* 158, 1415–1430. doi:10.1016/j.cell.2014.07.039

Xie, L., and Jakob, U. (2019). Inorganic polyphosphate, a multifunctional polyanionic protein scaffold. *J. Biol. Chem.* 294, 2180–2190. doi:10.1074/jbc.REV118.002808

Yoneda, T., Benedetti, C., Urano, F., Clark, S. G., Harding, H. P., and Ron, D. (2004). Compartment-specific perturbation of protein handling activates genes encoding mitochondrial chaperones. *J. Cell Sci.* 117, 4055–4066. doi:10.1242/jcs.01275

Yoo, N. G., Dogra, S., Meinen, B. A., Tse, E., Haefliger, J., Southworth, D. R., et al. (2018). Polyphosphate stabilizes protein unfolding intermediates as soluble amyloid-like oligomers. *J. Mol. Biol.* 430, 4195–4208. doi:10.1016/j.jmb.2018.08.016

Yoshii, S. R., Kishi, C., Ishihara, N., and Mizushima, N. (2011). Parkin mediates proteasome-dependent protein degradation and rupture of the outer mitochondrial membrane. *J. Biol. Chem.* 286, 19630–19640. doi:10.1074/jbc.M110.209338

Youle, R. J., and Narendra, D. P. (2011). Mechanisms of mitophagy. *Nat. Rev. Mol. Cell Biol.* 12, 9–14. doi:10.1038/nrm3028

Yu, X., Xu, X., Dong, W., Yang, C., Luo, Y., He, Y., et al. (2022). DDIT3/CHOP mediates the inhibitory effect of ER stress on chondrocyte differentiation by AMPKα-SIRT1 pathway. *Biochim. Biophys. Acta Mol. Cell Res.* 1869, 119265. doi:10.1016/j.bbamcr.2022.119265

Zhang, J., Xiang, H., Liu, J., Chen, Y., and Liu, B. (2020). Mitochondrial Sirtuin 3: new emerging biological function and therapeutic target. *Theranostics* 10, 8315–8342. doi:10.7150/thno.45922

Zhang, Y., Wu, Y., Zhang, M., Li, Z., Liu, B., Liu, H., et al. (2023). Synergistic mechanism between the endoplasmic reticulum and mitochondria and their crosstalk with other organelles. *Cell Death Discov.* 9, 51. doi:10.1038/s41420-023-01353-w

Zhao, Q., Wang, J., Levichkin, I. V., Stasinopoulos, S., Ryan, M. T., and Hoogenraad, N. J. (2002). A mitochondrial specific stress response in mammalian cells. *EMBO J.* 21, 4411–4419. doi:10.1093/emboj/cdf445

frontiers | Frontiers in Molecular Biosciences

TYPE Review
PUBLISHED 12 August 2024
DOI 10.3389/fmolb.2024.1455817

OPEN ACCESS

EDITED BY
Emily Sontag,
Marquette University, United States

REVIEWED BY
Carmen Ruger-Herreros,
University of Seville, Spain
Cassandra Terry,
London Metropolitan University,
United Kingdom

*CORRESPONDENCE
Jana Schepers,
jana.schepers@uni-mainz.de
Christian Behl,
cbehl@uni-mainz.de

†These authors share first authorship

RECEIVED 27 June 2024
ACCEPTED 26 July 2024
PUBLISHED 12 August 2024

CITATION
Schepers J, Löser T and Behl C (2024) Lipids and α-Synuclein: adding further variables to the equation.
Front. Mol. Biosci. 11:1455817.
doi: 10.3389/fmolb.2024.1455817

Lipids and α-Synuclein: adding further variables to the equation

Jana Schepers*†, Timo Löser† and Christian Behl*

The Autophagy Lab, Institute of Pathobiochemistry, University Medical Center of the Johannes Gutenberg University Mainz, Mainz, Germany

Aggregation of alpha-Synuclein (αSyn) has been connected to several neurodegenerative diseases, such as Parkinson's disease (PD), dementia with Lewy Bodies (DLB), and multiple system atrophy (MSA), that are collected under the umbrella term *synucleinopathies*. The membrane binding abilities of αSyn to negatively charged phospholipids have been well described and are connected to putative physiological functions of αSyn. Consequently, αSyn-related neurodegeneration has been increasingly connected to changes in lipid metabolism and membrane lipid composition. Indeed, αSyn aggregation has been shown to be triggered by the presence of membranes *in vitro*, and some genetic risk factors for PD and DLB are associated with genes coding for proteins directly involved in lipid metabolism. At the same time, αSyn aggregation itself can cause alterations of cellular lipid composition and brain samples of patients also show altered lipid compositions. Thus, it is likely that there is a reciprocal influence between cellular lipid composition and αSyn aggregation, which can be further affected by environmental or genetic factors and ageing. Little is known about lipid changes during physiological ageing and regional differences of the lipid composition of the aged brain. In this review, we aim to summarise our current understanding of lipid changes in connection to αSyn and discuss open questions that need to be answered to further our knowledge of αSyn related neurodegeneration.

KEYWORDS

alpha-Synuclein, Parkinson's disease, DLB, MSA, membrane lipids, lipid metabolism

1 Introduction

With approximately 50% of the dry weight of the human brain being lipids, it has one of the highest lipid contents in the human body (Hamilton et al., 2007; Bruce et al., 2017). Strikingly, lipid changes in Alzheimer's disease (AD) have already been described by Alois Alzheimer upon discovery (Alzheimer et al., 1995) but have not been consequently investigated at that time, perhaps partly due to the lack of adequate methodology. Nowadays, changes in lipid metabolism of the brain are implicated in several neurodegenerative diseases such as, among others, AD, Parkinson's disease (PD), and amyotrophic lateral sclerosis (ALS) (Wei et al., 2023). For example, it was shown that the lipid metabolism in AD brain tissue is changed, including changes in the fatty acid composition (Nasaruddin et al., 2016; Yin, 2023), accumulation of cholesterol (Xiong et al., 2008; Ahmed et al., 2024), and the presence of the lipoprotein APOE4 isoform as risk factor for AD (Zhu et al., 2015; Lefterov et al., 2019; Miranda et al., 2022; Pires and Rego, 2023; Lozupone and Panza, 2024).

In this review, we focus on α-Synuclein (αSyn) and its growing connection to lipids, not only in the context of its putative physiological functions but also during neurodegenerative

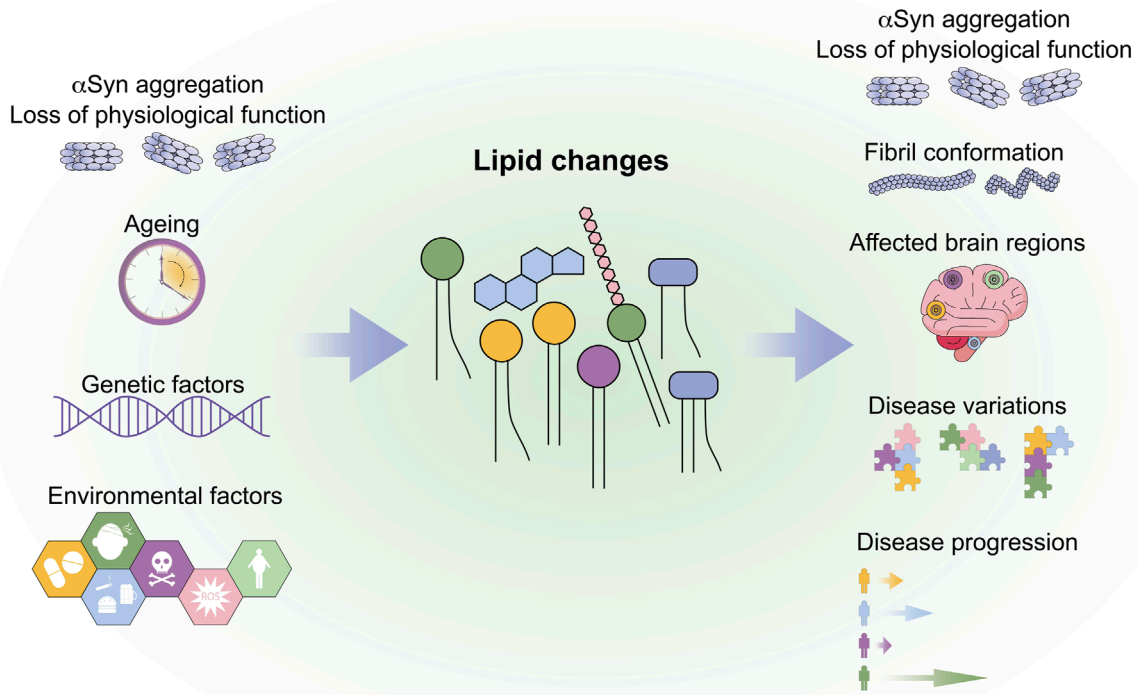

GRAPHICAL ABSTRACT
The graphical abstract summarises factors that might lead to lipid changes and possible influences of lipid changes on synucleinopathies.

processes. Aggregation of αSyn in different neuronal tissues is associated with different neurodegenerative diseases that are collected under the term synucleinopathies. These include, among others, PD, dementia with Lewy Bodies (DLB), and multiple system atrophy (MSA) (Calabresi et al., 2023). To understand disease formation and progression, a lot of successful research has already been conducted, connecting αSyn-aggregation and neurodegeneration to mitochondrial dysfunction and oxidative stress, lysosomal dysfunction, inflammatory processes, and a perturbed Ca^{2+} homeostasis and excitotoxicity (Rocha et al., 2018; Wang et al., 2020; Sahoo et al., 2022; Lyra et al., 2023; Forloni, 2023; Rcom-H'cheo-Gauthier et al., 2016). However, more recently, the link between PD pathogenesis and lipids has gained more and more attention (reviewed in (Alecu and Bennett, 2019; Fanning et al., 2020; Battis et al., 2023; Flores-Leon and Outeiro, 2023)). For example, it was shown that Lewy Bodies (LBs) contain an abundancy of different membranes (Shahmoradian et al., 2019).

We focus on lipid changes and its impact on synucleinopathies, summarising how changes in membrane lipids might contribute to disease progression and whether differences in the membrane composition could contribute to differences in aggregate conformation and localisation. We summarise putative physiological functions of αSyn in connection to membrane lipids as well as lipid-associated processes and discuss lipid changes connected to PD, DLB, and MSA. It is important to keep in mind that, while these three diseases are distinguishable from each other, especially PD and DLB share overlapping disease phenotypes and risk factors (Calabresi et al., 2023). Thus, we compare common factors connecting lipid metabolism that might play a role in all three synucleinopathies but also discuss differences.

As ageing is known to be connected to neurodegenerative synucleinopathies (Poewe et al., 2022; Calabresi et al., 2023), we further discuss current knowledge of changes of the lipid composition of the aged brain. To date, little is known about lipid changes in the brain during physiological ageing even though it might be possible that changes in the regional lipid composition of the brain might explain why different brain regions are affected in different patients. Whether synucleinopathies are induced by age-related lipid changes in the brain remains unclear.

It is known that αSyn forms amyloid fibrils that are rich in β-sheets during pathological processes. During amyloid fibril formation, the structurally disordered αSyn monomers oligomerise to form aggregates that grow into β-sheet rich *protofibrils*. These protofibrils grow to form long amyloid fibrils, that can be detected in LBs (Ghosh et al., 2017; Alam et al., 2019; Mehra et al., 2021). It is known that these amyloid fibrils can adapt different conformations, referred to as *strains* (Bousset et al., 2013). In this review, we address aggregation formation of αSyn in the presence of lipids and discuss how conformational variations of αSyn *strains*, might, to a certain extent, depend on the lipid environment.

To date, there are no disease-modifying treatments available for PD, DLB, and MSA. For PD, the use of L-Dopa to restore

dopaminergic function, developed in the 1960s (Cotzias et al., 1967), is still the most common treatment (Fernagut et al., 2014; Stoker and Barker, 2020). Developing alternative treatments and ways to detect pathological events earlier is urgently needed. Thus, understanding the connection between lipid changes, αSyn aggregation, and disease progression has the potential to open new, possible ways of disease-modification and earlier detection.

2 Alpha-Synuclein

αSyn is a 14 kDa protein of the small synuclein protein family, which was initially described in the Pacific electric ray *Tetronarce californica* in 1988 and is evolutionary highly conserved (Figure 1A) (Maroteaux et al., 1988; Zhu and Fink, 2003). In humans, the *SNCA* gene, which spans five canonical exons and is located on the PARK1/4 locus of chromosome 4, encodes αSyn. The full-length protein consists of 140 amino acids (aa) and can be divided into three domains (Figure 1B) (Emamzadeh, 2016).

Residues 1–60 form the positively charged N-terminus, which, because of its amphipathic nature, allows interactions with membrane lipids (Bartels et al., 2010; Pirc and Ulrih, 2015). The high amount of lysine residues conducts interactions with anionic lipids, such as phosphatidic acid, phosphatidylinositol, as well as highly negative phosphoinositide phosphates (Middleton and Rhoades, 2010; Jacob et al., 2021a). Upon membrane binding, the coiled N-terminus transforms into a α-helical structure (Figure 1C) (Bussell and Eliezer, 2003; Bodner et al., 2009). Besides an electrostatic interplay, the robustness of this membrane-binding α-helix is strongly dependent on the amount of lipid molecules per protein (Shvadchak et al., 2011; Roeters et al., 2023). The transition from random coil to helix is facilitated by multiple, imperfect repeats of 11 aa, containing a highly conserved KTKEGV motif. Lipid-binding motifs with high similarity were found in apolipoproteins, such as ApoA-I, which also forms α-helices upon membrane binding (Segrest et al., 1990; George et al., 1995). Two of these KTKEGV repeats in αSyn also reach into the second protein domain, the 35 aa long non-amyloid-β component (NAC) (Ueda et al., 1993). In early studies, this domain was found to be prone to aggregation, presumably because of an 11-residue core region, the so-called NACore. Its β-strand structure tends to stack into multiple β-sheets and induces amyloidogenic protein aggregation (Rodriguez et al., 2015; Tuttle et al., 2016; Xu et al., 2016). *In vitro* studies revealed numerous factors that affect the kinetics of αSyn fibril formation. Endogenous factors for αSyn nucleation include protein modifications and truncations, as well as the presence of lipids and membranes (Galvagnion et al., 2015; Ghosh et al., 2017). Environmental factors, such as metals, pesticides, pH, and temperature changes were also found to promote *in vitro* fibrillation (Morris and Finke, 2009; Ghosh et al., 2017). The third protein domain is the anionic C-terminus, which consists of the remaining 46 aa. It is a proline-rich, intrinsically disordered region (random coil) in which around one third of residues are acidic. This comparatively flexible region was found to be a target for multiple post-translational modifications (PTMs), and the central domain for protein-protein interactions (Cole et al., 2002; Oueslati et al., 2010; Manzanza et al., 2021). The majority of investigated PTMs introduced in αSyn were found to inhibit protein function and enhance its susceptibility to pathological aggregation (Zhang et al., 2019). However, recent studies have identified several physiological functions of C-terminal modifications (Figure 1B). For instance, SUMOylation of lysine residues K96 and K102 is required for the nuclear translocation of αSyn (Krumova et al., 2011; Ryu et al., 2019). Additionally, phosphorylation of tyrosine Y125 has been shown to modulate the interaction between αSyn and phospholipase D in human embryonic kidney cells (HEK-293) (Ahn et al., 2002). Recently, it has been shown that phosphorylation at serine S129, which is predominantly related to αSyn pathology, might also regulate αSyn function in healthy cells (Ramalingam et al., 2023).

Exclusively found in vertebrates, αSyn is localised in several different regions of the brain, such as the *substantia nigra*, the cerebral cortex, and hippocampus, among others (Taguchi et al., 2016). Localisation of αSyn in presynaptic terminals as well as its co-localisation with synaptic vesicles (Maroteaux et al., 1988; Bayer et al., 1999; Taguchi et al., 2016) led researchers to believe that αSyn might play an important role in neurotransmission. In the following years, many studies helped elucidate the transport route of αSyn from its synthesis in the cell soma to presynaptic axon terminals and its interactions with different proteins and whole organelles.

3 From synthesis to function – interactions of αSyn across the neuron

Since αSyn lacks a canonical translocon sequence, *de novo* biosynthesis of αSyn is most likely directed into the cytoplasm. In the neuronal soma, αSyn is able to interact with a variety of organelles (reviewed in (Bernal-Conde et al., 2019)). Localisation into the nucleus is facilitated via C-terminal SUMOylation and subsequent translocation by karyopherin α6 (Ryu et al., 2019). Because of its small size (<40 kDa), diffusion through the nuclear pore complex inside the nucleus might also be possible (Timney et al., 2016). αSyn can affect DNA persistence length, i.e., physical stiffness, and accessibility for transcription factors, either by direct electrostatic interactions with the DNA backbone, or indirectly, by retaining epigenetic proteins (e.g., histone-modifying enzymes) from entering the nucleus (Desplats et al., 2011; Jiang et al., 2018; Surguchov, 2023). It was observed that these interactions influence DNA condensation through H3K9 methylation and altered histone acetylation (Kontopoulos et al., 2006; Sugeno et al., 2016).

Outside the nucleus, αSyn is found at the outer mitochondrial membrane as well as in mitochondrial sub-compartments (Cole et al., 2008; Devi et al., 2008; Georgas et al., 2009; Menges et al., 2017). At the outer membrane, αSyn suppresses mitochondrial fusion events, which is suggested to benefit the transport of small mitochondrial fragments across the axon (Nakamura et al., 2011; Saxton and Hollenbeck, 2012; Bernal-Conde et al., 2020). However, another study found that drastically changed fusion-fission rates, induced by αSyn overexpression, impair axonal transport (Pozo Devoto et al., 2017). Once inside the mitochondrion, the largest proportion of αSyn accumulates at the inner mitochondrial membrane (IMM), where it most likely interacts with the highly anionic mitochondrial signature phospholipid cardiolipin (Cole et al., 2008; Dudek, 2017; Ryan et al., 2018). This IMM-localisation was mainly found around the electron

10.3389/fmolb.2024.1455817

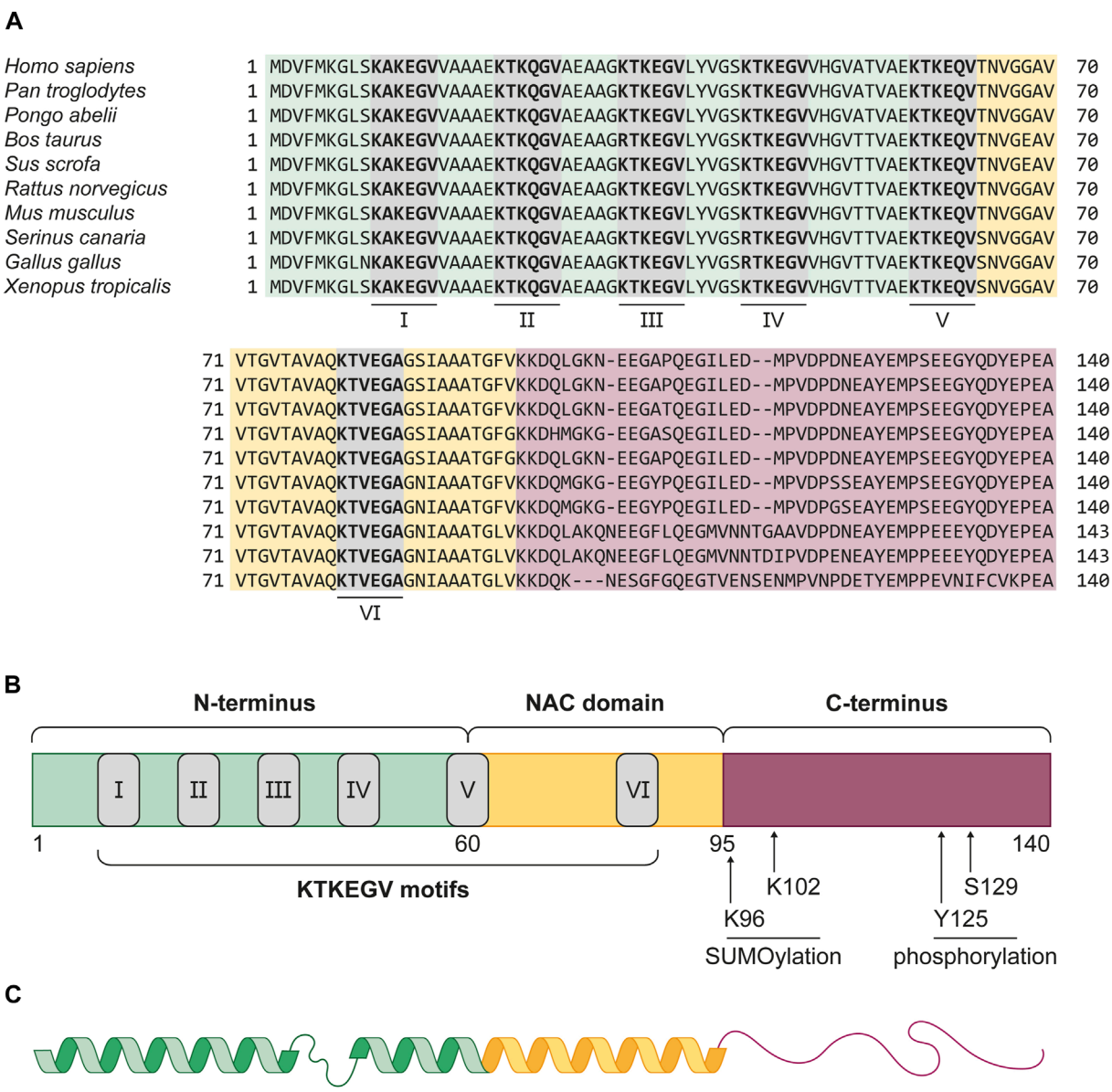

FIGURE 1
Evolutionary conservation and structure of αSyn. **(A)** Protein sequence alignment of αSyn in vertebrae species *Homo sapiens* (human), *Pan troglodytes* (chimpanzee), *Pongo abelii* (sumatran orangutan), *Bos taurus* (cattle), *Sus scrofa* (wild boar), *Rattus norvegicus* (common rat), *Mus musculus* (house mouse), *Serinus canaria* (atlantic canary), *Gallus gallus* (chicken), and *Xenopus tropicalis* (western clawed frog). The alignment shows a high conservation of the protein across all listed species, especially in the amphipathic N-terminus (green) and NAC domain (yellow). The six KTKEGV motifs (grey boxes), numbered I-VI, show close similarity, with only two differences. In cattle, the first arginine residue in the third motif (III) replaces the chemically very similar lysine residue. The same is observed for the first aa of the fourth KTKEGV motif (IV) in both bird species. In birds, the αSyn protein is also three aa longer than in the other listed organisms. **(B)** αSyn can be structurally divided into the amphipathic N-terminus (green, 1–60 aa), the aggregation promoting NAC-domain (yellow, 61–95 aa) and the acidic C-terminus (red, 96–140 aa) which facilitates protein-protein interactions. The grey boxes depict the KTKEGV motifs, which promote membrane association. At the C-terminus, four post-translational modifications, K96 and K102 SUMOylation, as well as Y125 and S129 phosphorylation, are displayed. These post-translational modifications are suggested to serve physiological functions of αSyn inside the cell. Phosphorylation at S129 is also associated with αSyn pathology. **(C)** Representation αSyn's secondary structure in the presence of membrane lipids. The N-terminus and NAC domain form an interrupted α-helix which binds to highly curved membranes. The proline-rich C-terminus is considered as intrinsically disordered and flexible.

transport chain (ETC), which is most likely due to its cardiolipin-rich environment (Paradies et al., 2014). The physiological function of αSyn at the ETC is not fully understood, but several lines of evidence suggest that αSyn might stabilise complex I-III electron transfer (Ellis et al., 2005; Devi et al., 2008).

One of the most important processes that αSyn interferes with is vesicular trafficking between the endoplasmic reticulum (ER), the Golgi apparatus (Golgi), and the endosomal shuttle network (Thayanidhi et al., 2010; Teixeira et al., 2021). In several PD models, αSyn was found to interact with membrane fusion

factor Rab1 and its homologues, which are associated with ER-Golgi trafficking (Cooper et al., 2006). While the study from Cooper et al. (2006) mainly focused on the detrimental interplay of αSyn with proteins involved in ER-GA transport, previous studies suggested a physiological function of αSyn for *soluble N-ethylmaleimide-sensitive-factor attachment receptor* (SNARE)-dependent membrane fusion events (Burré et al., 2010; Yoo et al., 2023). Accordingly, experiments in *S. cerevisiae* expressing human αSyn showed that the Rab1 homologue Ypt1 colocalises with cytosolic αSyn-accumulations (Soper et al., 2011). Human wild-type αSyn also co-localises with several other yeast Rab proteins, involved in intra-Golgi trafficking, such as Ypt6, Ypt31, and Ypt32 (Soper et al., 2011). In the endo-lysosomal system, αSyn was found to be in close proximity to transport vesicles (Lee et al., 2011; Huang et al., 2019) as well as important factors, such as RAB5A, RAB7, and RAB11A, which play a role in endosomal trafficking (Hasegawa et al., 2011). αSyn being involved in this pathway is supported by the high amounts of anionic, phosphorylated phosphoinositides that comprise endosomal transport vesicles, to which αSyn demonstrates an exceptionally high affinity (Jacob et al., 2021b; Choong et al., 2023).

One of the earliest discovered key functions of αSyn is its involvement in synaptic vesicle trafficking and exocytosis at the pre-synapse (reviewed in (Sharma and Burré, 2023; Nordengen and Morland, 2024)). In fact, the majority of αSyn is found at pre-synaptic axon terminals in adult animals (Maroteaux et al., 1988; Hsu et al., 1998). In order to reach its destination, αSyn is transported along the axon via the slow component b (SCb) (Tang et al., 2012). Besides αSyn, SCb was shown to mainly transport proteins critical for axon growth and regeneration, as well as synaptic function (Roy et al., 2007). Interestingly, the translocation of αSyn to the synapse is also dependent on its association with lipid rafts (Fortin et al., 2004).

At the axon terminal, αSyn was found to play an important, but not essential, role in the life cycle of synaptic vesicles (SV), primarily, but not exclusively, in dopaminergic neurons (reviewed in (Nordengen and Morland, 2024)). During preparation of SV secretion, αSyn participates in different steps, such as monoamine transmitter loading, vesicle docking and - priming (Pifl et al., 2014; Huang et al., 2019). In vesicle priming, αSyn was shown to interact with different proteins that facilitate the fusion of SV and the plasma membrane, e.g., SNARE proteins and the previously mentioned Rab proteins (Burré et al., 2010; Lou et al., 2017). In these processes, the N-terminus of αSyn is proposed to remain in close proximity to the SV membranes, due to its high affinity to anionic and highly curved membranes, while the C-terminus is thought to interact with other proteins (Jensen et al., 1999; Payton et al., 2004; McFarland et al., 2008). Recent data in different cell types show that the localisation of αSyn to the plasma membrane is highly dependent on the abundance of phosphatidylinositol polyphosphates, namely, phosphatidylinositol bisphosphates (PIP2) and phosphatidylinositol trisphosphates (PIP3) (Jacob et al., 2021b). Subsequently, αSyn is also involved in the fusion of SVs and, thereby, the release of neurotransmitters. The presence of αSyn was shown to expand the exocytotic fusion pore at the synapse, favouring full membrane fusion over the faster "kiss-and-run" mechanism (Khounlo et al., 2021). In order to keep the SV pools balanced, αSyn was suggested to aid with endocytosis by introducing higher curvature to the synaptic plasma membrane (Westphal and Chandra, 2013).

αSyn demonstrates a high variety of localisations and putative physiological functions across the neuron, from soma to axon terminal (Summarised in Figure 2). In PD and LBD, aggregated forms of αSyn that contribute to disease pathology were found to be in close proximity to the beforementioned organelles and pathways (Miraglia et al., 2018; Moors et al., 2021). This underlines the importance of a strict regulation of putative physiological functions of αSyn in affected cellular compartments. Even though interactions with multiple organelles and transport pathways may appear arbitrary at first glance, a shared characteristic unites these diverse localisations of αSyn. αSyn seems to play a key role in general vesicle organisation and membrane fusion events. This was especially observed in highly curved membrane regions rich in anionic phospholipids, such as SVs, general endolysosomal vesicles, or even mitochondria with externalised cardiolipin (Ryan et al., 2018). Given that the above described αSyn-membrane interactions play such a considerable role in αSyn's putative impact on a variety of neuronal functions, dysregulation of these interactions might be likely to contribute to the generation and/or progression of αSyn related neurodegenerative diseases.

4 Synucleinopathies and lipids

4.1 PD and lipid changes

The most common synucleinopathy is PD, which is commonly associated with neurodegeneration of dopaminergic neurons in the substantia nigra (SN) and the formation of LBs (Kalia and Lang, 2015). Analyses of patient tissue have revealed that the lipid composition of the brain is changed. These changes include, for example, an increase of diacylglycerols (DAGs) in the frontal cortex of PD patients (Wood et al., 2018). Lipidomic analysis of the visual cortex of PD patients revealed a dramatically altered lipid profile when compared to control brains. These changes include a decrease of unsaturated phosphatidylethanolamine (PE) and differences in the amount of phosphatidylinositol (PI), depending on its fatty acid (FA) chain lengths (Cheng et al., 2011). Similar observations were made when lipidomic analyses were performed upon expression of αSyn in several model systems, where an increase in DAG together with a decrease of several membrane lipid species such as phosphatidylserine (PS) and PI was found (Fanning et al., 2019). Taken together, this suggests that αSyn (-aggregation) may change the lipid composition of the brain.

It is also known that αSyn-lipid interactions depend on the membrane lipid composition. For example, it was shown that increasing the amount of negatively charged gangliosides (GMs) of small unilamellar vesicles (SUVs) *in vitro* increased membrane binding of αSyn (Man et al., 2021). Further *in vitro* studies revealed that the amount of anionic lipids is crucial for αSyn-membrane interactions (Davidson et al., 1998; Andersson et al., 2024) and that more αSyn is able to bind to anionic deformable SUVs, showing that the charge, the flexibility, and the curvature of membranes influence αSyn binding (Andersson et al., 2024; Makasewicz et al., 2024). Furthermore, the interaction of αSyn with membrane lipids was proposed to contribute to aggregate formation (Auluck et al., 2010;

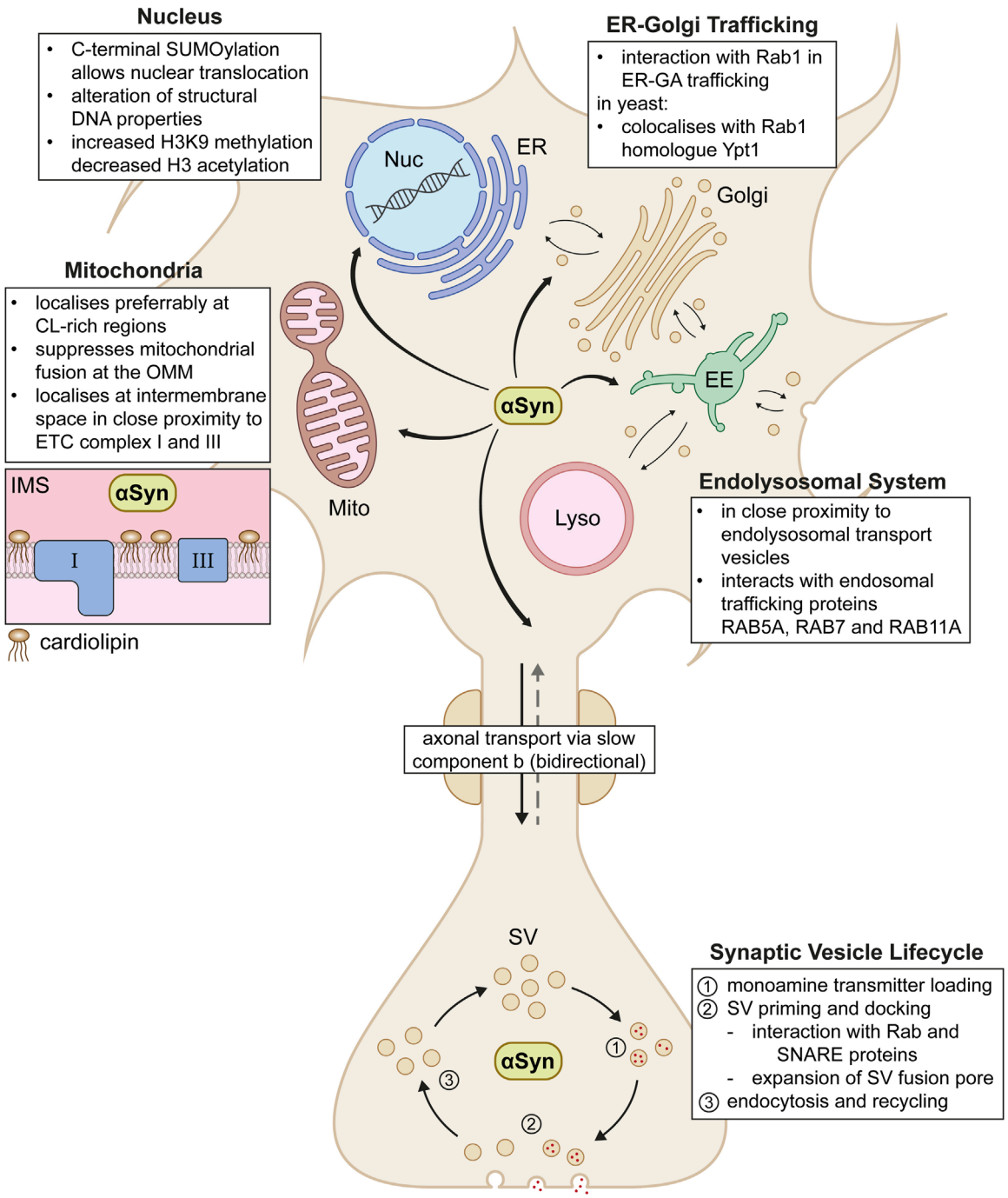

FIGURE 2
Proposed physiological interactions of αSyn across the neuron. In the cell, αSyn acts in various compartments including the nucleus (Nuc), endoplasmic reticulum (ER), Golgi apparatus (Golgi), early endosomes (EE), lysosomes (Lyso) and mitochondria (Mito). In mitochondria, αSyn localises in the intermembrane space (IMS) in close proximity to electron chain complex I and III (box on the left). αSyn shuttles between soma and synapse via axonal transport via the slow component b. At the synapse, αSyn plays a role in various steps of the entire life cycle of synaptic vesicles (SV). Further interaction details are depicted as text boxes in the figure.

Galvagnion et al., 2015). However, other studies have shown that this interaction can prevent αSyn fibril formation (Zhu and Fink, 2003; Martinez et al., 2007). It is important to note that these studies have all been conducted *in vitro* and in correlation with different lipid compositions. While the ratio of PS, phosphatidylcholine (PC), and PE contributed to amyloid aggregation (Galvagnion et al., 2015), interaction with the ganglioside GM1 inhibited it (Martinez et al., 2007). Indeed, GM1 levels were shown to be decreased in brains

of PD patients (Hadaczek et al., 2015). Studies on mice deficient for the GM2-synthase, were shown to exhibit PD-like symptoms, which could be alleviated by treatment with LIGA-20, an analogue of GM1 that is able to cross the blood brain barrier (BBB) (Wu et al., 2011). Therefore, the overall lipid composition might not only have a great influence on αSyn membrane interaction but also on αSyn oligomerisation and fibril formation, by either inducing or preventing it. Interestingly, PD-associated mutations of αSyn have been shown to exhibit differential membrane interaction properties (Battis et al., 2023).

Furthermore, some genetic risk factors for PD that are involved in membrane lipid metabolism continue to be identified. One of the most prominent examples are mutations of the *GBA1* gene, coding for the hydrolase glucocerebrosidase (GCase) (Aharon-Peretz et al., 2004; Neumann et al., 2009; Galper et al., 2022; Flores-Leon and Outeiro, 2023). *GBA1* mutations include T369M, T297S, and E326K, among others and cause a reduced activity of the lysosomal GCase (Dos Santos et al., 2024). This is associated with an increased risk for PD (Flores-Leon and Outeiro, 2023; Dos Santos et al., 2024). The GCase hydrolyses glucoceramide to glucose and ceramide in the lysosome and, thus, plays a role in sphingolipid metabolism (Gegg et al., 2022). However, the exact mechanisms of how this leads to PD are still unclear. It is thought that a reduced activity of the GCase inhibits lysosomal function and, thereby, leads to an increased amount of protein aggregation, including aggregation of αSyn (Johnson et al., 2020). It was further shown that αSyn aggregation depends on the FA chain length of GCase substrates; only FA chains longer than C22 induced aggregation (Fredriksen et al., 2021). Conversely, GCase activation enhanced lysosomal activity, which induced clearance of αSyn aggregates (Mazzulli et al., 2016). Interestingly, homozygous mutations of *GBA1* are known to cause Gaucher's disease (GD), in which symptoms overlap with symptoms known in PD (Johnson et al., 2020).

Another risk factor for PD that is associated with lipid metabolism is Synaptojanin 1 (SYNJ1), which is a PIP-phosphatase (Krebs et al., 2013; Quadri et al., 2013; Olgiati et al., 2014; Ben Romdhan et al., 2018; Schechter and Sharon, 2021). SYNJ1 is part of several pathways involving vesicular structures such as endocytosis (Perera et al., 2006), endosomal trafficking (Watanabe et al., 2018), and autophagy (George et al., 2016; Vanhauwaert et al., 2017). Mutations in SYNJ1's PIP-phosphatase domain but also other domains are associated with an increased risk for developing PD (Ben Romdhan et al., 2018; Taghavi et al., 2018; Schechter and Sharon, 2021). Again, the exact mechanisms that cause an increased risk for PD are still unclear. It is thought that synaptic dysfunction, caused by SYNJ1 mutations, may trigger neurotoxicity (Brooker et al., 2024). Additionally, mutations of *SH3GL2*, which encodes for the SYNJ1 binding partner endophilin A1, have also been identified as risk factors for PD (Nalls et al., 2019; Brooker et al., 2024). Similarly, mutations in *LRRK2*, a protein kinase that phosphorylates SYNJ1 and is involved in endocytosis (Pan et al., 2017; Schechter and Sharon, 2021) and autophagy (reviewed in (Madureira et al., 2020)) have been identified as risk factors for PD (Summarised in Table 1). Again, detailed molecular mechanisms remain unclear. Taken together, dysregulation of lipid homeostasis, whether directly or indirectly, is likely to affect cellular function and, thus, contributes to PD formation and/or progression.

As most data on αSyn and lipid homeostasis exist in the context of PD, little is known about lipid changes, maybe even in other brain regions, that may also be altered in other synucleinopathies. The question here is whether similar changes in lipid composition might be a common factor in all synucleinopathies and whether changes occur in different regions of the brain, which might explain the differences between the synucleinopathies. Lastly, whether and how the lipid composition influences aggregate conformation known to vary in different synucleinopathies still needs to be investigated.

4.2 DLB and lipid changes

Formation of LBs and a loss of dopaminergic neurons of the SN, together with a reduction of cortical neurons and neurons of the limbic system, are commonly associated with DLB (Outeiro et al., 2019). In DLB, LBs can also be found in different regions of the brain besides the SN, such as the neocortex and the limbic system (Outeiro et al., 2019). There is still very little data connecting changes in lipid homeostasis to DLB but a few genetic risk factors are known that overlap with risk factors for PD.

The most common genetic risk factors for DLB, shared with PD, are mutations of *GBA1*, causing changes in the functionality of the GCase, a dysregulation of sphingolipid metabolism, and changes in autophagy function (see above) (Lee et al., 2021). It was suggested that mutations of *GBA1* may even have a stronger association to DLB than to PD (Nalls et al., 2013; Lee et al., 2021). Another risk factor involved in lipid homeostasis that is associated with DLB is the presence of the *APOE ε4* isoform of the apolipoprotein E (APOE) (Tsuang et al., 2013; Bras et al., 2014). APOE has three isoforms (ε2, ε3, and ε4) and is mainly expressed in astrocytes. It plays a role in cholesterol and lipid transport across the brain, which is important for neuronal function (Yamazaki et al., 2019; Jin et al., 2022). Interestingly, the presence of the *APOE ε4* isoform has also been associated with Alzheimer's Disease (AD) (Lee et al., 2021; Pires and Rego, 2023; Fortea et al., 2024; Lozupone and Panza, 2024). An inefficient lipid transport from astrocytes to neurons is known to change neuronal lipid composition (Lefterov et al., 2019; Miranda et al., 2022). Interestingly, it was found in the context of AD, that carriers of the *APOE ε4* allele have reduced levels of PIP2, which was explained by a decreased degradation of the *SYNJ1* mRNA (Zhu et al., 2015). As mentioned above, mutations in *SYNJ1* itself are known risk factors for PD (Krebs et al., 2013; Quadri et al., 2013; Olgiati et al., 2014; Ben Romdhan et al., 2018; Schechter and Sharon, 2021), however, whether this is also the case for DLB is still unclear. Further research into a possible connection of *SYNJ1* mutations and DLB would help to clarify this. Maybe unsurprisingly, DLB is often not clearly distinguishable from AD (dementia only) or PD (Parkinsonism with dementia) (Noe et al., 2004; Jellinger and Korczyn, 2018; Nedelec et al., 2023) (Summarised in Table 1).

In general, the presence of αSyn itself is already changing the cellular lipid composition (see above), and, thus, it might be likely that this is also the case in other synucleinopathies. The combination of genetic factors that change the cellular lipid profile might be one of the factors leading to or accelerating disease progression.

TABLE 1 Summary of lipid-related connections to αSyn pathology in PD, DLB, and MSA.

α-Synucleinopathy	Affected brain region	Connection to lipids (including genetic factors)	Aggregates found	References
Parkinson's Disease (PD)	• Dopaminergic neurons of the substantia nigra (pars compacta)	*Patient data* • Increase of DAG in the frontal cortex of PD patients • General change of the lipid profile of the visual cortex of PD patients including a decrease of unsaturated PE and FA-chain length dependent changes in the amounts of PI • Decrease of GM1 in brains of PD patients *In vitro studies* • αSyn has a higher binding affinity to negatively charged/anionic membrane lipids and to vesicular membranes • PS, PC, and PE to αSyn ratio contributes to amyloid aggregation • GM1 inhibits amyloid aggregation *In vivo studies* • Increase of DAG, decrease of PS and PI • GM2-synthase deficient mice show PD-like symptoms, which can be alleviated by GM1-analogue treatment *Genetic risk factors* • Mutations of *GBA1* • Mutations of *SH3GL2* • Mutations of *LRRK2*	• Formation of Lewy Bodies (LBs) and Lewy Neurites • Aggregates contain a Lewy fold: three layered aggregates comprised of residues 31–100 of αSyn that form a total of 9 β-sheet strands	Davidson et al. (1998), Aharon-Peretz et al. (2004), Martinez et al. (2007), Neumann et al. (2009), Cheng et al. (2011), Wu et al. (2011), Krebs et al. (2013), Quadri et al. (2013), Olgiati et al. (2014), Galvagnion et al. (2015), Hadaczek et al. (2015), Kalia and Lang (2015), Ben Romdhan et al. (2018), Wood et al. (2018), Fanning et al. (2019), Johnson et al. (2020), Man et al. (2021), Schechter and Sharon (2021), Galper et al. (2022), Gegg et al. (2022), Yang et al. (2022), Flores-Leon and Outeiro (2023), Andersson et al. (2024), Dos Santos et al. (2024), Makasewicz et al. (2024)
Dementia with Lewy Bodies (DLB)	• Neocortex • Limbic system • Dopaminergic neurons of the substantia nigra (pars compacta)	*Patient data* • Decrease of several phospholipids in brains of *APOEε4* carriers (in the context of AD) • In the context of AD: reduced levels of PIP2 *In vivo studies* • In the context of APOE ε4 KI mice: reduced levels of PIP2 and reduced degradation of *SYNJ1*mRNA *Genetic risk factors* • Mutations of *GBA1* • Carriers of *APOEε4*	• Formation of LBs and LNs • Aggregates contain a Lewy fold: three layered aggregates comprised of residues 31–100 of αSyn that form a total of 9 β-sheet strands	Nalls et al. (2013), Zhu et al. (2015), Lefterov et al. (2019), Outeiro et al. (2019), Lee et al. (2021), Yang et al. (2022)
Multiple System Atrophy (MSA)	• MSA-P (with parkinsonism): midbrain and basal ganglia • MSA-C (with cerebral ataxia): midbrain, cerebellum, and brainstem	*Patient data* • Low serum levels of cholesterol, LDL-C, HDL-C (lower in MSA-C patients), and TG are associated with both, MSA-C and MSA-P, but have no effect on disease progression *In vivo studies* • Transcriptome analysis of striatal astrocytes of a MSA mouse model revealed a downregulation of genes involved in lipid metabolism *Genetic risk factors* • inconclusive • weak connection to APOE ε4	• Formation of glial cytoplasmic inclusions (GCIs) in oligodendrocytes • Aggregates form asymmetrical Type I or Type II filaments • Type I filaments are made of two protofibrils: PF-1A is formed by residues 14–94 and contains 12 β-sheets and PF-1B is formed by residues 21–99 and contains ten β-sheets • Type II filaments are made of two protofibrils: PF-IIA is formed by residues 14–94 and also contains 12 β-sheets but has a different conformation to PF-IA. PF-IIB is formed by residues 36–99 and contains nine β-sheets	Lee et al. (2009), Cao et al. (2014), Robinson et al. (2018), Schweighauser et al. (2020), Poewe et al. (2022), So and Watts (2023), Schneider et al. (2024)

4.3 MSA and lipid changes

MSA is a rare neurodegenerative synucleinopathy and, in contrast to PD and DLB, associated with the formation of αSyn aggregates in oligodendrocytes referred to as glial cytoplasmic inclusions (GCIs) (Spillantini et al., 1998; Poewe et al., 2022). One of the hallmarks of MSA is a demyelination of neurons, which is connected to GCI-formation (Poewe et al., 2022). Myelin, multiple layers of membranes looped around the axon, contains a higher proportion of cholesterol and glycolipids (e.g., glycosylceramide) than other cellular membranes (Baumann and Pham-Dinh, 2001; Poitelon et al., 2020).

Little is known about the connections between GCI formation and the unique lipid composition of myelin sheaths in the context of MSA. It was shown that lower cholesterol levels and lower levels of LDL-C and HDL-C in patient serum have been connected to an increased risk of developing MSA (Lee et al., 2009; Cao et al., 2014). However, it is known that lipoproteins carrying cholesterol outside the central nervous system do not cross the blood brain barrier (BBB) and that cholesterol in the brain is mainly synthesised in astrocytes (Bleasel et al., 2014; Pifferi et al., 2021; Li et al., 2022). Thus, the connections between serum cholesterol levels and lipid changes in the brain during MSA remain elusive on a molecular level. In an MSA mouse model, transcriptome analyses of astrocytes implicated a dysregulation of cellular lipid metabolism (Schneider et al., 2024). This might point towards a changed lipid homeostasis in MSA but needs to be investigated more thoroughly.

Genetic risk factors for MSA that connect to lipid homeostasis are currently unknown. There are inconclusive studies on the genetic background of MSA (Poewe et al., 2022). Interestingly, one study suggests that the frequency of MSA-patients carrying the *APOE ε2* isoform is lower than the frequency of MSA patients carrying the *APOE ε4* isoform (Robinson et al., 2018) (Summarised in Table 1).

Taken together, MSA remains the rarest and, in terms of connection to lipids, the most elusive synucleinopathy, mostly due to the inconclusive evidence for a genetic background. Nevertheless, more research effort has to be directed towards understanding the differences or similarities between PD, DLB, and MSA.

5 Lipid changes in physiological ageing

Given that ageing is one of the biggest risk factors for developing neurodegenerative diseases such as PD, and that most neurodegenerative diseases occur sporadically, it is of great interest to understand lipid changes in the aged brain. While there has been a lot of research effort to better understand disease-related lipid changes in the brain, less is known about the possible lipid changes during physiological ageing. Very early studies analysing whole brains have described a general decline of total lipids with age (Rouser and Yamamoto, 1968; Mesa-Herrera et al., 2019). Later, analyses of white matter and cerebral cortices of the temporal and frontal lobes confirmed these findings (Svennerholm et al., 1991). More specific analyses of lipid classes revealed, for example, a reduction of polyunsaturated fatty acids (PUFAs) in the orbitofrontal cortex with age (McNamara et al., 2008). A more recent study has found that, while the overall lipid concentrations in the prefrontal cortex remain at a similar level with age, the lipid profile itself undergoes changes with a transition point of about 50–55 years of age. Some affected pathways were shown to be unsaturated fatty acid biosynthesis and glycerolipid metabolism, with differences between males and females (Yu et al., 2020). Interestingly, regional lipid profile diversity was also shown to change with age (Mota-Martorell et al., 2022). However, given the complexity of the brain, lipid changes in the physiologically ageing brain are still not clearly understood. Being able to differentiate between changes in healthy ageing and changes that might be part of, or even precede, pathological processes of neurodegeneration is of great importance to prevent and/or treat these diseases.

In an effort to find potential disease markers for PD, a significant amount of research has been focusing on lipidomic analyses of patient serum. For example, serum analyses of patients carrying the A53T mutation of *SNCA* revealed an increase of diacylglycerol, triacylglycerol, and PC (Avisar et al., 2022). Similarly, a decrease of serum levels of HDL-C was found in patients with PD (Choe et al., 2021). Furthermore, patients carrying a mutation in *LRRK2* showed changes in ceramide (Cer), TAG, sphingomyelin, PC, and lyso-phosphatidylethanolamine (LPE) (Galper et al., 2022). Analysis of samples from patients with idiopathic PD showed similar findings with lower levels of PS, some Cer species, and Sphingomyelin (SM) (Dahabiyeh et al., 2023). While these findings might pave the path to potential serum markers for disease, this is only the beginning of more extensive research to come. The challenge here is to find common markers that are reliably enough for all variants of PD, as it is a disease caused by multiple factors, many of which have not yet been completely understood.

6 Lipid interactions and possible influences on aggregate formation

Interestingly, it is known that different synucleinopathies exhibit different fibrillar αSyn conformations. These conformational differences are referred to as αSyn strains and, similarly to what is already known in prion diseases, they show different characteristics in terms of disease progression (Prusiner, 2012; Bousset et al., 2013; Peng et al., 2018; Woerman et al., 2019). When comparing LBs to GCIs from MSA patients, for example, the conformation of the accumulations was shown to be clearly distinct from each other (Peng et al., 2018; Shahnawaz et al., 2020). Indeed, two types of filaments were found in MSA patient brain extracts: Type I filaments were larger and showed a distinct folding when compared to the smaller Type II filaments. Both filaments were found to be asymmetrical and made of two protofilaments each. These protofilaments contain between 9 and 12 β-sheets (Schweighauser et al., 2020; So and Watts, 2023). αSyn filaments derived from patients with DLB or PD, on the other hand, showed identical conformations containing an ordered core called the *Lewy fold*, which is a three-layered aggregate with a total of nine β-sheets formed by residues 31–100 (Table 1) (Yang et al., 2022). *In vitro*, recombinant αSyn showed a larger variation in aggregate conformation, depending on chemical conditions under which the aggregations were formed (So and Watts, 2023). These variants exhibited different effectivities of prion-like seeding properties

(Walker and Jucker, 2015; Goedert et al., 2017), e.g., the propagation from cell to cell within the brain (Torre-Muruzabal et al., 2023).

However, the reason for these conformational differences that cause different disease phenotypes in synucleinopathies are not well understood. It is known that αSyn aggregation can be triggered by interaction with lipids (Makasewicz et al., 2024). Using *in vitro* membrane models including small unilamellar vesicles (SUVs), giant unilamellar vesicles (GUVs), and flat supported lipid bilayers, it was shown that lipid interaction of αSyn can induce nucleation of aggregates (Grey et al., 2011; Galvagnion et al., 2015; Makasewicz et al., 2021; Dear et al., 2024). These processes are dependent on the lipid composition of the vesicular structures investigated, the amount of negatively charged lipids, membrane fluidity, and membrane curvature (reviewed in (Makasewicz et al., 2024)).

Furthermore, familial variants of αSyn are found to be N-terminally acetylated in LBs (Anderson et al., 2006). Recently, it was shown that N-terminal acetylation of familial variants of αSyn can change the structure of the fibrillar aggregates and the lipid binding properties individually for each investigated variant (Bell et al., 2023). These findings point towards highly complex processes involved in the formation of synucleinopathies, implicating, among others, lipid composition, post-translational modifications, and possible mutations of *SNCA*.

Based on this, it might not be unlikely that changes in cellular lipid composition, occurring with age, through mutations in genes involved in lipid homeostasis, or through individual lifestyle and environmental factors, influence disease onset, variation, severity, and progression. Thinking a little further, this might even mean that differences of lipid compositions within a single brain (Mota-Martorell et al., 2022) could explain regional specificity of protein aggregates and symptom-phenotype variations. Indeed, it was recently found that distinct aggregate variants can be found in different brain regions (Wiseman et al., 2024). Taken together, understanding changes in the lipid composition of different brain regions and how this affects disease is likely to be one of the significant steps towards understanding the progression and onset of synucleinopathies. An improved understanding of the underlying processes will open new paths towards treatment or even disease prevention.

7 Discussion

The putative physiological functions and membrane binding properties of αSyn and processes during neurodegeneration are strongly connected to lipid changes in the brain. While synucleinopathies are all known to be multifactorial neurodegenerative diseases, it is possible that some of the factors currently recognised as contributing to disease development and progression might be rooted in changes in lipid metabolism or membrane lipid composition (Reviewed in (Flores-Leon and Outeiro, 2023)). For example, it was shown that a lack of the well-established risk factor for PD *PINK1* causes an accumulation of ceramides in the mitochondrial membrane, inhibiting β-oxidation and causing degradation of mitochondria via mitophagy (Vos et al., 2021; Flores-Leon and Outeiro, 2023). Even though the exact physiological roles of αSyn still remain to be determined, much progress has been made. With the help of advanced analytical methods, understanding the connection between lipid changes (storage, metabolism, lipid rafts, membrane composition) and αSyn is of importance to provide a deeper insight into the ever-increasing complexity of synucleinopathies.

Individual genetic risk factors, environmental and nutritional factors, and ageing, might all have an impact on the lipid composition of the brain. To date, very little is known about lipid-changes during physiological ageing although understanding these processes might be key to develop new research approaches for prevention or treatment of synucleinopathies. Furthermore, being able to distinguish between physiological lipid changes and alterations that contribute to disease progression will contribute substantially to future research of neurodegeneration. More progress is needed to understand regional lipid changes and their potential impact on disease development. Considering that these changes may result from a combination of several factors that are likely to be individual for each affected person, personalised assessments and treatments should be considered in the future. If different lipid compositions affect aggregate conformation and, with that, influence the rate of disease progression and spread throughout the brain, it might potentially open new ways of disease prevention or inspire novel therapeutical approaches.

A lot of research has already been conducted on future therapeutical or preventative treatments. One approach, for example, is the use of lipidic nanoparticles for drug delivery (Tsakiri et al., 2024), which could be adapted for targeting lipid changes in the brain, a concept referred to as *membrane lipid therapy* (Escriba et al., 2015). However, for that, we require a deeper understanding of the molecular mechanisms of lipid changes in synucleinopathies. Other major challenges that need to be addressed are ways to diagnose and classify neurodegenerative diseases such as synucleinopathies earlier and before the onset of clinical symptoms. Here, we can expand on the research efforts into finding reliable early biomarkers for PD such as, for example, αSyn seeding assays of cerebrospinal fluid (Orru et al., 2021; Rutledge et al., 2024).

Although a lot of factors connected to disease formation are already well understood, the influence of lipids on these processes have only recently gained more attention. Taken together, future research efforts should be made to (i) better understand differences between lipid changes that occur during physiological aging and lipid changes associated with pathological processes; (ii) to understand how regional differences in the lipid composition might contribute to aggregate localisation and conformation and, with that, influence the speed of disease progression and symptom variations; (iii) and to find reliable markers that can detect pathological processes earlier. Viewing synucleinopathies through the lens of lipid alterations alongside other well-established disease contributors possibly holds the potential to find novel approaches in disease diagnosis and therapy.

Author contributions

JS: Conceptualization, Visualization, Writing–original draft, Writing–review and editing. TL: Visualization, Writing–original

draft, Writing–review and editing. CB: Writing–review and editing.

Funding

The author(s) declare that financial support was received for the research, authorship, and/or publication of this article. This work was supported by the Hanna Bragard-Apfel Stiftung and the Peter-Beate-Heller-Stiftung des Stifterverbandes für die deutsche Wissenschaft.

Acknowledgments

We thank Fazilet Bekbulat for critical reading of the manuscript.

Conflict of interest

The authors declare that the research was conducted in the absence of any commercial or financial relationships that could be construed as a potential conflict of interest.

Publisher's note

All claims expressed in this article are solely those of the authors and do not necessarily represent those of their affiliated organizations, or those of the publisher, the editors and the reviewers. Any product that may be evaluated in this article, or claim that may be made by its manufacturer, is not guaranteed or endorsed by the publisher.

References

Aharon-Peretz, J., Rosenbaum, H., and Gershoni-Baruch, R. (2004). Mutations in the glucocerebrosidase gene and Parkinson's disease in Ashkenazi Jews. *N. Engl. J. Med.* 351, 1972–1977. doi:10.1056/NEJMoa033277

Ahmed, H., Wang, Y., Griffiths, W. J., Levey, A. I., Pikuleva, I., Liang, S. H., et al. (2024). Brain cholesterol and Alzheimer's disease: challenges and opportunities in probe and drug development. *Brain* 147, 1622–1635. doi:10.1093/brain/awae028

Ahn, B. H., Rhim, H., Kim, S. Y., Sung, Y. M., Lee, M. Y., Choi, J. Y., et al. (2002). alpha-Synuclein interacts with phospholipase D isozymes and inhibits pervanadate-induced phospholipase D activation in human embryonic kidney-293 cells. *J. Biol. Chem.* 277, 12334–12342. doi:10.1074/jbc.M110414200

Alam, P., Bousset, L., Melki, R., and Otzen, D. E. (2019). α-synuclein oligomers and fibrils: a spectrum of species, a spectrum of toxicities. *J. Neurochem.* 150, 522–534. doi:10.1111/jnc.14808

Alecu, I., and Bennett, S. A. L. (2019). Dysregulated lipid metabolism and its role in α-synucleinopathy in Parkinson's disease. *Front. Neurosci.* 13, 328. doi:10.3389/fnins.2019.00328

Alzheimer, A., Stelzmann, R. A., Schnitzlein, H. N., and Murtagh, F. R. (1995). An English translation of Alzheimer's 1907 paper, "Uber eine eigenartige Erkankung der Hirnrinde. *Clin. Anat.* 8, 429–431. doi:10.1002/ca.980080612

Anderson, J. P., Walker, D. E., Goldstein, J. M., de Laat, R., Banducci, K., Caccavello, R. J., et al. (2006). Phosphorylation of Ser-129 is the dominant pathological modification of alpha-synuclein in familial and sporadic Lewy body disease. *J. Biol. Chem.* 281, 29739–29752. doi:10.1074/jbc.M600933200

Andersson, A., Linse, S., Sparr, E., Fornasier, M., and Jonsson, P. (2024). The density of anionic lipids modulates the adsorption of α-Synuclein onto lipid membranes. *Biophys. Chem.* 305, 107143. doi:10.1016/j.bpc.2023.107143

Auluck, P. K., Caraveo, G., and Lindquist, S. (2010). α-Synuclein: membrane interactions and toxicity in Parkinson's disease. *Annu. Rev. Cell Dev. Biol.* 26, 211–233. doi:10.1146/annurev.cellbio.042308.113313

Avisar, H., Guardia-Laguarta, C., Surface, M., Papagiannakis, N., Maniati, M., Antonellou, R., et al. (2022). Lipid level alteration in human and cellular models of alpha synuclein mutations. *NPJ Park. Dis.* 8, 52. doi:10.1038/s41531-022-00313-y

Bartels, T., Ahlstrom, L. S., Leftin, A., Kamp, F., Haass, C., Brown, M. F., et al. (2010). The N-terminus of the intrinsically disordered protein α-synuclein triggers membrane binding and helix folding. *Biophys. J.* 99, 2116–2124. doi:10.1016/j.bpj.2010.06.035

Battis, K., Xiang, W., and Winkler, J. (2023). The bidirectional interplay of a-synuclein with lipids in the central nervous system and its implications for the pathogenesis of Parkinson's disease. *Int. J. Mol. Sci.* 24, 13270. doi:10.3390/ijms241713270

Baumann, N., and Pham-Dinh, D. (2001). Biology of oligodendrocyte and myelin in the mammalian central nervous system. *Physiol. Rev.* 81, 871–927. doi:10.1152/physrev.2001.81.2.871

Bayer, T. A., Jakala, P., Hartmann, T., Egensperger, R., Buslei, R., Falkai, P., et al. (1999). Neural expression profile of alpha-synuclein in developing human cortex. *Neuroreport* 10, 2799–2803. doi:10.1097/00001756-199909090-00019

Bell, R., Castellana-Cruz, M., Nene, A., Thrush, R. J., Xu, C. K., Kumita, J. R., et al. (2023). Effects of N-terminal acetylation on the aggregation of disease-related α-synuclein variants. *J. Mol. Biol.* 435, 167825. doi:10.1016/j.jmb.2022.167825

Ben Romdhan, S., Sakka, S., Farhat, N., Triki, S., Dammak, M., and Mhiri, C. (2018). A novel SYNJ1 mutation in a Tunisian family with Juvenile Parkinson's disease associated with epilepsy. *J. Mol. Neurosci.* 66, 273–278. doi:10.1007/s12031-018-1167-2

Bernal-Conde, L. D., Ramos-Acevedo, R., Reyes-Hernandez, M. A., Balbuena-Olvera, A. J., Morales-Moreno, I. D., Arguero-Sanchez, R., et al. (2019). Alpha-synuclein physiology and pathology: a perspective on cellular structures and organelles. *Front. Neurosci.* 13, 1399. doi:10.3389/fnins.2019.01399

Bernal-Conde, L. D., Ramos-Acevedo, R., Reyes-Hernández, M. A., Balbuena-Olvera, A. J., Morales-Moreno, I. D., Argüero-Sánchez, R., et al. (2020). Alpha-synuclein physiology and pathology: a perspective on cellular structures and organelles. *Front. Neurosci.* 13. doi:10.3389/fnins.2019.01399

Bleasel, J. M., Wong, J. H., Halliday, G. M., and Kim, W. S. (2014). Lipid dysfunction and pathogenesis of multiple system atrophy. *Acta Neuropathol. Commun.* 2, 15. doi:10.1186/2051-5960-2-15

Bodner, C. R., Dobson, C. M., and Bax, A. (2009). Multiple tight phospholipid-binding modes of alpha-synuclein revealed by solution NMR spectroscopy. *J. Mol. Biol.* 390, 775–790. doi:10.1016/j.jmb.2009.05.066

Bousset, L., Pieri, L., Ruiz-Arlandis, G., Gath, J., Jensen, P. H., Habenstein, B., et al. (2013). Structural and functional characterization of two alpha-synuclein strains. *Nat. Commun.* 4, 2575. doi:10.1038/ncomms3575

Bras, J., Guerreiro, R., Darwent, L., Parkkinen, L., Ansorge, O., Escott-Price, V., et al. (2014). Genetic analysis implicates APOE, SNCA and suggests lysosomal dysfunction in the etiology of dementia with Lewy bodies. *Hum. Mol. Genet.* 23, 6139–6146. doi:10.1093/hmg/ddu334

Brooker, S. M., Naylor, G. E., and Krainc, D. (2024). Cell biology of Parkinson's disease: mechanisms of synaptic, lysosomal, and mitochondrial dysfunction. *Curr. Opin. Neurobiol.* 85, 102841. doi:10.1016/j.conb.2024.102841

Bruce, K. D., Zsombok, A., and Eckel, R. H. (2017). Lipid processing in the brain: a key regulator of systemic metabolism. *Front. Endocrinol. (Lausanne)* 8, 60. doi:10.3389/fendo.2017.00060

Burré, J., Sharma, M., Tsetsenis, T., Buchman, V., Etherton, M. R., and Südhof, T. C. (2010). Alpha-synuclein promotes SNARE-complex assembly *in vivo* and *in vitro*. *Science* 329, 1663–1667. doi:10.1126/science.1195227

Bussell, R., and Eliezer, D. (2003). A structural and functional role for 11-mer repeats in α-synuclein and other exchangeable lipid binding proteins. *J. Mol. Biol.* 329, 763–778. doi:10.1016/s0022-2836(03)00520-5

Calabresi, P., Mechelli, A., Natale, G., Volpicelli-Daley, L., Di Lazzaro, G., and Ghiglieri, V. (2023). Alpha-synuclein in Parkinson's disease and other synucleinopathies: from overt neurodegeneration back to early synaptic dysfunction. *Cell death Dis.* 14, 176. doi:10.1038/s41419-023-05672-9

Cao, B., Guo, X., Chen, K., Song, W., Huang, R., Wei, Q. Q., et al. (2014). Serum lipid levels are associated with the prevalence but not with the disease progression of multiple system atrophy in a Chinese population. *Neurol. Res.* 36, 150–156. doi:10.1179/1743132813y.0000000277

Cheng, D., Jenner, A. M., Shui, G., Cheong, W. F., Mitchell, T. W., Nealon, J. R., et al. (2011). Lipid pathway alterations in Parkinson's disease primary visual cortex. *PloS one* 6, e17299. doi:10.1371/journal.pone.0017299

Choe, C. U., Petersen, E., Lezius, S., Cheng, B., Schulz, R., Buhmann, C., et al. (2021). Association of lipid levels with motor and cognitive function and decline in

advanced Parkinson's disease in the Mark-PD study. *Park. Relat. Disord.* 85, 5–10. doi:10.1016/j.parkreldis.2021.02.007

Choong, C.-J., Aguirre, C., Kakuda, K., Beck, G., Nakanishi, H., Kimura, Y., et al. (2023). Phosphatidylinositol-3, 4, 5-trisphosphate interacts with alpha-synuclein and initiates its aggregation and formation of Parkinson's disease-related fibril polymorphism. *Acta Neuropathol.* 145, 573–595. doi:10.1007/s00401-023-02555-3

Cole, N. B., DiEuliis, D., Leo, P., Mitchell, D. C., and Nussbaum, R. L. (2008). Mitochondrial translocation of alpha-synuclein is promoted by intracellular acidification. *Exp. Cell Res.* 314, 2076–2089. doi:10.1016/j.yexcr.2008.03.012

Cole, N. B., Murphy, D. D., Grider, T., Rueter, S., Brasaemle, D., and Nussbaum, R. L. (2002). Lipid droplet binding and oligomerization properties of the Parkinson's disease protein alpha-synuclein. *J. Biol. Chem.* 277, 6344–6352. doi:10.1074/jbc.M108414200

Cooper, A. A., Gitler, A. D., Cashikar, A., Haynes, C. M., Hill, K. J., Bhullar, B., et al. (2006). Alpha-synuclein blocks ER-golgi traffic and Rab1 rescues neuron loss in Parkinson's models. *Science* 313, 324–328. doi:10.1126/science.1129462

Cotzias, G. C., Van Woert, M. H., and Schiffer, L. M. (1967). Aromatic amino acids and modification of parkinsonism. *N. Engl. J. Med.* 276, 374–379. doi:10.1056/nejm196702162760703

Dahabiyeh, L. A., Nimer, R. M., Rashed, M., Wells, J. D., and Fiehn, O. (2023). Serum-based lipid panels for diagnosis of idiopathic Parkinson's disease. *Metabolites* 13, 990. doi:10.3390/metabo13090990

Davidson, W. S., Jonas, A., Clayton, D. F., and George, J. M. (1998). Stabilization of alpha-synuclein secondary structure upon binding to synthetic membranes. *J. Biol. Chem.* 273, 9443–9449. doi:10.1074/jbc.273.16.9443

Dear, A. J., Teng, X., Ball, S. R., Lewin, J., Horne, R. I., Clow, D., et al. (2024). Molecular mechanism of α-synuclein aggregation on lipid membranes revealed. *Chem. Sci.* 15, 7229–7242. doi:10.1039/d3sc05661a

Desplats, P., Spencer, B., Coffee, E., Patel, P., Michael, S., Patrick, C., et al. (2011). Alpha-synuclein sequesters Dnmt1 from the nucleus: a novel mechanism for epigenetic alterations in Lewy body diseases. *J. Biol. Chem.* 286, 9031–9037. doi:10.1074/jbc.C110.212589

Devi, L., Raghavendran, V., Prabhu, B. M., Avadhani, N. G., and Anandatheerthavarada, H. K. (2008). Mitochondrial import and accumulation of alpha-synuclein impair complex I in human dopaminergic neuronal cultures and Parkinson disease brain. *J. Biol. Chem.* 283, 9089–9100. doi:10.1074/jbc.M710012200

Dos Santos, J. C. C., Mano, G. B. C., da Cunha Barreto-Vianna, A. R., Garcia, T. F. M., de Vasconcelos, A. V., Sa, C. S. G., et al. (2024). The molecular impact of glucosylceramidase beta 1 (Gba1) in Parkinson's disease: a new genetic state of the art. *Mol. Neurobiol.* doi:10.1007/s12035-024-04008-8

Dudek, J. (2017). Role of cardiolipin in mitochondrial signaling pathways. *Front. Cell Dev. Biol.* 5, 90. doi:10.3389/fcell.2017.00090

Ellis, C. E., Murphy, E. J., Mitchell, D. C., Golovko, M. Y., Scaglia, F., Barceló-Coblijn, G. C., et al. (2005). Mitochondrial lipid abnormality and electron transport chain impairment in mice lacking α-synuclein. *Mol. Cell. Biol.* 25, 10190–10201. doi:10.1128/mcb.25.22.10190-10201.2005

Emamzadeh, F. N. (2016). Alpha-synuclein structure, functions, and interactions. *J. Res. Med. Sci.* 21, 29. doi:10.4103/1735-1995.181989

Escriba, P. V., Busquets, X., Inokuchi, J., Balogh, G., Torok, Z., Horvath, I., et al. (2015). Membrane lipid therapy: modulation of the cell membrane composition and structure as a molecular base for drug discovery and new disease treatment. *Prog. Lipid Res.* 59, 38–53. doi:10.1016/j.plipres.2015.04.003

Fanning, S., Haque, A., Imberdis, T., Baru, V., Barrasa, M. I., Nuber, S., et al. (2019). Lipidomic analysis of α-synuclein neurotoxicity identifies stearoyl CoA desaturase as a target for Parkinson treatment. *Mol. Cell* 73, 1001–1014 e8. doi:10.1016/j.molcel.2018.11.028

Fanning, S., Selkoe, D., and Dettmer, U. (2020). Parkinson's disease: proteinopathy or lipidopathy? *NPJ Park. Dis.* 6, 3. doi:10.1038/s41531-019-0103-7

Fernagut, P. O., Dehay, B., Maillard, A., Bezard, E., Perez, P., Pavy-Le Traon, A., et al. (2014). Multiple system atrophy: a prototypical synucleinopathy for disease-modifying therapeutic strategies. *Neurobiol. Dis.* 67, 133–139. doi:10.1016/j.nbd.2014.03.021

Flores-Leon, M., and Outeiro, T. F. (2023). More than meets the eye in Parkinson's disease and other synucleinopathies: from proteinopathy to lipidopathy. *Acta Neuropathol.* 146, 369–385. doi:10.1007/s00401-023-02601-0

Forloni, G. (2023). Alpha synuclein: neurodegeneration and inflammation. *Int. J. Mol. Sci.* 24, 5914. doi:10.3390/ijms24065914

Fortea, J., Pegueroles, J., Alcolea, D., Belbin, O., Dols-Icardo, O., Vaqué-Alcázar, L., et al. (2024). APOE4 homozygozity represents a distinct genetic form of Alzheimer's disease. *Nat. Med.* 30, 1284–1291. doi:10.1038/s41591-024-02931-w

Fortin, D. L., Troyer, M. D., Nakamura, K., Kubo, S., Anthony, M. D., and Edwards, R. H. (2004). Lipid rafts mediate the synaptic localization of alpha-synuclein. *J. Neurosci. official J. Soc. Neurosci.* 24, 6715–6723. doi:10.1523/JNEUROSCI.1594-04.2004

Fredriksen, K., Aivazidis, S., Sharma, K., Burbidge, K. J., Pitcairn, C., Zunke, F., et al. (2021). Pathological α-syn aggregation is mediated by glycosphingolipid chain length and the physiological state of α-syn *in vivo*. *Proc. Natl. Acad. Sci. U. S. A.* 118, e2108489118. doi:10.1073/pnas.2108489118

Galper, J., Dean, N. J., Pickford, R., Lewis, S. J. G., Halliday, G. M., Kim, W. S., et al. (2022). Lipid pathway dysfunction is prevalent in patients with Parkinson's disease. *Brain* 145, 3472–3487. doi:10.1093/brain/awac176

Galvagnion, C., Buell, A. K., Meisl, G., Michaels, T. C., Vendruscolo, M., Knowles, T. P., et al. (2015). Lipid vesicles trigger α-synuclein aggregation by stimulating primary nucleation. *Nat. Chem. Biol.* 11, 229–234. doi:10.1038/nchembio.1750

Gegg, M. E., Menozzi, E., and Schapira, A. H. V. (2022). Glucocerebrosidase-associated Parkinson disease: pathogenic mechanisms and potential drug treatments. *Neurobiol. Dis.* 166, 105663. doi:10.1016/j.nbd.2022.105663

Georgas, K., Rumballe, B., Valerius, M. T., Chiu, H. S., Thiagarajan, R. D., Lesieur, E., et al. (2009). Analysis of early nephron patterning reveals a role for distal RV proliferation in fusion to the ureteric tip via a cap mesenchyme-derived connecting segment. *Dev. Biol.* 332, 273–286. doi:10.1016/j.ydbio.2009.05.578

George, A. A., Hayden, S., Stanton, G. R., and Brockerhoff, S. E. (2016). Arf6 and the 5'phosphatase of synaptojanin 1 regulate autophagy in cone photoreceptors. *Bioessays* 38 (Suppl. 1), S119–S135. doi:10.1002/bies.201670913

George, J. M., Jin, H., Woods, W. S., and Clayton, D. F. (1995). Characterization of a novel protein regulated during the critical period for song learning in the zebra finch. *Neuron* 15, 361–372. doi:10.1016/0896-6273(95)90040-3

Ghosh, D., Mehra, S., Sahay, S., Singh, P. K., and Maji, S. K. (2017). α-synuclein aggregation and its modulation. *Int. J. Biol. Macromol.* 100, 37–54. doi:10.1016/j.ijbiomac.2016.10.021

Goedert, M., Masuda-Suzukake, M., and Falcon, B. (2017). Like prions: the propagation of aggregated tau and α-synuclein in neurodegeneration. *Brain* 140, 266–278. doi:10.1093/brain/aww230

Grey, M., Linse, S., Nilsson, H., Brundin, P., and Sparr, E. (2011). Membrane interaction of α-synuclein in different aggregation states. *J. Park. Dis.* 1, 359–371. doi:10.3233/JPD-2011-11067

Hadaczek, P., Wu, G., Sharma, N., Ciesielska, A., Bankiewicz, K., Davidow, A. L., et al. (2015). GDNF signaling implemented by GM1 ganglioside; failure in Parkinson's disease and GM1-deficient murine model. *Exp. Neurol.* 263, 177–189. doi:10.1016/j.expneurol.2014.10.010

Hamilton, J. A., Hillard, C. J., Spector, A. A., and Watkins, P. A. (2007). Brain uptake and utilization of fatty acids, lipids and lipoproteins: application to neurological disorders. *J. Mol. Neurosci.* 33, 2–11. doi:10.1007/s12031-007-0060-1

Hasegawa, T., Konno, M., Baba, T., Sugeno, N., Kikuchi, A., Kobayashi, M., et al. (2011). The AAA-ATPase VPS4 regulates extracellular secretion and lysosomal targeting of α-synuclein. *PloS one* 6, e29460. doi:10.1371/journal.pone.0029460

Hsu, L. J., Mallory, M., Xia, Y., Veinbergs, I., Hashimoto, M., Yoshimoto, M., et al. (1998). Expression pattern of synucleins (non-Abeta component of Alzheimer's disease amyloid precursor protein/alpha-synuclein) during murine brain development. *J. Neurochem.* 71, 338–344. doi:10.1046/j.1471-4159.1998.71010338.x

Huang, M., Wang, B., Li, X., Fu, C., Wang, C., and Kang, X. (2019). α-Synuclein: a multifunctional player in exocytosis, endocytosis, and vesicle recycling. *Front. Neurosci.* 13, 28. doi:10.3389/fnins.2019.00028

Jacob, R. S., Eichmann, C., Dema, A., Mercadante, D., and Selenko, P. (2021a). α-Synuclein plasma membrane localization correlates with cellular phosphatidylinositol polyphosphate levels. *eLife* 10, e61951. doi:10.7554/eLife.61951

Jacob, R. S., Eichmann, C., Dema, A., Mercadante, D., and Selenko, P. (2021b). α-Synuclein plasma membrane localization correlates with cellular phosphatidylinositol polyphosphate levels. *Elife* 10, e61951. doi:10.7554/eLife.61951

Jellinger, K. A., and Korczyn, A. D. (2018). Are dementia with Lewy bodies and Parkinson's disease dementia the same disease? *BMC Med.* 16, 34. doi:10.1186/s12916-018-1016-8

Jensen, P. H., Hager, H., Nielsen, M. S., Højrup, P., Gliemann, J., and Jakes, R. (1999). alpha-synuclein binds to Tau and stimulates the protein kinase A-catalyzed tau phosphorylation of serine residues 262 and 356. *J. Biol. Chem.* 274, 25481–25489. doi:10.1074/jbc.274.36.25481

Jiang, K., Rocha, S., Westling, A., Kesarimangalam, S., Dorfman, K. D., Wittung-Stafshede, P., et al. (2018). Alpha-synuclein modulates the physical properties of DNA. *Chemistry* 24, 15685–15690. doi:10.1002/chem.201803933

Jin, Y., Li, F., Sonoustoun, B., Kondru, N. C., Martens, Y. A., Qiao, W., et al. (2022). APOE4 exacerbates α-synuclein seeding activity and contributes to neurotoxicity in Alzheimer's disease with Lewy body pathology. *Acta Neuropathol.* 143, 641–662. doi:10.1007/s00401-022-02421-8

Johnson, P. H., Weinreb, N. J., Cloyd, J. C., Tuite, P. J., and Kartha, R. V. (2020). GBA1 mutations: prospects for exosomal biomarkers in α-synuclein pathologies. *Mol. Genet. Metab.* 129, 35–46. doi:10.1016/j.ymgme.2019.10.006

Kalia, L. V., and Lang, A. E. (2015). Parkinson's disease. *Lancet* 386, 896–912. doi:10.1016/s0140-6736(14)61393-3

Khounlo, R., Hawk, B. J. D., Khu, T.-M., Yoo, G., Lee, N. K., Pierson, J., et al. (2021). Membrane binding of α-synuclein stimulates expansion of SNARE-dependent fusion pore. *Front. Cell Dev. Biol.* 9, 663431. doi:10.3389/fcell.2021.663431

Kontopoulos, E., Parvin, J. D., and Feany, M. B. (2006). Alpha-synuclein acts in the nucleus to inhibit histone acetylation and promote neurotoxicity. *Hum. Mol. Genet.* 15, 3012–3023. doi:10.1093/hmg/ddl243

Krebs, C. E., Karkheiran, S., Powell, J. C., Cao, M., Makarov, V., Darvish, H., et al. (2013). The Sac1 domain of *<scp>SYNJ</scp> 1* identified mutated in a family with early-onset progressive P arkinsonism with generalized seizures. *Hum. Mutat.* 34, 1200–1207. doi:10.1002/humu.22372

Krumova, P., Meulmeester, E., Garrido, M., Tirard, M., Hsiao, H. H., Bossis, G., et al. (2011). Sumoylation inhibits alpha-synuclein aggregation and toxicity. *J. Cell Biol.* 194, 49–60. doi:10.1083/jcb.201010117

Lee, H. J., Kang, S. J., Lee, K., and Im, H. (2011). Human α-synuclein modulates vesicle trafficking through its interaction with prenylated Rab acceptor protein 1. *Biochem. Biophys. Res. Commun.* 412, 526–531. doi:10.1016/j.bbrc.2011.07.028

Lee, J. Y., Marian, O. C., and Don, A. S. (2021). Defective lysosomal lipid catabolism as a common pathogenic mechanism for dementia. *Neuromolecular Med.* 23, 1–24. doi:10.1007/s12017-021-08644-4

Lee, P. H., Lim, T. S., Shin, H. W., Yong, S. W., Nam, H. S., and Sohn, Y. H. (2009). Serum cholesterol levels and the risk of multiple system atrophy: a case-control study. *Mov. Disord.* 24, 752–758. doi:10.1002/mds.22459

Lefterov, I., Wolfe, C. M., Fitz, N. F., Nam, K. N., Letronne, F., Biedrzycki, R. J., et al. (2019). APOE2 orchestrated differences in transcriptomic and lipidomic profiles of postmortem AD brain. *Alzheimers Res. Ther.* 11, 113. doi:10.1186/s13195-019-0558-0

Li, D., Zhang, J., and Liu, Q. (2022). Brain cell type-specific cholesterol metabolism and implications for learning and memory. *Trends Neurosci.* 45, 401–414. doi:10.1016/j.tins.2022.01.002

Lou, X., Kim, J., Hawk, B. J., and Shin, Y.-K. (2017). α-Synuclein may cross-bridge v-SNARE and acidic phospholipids to facilitate SNARE-dependent vesicle docking. *Biochem. J.* 474, 2039–2049. doi:10.1042/BCJ20170200

Lozupone, M., and Panza, F. (2024). Impact of apolipoprotein E isoforms on sporadic Alzheimer's disease: beyond the role of amyloid beta. *Neural Regen. Res.* 19, 80–83. doi:10.4103/1673-5374.375316

Lyra, P., Machado, V., Rota, S., Chaudhuri, K. R., Botelho, J., and Mendes, J. J. (2023). Revisiting alpha-synuclein pathways to inflammation. *Int. J. Mol. Sci.* 24, 7137. doi:10.3390/ijms24087137

Madureira, M., Connor-Robson, N., and Wade-Martins, R. (2020). LRRK2: autophagy and lysosomal activity. *Front. Neurosci.* 14, 498. doi:10.3389/fnins.2020.00498

Makasewicz, K., Linse, S., and Sparr, E. (2024). Interplay of α-synuclein with lipid membranes: cooperative adsorption, membrane remodeling and coaggregation. *JACS Au* 4, 1250–1262. doi:10.1021/jacsau.3c00579

Makasewicz, K., Wennmalm, S., Stenqvist, B., Fornasier, M., Andersson, A., Jonsson, P., et al. (2021). Cooperativity of α-synuclein binding to lipid membranes. *ACS Chem. Neurosci.* 12, 2099–2109. doi:10.1021/acschemneuro.1c00006

Man, W. K., Tahirbegi, B., Vrettas, M. D., Preet, S., Ying, L., Vendruscolo, M., et al. (2021). The docking of synaptic vesicles on the presynaptic membrane induced by α-synuclein is modulated by lipid composition. *Nat. Commun.* 12, 927. doi:10.1038/s41467-021-21027-4

Manzanza, N. O., Sedlackova, L., and Kalaria, R. N. (2021). Alpha-synuclein post-translational modifications: implications for pathogenesis of Lewy body disorders. *Front. Aging Neurosci.* 13, 690293. doi:10.3389/fnagi.2021.690293

Maroteaux, L., Campanelli, J. T., and Scheller, R. H. (1988). Synuclein: a neuron-specific protein localized to the nucleus and presynaptic nerve terminal. *J. Neurosci. official J. Soc. Neurosci.* 8, 2804–2815. doi:10.1523/jneurosci.08-08-02804.1988

Martinez, Z., Zhu, M., Han, S., and Fink, A. L. (2007). GM1 specifically interacts with alpha-synuclein and inhibits fibrillation. *Biochemistry* 46, 1868–1877. doi:10.1021/bi061749a

Mazzulli, J. R., Zunke, F., Tsunemi, T., Toker, N. J., Jeon, S., Burbulla, L. F., et al. (2016). Activation of β-glucocerebrosidase reduces pathological α-synuclein and restores lysosomal function in Parkinson's patient midbrain neurons. *J. Neurosci.* 36, 7693–7706. doi:10.1523/JNEUROSCI.0628-16.2016

McFarland, M. A., Ellis, C. E., Markey, S. P., and Nussbaum, R. L. (2008). Proteomics analysis identifies phosphorylation-dependent alpha-synuclein protein interactions. *Mol. Cell. Proteomics* 7, 2123–2137. doi:10.1074/mcp.M800116-MCP200

McNamara, R. K., Liu, Y., Jandacek, R., Rider, T., and Tso, P. (2008). The aging human orbitofrontal cortex: decreasing polyunsaturated fatty acid composition and associated increases in lipogenic gene expression and stearoyl-CoA desaturase activity. *Prostagl. Leukot. Essent. Fat. Acids* 78, 293–304. doi:10.1016/j.plefa.2008.04.001

Mehra, S., Gadhe, L., Bera, R., Sawner, A. S., and Maji, S. K. (2021). Structural and functional insights into α-synuclein fibril polymorphism. *Biomolecules* 11, 1419. doi:10.3390/biom11101419

Menges, S., Minakaki, G., Schaefer, P. M., Meixner, H., Prots, I., Schlötzer-Schrehardt, U., et al. (2017). Alpha-synuclein prevents the formation of spherical mitochondria and apoptosis under oxidative stress. *Sci. Rep-Uk* 7, 42942. doi:10.1038/srep42942

Mesa-Herrera, F., Taoro-Gonzalez, L., Valdes-Baizabal, C., Diaz, M., and Marin, R. (2019). Lipid and lipid raft alteration in aging and neurodegenerative diseases: a window for the development of new biomarkers. *Int. J. Mol. Sci.* 20, 3810. doi:10.3390/ijms20153810

Middleton, E. R., and Rhoades, E. (2010). Effects of curvature and composition on α-synuclein binding to lipid vesicles. *Biophys. J.* 99, 2279–2288. doi:10.1016/j.bpj.2010.07.056

Miraglia, F., Ricci, A., Rota, L., and Colla, E. (2018). Subcellular localization of alpha-synuclein aggregates and their interaction with membranes. *Neural Regen. Res.* 13, 1136–1144. doi:10.4103/1673-5374.235013

Miranda, A. M., Ashok, A., Chan, R. B., Zhou, B., Xu, Y., McIntire, L. B., et al. (2022). Effects of APOE4 allelic dosage on lipidomic signatures in the entorhinal cortex of aged mice. *Transl. Psychiatry* 12, 129. doi:10.1038/s41398-022-01881-6

Moors, T. E., Maat, C. A., Niedieker, D., Mona, D., Petersen, D., Timmermans-Huisman, E., et al. (2021). The subcellular arrangement of alpha-synuclein proteoforms in the Parkinson's disease brain as revealed by multicolor STED microscopy. *Acta Neuropathol.* 142, 423–448. doi:10.1007/s00401-021-02329-9

Morris, A. M., and Finke, R. G. (2009). Alpha-synuclein aggregation variable temperature and variable pH kinetic data: a re-analysis using the Finke-Watzky 2-step model of nucleation and autocatalytic growth. *Biophys. Chem.* 140, 9–15. doi:10.1016/j.bpc.2008.11.003

Mota-Martorell, N., Andres-Benito, P., Martin-Gari, M., Galo-Licona, J. D., Sol, J., Fernandez-Bernal, A., et al. (2022). Selective brain regional changes in lipid profile with human aging. *Geroscience* 44, 763–783. doi:10.1007/s11357-022-00527-1

Nakamura, K., Nemani, V. M., Azarbal, F., Skibinski, G., Levy, J. M., Egami, K., et al. (2011). Direct membrane association drives mitochondrial fission by the Parkinson disease-associated protein alpha-synuclein. *J. Biol. Chem.* 286, 20710–20726. doi:10.1074/jbc.M110.213538

Nalls, M. A., Blauwendraat, C., Vallerga, C. L., Heilbron, K., Bandres-Ciga, S., Chang, D., et al. (2019). Identification of novel risk loci, causal insights, and heritable risk for Parkinson's disease: a meta-analysis of genome-wide association studies. *Lancet Neurol.* 18, 1091–1102. doi:10.1016/S1474-4422(19)30320-5

Nalls, M. A., Duran, R., Lopez, G., Kurzawa-Akanbi, M., McKeith, I. G., Chinnery, P. F., et al. (2013). A multicenter study of glucocerebrosidase mutations in dementia with Lewy bodies. *JAMA Neurol.* 70, 727–735. doi:10.1001/jamaneurol.2013.1925

Nasaruddin, M. L., Holscher, C., Kehoe, P., Graham, S. F., and Green, B. D. (2016). Wide-ranging alterations in the brain fatty acid complement of subjects with late Alzheimer's disease as detected by GC-MS. *Am. J. Transl. Res.* 8, 154–165.

Nedelec, T., Couvy-Duchesne, B., Darves-Bornoz, A., Couronne, R., Monnet, F., Gantzer, L., et al. (2023). A comparison between early presentation of dementia with Lewy bodies, alzheimer's disease, and Parkinson's disease: evidence from routine primary care and UK biobank data. *Ann. Neurol.* 94, 259–270. doi:10.1002/ana.26670

Neumann, J., Bras, J., Deas, E., O'Sullivan, S. S., Parkkinen, L., Lachmann, R. H., et al. (2009). Glucocerebrosidase mutations in clinical and pathologically proven Parkinson's disease. *Brain* 132, 1783–1794. doi:10.1093/brain/awp044

Noe, E., Marder, K., Bell, K. L., Jacobs, D. M., Manly, J. J., and Stern, Y. (2004). Comparison of dementia with Lewy bodies to Alzheimer's disease and Parkinson's disease with dementia. *Mov. Disord.* 19, 60–67. doi:10.1002/mds.10633

Nordengen, K., and Morland, C. (2024). From synaptic physiology to synaptic pathology: the enigma of α-synuclein. *Int. J. Mol. Sci.* 25, 986. doi:10.3390/ijms25020986

Olgiati, S., De Rosa, A., Quadri, M., Criscuolo, C., Breedveld, G. J., Picillo, M., et al. (2014). PARK20 caused by SYNJ1 homozygous Arg258Gln mutation in a new Italian family. *Neurogenetics* 15, 183–188. doi:10.1007/s10048-014-0406-0

Orru, C. D., Ma, T. C., Hughson, A. G., Groveman, B. R., Srivastava, A., Galasko, D., et al. (2021). A rapid α-synuclein seed assay of Parkinson's disease CSF panel shows high diagnostic accuracy. *Ann. Clin. Transl. Neurol.* 8, 374–384. doi:10.1002/acn3.51280

Oueslati, A., Fournier, M., and Lashuel, H. A. (2010). "Chapter 7 - role of post-translational modifications in modulating the structure, function and toxicity of α-synuclein: implications for Parkinson's disease pathogenesis and therapies," in *Progress in brain research*. Editors A. Björklund, and M. A. Cenci (Elsevier), 115–145.

Outeiro, T. F., Koss, D. J., Erskine, D., Walker, L., Kurzawa-Akanbi, M., Burn, D., et al. (2019). Dementia with Lewy bodies: an update and outlook. *Mol. Neurodegener.* 14, 5. doi:10.1186/s13024-019-0306-8

Pan, P. Y., Li, X., Wang, J., Powell, J., Wang, Q., Zhang, Y., et al. (2017). Parkinson's disease-associated LRRK2 hyperactive kinase mutant disrupts synaptic vesicle trafficking in ventral midbrain neurons. *J. Neurosci. official J. Soc. Neurosci.* 37, 11366–11376. doi:10.1523/JNEUROSCI.0964-17.2017

Paradies, G., Paradies, V., De Benedictis, V., Ruggiero, F. M., and Petrosillo, G. (2014). Functional role of cardiolipin in mitochondrial bioenergetics. *Biochim. Biophys. Acta (BBA) - Bioenerg.* 1837, 408–417. doi:10.1016/j.bbabio.2013.10.006

Payton, J. E., Perrin, R. J., Woods, W. S., and George, J. M. (2004). Structural determinants of PLD2 inhibition by α-synuclein. *J. Mol. Biol.* 337, 1001–1009. doi:10.1016/j.jmb.2004.02.014

Peng, C., Gathagan, R. J., Covell, D. J., Medellin, C., Stieber, A., Robinson, J. L., et al. (2018). Cellular milieu imparts distinct pathological α-synuclein strains in α-synucleinopathies. *Nature* 557, 558–563. doi:10.1038/s41586-018-0104-4

Perera, R. M., Zoncu, R., Lucast, L., De Camilli, P., and Toomre, D. (2006). Two synaptojanin 1 isoforms are recruited to clathrin-coated pits at different stages. *Proc. Natl. Acad. Sci. U. S. A.* 103, 19332–19337. doi:10.1073/pnas.0609795104

Pifferi, F., Laurent, B., and Plourde, M. (2021). Lipid transport and metabolism at the blood-brain interface: implications in health and disease. *Front. Physiol.* 12, 645646. doi:10.3389/fphys.2021.645646

Pifl, C., Rajput, A., Reither, H., Blesa, J., Cavada, C., Obeso, J. A., et al. (2014). Is Parkinson's disease a vesicular dopamine storage disorder? Evidence from a study in isolated synaptic vesicles of human and nonhuman primate striatum. *J. Neurosci.* 34, 8210–8218. doi:10.1523/JNEUROSCI.5456-13.2014

Pirc, K., and Ulrih, N. P. (2015). α-Synuclein interactions with phospholipid model membranes: key roles for electrostatic interactions and lipid-bilayer structure. *Biochim. Biophys. acta* 1848, 2002–2012. doi:10.1016/j.bbamem.2015.06.021

Pires, M., and Rego, A. C. (2023). Apoe4 and alzheimer's disease pathogenesis-mitochondrial deregulation and targeted therapeutic strategies. *Int. J. Mol. Sci.* 24, 778. doi:10.3390/ijms24010778

Poewe, W., Stankovic, I., Halliday, G., Meissner, W. G., Wenning, G. K., Pellecchia, M. T., et al. (2022). Multiple system atrophy. *Nat. Rev. Dis. Prim.* 8, 56. doi:10.1038/s41572-022-00382-6

Poitelon, Y., Kopec, A. M., and Belin, S. (2020). Myelin fat facts: an overview of lipids and fatty acid metabolism. *Cells* 9, 812. doi:10.3390/cells9040812

Pozo Devoto, V. M., Dimopoulos, N., Alloatti, M., Pardi, M. B., Saez, T. M., Otero, M. G., et al. (2017). αSynuclein control of mitochondrial homeostasis in human-derived neurons is disrupted by mutations associated with Parkinson's disease. *Sci. Rep.* 7, 5042. doi:10.1038/s41598-017-05334-9

Prusiner, S. B. (2012). Cell biology. A unifying role for prions in neurodegenerative diseases. *Science* 336, 1511–1513. doi:10.1126/science.1222951

Quadri, M., Fang, M., Picillo, M., Olgiati, S., Breedveld, G. J., Graafland, J., et al. (2013). Mutation in the SYNJ1 gene associated with autosomal recessive, early-onset Parkinsonism. *Hum. Mutat.* 34, 1208–1215. doi:10.1002/humu.22373

Ramalingam, N., Jin, S. X., Moors, T. E., Fonseca-Ornelas, L., Shimanaka, K., Lei, S., et al. (2023). Dynamic physiological α-synuclein S129 phosphorylation is driven by neuronal activity. *Npj Park. Dis.* 9, 4. doi:10.1038/s41531-023-00444-w

Rcom-H'cheo-Gauthier, A. N., Osborne, S. L., Meedeniya, A. C., and Pountney, D. L. (2016). Calcium: alpha-synuclein interactions in alpha-synucleinopathies. *Front. Neurosci.* 10, 570. doi:10.3389/fnins.2016.00570

Robinson, J. L., Lee, E. B., Xie, S. X., Rennert, L., Suh, E., Bredenberg, C., et al. (2018). Neurodegenerative disease concomitant proteinopathies are prevalent, age-related and APOE4-associated. *Brain* 141, 2181–2193. doi:10.1093/brain/awy146

Rocha, E. M., De Miranda, B., and Sanders, L. H. (2018). Alpha-synuclein: pathology, mitochondrial dysfunction and neuroinflammation in Parkinson's disease. *Neurobiol. Dis.* 109, 249–257. doi:10.1016/j.nbd.2017.04.004

Rodriguez, J. A., Ivanova, M. I., Sawaya, M. R., Cascio, D., Reyes, F. E., Shi, D., et al. (2015). Structure of the toxic core of α-synuclein from invisible crystals. *Nature* 525, 486–490. doi:10.1038/nature15368

Roeters, S. J., Strunge, K., Pedersen, K. B., Golbek, T. W., Bregnhøj, M., Zhang, Y., et al. (2023). Elevated concentrations cause upright alpha-synuclein conformation at lipid interfaces. *Nat. Commun.* 14, 5731. doi:10.1038/s41467-023-39843-1

Rouser, G., and Yamamoto, A. (1968). Curvilinear regression course of human brain lipid composition changes with age. *Lipids* 3, 284–287. doi:10.1007/BF02531202

Roy, S., Winton, M. J., Black, M. M., Trojanowski, J. Q., and Lee, V. M. (2007). Rapid and intermittent cotransport of slow component-b proteins. *J. Neurosci. official J. Soc. Neurosci.* 27, 3131–3138. doi:10.1523/JNEUROSCI.4999-06.2007

Rutledge, J., Lehallier, B., Zarifkar, P., Losada, P. M., Shahid-Besanti, M., Western, D., et al. (2024). Comprehensive proteomics of CSF, plasma, and urine identify DDC and other biomarkers of early Parkinson's disease. *Acta Neuropathol.* 147, 52. doi:10.1007/s00401-024-02706-0

Ryan, T., Bamm, V. V., Stykel, M. G., Coackley, C. L., Humphries, K. M., Jamieson-Williams, R., et al. (2018). Cardiolipin exposure on the outer mitochondrial membrane modulates α-synuclein. *Nat. Commun.* 9, 817. doi:10.1038/s41467-018-03241-9

Ryu, S., Baek, I., and Liew, H. (2019). Sumoylated α-synuclein translocates into the nucleus by karyopherin α6. *Mol. Cell. Toxicol.* 15, 103–109. doi:10.1007/s13273-019-0012-1

Sahoo, S., Padhy, A. A., Kumari, V., and Mishra, P. (2022). Role of ubiquitin-proteasome and autophagy-lysosome pathways in α-synuclein aggregate clearance. *Mol. Neurobiol.* 59, 5379–5407. doi:10.1007/s12035-022-02897-1

Saxton, W. M., and Hollenbeck, P. J. (2012). The axonal transport of mitochondria. *J. Cell Sci.* 125, 2095–2104. doi:10.1242/jcs.053850

Schechter, M., and Sharon, R. (2021). An emerging role for phosphoinositides in the pathophysiology of Parkinson's disease. *J. Park. Dis.* 11, 1725–1750. doi:10.3233/JPD-212684

Schneider, Y., Gauer, C., Andert, M., Hoffmann, A., Riemenschneider, M. J., Krebs, W., et al. (2024). Distinct forebrain regions define a dichotomous astrocytic profile in multiple system atrophy. *Acta Neuropathol. Commun.* 12, 1. doi:10.1186/s40478-023-01699-3

Schweighauser, M., Shi, Y., Tarutani, A., Kametani, F., Murzin, A. G., Ghetti, B., et al. (2020). Structures of α-synuclein filaments from multiple system atrophy. *Nature* 585, 464–469. doi:10.1038/s41586-020-2317-6

Segrest, J. P., De Loof, H., Dohlman, J. G., Brouillette, C. G., and Anantharamaiah, G. M. (1990). Amphipathic helix motif: classes and properties. *Proteins Struct. Funct. Bioinforma.* 8, 103–117. doi:10.1002/prot.340080202

Shahmoradian, S. H., Lewis, A. J., Genoud, C., Hench, J., Moors, T. E., Navarro, P. P., et al. (2019). Lewy pathology in Parkinson's disease consists of crowded organelles and lipid membranes. *Nat. Neurosci.* 22, 1099–1109. doi:10.1038/s41593-019-0423-2

Shahnawaz, M., Mukherjee, A., Pritzkow, S., Mendez, N., Rabadia, P., Liu, X., et al. (2020). Discriminating α-synuclein strains in Parkinson's disease and multiple system atrophy. *Nature* 578, 273–277. doi:10.1038/s41586-020-1984-7

Sharma, M., and Burré, J. (2023). α-Synuclein in synaptic function and dysfunction. *Trends Neurosci.* 46, 153–166. doi:10.1016/j.tins.2022.11.007

Shvadchak, V. V., Yushchenko, D. A., Pievo, R., and Jovin, T. M. (2011). The mode of α-synuclein binding to membranes depends on lipid composition and lipid to protein ratio. *FEBS Lett.* 585, 3513–3519. doi:10.1016/j.febslet.2011.10.006

So, R. W. L., and Watts, J. C. (2023). α-Synuclein conformational strains as drivers of phenotypic heterogeneity in neurodegenerative diseases. *J. Mol. Biol.* 435, 168011. doi:10.1016/j.jmb.2023.168011

Soper, J. H., Kehm, V., Burd, C. G., Bankaitis, V. A., and Lee, V. M. Y. (2011). Aggregation of α-synuclein in *S. cerevisiae* is associated with defects in endosomal trafficking and phospholipid biosynthesis. *J. Mol. Neurosci.* 43, 391–405. doi:10.1007/s12031-010-9455-5

Spillantini, M. G., Crowther, R. A., Jakes, R., Cairns, N. J., Lantos, P. L., and Goedert, M. (1998). Filamentous alpha-synuclein inclusions link multiple system atrophy with Parkinson's disease and dementia with Lewy bodies. *Neurosci. Lett.* 251, 205–208. doi:10.1016/s0304-3940(98)00504-7

Stoker, T. B., and Barker, R. A. (2020). Recent developments in the treatment of Parkinson's Disease. *F1000Res* 9, 862. doi:10.12688/f1000research.25634.1

Sugeno, N., Jäckel, S., Voigt, A., Wassouf, Z., Schulze-Hentrich, J., and Kahle, P. J. (2016). α-Synuclein enhances histone H3 lysine-9 dimethylation and H3K9me2-dependent transcriptional responses. *Sci. Rep.* 6, 36328. doi:10.1038/srep36328

Surguchov, A. (2023). α-Synuclein and mechanisms of epigenetic regulation. *Brain Sci.* 13, 150. doi:10.3390/brainsci13010150

Svennerholm, L., Bostrom, K., Helander, C. G., and Jungbjer, B. (1991). Membrane lipids in the aging human brain. *J. Neurochem.* 56, 2051–2059. doi:10.1111/j.1471-4159.1991.tb03466.x

Taghavi, S., Chaouni, R., Tafakhori, A., Azcona, L. J., Firouzabadi, S. G., Omrani, M. D., et al. (2018). A clinical and molecular genetic study of 50 families with autosomal recessive parkinsonism revealed known and novel gene mutations. *Mol. Neurobiol.* 55, 3477–3489. doi:10.1007/s12035-017-0535-1

Taguchi, K., Watanabe, Y., Tsujimura, A., and Tanaka, M. (2016). Brain region-dependent differential expression of alpha-synuclein. *J. Comp. Neurol.* 524, 1236–1258. doi:10.1002/cne.23901

Tang, Y., Das, U., Scott, D. A., and Roy, S. (2012). The slow axonal transport of alpha-synuclein–mechanistic commonalities amongst diverse cytosolic cargoes. *Cytoskelet. Hob.* 69, 506–513. doi:10.1002/cm.21019

Teixeira, M., Sheta, R., Idi, W., and Oueslati, A. (2021). Alpha-synuclein and the endolysosomal system in Parkinson's disease: guilty by association. *Biomolecules* 11, 1333. doi:10.3390/biom11091333

Thayanidhi, N., Helm, J. R., Nycz, D. C., Bentley, M., Liang, Y., and Hay, J. C. (2010). Alpha-synuclein delays endoplasmic reticulum (ER)-to-Golgi transport in mammalian cells by antagonizing ER/Golgi SNAREs. *Mol. Biol. Cell* 21, 1850–1863. doi:10.1091/mbc.e09-09-0801

Timney, B. L., Raveh, B., Mironska, R., Trivedi, J. M., Kim, S. J., Russel, D., et al. (2016). Simple rules for passive diffusion through the nuclear pore complex. *J. Cell Biol.* 215, 57–76. doi:10.1083/jcb.201601004

Torre-Muruzabal, T., Van der Perren, A., Coens, A., Gelders, G., Janer, A. B., Camacho-Garcia, S., et al. (2023). Host oligodendrogliopathy and α-synuclein strains dictate disease severity in multiple system atrophy. *Brain* 146, 237–251. doi:10.1093/brain/awac061

Tsakiri, M., Tsichlis, I., Zivko, C., Demetzos, C., and Mahairaki, V. (2024). Lipidic nanoparticles, extracellular vesicles and hybrid platforms as advanced medicinal products: future therapeutic prospects for neurodegenerative diseases. *Pharmaceutics* 16, 350. doi:10.3390/pharmaceutics16030350

Tsuang, D., Leverenz, J. B., Lopez, O. L., Hamilton, R. L., Bennett, D. A., Schneider, J. A., et al. (2013). APOE ε4 increases risk for dementia in pure synucleinopathies. *JAMA Neurol.* 70, 223–228. doi:10.1001/jamaneurol.2013.600

Tuttle, M. D., Comellas, G., Nieuwkoop, A. J., Covell, D. J., Berthold, D. A., Kloepper, K. D., et al. (2016). Solid-state NMR structure of a pathogenic fibril of full-length human α-synuclein. *Nat. Struct. Mol. Biol.* 23, 409–415. doi:10.1038/nsmb.3194

Ueda, K., Fukushima, H., Masliah, E., Xia, Y., Iwai, A., Yoshimoto, M., et al. (1993). Molecular cloning of cDNA encoding an unrecognized component of amyloid in Alzheimer disease. *Proc. Natl. Acad. Sci. U. S. A.* 90, 11282–11286. doi:10.1073/pnas.90.23.11282

Vanhauwaert, R., Kuenen, S., Masius, R., Bademosi, A., Manetsberger, J., Schoovaerts, N., et al. (2017). The SAC1 domain in synaptojanin is required for autophagosome maturation at presynaptic terminals. *EMBO J.* 36, 1392–1411. doi:10.15252/embj.201695773

Vos, M., Dulovic-Mahlow, M., Mandik, F., Frese, L., Kanana, Y., Haissatou Diaw, S., et al. (2021). Ceramide accumulation induces mitophagy and impairs β-oxidation in PINK1 deficiency. *Proc. Natl. Acad. Sci. U. S. A.* 118, e2025347118. doi:10.1073/pnas.2025347118

Walker, L. C., and Jucker, M. (2015). Neurodegenerative diseases: expanding the prion concept. *Annu. Rev. Neurosci.* 38, 87–103. doi:10.1146/annurev-neuro-071714-033828

Wang, R., Sun, H., Ren, H., and Wang, G. (2020). α-Synuclein aggregation and transmission in Parkinson's disease: a link to mitochondria and lysosome. *Sci. China Life Sci.* 63, 1850–1859. doi:10.1007/s11427-020-1756-9

Watanabe, S., Mamer, L. E., Raychaudhuri, S., Luvsanjav, D., Eisen, J., Trimbuch, T., et al. (2018). Synaptojanin and endophilin mediate neck formation during ultrafast endocytosis. *Neuron* 98, 1184–1197 e6. doi:10.1016/j.neuron.2018.06.005

Wei, J., Wong, L. C., and Boland, S. (2023). Lipids as emerging biomarkers in neurodegenerative diseases. *Int. J. Mol. Sci.* 25, 131. doi:10.3390/ijms25010131

Westphal, C. H., and Chandra, S. S. (2013). Monomeric synucleins generate membrane curvature. *J. Biol. Chem.* 288, 1829–1840. doi:10.1074/jbc.M112.418871

Wiseman, J. A., Murray, H. C., Faull, R., Dragunow, M., Turner, C. P., Dieriks, B. V., et al. (2024). Aggregate-prone brain regions in Parkinson's disease are rich in unique N-terminus α-synuclein conformers with high proteolysis susceptibility. *NPJ Park. Dis.* 10, 1. doi:10.1038/s41531-023-00614-w

Woerman, A. L., Oehler, A., Kazmi, S. A., Lee, J., Halliday, G. M., Middleton, L. T., et al. (2019). Multiple system atrophy prions retain strain specificity after serial propagation in two different Tg(SNCA ∗ A53T) mouse lines. *Acta Neuropathol.* 137, 437–454. doi:10.1007/s00401-019-01959-4

Wood, P. L., Tippireddy, S., Feriante, J., and Woltjer, R. L. (2018). Augmented frontal cortex diacylglycerol levels in Parkinson's disease and Lewy Body Disease. *PloS one* 13, e0191815. doi:10.1371/journal.pone.0191815

Wu, G., Lu, Z. H., Kulkarni, N., Amin, R., and Ledeen, R. W. (2011). Mice lacking major brain gangliosides develop parkinsonism. *Neurochem. Res.* 36, 1706–1714. doi:10.1007/s11064-011-0437-y

Xiong, H., Callaghan, D., Jones, A., Walker, D. G., Lue, L. F., Beach, T. G., et al. (2008). Cholesterol retention in Alzheimer's brain is responsible for high beta- and gamma-secretase activities and Abeta production. *Neurobiol. Dis.* 29, 422–437. doi:10.1016/j.nbd.2007.10.005

Xu, L., Nussinov, R., and Ma, B. (2016). Coupling of the non-amyloid-component (NAC) domain and the KTK(E/Q)GV repeats stabilize the α-synuclein fibrils. *Eur. J. Med. Chem.* 121, 841–850. doi:10.1016/j.ejmech.2016.01.044

Yamazaki, Y., Zhao, N., Caulfield, T. R., Liu, C. C., and Bu, G. (2019). Apolipoprotein E and Alzheimer disease: pathobiology and targeting strategies. *Nat. Rev. Neurol.* 15, 501–518. doi:10.1038/s41582-019-0228-7

Yang, Y., Shi, Y., Schweighauser, M., Zhang, X., Kotecha, A., Murzin, A. G., et al. (2022). Structures of α-synuclein filaments from human brains with Lewy pathology. *Nature* 610, 791–795. doi:10.1038/s41586-022-05319-3

Yin, F. (2023). Lipid metabolism and Alzheimer's disease: clinical evidence, mechanistic link and therapeutic promise. *FEBS J.* 290, 1420–1453. doi:10.1111/febs.16344

Yoo, G., Shin, Y.-K., and Lee, N. K. (2023). The role of α-synuclein in SNARE-mediated synaptic vesicle fusion. *J. Mol. Biol.* 435, 167775. doi:10.1016/j.jmb.2022.167775

Yu, Q., He, Z., Zubkov, D., Huang, S., Kurochkin, I., Yang, X., et al. (2020). Lipidome alterations in human prefrontal cortex during development, aging, and cognitive disorders. *Mol. Psychiatry* 25, 2952–2969. doi:10.1038/s41380-018-0200-8

Zhang, J. M., Li, X. P., and Li, J. D. (2019). The roles of post-translational modifications on α-synuclein in the pathogenesis of Parkinson's diseases. *Front. Neurosci.* 13, 381. doi:10.3389/fnins.2019.00381

Zhu, L., Zhong, M., Elder, G. A., Sano, M., Holtzman, D. M., Gandy, S., et al. (2015). Phospholipid dysregulation contributes to ApoE4-associated cognitive deficits in Alzheimer's disease pathogenesis. *Proc. Natl. Acad. Sci. U. S. A.* 112, 11965–11970. doi:10.1073/pnas.1510011112

Zhu, M., and Fink, A. L. (2003). Lipid binding inhibits alpha-synuclein fibril formation. *J. Biol. Chem.* 278, 16873–16877. doi:10.1074/jbc.M210136200

frontiers | Frontiers in Molecular Biosciences

TYPE Mini Review
PUBLISHED 04 February 2025
DOI 10.3389/fmolb.2025.1550815

OPEN ACCESS

EDITED BY
Verena Kohler,
Umeå University, Sweden

REVIEWED BY
Kazuchika Nishitsuji,
Wakayama Medical University, Japan

*CORRESPONDENCE
Motoyuki Itoh,
mito@chiba-u.jp

RECEIVED 24 December 2024
ACCEPTED 20 January 2025
PUBLISHED 04 February 2025

CITATION
Suzuki S and Itoh M (2025) Synergistic effects of mutation and glycosylation on disease progression.
Front. Mol. Biosci. 12:1550815.
doi: 10.3389/fmolb.2025.1550815

Synergistic effects of mutation and glycosylation on disease progression

Shodai Suzuki[1] and Motoyuki Itoh[1,2,3]*

[1]Department of Biochemistry, Graduate School of Pharmaceutical Sciences, Chiba University, Chiba, Japan, [2]Research Institute of Disaster Medicine, Chiba University, Chiba, Japan, [3]Health and Disease Omics Center, Chiba University, Chiba, Japan

Glycosylation, a post-translational modification, plays a crucial role in proper localization and function of proteins. It is regulated by multiple glycosyltransferases and can be influenced by various factors. Inherited missense mutations in glycosylated proteins such as NOTCH3, Low-density lipoprotein receptor (LDLR), and Amyloid precursor protein (APP) could affect their glycosylation states, leading to cerebral small vessel disease, hypercholesterolemia, and Alzheimer's disease, respectively. Additionally, physiological states and aging-related conditions can affect the expression levels of glycosyltransferases. However, the interplay between mutations in glycosylated proteins and changes in their glycosylation levels remains poorly understood. This mini-review summarizes the effects of glycosylation on transmembrane proteins with pathogenic mutations, including NOTCH3, LDLR, and APP. We highlight the synergistic contributions of missense amino acids in the mutant proteins and alterations in their glycosylation states to their molecular pathogenesis.

KEYWORDS

glycosylation, mutation, aging, Notch3, LDLR, APP, CADASIL, familial hypercholesterolemia

1 Introduction

Glycosylation, a post-translational modification involving the addition of sugar chains to proteins, is categorized into *N*- and *O*-linked glycosylation. This process regulates protein folding, processing, transport, function, interactions, and turnover. Various glycosyltransferases are responsible for transferring glycans to proteins.

Abnormal glycosylation, driven by multiple factors, can lead to numerous pathogenic processes. The primary genetic pathology associated with aberrant glycosylation is congenital disorders of glycosylation (CDG). CDG involves loss-of-function mutations in genes related to the synthesis and transfer of glycan, often leading to developmental and neurological diseases (Reily et al., 2019). In contrast, some missense mutations in genes encoding glycosylated proteins, such as transmembrane proteins, can affect their glycosylation states and lead to pathogenesis. For example, missense mutations in NOTCH3 alter its *O*-glycosylation states and lead to cerebral autosomal dominant arteriopathy with subcortical infarcts and leukoencephalopathy (CADASIL) (Joutel et al., 1996; Arboleda-Velasquez et al., 2005; Suzuki et al., 2024). In addition, Low-density lipoprotein receptor (LDLR) and Amyloid precursor protein

(APP) are also glycosylated proteins and their glycosylation levels could be affected by mutations related with inherited diseases, familial hypercholesterolemia (FH) and familial Alzheimer's disease (FAD), respectively (Akasaka-Manya et al., 2008; Pedersen et al., 2014; Akasaka-Manya and Manya, 2020). Physiological aspects also influence glycosylation states. Expression levels of glycosyltransferases vary among different tissues and cell types (Indellicato and Trinchera, 2021; Sobral et al., 2022). Furthermore, degenerative conditions, such as aging, can alter the expression of glycosyltransferases (Vanhooren et al., 2011; Oinam et al., 2020; Sobral et al., 2022), the amounts of sugar-nucleotides as glycan sources (Imae et al., 2024), and thereby protein glycosylation states (Sato and Endo, 2010; Itakura et al., 2016; Gudelj et al., 2018; Zhang et al., 2024). However, the relationship between missense mutations in glycosylated proteins and changes in their glycosylation states is not fully understood.

This mini-review summarizes how mutations and glycosylation in the transmembrane proteins contribute to the pathogenesis, with a focus on NOTCH3, Low-density lipoprotein receptor (LDLR), and Amyloid precursor protein (APP). These examples highlight the synergistic roles of missense amino acids and the protein glycosylation changes in disease progression.

2 NOTCH3 and cerebral autosomal dominant arteriopathy with subcortical infarcts and leukoencephalopathy (CADASIL)

2.1 Effects of glycosylation on NOTCH3 functions and proteostasis

The *NOTCH3* gene encodes a single transmembrane receptor involved primarily in differentiation and survival of vascular smooth muscle cells (VSMCs) and pericytes in the adult vasculature (Domenga et al., 2004; Liu et al., 2010; Wang et al., 2014; Henshall et al., 2015; Vanlandewijck et al., 2018). NOTCH3 is one of NOTCH family (NOTCH1-4) and features 34 epidermal growth factor (EGF)-like repeats in its extracellular domain, including binding sites for canonical Notch ligands, such as Jagged (JAG)-1 and −2, and Delta-like ligands (DLL)-1 and −4 (Figure 1A) (Bray, 2006; Bray, 2016). The interaction between the NOTCH receptors and ligands triggers the dissociation of the extracellular and intracellular domain, which induces the upregulation of downstream gene expression (Nichols et al., 2007; Meloty-Kapella et al., 2012). The NOTCH3 ectodomain is endocytosed by JAG1 and DLL4 (Watanabe et al., 2011; Suzuki et al., 2021; Suzuki et al., 2024). In each EGF-like repeat of NOTCH, three disulfide bonds form between C^1-C^3, C^2-C^4 and C^5-C^6, where the number on cysteine denote their position within an EGF-like repeat. Moreover, NOTCH EGF-like repeats can be modulated by *O*-glycosylation, such as *O*-fucose, *O*-glucose, and *O*-*N*-acetylglucosamine (*O*-GlcNAc), which are modified by Protein *O*-fucosyltransferase 1 (POFUT1) (Moloney et al., 2000; Wang et al., 2001; Stahl et al., 2008), Protein *O*-glucosyltransferase 1-3 (POGLUT1-3) (Wang et al., 2001; Acar et al., 2008; Takeuchi et al., 2018), and EGF domain-specific *O*-linked *N*-acetylglucosamine transferase (EOGT) (Matsuura et al., 2008; Sakaidani et al., 2012), respectively (Figure 1A). The *O*-glycans are linked to serine or threonine within the cysteine-flanked consensus sequences of EGF-like repeats. Specifically, *O*-fucose attaches at C^2XXXXS/TC^3, *O*-glucose at C^1XSXA/PC^2 and $C^3XNTXGSFXC^4$, and *O*-GlcNAc at $C^5XXGY/FS/TGXXXC^6$ and $C^5XXGY/FS/TGXXC^6$ (Varshney and Stanley, 2018; Urata and Takeuchi, 2019). The POFUT1-mediated *O*-fucose modification regulates the trafficking and binding ability of Notch receptors (Okamura and Saga, 2008; Stahl et al., 2008). POFUT1 also functions as a glycosyltransferase-independent chaperone, helping Notch folding (Okajima et al., 2005). Monosaccharide *O*-fucose can be elongated to a tetrasaccharide with GlcNAc, galactose, and neuraminic acid, which are added by β-1,3-*N*-acetylglucosaminyltranseferase (Fringe), β-4-galactosyltranseferase, and sialyltransferase, respectively (Brückner et al., 2000; Moloney et al., 2000). Fringe modulates ligand-binding ability and signaling activity (Brückner et al., 2000; Moloney et al., 2000; Yang et al., 2005; Taylor et al., 2014; Kakuda and Haltiwanger, 2017; Kakuda et al., 2020; Suzuki et al., 2024). There are three homologs in mammals: Lunatic fringe (LFNG), Manic fringe (MFNG), and Radical fringe (RFNG), which glycosylate NOTCH at common and unique sets of sites. LFNG and MFNG inhibit the JAG1-dependent activity of NOTCH1, but RFNG enhances it (Moloney et al., 2000; Kakuda and Haltiwanger, 2017). Among three homologs, our recent study has demonstrated that a human pericyte cell line expresses RFNG at a higher level compared to LFNG and MFNG, and long-term culture-induced senescence increases RFNG in pericytes (Suzuki et al., 2024). Overexpression of RFNG in a NOTCH3-expressing HeLa cell line impairs JAG1-NOTCH3 but enhances DLL4-NOTCH3 activity (Suzuki et al., 2024). These findings suggest that RFNG can regulate the NOTCH3 function and turnover under cerebral microenvironment and aging conditions. Moreover, given that *O*-glucose and *O*-GlcNAc regulates the folding and transport of NOTCH1 (Takeuchi et al., 2017; Ogawa et al., 2020; Zhang et al., 2022), the three types of *O*-glycan may cooperatively play roles in NOTCH3 signaling function and proteostasis.

2.2 Roles of glycosylation in CADASIL pathogenesis

Mutations in *NOTCH3* gene cause Cerebral Autosomal Dominant Arteriopathy with Subcortical Infarcts and Leukoencephalopathy (CADASIL), a cerebral small vessel disease marked by recurrent ischemic strokes and vascular dementia (Joutel et al., 1996; Yamamoto et al., 2023; Mizuta et al., 2024). The disease is characterized by the degeneration of mural cells and the abnormal deposition of granular osmiophilic material (GOM), containing NOTCH3 protein as a main component (Ruchoux et al., 1995; Mayer et al., 1999; Joutel et al., 2000; Ishiko et al., 2006; Tikka et al., 2009; Lewandowska et al., 2011; Morroni et al., 2013). Based on investigations with disease model animals, the pathological features of CADASIL appear in an age-dependent manner (Joutel et al., 2010; Ghosh et al., 2015; Gravesteijn et al., 2019). High-risk pathogenic mutations are clustered within the EGF-like repeats 1 to 6, which are not ligand-binding domain (Rutten et al., 2016; Hack et al., 2023) (Figure 1A).

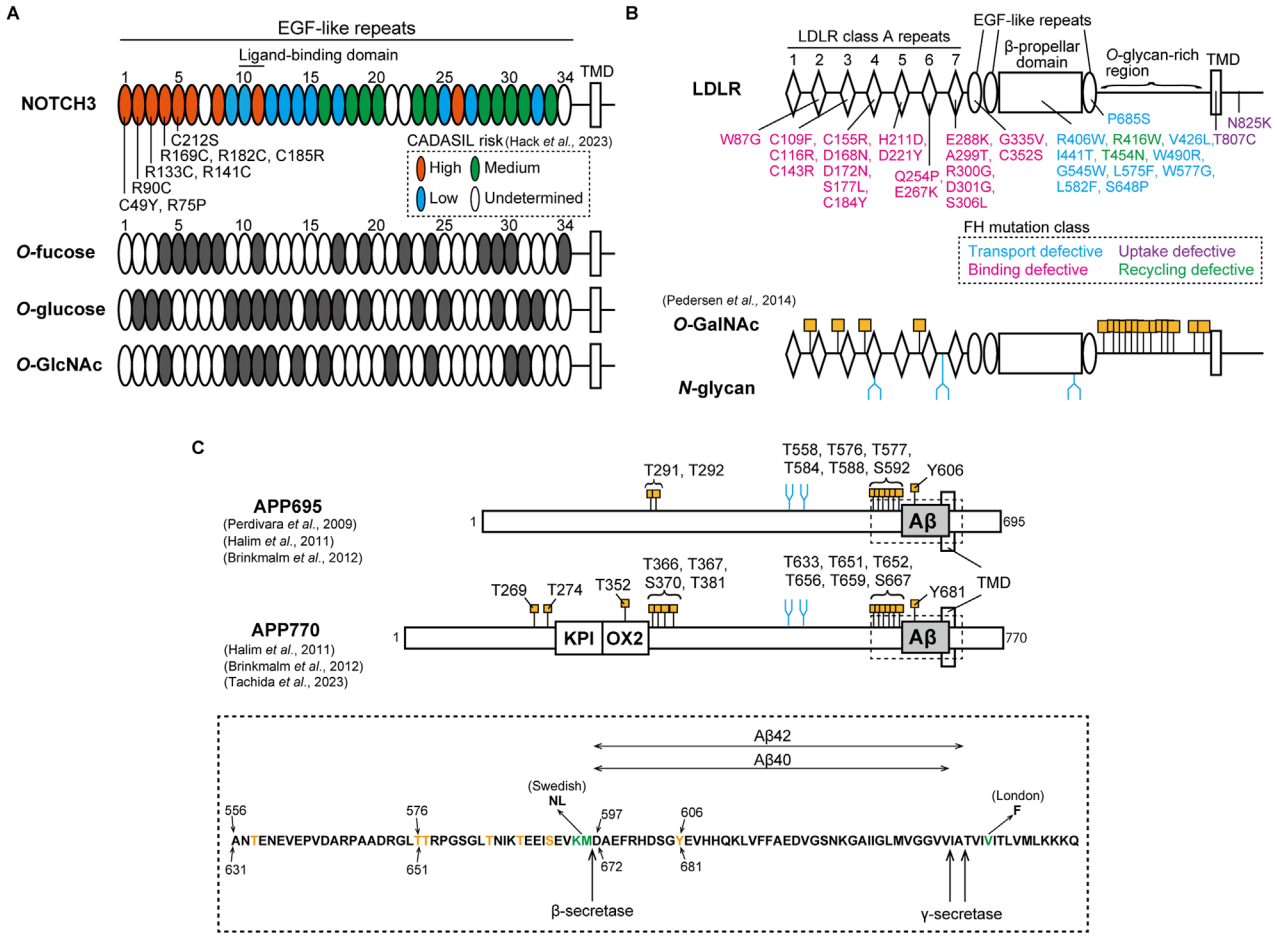

FIGURE 1
Pathological mutation and glycosylation amino acid sites of NOTCH3, LDLR, and APP. **(A)** Upper: NOTCH3 consists of 34 EGF-like repeats in its ectodomain, as shown in an oval. The ligand-binding domain exists in EGF-like repeats 10 and 11. EGF-like repeats at which cysteine-altering mutations are associated with high, medium, low and undetermined risks for CADASIL are shown in orange, green, cyan, and white, respectively, as classified in a recent study (Hack et al., 2023). Representative pathogenic mutations in EGF-like repeats 1 to 5 are shown. TMD represents transmembrane domain. Below: EGF-like repeats that harbor the consensus sites for *O*-fucose (C^2XXXXS/TC^3), *O*-glucose (C^1XSXA/PC^2 and $C^3XNTXGSFXC^4$), and *O*-GlcNAc ($C^5XXGY/FS/TGXXXC^6$ and $C^5XXGY/FS/TGXXC^6$) are shown in gray. **(B)** Upper: LDLR consists of 7 class A repeats with the linker region, a β-propeller domain surrounded by two and one EGF-like repeats, an *O*-glycan-rich domain, a transmembrane domain, and an intracellular domain. The ligand-binding domain exists in the class A repeats. FH-causing missense mutations are shown in cyan, magenta, purple, and green, depending on functional phenotypes with defects in transport, binding, uptake, and recycling, respectively. TMD represents transmembrane domain. Below: *O*-GalNAc and *N*-glycan modification sites in the LDLR as identified by Pedersen et al. (2014). *O*-GalNAc is modified at four consensus sites, XX-C^6-XXXT-C^1-XX, within linker regions between the class A repeats and at multiple sites of the *O*-glycan-rich domain, as shown in orange. *N*-glycan is also attached to three sites in the class A repeats and the β-propeller domain, as represented in blue. **(C)** Upper: APP isoforms, APP695 and APP770. Compared to APP695, APP770 has KPI and OX2 domains. Aβ, as shown in gray, is cleaved by β- and γ-secretase. *O*-GalNAc and *N*-glycan are attached to specific sites, as shown in orange and blue, respectively (Perdivara et al., 2009; Halim et al., 2011; Brinkmalm et al., 2012; Tachida et al., 2023). TMD represents the transmembrane domain. Below: amino acid sequences including the Aβ region, as highlighted in the upper figure by a dotted box. Threonine, serine, and tyrosine residues modified with *O*-GalNAc are shown in orange. The amino acids shown in green are mutated sites observed in FAD Swedish and London families. The amino acid positions for APP695 and APP770 are described at the upper and bottom sides, respectively.

Furthermore, most CADASIL mutations alter cysteine residues, inducing aggregation. NOTCH3 C49Y, R90C, R133C, R141C, and C183R mutations result in the multimerization of the EGF-like repeats 1-3 and 1-5 fragmented protein due to abnormal disulfide bond formation (Opherk et al., 2009; Duering et al., 2011; Young et al., 2022). Despite the tendency of NOTCH3 R133C and C185R to accumulate within the endoplasmic reticulum and at the cell membrane (Takahashi et al., 2010; Watanabe et al., 2011; Suzuki et al., 2024), our research indicates that this accumulation is influenced by the cellular environment as well as the mutation itself (Suzuki et al., 2021). In addition, signaling defects in NOTCH3 mutants might also play a role in disease pathogenesis, which remains a topic of debate (Joutel et al., 2004; Peters et al., 2004; Jin et al., 2008; Dupré et al., 2024; Romay et al., 2024). Taking all factors into account, the cellular accumulation and signaling defects of NOTCH3 CADASIL mutant proteins may be contingent on cellular conditions, including the glycosylation states of NOTCH3. Since the *O*-glycan consensus sequences of NOTCH include cysteine residues at defined positions, numerous pathogenic cysteine-altering mutations can change NOTCH3 glycosylation

states, leading to abnormal function and turnover. POFUT1 does not facilitate the folding of a CADASIL-like *Drosophila* Notch mutant C599Y, which corresponds to C542Y in human NOTCH3, in comparison to the wild-type Notch (Okajima et al., 2005). Mouse NOTCH3 CADASIL-like mutants R91C, R170C, and C213S (corresponding to R90C, R169C, and C212S in human NOTCH3, respectively), exhibit impairment of LFNG-mediated modification in the NOTCH3 EGF-like domains 1 to 5 (Arboleda-Velasquez et al., 2005). LFNG tends to increase the aggregation propensity of NOTCH3 C185R but not that of NOTCH3 WT (Suzuki et al., 2021). Our recent study has demonstrated that an increase in RFNG expression leads to a greater reduction in signaling activity and turnover of NOTCH3 R141C and C185R compared to the WT (Suzuki et al., 2024). Furthermore, LC-MS/MS analysis demonstrated that RFNG modifies NOTCH3 C185R at a lesser extent to the WT in the EGF-like repeat 4 but to a similar extent in the EGF-like repeat-11 (Suzuki et al., 2024). Given that specific *O*-fucose sites on NOTCH1 play unique roles in how Fringe modulates NOTCH1 activity through *O*-fucose elongation (Kakuda and Haltiwanger, 2017), reduced RFNG-mediated glycosylation in NOTCH3 C185R EGF-like repeat 4, compared to NOTCH3 WT, may lead to impaired signaling activity and increased resistance to degradation of NOTCH3 C185R. Furthermore, investigating the NOTCH3 EGF-like domains linked to CADASIL risk and their glycosylation consensus sites may explain the high risk for CADASIL (57) (Figure 1A). For example, patients with NOTCH3 R182C mutation in the EGF-like domain 4 have a higher accumulation of NOTCH3 protein around the vessels compared to those with R141C in EGF-like repeat 3 and R75P in EGF-like repeat 1 (Ishiyama et al., 2024). This may potentially be attributed to the unique positioning of the EGF-like domain 4, which has three types of *O*-glycosylation consensus amino acid sequences (Figure 1A). On the other hand, the modification of NOTCH1 EGF-like domains by Fringe varies with cell type (Matsumoto et al., 2022). Therefore, comprehensive analyses are needed to investigate the *O*-glycosylation states of NOTCH3 in specific cell types, such as vascular muscle cells and pericytes, as well as under senescent conditions.

3 Low-density lipoprotein receptor (LDLR) and familial hypercholesterolemia (FH)

3.1 Roles of glycosylation on LDLR functions and transport

The low-density lipoprotein receptor (LDLR) is a transmembrane receptor expressed in many types of cells, regulating plasma cholesterol levels (Goldstein and Brown, 1985). The extracellular region at the N-terminal domain harbors seven LDLR class A repeats, each of which is a cysteine-rich module with three disulfide bonds. Additionally, there are three EGF-like repeats along with a β-propeller domain and clustered *O*-glycan-rich sites (Figure 1B). LDLR-mediated cholesterol maintenance begins with LDLR binding to plasma LDL, a circulating cholesterol carrier containing apolipoprotein families such as apolipoprotein B (APOB), and subsequently undergoing clathrin-mediated endocytosis (Goldstein and Brown, 1985; Esser et al., 1988; Russell et al., 1989). The binding of LDLR to LDL involves the LDLR class A repeats 1-7, among which deletion of class A repeat-5 impacts LDLR binding ability the most (Russell et al., 1989). After transport to endosomes, the acidic conditions enable the EGF-like repeats and β-propeller domains of LDLR to change conformation (Davis et al., 1987; Klee and Zimmermann, 2019). This results in the dissociation of LDLR-LDL complex and subsequent recycling of LDLR to the cell membrane (Davis et al., 1987). LDLR is known to be modified with both *O*- and *N*-glycans (Cummings et al., 1983; Pedersen et al., 2014) (Figure 1B). Defects in producing UDP-*N*-acetylgalactosamine (GalNAc) lead to reduced expression of LDLR at the cell membrane, suggesting that mucin-type *O*-GalNAc modification of LDLR is required for the stabilization (Kozarsky et al., 1988). Mass spectrometric analysis showed that the linker domains between the class A repeats are modified with *O*-GalNAc at threonine residues in the consensus sequence XX-C^{6}-XXXT-C^{1}-XX (Figure 1B) (Pedersen et al., 2014). Among the polypeptide *N*-acetylgalactosaminyltransferase family (ppGalNAc-Ts), ppGalNAc-T11 mainly regulates *O*-GalNAc modification in LDLR (Pedersen et al., 2014). Furthermore, the *O*-GalNAc in the linker regions regulates LDLR affinity for LDL (Wang et al., 2018). In contrast, the *O*-glycan-rich region stabilizes the protein structure but does not affect binding affinity for LDL (Davis et al., 1986a). LDLR class A repeats and β-propeller domain are also modified with *N*-glycans (Figure 1B), but their functions remain unclear (Pedersen et al., 2014).

3.2 Relevance of glycosylation with FH pathogenesis

LDLR variants are associated with familial hypercholesterolemia (FH), leading to arteriosclerosis and myocardial infarction (Goldstein and Brown, 1985). Aging plays a key role in causing coronary heart disease in FH (Mabuchi et al., 1989; Perak et al., 2016). Although FH pathogenic mutations are widely reported in *LDLR* without a hot spot (Vrablik et al., 2020), FH mutations in the class A repeat 5 are abundant and lead to higher LDL-cholesterol levels in blood than those in other domains (Gudnason et al., 1994; Day et al., 1997). Based on structural and functional analysis, the mutations are classified into classes 1 to 5 (Tolleshaug et al., 1983; Etxebarria et al., 2015; Benito-Vicente et al., 2018; Banerjee et al., 2019; Alves et al., 2021; Graça et al., 2022). Class 1: the null alleles do not produce LDLR, resulting in no visible protein bands on polyacrylamide gel electrophoresis (Tolleshaug et al., 1983). Class 2: transport-defective alleles express the glycosylation-immature form due to retention in the endoplasmic reticulum (Tolleshaug et al., 1983; Etxebarria et al., 2015; Benito-Vicente et al., 2018; Banerjee et al., 2019; Kizhakkedath et al., 2019; Alves et al., 2021; Graça et al., 2022). Class 3: binding-deficient alleles produce mature LDLR transported to the cell membrane, but impair its binding ability to LDL (Tolleshaug et al., 1983; Etxebarria et al., 2015; Benito-Vicente et al., 2018; Banerjee et al., 2019; Alves et al., 2021; Graça et al., 2022). Class 4: internalization-deficient alleles exhibit low endocytosis of LDLR (Lehrman et al., 1985; Davis et al., 1986b; Benito-Vicente et al., 2018). Class 5: recycling-defective mutations in the β-propeller domain impair the recycling pathway after the dissociation of the LDLR-LDL complex (Benito-Vicente et al., 2018;

Banerjee et al., 2019). While the LDLR variants affect 55% of amino acids located within five or fewer residues from glycosylation sites (Klee and Zimmermann, 2019), the precise mechanisms by which the missense mutations in LDLR affect its glycosylation, thereby leading to insufficient binding, uptake, and recycling phenotypes, remain unclear. One possibility is that cysteine-altering mutations could affect the structure of the consensus *O*-GalNAc amino acid sequence in the class A linker regions. This may result in reduced *O*-GalNAc modification and thereby less binding ability of LDLR (Figure 1B) (Wang et al., 2018). Cysteine-sparing mutations in *LDLR* may also cause abnormal disulfide bonds, as seen in mutations in *NOTCH3,* and subsequently reduced glycosylation (Wollenweber et al., 2015). Additionally, aging-mediated expression changes in ppGalNAc-Ts and mutations in *LDLR* may cooperatively contribute to pathogenesis (Sobral et al., 2022). Comprehensive investigation of glycosylation in LDLR mutants, under conditions with aging and various cell types, may help in understanding of the glycosylation-mediated mechanisms underlying FH pathogenesis.

4 Amyloid precursor protein (APP) and familial Alzheimer's disease (FAD)

4.1 Effects of glycosylation on APP transport and processing

The amyloid precursor protein (APP) is a transmembrane protein involved in Alzheimer's disease through the production of amyloid-β (Aβ). APP exists in three isoforms: APP695, APP751, and APP770. APP695 is predominantly expressed in mature neurons, while APP770 is expressed in brain endothelial cells (Wertkin et al., 1993; Kitazume et al., 2010). APP undergoes amyloidogenic and non-amyloidogenic pathways, regulated by different processing enzymes. The amyloidogenic process initiates with cleavage by β-secretase 1 (BACE1) in the Goldi complex and endosome, leading to the release of the toxic peptide Aβ through subsequent processing by γ-secretase. In the non-amyloidogenic pathway, APP is cleaved by α-secretase and γ-secretase, producing the extracellular soluble APP-α protein. These distinct processing pathways are regulated by *N*- and *O*-linked glycosylation attached to APP (Figure 1C) (Akasaka-Manya and Manya, 2020). APP has two *N*-glycosylation sites, and APP695 mutants deficient in *N*-glycosylation show impaired transport to the cell membrane (Yazaki et al., 1996; Tsatsanis et al., 2019). β-galactoside α2,6-sialyltransferase (ST6Gal-I) adds sialic acid to the terminal galactose of *N*-linked glycans. Overexpression of ST6Gal-I enhances both α-cleavage and β-cleavage of APP695 by increasing its sialylation, resulting in elevated Aβ release (Nakagawa et al., 2006). The bisecting GlcNAc, a form of *N*-linked glycan, is modified by GnT-III. Overexpression of GnT-III reduces Aβ secretion in Neuro2a cells through increased glycosylation of APP695 and BACE1, indicating that increased bisecting GlcNAc on APP695 and BACE1 is protective against Aβ production (Akasaka-Manya et al., 2010). Mass spectrometry analyses show that APP has threonine and serine sites modified with *O*-GalNAc glycans (Perdivara et al., 2009; Halim et al., 2011; Brinkmalm et al., 2012; Tachida et al., 2023) (Figure 1C). The *O*-glycan-deficient mutation in APP695 causes retention in the endoplasmic reticulum, impairing the processing pathways (Tomita et al., 1998). ppGalNAc-T6 glycosylates APP695 at T577, promoting α-cleavage but not β-cleavage. This results in decreased Aβ release (Akasaka-Manya et al., 2017). ppGalNAc-T2 also regulates Aβ production from APP695 (Liu et al., 2017) and APP770 (Tachida et al., 2023). Moreover, Aβ peptide purified from human cerebrospinal fluid, which may be derived from all APP isoforms, contains the unique *O*-GalNAc modification at the tyrosine residue, APP695 Y606 and APP770 Y681, respectively (Halim et al., 2011; Brinkmalm et al., 2012). This modification regulates the secondary structure and processing efficiency of the APP fragment (Singh et al., 2021). Similar to the Notch protein, the extracellular domain of APP695 could be modified with *O*-GlcNAc at the threonine residues, T291, T292, and T576 (Chun et al., 2017). *O*-GlcNAcase inhibition with PUGNAc, which enhances *O*-GlcNAcylation on APP695, reduces Aβ release by decreasing APP695 internalization from the cell membrane (Jacobsen and Iverfeldt, 2011; Chun et al., 2015). The glycosyltransferase for APP695 *O*-GlcNAcylation has not been identified yet, but EOGT could play a role (Akasaka-Manya and Manya, 2020). On the other hand, the effects of *O*-glycosylation on processing and transport differ between APP695 and APP770 (Tachida et al., 2023). Accordingly, the diverse *N*- and *O*-glycosylation at multiple amino acid sites regulate the folding, cellular localization, and cleavage pathways of APP695 and APP770 in distinct ways, thereby controlling Aβ release.

4.2 Impacts of glycosylation on Aβ production from APP pathogenic mutants

Mutations in the *APP* gene cause familial Alzheimer's disease (FAD). The APP695 K595N and M596L mutations, known as the Swedish mutation, exhibit higher cleavage efficiency by BACE1 compared to wild-type APP, leading to increased Aβ production (Citron et al., 1992; Perez et al., 1996; Thinakaran et al., 1996). APP produces different Aβ forms, Aβ40 and Aβ42, with the latter being less soluble (Burdick et al., 1992; Jarrett et al., 1993). The APP695 London-type mutation, V642F, located near the γ-secretase site, increases Aβ42 release but not Aβ40 (Suzuki et al., 1994). APP695 Swedish and London-type mutants exhibit increased bisecting GlcNAc and core fucose in *N*-glycans (Akasaka-Manya et al., 2008). Although bisecting GlcNAc protects against Aβ production in APP WT (Akasaka-Manya et al., 2010), the effects of enhanced *N*-glycosylation of APP Swedish and London mutants on additional Aβ production remain unknown. BACE1 can directly reduce ST6Gal-I activity through its cleavage, which competes with APP695 WT as a BACE1 substrate (Kitazume et al., 2001). However, the APP695 Swedish mutant cannot reduce ST6Gal-I activity compared to APP WT, potentially increasing Aβ production due to enhanced sialylation (Kitazume et al., 2001; Nakagawa et al., 2006). Furthermore, APP770 Y681 *O*-GalNAcylation increases β-cleavage of the Swedish mutant but not that of WT, indicating the synergistic contributions of APP Swedish mutation and the *O*-GalNAc modification at the tyrosine to Aβ production (Singh et al., 2021). Therefore, *N*-glycan and *O*-glycosylation can impact Aβ production from APP FAD mutant proteins, in addition to the effects of mutations themselves. Future work is required to determine the glycosylation states of APP FAD mutants in different cell types such as neurons and cerebral endothelial cells.

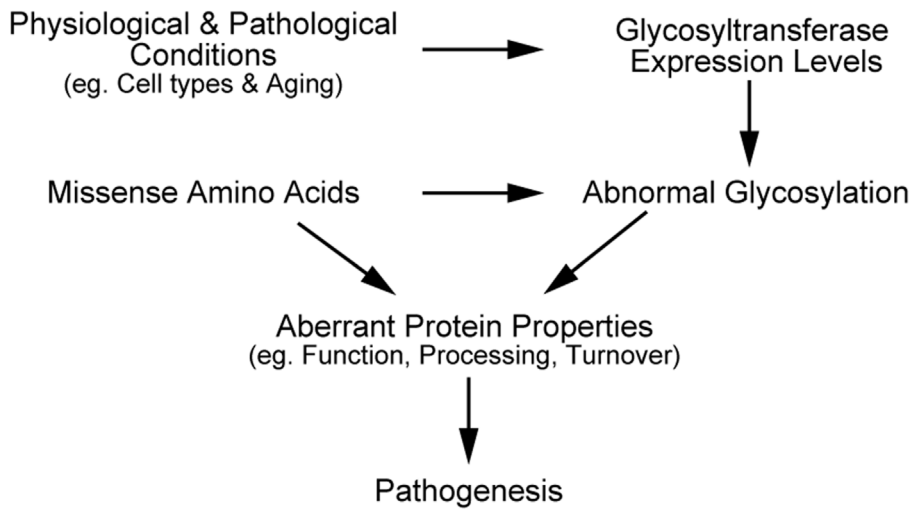

FIGURE 2
Schematic illustration explaining synergistic effects of mutation and glycosylation on disease progression.

5 Summary and conclusion

In this review, we have outlined the impacts of *O*- and *N*-linked glycosylation on the function, processing, and turnover of pathogenic mutants, including NOTCH3, LDLR, and APP. Missense mutations in the transmembrane proteins can alter their glycosylation states, partly due to structural disturbances around glycosylated sites. The variants can change the protein localization of proteins, resulting in glycosylation pattern that differ from the wild-type. Moreover, cell types and aging are known to affect expression levels of glycosyltransferases such as radical fringe and ppGalNAc-Ts (Sobral et al., 2022; Suzuki et al., 2024), and consequently change the glycosylation levels of NOTCH3, LDLR, and APP. Therefore, missense amino acids, physiological and pathological changes of glycosyltransferases expression, and abnormal glycosylation in mutant proteins can synergistically contribute to pathogenesis (Figure 2). Employing state-of-the-art techniques to detect *N*- and *O*-glycosylation and investigating the combined effects of glycosylation and mutations could enhance our understanding of molecular pathogenic mechanisms. Meanwhile, it is crucial to determine the glycosylation states of mutant proteins with an appropriate experimental design, considering both physiological and pathogenic conditions.

Author contributions

SS: Conceptualization, Funding acquisition, Resources, Writing–original draft, Writing–review and editing. MI: Conceptualization, Funding acquisition, Resources, Supervision, Writing–review and editing.

Funding

The author(s) declare that financial support was received for the research, authorship, and/or publication of this article. This research was supported by JSPS KAKENHI Grant Number JP22KJ0484 (to S.S.), JP21H02621 (to M.I.), and Grants-in-Aid for Students in Innovative Medicine CHIBA Doctoral WISE Program (to S.S.).

Conflict of interest

The authors declare that the research was conducted in the absence of any commercial or financial relationships that could be construed as a potential conflict of interest.

Generative AI statement

The author(s) declare that Generative AI was used in the creation of this manuscript. Generative AI Microsoft Copilot was used to help English proofreading.

Publisher's note

All claims expressed in this article are solely those of the authors and do not necessarily represent those of their affiliated organizations, or those of the publisher, the editors and the reviewers. Any product that may be evaluated in this article, or claim that may be made by its manufacturer, is not guaranteed or endorsed by the publisher.

References

Acar, M., Jafar-Nejad, H., Takeuchi, H., Rajan, A., Ibrani, D., Rana, N. A., et al. (2008). Rumi is a CAP10 domain glycosyltransferase that modifies notch and is required for notch signaling. *Cell* 132, 247–258. doi:10.1016/J.CELL.2007.12.016

Akasaka-Manya, K., Kawamura, M., Tsumoto, H., Saito, Y., Tachida, Y., Kitazume, S., et al. (2017). Excess APP O-glycosylation by GalNAc-T6 decreases Aβ production. *J. Biochem.* 161, 99–111. doi:10.1093/jb/mvw056

Akasaka-Manya, K., and Manya, H. (2020). The role of APP O-glycosylation in Alzheimer's disease. *Biomolecules* 10, 1569–1614. doi:10.3390/BIOM10111569

Akasaka-Manya, K., Manya, H., Sakurai, Y., Wojczyk, B. S., Kozutsumi, Y., Saito, Y., et al. (2010). Protective effect of N-glycan bisecting GlcNAc residues on beta-amyloid production in Alzheimer's disease. *Glycobiology* 20, 99–106. doi:10.1093/GLYCOB/CWP152

Akasaka-Manya, K., Manya, H., Sakurai, Y., Wojczyk, B. S., Spitalnik, S. L., and Endo, T. (2008). Increased bisecting and core-fucosylated N-glycans on mutant human amyloid precursor proteins. *Glycoconj J.* 25, 775–786. doi:10.1007/s10719-008-9140-x

Alves, A. C., Azevedo, S., Benito-Vicente, A., Graça, R., Galicia-Garcia, U., Barros, P., et al. (2021). LDLR variants functional characterization: contribution to variant classification. *Atherosclerosis* 329, 14–21. doi:10.1016/j.atherosclerosis.2021.06.001

Arboleda-Velasquez, J. F., Rampal, R., Fung, E., Darland, D. C., Liu, M., Martinez, M. C., et al. (2005). CADASIL mutations impair Notch3 glycosylation by Fringe. *Hum. Mol. Genet.* 14, 1631–1639. doi:10.1093/hmg/ddi171

Banerjee, P., Chan, K. C., Tarabocchia, M., Benito-Vicente, A., Alves, A. C., Uribe, K. B., et al. (2019). Functional analysis of LDLR (low-density lipoprotein receptor) variants in patient lymphocytes to assess the effect of evinacumab in homozygous familial hypercholesterolemia patients with a spectrum of LDLR activity. *Arterioscler. Thromb. Vasc. Biol.* 39, 2248–2260. doi:10.1161/ATVBAHA.119.313051

Benito-Vicente, A., Uribe, K. B., Jebari, S., Galicia-Garcia, U., Ostolaza, H., and Martin, C. (2018). Validation of LDLr activity as a tool to improve genetic diagnosis of familial hypercholesterolemia: a retrospective on functional characterization of LDLr variants. *Int. J. Mol. Sci.* 19, 1676–1719. doi:10.3390/IJMS19061676

Bray, S. J. (2006). Notch signalling: a simple pathway becomes complex. *Nat. Rev. Mol. Cell Biol.* 7, 678–689. doi:10.1038/nrm2009

Bray, S. J. (2016). Notch signalling in context. *Nat. Rev. Mol. Cell Biol.* 17 (11), 722–735. doi:10.1038/nrm.2016.94

Brinkmalm, G., Portelius, E., Öhrfelt, A., Mattsson, N., Persson, R., Gustavsson, M. K., et al. (2012). An online nano-LC-ESI-FTICR-MS method for comprehensive characterization of endogenous fragments from amyloid β and amyloid precursor protein in human and cat cerebrospinal fluid. *J. Mass Spectrom.* 47, 591–603. doi:10.1002/jms.2987

Brückner, K., Perez, L., Clausen, H., and Cohen, S. (2000). Glycosyltransferase activity of fringe modulates notch–delta interactions. *Nature* 406, 411–415. doi:10.1038/35019075

Burdick, D., Soreghan, B., Kwon, M., Kosmoski, J., Knauer, M., Henschen, A., et al. (1992). Assembly and aggregation properties of synthetic Alzheimer's A4/beta amyloid peptide analogs. *J. Biol. Chem.* 267, 546–554. doi:10.1016/s0021-9258(18)48529-8

Chun, Y. S., Kwon, O. H., and Chung, S. (2017). O-GlcNAcylation of amyloid-β precursor protein at threonine 576 residue regulates trafficking and processing. *Biochem. Biophys. Res. Commun.* 490, 486–491. doi:10.1016/J.BBRC.2017.06.067

Chun, Y. S., Park, Y., Oh, H. G., Kim, T. W., Yang, H. O., Park, M. K., et al. (2015). O-GlcNAcylation promotes non-amyloidogenic processing of amyloid-β protein precursor via inhibition of endocytosis from the plasma membrane. *J. Alzheimer's Dis.* 44, 261–275. doi:10.3233/JAD-140096

Citron, M., Ohersdorf, T., Haass, C., Mcconlogue, L., Hung, A. Y., Seubert, P., et al. (1992). Mutation of the β-amyloid precursor protein in familial Alzheimer's disease increases β-protein production. *Nature* 360, 1991–1993. doi:10.1038/360672a0

Cummings, R. D., Kornfeld, S., Schneider, W. J., Hobgood, K. K., Tolleshaug, H., Brown, M. S., et al. (1983). Biosynthesis of N- and O-linked oligosaccharides of the low density lipoprotein receptor. *J. Biol. Chem.* 258, 15261–15273. doi:10.1016/S0021-9258(17)43802-6

Davis, C. G., Elhammer, A., Russell, D. W., Schneider, W. J., Kornfeld, S., Brown, M. S., et al. (1986a). Deletion of clustered O-linked carbohydrates does not impair function of low density lipoprotein receptor in transfected fibroblasts. *J. Biol. Chem.* 261, 2828–2838. doi:10.1016/S0021-9258(17)35862-3

Davis, C. G., Goldstein, J. L., Südhof, T. C., Anderson, R. G. W., Russell, D. W., and Brown, M. S. (1987). Acid-dependent ligand dissociation and recycling of LDL receptor mediated by growth factor homology region. *Nature* 326, 760–765. doi:10.1038/326760a0

Davis, C. G., Lehrman, M. A., Russell, D. W., Anderson, R. G. W., Brown, M. S., and Goldstein, J. L. (1986b). The J. D. mutation in familial hypercholesterolemia: amino acid substitution in cytoplasmic domain impedes internalization of LDL receptors. *Cell* 45, 15–24. doi:10.1016/0092-8674(86)90533-7

Day, I. N. M., Whittall, R. A., O'Dell, S. D., Haddad, L., Bolla, M. K., Gudnason, V., et al. (1997). Spectrum of LDL receptor gene mutations in heterozygous familial hypercholesterolemia. *Hum. Mutat.* 10, 116–127. doi:10.1002/(SICI)1098-1004(1997)10:2<116::AID-HUMU4>3.0.CO;2-I

Domenga, V., Fardoux, P., Lacombe, P., Monet, M., Maciazek, J., Krebs, L. T., et al. (2004). Notch3 is required for arterial identity and maturation of vascular smooth muscle cells. *Genes Dev.* 18, 2730–2735. doi:10.1101/gad.308904

Duering, M., Karpinska, A., Rosner, S., Hopfner, F., Zechmeister, M., Peters, N., et al. (2011). Co-aggregate formation of CADASIL-mutant NOTCH3: a single-particle analysis. *Hum. Mol. Genet.* 20, 3256–3265. doi:10.1093/hmg/ddr237

Dupré, N., Gueniot, F., Domenga-Denier, V., Dubosclard, V., Nilles, C., Hill-Eubanks, D., et al. (2024). Protein aggregates containing wild-type and mutant NOTCH3 are major drivers of arterial pathology in CADASIL. *J. Clin. Investigation* 134, e175789. doi:10.1172/JCI175789

Esser, V., Limbird, L. E., Brown, M. S., Goldstein, J. L., and Russell, D. W. (1988). Mutational analysis of the ligand binding domain of the low density lipoprotein receptor. *J. Biol. Chem.* 263, 13282–13290. doi:10.1016/S0021-9258(18)37702-0

Etxebarria, A., Benito-Vicente, A., Stef, M., Ostolaza, H., Palacios, L., and Martin, C. (2015). Activity-associated effect of LDL receptor missense variants located in the cysteine-rich repeats. *Atherosclerosis* 238, 304–312. doi:10.1016/J.ATHEROSCLEROSIS.2014.12.026

Ghosh, M., Balbi, M., Hellal, F., Dichgans, M., Lindauer, U., and Plesnila, N. (2015). Pericytes are involved in the pathogenesis of CADASIL. *Ann. Neurol.*, 1–39. doi:10.1002/ana.24512

Goldstein, J. L., and Brown, M. S. (1985). The ldl receptor and the regulation of cellular cholesterol metabolism. *J. Cell Sci.* 1985, 131–137. doi:10.1242/JCS.1985.SUPPLEMENT_3.13

Graça, R., Alves, A. C., Zimon, M., Pepperkok, R., and Bourbon, M. (2022). Functional profiling of LDLR variants: important evidence for variant classification: functional profiling of LDLR variants. *J. Clin. Lipidol.* 16, 516–524. doi:10.1016/j.jacl.2022.04.005

Gravesteijn, G., Munting, L. P., Overzier, M., Mulder, A. A., Hegeman, I., Derieppe, M., et al. (2019). Progression and classification of granular osmiophilic material (GOM) deposits in functionally characterized human NOTCH3 transgenic mice. *Transl. Stroke Res.* 11, 517–527. doi:10.1007/s12975-019-00742-7

Gudelj, I., Lauc, G., and Pezer, M. (2018). Immunoglobulin G glycosylation in aging and diseases. *Cell Immunol.* 333, 65–79. doi:10.1016/J.CELLIMM.2018.07.009

Gudnason, V., Day, I. N. M., and Humphries, S. E. (1994). Effect on plasma lipid levels of different classes of mutations in the low-density lipoprotein receptor gene in patients with familial hypercholesterolemia. *Arterioscler. Thromb. Vasc. Biol.* 14, 1717–1722. doi:10.1161/01.ATV.14.11.1717

Hack, R. J., Gravesteijn, G., Cerfontaine, M. N., Santcroos, M. A., Gatti, L., Kopczak, A., et al. (2023). Three-tiered EGFr domain risk stratification for individualized NOTCH3-small vessel disease prediction. *Brain* 146, 2913–2927. doi:10.1093/BRAIN/AWAC486

Halim, A., Brinkmalm, G., Rüetschi, U., Westman-Brinkmalm, A., Portelius, E., Zetterberg, H., et al. (2011). Site-specific characterization of threonine, serine, and tyrosine glycosylations of amyloid precursor protein/amyloid beta-peptides in human cerebrospinal fluid. *Proc. Natl. Acad. Sci. U. S. A.* 108, 11848–11853. doi:10.1073/pnas.1102664108

Henshall, T. L., Keller, A., He, L., Johansson, B. R., Wallgard, E., Raschperger, E., et al. (2015). Notch3 is necessary for blood vessel integrity in the central nervous system. *Arterioscler. Thromb. Vasc. Biol.* 35, 409–420. doi:10.1161/ATVBAHA.114.304849

Imae, R., Manya, H., Tsumoto, H., Umezawa, K., Miura, Y., and Endo, T. (2024). Changes in the amount of nucleotide sugars in aged mouse tissues. *Glycobiology* 34, cwae032–13. doi:10.1093/glycob/cwae032

Indellicato, R., and Trinchera, M. (2021). Epigenetic regulation of glycosylation in cancer and other diseases. *Int. J. Mol. Sci.* 22, 2980–3016. doi:10.3390/ijms22062980

Ishiko, A., Shimizu, A., Nagata, E., Takahashi, K., Tabira, T., and Suzuki, N. (2006). Notch3 ectodomain is a major component of granular osmiophilic material (GOM) in CADASIL. *Acta Neuropathol.* 112, 333–339. doi:10.1007/s00401-006-0116-2

Ishiyama, H., Kim, H., Saito, S., Takeda, S., Takegami, M., Yamamoto, Y., et al. (2024). Pro-hemorrhagic cerebral autosomal dominant arteriopathy with subcortical infarcts and leukoencephalopathy associated with NOTCH3 p.R75P mutation with low vascular NOTCH3 aggregation property. *Ann. Neurol.* 95, 1040–1054. doi:10.1002/ANA.26916

Itakura, Y., Sasaki, N., Kami, D., Gojo, S., Umezawa, A., and Toyoda, M. (2016). N- and O-glycan cell surface protein modifications associated with cellular senescence and human aging. *Cell Biosci.* 6, 14–11. doi:10.1186/s13578-016-0079-5

Jacobsen, K. T., and Iverfeldt, K. (2011). O-GlcNAcylation increases non-amyloidogenic processing of the amyloid-β precursor protein (APP). *Biochem. Biophys. Res. Commun.* 404, 882–886. doi:10.1016/J.BBRC.2010.12.080

Jarrett, J. T., Berger, E. P., and Lansbury, P. T. (1993). The carboxy terminus of the beta amyloid protein is critical for the seeding of amyloid formation: implications for the pathogenesis of Alzheimer's disease. *Biochemistry* 32, 4693–4697. doi:10.1021/bi00069a001

Jin, S., Hansson, E. M., Tikka, S., Lanner, F., Sahlgren, C., Farnebo, F., et al. (2008). Notch signaling regulates platelet-derived growth factor receptor-beta expression in vascular smooth muscle cells. *Circ. Res.* 102, 1483–1491. doi:10.1161/CIRCRESAHA.107.167965

Joutel, A., Andreux, F., Gaulis, S., Domenga, V., Cecillon, M., Battail, N., et al. (2000). The ectodomain of the Notch3 receptor accumulates within the cerebrovasculature of CADASIL patients. *J. Clin. Invest.* 105, 597–605. doi:10.1172/JCI8047

Joutel, A., Corpechot, C., Ducros, A., Vahedi, K., Chabriat, H., Mouton, P., et al. (1996). Notch3 mutations in CADASIL, a hereditary adult-onset condition causing stroke and dementia. *Nature* 383, 707–710. doi:10.1038/383707a0

Joutel, A., Monet, M., Domenga, V., Riant, F., and Tournier-Lasserve, E. (2004). Pathogenic mutations associated with cerebral autosomal dominant arteriopathy with subcortical infarcts and leukoencephalopathy differently affect Jagged1 binding and Notch3 activity via the RBP/JK signaling pathway. *Am. J. Hum. Genet.* 74, 338–347. doi:10.1086/381506

Joutel, A., Monet-Leprêtre, M., Gosele, C., Baron-Menguy, C., Hammes, A., Schmidt, S., et al. (2010). Cerebrovascular dysfunction and microcirculation rarefaction precede white matter lesions in a mouse genetic model of cerebral ischemic small vessel disease. *J. Clin. Investigation* 120, 433–445. doi:10.1172/JCI39733

Kakuda, S., and Haltiwanger, R. S. (2017). Deciphering the fringe-mediated notch code: identification of activating and inhibiting sites allowing discrimination between ligands. *Dev. Cell* 40, 193–201. doi:10.1016/J.DEVCEL.2016.12.013

Kakuda, S., LoPilato, R. K., Ito, A., and Haltiwanger, R. S. (2020). Canonical Notch ligands and Fringes have distinct effects on NOTCH1 and NOTCH2. *J. Biol. Chem.* 295, 14710–14722. doi:10.1074/jbc.RA120.014407

Kitazume, S., Tachida, Y., Kato, M., Yamaguchi, Y., Honda, T., Hashimoto, Y., et al. (2010). Brain endothelial cells produce amyloid β from amyloid precursor protein 770 and preferentially secrete the O-glycosylated form. *J. Biol. Chem.* 285, 40097–40103. doi:10.1074/JBC.M110.144626

Kitazume, S., Tachida, Y., Oka, R., Shirotani, K., Saido, T. C., and Hashimoto, Y. (2001). Alzheimer's beta-secretase, beta-site amyloid precursor protein-cleaving enzyme, is responsible for cleavage secretion of a Golgi-resident sialyltransferase. *Proc. Natl. Acad. Sci. U. S. A.* 98, 13554–13559. doi:10.1073/pnas.241509198

Kizhakkedath, P., John, A., Al-Sawafi, B. K., Al-Gazali, L., and Ali, B. R. (2019). Endoplasmic reticulum quality control of LDLR variants associated with familial hypercholesterolemia. *FEBS Open Bio* 9, 1994–2005. doi:10.1002/2211-5463.12740

Klee, E. W., and Zimmermann, M. T. (2019). Molecular modeling of LDLR aids interpretation of genomic variants. *J. Mol. Med.* 97, 533–540. doi:10.1007/s00109-019-01755-3

Kozarsky, K., Kingsley, D., and Krieger, M. (1988). Use of a mutant cell line to study the kinetics and function of O-linked glycosylation of low density lipoprotein receptors. *Proc. Natl. Acad. Sci.* 85, 4335–4339. doi:10.1073/PNAS.85.12.4335

Lehrman, M. A., Goldstein, J. L., Brown, M. S., Russell, D. W., and Schneider, W. J. (1985). Internalization-defective LDL receptors produced by genes with nonsense and frameshift mutations that truncate the cytoplasmic domain. *Cell* 41, 735–743. doi:10.1016/S0092-8674(85)80054-4

Lewandowska, E., Dziewulska, D., Parys, M., and Pasennik, E. (2011). Ultrastructure of granular osmiophilic material deposits (GOM) in arterioles of CADASIL patients. *Folia Neuropathol.* 49, 174–180.

Liu, F., Xu, K., Xu, Z., De Las Rivas, M., Wang, C., Li, X., et al. (2017). The small molecule luteolin inhibits N-acetyl-α-galactosaminyltransferases and reduces mucin-type O-glycosylation of amyloid precursor protein. *J. Biol. Chem.* 292, 21304–21319. doi:10.1074/JBC.M117.814202

Liu, H., Zhang, W., Kennard, S., Caldwell, R. B., and Lilly, B. (2010). Notch3 is critical for proper angiogenesis and mural cell investment. *Circ. Res.* 107, 860–870. doi:10.1161/CIRCRESAHA.110.218271

Mabuchi, H., Koizumi, J., Shimizu, M., and Takeda, R. (1989). Development of coronary heart disease in familial hypercholesterolemia. *Circulation* 79, 225–232. doi:10.1161/01.cir.79.2.225

Matsumoto, K., Kumar, V., Varshney, S., Nairn, A. V., Ito, A., Pennarubia, F., et al. (2022). Fringe GlcNAc-transferases differentially extend O-fucose on endogenous NOTCH1 in mouse activated T cells. *J. Biol. Chem.* 298, 102064. doi:10.1016/J.JBC.2022.102064

Matsuura, A., Ito, M., Sakaidani, Y., Kondo, T., Murakami, K., Furukawa, K., et al. (2008). O-linked N-acetylglucosamine is present on the extracellular domain of notch receptors. *J. Biol. Chem.* 283, 35486–35495. doi:10.1074/jbc.M806202200

Mayer, M., Straube, A., Bruening, R., Uttner, I., Pongratz, D., Gasser, T., et al. (1999). Muscle and skin biopsies are a sensitive diagnostic tool in the diagnosis of CADASIL. *J. Neurol.* 246, 526–532. doi:10.1007/s004150050398

Meloty-Kapella, L., Shergill, B., Kuon, J., Botvinick, E., and Weinmaster, G. (2012). Notch ligand endocytosis generates mechanical pulling force dependent on dynamin, epsins, and actin. *Dev. Cell* 22, 1299–1312. doi:10.1016/J.DEVCEL.2012.04.005

Mizuta, I., Nakao-Azuma, Y., Yoshida, H., Yamaguchi, M., and Mizuno, T. (2024). Progress to clarify how NOTCH3 mutations lead to CADASIL, a hereditary cerebral small vessel disease. *Biomolecules* 14, 127. doi:10.3390/BIOM14010127

Moloney, D. J., Panin, V. M., Johnston, S. H., Chen, J., Shao, L., Wilson, R., et al. (2000). Fringe is a glycosyltransferase that modifies Notch. *Nature* 406, 369–375. doi:10.1038/35019000

Morroni, M., Marzioni, D., Ragno, M., di Bella, P., Cartechini, E., Pianese, L., et al. (2013). Role of electron microscopy in the diagnosis of cadasil syndrome: a study of 32 patients. *PLoS One* 8, e65482. doi:10.1371/JOURNAL.PONE.0065482

Nakagawa, K., Kitazume, S., Oka, R., Maruyama, K., Saido, T. C., Sato, Y., et al. (2006). Sialylation enhances the secretion of neurotoxic amyloid-beta peptides. *J. Neurochem.* 96, 924–933. doi:10.1111/j.1471-4159.2005.03595.x

Nichols, J. T., Miyamoto, A., Olsen, S. L., D'Souza, B., Yao, C., and Weinmaster, G. (2007). DSL ligand endocytosis physically dissociates Notch1 heterodimers before activating proteolysis can occur. *J. Cell Biol.* 176, 445–458. doi:10.1083/jcb.200609014

Ogawa, M., Tashima, Y., Sakaguchi, Y., Takeuchi, H., and Okajima, T. (2020). Contribution of extracellular O-GlcNAc to the stability of folded epidermal growth factor-like domains and Notch1 trafficking. *Biochem. Biophys. Res. Commun.* 526, 184–190. doi:10.1016/J.BBRC.2020.03.066

Oinam, L., Changarathil, G., Raja, E., Ngo, Y. X., Tateno, H., Sada, A., et al. (2020). Glycome profiling by lectin microarray reveals dynamic glycan alterations during epidermal stem cell aging. *Aging Cell* 19, 131900–e13213. doi:10.1111/acel.13190

Okajima, T., Xu, A., Lei, L., and Irvine, K. D. (2005). Chaperone activity of protein O-fucosyltransferase 1 promotes notch receptor folding. *Sci. (1979)* 307, 1599–1603. doi:10.1126/science.1108995

Okamura, Y., and Saga, Y. (2008). Pofut1 is required for the proper localization of the Notch receptor during mouse development. *Mech. Dev.* 125, 663–673. doi:10.1016/J.MOD.2008.04.007

Opherk, C., Dichgans, M., Bader, B., Giese, A., Karpinska, A., Duering, M., et al. (2009). CADASIL mutations enhance spontaneous multimerization of NOTCH3. *Hum. Mol. Genet.* 18, 2761–2767. doi:10.1093/hmg/ddp211

Pedersen, N. B., Wang, S., Narimatsu, Y., Yang, Z., Halim, A., Schjoldager, K. T. B. G., et al. (2014). Low density lipoprotein receptor class A repeats are O-glycosylated in linker regions. *J. Biol. Chem.* 289, 17312–17324. doi:10.1074/JBC.M113.545053

Perak, A. M., Ning, H., De Ferranti, S. D., Gooding, H. C., Wilkins, J. T., and Lloyd-Jones, D. M. (2016). Long-term risk of atherosclerotic cardiovascular disease in US adults with the familial hypercholesterolemia phenotype. *Circulation* 134, 9–19. doi:10.1161/CIRCULATIONAHA.116.022335

Perdivara, I., Petrovich, R., Allinquant, B., Deterding, L. J., Tomer, K. B., and Przybylski, M. (2009). Elucidation of O-glycosylation structures of the β-amyloid precursor protein by liquid chromatography - mass spectrometry using electron transfer dissociation and collision induced dissociation. *J. Proteome Res.* 8, 3786. doi:10.1021/pr9001096

Perez, R. G., Squazzo, S. L., and Koo, E. H. (1996). Enhanced release of amyloid beta-protein from codon 670/671 "Swedish" mutant beta-amyloid precursor protein occurs in both secretory and endocytic pathways. *J. Biol. Chem.* 271, 9100–9107. doi:10.1074/jbc.271.15.9100

Peters, N., Opherk, C., Zacherle, S., Capell, A., Gempel, P., and Dichgans, M. (2004). CADASIL-associated Notch3 mutations have differential effects both on ligand binding and ligand-induced Notch3 receptor signaling through RBP-Jk. *Exp. Cell Res.* 299, 454–464. doi:10.1016/J.YEXCR.2004.06.004

Reily, C., Stewart, T. J., Renfrow, M. B., and Novak, J. (2019). Glycosylation in health and disease. *Nat. Rev. Nephrol.* 15, 346–366. doi:10.1038/s41581-019-0129-4

Romay, M. C., Knutsen, R. H., Ma, F., Mompeón, A., Hernandez, G. E., Salvador, J., et al. (2024). Age-related loss of Notch3 underlies brain vascular contractility deficiencies, glymphatic dysfunction, and neurodegeneration in mice. *J. Clin. Investigation* 134, e166134. doi:10.1172/JCI166134

Ruchoux, M. M., Guerouaou, D., Vandenhaute, B., Pruvo, J. P., Vermersch, P., and Leys, D. (1995). Systemic vascular smooth muscle cell impairment in cerebral autosomal dominant arteriopathy with subcortical infarcts and leukoencephalopathy. *Acta Neuropathol.* 89, 500–512. doi:10.1007/BF00571504

Russell, D. W., Brown, M. S., and Goldstein, J. L. (1989). Different combinations of cysteine-rich repeats mediate binding of low density lipoprotein receptor to two different proteins. *J. Biol. Chem.* 264, 21682–21688. doi:10.1016/S0021-9258(20)88240-4

Rutten, J. W., Dauwerse, H. G., Gravesteijn, G., van Belzen, M. J., van der Grond, J., Polke, J. M., et al. (2016). Archetypal NOTCH3 mutations frequent in public exome: implications for CADASIL. *Ann. Clin. Transl. Neurol.* 3, 844–853. doi:10.1002/acn3.344

Sakaidani, Y., Ichiyanagi, N., Saito, C., Nomura, T., Ito, M., Nishio, Y., et al. (2012). O-linked-N-acetylglucosamine modification of mammalian Notch receptors by an atypical O-GlcNAc transferase Eogt1. *Biochem. Biophys. Res. Commun.* 419, 14–19. doi:10.1016/J.BBRC.2012.01.098

Sato, Y., and Endo, T. (2010). Alteration of brain glycoproteins during aging. *Geriatr. Gerontol. Int.* 10, S32–S40. doi:10.1111/J.1447-0594.2010.00602.X

Singh, Y., Ormaza, D., Massetti, A., Minond, D., and Cudic, M. (2021). Tyrosine O-GalNAc alters the conformation and proteolytic susceptibility of APP model glycopeptides. *ACS Chem. Neurosci.* 12, 2974–2980. doi:10.1021/acschemneuro.1c00387

Sobral, D., Francisco, R., Duro, L., Videira, P. A., and Grosso, A. R. (2022). Concerted regulation of glycosylation factors sustains tissue identity and function. *Biomedicines* 10, 1805. doi:10.3390/biomedicines10081805

Stahl, M., Uemura, K., Ge, C., Shi, S., Tashima, Y., and Stanley, P. (2008). Roles of Pofut1 and O-fucose in mammalian notch signaling. *J. Biol. Chem.* 283, 13638–13651. doi:10.1074/JBC.M802027200

Suzuki, N., Cheung, T. T., Cai, X.-D., Odaka, A., Otvos, L., Eckman, C., et al. (1994). An increased percentage of long amyloid beta protein secreted by familial amyloid beta protein precursor (beta APP717) mutants. *Sci. (1979)* 264, 1336–1340. doi:10.1126/science.8191290

Suzuki, S., Hiura, S., Mashiko, T., Matsumoto, T., and Itoh, M. (2021). Lunatic fringe promotes the aggregation of CADASIL NOTCH3 mutant proteins. *Biochem. Biophys. Res. Commun.* 557, 302–308. doi:10.1016/j.bbrc.2021.04.031

Suzuki, S., Mashiko, T., Tsukamoto, Y., Oya, M., Kotani, Y., Okawara, S., et al. (2024). The N-acetylglucosaminyltransferase Radical fringe contributes to defects in JAG1-dependent turnover and signaling of NOTCH3 CADASIL mutants. *J. Biol. Chem.* 300, 107787. doi:10.1016/J.JBC.2024.107787

Tachida, Y., Iijima, J., Takahashi, K., Suzuki, H., Kizuka, Y., Yamaguchi, Y., et al. (2023). O-GalNAc glycosylation determines intracellular trafficking of APP and Aβ production. *J. Biol. Chem.* 299, 104905. doi:10.1016/J.JBC.2023.104905

Takahashi, K., Adachi, K., Yoshizaki, K., Kunimoto, S., Kalaria, R. N., and Watanabe, A. (2010). Mutations in NOTCH3 cause the formation and retention of aggregates in the endoplasmic reticulum, leading to impaired cell proliferation. *Hum. Mol. Genet.* 19, 79–89. doi:10.1093/hmg/ddp468

Takeuchi, H., Schneider, M., Williamson, D. B., Ito, A., Takeuchi, M., Handford, P. A., et al. (2018). Two novel protein O-glucosyltransferases that modify sites distinct from POGLUT1 and affect Notch trafficking and signaling. *Proc. Natl. Acad. Sci. U. S. A.* 115, E8395–E8402. doi:10.1073/pnas.1804005115

Takeuchi, H., Yu, H., Hao, H., Takeuchi, M., Ito, A., Li, H., et al. (2017). O-Glycosylation modulates the stability of epidermal growth factor-like repeats and thereby regulates Notch trafficking. *J. Biol. Chem.* 292, 15964–15973. doi:10.1074/jbc.M117.800102

Taylor, P., Takeuchi, H., Sheppard, D., Chillakuri, C., Lea, S. M., Haltiwanger, R. S., et al. (2014). Fringe-mediated extension of O-linked fucose in the ligand-binding region of Notch1 increases binding to mammalian Notch ligands. *Proc. Natl. Acad. Sci. U. S. A.* 111, 7290–7295. doi:10.1073/pnas.1319683111

Thinakaran, G., Teplow, D. B., Siman, R., Greenberg, B., and Sisodiat, S. S. (1996). Metabolism of the "Swedish" amyloid precursor protein variant in neuro2a (N2a) cells: evidence that cleavage at the "β-secretase" site occurs in the Golgi apparatus. *J. Biol. Chem.* 271, 9390–9397. doi:10.1074/jbc.271.16.9390

Tikka, S., Mykknen, K., Ruchoux, M. M., Bergholm, R., Junna, M., Pyhnen, M., et al. (2009). Congruence between NOTCH3 mutations and GOM in 131 CADASIL patients. *Brain* 132, 933–939. doi:10.1093/brain/awn364

Tolleshaug, H., Hobgood, K. K., Brown, M. S., and Goldstein, J. L. (1983). The LDL receptor locus in familial hypercholesterolemia: multiple mutations disrupt transport and processing of a membrane receptor. *Cell* 32, 941–951. doi:10.1016/0092-8674(83)90079-X

Tomita, S., Kirino, Y., and Suzuki, T. (1998). Cleavage of Alzheimer's amyloid precursor protein (APP) by secretases occurs after O-glycosylation of APP in the protein secretory pathway. Identification of intracellular compartments in which APP cleavage occurs without using toxic agents that interfere with protein metabolism. *J. Biol. Chem.* 273, 6277–6284. doi:10.1074/jbc.273.11.6277

Tsatsanis, A., Dickens, S., Kwok, J. C. F., Wong, B. X., and Duce, J. A. (2019). Post translational modulation of β-amyloid precursor protein trafficking to the cell surface alters neuronal iron homeostasis. *Neurochem. Res.* 44, 1367–1374. doi:10.1007/s11064-019-02747-y

Urata, Y., and Takeuchi, H. (2019). Effects of Notch glycosylation on health and diseases. *Dev. Growth Differ.* 62, 35–48. doi:10.1111/dgd.12643

Vanhooren, V., Dewaele, S., Kuro-o, M., Taniguchi, N., Dollé, L., van Grunsven, L. A., et al. (2011). Alteration in N-glycomics during mouse aging: a role for FUT8. *Aging Cell* 10, 1056–1066. doi:10.1111/j.1474-9726.2011.00749.x

Vanlandewijck, M., He, L., Mäe, M. A., Andrae, J., Ando, K., Del Gaudio, F., et al. (2018). A molecular atlas of cell types and zonation in the brain vasculature. *Nature* 554, 475–480. doi:10.1038/nature25739

Varshney, S., and Stanley, P. (2018). Multiple roles for O-glycans in Notch signalling. *FEBS Lett.* 592, 3819–3834. doi:10.1002/1873-3468.13251

Vrablik, M., Tichý, L., Freiberger, T., Blaha, V., Satny, M., and Hubacek, J. A. (2020). Genetics of familial hypercholesterolemia: new insights. *Front. Genet.* 11, 574474. doi:10.3389/fgene.2020.574474

Wang, S., Mao, Y., Narimatsu, Y., Ye, Z., Tian, W., Goth, C. K., et al. (2018). Site-specific O-glycosylation of members of the low-density lipoprotein receptor superfamily enhances ligand interactions. *J. Biol. Chem.* 293, 7408–7422. doi:10.1074/JBC.M117.817981

Wang, Y., Shao, L., Shi, S., Harris, R. J., Spellman, M. W., Stanley, P., et al. (2001). Modification of epidermal growth factor-like repeats witho-fucose: molecular cloning and expression of A novel gdp-fucose proteino-fucosyltransferase. *J. Biol. Chem.* 276, 40338–40345. doi:10.1074/JBC.M107849200

Wang, Y. Y., Pan, L. Y., Moens, C. B., and Appel, B. (2014). Notch3 establishes brain vascular integrity by regulating pericyte number. *Dev. Camb.* 141, 307–317. doi:10.1242/dev.096107

Watanabe, Y., Mizuno, T., Tanaka, M., Watanabe-Hosomi, A., and Nakagawa, M. (2011). Transendocytosis is impaired in CADASIL-mutant NOTCH3. *Exp. Neurol.* 233, 303–311. doi:10.1016/j.expneurol.2011.10.020

Wertkin, A. M., Turner, R. S., Pleasure, S. J., Golde, T. E., Younkin, S. G., Trojanowski, J. Q., et al. (1993). Human neurons derived from a teratocarcinoma cell line express solely the 695-amino acid amyloid precursor protein and produce intracellular beta-amyloid or A4 peptides. *Proc. Natl. Acad. Sci. U. S. A.* 90, 9513–9517. doi:10.1073/pnas.90.20.9513

Wollenweber, F. A., Hanecker, P., Bayer-Karpinska, A., Malik, R., Bäzner, H., Moreton, F., et al. (2015). Cysteine-sparing CADASIL mutations in NOTCH3 show proaggregatory properties *in vitro*. *Stroke* 46, 786–792. doi:10.1161/STROKEAHA.114.007472

Yamamoto, Y., Liao, Y. C., Lee, Y. C., Ihara, M., and Choi, J. C. (2023). Update on the epidemiology, pathogenesis, and biomarkers of cerebral autosomal dominant arteriopathy with subcortical infarcts and leukoencephalopathy. *J. Clin. Neurology* 19, 12–27. doi:10.3988/JCN.2023.19.1.12

Yang, L. T., Nichols, J. T., Yao, C., Manilay, J. O., Robey, E. A., and Weinmaster, G. (2005). Fringe glycosyltransferases differentially modulate Notch1 proteolysis induced by Delta1 and Jagged1. *Mol. Biol. Cell* 16, 927–942. doi:10.1091/mbc.E04-07-0614

Yazaki, M., Tagawa, K., Maruyama, K., Sorimachi, H., Tsuchiya, T., Ishiura, S., et al. (1996). Mutation of potential N-linked glycosylation sites in the Alzheimer's disease amyloid precursor protein (APP). *Neurosci. Lett.* 221, 57–60. doi:10.1016/S0304-3940(96)13285-7

Young, K. Z., Rojas Ramírez, C., Keep, S. G., Gatti, J. R., Lee, S. J., Zhang, X., et al. (2022). Oligomerization, trans-reduction, and instability of mutant NOTCH3 in inherited vascular dementia. *Commun. Biol.* 5, 331–412. doi:10.1038/s42003-022-03259-2

Zhang, A., Tsukamoto, Y., Takeuchi, H., Nishiwaki, K., Tashima, Y., and Okajima, T. (2022). Secretory expression of mammalian NOTCH tandem epidermal growth factor-like repeats based on increased O-glycosylation. *Anal. Biochem.* 656, 114881. doi:10.1016/J.AB.2022.114881

Zhang, W., Chen, T., Zhao, H., and Ren, S. (2024). Glycosylation in aging and neurodegenerative diseases. *Acta Biochim. Biophys. Sin. (Shanghai)* 56, 1208–1220. doi:10.3724/ABBS.2024136

frontiers | Frontiers in Molecular Biosciences

TYPE Review
PUBLISHED 05 March 2025
DOI 10.3389/fmolb.2025.1554717

OPEN ACCESS

EDITED BY
Venkateswarlu Kanamarlapudi,
Swansea University Medical School,
United Kingdom

REVIEWED BY
Jonathan Barlow,
University of Birmingham, United Kingdom
Bhavani Shankar Sahu,
National Brain Research Centre (NBRC), India
Rosaria Di Martino,
National Research Council (CNR), Italy

*CORRESPONDENCE
Anoop Arunagiri,
arunagiri@etsu.edu
Srivastav Ranganathan,
sranga88@pks.mpg.de

RECEIVED 02 January 2025
ACCEPTED 13 February 2025
PUBLISHED 05 March 2025

CITATION
Zavarzadeh PG, Panchal K, Bishop D, Gilbert E, Trivedi M, Kee T, Ranganathan S and Arunagiri A (2025) Exploring proinsulin proteostasis: insights into beta cell health and diabetes.
Front. Mol. Biosci. 12:1554717.
doi: 10.3389/fmolb.2025.1554717

Exploring proinsulin proteostasis: insights into beta cell health and diabetes

Parisima Ghaffarian Zavarzadeh[1], Kathigna Panchal[1], Dylan Bishop[1], Elizabeth Gilbert[1], Mahi Trivedi[1], Tovaria Kee[1], Srivastav Ranganathan[2]* and Anoop Arunagiri[1]*

[1]Department of Biological Sciences, East Tennessee State University, Johnson City, TN, United States, [2]Max Planck Institute for the Physics of Complex Systems, Dresden, Germany

Proinsulin misfolding is central to diabetes. This review examines the cellular mechanisms regulating proinsulin proteostasis in pancreatic β-cells, encompassing genetic factors such as insulin gene mutations, and exploring the roles of endoplasmic reticulum (ER) stress and the unfolded protein response (UPR), ER redox balance, mitochondrial function, and the influence of extrinsic factors. Mutations in the INS gene, particularly those affecting cysteine residues, impair folding and disulfide bond formation, often exhibiting dominant-negative effects on the wild-type proinsulin. The importance of ER quality control mechanisms, including chaperones and oxidoreductases, in facilitating proper folding and degradation of misfolded proinsulin is emphasized. Disruptions in these systems, due to genetic mutations, ER stress, or impaired ER-to-Golgi trafficking, lead to proinsulin accumulation and β-cell dysfunction. The unfolded protein response (UPR), especially the PERK and IRE1α-XBP1 pathways, emerges as a central regulator of protein synthesis and ER stress management. The review also discusses the role of mitochondrial health, ER redox state, and extrinsic factors such as diet and medications in influencing proinsulin proteostasis. Finally, the structural insights from NMR and molecular dynamics simulations are discussedhighlighting the dynamics of misfolding and underscoring the importance of disulfide bonds. These mechanistic insights suggest innovative strategies targeting thiol/disulfide redox systems in cells to mitigate protein misfolding diseases including diabetes.

KEYWORDS

proinsulin folding, trafficking, beta cells, proteostasis, insulin biosynthesis, diabetes

1 Introduction

Proinsulin, the established insulin precursor, is produced and folded within pancreatic β-cells' endoplasmic reticulum (ER). The folded proinsulin trafficks from the ER to Golgi and is further processed to produce equimolar insulin and C-peptide, both of which are subsequently stored in secretory granules in the β-cells (Kitabchi, 1977). Proinsulin comprises 86 amino acids organized into three chains: B-chain, C-peptide, and A-chain. Critical disulfide bonds, A6-A11 (intra-chain), B7-A7, and B19-A20 (both inter-chain), ensure the

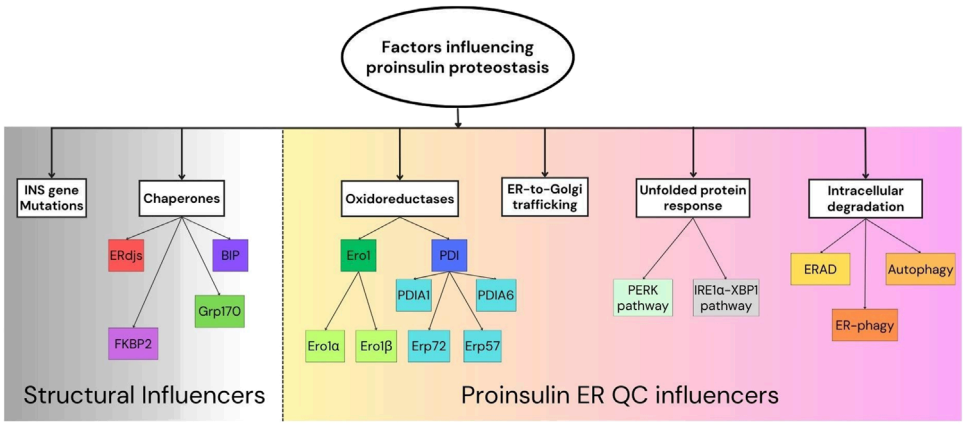

FIGURE 1
Factors influencing proinsulin proteostasis.Schematic representation of the proinsulin proteostasis "influencers" broadly divided into structural influencers (*left*) and proinsulin ER quality control (QC) mechanisms (*right*). Key components involved in proinsulin folding and ER quality control are shown.

native folding of proinsulin (Gupta, 2022; Haataja et al., 2016). To maintain insulin levels, pancreatic *β*-cells must also regulate proinsulin production. Proinsulin is inherently prone to misfolding, with a subset of molecules particularly susceptible to this during their synthesis. Misfolded proinsulin is generally degraded via ER-associated protein degradation (ERAD) or reticulophagy. Mutant INS-gene-induced Diabetes of Youth (MIDY), a subtype of Maturity-Onset Diabetes of the Young (MODY), caused by insulin (INS) gene mutations is historically featured proinsulin misfolding (Liu et al., 2010a; Sun et al., 2020; Haataja et al., 2021). However, proinsulin misfolding is not exclusively a consequence of genetic mutations in the INS gene. Non-mutated, wild-type (WT) proinsulin can also misfold when the ER "folding environment" becomes unfavorable, such as during ER stress. Notably, β-cell failure in type 2 diabetes (T2D), which lacks INS gene mutations, is also associated with ER stress and proinsulin misfolding. This suggests a bidirectional relationship between proinsulin misfolding and ER stress, both of which can lead to β-cell dysfunction and the development of diabetes (Laybutt et al., 2007; Arunagiri et al., 2019). Mitochondrial dysfunction and reduced cellular energy can also contribute to proinsulin misfolding (Arunagiri et al., 2024). Observation of proinsulin misfolding in prediabetic T2D rodent models (Arunagiri et al., 2019) suggests that patients with early-stage T2D and dysglycemia may exhibit proinsulin misfolding before complete *β*-cell failure. Recent research has significantly advanced our understanding of proinsulin misfolding under *β*-cell stress and in different forms of diabetes (Sun et al., 2020; Arunagiri et al., 2019; Arunagiri et al., 2024). This review will provide a comprehensive overview of the latest findings, examining genetic and cellular factors that impact proinsulin proteostasis—synthesis, folding, trafficking, and degradation, in the context of diabetes pathophysiology. Section 2 below focuses on INS gene mutations that cause proinsulin misfolding. Sections 3 through 8 then discuss the mechanisms that regulate proinsulin quality control in β-cells (Figure 1). Finally, Section 9 explores the structural basis of proinsulin misfolding.

2 MODY mutations

Maturity-Onset Diabetes of the Young (MODY) is a distinct group of monogenic diabetes subtypes, separate from type 1 (autoimmune) and type 2 (polygenic/environmental) diabetes (Hoffman et al., 2025; Antal, 2021). Accounting for 1%–5% of all diabetes cases, MODY is the most common form of monogenic diabetes, characterized by autosomal dominant inheritance and typically presenting before age 25 (Hoffman et al., 2025; Antal, 2021). Caused by heterozygous mutations in various genes affecting insulin secretion, MODY can exhibit a wide range of clinical presentations. Accurate diagnosis is crucial due to subtype-specific treatment responses, complication rates, and extra-pancreatic manifestations. While initially described in non-obese individuals, MODY has been reported across various racial groups (Hoffman et al., 2025). It is estimated that MODY accounts for 6.5% of antibody-negative diabetes in children (Hoffman et al., 2025). Advanced genetic testing has identified numerous MODY genes and subtypes, improving our understanding of these disorders (Hoffman et al., 2025; Antal, 2021). Some of the key MODY subtypes (Hoffman et al., 2025; Antal, 2021) influencing *β*-cell function or pancreas development include:

a) GCK MODY (MODY 2): GCK gene (7p15-p13), glucokinase. Regulates insulin secretion. Higher fasting glucose. Mild, non-progressive hyperglycemia, often asymptomatic.
b) HNF1A MODY (MODY 3): HNF1A gene (12q24.2), HNF1alpha protein. Regulates transcription in various tissues. Impaired glucose metabolism in *β*-cells. Progressive *β*-cell dysfunction. Decreased renal glycosuria threshold.
c) PDX1/IPF1-MODY (MODY 4): PDX1 gene (13q12.2), PDX1 protein. Crucial for pancreatic/*β*-cell development and insulin gene expression.
d) NEUROD1 MODY (MODY 6): NEUROD1 gene (2q32), NeuroD1 protein. Affects pancreatic/neuronal development.
e) KLF11 MODY (MODY 7): KLF11 gene (2q25), KLF11 protein. Regulates PDX1 and insulin gene expression.

f) PAX4 MODY (MODY 9): PAX4 gene (7q32), PAX4 protein. Essential for β-cell formation.
g) INS MODY (MODY 10): INS gene (11p15.5), preproinsulin. Mutations lead to misfolded proinsulin.
h) ABCC8 MODY (MODY 12): ABCC8 gene (11p15), SUR1 protein. Regulates insulin secretion. Associated with neonatal diabetes/hypoglycemia. Responsive to sulfonylureas.
i) KCNJ11 MODY (MODY 13): KCNJ11 gene (11p15), KIR 6.2 protein. Regulates insulin secretion. Associated with neonatal diabetes/hypoglycemia. Responsive to sulfonylureas.
j) APPL1 MODY (MODY 14): APPL1 gene (3p14.3), APPL1 protein. Involved in insulin signaling and β-cell survival.

While INS MODY, caused by mutations directly within the insulin gene, represents the most direct link to proinsulin proteostasis, the influence of other MODY subtypes on this crucial process deserves further scrutiny. The intricate gene regulatory and protein interaction network within β-cells suggests that disruptions in other MODY-related genes could indirectly impact proinsulin proteostasis. Transcription factors like HNF1A, GCK and PDX1, implicated in various MODY subtypes, orchestrate the expression of numerous genes essential for β-cell function, potentially altering those involved in proinsulin folding and/or processing. For instance, recent research in HNF1A-MODY has revealed impaired insulin secretion and abnormal insulin granule accumulation linked to reduced CACNA1A and SYT13 expression (Gonzalez et al., 2022), respectively. These findings raise the intriguing possibility of a connection to proinsulin trafficking or processing, echoing previously established links between ER calcium imbalances and proinsulin proteostasis. Disruptions in ER calcium homeostasis, whether due to PERK deficiency affecting proinsulin synthesis and folding (Sowers et al., 2018), or SERCA2 knockout impairing proinsulin processing (Iida et al., 2023), can significantly impact β-cell function. The observed calcium dysregulation in HNF1A-MODY suggests a similar pathway may be involved, though further investigation is required. Another gene, glucokinase (GCK/MODY 2), while primarily known for its role in glucose-stimulated insulin secretion, also plays a crucial role in β-cell mass and survival (Matschinsky and Wilson, 2019). Studies suggest that while GCK activation can have proliferative effects on β-cells (Wei et al., 2009), a prolonged activation can lead to β-cell failure due to increased ER stress (Tornovsky-Babeay et al., 2021). This delicate balance of GCK activity suggests a link to proinsulin proteostasis, as altered GCK activity could influence insulin biosynthesis and secretion, potentially impacting upstream proinsulin synthesis (and folding). Finally, studies on PDX1 (MODY 4), a transcription factor crucial for β-cell development and function, have revealed its importance in managing ER stress, a key player in proinsulin proteostasis. Research has shown that Pdx1 levels are maintained during ER stress through a specialized translational mechanism, allowing the β-cell to adapt to the stress (Templin et al., 2014; Sachdeva et al., 2009). Importantly, Pdx1 also regulates a several ER-related genes, including those involved in disulfide bond formation (e.g.,. Ero1β), protein folding (BiP), and the UPR itself (Sachdeva et al., 2009). Pdx1 deficiency leads to increased ER stress, highlighting its critical role in maintaining ER homeostasis. Given the strong links recently established between ER homeostasis and proinsulin folding and trafficking (Arunagiri et al., 2019; Arunagiri et al., 2024; Rohli et al., 2024), it is highly likely that PDX1 plays a significant role in proinsulin proteostasis. Notwithstanding the foregoing, the precise mechanisms and extent of these indirect effects from various MODY subtypes remain to be fully elucidated. While different MODY subtypes could potentially influence proinsulin proteostasis (with limited published data available), extensive literature supports the fact that INS MODY (MODY 10) most directly relates to proinsulin folding and trafficking because mutations in the *INS* gene can result in proinsulin structural defects and cause misfolding. The following subsection is dedicated to exploring this critical link.

2.1 MIDY (MODY 10)/INS gene mutations

Mutations in the INS gene can cause Mutant INS-gene-induced Diabetes of Youth (MIDY) by disrupting the proper folding of proinsulin. The misfolded mutant proinsulins containing free cysteine residues can oligomerize via intermolecular disulfide bridges (Sun et al., 2020; Haataja et al., 2021). Besides that they form disulfide bonds with WT proinsulin, resulting in the formation of hetero-oligomers within the β-cells (Sun et al., 2020). Regardless of whether the mutation introduces or eliminates a free cysteine residue, the mutated proinsulin tends to sequester WT proinsulin through intermolecular bonding. This dominant-negative effect of the mutant on WT proinsulin occludes ER-to-Golgi export of WT proinsulin, potentially impairing insulin production in the β-cell. This interplay between mutant and WT proinsulin underlies the pathogenesis of MIDY (Liu et al., 2010a).

MIDY can be categorized based on mutation type, as not all INS mutations lead to the disease. Several missense mutations (Figure 2) can affect proinsulin folding and cause MIDY (Liu et al., 2010a; Haataja et al., 2021). These mutations disrupt critical disulfide bonds necessary for proper protein folding. While different mutations have varying effects on proinsulin folding, alterations in highly conserved residues are more strongly associated with the MIDY phenotype (Liu et al., 2010b). Alternatively, MIDY may be categorized based on the impact of the mutation on proinsulin biosynthesis and folding. Although INS gene mutations can impair proinsulin folding, their severity and specific effects vary. For instance, the C43G mutation disrupts the formation of the B19-A20 disulfide bond, one of the earliest bonds formed in native proinsulin, significantly affecting its folding and secretion. In contrast, the G32R and Y108C mutations produce proinsulin that can enter the secretory pathway but is functionally compromised. The severity of the mutations can indirectly be assessed by measuring the amount of intracellular and extracellular (secreted) insulin or C-peptide (Park et al., 2010).

Mutations within the proinsulin sequence, particularly on the B- and A-chains, can disrupt folding in MIDY. This is especially true for mutations in conserved residues like HisB5 and GlyB8, which are critical for proper folding of proinsulin. The limited potential for compensatory mutations due to the conservative nature of the proinsulin sequence further exacerbates the deleterious effects of misfolding, leading to clinical diabetes (Weiss, 2013). A prime example is Tyrosine-B16 (Tyr-B16), a crucial residue for normal proinsulin dimerization. While mutations like Y(B16)D or Y(B16)A primarily affect interactions and lead to dimerization without directly impacting folding or secretion, the Y(B16)P mutation specifically induces misfolding. Additionally, Tyr-B16

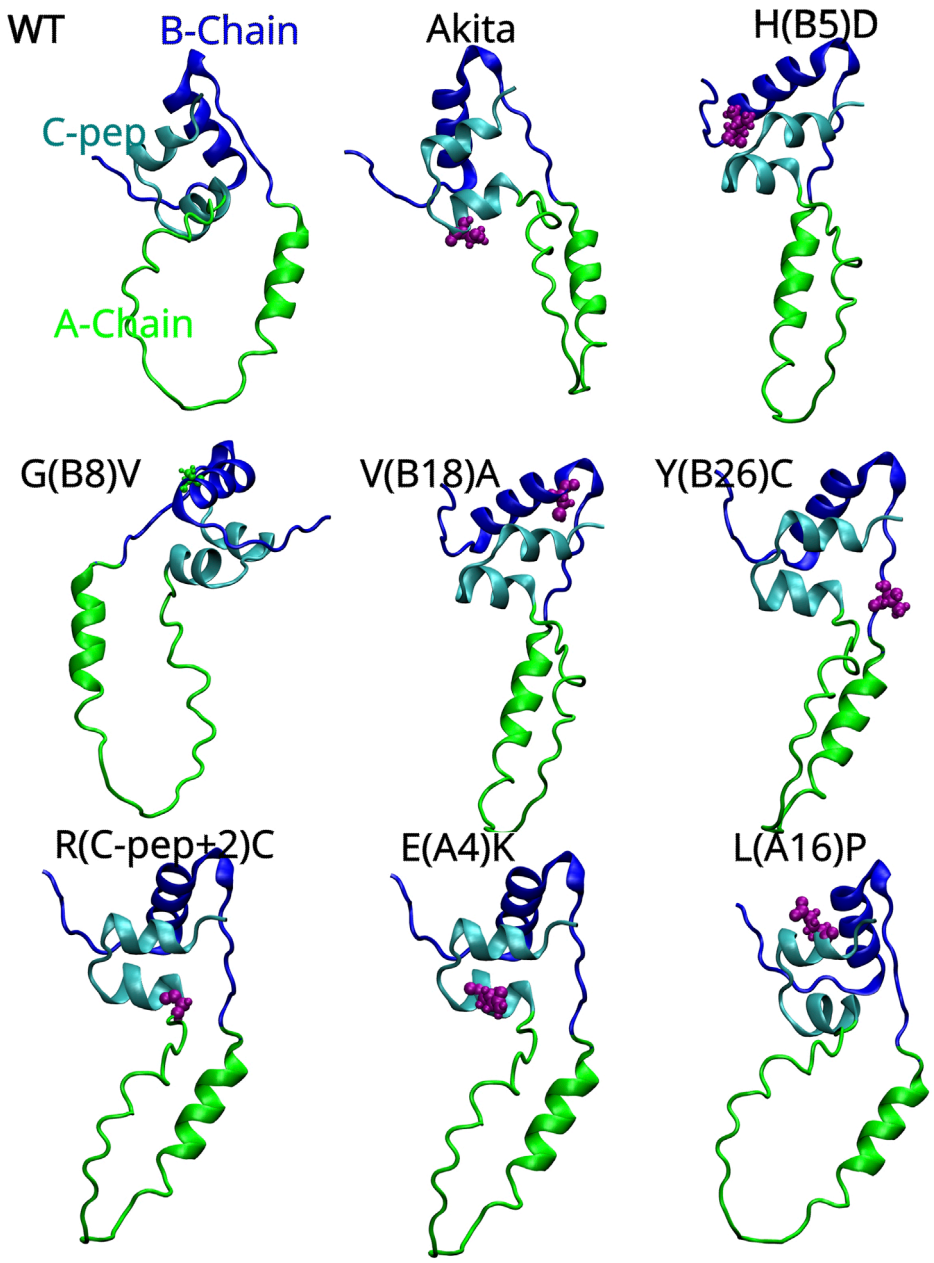

FIGURE 2
AlphaFold-predicted 3D structures of human proinsulin with the A-Chain, B-Chain and C-peptide represented as green, blue and cyan colored ribbons respectively. The locations of the *Akita* (C (A7)Y) and MIDY mutations are shown in pink color and van der Waals spheres showing their 3D location with respect to the three key regions of proinsulin. The proinsulin mutant nomenclature is as follows: H(B5)D means Histidine, which is the fifth amino acid on the B-chain, is replaced with Aspartic acid.

can contribute to the dominant-negative effect by facilitating interactions between WT and misfolded proinsulin. This effect is particularly pronounced in the C(A7)Y *Akita* mutation, which introduces a free cysteine residue and promotes the formation of disulfide-linked oligomers that impair the secretion of WT proinsulin. Interestingly, substituting Tyr-B16 with Ala, Asp, or Pro can mitigate this dominant-negative effect by preventing these aberrant interactions (Sun et al., 2020). Mutations affecting non-cysteine residues can also disrupt proinsulin folding and secretion. For instance, the G(B23)V mutation hinders the proper assembly of the A and B chains, preventing the formation of disulfide bonds. This finding suggests that mutations outside of cysteine residues can still impair proinsulin structure, and thereby the structure of insulin, and possibly its function too (Liu et al., 2010a). Several non-cysteine mutations have been shown to block proinsulin secretion from the ER. Some of these mutations, such as those affecting the Cys (A6)–Cys (A11) bond, disrupt proper folding and trafficking. However, the severity of these mutations varies. While some, like V(B18)A and E(A4)K, can partially escape quality control and be secreted, others, such as L(A16)P and H(B5)D, have more severe

effects and are largely retained in the ER (Haataja et al., 2021), indicating that the amino acid substitution and the position of substitution on proinsulin (primary sequence) plays a pivotal role in determining the magnitude of misfolding and proteotoxicity. Different mutations can impair proinsulin folding, trafficking, and ER stress response, leading to varying degrees of diabetes severity. While some mutations, such as G(B20)R and P(B28)L, have milder effects and are associated with the disease, others, like C(A7)Y, have more severe consequences. The G(B20)R mutation interestingly leads to increased binding affinity of proinsulin to the insulin receptor but disrupts protein folding and trafficking, ultimately leading to reduced insulin secretion and contributing to the development of diabetes (Wang et al., 2020). It was recently realized that regardless of the mutation location within the proinsulin sequence, misfolding often involves the formation of disulfide-linked oligomers through interactions with free thiol groups on the proinsulin molecule (Haataja et al., 2021).

These studies overall emphasize the importance of understanding the mechanisms underlying proinsulin misfolding and the impact of specific mutations on proinsulin structure, insulin production and secretion. By elucidating these mechanisms, researchers may be able to develop novel therapy for treating diabetes caused by INS gene mutations (Haataja et al., 2021). The proposed strategies along these lines include i) a combination of CRISPR/Cas9 and stem technology to replace deleterious mutations implicated in MIDY (Balboa et al., 2018) or ii) devising approaches to target free thiols in proinsulin to mitigate intermolecular disulfide pairings (Haataja et al., 2021).

Proinsulin folding and trafficking, in addition to being affected by INS gene mutations, are also heavily influenced by the ER microenvironment. The ER's resident proteins and processes directly or indirectly impact proinsulin folding. After a brief overview of ER stress and the unfolded protein response, the following sections will delve into these influential factors.

3 ER stress and Unfolded Protein Response (UPR)

The ER is a vital organelle responsible for numerous cellular functions, including protein folding, lipid synthesis, and calcium regulation (Lodish et al., 2021). ER stress arises when these functions are disrupted, often due to an accumulation of misfolded or unfolded proteins in the ER lumen. This protein buildup, known as proteotoxicity, overwhelms the ER's capacity to properly fold proteins (Oakes and Papa, 2015). While proteotoxicity is a common cause, other stressors like disruptions in lipid metabolism, glucose regulation, or calcium homeostasis can also trigger ER stress. Essentially, anything that throws the delicate balance of the ER's functions off can lead to stress. The cell's primary response to ER stress is the Unfolded Protein Response (UPR) (Ron and Walter, 2007). The UPR is a complex signaling pathway with the goal of restoring ER homeostasis. It has three main branches, each activated by distinct transmembrane proteins in the ER membrane:

i. IRE1α: When activated by unfolded proteins (indirectly via BiP, as discussed below), IRE1α splices XBP1 mRNA, which then encodes a transcription factor that upregulates genes involved in protein folding and ER-associated degradation (ERAD) (Ron and Walter, 2007; Hetz et al., 2020).
ii. PERK: PERK phosphorylates eIF2α, a protein involved in translation initiation. This phosphorylation has a dual effect: it reduces overall protein synthesis, lessening the burden on the ER, and it selectively increases the translation of certain mRNAs, including ATF4, which encodes a transcription factor that induces genes involved in protein folding, autophagy and antioxidative response (Hetz et al., 2020).
iii. ATF6: ATF6 is a transmembrane protein that, when activated by ER stress, translocates to the Golgi apparatus. In the Golgi, it is cleaved, releasing the active ATF6 fragment, which then travels to the nucleus to activate the transcription of genes involved in protein folding, ER/Golgi biogenesis and ERAD (Hetz et al., 2020).

The role of BiP in the UPR. BiP (Binding immunoglobulin protein), also known as GRP78, is a major ER chaperone. It belongs to the Hsp70 family of proteins and plays a crucial role in protein quality control within the ER, mostly by activating the three UPR branches, as highlighted below.

(a) BiP acts as a key regulator of the IRE1α branch of the UPR. The two models describe how BiP interacts with IRE1α: (1) The "BiP competition" model (Adams et al., 2019): In the absence of ER stress, BiP is bound to IRE1α, keeping it inactive. When unfolded proteins accumulate in the ER, BiP preferentially binds to these unfolded proteins, effectively "competing" for BiP. This dissociation of BiP from IRE1α allows IRE1α to become activated and initiate the UPR signaling cascade, and (2) A second model suggests that BiP directly senses the presence of unfolded proteins and then transmits this information to IRE1α, leading to its activation. Essentially, BiP acts as a sensor of ER stress and relays this information to IRE1α (Carrara et al., 2015; Kopp et al., 2018). Regardless of the precise mechanism, BiP's interaction with IRE1α is essential for initiating the UPR in response to ER stress. It acts as a molecular switch, linking the presence of unfolded proteins to the activation of the UPR pathway.
(b) PERK, like IRE1, relies on the chaperone protein BiP for its activation (Carrara et al., 2015). BiP normally binds to the luminal domains of both IRE1 and PERK, keeping them inactive. However, when unfolded proteins accumulate in the ER lumen, BiP's affinity for these unfolded proteins surpasses its affinity for IRE1 or PERK. BiP dissociates from PERK (and IRE1) and binds to the unfolded proteins. This release of BiP from PERK allows PERK molecules to oligomerize and become trans-phosphorylated, which is the crucial step that activates PERK (Cui et al., 2011). BiP's binding to PERK is thought to sterically hinder the oligomerization process, preventing PERK from coming together to activate itself (Bertolotti et al., 2000). Once PERK is activated through this BiP-mediated release and oligomerization, it proceeds to phosphorylate eIF2α, leading to the downstream effects on translation (Harding et al., 1999).
(c) BiP regulates of ATF6 activation. BiP binds to ATF6's luminal domain, utilizing its peptide-binding domain in a manner similar to its interaction with unfolded proteins, forming a stable complex. This binding serves to inhibit ATF6 activation by preventing its transport to the Golgi apparatus, where it

undergoes proteolytic cleavage to become active (Shen et al., 2005). During ER stress, BiP's higher affinity for accumulating unfolded proteins leads to its release from ATF6. This release is not a passive consequence of competition but is actively triggered by specific sequences within ATF6. Once freed from BiP, ATF6 can then translocate to the Golgi, where it is cleaved and becomes transcriptionally active (Shen et al., 2005). Therefore, BiP functions as a master regulator of the ATF6 branch of the UPR, maintaining ATF6 in an inactive state within the ER under non-stressful conditions and releasing it only when ER stress signals the necessity for UPR activation to restore cellular homeostasis.

In addition to BiP, several other ER chaperones contribute to quality control within the ER. Given this review's focus on the β-cell ER and proinsulin proteostasis, the following subsection will introduce and describe the roles of key chaperones found in the β-cell ER, beginning with BiP. The individual branches of the unfolded protein response will then be discussed. Finally, we will explore the connection between proinsulin synthesis and the UPR in β-cells, followed by a separate discussion of the relationship between calcium homeostasis and the UPR in these cells.

3.1 ER chaperones

3.1.1 BiP

Chaperones are essential proteins that assist in proper protein folding within the cell. Among these, BiP, a member of the HSP70 family residing in the ER, plays a pivotal role. BiP interacts with various co-chaperone families, such as the DnaJ/HSP40 family, which stimulate its ATPase activity (Pobre et al., 2019). Extensive research has demonstrated BiP's function in facilitating proper proinsulin folding. A study employed nonreducing Tris-Tricine-urea-SDS-PAGE, a technique sensitive to disulfide mispairing, to investigate the folding differences between wild-type (WT) and mutant proinsulin (Liu et al., 2005). To track proinsulin, insulin, and conversion intermediates, a 5 and 30-min chase medium was analyzed using immunoprecipitation. This study identified two bands migrating slower than native proinsulin. One of these bands co-precipitated with BiP upon anti-BiP immunoprecipitation. Notably, these slow-migrating bands failed to convert to insulin during the chase. Their association with BiP suggests abnormal conformations, leading to their recognition by the ER quality control system. This system could either refold misfolded proinsulin oligomers or facilitate their degradation (Liu et al., 2005). Another early study on the *Akita* mouse model revealed decreased secretory granules and insulin levels, which could be attributed to lower WT proinsulin levels in the β-cell. Furthermore, the ER lumen was enlarged to accommodate the abundant misfolded proinsulin. The presence of high molecular weight proinsulin in the ER coincided with BiP overexpression likely for the degradation of these misfolded proinsulin molecules. In other words, the ER accumulation of proinsulin is possibly mitigated by BiP (Wang et al., 1999). Finally, a recent study highlighted BiP's role in proinsulin folding by treating a rodent *β*-cell line with the bacterial SubAB protease, which targets and cleaves BiP's "linker" region (Arunagiri et al., 2019). This treatment resulted in large, disulfide-linked proinsulin complexes retained within the ER, as confirmed by immunoblotting and immunostaining. These findings strongly suggest that BiP plays a crucial role in either refolding or degrading misfolded WT proinsulin, thereby maintaining ER homeostasis. While elevated levels of BiP co-chaperone, p58ipk, have been observed in diabetic rodent models (Laybutt et al., 2007; Arunagiri et al., 2019), it is not known whether BiP protein levels rise. Further comprehensive studies are required to clarify the precise timing of the changes in ER chaperone levels during disease progression.

3.1.2 ER DnaJ-like (ERdj) family members

These ERdjs function as co-chaperones for BiP. One specific ERdj, ERdj3, is found ubiquitously throughout the body, with highest expression in secretory tissues (Shen and Hendershot, 2005). This is one of the mammalian ER DnaJ homologous that stimulates the BiP ATPase activity. Studies reveal high expression levels of ERdj3 in the pancreas, suggesting it may specifically interact with proinsulin during its production. Notably, co-immunoprecipitation experiments using an *Akita* mouse *β*-cell line harboring the proinsulin mutation (C (A7)Y, described earlier) showed that ERdj3 associates with both wild-type and mutated proinsulin (Gorasia et al., 2016). Another ERdj linked to insulin biosynthesis is ERdj4. Inactivation of the ERdj4 gene in mice resulted in chronic ER stress and *β*-cell loss, mimicking diabetic conditions (Fritz et al., 2014). Overall, understanding the function of ERdjs, particularly ERdj3 and ERdj4, holds promise for developing strategies to prevent *β*-cell dysfunction and improve glucose control in metabolic disorders like type 2 diabetes.

3.1.3 Grp170

Grp170, a chaperone with unique properties, contributes to proinsulin quality control. While Grp170 can interact with BiP and influence its function, it appears to have independent roles in proinsulin handling, especially in misfolded *Akita* proinsulin. Grp170 specifically targets high-molecular-weight aggregates of *Akita* proinsulin for degradation (Cunningham et al., 2017). (Cunningham et al., 2019) reported that the ER employs two proteins, Grp170 and Reticulon 3 (RTN3), to address proinsulin aggregation. Grp170 prevents aggregation, while RTN3 facilitates the removal of aggregates via ER-phagy (Cunningham et al., 2019). These combined efforts reduce aggregate burden, restore WT proinsulin transport, and alleviate ER stress. Grp170 preferentially binds to aggregation-prone amino acid sequences, which may be exposed on the surface of *Akita* proinsulin aggregates. This interaction could promote the formation of smaller, oligomeric species that are more amenable to ERAD or refolding. The exact mechanism by which Grp170 targets *Akita* aggregates remains unclear. Understanding this interaction is crucial for elucidating the role of Grp170 in mitigating ER stress and preventing the accumulation of proinsulin aggregates in MIDY.

3.1.4 *FK506-Binding* protein 2 (FKBP2)

FKBP2, a proline isomerase residing in the ER, plays a crucial role in proinsulin folding (Hoefner et al., 2023). It interacts with both proinsulin and the Grp94 chaperone, suggesting a chaperone-like function. This makes it a potential biomarker for early diabetes diagnosis and a target for improving proinsulin folding. Studies carried out by (Hoefner et al., 2023) using FKBP2 knockout (KO)

models highlight its importance. In the FKBP2 KO, a significant increase in misfolded, poorly soluble proinsulin, alongside a decrease in overall ER proinsulin levels was observed, implying that misfolded proinsulin might be degraded promptly rather than aggregating. Interestingly, FKBP2 KO also triggered apoptosis in β-cells without inducing ER stress responses. FKBP2 appears to preferentially bind to unfolded, reduced proinsulin–specifically before disulfide bond formation–emphasizing its critical role in this early folding step. This aligns with the observation in FKBP2 KO models, where misfolded proinsulin formed disulfide-linked dimers and multimers (Hoefner et al., 2023). Paradoxically, FKBP2 was found to be overexpressed in β-cells of T2D patients. It was found that FKBP2 isomerizes a specific proline residue (P28) at position 28 of the proinsulin B-chain, and this isomerization, particularly converting cis-proline to the trans conformation, is crucial for releasing proinsulin from misfolded states. This is supported by proinsulin misfolding increases when FKBP2 is deficient, as evidenced by CRISPR/Cas9 KO of FKBP2 in INS-1E cells, which reduced intracellular proinsulin and insulin levels. It is clear from these findings that there is a complex relationship between FKBP2 and proinsulin folding in β-cells, with potential implications for both diagnosis and treatment of diabetes (Hoefner et al., 2023).

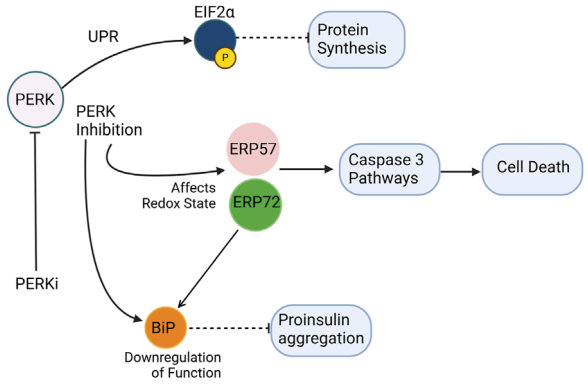

FIGURE 3
PERK inhibition disrupts ER homeostasis and promotes proinsulin misfolding. PERKi (PERK inhibitor) impairs translational attenuation, alters the ER redox environment, and downregulates chaperone function. Specifically, PERKi prevents the phosphorylation of eIF2α, leading to increased protein synthesis and exacerbating ER stress. Additionally, PERKi can affect the redox state of ER oxidoreductases like Erp72 and Erp57, potentially reducing the activity of the ER chaperone BiP. These combined effects result in the accumulation of misfolded proinsulin, contributing to ER dyshomeostasis in β-cells. Separately, Erp57 suppression results in elevated cleaved Caspase-3, indicating increased apoptosis. *Dashed inhibitory arrows indicated weakened effects.*

3.2 Role of the individual UPR branches in proinsulin proteostasis

The β-cell UPR arms play a crucial role in maintaining proinsulin folding and trafficking. Here, we explore the specific contributions of the PERK, IRE1α–XBP1 and ATF6 pathways, and highlight the influence of UPR in proinsulin synthesis and ER calcium homeostasis.

3.2.1 PERK

The PERK pathway plays a central role in maintaining proinsulin production and folding within the ER (Figure 3). The PERK/eIF2α pathway involves the phosphorylation of EIF2α by PERK kinase activity, which is crucial for protein translation in cells (Shi et al., 1998). Dysregulated eIF2α phosphorylation has been implicated in monogenic and polygenic diabetes, as β-cells in these conditions exhibit markers of unresolved ER stress (Cnop et al., 2017). The phosphorylation of eIF2α slows global protein synthesis during ER stress, allowing for the selective translation of stress-response proteins like ATF4. However, excessive or insufficient phosphorylation of eIF2α can impair β-cell survival, highlighting the delicate balance required for proper UPR signaling. A selective small molecule inhibitor, PERKi, was shown to acutely inhibit PERK's ability to phosphorylate eIF2a thereby having immediate effects on protein synthesis in normal β-cells. This acute inhibition of PERK was suggested to result in the deregulation of protein synthesis causing misfolded proinsulin to accumulate (Harding et al., 2012). However, the detection of misfolded proinsulin by biochemical means revealed that the aggregation of proinsulin did not occur immediately in β-cells treated with PERKi, but took at least 10–12 h (Arunagiri et al., 2019). Does this mean that the PERKi-mediated ER build-up of proinsulin is independent of the protein synthesis defects resulting from PERK inhibition? A separate study by Sowers et al., 2018 highlighted that PERK could modulate the function of the ER chaperone BiP by regulating its glucose-dependent activity (Sowers et al., 2018). Disrupting this balance through PERK inhibition negatively affects BiP function, and both upregulation and downregulation of BiP can trigger proinsulin aggregation. Interestingly, while overexpression of ERp72 can rescue proinsulin from aggregation, its role seems less critical compared to BiP (Sowers et al., 2018). PERK-deficient mice models exhibit diabetic characteristics and increased vulnerability to proinsulin misfolding. This suggests that PERK dysfunction initiates ER stress, which in turn contributes to proinsulin misfolding, and the observed proinsulin aggregation might be a consequence of the inhibited pathway leading to an accumulation of abundant newly synthesized proinsulin over time in the ER (Sowers et al., 2018).

3.2.2 IRE1α–XBP1 pathway

UPR triggers IRE1α–XBP1 pathway and the activation of IRE1α′s RNase domain by ER stress causes the cleaving of unspliced XBP1 (XBP1u) mRNA (X-box-binding protein 1). The spliced form, XBP1s, then acts as a transcriptional activator that upregulates specific gene encoding ER chaperones, ERAD proteins, and lipid synthesis enzymes. Tsuchiya et al., 2018 suggested that the IRE1α–XBP1pathway controls the expression of several protein disulfide isomerases (PDIs), including PDI, PDIR, P5, ERp44, and ERp46, which are essential for the oxidative folding of proinsulin (Tsuchiya et al., 2018). It was shown that inactivation of the IRE1α-XBP1 pathway leads to decreased expression of these PDIs, resulting in impaired proinsulin folding and reduced insulin production. Conversely, overexpression of these PDIs can restore insulin secretion. These findings highlight the importance of the IRE1α-XBP1 pathway in regulating proinsulin folding and the essential role of PDIs in this process (Tsuchiya et al., 2018) (Figure 4). Additionally, the deletion of Xbp1 in mouse β-cells primarily affects

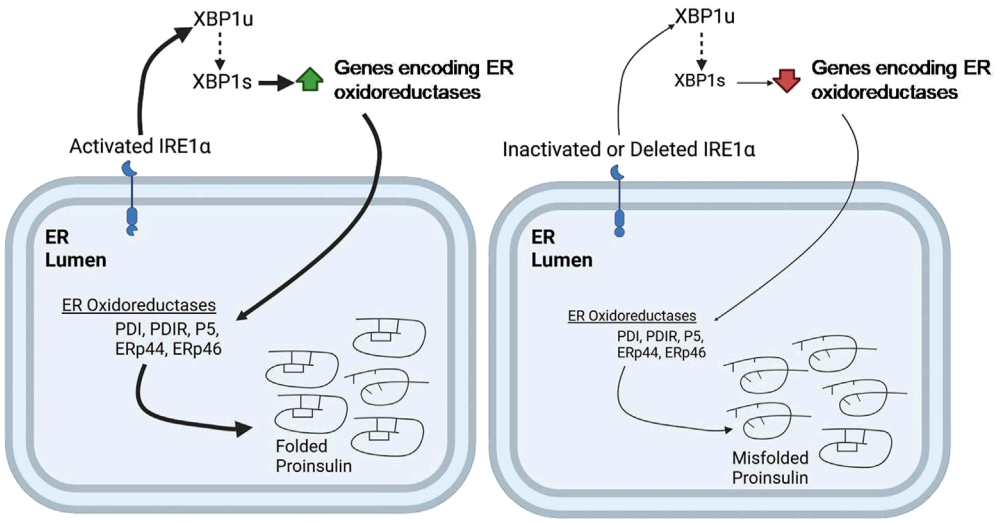

FIGURE 4
IRE1α deficiency impairs ER oxidative folding of proinsulin. IRE1α activation in pancreatic β-cells promotes XBP1 splicing, leading to increased expression of the indicated ER oxidoreductases, which enhances proinsulin folding (*Left*). In contrast, IRE1α inactivation or knockdown impairs XBP1 splicing, leading to decreased expression of ER oxidoreductases, which results in defective oxidative protein folding, particularly of proinsulin, in the β-cell ER (*right*). *Thickness of the arrows signifies the efficiency or magnitude of the processes.*

the expression of mRNA encoding insulin, impacting its processing and secretion (Tsuchiya et al., 2018). This further underscores the complex role of the IRE1α-XBP1 pathway in maintaining β-cell function and insulin production.

3.2.3 ATF6 pathway

ATF6, a key component of the UPR and the third major arm alongside PERK and IRE1, plays a critical role in maintaining pancreatic β-cell health. Studies reveal that key UPR components, including ATF6 and sXBP1, are progressively downregulated in β-cells of both mouse models and human T1D patients, implicating UPR dysfunction in the disease process (Engin et al., 2013). This dysfunction is particularly important in the β-cells because proper folding and trafficking of proinsulin depends heavily on ER homeostasis. The accumulation of misfolded proinsulin can trigger ER stress, potentially exacerbating UPR dysfunction. Conversely, a compromised UPR, particularly the ATF6 pathway, may impair the ER's capacity to correctly handle proinsulin, creating a vicious cycle. The chemical chaperone TUDCA shows promise in mitigating this dysfunction, preventing T1D development in mouse models by reducing disease incidence, preserving insulin production, and mitigating immune cell infiltration (insulitis) without broadly suppressing the immune system (Engin et al., 2013). Interestingly, TUDCA's benefits depend on ATF6; in β-cell specific ATF6mice, TUDCA's protective effects are abolished, highlighting ATF6's crucial role in TUDCA's mechanism (Engin et al., 2013). TUDCA appears to preserve ATF6 expression and function, essential for β-cell survival under ER stress and immune attack. Furthermore, overexpressing ATF6 in β-cells provides partial protection against ER stress and cytokine-induced death, reinforcing its importance in β-cell resilience (Engin et al., 2013). Beyond its role in T1D, ATF6 also plays a key role in β-cell proliferation (Sharma et al., 2015). Mild ER stress, activating the UPR, promotes glucose-dependent β-cell proliferation, and this effect is specifically driven by ATF6. Inhibiting ATF6 reduces proliferation, while overexpressing ATF6 increases β-cell division in both mouse and human β-cells (Sharma et al., 2015). Moreover, ATF6 acts as a central regulator within the broader UPR, controlling the transcriptional output of multiple UPR pathways, including XBP1, and playing a vital role in managing ER stress (Sharma et al., 2020). ATF6 is not only essential for the induction of its own target genes, but also required for the expression of genes targeted by the XBP1 pathway. This means that even though XBP1 activation (Xbp1 splicing) can proceed independently of ATF6, the subsequent upregulation of XBP1 target genes—crucial for alleviating ER stress—is heavily dependent on ATF6's presence (Sharma et al., 2020). XBP1s regulates the expression of ER chaperones and protein disulfide isomerases (PDIs) (see section 3.2.2 or Figure 4), both of which, are essential for proper proinsulin foldingin β-cells. Given proinsulin folding relies on this coordinated UPR activity, including the ATF6 and IRE1α-XBP1 pathways, targeting the UPR, and specifically these pathways, offers a novel therapeutic avenue for diabetes.

3.2.4 Proinsulin synthesis and UPR

Glucose elevation stimulates proinsulin translation in *β*-cells to meet increased insulin demand. However, in diabetic conditions, high proinsulin levels are observed despite diminished insulin secretion, suggesting a compensatory upregulation of proinsulin synthesis. This phenomenon, characterized by increased proinsulin production alongside reduced insulin secretion, has been documented in both human and rodent models (Ward et al., 1987; Leahy, 1993; Uchizono et al., 2007; Halban et al., 1983). The surge in proinsulin synthesis can overwhelm the ER's folding capacity, leading to proinsulin misfolding and ultimately inducing the UPR. One of the key UPR sensors, PERK, regulates protein

synthesis in cells. From a proinsulin synthesis perspective, the mechanism by which PERK inhibition leads to proinsulin misfolding/aggregation remains unclear, however as discussed in Section 6.1, aggregation likely arises from either excessive proinsulin production, impaired folding machinery, or a combination of both (Sowers et al., 2018). Recent studies have identified OSGEP as a key regulator of proinsulin translation and ER stress homeostasis in β-cells. OSGEP deletion in mice leads to impaired proinsulin translation and increased ER stress, resulting in glucose intolerance and hyperglycemia. These findings suggest that OSGEP may play a role in maintaining proinsulin proteostasis and β-cell function, particularly under conditions of high glucose and insulin demand (Liu et al., 2024).

3.2.5 *ER* calcium homeostasis and UPR

ER calcium homeostasis is crucial for proper *β*-cell function and insulin production. SERCA2 (Sarco/endoplasmic reticulum calcium ATPase 2), an ER-localized calcium pump, plays a key role in maintaining ER calcium stores. (Iida et al., 2023) investigated the role of SERCA2 in pancreatic *β*-cell function and insulin production, finding that *β*-cell-specific SERCA2 knockout mice and human islets exposed to high glucose and palmitate exhibited impaired calcium signaling, altered proinsulin processing, and reduced insulin secretion (Iida et al., 2023). This highlights the importance of ER calcium homeostasis in maintaining *β*-cell function and insulin production. This study raises a question of whether ER calcium imbalance directly affects proinsulin folding. Interestingly, PERK inhibition, which perturbs proinsulin synthesis and folding (discussed earlier), was also found to interfere with calcium fluxes in the cells (Sowers et al., 2018; Wang et al., 2013), indicating a potential connection between UPR, calcium balance, and proinsulin proteostasis in *β*-cells. A good example for this is the close connection between ER calcium levels, BiP, and proinsulin folding, with BiP acting as a central component in this relationship. The ER carefully controls its calcium levels through a balance of calcium entry, removal, and buffering. In addition to the cell signaling role, calcium regulation very likely supports ER's protein-folding machinery through ER-resident chaperones like BiP. While some studies explore its potential contribution to ER calcium storage (Lievremont et al., 1997), its well-established function is as a chaperone, assisting in the correct folding of newly synthesized proteins, including proinsulin. As discussed in section 3.1.1, BiP helps prevent proinsulin from misfolding and clumping together (Arunagiri et al., 2019). Correct calcium levels are needed for BiP to work efficiently (Preissler et al., 2020). Additionally, BiP itself can be targeted by toxins like SubAB (see section 3.1.1). When SubAB cleaves BiP, proinsulin misfolding occurs, independent of calcium levels. To sum up, maintaining correct calcium levels is important for BiP function, and BiP is essential for proper proinsulin folding. Problems at any point in this system—whether through direct calcium imbalance or BiP destruction—can lead to ER stress, activation of the UPR, and impaired proinsulin handling in the *β*-cells. While the calcium-dependent ER chaperone calreticulin (Michalak, 2024) might play a role in proinsulin proteostasis in *β*-cells, its precise function along these lines remains unknown and requires further investigation.

Given ER stress and UPR activation are so closely tied to calcium homeostasis, it is crucial to understand the dynamics of UPR activation in response to varying degrees of calcium depletion. A recent study by Pontisso et al. (2024) has shed light on this relationship, examining the early activation of UPR pathways in response to moderate ER calcium depletion. It was demonstrated that IRE1 demonstrates the fastest and most sensitive response, reaching peak phosphorylation rapidly, while PERK activation is slower and less sensitive, increasing gradually over time (Pontisso et al., 2024). ATF6 activation mirrors PERK's pattern but exhibits bimodal dose sensitivity. Importantly, the study also found that IRE1 and PERK activation is reversible upon restoration of ER calcium levels, with phosphorylation decreasing and returning to basal levels when the calcium depletion inducer is removed (Pontisso et al., 2024). However, computational modeling, while predicting this reversibility, underestimated the speed of deactivation, suggesting the involvement of additional regulatory mechanisms, such as phosphatase activity, in the rapid recovery of IRE1 and PERK. Mechanistically, the study proposes that differences in the early steps following BiP unbinding, specifically variations in BiP affinity and oligomerization states, contribute to the distinct activation kinetics observed for each UPR branch, with IRE1 exhibiting a lower BiP affinity and autophosphorylating in larger oligomers compared to PERK (Pontisso et al., 2024).

From a *β*-cell perspective, these dynamics are critical. The ability of the UPR to sense and respond to even moderate calcium fluctuations allows *β*-cells to fine-tune their protein folding machinery and maintain proinsulin homeostasis. However, excessive calcium dysregulation, such as that seen in type 2 diabetes (Becerra-Tomas et al., 2014), can lead to persistent UPR activation, overwhelming the *β*-cell's capacity to cope with ER stress. Such a stress coupled with the observed discrepancies in UPR deactivation kinetics, can disrupt proinsulin folding and/or processing and impair insulin production, and ultimately contribute to *β*-cell failure.

4 Oxidoreductases and related proteins

4.1 Protein disulfide isomerases (PDI)

PDI, a member of the ER oxidoreductase family, plays a critical role in protein folding within the ER. PDI itself is a complex enzyme system, with isoforms like PDIA1, PDIA6, Erp72, and Erp57 contributing to its function (Rajpal et al., 2012). Highly expressed in pancreatic *β*-cells, PDI directly influences disulfide bond formation in target proteins like proinsulin (Figure 5), making it crucial for proper insulin production. PDI participates in protein folding by acting as a "redox-active chaperone", both preventing protein aggregation and catalyzing the formation, breakage, and rearrangement of disulfide bonds, which are vital for achieving the final protein structure. PDI is essential for efficient proinsulin refolding, acting as both a chaperone and isomerase (Winter et al., 2002). PDI's chaperone activity is crucial in the first few seconds to prevent proinsulin aggregation, while its isomerase activity, though most effective early, can still improve folding later. Aggregation occurs rapidly at the start of refolding, and PDI's chaperone function directly suppresses it, enabling the isomerase activity to correct disulfide bonds (Winter et al.,

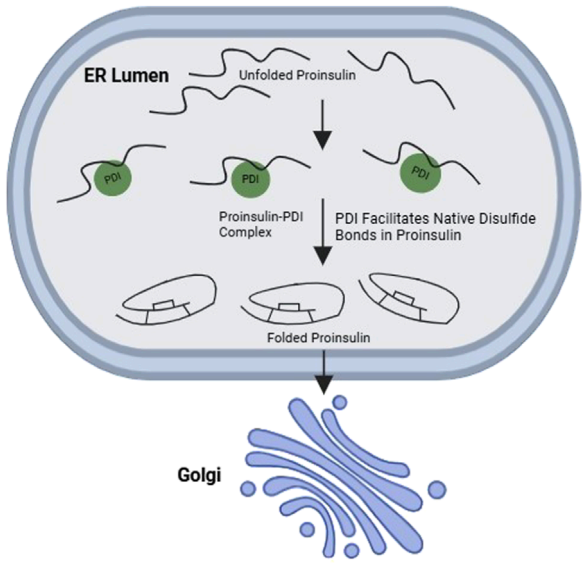

FIGURE 5
Interaction between PDI and wild-type proinsulin promotes oxidative folding of proinsulin. PDI, a major ER oxidoreductase, promotes the native disulfide bond formation in proinsulin, thereby facilitating its ER-to-Golgi transport in in β-cells.

2002). Inhibiting PDI's chaperone function with genistein increases aggregation and reduces yield, highlighting its importance for efficient proinsulin maturation. Essentially, PDI acts early to prevent aggregation and later to correct disulfide bonds, ensuring high-yield proinsulin folding (Winter et al., 2002). Further studies using a mutant PDI lacking the peptide binding domain (PDI-aba'c) shed light on its specific roles. This mutant PDI retained its redox potential but lacked chaperone activity due to the absence of the b' domain and its peptide binding ability (Winter et al., 2011). Interestingly, PDI-aba'c still increased proinsulin folding and yield, suggesting that in a fully oxidized environment, PDI's primary function might be rearranging disulfide bonds, not necessarily binding to unfolded proteins. Further research is needed to fully understand the nuances of PDI function in *β*-cells and its potential as a therapeutic target for pancreatic *β*-cell dysfunction.

4.1.1 PDIA1

PDIA1, a member of the PDI family facilitates the formation of correct disulfide bonds within proteins. A recent study showed that PDIA1 is essential for proper insulin production under metabolic stress conditions (Jang et al., 2019). β-cells lacking PDIA1 exhibit a range of impairments, including the accumulation of misfolded proinsulin aggregates, disruptions in the transport of vesicles from the ER to the Golgi apparatus, and a decrease in insulin granule content. These findings underscore the critical role of PDIA1 in the oxidative maturation of proinsulin within the ER. In response to PDIA1 deficiency, β-cells attempt to compensate by overexpressing BiP, possibly to refold the largely misfolded proinsulin. Overall, PDIA1's disulfide isomerase activity helps lessen misfolded proteins and maintain ER homeostasis.

4.1.2 PDIA6

Another PDI family member, PDIA6, exhibits a unique function. In a study comparing different PDIs, only PDIA6 was found to preferentially interact with misfolded *Akita* proinsulin (Gorasia et al., 2016). This interaction was confirmed in βTC-6 β-cell lines. Like other PDIs, PDIA6 possesses oxidoreductase activity and is induced under unfolded protein response (UPR) conditions. Notably, PDIA6 activity was significantly higher in cells containing misfolded *Akita* proinsulin compared to wild-type proinsulin, with expression levels increasing 10-fold (Gorasia et al., 2016). These findings suggest that PDIA6 plays a role in processing specifically misfolded proinsulin. Recent research (Yassin et al., 2024) has illuminated PDIA6's broader role in the ER stress response, particularly within the context of selective ER retention (sERr) (Yassin et al., 2024). This process can involve the formation of large disulfide-bonded complexes, a phenomenon also observed with misfolded proinsulin. It was demonstrated that while ERp44 (another PDI family member) promotes sERr and increases the size of these complexes, PDIA6 acts antagonistically. Despite constitutively interacting with ERp44 via disulfide bonds, PDIA6 deletion slows down recovery from sERr, suggesting that PDIA6 facilitates the release of retained proteins (Yassin et al., 2024). PDIA6 may play a similar role in proinsulin proteostasis, promoting the processing or degradation of misfolded proinsulin and ensuring proper handling of the ER retained species.

4.1.3 Erp72

Erp72, is involved in the PERK pathway, a signaling cascade activated during ER stress (Wang et al., 2014; Gupta et al., 2010; Feng et al., 2009). Suppression of PERK activity (by C-terminus deletion) caused a 3.3-fold increase in Erp72 protein levels (Gupta et al., 2010), which could result in impaired ERAD given Erp72 is a negative regulator of retrotranslocation (Forster et al., 2006). If the increased expression of ERp72 also increases ER retention of secretory proteins such as proinsulin, this would indicate a trafficking defect. Interestingly, ablation of PERK in INS1 832/13 β-cell lines showed a significant alteration in the redox state of Erp72 (Feng et al., 2009). This finding suggests that the protein quantity and its proper folded state with the correct redox balance are essential for Erp72 function. Additionally, manipulating Erp72 expression in PERKi cells demonstrated a partial rescue of the impaired ER function. Both overexpression and reduced activity of Erp72 showed positive effects, suggesting a complex regulatory role. However, combined siRNA knockdown of both BiP and Erp72 revealed a more dominant role for BiP in maintaining ER function (Sowers et al., 2018).

4.1.4 Erp57

Similar to Erp72, Erp57 exhibits a disrupted redox state in PERKi models without changes in protein levels (Sowers et al., 2018). However, other studies suggest a different role for Erp57. Overexpression of Erp57 contributes to β-cell survival, potentially linking it to the observed autophagy in β-cells of type 2 diabetes islets. Additionally, suppression of the Erp57 led to increased levels of cleaved Caspase-3, a protein involved in

apoptosis (Yamamoto et al., 2014). These findings suggest Erp57's function in promoting β-cell survival.

4.2 ER oxidoreductin 1 (Ero1)

Other oxidoreductase families exist outside of the PDI family, including Ero1. Pancreatic *β*-cells express two forms of the oxidoreductase Ero1: Ero1α and Ero1β. Unlike the ubiquitously expressed Ero1α, Ero1β expression is very limited among cell types but is well expressed in pancreatic *β*-cells (Cabibbo et al., 2000; Ramming and Appenzeller-Herzog, 2012; Zito et al., 2010), suggesting that it might play a role in proinsulin folding. Both Ero1α and Ero1β contribute to proinsulin folding and can positively influence native proinsulin anterograde export through different mechanisms.

4.2.1 ER oxidoreductin 1β (ERO1β)

Ero1β is a pancreas-specific disulfide oxidase (Zito et al., 2010)that is upregulated in response to ER stress. It has been observed to promote insulin synthesis in *β*-cells and contribute to glucose homeostasis (Zito et al., 2010). Overexpression of ERO1β in *β*-cells leads to improved proinsulin folding, enhanced ER-to-Golgi trafficking, and increased insulin production. However, knockout of this gene in mice did not result in severe proinsulin misfolding (Zito et al., 2010), suggesting that other oxidoreductases can compensate for its absence and provide an oxidative environment for the ER. Proinsulin misfolding and ER stress are implicated in the development and progression of diabetes. Interestingly, while ERO1β overexpression leads to increased expression of UPR genes and ER enlargement, indicating ER stress, its expression decreases in the *Akita* mouse model, which exhibits increased ER stress. This decrease might be due to the reduced β-cell mass in this model. The expression of ERO1β gradually declines with age in *Akita* mice, correlating with increased glucose intolerance (Zito et al., 2010). This contrasts with the increased expression of other UPR genes, suggesting a unique function for ERO1β in ER stress response. It is hypothesized that decreased ERO1β expression might contribute to the progression of diabetes and β-cell dysfunction by exacerbating ER stress. However, manipulating ERO1β expression, such as overexpression, might not ameliorate β-cell function and could even worsen ER stress (Awazawa et al., 2014). These findings highlight the importance of maintaining a balanced level of ERO1β to preserve ER homeostasis and β-cell function for insulin synthesis.

4.2.2 *ER* oxidoreductin *1α (Ero1α)*

In contrast to ERO1β, oxidoreductase Ero1α is ubiquitously expressed in various cell types. Increasing the expression of Ero1α can limit ER stress by enhancing ER oxidation and modifying the folding of proinsulin. Studies carried out by (Wright et al., 2013) (Wright et al., 2013) has shown that different variants of Ero1α, including wild-type and variants lacking regulatory disulfides, can modify the folding of misfolded proinsulin-G(B23)V mutant, leading to its secretion. Overexpression of Ero1α can limit proinsulin misfolding and its negative consequences. This increase is beneficial for exporting wild-type proinsulin in cells that express both wild-type and misfolded mutant proinsulin (Wright et al., 2013), emphasizing Ero1α′s ability of tone down the dominant negative effect of the mutant over the wild-type proinsulin. These properties make Ero1α a potential therapeutic target for MIDY.

4.3 Peroxiredoxin 4 (PRDX4)

PRDX4, an ER-localized protein has been reported to interact with both native and misfolded proinsulin, facilitating proper disulfide bond formation (Tran et al., 2020). A study by (Tran et al., 2020) (Tran et al., 2020) revealed that PRDX4's interaction with the ER chaperone BiP is independent of proinsulin folding, and PRDX4 binding to proinsulin is independent of BiP, which suggests complex interactions between these proteins in the ER. The work also explores the impact of glucose levels on PRDX4 activity (Tran et al., 2020). While high glucose levels increase insulin secretion in Min6 cells, they also lead to increased sulfonylation of PRDX4. Sulfonylation-mediated inactivation of PRDX4 could reduce its ability to protect proinsulin from oxidative damage and misfolding. However, in human islets, the increase in glucose does not significantly affect PRDX4 sulfonylation (Tran et al., 2020). This difference raises questions about the role of PRDX4 in T2D patients and its potential as a biomarker for oxidative stress in *β*-cells. Overall, PRDX4 appears to influence proinsulin proteostasis; however, more research is needed to elucidate its potential implications in diabetes.

5 Proinsulin anterograde trafficking

5.1 ER-to-Golgi trafficking

Beyond genetic mutations in the INS gene and dysfunctions of chaperones and oxidoreductases, impaired ER-to-Golgi trafficking can significantly impact proinsulin folding and aggregation. A complex machinery, including proteins like Sar1, Sec23, Sec24, Sec13, and Sec31, is involved in the formation of COPII vesicles, which mediate this transport (Fromme et al., 2008; Tang and Ginsburg, 2023). The small GTPase Sar1 plays a pivotal role in regulating coat assembly and disassembly. This trafficking step, while occurring after proinsulin folding, can exert a negative feedback loop on ER homeostasis, potentially increasing misfolded proinsulin (Arunagiri et al., 2024). Studies using non-reducing SDS-PAGE/immunoblotting have revealed the formation of proinsulin oligomers associated with impaired ER-to-Golgi transport (Arunagiri et al., 2024). Brefeldin A (BFA) is a well-known pharmacological inhibitor of ER-to-Golgi transport. It indirectly restricts the association of the COPI coat. When cultured β-cells or purified human/rodent islets were treated with BFA, it led to the accumulation of misfolded proinsulin in the ER (Arunagiri et al., 2024; Zhu et al., 2019). Likewise, the mutations in genes encoding proteins involved in COPII vesicle formation, such as Sar1 or YIPF5, can disrupt ER-to-Golgi trafficking. While the YIPF5-I98S mutation, implicated in neonatal diabetes, impairs proinsulin trafficking from the ER to the Golgi leading to proinsulin misfolding in stem cell-derived *β*-cell-like clusters

(Arunagiri et al., 2024; De Franco et al., 2020), the Sar1 mutation or deficiency in β-cells has been shown to cause proinsulin misfolding, trafficking and maturation defects (Zhu et al., 2019; Fang et al., 2015). The defective ER export is hence proposed to be a major contributor to ER stress induced by misfolded proinsulin. A recent work supporting these findings came from a study centered on IER3IP1, a protein involved in proinsulin ER-to-Golgi trafficking. IER3IP1 is highly expressed in β cells, and mutations in IER3IP1 can lead to impaired proinsulin trafficking, ER stress, and β-cell dysfunction (Yang et al., 2022). Moreover, IER3IP1 mutations (such as the IER3IP1V21G variant) can cause proinsulin accumulation in the ER, reduced insulin secretion, and increased ER stress. In agreement with this, the CRISPR-Cas9-mediated IER3IP1 KO cells exhibited impaired proinsulin trafficking, as evidenced by reduced colocalization of proinsulin with Golgi markers and increased ER retention. The knockout model also showed an increased ER stress. Overall, these findings highlight the importance of proper ER-to-Golgi trafficking for proinsulin proteostasis and insulin production in β-cells.

5.2 Golgi export of proinsulin

Recent work by Boyer et al. (2023) has highlighted the importance of synchronized proinsulin trafficking and the impact of delayed Golgi export on β-cell function and diabetes pathogenesis. The concept of synchronized trafficking emphasizes the coordinated movement of proinsulin through the secretory pathway, from ER exit to Golgi transit, insulin granule formation, and ultimately secretion. This study, using the novel proCpepRUSH reporter and RUSH system, provides a beautiful example of visualizing and quantifying this synchronization, revealing the precise sequence of key events. Specifically, they observed proinsulin's progression from the ER to the Golgi, followed by its condensation within the Golgi, and subsequent appearance in mature insulin granules, mirroring the known timeline of proinsulin processing (Boyer et al., 2023). Interestingly, this research demonstrates defects in proinsulin export from the Golgi in both dietary (Western diet) and genetic (db/db) models of diabetes. In these models, proinsulin accumulates in the Golgi, evidenced by increased proCpepRUSH signal proximal to the Golgi, and TIRF microscopy confirmed a decrease in proinsulin at the plasma membrane, suggesting impaired insulin granule delivery. This delay is linked to significant structural changes in the Golgi, including dilated cisternae, fewer cisternae per stack, and increased vesiculation, observed using electron microscopy (Boyer et al., 2023). These structural alterations likely disrupt proinsulin processing and packaging, as the study showed proCpepRUSH processing occurs post-Golgi exit, within the maturing granules. The extended chase experiments in the study further revealed that while the initial Golgi export was delayed, the proinsulin eventually reached its final destination, suggesting a kinetic delay rather than a complete block (Boyer et al., 2023). Thus, by highlighting both the synchronized nature of proinsulin trafficking and the specific vulnerability of Golgi export, this work emphasizes the complex relationship between these processes and their importance for glucose homeostasis, suggesting the Golgi as a potential target for diabetes interventions.

6 Proinsulin intracellular degradation

Misfolded proinsulin accumulation can lead to ER stress and impaired β-cell function. Hence, several degradation pathways work in concert to eliminate misfolded proinsulin.

6.1 *ER*-Associated *degradation (ERAD)*

ERAD is a highly regulated process that targets misfolded proteins for degradation by the proteasome (McCracken and Brodsky, 2003; Krshnan et al., 2022). Misfolded proinsulin in the ER should befirst unfolded, and chaperoned to the ERAD complex (by BiP) to be then transported back to the cytosol (retrotranslocation) and marked for proteasomal degradation via ubiquitination. These steps essentially describe the ERAD of proinsulin in β-cells. Derlin-2, HRD1, and p97 are key components of the ERAD pathway (Hoelen et al., 2015). The knockdown of these proteins leads to increased proinsulin levels, suggesting their involvement in its degradation. Furthermore, SEL1L, another ERAD component, has been shown to play a critical role in proinsulin processing and degradation (Hu et al., 2019). SEL1L-deficient pancreatic β-cells exhibit impaired proinsulin processing and increased degradation of wild-type and folding-deficient mutant proinsulin. These findings highlight the importance of ERAD in maintaining proinsulin homeostasis. Moreover, acute inhibition of the proteasome (using MG132) leads to increased proinsulin levels and accumulation of misfolded proteins in the ER, further supporting the role of proteasomal degradation in proinsulin quality control (Xu et al., 2022). Recent research has also unveiled a link between proinsulin degradation and the development of autoimmunity. The ERAD enzyme UBE2G2 is involved in proinsulin degradation and the subsequent presentation of the PPIB10-18 autoantigen (Cremer et al., 2024). Misfolded proinsulin triggers UPR, leading to ERAD-mediated dislocation of proinsulin (to relieve ER stress). By degrading proinsulin, ERAD machinery (HRD1/UBE2G2 ubiquitination complex) may contribute to the generation of proinsulin B-chain autoantigens, which can trigger autoreactive $CD8^+$ T cell responses (Cremer et al., 2024). This suggests that reducing the proinsulin degradation load on ERAD, potentially by improving the β-cell's oxidative folding environment, could help alleviate the risk of autoimmunity. Collectively, these studies provide valuable insights into the complex mechanisms regulating proinsulin degradation in pancreatic β-cells.

6.2 Autophagy

Autophagy, a cellular process that involves the formation of autophagosomes to engulf and degrade cellular components, including misfolded proteins, can be activated as a compensatory mechanism when the ERAD pathway is compromised. Chloroquine treatment of purified rodent islets resulted in the accumulation of misfolded proinsulin, suggesting that autophagic pathways may be involved in the disposal of misfolded proinsulin (Shrestha et al., 2023). More recent studies surprisingly showed that chloroquine exposure on pancreatic β-cells led to proinsulin misfolding and its accumulation in the ER (Xu et al., 2024) instead of autophagosomes.

This raises questions about the precise role of autophagy in proinsulin clearance and the specificity of chloroquine's effects in β-cells (discussed in Section 9.3c).

6.3 ER-Phagy

ER-phagy, also known as reticulophagy, is a specialized form of autophagy for eliminating misfolded proinsulin. When misfolded proinsulin aggregates form, chaperones like Grp170 attempt to bind and prevent further aggregation (Cunningham et al., 2017). If this fails, ER-phagy kicks in. Here, a protein called Reticulon-3 (RTN3) plays a critical role (Cunningham et al., 2019). However, studies suggest RTN3 might not have direct access to the part of the ER (ER lumen) where proinsulin resides. This is where another protein, PGRMC1, comes in. Located within the ER lumen, PGRMC1 acts as a bridge between misfolded proinsulin and RTN3, facilitating their interaction and subsequent degradation by lysosomes. Notably, PGRMC1 exhibits size selectivity, preferentially targeting smaller misfolded mutant proinsulins (Chen et al., 2021). Chemically interfering with PGRMC1 function was found to partially restore insulin storage capacity by blocking the ER-phagic degradation pathway for both wild-type and mutant forms of proinsulin (Chen et al., 2021).

A well-coordinated functioning of ERAD, autophagy, and ER-phagy ensures the elimination of misfolded or excess proinsulin in *β*-cells. Understanding these degradation pathways can provide insights into the pathogenesis of diabetes and identify potential interventions.

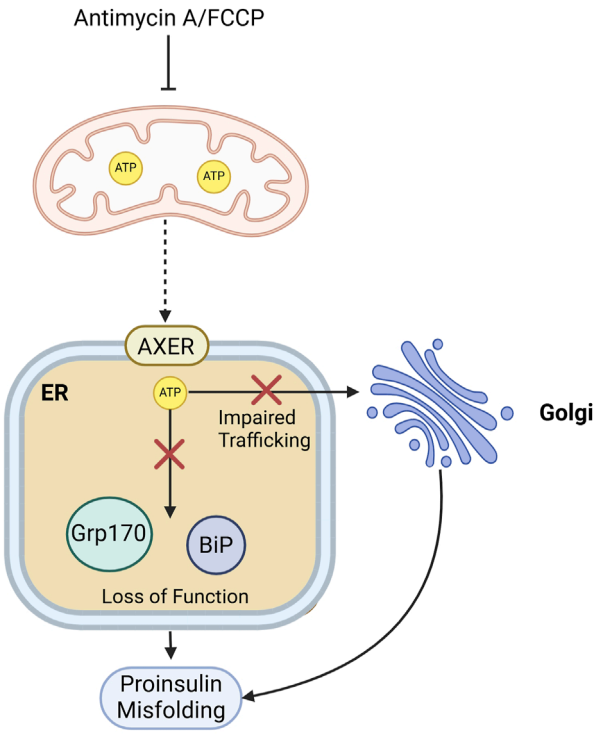

FIGURE 6
Mitochondrial energy supply supports proinsulin folding and ER-to-Golgi transport. Mitochondrial ATP depletion in β-cells by Antimycin A or FCCP treatment, could impact proinsulin folding by affecting the function of ATP-dependent ER chaperones like BiP or by impairing proinsulin trafficking from the ER to the Golgi.*Red crosses indicate blocked pathways, and dashed arrow indicated impaired mitochondria-to-ER ATP shuttling.*

7 Role of mitochondria in proinsulin proteostasis

Mitochondria are important for maintaining proinsulin proteostasis in *β*-cells. By regulating cellular redox donor cycles, particularly NADPH and thioredoxin, mitochondria influence the redox environment of the ER. Recent research by (Rohli et al., 2024) revealed that proper mitochondrial function is crucial for maintaining ER redox balance, which supports NADPH-dependent redox cycles essential for proinsulin folding and trafficking (Rohli et al., 2024). The authors find that mitochondrial dysfunction and metabolic inhibition lead to ER hyperoxidation. NADPH and thioredoxin are vital in sustaining ER redox homeostasis, and suppressing thioredoxin-interacting protein (Txnip) can restore ER function and proinsulin trafficking. Moreover, it is proposed that β-cell deterioration in T2D is associated with both mitochondrial dysfunction and redox imbalance, affecting proinsulin maturation and insulin granule stores, contributing to diabetes progression (Rohli et al., 2024). Targeting redox pathways, particularly through antioxidant interventions like TXNIP inhibition, is suggested as a means to enhance β-cell health and function.An independent study by Arunagiri, et al. (2024) pointed out that the blocking of ATP production in the mitochondria using Antimycin A or FCCP in Min6 cells leads to proinsulin misfolding (Arunagiri et al., 2024), most likely due to the unavailability of ATP for the ER chaperone functioning. ATP is known to shuttle from mitochondria to the ER via an ER membrane channel called AXER (Klein et al., 2018; Yong et al., 2019). In addition to ATP supply to the ER, ATP production is also important for the anterograde trafficking of the proteins in cells (Jamieson and Palade, 1968). Depletion of ATP in *β*-cellscould therefore potentially impair proinsulin ER-to-Golgi trafficking, and this trafficking defect in turn might cause a folding problem (Figure 6), as described in section 5. Targeting the ER-mitochondrial interactions may offer a potential approach for managing type 2 diabetes by improving β-cell function.

8 Extrinsic factors

Beyond the intrinsic cellular factors discussed in the preceding sections, extrinsic factors, including dietary intake and prescribed medications, can significantly impact proinsulin proteostasis and subsequent insulin biosynthesis within *β*-cells.

8.1 Nutrient/diet

Nutrient availability, particularly during feeding cycles significantly impacts proinsulin synthesis. Rapid dephosphorylation of the translation initiation factor eIF2α, induced by nutrient intake, precedes a surge in proinsulin levels. Conversely,

rephosphorylation of eIF2α during fasting periods correlates with a decrease in proinsulin levels (Xu et al., 2023). Subthreshold genetic predisposition to proinsulin misfolding can remain silent until triggered by a high-fat diet (HFD). Male mice with this predisposition (carrying a MIDY-like INS gene mutation, R (B22)E) exhibit glucose intolerance and rapidly develop frank diabetes upon HFD exposure, but do not develop diabetes when on a regular diet (Alam et al., 2021). A rapid increase in proinsulin misfolding and a decline in insulin production in the model are associated with dramatic pancreatic pathology (Alam et al., 2021). These findings underscore the critical role of dietary factors in regulating proinsulin synthesis folding, and, ultimately, insulin production. Identifying the mechanisms protecting females from diabetes in this model could offer novel preventative strategies for both sexes.

8.2 Hormones and drugs

8.2.1 Estrogen

The protective effect of estrogen against diabetes in women has been previously reported, but the underlying mechanisms remained unclear. To address this, (Xu et al., 2018) administered Conjugated Estrogens (CE) in *Akita* mice (Xu et al., 2018). CE, through its primary receptor ERα, was suggested to stabilize the ERAD pathway and reduce ER stress in β-cells. ERAD degraders, such as HRD1 and SEL1L, prevent the premature degradation of functional proteins. CE activation of ERα stabilizes these proteins by inhibiting their proteasomal degradation mediated by UBC6e, the only ubiquitin-conjugating enzyme localized to the ER. When ERα is absent, UBC6e expression increases, and this causes the degradation of ERAD components and the accumulation of misfolded proinsulin. To sum up, estrogen restores *β*-cell function by modulating the proinsulin degradation pathway (Xu et al., 2018).

8.3 Olanzapine

Olanzapine, a medication commonly used to treat schizophrenia, can have unexpected consequences beyond its intended therapeutic effects. In addition to its well-known association with weight gain, olanzapine can impede the normal function of pancreatic *β*-cells. By interfering with the normal folding and processing of proinsulin, olanzapine was reported to impair insulin production by unknown mechanisms (Ninagawa et al., 2020). This observation suggests that olanzapine administration can lead to the development of diabetes, even in patients who do not experience significant weight gain, a more commonly recognized side effect of the drug.

8.4 Chloroquine

Chloroquine, a common antimalarial medication, also affects cellular processes beyond its intended use. In a study by (Xu et al., 2024), it was found that chloroquine disrupts the proper folding of proinsulin in the pancreatic β-cells, causing misfolded proinsulin to accumulate in the ER. This accumulation was not due to autophagy inhibition or chloroquine's pH effects but resulted from impaired interaction between proinsulin and PDI (Xu et al., 2024). Consequently, the production of mature insulin is significantly decreased, potentially impairing glucose metabolism and, in severe cases, contributing to diabetes development. These findings highlight the need for caution with chloroquine in diabetes treatment. Its effects on pancreatic β-cells necessitate further investigation to understand its safety and efficacy.

9 Proinsulin folding landscape in the context of native function and dysfunction

Considering the importance of proinsulin proteostasis in β-cells, exploring the interplay between protein structure and disease becomes crucial. This naturally leads to the question: What is the structural basis of proinsulin misfolding in diabetes? This is an area of active investigation, with biophysical techniques like NMR, X-ray crystallography, and molecular dynamics (MD) simulations playing a vital role in uncovering the underlying protein dynamics.

9.1 Inter- and intra-chain disulfide bonds and their roles in proinsulin folding and ER export

The B- and A-chains of proinsulin form the insulin core, which is stabilized by three disulfide bonds: (i) A6–A11 (intra-A-chain), (ii) A7–B7 (inter-chain), and (iii) A20–B19 (inter-chain, stabilizing the insulin core). These disulfide bonds must form in a sequential and cooperative manner to ensure proper folding. Incorrect disulfide pairing can result in folding defects and ER retention as indicated earlier. The folding process of proinsulin is guided by a combination of intramolecular disulfide bond formation, C-peptide-mediated structural organization (Ksenofontova et al., 2014; Jung et al., 2017), and interactions with other proteins and chaperones. Insights from NMR unveil that most crystal structure hydrogen bonds in insulin are transient in solution, with stable bonds primarily around the B19-A20 disulfide bridge, a potential folding nucleus (Hua et al., 2011; Gorai and Vashisth, 2022). The Cys (B19)–Cys (A20) bond plays a pivotal role in facilitating the formation of other disulfide bridges (Haataja et al., 2016). Given the importance of these disulfide bonds in proinsulin folding, it is crucial to examine their specific roles in secretion. Notably, the Cys (B7)–Cys (A7) and Cys (B19)–Cys (A20) bonds are essential for export from the ER. While the Cys (A6)–Cys (A11) bond is crucial for insulin stability, it is dispensable for proinsulin export (Haataja et al., 2016), and mutations lacking this bond still achieve efficient secretion.

9.2 Proinsulin B- and A-chain substitutions influence proinsulin folding

MD simulations have been instrumental in revealing the remarkable flexibility of insulin's B-chain (Papaioannou et al., 2015). They pinpoint how the B-chain switches between its active (T-state) and inactive (Rf-state) conformations (Kosinova et al., 2014), highlighting the significance of localized interactions and a

hinge mechanism involving Phe24 in orchestrating receptor binding (Papaioannou et al., 2015). The N-terminal segment of the B-chain (B1–B8) plays a critical role in guiding disulfide bond formation. Studies show that mutations in this region, such as PheB1 deletion, impair folding efficiency and increase misfolding rates (Liu et al., 2010c). The inability to adopt native conformations due to mutations or mispaired disulfide bonds could result in loss of folding efficiency resulting in misfolding. Mutations affecting PheB24 (e.g., PheB24 → TyrB24) impair folding, despite having minimal effects on insulin receptor binding (Rege et al., 2020).

In MIDY, the aberrant B-chain interactions are responsible for the dominant-negative effect of MIDY mutant on WT proinsulin (Sun et al., 2020) (discussed in section 2). The B9-B19 α-helix (residues 8–29), normally facilitating proinsulin homodimerization for proper processing, becomes a site of pathological heterodimerization in MIDY (Sun et al., 2020). Mutations like C(A7)Y lead to misfolding, creating a mutant proinsulin that interacts with wild-type proinsulin, disrupting its ER export and processing. Importantly, Tyr-B16, a key residue in the dimerization interface, is essential for this pathological interaction. While mutations like Y(B16)D/A impair homodimerization, they also weaken the mutant-wild-type interaction when combined with a MIDY mutation (Sun et al., 2020). Disruption of the α-helix (Y(B16)P) impairs folding but does not cause the same dominant-negative effect as the *Akita* mutation, highlighting the specific nature of the pathogenic interaction. The misfolded MIDY mutant, via its B-chain including Tyr-B16, "hijacks" wild-type proinsulin, preventing its maturation and causing insulin deficiency (Sun et al., 2020).

The A-chain of proinsulin consists of two α-helices (A1–A8 and A12–A20), which remain largely conserved during the transition from proinsulin to insulin (Yang et al., 2010). However, the A-chain exhibits significant local flexibility in proinsulin, particularly around the A1–A8 segment, which does not assume a fully stable α-helical conformation in the precursor molecule. This flexibility likely facilitates proper folding and disulfide bond formation, ensuring that proinsulin reaches its native state efficiently before cleavage into insulin. The A-chain participates in all three disulfide bonds in proinsulin (B19-A20, B7-A7 and A6-A11). These bonds help stabilize the structure, preventing misfolding and aggregation. However, mutations affecting cysteine residues in the A-chain such as the *Akita* mutation C(A7)Y can lead to incorrect disulfide pairing, resulting in proinsulin misfolding and retention in the ER (Zuber et al., 2004) and β-cell dysfunction, and the C (A6)S MIDY mutation results in loss of the A6-A11 intra-chain bond, destabilizing the α-helices of the A-chain. Likewise, a mutation that might disrupt the A20-B19 inter-chain bond would not only impair insulin core stability and receptor-binding ability, but also significantly affect proinsulin folding.

Mutations at key hydrophobic residues within the A-chain (such as A2, A8, A13, and A19) affect the packing of α-helices, causing (a) Reduced structural integrity of the insulin core, and (b) Lower affinity for the insulin receptor due to altered surface properties. For instance, V(A3)L mutation would destabilize A-chain helix, impairing receptor interactions and reducing insulin bioactivity (Nishi and Nanjo, 2011). While mutations at the interface between the A- and B-chains, which can disrupt intermolecular hydrogen bonding and van der Waals interactions, specific mutation on the A-chain specifically could have different outcomes on proinsulin structure and trafficking. For example, Y(A19)C increases misfolding risk and causes partial ER retention of the protein (Rajan et al., 2010). On the other hand, mutating E(A17) disrupts protein sorting to the regulatory secretory pathway, indicating this A-chain residue is critical for efficient sorting (Dhanvantari et al., 2003).

9.3 The structural implication of the flexible C-peptide

Proinsulin and insulin share a key ability to form hexamers in the presence of zinc, which is crucial for efficient storage and secretion (Pekar and Frank, 1972). However, proinsulin hexamers are more dynamic than insulin hexamers, likely due to the structural interference of the C-peptide. This dynamic equilibrium affects the rate of proinsulin processing and insulin secretion. Unlike insulin, which is prone to amyloid fibrillation, proinsulin is highly resistant to fibrillation (Huang et al., 2005), and this protection is provided by the C-peptide, which prevents the β-sheet stacking required for amyloid formation (Huang et al., 2005). Crystallographic studies confirm that the insulin core in proinsulin adopts a conformation similar to mature insulin (Frank et al., 1972), though with greater flexibility due to the presence of the C-peptide, which aids in the alignment of folding intermediates (Jung et al., 2017). This mobility of the C-peptide facilitates the crucial pairing of cysteine residues for disulfide bond formation, essential for the correct folding of insulin's A- and B-chains (Ksenofontova et al., 2014; Jung et al., 2017). The C-peptide guides correct folding but do not participate in insulin receptor binding, making it dispensable after proinsulin is processed into insulin. Evolutionary analysis of the proinsulin sequences from mammals, reptiles and birds by Landreh and Jornvall (2015) reveal a remarkable evolutionary and structural flexibility of the C-peptide, which exhibits a much higher sequence variation than other regions of the protein (Landreh and Jornvall, 2015). The A- and B-chains of insulin on the other hand exhibit a high degree of evolutionary conservation across species (Landreh and Jornvall, 2015). This difference in conservation levels influences the structural role, biochemical interactions, and evolutionary flexibility of C-peptide, allowing proinsulin to behave differently from insulin. The C-peptide is also home to fewer disease mutations compared to the A- and B- chains which show tight evolutionary conservation.

10 Discussion and future perspectives

This review enunciates the complex network of genetic and cellular factors governing proinsulin proteostasis in pancreatic β-cells (Figure 7; Table 1) and its crucial role in diabetes. INS gene mutations, especially those impacting cysteine residues and conserved regions, directly impair proinsulin folding and disulfide bond formation, often exhibiting a dominant-negative effect (Liu et al., 2010a; Haataja et al., 2021). This underscores the importance of ER quality control mechanisms, involving a network of chaperones (BiP, ERdjs, Grp170, FKBP2) and oxidoreductases (PDIs and Ero1s) that facilitate proper folding, prevent aggregation, and target misfolded proinsulin for degradation. Disruptions to these systems, whether through genetic mutations, ER stress, or

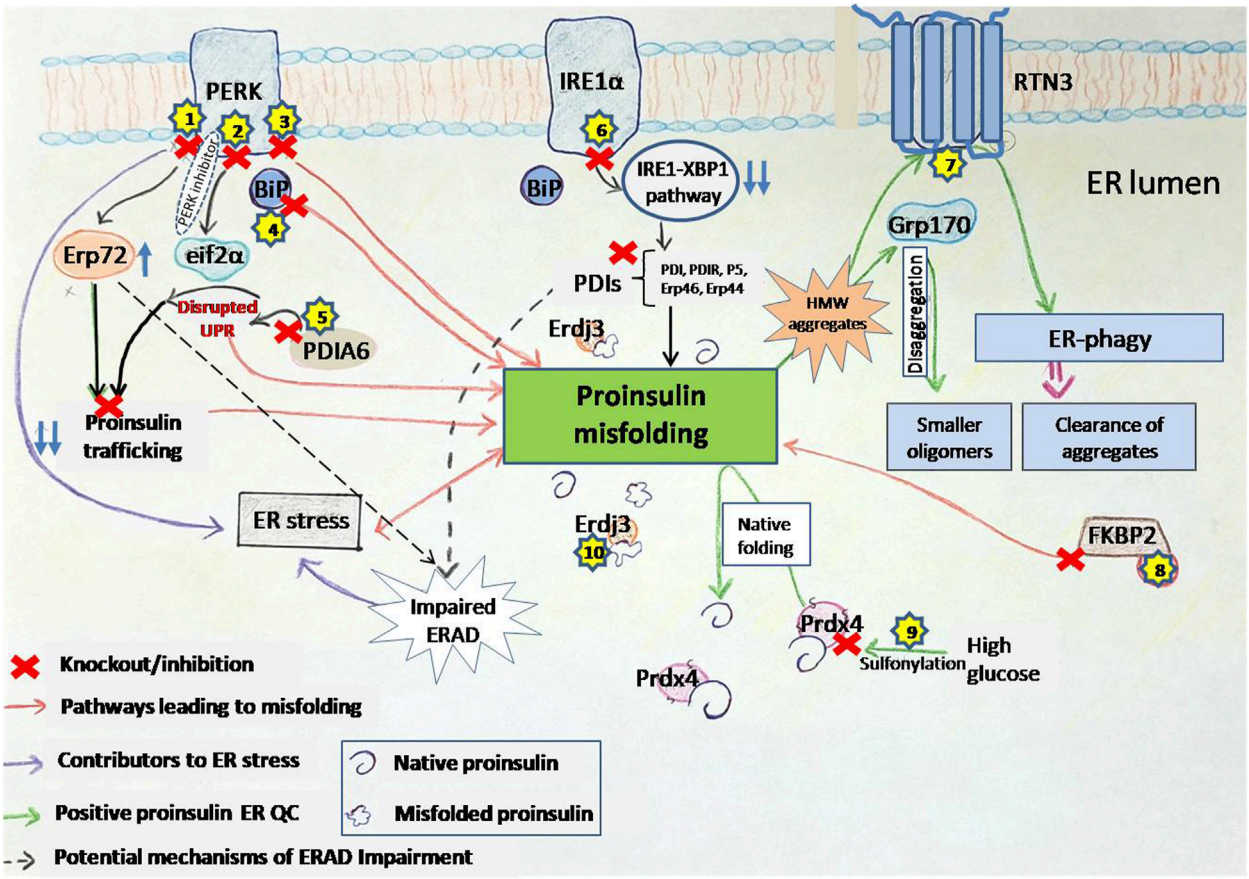

FIGURE 7
Orchestrating proinsulin proteostasis in β-cells: Molecular Chaperones, oxidoreductases, and the UPR. (1) PERK ablation, leading to Erp72 upregulation, may impair proinsulin degradation or trafficking. Independently, PERK inhibition can induce ER stress in β-cells, (2) PERK inhibition (by PERKi) prevents eIF2α phosphorylation, negatively impacting the UPR primarily through dysregulation of protein synthesis, (3) Treatment of β-cells with PERKi for 10–12 h induces proinsulin misfolding, (4) BiP inactivation (by SubAB or PERK inhibition) impairs proinsulin folding in β-cells, (5) PDIA6 deletion may impair both the UPR and proinsulin trafficking; Defective proinsulin trafficking could hinder proinsulin folding in the ER, (6) Inhibition of the IRE1α-XBP1 pathway deregulates PDI activity in β-cells, potentially impeding proinsulin folding or disrupting ERAD through impaired PDI-mediated retrotranslocation, (7) Grp170 either directly targets mutant high-molecular weight (HMW) proinsulin aggregates or collaborates with reticulon 3 (RTN3), which engages with PGRMC1 on the ER luminal side (not shown), to clear aggregates via ER-phagy in the cytosol, (8) FBKBP2 knockout results in proinsulin misfolding, (9) Highglucose-induced sulfonylation of PRDX4 impairs its protective function against proinsulin misfolding, (10) Erdj3 may promote proinsulin folding by acting as a co-chaperone with BiP.

impaired ER-to-Golgi trafficking, lead to proinsulin accumulation and *β*-cell dysfunction. The UPR, particularly the PERK and IRE1α-XBP1 pathways, emerges as a central regulator, balancing protein synthesis with ER stress management. Notably, PERK inhibition's delayed effect on proinsulin aggregation suggests downstream effects on chaperone function, especially BiP (Sowers et al., 2018). On the other hand, the IRE1α-XBP1 pathway's regulation of PDI expression highlights the importance of oxidative folding regulated through UPR elements (Tsuchiya et al., 2018). Furthermore, the collective action of ERAD, autophagy, and ER-phagy demonstrates a sophisticated yet vulnerable protein quality control system in β-cells. Mitochondrial health and ER redox state add further complexity, suggesting that targeting mitochondrial dysfunction could indirectly improve proinsulin folding. Extrinsic factors like diet, estrogen, and medications like olanzapine and chloroquine further emphasize the vulnerability of proinsulin proteostasis (Xu et al., 2023; Alam et al., 2021; Xu et al., 2018; Ninagawa et al., 2020). The discovery of OSGEP as a key regulator of proinsulin translation and ER stress homeostasis (Liu et al., 2024) along with the paradoxical overexpression of FKBP2 in T2D (Hoefner et al., 2023), present compelling avenues for future research in diabetes intervention. Likewise, the potential link between ERAD and autoimmunity (Cremer et al., 2024) suggests a connection between proinsulin misfolding and T1D, warranting further exploration.

INS gene mutations result in mispaired or unpaired cysteines lead to ER retention of misfolded proinsulin, triggering ER stress (Liu et al., 2010a; Haataja et al., 2021) and β-cell dysfunction—a hallmark of MIDY (discussed in section 2). Similar misfolding involving aberrant disulfide bonding (mostly intermolecular) has been observed in WT proinsulin when the ER oxidative folding environment is unfavorable (Arunagiri et al., 2024). Modifying these disulfide interactions could therefore potentially improve native folding or alleviate dominant-negative effects (in case of MIDY

TABLE 1 A summary of representative factors influencing proinsulin proteostasis in β-cells.

Factors	Role in proinsulin proteostasis	Model organisms or cell lines used	Key references and further reading
INS gene mutations	Mutations in the INS gene can disrupt proinsulin folding, leading to misfolded mutant proteins that can form harmful aggregates and trap healthy proinsulin molecules within β-cell ER, ultimately impairing insulin production and contributing MIDY	Rat or mouse pancreatic β-cell lines (INS1 cells, Min6 cells), HEK 293T cells, Akita mouse model, mouse islets	Liu et al. (2010a), Sun et al. (2020), Haataja et al. (2021), Liu et al. (2010b)
ER Chaperones			
BiP	• BiP is upregulated in response to ER stress likely caused by misfolded proinsulin • BiP interacts with misfolded proinsulin • Disruption of BiP function leads to proinsulin aggregation	C57BL/KsJ db/db mice, mouse pancreatic islets, human pancreatic islets, rat pancreatic β-cell lines	Laybutt et al. (2007), Arunagiri et al. (2019), Liu et al. (2005), Wang et al. (1999)
ERdj3	ERdj3 interacts with both wild-type and mutant proinsulin, potentially by assisting BiP in proinsulin quality control	Insulinoma cell lines	Gorasia et al. (2016)
Grp170	• Grp170 specifically targets aggregated mutant proinsulin for degradation • Working in concert with RTN3, Grp170 manages proinsulin aggregates	Rat INS-1 832/13 cell line, HEK 293T cells	Cunningham et al. (2017), Cunningham et al. (2019)
FKBP2	• FKBP2 is crucial for early proinsulin folding and prevents aggregation • Isomerization at proinsulin P28 by FKBP2 facilitates release from misfolded states	Rat insulinoma INS-1E cells	Hoefner et al. (2023)
Unfolded Protein Response			
PERK	• PERK-mediated eIF2α phosphorylation regulates proinsulin translation • PERK influences BiP function, impacting proinsulin aggregation • PERKi treatment of β-cell or islets leads to proinsulin misfolding	HEK 293T cells, INS1E cells	Arunagiri et al. (2019), Sowers et al. (2018), Harding et al. (2012)
IRE1α–XBP1 Pathway	IRE1α–XBP1 pathway is essential for maintaining β-cell function and insulin production. This pathway regulates the expression of PDIs crucial for proinsulin folding	INS1 832/13 and Min6 cells, mouse models, mouse pancreatic islets, human pancreatic islets, Rat pancreatic β-cell lines INS1E and INS-832/13	Tsuchiya et al. (2018)
Proinsulin Synthesis	Glucose stimulates proinsulin synthesis. Increased proinsulin synthesis can overwhelm the ER's folding capacity, leading to misfolding and UPR induction	Rat INS1 832/13 and mouse Min6 cells, rat Islets	Sowers et al. (2018), Harding et al. (2012), Ward et al., 1987; Leahy (1993), Uchizono et al. (2007), Halban et al. (1983)
ER Calcium Homeostasis	• Deficiency of ER calcium pump, SERCA2, impairs calcium signaling, proinsulin processing, and insulin secretion • PERK inhibition interferes with calcium fluxes and proinsulin folding in β-cells	βSERCA2KO mice, INS-1 cell line, Human pancreatic islets, INS1 832/13 and Min6 cells, Islets from C57BL6/J mice	Sowers et al. (2018), Iida et al. (2023), Wang et al. (2013)

(Continued on the following page)

TABLE 1 (*Continued*) A summary of representative factors influencing proinsulin proteostasis in β-cells.

Factors	Role in proinsulin proteostasis	Model organisms or cell lines used	Key references and further reading
Oxidoreductases			
PDI	PDIs are crucial for proper disulfide bond formation in proinsulin. Independent studies on PDI family members have suggested a positive influence of the protein on proinsulin trafficking. Representative PDI family members and their reported functions in β-cells are listed below • PDIA1 deficiency leads to misfolded proinsulin aggregates and decreased insulin secretion • PDIA6 interacts with misfolded proinsulin and has higher activity in cells containing this misfolded protein • Erp72 function depends on both its quantity and proper folded state with the correct redox balance. It is involved in the PERK stress signaling pathway	INS1 832/13 and Min6 cells, 293 and HepG2 cells, HEK 293T cells, C57BL/6 mice	Sowers et al. (2018), Rajpal et al. (2012), Jang et al. (2019), He et al. (2015)
Ero1β	• Ero1β promotes proinsulin folding and insulin synthesis • While reduced Ero1β expression can mitigate the effects of misfolded proinsulin in cultured Min6 cells, this protective effect is not observed in pancreatic islets *in vivo* • Ero1β expression is complexly regulated in diabetes	INS1 and 293 cells, 293 and HepG2 cells, Min6 cells, *Akita* mice, Islets from wild-type and ERO1-β mutant mice	Rajpal et al. (2012), Zito et al. (2010)
Ero1 α	Ero1α improves WT and mutant proinsulin folding and secretion	293T cells, rat insulinoma cells	Wright et al. (2013)
Extrinsic factors			
Nutrient/Diet	• Nutrient cycles regulate proinsulin synthesis via eIF2α phosphorylation • A high-fat diet can trigger diabetes in genetically predisposed rodent model by exacerbating proinsulin misfolding	Rat or mouse pancreatic β cell lines, HEK 293T cells, mouse islets	Xu et al. (2023), Alam et al. (2021)
Estrogen	Estrogen, acting via ERα, protects against diabetes by stabilizing the ERAD pathway, preventing premature degradation of functional proteins and mitigating ER stress caused by misfolded proinsulin	Male and female heterozygous *Akita*, Mouse islet, Human islets	Xu et al. (2018)
Olanzapine	Olanzapine interferes with proper disulfide bond formation in proinsulin, leading to misfolding and ER retention	MIN6 cells, Male BALB/c mice, mouse pancreatic islets	Ninagawa et al. (2020)
Chloroquine	Chloroquine disrupts proinsulin folding in β-cells by impairing proinsulin-PDI interaction	Pancreatic β-cells	Xu et al. (2024)

mutants) and improve insulin biosynthesis and secretion, offering exciting restorative possibilities.

The importance of disulfide bonds extends beyond proinsulin. Crystallins, essential for lens transparency, rely on precise disulfide formation for stability. Similar to proinsulin, misfolded crystallins with aberrant disulfide bonds aggregate, leading to cataracts (Serebryany et al., 2024). Mutations in γD-crystallin, for example, have been linked to non-native disulfide bonding, causing structural destabilization and cataractogenesis (Serebryany et al., 2018). These parallels highlight the importance of precise cysteine pairing in protein folding and function (Narayan, 2021). The "combinatorial" nature of disulfide bonds in protein sequences with multiple cysteines underscores their importance in diverse biological systems. Incorrect pairing in crystallins, as in proinsulin, compromises functionality, emphasizing the universal challenges of achieving the correct disulfide topology.

Advances in recombinant insulin production leverage insights into proinsulin structure. Studies on artificial leader peptides fused to proinsulin have shown that subtle sequence variations can significantly impact folding, cleavage efficiency and expression levels in bacterial systems (Jung et al., 2017). Computational modeling approaches predict how these sequences affect protease accessibility and insulin maturation, offering promising strategies to enhance production (Jung et al., 2017).

The insights into the structural basis of proinsulin misfolding and the multifaceted interaction of cellular factors influencing proteostasis pave the way for novel interventions strategies. Targeting disulfide redox systems in particular, offers a promising approach for mitigating proinsulin misfolding in β-cells.

Traditional models used in β-cell biology, typically involving animal cells or immortalized cell lines (shown in Table 1), often do not accurately replicate human β-cell physiology. This shortcoming significantly impedes the translation of research into effective diabetes therapies. Human β-cells exhibit unique features in gene expression, signaling pathways, and pancreatic islet interactions that animal models and cell lines cannot fully emulate. While useful for preliminary studies, these simplified models do not capture the complex environment and responses of human β-cells *in vivo*.

To address this translational gap, researchers are increasingly turning to human-derived tissues. Stem cell-derived β-cell-like clusters (SC-βLCs), derived from pluripotent stem cells, offer a more physiologically relevant 3D model. These clusters demonstrate key β-cell functions, such as glucose-stimulated insulin secretion, and show great promise for drug screening, disease modeling, and potential cell replacement therapies. They provide a controlled and scalable system compared to primary human tissue. An example SC-βLCs is breifly highlighted in proinsulin anterograde trafficking (Section 5). Additionally, human pancreatic tissue slices and isolated islets, sourced from deceased donors with ethical adherence, offer insights into native β-cell function within their natural microenvironment. Studying these tissues enables researchers to explore β-cell interactions with other islet cell types, modulation by surrounding tissue architecture, and disruptions in conditions like type 2 diabetes. These tissues present a more complex and realistic picture of β-cell physiology than *in vitro* models.

By prioritizing human-derived models—SC-βLCs, pancreatic tissue slices, and isolated islets—β-cell biologists are making significant strides in understanding human β-cell physiology. This research is crucial for developing more effective and targeted diabetes therapies. These models facilitate a deeper understanding of disease mechanisms, identification of novel drug targets, and development of personalized medicine approaches tailored to individual patient needs. Ultimately, this shift toward human-relevant models promises to accelerate the development of better treatments and improve the lives of those with diabetes.

The complex challenge of proinsulin proteostasis demands a holistic and integrated approach for future therapies. This necessitates investigations in human tissues and the development of interventions that target not only the proinsulin protein itself, but also the interconnected cellular networks governing the UPR, mitochondrial function, and ER redox and calcium homeostasis.

Author contributions

PZ: Visualization, Writing–original draft, Writing–review and editing. KP: Writing–original draft, Writing–review and editing. DB: Visualization, Writing–review and editing. EG: Visualization, Writing–review and editing. MT: Writing–review and editing. TK: Writing–review and editing. SR: Conceptualization, Writing–review and editing. AA: Conceptualization, Supervision, Writing–original draft, Writing–review and editing, Visualization.

Funding

The author(s) declare that financial support was received for the research, authorship, and/or publication of this article. East Tennessee State University (AA), and Max Planck Institute for the Physics of Complex Systems (SR).

Conflict of interest

The authors declare that the research was conducted in the absence of any commercial or financial relationships that could be construed as a potential conflict of interest.

Generative AI statement

The author(s) declare that no Generative AI was used in the creation of this manuscript.

Publisher's note

References

Adams, C. J., Kopp, M. C., Larburu, N., Nowak, P. R., and Ali, M. M. U. (2019). Structure and molecular mechanism of ER stress signaling by the unfolded protein response signal activator IRE1. *Front. Mol. Biosci.* 6, 11. doi:10.3389/fmolb.2019.00011

Alam, M., Arunagiri, A., Haataja, L., Torres, M., Larkin, D., Kappler, J., et al. (2021). Predisposition to proinsulin misfolding as a genetic risk to diet-induced diabetes. *Diabetes* 70, 2580–2594. doi:10.2337/db21-0422

Antal, Z. (2021). Maturity-onset diabetes of the Young (MODY): genetic causes, clinical characteristics, considerations for testing, and treatment options. *Endocrines* 2, 485–501. doi:10.3390/endocrines2040043

Arunagiri, A., Alam, M., Haataja, L., Draz, H., Alasad, B., Samy, P., et al. (2024). Proinsulin folding and trafficking defects trigger a common pathological disturbance of endoplasmic reticulum homeostasis. *Protein Sci.* 33, e4949. doi:10.1002/pro.4949

Arunagiri, A., Haataja, L., Pottekat, A., Pamenan, F., Kim, S., Zeltser, L. M., et al. (2019). Proinsulin misfolding is an early event in the progression to type 2 diabetes. *Elife* 8, e44532. doi:10.7554/eLife.44532

Awazawa, M., Futami, T., Sakada, M., Kaneko, K., Ohsugi, M., Nakaya, K., et al. (2014). Deregulation of pancreas-specific oxidoreductin ERO1β in the pathogenesis of diabetes mellitus. *Mol. Cell Biol.* 34, 1290–1299. doi:10.1128/MCB.01647-13

Balboa, D., Saarimäki-Vire, J., Borshagovski, D., Survila, M., Lindholm, P., Galli, E., et al. (2018). Insulin mutations impair beta-cell development in a patient-derived iPSC model of neonatal diabetes. *Elife* 7, e38519. doi:10.7554/eLife.38519

Becerra-Tomas, N., Estruch, R., Bulló, M., Casas, R., Díaz-López, A., Basora, J., et al. (2014). Increased serum calcium levels and risk of type 2 diabetes in individuals at high cardiovascular risk. *Diabetes Care* 37, 3084–3091. doi:10.2337/dc14-0898

Bertolotti, A., Zhang, Y., Hendershot, L. M., Harding, H. P., and Ron, D. (2000). Dynamic interaction of BiP and ER stress transducers in the unfolded-protein response. *Nat. Cell Biol.* 2, 326–332. doi:10.1038/35014014

Boyer, C. K., Bauchle, C. J., Zhang, J., Wang, Y., and Stephens, S. B. (2023). Synchronized proinsulin trafficking reveals delayed Golgi export accompanies β-cell secretory dysfunction in rodent models of hyperglycemia. *Sci. Rep.* 13, 5218. doi:10.1038/s41598-023-32322-z

Cabibbo, A., Pagani, M., Fabbri, M., Rocchi, M., Farmery, M. R., Bulleid, N. J., et al. (2000). ERO1-L, a human protein that favors disulfide bond formation in the endoplasmic reticulum. *J. Biol. Chem.* 275, 4827–4833. doi:10.1074/jbc.275.7.4827

Carrara, M., Prischi, F., Nowak, P. R., Kopp, M. C., and Ali, M. M. (2015). Noncanonical binding of BiP ATPase domain to Ire1 and Perk is dissociated by unfolded protein CH1 to initiate ER stress signaling. *Elife* 4, e03522. doi:10.7554/eLife.03522

Chen, Y. J., Knupp, J., Arunagiri, A., Haataja, L., Arvan, P., and Tsai, B. (2021). PGRMC1 acts as a size-selective cargo receptor to drive ER-phagic clearance of mutant prohormones. *Nat. Commun.* 12, 5991. doi:10.1038/s41467-021-26225-8

Cnop, M., Toivonen, S., Igoillo-Esteve, M., and Salpea, P. (2017). Endoplasmic reticulum stress and eIF2α phosphorylation: the Achilles heel of pancreatic β cells. *Mol. Metab.* 6, 1024–1039. doi:10.1016/j.molmet.2017.06.001

Cremer, T., Hoelen, H., van de Weijer, M. L., Janssen, G. M., Costa, A. I., van Veelen, P. A., et al. (2024). Proinsulin degradation and presentation of a proinsulin B-chain autoantigen involves ER-associated protein degradation (ERAD)-enzyme UBE2G2. *PLoS One* 19, e0287877. doi:10.1371/journal.pone.0287877

Cui, W., Li, J., Ron, D., and Sha, B. (2011). The structure of the PERK kinase domain suggests the mechanism for its activation. *Acta Crystallogr. D. Biol. Crystallogr.* 67, 423–428. doi:10.1107/S0907444911006445

Cunningham, C. N., He, K., Arunagiri, A., Paton, A. W., Paton, J. C., Arvan, P., et al. (2017). Chaperone-driven degradation of a misfolded proinsulin mutant in parallel with restoration of wild-type insulin secretion. *Diabetes* 66, 741–753. doi:10.2337/db16-1338

Cunningham, C. N., Williams, J. M., Knupp, J., Arunagiri, A., Arvan, P., and Tsai, B. (2019). Cells deploy a two-pronged strategy to rectify misfolded proinsulin aggregates. *Mol. Cell* 75, 442–456. doi:10.1016/j.molcel.2019.05.011

De Franco, E., Lytrivi, M., Ibrahim, H., Montaser, H., Wakeling, M. N., Fantuzzi, F., et al. (2020). YIPF5 mutations cause neonatal diabetes and microcephaly through endoplasmic reticulum stress. *J. Clin. Invest* 130, 6338–6353. doi:10.1172/JCI141455

Dhanvantari, S., Shen, F. S., Adams, T., Snell, C. R., Zhang, C., Mackin, R. B., et al. (2003). Disruption of a receptor-mediated mechanism for intracellular sorting of proinsulin in familial hyperproinsulinemia. *Mol. Endocrinol.* 17, 1856–1867. doi:10.1210/me.2002-0380

Engin, F., Yermalovich, A., Nguyen, T., Ngyuen, T., Hummasti, S., Fu, W., et al. (2013). Restoration of the unfolded protein response in pancreatic β cells protects mice against type 1 diabetes. *Sci. Transl. Med.* 5, 211ra156. doi:10.1126/scitranslmed.3006534

Fang, J., Liu, M., Zhang, X., Sakamoto, T., Taatjes, D. J., Jena, B. P., et al. (2015). COPII-dependent ER export: a critical component of insulin biogenesis and β-cell ER homeostasis. *Mol. Endocrinol.* 29, 1156–1169. doi:10.1210/me.2015-1012

Feng, D., Wei, J., Gupta, S., McGrath, B. C., and Cavener, D. R. (2009). Acute ablation of PERK results in ER dysfunctions followed by reduced insulin secretion and cell proliferation. *BMC Cell Biol.* 10, 61. doi:10.1186/1471-2121-10-61

Forster, M. L., Sivick, K., Park, Y. N., Arvan, P., Lencer, W. I., and Tsai, B. (2006). Protein disulfide isomerase-like proteins play opposing roles during retrotranslocation. *J. Cell Biol.* 173, 853–859. doi:10.1083/jcb.200602046

Frank, B. H., Pekar, A. H., and Veros, A. J. (1972). Insulin and proinsulin conformation in solution. *Diabetes* 21, 486–491. doi:10.2337/diab.21.2.s486

Fritz, J. M., Dong, M., Apsley, K. S., Martin, E. P., Na, C. L., Sitaraman, S., et al. (2014). Deficiency of the BiP cochaperone ERdj4 causes constitutive endoplasmic reticulum stress and metabolic defects. *Mol. Biol. Cell* 25, 431–440. doi:10.1091/mbc.E13-06-0319

Fromme, J. C., Orci, L., and Schekman, R. (2008). Coordination of COPII vesicle trafficking by Sec23. *Trends Cell Biol.* 18, 330–336. doi:10.1016/j.tcb.2008.04.006

Gonzalez, B. J., Zhao, H., Niu, J., Williams, D. J., Lee, J., Goulbourne, C. N., et al. (2022). Reduced calcium levels and accumulation of abnormal insulin granules in stem cell models of HNF1A deficiency. *Commun. Biol.* 5, 779. doi:10.1038/s42003-022-03696-z

Gorai, B., and Vashisth, H. (2022). Progress in simulation studies of insulin structure and function. *Front. Endocrinol. (Lausanne)* 13, 908724. doi:10.3389/fendo.2022.908724

Gorasia, D. G., Dudek, N. L., Safavi-Hemami, H., Perez, R. A., Schittenhelm, R. B., Saunders, P. M., et al. (2016). A prominent role of PDIA6 in processing of misfolded proinsulin. *Biochim. Biophys. Acta* 1864, 715–723. doi:10.1016/j.bbapap.2016.03.002

Gupta, A. (2022). in *Biosynthesis of insulin 71-133* (Elsevier).

Gupta, S., McGrath, B., and Cavener, D. R. (2010). PERK (EIF2AK3) regulates proinsulin trafficking and quality control in the secretory pathway. *Diabetes* 59, 1937–1947. doi:10.2337/db09-1064

Haataja, L., Arunagiri, A., Hassan, A., Regan, K., Tsai, B., Dhayalan, B., et al. (2021). Distinct states of proinsulin misfolding in MIDY. *Cell Mol. Life Sci.* 78, 6017–6031. doi:10.1007/s00018-021-03871-1

Haataja, L., Manickam, N., Soliman, A., Tsai, B., Liu, M., and Arvan, P. (2016). Disulfide mispairing during proinsulin folding in the endoplasmic reticulum. *Diabetes* 65, 1050–1060. doi:10.2337/db15-1345

Halban, P. A., Bonner-Weir, S., and Weir, G. C. (1983). Elevated proinsulin biosynthesis *in vitro* from a rat model of non-insulin-dependent diabetes mellitus. *Diabetes* 32, 277–283. doi:10.2337/diab.32.3.277

Harding, H. P., Zhang, Y., and Ron, D. (1999). Protein translation and folding are coupled by an endoplasmic-reticulum-resident kinase. *Nature* 397, 271–274. doi:10.1038/16729

Harding, H. P., Zyryanova, A. F., and Ron, D. (2012). Uncoupling proteostasis and development *in vitro* with a small molecule inhibitor of the pancreatic endoplasmic reticulum kinase, PERK. *J. Biol. Chem.* 287, 44338–44344. doi:10.1074/jbc.M112.428987

He, K., Cunningham, C. N., Manickam, N., Liu, M., Arvan, P., and Tsai, B. (2015). PDI reductase acts on Akita mutant proinsulin to initiate retrotranslocation along the Hrd1/Sel1L-p97 axis. *Mol. Biol. Cell* 26, 3413–3423. doi:10.1091/mbc.E15-01-0034

Hetz, C., Zhang, K., and Kaufman, R. J. (2020). Mechanisms, regulation and functions of the unfolded protein response. *Nat. Rev. Mol. Cell Biol.* 21, 421–438. doi:10.1038/s41580-020-0250-z

Hoefner, C., Bryde, T. H., Pihl, C., Tiedemann, S. N., Bresson, S. E., Hotiana, H. A., et al. (2023). FK506-Binding protein 2 participates in proinsulin folding. *Biomolecules* 13, 152. doi:10.3390/biom13010152

Hoelen, H., Zaldumbide, A., van Leeuwen, W. F., Torfs, E. C. W., Engelse, M. A., Hassan, C., et al. (2015). Proteasomal degradation of proinsulin requires derlin-2, HRD1 and p97. *PLoS One* 10, e0128206. doi:10.1371/journal.pone.0128206

Hoffman, L. S., Fox, T. J., Anastasopoulou, C., and Jialal, I. (2025). Maturity onset diabetes in the Young.

Hu, Y., Gao, Y., Zhang, M., Deng, K. Y., Singh, R., Tian, Q., et al. (2019). Endoplasmic reticulum-associated degradation (ERAD) has a critical role in supporting glucose-stimulated insulin secretion in pancreatic β-cells. *Diabetes* 68, 733–746. doi:10.2337/db18-0624

Hua, Q. X., Jia, W., and Weiss, M. A. (2011). Conformational dynamics of insulin. *Front. Endocrinol. (Lausanne)* 2, 48. doi:10.3389/fendo.2011.00048

Huang, K., Dong, J., Phillips, N. B., Carey, P. R., and Weiss, M. A. (2005). Proinsulin is refractory to protein fibrillation: topological protection of a precursor protein from cross-beta assembly. *J. Biol. Chem.* 280, 42345–42355. doi:10.1074/jbc.M507110200

Iida, H., Kono, T., Lee, C. C., Krishnan, P., Arvin, M. C., Weaver, S. A., et al. (2023). SERCA2 regulates proinsulin processing and processing enzyme maturation in pancreatic beta cells. *Diabetologia* 66, 2042–2061. doi:10.1007/s00125-023-05979-4

Jamieson, J. D., and Palade, G. E. (1968). Intracellular transport of secretory proteins in the pancreatic exocrine cell. IV. Metabolic requirements. *J. Cell Biol.* 39, 589–603. doi:10.1083/jcb.39.3.589

Jang, I., Pottekat, A., Poothong, J., Yong, J., Lagunas-Acosta, J., Charbono, A., et al. (2019). PDIA1/P4HB is required for efficient proinsulin maturation and ß cell health in response to diet induced obesity. *Elife* 8, e44528. doi:10.7554/eLife.44528

Jung, S. H., Kim, C. K., Lee, G., Yoon, J., and Lee, M. (2017). Structural analysis of recombinant human preproinsulins by structure prediction, molecular dynamics, and protein-protein docking. *Genomics Inf.* 15, 142–146. doi:10.5808/GI.2017.15.4.142

Kitabchi, A. E. (1977). Proinsulin and C-peptide: a review. *Metabolism* 26, 547–587. doi:10.1016/0026-0495(77)90099-3

Klein, M. C., Zimmermann, K., Schorr, S., Landini, M., Klemens, P. A. W., Altensell, J., et al. (2018). AXER is an ATP/ADP exchanger in the membrane of the endoplasmic reticulum. *Nat. Commun.* 9, 3489. doi:10.1038/s41467-018-06003-9

Kopp, M. C., Nowak, P. R., Larburu, N., Adams, C. J., and Ali, M. M. (2018). *In vitro* FRET analysis of IRE1 and BiP association and dissociation upon endoplasmic reticulum stress. *Elife* 7, e30257. doi:10.7554/eLife.30257

Kosinova, L., Veverka, V., Novotná, P., Collinsová, M., Urbanová, M., Moody, N. R., et al. (2014). Insight into the structural and biological relevance of the T/R transition of the N-terminus of the B-chain in human insulin. *Biochemistry* 53, 3392–3402. doi:10.1021/bi500073z

Krshnan, L., van de Weijer, M. L., and Carvalho, P. (2022). Endoplasmic reticulum-associated protein degradation. *Cold Spring Harb. Perspect. Biol.* 14, a041247. doi:10.1101/cshperspect.a041247

Ksenofontova, O. I., Romanovskaya, E. V., and Stefanov, V. E. (2014). Study of conformational mobility of insulin, proinsulin, and insulin-like growth factors. *J. Evol. Biochem. Phys.* 50, 42–48. doi:10.1134/s002209301401006x

Landreh, M., and Jornvall, H. (2015). C-peptide evolution: generation from few structural restrictions of bioactivities not necessarily functional. *FEBS Lett.* 589, 415–418. doi:10.1016/j.febslet.2015.01.006

Laybutt, D. R., Preston, A. M., Akerfeldt, M. C., Kench, J. G., Busch, A. K., Biankin, A. V., et al. (2007). Endoplasmic reticulum stress contributes to beta cell apoptosis in type 2 diabetes. *Diabetologia* 50, 752–763. doi:10.1007/s00125-006-0590-z

Leahy, J. L. (1993). Increased proinsulin/insulin ratio in pancreas extracts of hyperglycemic rats. *Diabetes* 42, 22–27. doi:10.2337/diab.42.1.22

Lievremont, J. P., Rizzuto, R., Hendershot, L., and Meldolesi, J. (1997). BiP, a major chaperone protein of the endoplasmic reticulum lumen, plays a direct and important role in the storage of the rapidly exchanging pool of Ca2+. *J. Biol. Chem.* 272, 30873–30879. doi:10.1074/jbc.272.49.30873

Liu, M., Haataja, L., Wright, J., Wickramasinghe, N. P., Hua, Q. X., Phillips, N. F., et al. (2010a). Mutant INS-gene induced diabetes of youth: proinsulin cysteine residues impose dominant-negative inhibition on wild-type proinsulin transport. *PLoS One* 5, e13333. doi:10.1371/journal.pone.0013333

Liu, M., Hodish, I., Haataja, L., Lara-Lemus, R., Rajpal, G., Wright, J., et al. (2010b). Proinsulin misfolding and diabetes: mutant INS gene-induced diabetes of youth. *Trends Endocrinol. Metab.* 21, 652–659. doi:10.1016/j.tem.2010.07.001

Liu, M., Hua, Q. x., Hu, S. Q., Jia, W., Yang, Y., Saith, S. E., et al. (2010c). Deciphering the hidden informational content of protein sequences: foldability of proinsulin hinges on a flexible arm that is dispensable in the mature hormone. *J. Biol. Chem.* 285, 30989–31001. doi:10.1074/jbc.M110.152645

Liu, M., Li, Y., Cavener, D., and Arvan, P. (2005). Proinsulin disulfide maturation and misfolding in the endoplasmic reticulum. *J. Biol. Chem.* 280, 13209–13212. doi:10.1074/jbc.C400475200

Liu, Y., Yang, X., Zhou, J., Yang, H., Yang, R., Zhu, P., et al. (2024). OSGEP regulates islet β-cell function by modulating proinsulin translation and maintaining ER stress homeostasis in mice. *Nat. Commun.* 15, 10479. doi:10.1038/s41467-024-54905-8

Lodish, H., Berk, A., Kaiser, C., Krieger, M., Bretscher, A., Ploegh, H., et al. (2021). *Molecular Cell Biology*, Editors. Ninth B. Anna, L. Maria, M. Susan, and Z. Michael (W. H. Freeman Macmillan Learning).

Matschinsky, F. M., and Wilson, D. F. (2019). The central role of glucokinase in glucose homeostasis: a perspective 50 Years after demonstrating the presence of the enzyme in islets of langerhans. *Front. Physiol.* 10, 148. doi:10.3389/fphys.2019.00148

McCracken, A. A., and Brodsky, J. L. (2003). Evolving questions and paradigm shifts in endoplasmic-reticulum-associated degradation (ERAD). *Bioessays* 25, 868–877. doi:10.1002/bies.10320

Michalak, M. (2024). Calreticulin: endoplasmic reticulum Ca(2+) gatekeeper. *J. Cell Mol. Med.* 28, e17839. doi:10.1111/jcmm.17839

Narayan, M. (2021). The Formation of native disulfide bonds: treading a fine line in protein folding. *Protein J.* 40, 134–139. doi:10.1007/s10930-021-09976-7

Ninagawa, S., Tada, S., Okumura, M., Inoguchi, K., Kinoshita, M., Kanemura, S., et al. (2020). Antipsychotic olanzapine-induced misfolding of proinsulin in the endoplasmic reticulum accounts for atypical development of diabetes. *Elife* 9, e60970. doi:10.7554/eLife.60970

Nishi, M., and Nanjo, K. (2011). Insulin gene mutations and diabetes. *J. Diabetes Investig.* 2, 92–100. doi:10.1111/j.2040-1124.2011.00100.x

Oakes, S. A., and Papa, F. R. (2015). The role of endoplasmic reticulum stress in human pathology. *Annu. Rev. Pathol.* 10, 173–194. doi:10.1146/annurev-pathol-012513-104649

Papaioannou, A., Kuyucak, S., and Kuncic, Z. (2015). Molecular dynamics simulations of insulin: elucidating the conformational changes that enable its binding. *PLoS One* 10, e0144058. doi:10.1371/journal.pone.0144058

Park, S. Y., Ye, H., Steiner, D. F., and Bell, G. I. (2010). Mutant proinsulin proteins associated with neonatal diabetes are retained in the endoplasmic reticulum and not efficiently secreted. *Biochem. Biophys. Res. Commun.* 391, 1449–1454. doi:10.1016/j.bbrc.2009.12.090

Pekar, A. H., and Frank, B. H. (1972). Conformation of proinsulin. A comparison of insulin and proinsulin self-association at neutral pH. *Biochemistry* 11, 4013–4016. doi:10.1021/bi00772a001

Pobre, K. F. R., Poet, G. J., and Hendershot, L. M. (2019). The endoplasmic reticulum (ER) chaperone BiP is a master regulator of ER functions: getting by with a little help from ERdj friends. *J. Biol. Chem.* 294, 2098–2108. doi:10.1074/jbc.REV118.002804

Pontisso, I., Ornelas-Guevara, R., Chevet, E., Combettes, L., and Dupont, G. (2024). Gradual ER calcium depletion induces a progressive and reversible UPR signaling. *PNAS Nexus* 3, pgae229. doi:10.1093/pnasnexus/pgae229

Preissler, S., Rato, C., Yan, Y., Perera, L. A., Czako, A., and Ron, D. (2020). Calcium depletion challenges endoplasmic reticulum proteostasis by destabilising BiP-substrate complexes. *Elife* 9, e62601. doi:10.7554/eLife.62601

Rajan, S., Eames, S. C., Park, S. Y., Labno, C., Bell, G. I., Prince, V. E., et al. (2010). *In vitro* processing and secretion of mutant insulin proteins that cause permanent neonatal diabetes. *Am. J. Physiol. Endocrinol. Metab.* 298, E403–E410. doi:10.1152/ajpendo.00592.2009

Rajpal, G., Schuiki, I., Liu, M., Volchuk, A., and Arvan, P. (2012). Action of protein disulfide isomerase on proinsulin exit from endoplasmic reticulum of pancreatic β-cells. *J. Biol. Chem.* 287, 43–47. doi:10.1074/jbc.C111.279927

Ramming, T., and Appenzeller-Herzog, C. (2012). The physiological functions of mammalian endoplasmic oxidoreductin 1: on disulfides and more. *Antioxid. Redox Signal* 16, 1109–1118. doi:10.1089/ars.2011.4475

Rege, N. K., Liu, M., Yang, Y., Dhayalan, B., Wickramasinghe, N. P., Chen, Y. S., et al. (2020). Evolution of insulin at the edge of foldability and its medical implications. *Proc. Natl. Acad. Sci. U. S. A.* 117, 29618–29628. doi:10.1073/pnas.2010908117

Rohli, K. E., Stubbe, N. J., Walker, E. M., Pearson, G. L., Soleimanpour, S. A., and Stephens, S. B. (2024). A metabolic redox relay supports ER proinsulin export in pancreatic islet β cells. *JCI Insight* 9, e178725. doi:10.1172/jci.insight.178725

Ron, D., and Walter, P. (2007). Signal integration in the endoplasmic reticulum unfolded protein response. *Nat. Rev. Mol. Cell Biol.* 8, 519–529. doi:10.1038/nrm2199

Sachdeva, M. M., Claiborn, K. C., Khoo, C., Yang, J., Groff, D. N., Mirmira, R. G., et al. (2009). Pdx1 (MODY4) regulates pancreatic beta cell susceptibility to ER stress. *Proc. Natl. Acad. Sci. U. S. A.* 106, 19090–19095. doi:10.1073/pnas.0904849106

Serebryany, E., Martin, R. W., and Takahashi, G. R. (2024). The functional significance of high cysteine content in eye lens gamma-crystallins. *Biomolecules* 14, 594. doi:10.3390/biom14050594

Serebryany, E., Yu, S., Trauger, S. A., Budnik, B., and Shakhnovich, E. I. (2018). Dynamic disulfide exchange in a crystallin protein in the human eye lens promotes cataract-associated aggregation. *J. Biol. Chem.* 293, 17997–18009. doi:10.1074/jbc.RA118.004551

Sharma, R. B., Darko, C., and Alonso, L. C. (2020). Intersection of the ATF6 and XBP1 ER stress pathways in mouse islet cells. *J. Biol. Chem.* 295, 14164–14177. doi:10.1074/jbc.RA120.014173

Sharma, R. B., O'Donnell, A. C., Stamateris, R. E., Ha, B., McCloskey, K. M., Reynolds, P. R., et al. (2015). Insulin demand regulates β cell number via the unfolded protein response. *J. Clin. Invest* 125, 3831–3846. doi:10.1172/JCI79264

Shen, J., Snapp, E. L., Lippincott-Schwartz, J., and Prywes, R. (2005). Stable binding of ATF6 to BiP in the endoplasmic reticulum stress response. *Mol. Cell Biol.* 25, 921–932. doi:10.1128/MCB.25.3.921-932.2005

Shen, Y., and Hendershot, L. M. (2005). ERdj3, a stress-inducible endoplasmic reticulum DnaJ homologue, serves as a cofactor for BiP's interactions with unfolded substrates. *Mol. Biol. Cell* 16, 40–50. doi:10.1091/mbc.e04-05-0434

Shi, Y., Vattem, K. M., Sood, R., An, J., Liang, J., Stramm, L., et al. (1998). Identification and characterization of pancreatic eukaryotic initiation factor 2 alpha-subunit kinase, PEK, involved in translational control. *Mol. Cell Biol.* 18, 7499–7509. doi:10.1128/mcb.18.12.7499

Shrestha, N., Torres, M., Zhang, J., Lu, Y., Haataja, L., Reinert, R. B., et al. (2023). Integration of ER protein quality control mechanisms defines β cell function and ER architecture. *J. Clin. Invest* 133, e163584. doi:10.1172/JCI163584

Sowers, C. R., Wang, R., Bourne, R. A., McGrath, B. C., Hu, J., Bevilacqua, S. C., et al. (2018). The protein kinase PERK/EIF2AK3 regulates proinsulin processing not via protein synthesis but by controlling endoplasmic reticulum chaperones. *J. Biol. Chem.* 293, 5134–5149. doi:10.1074/jbc.M117.813790

Sun, J., Xiong, Y., Li, X., Haataja, L., Chen, W., Mir, S. A., et al. (2020). Role of proinsulin self-association in mutant INS gene-induced diabetes of youth. *Diabetes* 69, 954–964. doi:10.2337/db19-1106

Tang, V. T., and Ginsburg, D. (2023). Cargo selection in endoplasmic reticulum-to-Golgi transport and relevant diseases. *J. Clin. Invest* 133, e163838. doi:10.1172/JCI163838

Templin, A. T., Maier, B., Tersey, S. A., Hatanaka, M., and Mirmira, R. G. (2014). Maintenance of Pdx1 mRNA translation in islet β-cells during the unfolded protein response. *Mol. Endocrinol.* 28, 1820–1830. doi:10.1210/me.2014-1157

Tornovsky-Babeay, S., Weinberg-Corem, N., Ben-Haroush Schyr, R., Avrahami, D., Lavi, J., Feleke, E., et al. (2021). Biphasic dynamics of beta cell mass in a mouse model of congenital hyperinsulinism: implications for type 2 diabetes. *Diabetologia* 64, 1133–1143. doi:10.1007/s00125-021-05390-x

Tran, D. T., Pottekat, A., Mir, S. A., Loguercio, S., Jang, I., Campos, A. R., et al. (2020). Unbiased profiling of the human proinsulin biosynthetic interaction network reveals a role for peroxiredoxin 4 in proinsulin folding. *Diabetes* 69, 1723–1734. doi:10.2337/db20-0245

Tsuchiya, Y., Saito, M., Kadokura, H., Miyazaki, J. I., Tashiro, F., Imagawa, Y., et al. (2018). IRE1-XBP1 pathway regulates oxidative proinsulin folding in pancreatic β cells. *J. Cell Biol.* 217, 1287–1301. doi:10.1083/jcb.201707143

Uchizono, Y., Alarcon, C., Wicksteed, B. L., Marsh, B. J., and Rhodes, C. J. (2007). The balance between proinsulin biosynthesis and insulin secretion: where can imbalance lead? *Diabetes Obes. Metab.* 9 (Suppl. 2), 56–66. doi:10.1111/j.1463-1326.2007.00774.x

Wang, H., Saint-Martin, C., Xu, J., Ding, L., Wang, R., Feng, W., et al. (2020). Biological behaviors of mutant proinsulin contribute to the phenotypic spectrum of diabetes associated with insulin gene mutations. *Mol. Cell Endocrinol.* 518, 111025. doi:10.1016/j.mce.2020.111025

Wang, J., Takeuchi, T., Tanaka, S., Kubo, S. K., Kayo, T., Lu, D., et al. (1999). A mutation in the insulin 2 gene induces diabetes with severe pancreatic beta-cell dysfunction in the Mody mouse. *J. Clin. Investigation* 103, 27–37. doi:10.1172/JCI4431

Wang, R., McGrath, B. C., Kopp, R. F., Roe, M. W., Tang, X., Chen, G., et al. (2013). Insulin secretion and Ca2+ dynamics in β-cells are regulated by PERK (EIF2AK3) in concert with calcineurin. *J. Biol. Chem.* 288, 33824–33836. doi:10.1074/jbc.M113.503664

Wang, R., Munoz, E. E., Zhu, S., McGrath, B. C., and Cavener, D. R. (2014). Perk gene dosage regulates glucose homeostasis by modulating pancreatic β-cell functions. *PLoS One* 9, e99684. doi:10.1371/journal.pone.0099684

Ward, W. K., LaCava, E. C., Paquette, T. L., Beard, J. C., Wallum, B. J., and Porte, D. (1987). Disproportionate elevation of immunoreactive proinsulin in type 2 (non-insulin-dependent) diabetes mellitus and in experimental insulin resistance. *Diabetologia* 30, 698–702. doi:10.1007/BF00296991

Wei, P., Shi, M., Barnum, S., Cho, H., Carlson, T., and Fraser, J. D. (2009). Effects of glucokinase activators GKA50 and LY2121260 on proliferation and apoptosis in pancreatic INS-1 beta cells. *Diabetologia* 52, 2142–2150. doi:10.1007/s00125-009-1446-0

Weiss, M. A. (2013). Diabetes mellitus due to the toxic misfolding of proinsulin variants. *FEBS Lett.* 587, 1942–1950. doi:10.1016/j.febslet.2013.04.044

Winter, J., Gleiter, S., Klappa, P., and Lilie, H. (2011). Protein disulfide isomerase isomerizes non-native disulfide bonds in human proinsulin independent of its peptide-binding activity. *Protein Sci.* 20, 588–596. doi:10.1002/pro.592

Winter, J., Klappa, P., Freedman, R. B., Lilie, H., and Rudolph, R. (2002). Catalytic activity and chaperone function of human protein-disulfide isomerase are required for the efficient refolding of proinsulin. *J. Biol. Chem.* 277, 310–317. doi:10.1074/jbc.M107832200

Wright, J., Birk, J., Haataja, L., Liu, M., Ramming, T., Weiss, M. A., et al. (2013). Endoplasmic reticulum oxidoreductin-1α (Ero1α) improves folding and secretion of mutant proinsulin and limits mutant proinsulin-induced endoplasmic reticulum stress. *J. Biol. Chem.* 288, 31010–31018. doi:10.1074/jbc.M113.510065

Xu, B., Allard, C., Alvarez-Mercado, A. I., Fuselier, T., Kim, J. H., Coons, L. A., et al. (2018). Estrogens promote misfolded proinsulin degradation to protect insulin production and delay diabetes. *Cell Rep.* 24, 181–196. doi:10.1016/j.celrep.2018.06.019

Xu, J., Zhu, R., Chen, Y., Li, X., Chen, X., Liu, M., et al. (2024). Chloroquine-induced proinsulin misfolding in the endoplasmic reticulum underlies the attenuation of mature insulin synthesis. *FASEB J.* 38, e70201. doi:10.1096/fj.202401945R

Xu, X., Arunagiri, A., Alam, M., Haataja, L., Evans, C. R., Zhao, I., et al. (2023). Nutrient-dependent regulation of β-cell proinsulin content. *J. Biol. Chem.* 299, 104836. doi:10.1016/j.jbc.2023.104836

Xu, X., Arunagiri, A., Haataja, L., Alam, M., Ji, S., Qi, L., et al. (2022). Proteasomal degradation of WT proinsulin in pancreatic beta cells. *J. Biol. Chem.* 298, 102406. doi:10.1016/j.jbc.2022.102406

Yamamoto, E., Uchida, T., Abe, H., Taka, H., Fujimura, T., Komiya, K., et al. (2014). Increased expression of ERp57/GRP58 is protective against pancreatic beta cell death caused by autophagic failure. *Biochem. Biophys. Res. Commun.* 453, 19–24. doi:10.1016/j.bbrc.2014.09.040

Yang, J., Zhen, J., Feng, W., Fan, Z., Ding, L., Yang, X., et al. (2022). IER3IP1 is critical for maintaining glucose homeostasis through regulating the endoplasmic reticulum function and survival of β cells. *Proc. Natl. Acad. Sci. U. S. A.* 119, e2204443119. doi:10.1073/pnas.2204443119

Yang, Y., Hua, Q. X., Liu, J., Shimizu, E. H., Choquette, M. H., Mackin, R. B., et al. (2010). Solution structure of proinsulin: connecting domain flexibility and prohormone processing. *J. Biol. Chem.* 285, 7847–7851. doi:10.1074/jbc.C109.084921

Yassin, O., Praveen, B., Darawshi, O., LaFramboise, T., Shmuel, M., Pattanayak, S. P., et al. (2024). Opposing regulation of endoplasmic reticulum retention under stress by ERp44 and PDIA6. *Biochem. J.* 481, 1921–1935. doi:10.1042/BCJ20240444

Yong, J., Bischof, H., Burgstaller, S., Siirin, M., Murphy, A., Malli, R., et al. (2019). Mitochondria supply ATP to the ER through a mechanism antagonized by cytosolic Ca^{2+} eLife 8, e49682. doi:10.7554/eLife.49682

Zhu, R., Li, X., Xu, J., Barrabi, C., Kekulandara, D., Woods, J., et al. (2019). Defective endoplasmic reticulum export causes proinsulin misfolding in pancreatic β cells. *Mol. Cell Endocrinol.* 493, 110470. doi:10.1016/j.mce.2019.110470

Zito, E., Chin, K. T., Blais, J., Harding, H. P., and Ron, D. (2010). ERO1-beta, a pancreas-specific disulfide oxidase, promotes insulin biogenesis and glucose homeostasis. *J. Cell Biol.* 188, 821–832. doi:10.1083/jcb.200911086

Zuber, C., Fan, J. Y., Guhl, B., and Roth, J. (2004). Misfolded proinsulin accumulates in expanded pre-Golgi intermediates and endoplasmic reticulum subdomains in pancreatic beta cells of Akita mice. *FASEB J.* 18, 917–919. doi:10.1096/fj.03-1210fje

frontiers | Frontiers in Molecular Biosciences

TYPE Correction
PUBLISHED 19 March 2025
DOI 10.3389/fmolb.2025.1592000

OPEN ACCESS

EDITED AND REVIEWED BY
Venkateswarlu Kanamarlapudi,
Swansea University Medical School,
United Kingdom

*CORRESPONDENCE
Anoop Arunagiri,
arunagiri@etsu.edu
Srivastav Ranganathan,
sranga88@pks.mpg.de

RECEIVED 11 March 2025
ACCEPTED 13 March 2025
PUBLISHED 19 March 2025

CITATION
Zavarzadeh PG, Panchal K, Bishop D, Gilbert E, Trivedi M, Kee T, Ranganathan S and Arunagiri A (2025) Corrigendum: Exploring proinsulin proteostasis: insights into beta cell health and diabetes.
Front. Mol. Biosci. 12:1592000.
doi: 10.3389/fmolb.2025.1592000

Corrigendum: Exploring proinsulin proteostasis: insights into beta cell health and diabetes

Parisima Ghaffarian Zavarzadeh[1], Kathigna Panchal[1], Dylan Bishop[1], Elizabeth Gilbert[1], Mahi Trivedi[1], Tovaria Kee[1], Srivastav Ranganathan[2]* and Anoop Arunagiri[1]*

[1]Department of Biological Sciences, East Tennessee State University, Johnson City, TN, United States, [2]Max Planck Institute for the Physics of Complex Systems, Dresden, Germany

KEYWORDS

proinsulin folding, trafficking, beta cells, proteostasis, insulin biosynthesis, diabetes

A Corrigendum on
Exploring proinsulin proteostasis: insights into beta cell health and diabetes

by Zavarzadeh PG, Panchal K, Bishop D, Gilbert E, Trivedi M, Kee T, Ranganathan S and Arunagiri A (2025). Front. Mol. Biosci. 12:1554717. doi: 10.3389/fmolb.2025.1554717

In the published article, there was an error in the legend for **Figure 7** as published. A sentence was incomplete in the 7th point in the legend. The corrected legend appears below.

"Orchestrating proinsulin proteostasis in β-cells: Molecular Chaperones, oxidoreductases, and the UPR. (1) PERK ablation, leading to Erp72 upregulation, may impair proinsulin degradation or trafficking. Independently, PERK inhibition can induce ER stress in β-cells, (2) PERK inhibition (by PERKi) prevents eIF2α phosphorylation, negatively impacting the UPR primarily through dysregulation of protein synthesis, (3) Treatment of β-cells with PERKi for 10–12 h induces proinsulin misfolding, (4) BiP inactivation (by SubAB or PERK inhibition) impairs proinsulin folding in β-cells, (5) PDIA6 deletion may impair both the UPR and proinsulin trafficking; Defective proinsulin trafficking could hinder proinsulin folding in the ER, (6) Inhibition of the IRE1α-XBP1 pathway deregulates PDI activity in β-cells, potentially impeding proinsulin folding or disrupting ERAD through impaired PDI-mediated retrotranslocation, (7) Grp170 either directly targets mutant high-molecular weight (HMW) proinsulin aggregates or collaborates with reticulon 3 (RTN3), which engages with PGRMC1 on the ER luminal side (not shown), to clear aggregates via ER-phagy in the cytosol, (8) FBKBP2 knockout results in proinsulin misfolding, (9) High-glucose-induced sulfonylation of PRDX4 impairs its protective function against proinsulin misfolding, (10) Erdj3 may promote proinsulin folding by acting as a co-chaperone with BiP."

The authors apologize for this error and state that this does not change the scientific conclusions of the article in any way. The original article has been updated.

Publisher's note

frontiers | Frontiers in Molecular Biosciences

TYPE Original Research
PUBLISHED 19 March 2025
DOI 10.3389/fmolb.2025.1567932

OPEN ACCESS

EDITED BY
Anoop Arunagiri,
East Tennessee State University, United States

REVIEWED BY
Danish Khan,
Stanford University, United States
Mustafi Raisa Amin,
Northeastern University, United States
Pilar Rivero-Rios,
University of Michigan, United States

*CORRESPONDENCE
Sanjeev K. Upadhyay,
sanjeev.kumar-biochem@msubaroda.ac.in
Bhavani Shankar Sahu,
bssahu@nbrc.ac.in
Ashwini Godbole,
ashwini.g@tdu.edu.in

†These authors have contributed equally to this work

RECEIVED 28 January 2025
ACCEPTED 28 February 2025
PUBLISHED 19 March 2025

CITATION
Simha PK, Mukherjee C, Kumar Gupta V, Bhatia K, Nagar P, ZA AN, Godbole A, Sahu BS and Upadhyay SK (2025) *Sida cordifolia* is efficacious in models of Huntington's disease by reducing ER stress.
Front. Mol. Biosci. 12:1567932.
doi: 10.3389/fmolb.2025.1567932

Sida cordifolia is efficacious in models of Huntington's disease by reducing ER stress

Prasanna K. Simha[1†], Chandramouli Mukherjee[2†], Vikas Kumar Gupta[3], Karishma Bhatia[3], Padmanabhi Nagar[4], Azeem Nazeer ZA[5], Ashwini Godbole[1*], Bhavani Shankar Sahu[2*] and Sanjeev K. Upadhyay[1,3*]

[1]Centre for Ayurveda Biology and Holistic Nutrition, University of Trans-Disciplinary Health Sciences and Technology (TDU), Bengaluru, India, [2]National Brain Research Centre, Gurugram, Haryana, India, [3]Department of Biochemistry, Faculty of Science, The Maharaja Sayajirao University of Baroda, Vadodara, Gujarat, India, [4]Department of Botany, Faculty of Science, The Maharaja Sayajirao University of Baroda, Vadodara, Gujarat, India, [5]Kerala Ayurveda Clinic, Bengaluru, India

Neurodegenerative disorders (NDs) are a major class of diseases where modern science has not succeeded in providing solutions to the desired levels. ER stress pathway is implicated in pathophysiology of several neurodegenerative disorders, especially those classified as proteinopathies. Several traditional medicines are used to treat neurodegeneration and *Sida cordifolia* (SC) is one of the common ingredients in formulations used for treating NDs and neuropathic pain. However, the mode of action is not clear. We studied the effectiveness of SC in Huntington's Disease (HD) model using *Caenorhabditis elegans* and mammalian cells. We used a transgenic *C. elegans* that expresses mutant huntingtin protein tagged with Yellow Fluorescent Protein (YFP) in their body wall muscle. In *C. elegans*, SC not only improved motility but also substantially increased the life span. Cell-based studies using inducible mutant Huntingtin protein (mHTT) with a long polyQ tail tagged with EGFP showed that SC profoundly modulates ER stress, reducing the stress caused by mHTT protein. The study showed that the mode of action of SC, at least partially, is through modulation of ER stress pathway, thereby normalizing the changes brought about by overexpression of mHTT.

KEYWORDS

***Sida cordifolia*, neurodegeneration, Huntington's disease, ER stress, ayurveda biology**

1 Introduction

Huntington's Disease (HD) is an autosomal dominant neurodegenerative disorder caused by the expansion of CAG trinucleotide repeats in the huntingtin (*Htt*) gene on chromosome 4. The disease is estimated to affect about 1 in 7,500 individuals in the population (Caron et al., 2018), being more prevalent in the Western population than in Asians (McColgan and Tabrizi, 2018). The mutant genes encode huntingtin protein with long tandem repeats of poly-glutamines (polyQ), typically more than 35 in a stretch. Longer CAG repeats cause earlier onset of disease and increased severity (McColgan and Tabrizi, 2018). The mutant protein misfolds and aggregates which is a cause for neurodegeneration (McColgan and Tabrizi, 2018). Cognitive, motor and psychological disturbances are

attributed to neuronal degeneration in the striatum, globus pallidus, subthalamic nucleus, thalamus, substantia nigra and hypothalamus of the brain (Caron et al., 2018).

Current treatments for HD are symptomatic and do not rectify the underlying causal cellular and molecular derangements. Symptomatic therapies include anti-dopaminergic agents and occasionally anti-depressants. Prolonged usage of these treatments in HD patients is associated with adverse effects (Ferguson et al., 2022) including diarrhea, nausea, vomiting, depression, Parkinsonism and suicidal tendencies (Paleacu, 2007; Yero and Rey, 2008). In animal models, azo-dye congo-red (Sánchez et al., 2003), disaccharide trehalose (Tanaka et al., 2004), and polyQ-binding peptide-1 (Nagai et al., 2003) have been reported to decrease the aggregation of mutant huntingtin protein, but none of these can cross the blood-brain barrier, impeding their development as therapeutics. Taken together, there remains an unmet need for new therapies to rectify the molecular derangements in HD, namely the aggregation of mutant huntingtin proteins and the toxic effects they cause in neurons.

Many cellular signal transduction pathways are implicated in HD. One cellular mechanism implicated in protein misfolding disorders involve the Endoplasmic Reticulum Unfolded Protein Response (ER-UPR). Studies have shown that chronic activation of the ER-UPR is a common feature of these diseases. In mammals, three main pathways, initiated by three different type-1 transmembrane proteins, namely: inositol – requiring protein – 1α (IRE -1α), protein kinase RNA-like ER kinase (PERK) and activating transcription factor-6 (ATF6), govern the ER-UPR. Manipulating these pathways using small molecules or genetic tools have shown to be effective in models of neurodegeneration (Hughes and Mallucci, 2019). In the case of HD, targeting XBP-1 is shown to be beneficial in animal models, and is thus being explored as a potential drug target (Vidal et al., 2012).

Ayurveda, an Indian traditional system of medicine has the pharmacopoeia of approximately 70,000 formulations. *Sida cordifolia* (Flannel Weed, *Bala*) (SC), a perennially growing shrub of the mallow family *Malvacea* native to India, is one of the most commonly used herbs in Ayurveda to treat diseases of the nervous system.

Ayurvedic formulations containing SC have been effectively used to treat pain, neurological diseases associated with tremors or movement disorders (Sati and Deole, 2020), Parkinson's Disease (Anjaneyulu et al., 2020) and arthritis (Das et al., 2021). Many of these ailments are degenerative in nature. Interestingly, in a case study with one patient of early onset HD, whole-system Ayurvedic treatment lead to reduction in involuntary movements, improved balance and gait (Malavika and Savitha, 2022). SC formed an important component of the treatment. This case report and observations from the practice of Ayurveda inspired us to determine if SC could reduce aggregation of mutant huntingtin protein in models of HD. It is interesting to note that in all the ailments, for which SC is prescribed in Ayurveda, ER-UPR is a key cellular pathway in their pathogenesis.

Acorus calamus (Sweet Flag, Muskrat root, *Vacha*) (AC), a plant from the family *Acoraceae*, is another neuroactive herb commonly used in Ayurveda. Unlike SC, AC is used for enhancing intelligence and treating epilepsy, speech disorders, which are non-degenerative in nature (Chunekar, 2004).

Here, we assessed the effect of methanolic extract of SC on cellular and molecular hallmarks in HD models. We chose to use AC, a differentially used herb, as a control to confirm the specificity of the SC effects. We used an animal model and a cell line model of HD. In *Caenorhabditis elegans* strains expressing a mutant huntingtin protein containing 40 tandem glutamines, the methanolic extract of SC, but not of AC, reduced aggregates of the polyQ-containing mutant huntingtin protein and thereby improved motility and prolonged life span of the nematode. In a transgenic mouse neuroblastoma cell line over-expressing a mutant huntingtin protein with 150 tandem glutamines, SC reduced aggregates of the polyQ-containing mutant protein by suppressing the Endoplasmic Reticulum Unfolded Protein Response (ER-UPR) triggered by aggregation. The results indicate that SC can be a source of novel therapeutics to inhibit aggregation of misfolded huntingtin proteins and the resulting neurodegenerative sequelae.

2 Materials and methods

2.1 Preparation of methanolic extract of *S. cordifolia* and *A. calamus*

Roots of SC (Specimen no. SANJ20/1) were obtained from herb collectors and rhizomes of AC (Specimen no. SANJ20/2) were obtained from Botanical Garden, MSU Baroda. The plant material was authenticated by Baro herbarium, Department of Botany, MSU Baroda.

The roots or rhizomes were thoroughly washed and dried, followed by powdering them coarsely. The plant root/rhizome powder and methanol (1:10 (w/v) root powder: methanol) was used for extraction using the soxhlet apparatus for 7–8 h. The extract was concentrated, and solvent was removed using a rotary evaporator and stored at −20°C for further use. TLC was run to check the quality of the extract. MTT assay was also performed to assess the toxicity (Supplementary Figure 5).

2.2 Culture and maintenance of *C. elegans*

The *C. elegans* strains N2 (wild type) and AM141 (rmls133 (unc54p::Q40::YFP); expressing Q40::YFP in body wall muscles of the nematode were procured from the *Caenorhabditis* Genetics Centre (CGC), University of Minnesota, United States. The worms were grown at 20°C on Nematode Growth Medium (NGM) seeded with *Escherichia coli* OP50 using standard protocols. All worm experiments were conducted in accordance with the internationally accepted principles and approved by institutional committee (IBSC/TDU/05/12/22).

2.3 Culture of N2a neuroblastoma cells over-expressing a mutant huntingtin protein with expanded polyQ, and treatment with extracts of *S. cordifolia*

Transgenic mouse N2a cells expressing an ecdysone-inducible truncated N-terminal huntingtin gene with 150 CAG repeats

attached to EGFP (HD 150Q) were a kind gift from Professor Nihar Jana's group, National Brain Research Center, Manesar, India. They were used to evaluate the effects of the *S. cordifolia* extract on huntingtin aggregates. The cells between passage numbers 2 to 10 were used for all experiments. They were cultured in 10% (v/v) FBS in DMEM, with 0.4 mg/mL Zeocin and 0.4 mg/mL G418 to its final concentration. For immunoblot experiments, 2×10^5 cells were plated in 6-well plates in replicates. Induction (with 1 µM Ponasterone A) and treatment (1, 5, and 10 µg/mL SC methanolic extract) were started simultaneously 24 h after plating. Media was replaced with fresh media every 24 h for 2 days, and after 48 h of initial treatment, the cells were harvested and lysed for immunoblot or PCR (Figure 4A).

2.4 PolyQ aggregates – imaging

2.4.1 In transgenic *C. elegans*

Age-synchronized AM141 worms were grown from embryo stage to Day 5 adult stage on freshly prepared NGM-OP50 plates (60 mm diameter) spotted with various concentrations (0.1 µg/mL, 1 µg/mL and 10 µg/mL) of methanolic extracts of SC or AC or vehicle control (DMSO). On Day 1, Day 3 and Day 5 of adulthood few of the worms were washed in M9 buffer and collected in sterile 1.5 mL microfuge tubes. 20 µL of 5 mM sodium azide solution was added to the worm suspension to paralyze them. The worms were then mounted on glass slides containing a 2% agar pad and covered using a cover slip (Pigazzini et al., 2020). The immobilized worms (up to 10 worms per group) were observed under a fluorescent microscope (Olympus BX41) equipped with a camera (Olympus DP72). The images were captured under a blue filter (excitation wavelength 455 nm–495 nm) using the Image-Pro Express software. The aggregates were defined as discrete structures with clear boundaries for counting puncta and quantified by measuring the average fluorescence intensity in the head region of the worm (up to the second pharyngeal bulb). The remaining worms were transferred to respective fresh drug containing/control plates every day to avoid starvation and mixing of the consecutive generations.

2.4.2 In cells over-expressing mutant huntingtin protein

2×10^4 cells were seeded in each well of 4 chamber slides, and after completion of treatment, cells were washed gently with PBS twice and then fixed using 4% PFA for 20 min. Thereafter, cells were mounted using DAPI containing mounting media (Fluorshield with DAPI SIGMA F6057-20 mL) using 24 mm*40 mm cover glass (blue-star) and imaged on the next day in 40x oil Zeiss-Apotome microscope.

2.5 Lifespan assay

Age-synchronized AM141 worms were grown on freshly prepared NGM-OP50 plates (60 mm diameter) spotted with various concentrations of preparation of *S. cordifolia* or *A. calamus* or vehicle control (DMSO), up to late L4 stage. The worms were then transferred to fresh drug-containing/control NGM-OP50 plates every day until all worms in the group were dead. Worms were considered dead if they did not move after being lightly prodded using a platinum wire worm pick (Cooper et al., 2015). Data was analyzed using OASIS 2 software to obtain Kaplan-Meyer survival curves and mean/median lifespan values (Han et al., 2016).

2.6 Thrashing assay

Age-synchronized N2 or AM141 worms were grown on control plates or on plate spotted with various concentrations of methanolic extracts of *S. cordifolia* or *A. calamus*, up to Day 5 adulthood. The worms were transferred to fresh drug containing/control NGM/OP50 plates every day using a worm pick. They were collected in M9 buffer and suspended in a 15 µL droplet of the buffer on a glass slide. Thrashing of the worms (up to 10 worms per group) was video recorded using a Levenhuk lite microscope camera, on days 1, 3 and 5 of adulthood. The thrashing was analyzed by counting the body bends manually (Currey and Liachko, 2021).

2.7 Worm development assay

Age-synchronized wild type (N2) worms were grown on fresh NGM/OP50 plates containing various concentrations (0.1 µg/mL, 1 µg/mL, 10 µg/mL) of methanolic extracts of *S. cordifolia* or *A. calamus* or vehicle control (DMSO) at 20°C from the embryo stage to Day 1 of adulthood. The larval stages 1, 2, 3, 4 and day 1 adult worms were imaged under Olympus IX71 microscope using the Olympus DP72 camera, at 26.5, 36, 45, 56, and 65 h respectively, from the embryo stage. Lengths of at least 10 worms per group were measured at each stage, using ImageJ software (Lee and Kang, 2017).

2.8 Worm fecundity assay

Age-synchronized wild type (N2) worms were grown on fresh NGM/OP50 plates containing various concentrations (0.1 µg/mL, 1 µg/mL, 10 µg/mL) of methanolic extracts of *S. cordifolia* or *A. calamus* or vehicle control (DMSO) at 20°C from the embryo stage to late L4 stage. 5 late L4 worms per group were then transferred to 5 fresh NGM/OP50 plates containing respective drugs or vehicle control, such that there was one worm per plate, and allowed to grow at 20°C, for the rest of the worm's reproductive cycle (days 1–5 of adulthood). The worms were transferred to fresh plates every day and the number of eggs laid per worm were counted each day under the microscope and the total number of eggs laid per worm throughout its reproductive cycle was counted (Ha et al., 2022).

2.9 Immunoblotting

Following completion of treatment, cells were lysed with RIPA lysis buffer (50 mM Tris, pH 7.4, 150 mM NaCl, 1 mM EDTA, 0.1% SDS, 1% Triton X-100, 1% sodium deoxycholate with, 1 mM phenylmethylsulphonyl fluoride, 2 mM Na_2VO_5, 1 mM NaF, 20 mM $Na_4P_2O_7$ as a phosphatase inhibitor cocktail) at 4°C. Lysates were collected, centrifuged at 14000 ×g for 15 min and the supernatant was collected. Total protein was estimated using

the BCA (Bicinchoninic Acid) method. 20 µg protein was loaded on SDS-PAGE and transferred to a nitrocellulose membrane. Membrane was blocked with 5% skimmed milk or 3% BSA (for phosphoprotein) for 2 h at room temperature. Membranes were then probed overnight with primary antibodies of anti-GFP (rabbit, 1:5,000), anti-GAPDH (Mouse, 1:8,000), anti-pEIF2α (rabbit, 1:2,500), anti-EIF2α (rabbit, 1:5,000), anti-IRE1α (Rabit, 1:5,000), Anti pIRE1α (rabbit, 1:2000), and washed with Tris-buffered saline, 0.1% Tween (TBST) and probed with HSP-tagged secondary antibody targeted against the host species of the primary (1:10,000). Blots were developed using Luminol and chemiluminescence images were captured using the Uvitec Cambridge gel doc instrument.

2.10 Quantitative polymerase chain reaction (qPCR)

Total RNA was extracted using TAKARA RNAiso, following the manufacturer's protocol. cDNA was prepared using BioRad iScript 5x RT supermix in a single-step reaction. qPCR was performed using iTaq SYBR green (BioRad) following the manufacturer's protocol in CFX96 (BioRad). In another set of reactions, the synthesized cDNA was used to check the expression of the GFP transcript by semiquantitative PCR using GTPCR master mix (TAKARA BIO) for the GFP-specific primer, normalized with GAPDH. Primers are listed in Supplementary Table 1.

2.11 Statistical analysis

Statistical comparisons between two groups were performed with students' unpaired t-tests when data were normally distributed with similar variances; otherwise, the Mann-Whitney test was performed to draw the significance. A p-value of 0.05 or less was considered statistically significant. Statistical analysis was performed using GraphPad Prism 8.0. The data are presented as means, and error bars show the standard error of the mean (SEM).

3 Results

3.1 Methanolic extract of SC inhibits aggregation of polyQ-expanded mutant huntingtin protein in the *C. elegans* model of HD

The toxic aggregation of misfolded mutant huntingtin proteins with expanded tandem repeats of polyQ in the central nervous system is the pathological hallmark of HD. The transgenic *C. elegans* strain expressing polyQ proteins is an excellent, widely established model studying cellular effects of aggregated proteins (Van Pelt and Truttmann, 2020). We investigated the possible therapeutic effect of SC and AC, in the AM141 strain of *C. elegans* which expresses a mutant huntingtin protein with 40 tandem glutamines (Q40::YFP) in body wall muscles (Morley et al., 2002). These worms accumulate the polyQ protein-aggregates as they age, which are seen as fluorescent punctae in the muscles (Figure 1A). We cultured these worms on fresh NGM/OP50 plates spotted with methanolic extracts of SC or AC. Worms treated with the SC extract, from embryo stage to day 1 adult stage (72 h at 20°C), showed about 20%–30% reduction in the number of YFP puncta (a measure of aggregated mutant huntingtin protein) as compared to vehicle/solvent (DMSO)-treated worms (Figures 1A, B; Supplementary Figure 1A). The average fluorescence levels of the puncta were also lower upon SC treatment (Figure 1C). This effect was specific to the SC extract, as the methanolic extract of AC did not reduce mutant huntingtin protein aggregation. We next performed imaging-based quantification of polyQ aggregates in worms at days 1, 3 and 5 of adulthood. Worms treated with 1 µg/mL SC significantly reduced fluorescence intensity of polyQ-YFP on day 1, and this effect gradually dissipated by day 5 (Figure 1D). Taken together, these results show that the SC extract (1 µg/mL) reduces aggregation of the mutant polyQ huntingtin protein. The treatment did not alter the development of the worms or their egg laying capacity (Supplementary Figures 1B, C).

3.2 SC treatment improves motility in the *C. elegans* model of HD

Caenorhabditis elegans swim by producing alternating C-shape and straight conformations called "thrashing" (Gjorgjieva et al., 2014). Aggregation of polyQ mutant huntingtin proteins in the body wall muscle leads to defects in thrashing. We performed the thrashing assay to investigate whether SC treatment improved motility of HD worms through its reduction of aggregated mutant huntingtin proteins. Worms grown on fresh NGM/OP50 plates containing different concentrations of SC or AC extracts were video graphed and their motility checked with the thrashing assay on days 1, 3 & 5 of adulthood. Treatment with SC (1 µg/mL), but not AC, restored motility of mutant worms to that of wild-type worms on day 1 (Figures 2A, B), the effect decreasing by day 5 (Figures 2C, D; Supplementary Figure 2).

3.3 SC treatment extends life span of HD model of *C. elegans*

Earlier studies showed that lifespan extension in neurodegenerative models of *C. elegans* is neuroprotective (Cooper et al., 2015). We investigated whether SC would extend the lifespan of *C. elegans*. Worms were treated with different concentrations of SC or AC extract on NGM OP50 plates from the embryo stage. SC extended the life span of AM141 worms expressing the 40Q mutant huntingtin protein, from 11.55 days in untreated worms to 17.07 days in SC-treated (1 µg/mL) worms (Figures 3A, D). In contrast, treatment with AC reduced life span of these worms (Figures 3B–D).

Although the fluorescence levels in worms are no different upon chronic (by day 5, Figure 1D) treatment with SC, the benefits of treatment last much longer as the worms are more motile (Figures 2C, D; Supplementary Figure 3) and live longer.

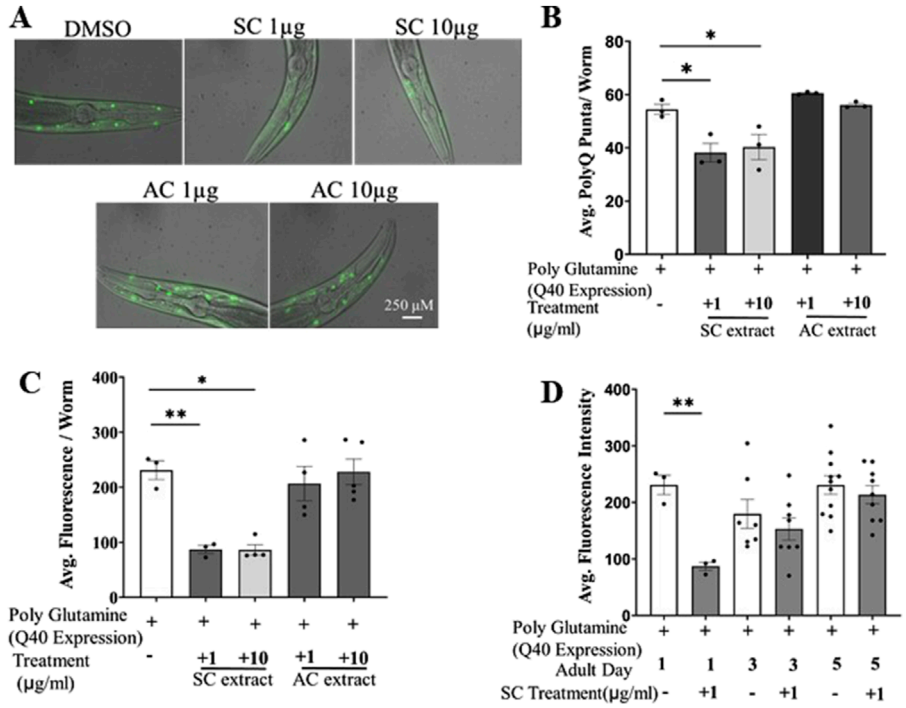

FIGURE 1
SC reduces polyQ aggregates in transgenic HD model of *C. elegans* (AM141). **(A)** Representative fluorescent microscopy images (day 1 adult worms) of poly Q aggregation in AM141 worms treated with SC or AC extracts **(B)** quantification of number of poly-Q puncta per worm (day1) (n = 3; for all the conditions) **(C)** average fluorescence intensity of poly-Q per worm **(D)** average fluorescence intensity of poly-Q in Day 1, Day3 and Day5 adult worms. (In all the graphs, each dot represents the mean of one experiment and a minimum of 3 means were considered for each graph. For each experiment 10 worms were used per group. Data represented as mean ± SEM,*p < 0.05,**p < 0.01).

3.4 SC reduces aggregation of mutant polyQ-containing huntingtin proteins in a mammalian system by reducing ER stress

We tested if SC could suppress aggregation of mutant huntingtin proteins in a mammalian system. For these studies we used the mouse transgenic N2a neuroblastoma cell line over-expressing an ecdysone-inducible mutant Huntingtin protein with an expanded polyQ repeat (150Q) attached to EGFP (HD150Q-EGFP) (Wang et al., 1999). Upon treatment of these cells with 1 µM Ponasterone A, analog of Ecdysone (Figure 4A), the HD150Q-EGFP mutant protein aggregated, visualized as increased GFP puncta by fluorescence microscopy. SC treatment significantly reduced HD150Q-EGFP aggregates (Figures 4B, C) by decreasing mutant protein levels (Figures 4E, F) without altering mRNA levels (transcription) (Figure 4D). We did not notice any change in puncta sizes (Supplementary Figure 4A).

We next determined if SC-mediated reduction of mutant huntingtin protein aggregation was due to modulation of the Endoplasmic Reticulum Unfolded Protein Response (ER-UPR). In mammals, three main pathways initiated by three different type-1 transmembrane proteins: inositol – requiring protein – 1α (IRE -1α), protein kinase RNA-like ER kinase (PERK) and activating transcription factor-6 (ATF6), govern ER-UPR. XBP-1, a transcription factor critical in this process, is induced by ATF6, spliced by IRE-1, and modulating XBP-1 is beneficial in animal models of HD (Vidal et al., 2012).

Ecdysone-induced aggregation of HD150Q-EGFP protein triggered ER-UPR as evidenced by increased phosphorylation of IRE-1α (Figures 5A, B), splicing of XBP-1 (Figure 5C) and activation of phospho-PERK-dependent phosphorylation of eIF2A (Figures 5E, F). Expression levels of BiP, an important chaperone in the ER stress response, was also reduced by SC treatment (Figure 5D). SC also suppressed other ER stress responses induced by HD150Q-EGFP protein aggregation including reduction of transcript levels of ATF4 and CHOP (Figures 5G, H). However, we did not find significant difference in GADD34 expression levels (Supplementary Figure 4B). CHOP, a protein linked to apoptosis (Oyadomari and Mori, 2004), is a key link between the ER stress pathway and apoptosis. SC-mediated reduction in CHOP raises the possibility that SC may inhibit apoptosis in stressed cells as a feature of neuroprotection.

4 Discussion

Here, we have explored the possibility of using Ayurvedic formulations for management and treatment of HD. Ayurveda uses SC containing formulation to treat neurodegenerative disorders, mainly targeting the weakness. We explored benefits of SC using an animal model of HD and suggest a mechanism based on the reduction of ER stress for the therapeutic effect. The

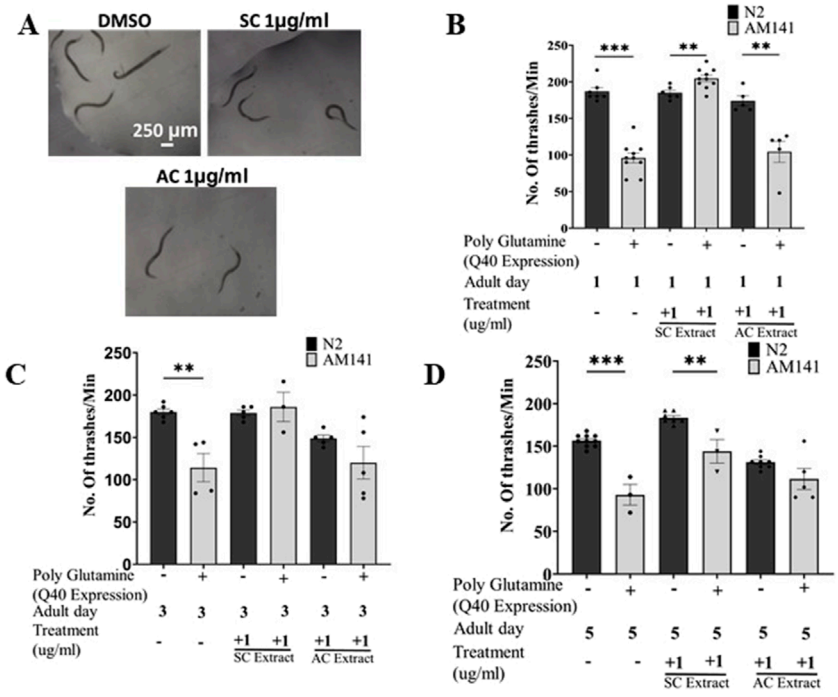

FIGURE 2
SC improves motility in HD model of *C. elegans*. **(A)** Representative images of thrashing of Day 1 adult AM141 worms Thrashing assay of N2 (wild type) and AM141 (HD model) worms treated with SC or AC extracts. Quantification of thrashing of **(B)** Day 1, **(C)** Day 3, and **(D)** Day 5 adult AM141 worms. (In all the graphs, each dot represents the mean of one experiment and a minimum of 3 means were considered for each graph. For each experiment 10 worms were used per group. Data represented as mean ± SEM,**p < 0.01*p < 0.05).

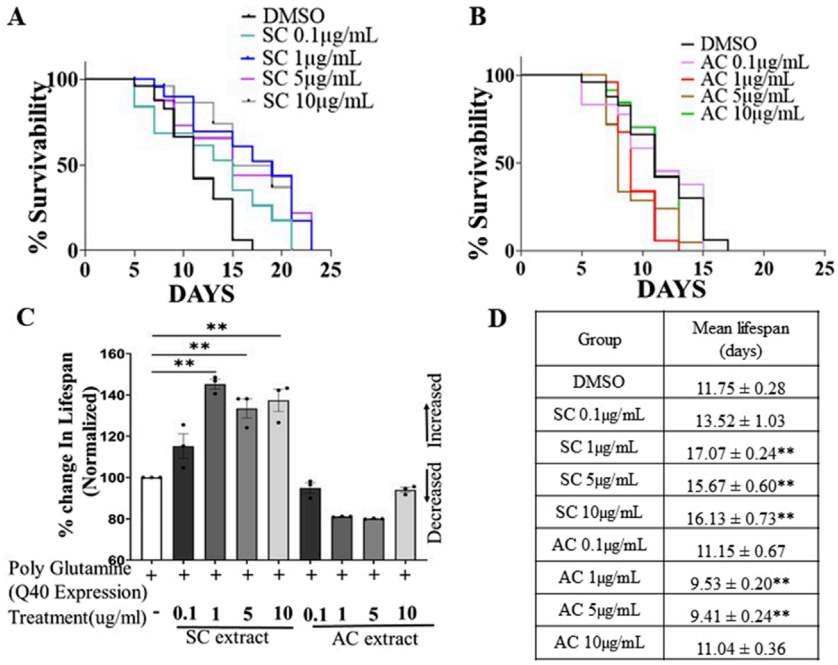

Group	Mean lifespan (days)
DMSO	11.75 ± 0.28
SC 0.1µg/mL	13.52 ± 1.03
SC 1µg/mL	17.07 ± 0.24**
SC 5µg/mL	15.67 ± 0.60**
SC 10µg/mL	16.13 ± 0.73**
AC 0.1µg/mL	11.15 ± 0.67
AC 1µg/mL	9.53 ± 0.20**
AC 5µg/mL	9.41 ± 0.24**
AC 10µg/mL	11.04 ± 0.36

FIGURE 3
SC improves lifespan of HD model of *C. elegans*. Survival curves of AM141 (HD model) worms **(A)** treated with SC extract **(B)** treated with AC extract. **(C)** Quantification of percentage change in lifespan of AM141 worms treated with SC or AC extracts n = 3 for all the condition). **(D)** Lifespan assay data of AM141 worms treated with SC or AC extract. n = 25 per group. Data are mean ± SD. *p < 0.05 **p < 0.01 and n-Individual Biological replicates).

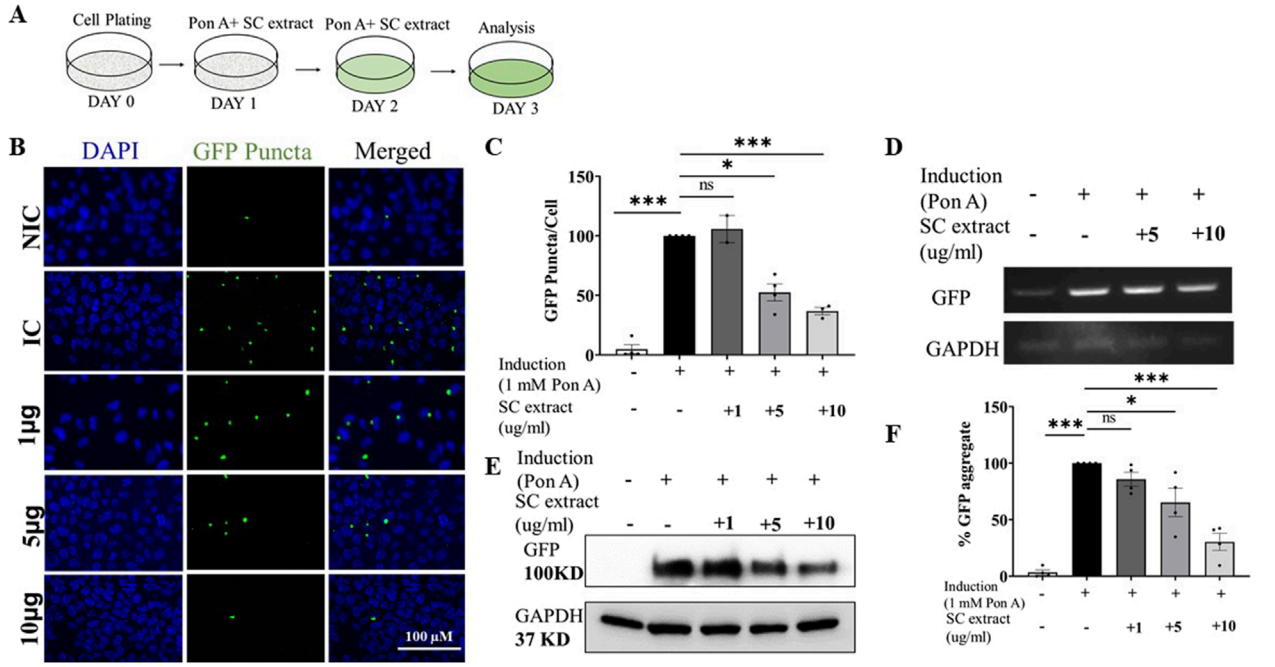

FIGURE 4
SC reduces protein aggregate in the poly-Q-EGFP expressing cells **(A)** Treatment protocol **(B)** Representative images of SC treated cells **(C)** Quantification of GFP-puncta per cell. (NIC, n = 3; IC, n = 4 SC 1 µg, n = 2; SC 5 µg, n = 4; SC 10 µg, n = 3) **(D)** Semi-quantitative PCR of GFP mRNA expression **(E)** Immunoblot of GFP protein **(F)** Quantification of immunoblots of GFP (n = 4 for all conditions). All data represented as mean ± SEM, $^{*}p < 0.05$, $^{**}p < 0.01$,$^{****}p < 0.001$ and ns is statistically non-significant and n = Individual biological replicate).

extract's mode of action, as indicated by our results is highlighted in a schematic in Figure 6. The extract likely contains several active ingredients that modulate multiple therapeutic targets. Such a multi-target therapeutic approach over single-target drugs is in line with current strategies being developed by the pharmaceutical industry. Future studies using fractionation of the extract coupled with cell and animal-based studies may help to identify active moieties within the extract and the molecular targets they modulate.

Huntington's, Alzheimer's, and Parkinson's disease are the most prevalent neurodegenerative disorders worldwide, for which many causative factors such as ageing, aggregation of certain proteins and specific genetic mutations are implicated. These factors lead to some common and distinct pathophysiological and clinical hallmarks. The research to develop treatment strategies often targets causative factors, like protein aggregation at cellular and molecular levels. Modern medicine's current treatment strategies for neurodegenerative diseases are mainly oriented towards symptomatic care. Therefore, there is an unmet need to develop sustainable solutions for management of neurodegenerative diseases. One of the efforts in this direction is exploring traditional knowledge of healthcare and medicine.

Many herbs and formulations have been used effectively for centuries for treatment of neurodegenerative and neurological diseases, but the bio-medical evidence for the effectiveness and mode of action is largely lacking. Based on knowledge of traditional medicine and modern drug discovery approaches, one can explore possibilities of finding newer molecules from scientifically validated herbal formulations (Rahmati et al., 2018). Investigating and verifying the efficacy of these formulations could help us understand and establish them as potential therapeutics, especially for current unmet health needs.

Taking clues from the concept and practice of Ayurveda, we hypothesized the effectiveness of SC in the chronic age-related process like protein aggregation and neurodegeneration. On the other hand, AC is used for non-degenerative neurological conditions and was hypothesized to have limited benefits on HD models. The results from the experiments in the study corroborated well with the hypothesis. SC showed protective effects in the transgenic Huntington's Disease model of *C. elegans*. Expression of polyQ disrupts the normal locomotor capacity of the worms, which was largely restored by SC treatment in HD worms (Figure 6). Furthermore, we show that SC increases the lifespan of the polyQ worms. Similar effects were not observed with treatment of AC. Surprisingly, worsening of movement in the worms treated with AC was observed on day 5 (Figure 2D). AC is described as very potent and excitatory, and the observed effects might be excitotoxicity. This will need further investigation.

The protective effect of SC was also visible in cellular models of HD (Figure 6). Using Neuro 2a cells expressing PolyQ-EGFP, we confirm that SC treatment reduces the polyQ protein amount and aggregation, as seen by immunoblotting and fluorescence microscopy respectively. We found that the SC affects at the post-transcription step in a fashion that reduces the total protein load of the PolyQ-EGFP, and consequently, reduces the aggregates. The

10.3389/fmolb.2025.1567932

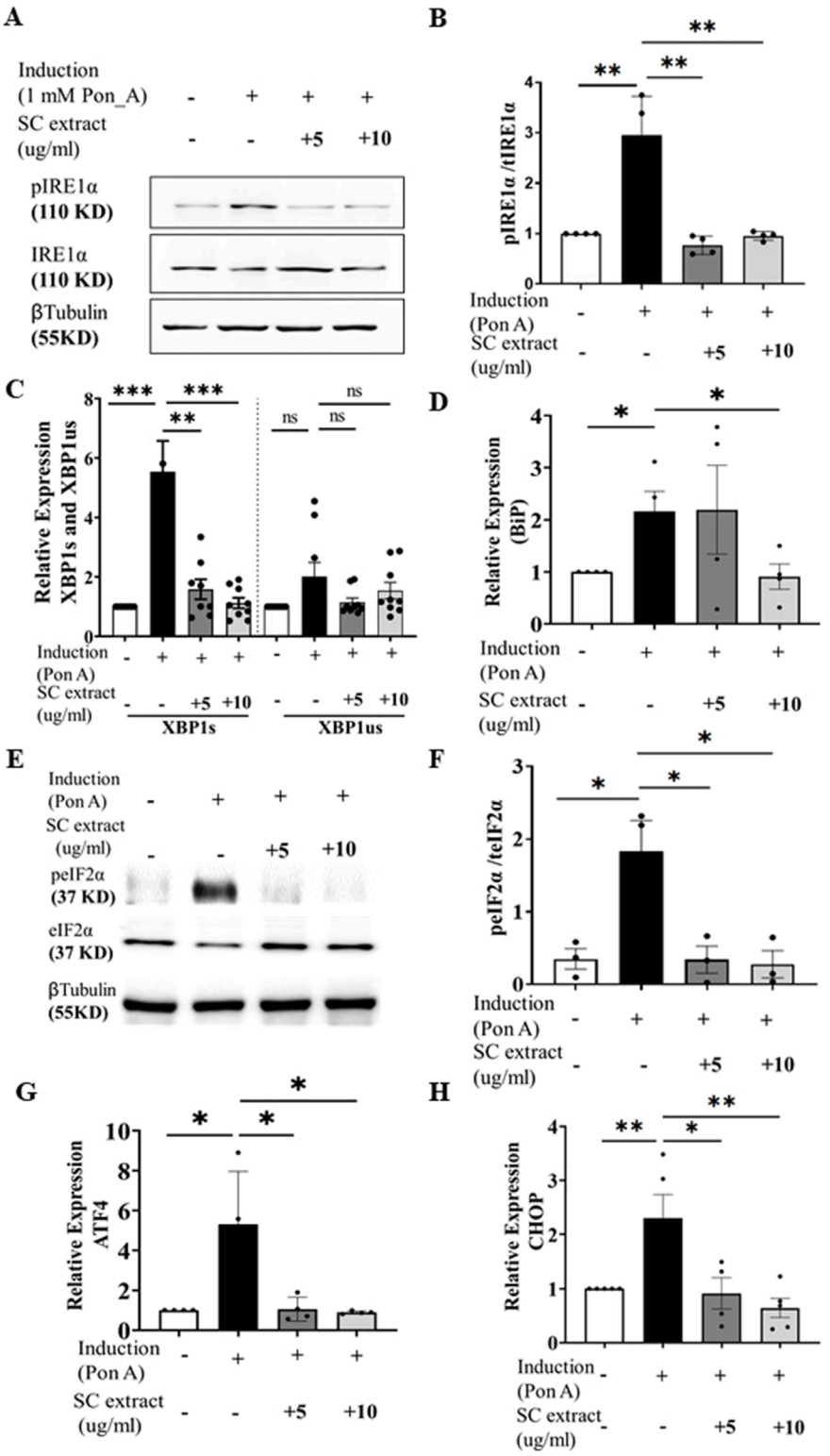

FIGURE 5
SC modulates ER stress pathway. **(A)** immunoblots of pIRE1α and IRE1α **(B)** and its quantification (n = 4 for all conditions) **(C)** Relative expression of XBP1s and XBP1us (n = 8 for all groups except SC10μg where n = 9) **(D)** Relative expression of bip (n = 4, for all conditions) **(E)** Representative Immunoblot of pEif2a and total Eif2a, **(F)** its quantification n = 3 for all condition), **(G)** Relative expression of ATF4 (n = 4 for all conditions) and **(H)** CHOP. (n = 4 for all conditions) (All data represented as mean ± SEM, *p < 0.05. **p < 0.01,****p < 0.001 and ns is statistically non-significant).

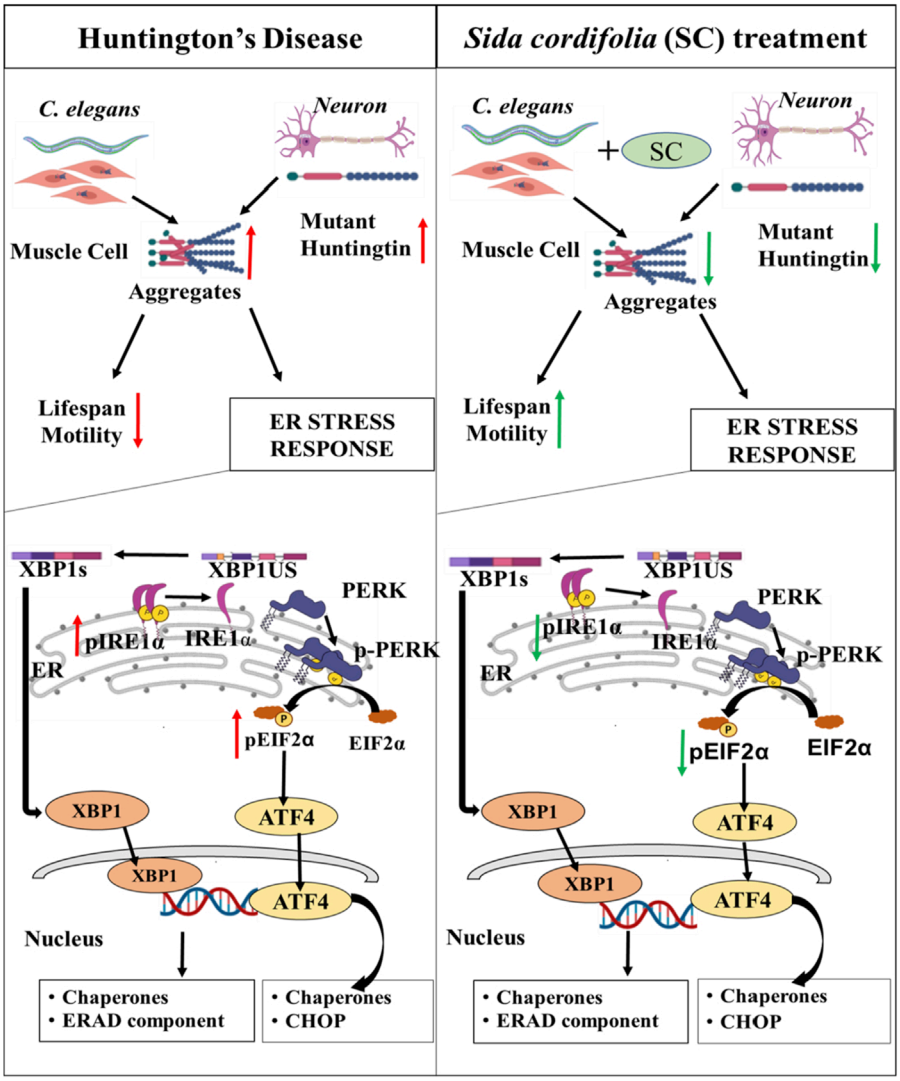

FIGURE 6
Sida cordifolia is efficacious in HD models by reducing ER stress. Reduces the aggregates in transgenic HD worm model expressing mutant protein (Q40::YFP) in their body wall muscle. This improves motility and enhances the lifespan of these worms. In neuroblastoma cells (N2a) expressing polyQ-EGFP SC treatment reduces the amount of mutant protein and thereby reducing the number of aggregates. This is accompanied by reduction in levels of key ER stress markers - Spliced XBP1s, pEIF2α and pIRE1α.

reduction of aggregates could be either the reduction in translation or the result of the removal of aggregates by the cells' stress-handling machinery. The reduction in translation looks less likely as the levels of p-eIF2α are reduced by SC treatment. Our study demonstrates an increase in the activity in IRE1α and eIF2α upon over-expressing the mutant HD protein. SC treatment reverses the pathway towards the control level as phospho-IRE1α and phospho-eIF2α protein levels revert to control levels. We observe these effects are translated to their respective downstream molecules, like XBP1s (downstream of IRE1α) and ATF4 and CHOP (downstream of eIF2α). The significant reduction in CHOP, a protein linked to DNA damage-induced apoptosis (Oyadomari and Mori, 2004) becomes very important as this is a key link between ER stress pathway and apoptosis. This observation is significant as it suggests that SC might reduce toxic effects by directly interfering with the apoptosis pathway in stressed cells for its neuroprotective effects. BiP, one of the primary players in the UPR and a key chaperone of ER, has been observed to be upregulated in stress conditions in several studies (Morris et al., 1997; Lei et al., 2017). Transcriptional regulation of genes to restore proteostasis in the ER is mediated by the XBP1 and ATF-6 branches of the UPR. Also, it is suggested that both BiP and XBP1 are target genes for ATF6. SC-mediated reduction in XBP-1 level agrees with the earlier finding where the loss of XBP1 was protective in the transgenic murine model of HD (Vidal et al., 2012). We guess these effects are because of enhanced clearance of the misfolded or aggregated protein, which needs further study. Also, we cannot distinguish between a mHtt specific effect or a general increased clearance of misfolded protein. Similarly, it remains to be seen whether the clearance is because of lysosomal or proteasomal degradation.

We noted a difference in effective doses in cell culture and *C. elegans*. We believe this might be due to different metabolizing enzymes or efflux pumps in worms and mammalian cell systems. The extract is more potent in the worms compared to N2a cells. Furthermore, molecular studies were done in the cell culture system partially because of possible signal dilution when we made protein extract or isolated mRNA from worms, as the body wall cells expressing transgenic protein form a small fraction of the entire worm.

Indian traditional medicine describes the role of SC in arthritis. A recent review enlists ER stress players as key targets for existing and potential drugs (Rahmati et al., 2018) in line with our findings. It is reassuring to see the specificity of the effect of herbs (SC and AC) in different types of biological conditions in agreement with the traditional knowledge. The methanol extract of SC likely contains several active ingredients that modulate multiple molecular targets. Future studies may help to identify active moieties within the extract and the molecular targets they modulate.

In summary, SC treatment reduces the aggregation of mutant polyQ-containing huntingtin proteins both in a *C. elegans* animal model and in a mouse neuroblastoma cell line. These effects are, at least in part, due to the suppression of various pathways in the ER stress response. Previously described experimental medications that reduced aggregation of mutant huntingtin protein in animal models (Nagai et al., 2003; Sánchez et al., 2003; Tanaka et al., 2004) had to be administered directly into the central nervous system because they were not able to penetrate the blood-brain-barrier. In contrast, the SC extract was effective in reducing aggregation of mutant huntingtin protein in *C. elegans* when applied into the growth medium, suggesting that it readily crosses the blood-brain-barrier. Further, oral administration of a SC-containing Ayurvedic formulation to a patient with juvenile-onset HD improved motor function, balance and gait without any adverse effects (Malavika and Savitha, 2022), again suggesting that SC-containing formulations can cross the blood-brain barrier giving hope for a safe therapeutic option for HD.

4.1 Preprint

A preprint has previously been published at bioRxiv (Simha et al., 2023).

Data availability statement

The original contributions presented in the study are included in the article/Supplementary Material, further inquiries can be directed to the corresponding authors.

Ethics statement

The manuscript presents research on animals that do not require ethical approval for their study.

Author contributions

PS: Data curation, Formal Analysis, Investigation, Methodology, Supervision, Validation, Writing–original draft. CM: Data curation, Formal Analysis, Investigation, Methodology, Supervision, Validation, Writing–original draft. VK: Formal Analysis, Investigation, Writing–review and editing, Methodology. KB: Formal Analysis, Investigation, Supervision, Writing–review and editing. PN: Methodology, Resources, Writing–review and editing. AZ: Writing–review and editing, Conceptualization. AG: Conceptualization, Data curation, Formal Analysis, Funding acquisition, Investigation, Methodology, Project administration, Resources, Supervision, Validation, Visualization, Writing–original draft. BS: Conceptualization, Data curation, Funding acquisition, Investigation, Methodology, Resources, Software, Supervision, Writing–original draft, Writing–review and editing, Formal Analysis, Project administration, Validation. SU: Conceptualization, Data curation, Formal Analysis, Funding acquisition, Investigation, Methodology, Project administration, Resources, Software, Supervision, Validation, Visualization, Writing–original draft, Writing–review and editing.

Funding

The author(s) declare that financial support was received for the research and/or publication of this article. The authors thank UGC for a start-up grant [F.4-5(185-FRP)/2015] to SKU, Pratiksha Trust for a research grant to AG and Ramalingaswami fellowship grant [BT/RLF/Re-entry/38/2016] to BSS.

Acknowledgments

We acknowledge the help extended by Anjaneyulu J, in collection and preparation of the SC extract. We thank Prof. George Chandy for providing valuable inputs to the project.

Conflict of interest

The authors declare that the research was conducted in the absence of any commercial or financial relationships that could be construed as a potential conflict of interest.

Generative AI statement

The author(s) declare that no Generative AI was used in the creation of this manuscript.

Publisher's note

All claims expressed in this article are solely those of the authors and do not necessarily represent those of

Supplementary Material

The Supplementary Material for this article can be found online at: https://www.frontiersin.org/articles/10.3389/fmolb.2025.1567932/full#supplementary-material

References

Anjaneyulu, J., R, V., and Godbole, A. (2020). Differential effect of Ayurvedic nootropics on *C. elegans* models of Parkinson's disease. *J. Ayurveda Integr. Med.* 11, 440–447. doi:10.1016/j.jaim.2020.07.006

Caron, N. S., Dorsey, E. R., and Hayden, M. R. (2018). Therapeutic approaches to huntington disease: from the bench to the clinic. *Nat. Rev. Drug Discov.* 17 (10), 729–750. doi:10.1038/nrd.2018.133

Chunekar, K. C. (2004). "Bhavaprakasa nighantu (Indian materia medica of sri bhavamisra)," in *Bhavaprakasa nighantu*. Editor G. S. Pandey (Varanasi: Indian Materia Medica of Sri Bhavamisra), 43.

Cooper, J. F., Dues, D. J., Spielbauer, K. K., Machiela, E., Senchuk, M. M., and Van Raamsdonk, J. M. (2015). Delaying aging is neuroprotective in Parkinson's disease: a genetic analysis in C. Elegans models. *Parkinson's Dis.* 1 (May), 15022. doi:10.1038/npjparkd.2015.22

Currey, H. N., and Liachko, N. F. (2021). Evaluation of motor impairment in c. Elegans models of amyotrophic lateral sclerosis. *J. Vis. Exp.* 2021 (175), 1–18. doi:10.3791/62699

Das, C., Bose, A., and Das, D. (2021). Ayurvedic Balarista ameliorate anti-arthritic activity in adjuvant induced arthritic rats by inhibiting pro-inflammatory cytokines and oxidative stress. *J. Tradit. Complement. Med.* 11, 228–237. doi:10.1016/j.jtcme.2020.04.006

Ferguson, M. W., Kennedy, C. J., Palpagama, T. H., Waldvogel, H. J., Faull, R. L. M., and Kwakowsky, A. (2022). Current and possible future therapeutic options for Huntington's disease. *J. Central Nerv. Syst. Dis.* 14, 11795735221092517. doi:10.1177/11795735221092517

Gjorgjieva, J., Biron, D., and Haspel, G. (2014). Overview articles 476. *BioScience* 64 (6), 476–486. doi:10.1093/biosci/biu058

Ha, N. M., Tran, S. H., Shim, Y. H., and Kang, K. (2022). *Caenorhabditis elegans* as a powerful tool in natural product bioactivity research. *Appl. Biol. Chem.* 65 (1), 18. doi:10.1186/s13765-022-00685-y

Han, S. K., Lee, D., Lee, H., Kim, D., Son, H. G., Yang, J. S., et al. (2016). OASIS 2: online application for survival analysis 2 with features for the analysis of maximal lifespan and healthspan in aging research. *Oncotarget* 7 (35), 56147–56152. doi:10.18632/ONCOTARGET.11269

Hughes, D., and Mallucci, G. R. (2019). The unfolded protein response in neurodegenerative disorders – therapeutic modulation of the PERK pathway. *FEBS J.* 286 (2), 342–355. doi:10.1111/FEBS.14422

Lee, S. Y., and Kang, K. (2017). Measuring the effect of chemicals on the growth and reproduction of caenorhabditis elegans. *J. Vis. Exp.* 2017 (128), 56437–56445. doi:10.3791/56437

Lei, Y., Wang, S., Ren, B., Wang, J., Chen, J., Lu, J., et al. (2017). CHOP favors endoplasmic reticulum stress-induced apoptosis in hepatocellular carcinoma cells via inhibition of autophagy. *PLOS ONE* 12 (8), e0183680. doi:10.1371/JOURNAL.PONE.0183680

Malavika, B., and Savitha, H. (2022). Effect of Ayurvedic interventions as add-on therapy in Huntington's disease: a case report. *J. Ayurveda Case Rep.* 5 (3), 116–121. doi:10.4103/jacr.jacr_78_21

McColgan, P., and Tabrizi, S. J. (2018). Huntington's disease: a clinical review. *Eur. J. Neurology* 25 (1), 24–34. doi:10.1111/ene.13413

Morley, J. F., Brignull, H. R., Weyers, J. J., and Morimoto, R. I. (2002). The threshold for polyglutamine-expansion protein aggregation and cellular toxicity is dynamic and influenced by aging in *Caenorhabditis elegans*. *Proc. Natl. Acad. Sci. U. S. A.* 99 (16), 10417–10422. doi:10.1073/pnas.152161099

Morris, J. A., Dorner, A. J., Edwards, C. A., Hendershot, L. M., and Kaufman, R. J. (1997). Immunoglobulin binding protein (BiP) function is required to protect cells from endoplasmic reticulum stress but is not required for the secretion of selective proteins. *J. Biol. Chem.* 272 (7), 4327–4334. doi:10.1074/JBC.272.7.4327

Nagai, Y., Fujikake, N., Ohno, K., Higashiyama, H., Popiel, H. A., Rahadian, J., et al. (2003). Prevention of polyglutamine oligomerization and neurodegeneration by the peptide inhibitor QBP1 in Drosophila. *Hum. Mol. Genet.* 12 (11), 1253–1259. doi:10.1093/hmg/ddg144

Oyadomari, S., and Mori, M. (2004). Roles of CHOP/GADD153 in endoplasmic reticulum stress. *Cell Death Differ.* 11, 381–389. doi:10.1038/sj.cdd.4401373

Paleacu, D. (2007). "Tetrabenazine in the treatment of Huntington's disease," in *Neuropsychiatry disease and treatment*.

Pigazzini, M. L., Gallrein, C., Iburg, M., Kaminski-Schierle, G., and Kirstein, J. (2020). Characterisation of amyloid structures in aging *C. elegans* using fluorescence lifetime imaging. *J. Vis. Exp. JoVE* (157), 61004. doi:10.3791/61004

Rahmati, M., Moosavi, M. A., and McDermott, M. F. (2018). ER stress: a therapeutic target in rheumatoid arthritis? *Trends Pharmacol. Sci.* 39 (7), 610–623. doi:10.1016/j.tips.2018.03.010

Sánchez, I., Mahlke, C., and Yuan, J. (2003). Pivotal role of oligomerization in expanded polyglutamine neurodegenerative disorders. *Nat. 2003* 421 (6921), 373–379. doi:10.1038/nature01301

Sati, R., and Deole, Y. S. (2020). *Vatarakta chikitsa adhyaya*. Jamnagar, Gujarat, India: Charak Samhita New Edition, 102. doi:10.47468/CSNE.2020.E01.S06.030

Simha, P. K., Mukherjee, C., Bhatia, K., Gupta, V. K., Sapariya, N. M., Nagar, P., et al. (2023). Sida cordifolia, a medicinal plant, is efficacious in models of Huntington's disease by reducing ER stress. *bioRxiv*. doi:10.1101/2023.11.01.565080

Tanaka, M., Machida, Y., Niu, S., Ikeda, T., Jana, N. R., Doi, H., et al. (2004). Trehalose alleviates polyglutamine-mediated pathology in a mouse model of Huntington disease. *Nat. Med.* 10 (2), 148–154. doi:10.1038/nm985

Van Pelt, K. M., and Truttmann, M. C. (2020). *Caenorhabditis elegans* as a model system for studying aging-associated neurodegenerative diseases. *Transl. Med. Aging* 4, 60–72. doi:10.1016/J.TMA.2020.05.001

Vidal, R. L., Figueroa, A., Court, F. A., Thielen, P., Molina, C., Wirth, C., et al. (2012). Targeting the UPR transcription factor XBP1 protects against Huntington's disease through the regulation of FoxO1 and autophagy. *Hum. Mol. Genet.* 21, 2245–2262. doi:10.1093/hmg/dds040

Wang, G. H., Mitsui, K., Kotliarova, S., Yamashita, A., Nagao, Y., Tokuhiro, S., et al. (1999). Caspase activation during apoptotic cell death induced by expanded polyglutamine in N2a cells. *NeuroReport* 10 (12), 2435–2438. doi:10.1097/00001756-199908200-00001

Yero, T., and Rey, J. A. (2008). Tetrabenazine (xenazine), an FDA-approved treatment option for Huntington's disease-related chorea. *Pharm. Ther.* 33, 690–694.

frontiers | Frontiers in Cell and Developmental Biology

TYPE Review
PUBLISHED 25 April 2025
DOI 10.3389/fcell.2025.1595121

OPEN ACCESS

EDITED BY
Anoop Arunagiri,
East Tennessee State University, United States

REVIEWED BY
Virginia Actis Dato,
University of California San Diego, United States
Renata Torres Da Costa,
Rutgers University Camden, United States
Deepti Dabral,
National Center for Advancing Translational Sciences (NIH), United States

*CORRESPONDENCE
Arunkumar Venkatesan,
venkatea@upstate.edu
Audrey M. Bernstein,
bernstea@upstate.edu

RECEIVED 17 March 2025
ACCEPTED 09 April 2025
PUBLISHED 25 April 2025

CITATION
Venkatesan A and Bernstein AM (2025) Protein misfolding and mitochondrial dysfunction in glaucoma.
Front. Cell Dev. Biol. 13:1595121.
doi: 10.3389/fcell.2025.1595121

Protein misfolding and mitochondrial dysfunction in glaucoma

Arunkumar Venkatesan[1]* and Audrey M. Bernstein[1,2]*

[1]Department of Ophthalmology and Visual Sciences, SUNY Upstate Medical University, Syracuse, NY, United States, [2]New York VA Healthcare, Syracuse VA Medical Center, Syracuse, NY, United States

Glaucoma is a leading cause of irreversible blindness worldwide. Elevated intraocular pressure caused by restricted outflow of the aqueous humor leads to the degeneration of retinal ganglion cells (RGCs) and their axons. Emerging evidence suggests that pathological mechanisms relating to protein folding and mitochondrial dysfunction are significant factors in the disease onset of different types of open-angle glaucoma. In this review, we discuss these defects in three distinct types of open-angle glaucoma: primary open-angle glaucoma (POAG), normal tension glaucoma (NTG), and exfoliation glaucoma (XFG). Genetic mutations linked to the previously mentioned open-angle glaucoma, including those in myocilin (MYOC), optineurin (OPTN), and lysyl oxidase 1 (LOXL1), disrupt protein folding and homeostasis, leading to endoplasmic reticulum stress, activation of the unfolded protein response and impaired autophagic protein degradation. These factors contribute to trabecular meshwork and retinal ganglion cell apoptosis. In addition to protein folding defects, mitochondrial dysfunction is also associated with the progression of trabecular meshwork damage and the death of RGCs. Factors such as oxidative stress, an altered mitochondrial fission-fusion balance, and mitophagy dysregulation make RGCs vulnerable and contribute to optic nerve degeneration. The crosstalk between protein folding and mitochondrial defects in glaucoma underscores the complexity of disease pathogenesis and offers potential targets for therapeutic intervention. Strategies aimed at restoring protein homeostasis, enhancing mitochondrial function, and mitigating cellular stress responses hold promise for neuroprotection in glaucoma.

KEYWORDS

er stress, upr, autophagy, mitochondrial dysfunction, POAG, NTG, XFG, glaucoma

Introduction

Glaucoma is a heterogeneous group of disorders characterized by gradual loss of peripheral-to-central vision due to optic neuropathy and the death of retinal ganglion cells (RGCs), leading to irreversible vision loss (Quigley, 1999; Allingham et al., 2009; Kwon et al., 2009). It is a leading cause of irreversible blindness, with over 60 million people affected worldwide, and its prevalence is estimated to increase to 111.8 million by 2040 (Tham et al., 2014). Elevated intraocular pressure (IOP) (≥22 mmHg) is a major risk factor for RGC loss and is often, but not always, associated with glaucoma. The trabecular meshwork (TM) and Schlemm's canal (SC) in the aqueous humor (AH) outflow pathway is a tissue that regulates

IOP via the effective discharge of AH produced by the ciliary body. However, an imbalance between the production and outflow of AH causes elevated IOP within the anterior chamber of the globe, and adverse mechanical pressure on the optic nerves (ON) causes optic neuropathy. This loss of RGCs is associated with structural changes to the optic nerve head (ONH) and loss of visual field (Kwon et al., 2009; Alvarado et al., 1984).

Glaucoma can be divided into primary and secondary forms. Primary open-angle glaucoma (POAG) is the most common type, in which the anterior chamber angle appears normal with increased IOP and no other underlying disease. Juvenile open-angle glaucoma (JOAG) presents at a much earlier age and is also characterized by higher IOP and a more severe progression compared to adult-onset POAG. Normal tension glaucoma (NTG) is a type of POAG marked by ON degeneration despite normal IOP (Rezaie et al., 2002). Exfoliation glaucoma (XFG) is a severe form of secondary glaucoma, with the elevation of IOP associated with the deposition of white, flaky aggregates in the anterior chamber of the eye (Dietze et al., 2024). Glaucoma is a multifactorial disease involving multiple genes and environmental factors in the disease pathogenesis (Wiggs, 2007). Recent advancements in genome-wide association studies (GWAS) and next-generation whole exome sequencing have broadened our understanding of the risk variants linked to various types of glaucoma (Huang et al., 2018). However, these genetic risk variants are often flipped in different populations, complicating the understanding of the disease (Wiggs and Pasquale, 2017).

Proteostasis is essential for cellular survival, and any perturbations in protein homeostasis can lead to diseases such as neurodegenerative, metabolic, and cardiovascular disorders (Balch et al., 2008). The endoplasmic reticulum (ER) organelle is a protein quality control system of the secretory pathway proteins, permitting only correctly folded proteins to exit the organelle. In contrast, misfolded proteins are degraded through ER-associated degradation (ERAD) and autophagy (Poothong et al., 2021). Mitochondria is a dynamic organelle and critical for cellular energy metabolism and apoptosis. Mitochondrial dysfunction is linked to a wide range of neurodegenerative pathologies, including Alzheimer's disease, Parkinson's disease, and amyotrophic lateral sclerosis (ALS) (Lin and Beal, 2006; Johri and Beal, 2012; Chen et al., 2023; Klemmensen et al., 2024). The close connection between ER and mitochondria is crucial for maintaining cellular homeostasis, particularly under stress conditions, as miscommunication could lead to metabolic diseases (Senft and Ronai, 2015). This review focuses on the protein folding and mitochondrial dysfunction defects caused by the pathogenic variants of POAG, NTG, and XFG glaucoma and provides new insights for targeted therapeutics.

Protein folding defects and neurodegeneration in glaucoma

The ER is a dynamic signaling organelle where proteins are co-translationally folded by the ER protein quality control (ERQC) mechanism with the assistance of resident glycan (calnexin (CNX), calreticulin (CRT)) and HSP (GRP78/BIP, GRP94) family chaperones. These proteins are stabilized through post-translational modifications (PTMs) such as N-glycosylation, lipidation, and disulfide bond formation (guided by PDI and ERO1), and only those that achieve their native conformation are exported via the secretory pathway. The ER also acts as an intracellular storage site for Ca^{2+} ($ERCa^{2+}$), crucial in influencing protein folding efficiency (Figure 1A) (Venkatesan et al., 2021). Proteins that do not achieve functional native conformation are prone to aggregation, where the misfolded monomer self-associates to form oligomers, further extending to create amyloid fibrils with a beta-sheet structure and well-organized amyloid plaques (Poothong et al., 2021). The accumulation of misfolded protein aggregates and unfolded proteins disrupts ER homeostasis, leading to stress in the ER and the development of diseases known as proteinopathy (Ganguly et al., 2017). As an adaptive reaction, ER stress triggers a sequence of cellular stress responses, including the unfolded protein response (UPR), pathways related to oxidative stress, and inflammatory responses to restore proteostasis and cellular homeostasis. BIP regulates UPR and activates three key signaling cascades: PERK, IRE1α, and ATF6 (Figure 1B). These cascades initiate a coordinated response, leading to distinct action branches that restore ER homeostasis by reducing protein synthesis, enhancing chaperone protein expression, and degrading misfolded proteins through ERAD. To alleviate ER stress, the PERK-ATF4-CHOP signaling cascade halts protein translation by activating the eIF2α and triggers apoptosis if the stress endures for an extended period. The IRE1α pathway, via the *XBP1* mRNA splicing, activates the promoters of genes related to ERQC and ERAD to induce ER homeostasis as an adaptive response. The ATF6 also activates an adaptive signaling pathway after being cleaved in the Golgi apparatus (Walter and Ron, 2011). When proteins are irreversibly misfolded and cannot be resolved through UPR pathways, the ubiquitin-proteasome-dependent ERAD pathway clears the abnormal proteins (Figure 1C). The ERAD pathway comprises four steps: recognizing misfolded proteins through the SEL1L-HRD1 translocation complex, retrotranslocating substrates to the cytosol using the cdc48/p97/VCP AAA-ATPase, re-ubiquitinating clients in the cytosol, and degrading them via proteasomes (Christianson and Carvalho, 2022). However, some large protein aggregates resistant to ERAD are degraded through lysosome-mediated autophagy. ER-phagy, a form of selective autophagy, uses specific ER membrane receptors, such as FAM134B, to identify sub-domains of the ER that contain misfolded aggregates, which are engulfed by autophagosomes through their interaction with LC3 (Figure 1D) (Mochida and Nakatogawa, 2022).

While the pathogenesis of glaucoma remains unclear, chronic ER stress induction is associated with TM and RGC dysfunction and results in increased IOP in both animal POAG glaucoma models and patients. Healthy TM cells are vulnerable to oxidative stress; for instance, exposure to tetra-butyl hydroperoxide triggers ATF4-mediated ER stress. Further activation of the UPR mediators eIF2α and CHOP triggers apoptosis and inflammatory cytokine production and contributes to IOP elevation (Ying et al., 2021). Additionally, inducing ER stress by overexpressing ATF4 led to TM dysfunction, resulting in elevated IOP and glaucomatous neurodegeneration in a mouse glaucoma model (Kasetti et al., 2020). Interestingly, markers of ER stress are found to be upregulated in TM tissues from patients with POAG. This heightened ER stress triggers the activation of oxidative stress and the PERK arm of the UPR pathway, leading to increased levels of ATF4 and CHOP

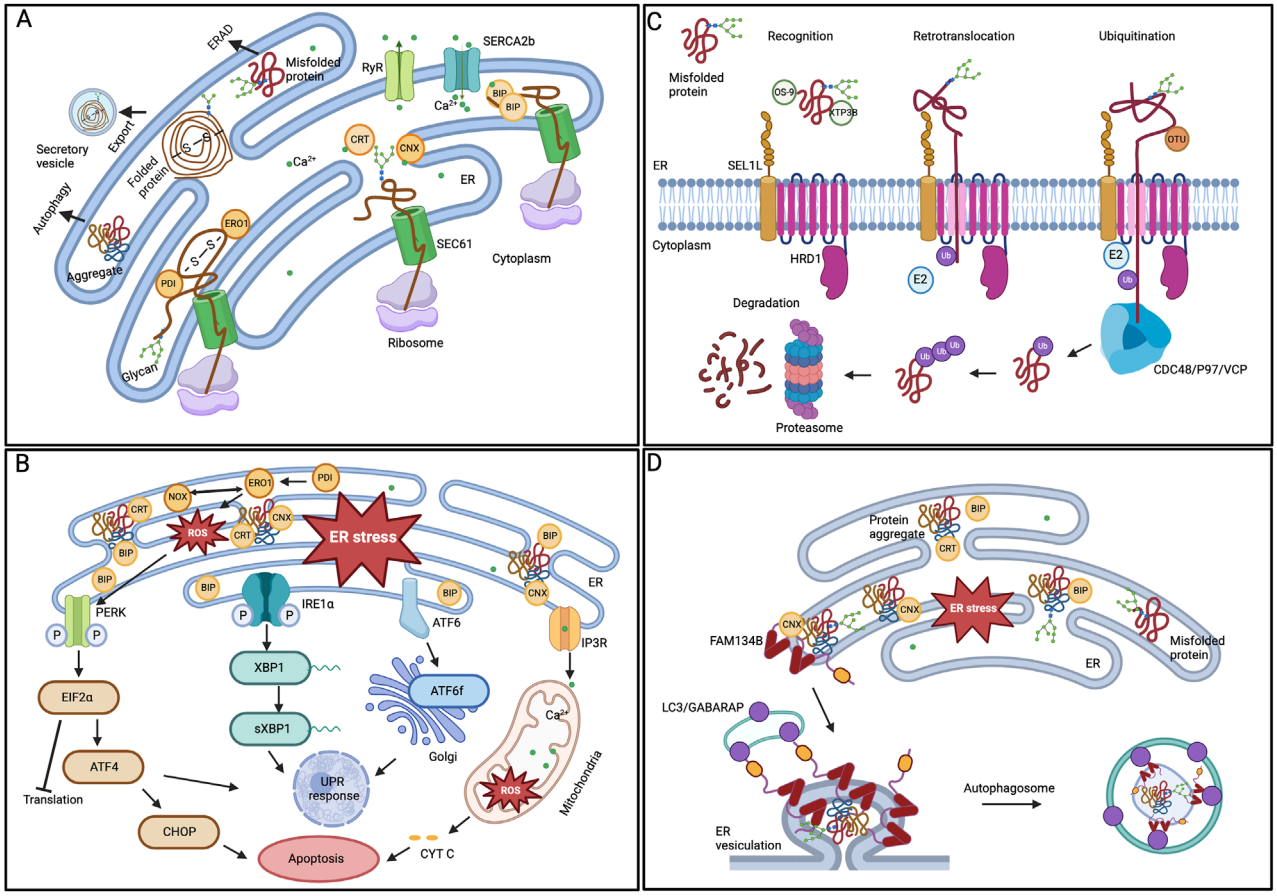

FIGURE 1
ER protein quality control mechanisms **(A)** Protein folding in ER lumen. Newly synthesized proteins that are translocated to the ER by the SEC61 translocon are folded by various ER chaperones. While the CRT/CNX cycle aids glycoproteins, PDI oxidizes cysteine residues to promote disulfide bond formation. Properly folded proteins can exit the organelle in vesicles. **(B)** ER stress and UPR activation. BIP removes its interaction from the three UPR signaling pathways in response to ER stress, initiating adaptive signaling. The PERK, IRE1α, and ATF6 pathways parallelly activate downstream modulators and regulate the gene expression to restore ER homeostasis. However, prolonged ER stress leads to the activation of cellular apoptosis. **(C)** ERAD degradation of substrate proteins. The ERAD substrates recognized by the chaperones are ubiquitinated and retro-translocated to the cytoplasm by the SEL1-HRD1 complex. In the cytoplasm, the CDC48/P97/VCP ATPase trims and re-ubiquitinates the substrates before being handed over to the proteasome for degradation. **(D)** ER-phagy mechanism. One of the ER-phagy receptors, FAM134B, identifies the ER subdomain that contains protein aggregates, aided by the chaperone CNX, for selective degradation. The receptor's oligomerization at the ER sheets' edge induces curvature in the ER membrane. Further, the interaction between the ER-phagy receptor and LC3/GABARAP facilitates the sequestration of ER regions within autophagosomes.

(Peters et al., 2015). This ER stress and activation of UPR could be one of the causes of dysregulated autophagy in glaucomatous TM cells (Porter et al., 2015). Likewise, the involvement of neuronal ER stress and CHOP activation in RGC death has been reported in chronic glaucoma models (Doh et al., 2010; Hu et al., 2012).

Prolonged activation of the UPR often triggers autophagy to restore homeostasis. Although the involvement of autophagy in ocular hypertension (OHT) and glaucoma is under investigation, alterations in autophagy vary by tissue type. While the anterior chamber tissues of the eye exhibited lower autophagic flux, the posterior chamber ON tissues demonstrated higher levels of autophagy in a DBA/2J (D2) spontaneous glaucoma mouse model (Hirt et al., 2018). Interestingly, autophagy deficiency with the gene knockout of *Atg4b*, a crucial autophagy gene involved in LC3 processing and autophagosome formation in chronic IOP elevation mouse models, resulted in normal IOP and protected against RGC death (Dixon et al., 2023). However, the role of autophagy is complicated as reduced autophagic flux is also associated with certain myocilin (MYOC) mutants that lead to protein aggregation, ER stress, UPR activations, and subsequent TM dysfunction (Kasetti et al., 2021; Yan et al., 2024).

In glaucoma, several lines of evidence indicate that genetic components play a crucial role. Multiple studies are increasingly reporting the involvement of several genetic variants in the pathogenesis of POAG, NTG, and XFG (Wiggs and Pasquale, 2017; Tirendi et al., 2023). Further research on these genetic risk variants has yielded new insights into the underlying molecular mechanisms relevant to glaucoma. In the following section, we will explore the protein folding defects caused by glaucoma risk variants, their impact on TM

dysfunction, and the survival of RGCs in various types of open-angle glaucoma.

Myocilin

Myocilin (MYOC) is commonly expressed in various ocular and non-ocular tissues. The TM was reported to show the highest level of myocilin expression among ocular tissues (Adam et al., 1997). Myocilin expression was also explicitly induced by stress conditions such as mechanical stretch, TGF β, and dexamethasone treatment (Tamm et al., 1999). Myocilin is a secreted glycoprotein encoded by the *MYOC* gene (Nguyen et al., 1998; Caballero and Borras, 2001) composed of an N-terminal coiled-coil (CC) region, which includes the leucine zipper (LZ) motifs. An unstructured linker connects this region to the C-terminal olfactomedin (OLF) homolog domain, which has a high-affinity Ca^{2+} binding site (Kubota et al., 1997; Donegan et al., 2012). The wild-type (WT) MYOC is often observed as a 55/57-kDa doublet in both TM cell lysates and in AH, indicating the protein's N-glycosylation at amino acid Asn57 (Shepard et al., 2003; Gobeil et al., 2004). However, the importance of MYOC N-glycosylation is not yet known. MYOC is secreted via the ER-Golgi secretory pathway. While the N-terminal CC region is sufficient to target the protein to the Golgi apparatus-mediated secretory compartment, the OLF domains are necessary for efficient secretion to the extracellular space (Stamer et al., 2006). The CC region shares the homology with Q-SNARE complexes and mediates interaction with the plasma membrane complexes while secreted out from cells (Dismuke et al., 2012). Several studies have investigated the mechanism of MYOC multimerization. Full-length MYOC has been shown to interact with itself to form MYOC homodimers. This homodimerization is mediated majorly by the residues in the LZ domain and the CC region and is independent of the OLF domain (Fautsch and Johnson, 2001; Wentz-Hunter et al., 2002). MYOC was also observed to form higher-order complexes (Nguyen et al., 1998) through disulfide crosslinking (Gobeil et al., 2004). In AH, MYOC presents as a multimeric large complex with bands ranging from 120 to 180 kDa (Gobeil et al., 2004). Although the full-length MYOC crystal structure remains unresolved, the C-terminal OLF domain crystal structure indicates it comprises a five-bladed β-propeller featuring a metal binding center in its highly conserved interior region (Donegan et al., 2015). Furthermore, the N-terminal CC region exhibits a Y-shaped parallel dimer-of-dimer structure. Additionally, the crystal structure of the mouse myocilin LZ domain shows a dimer cap formed through C-terminal disulfide bonds, which are typical of a canonical leucine zipper (Hill et al., 2017). Altogether, the full-length MYOC forms a Y-shaped dimer-of-dimers consisting of an N-terminal tetrameric stalk from the CC/LZ region, connected to the two C-terminal OLF domains.

Pathogenic MYOC variants in glaucoma

Mutations in the *MYOC* gene locus were the first glaucoma locus identified with a strong genetic link to POAG. *MYOC* genetic variants are estimated to account for about 4% of adult-onset POAG and >10% of autosomal dominant JOAG (Fingert et al., 1999; Aldred et al., 2004). Nearly 100 pathogenic variants in the *MYOC* gene have been found in a subset of patients with POAG (Fingert et al., 2002; Fingert et al., 1999), most of which cluster in exon 3, encoding the OLF domain. Recent studies also emphasize the accumulation of somatic *MYOC* mutations related to age in the onset of glaucoma (Sazhnyev et al., 2024). However, the observed *MYOC* gene variants in healthy control populations suggest that not all variants are pathogenic, but some are benign. While the physiological function of WT MYOC remains unclear, several mouse studies employing genetic strategies that either overexpress or disrupt *Myoc* gene expression did not lead to increased IOP or result in glaucoma (Kim et al., 2001; Gould et al., 2004; Gould et al., 2006). Also, haploinsufficiency of MYOC in patients due to either homozygous R46X truncation (Lam et al., 2000) or hemizygous interstitial deletion on 1q24-q26 does not cause glaucoma (Wiggs and Vollrath, 2001). Thus, the *MYOC* variants associated with glaucoma result from a toxic gain of function due to its misfolding (Zhou and Vollrath, 1999). The entire list of MYOC variants derived from extensive genome-sequencing projects can be found in the Genome Aggregation Database (gnomAD, https://gnomad.broadinstitute.org). Surprisingly, the MYOC β-propeller OLF domain accounts for over 90% of the reported missense and nonsense genetic variants. Based on various clinical and biochemical aspects of MYOC variants, Sclesi et al. categorize the pathogenicity of MYOC variants into three groups: pathogenic, likely pathogenic, and benign. The list of pathogenic variants includes C245Y, G246R, G252R, R272G, E323K, G364V, G367R, P370L, T377M, T377K, D380A, K423E, V426F, C433R, Y437H, I477N, I477S, Y479H, N480K, P481L, P481T, I499F, I499S, and S502P. The list of likely pathogenic variants includes V251A, P254R, L255P, P274R, Q337R, S341P, A363T, F369L, Y371D, T377R, D380H, D384G, E385K, T438I, N450Y, and L486F. Finally, the list of benign MYOC variants includes T293K, V329M, E352K, T353I, K398R, A445V, and K500R (Scelsi et al., 2021). Several studies showed that the disease-causing *MYOC* variants cause protein misfolding, amyloid-like aggregation, ER stress, and impaired secretion (Joe et al., 2003; Gobeil et al., 2004; Liu and Vollrath, 2004; Saccuzzo et al., 2024; Scelsi et al., 2023). In the following section, we will concentrate exclusively on specific MYOC variants that exhibit protein folding defects.

Impaired secretion of MYOC variants

Recent findings indicate that variants of MYOC, which misfold in the ER, are responsible for their harmful gain of function in POAG disease. MYOC secretion by the secretory TM cells is vital for extracellular matrix (ECM)-mediated cell adhesion. However, the disease-causing MYOC E300K, E323K, S341P, G364V, P370L, D380A, K423E, C433R, Y437H, N450Y, I477N missense, and Q368X nonsense variants impaired cellular secretion and were predominantly retained in the ER (Joe et al., 2003; Liu and Vollrath, 2004; Aroca-Aguilar et al., 2008; Zadoo et al., 2016; Yan et al., 2020; Zhou et al., 2022a; Scelsi et al., 2023; Yan et al., 2024). In certain instances, mutant MYOC exhibits a dominant-negative effect by oligomerizing with WT, impacting WT MYOC secretion (Gobeil et al., 2004). Also, the MYOC levels were reduced in the POAG patients' AH (Jacobson et al., 2001). Thus, the MYOC variants

are misfolded, fail to pass the ER quality control mechanisms, and are retained in the ER, as evidenced by their prolonged interactions with ER chaperones such as BIP, PDI, CRT, and ERP57 (Joe et al., 2003; Scelsi et al., 2023; Liu and Vollrath, 2004). In some cases, the mutations caused the misfolding of the protein by hindering its Ca^{2+} binding ability (D380A) or leading to aberrant disulfide bond formation (C433R) due to insufficient cysteine or altered protein stability and aggregation (E300K, G364V, Q368X, P370L, D380A, K423E, Y437H).

The lack of secretion led to the accumulation of misfolded MYOC variants in the ER of TM cells, causing ER stress and triggering UPR pathway activation. Notably, the WT MYOC also inhibited secretion under conditions of ER Ca^{2+} depletion that induce ER stress (Saccuzzo et al., 2022). Studies involving the expression of MYOC S341P, Q368X, P370L, Y437H, N450Y, and I477N variants have demonstrated the upregulation of the ER stress marker BIP (Joe and Tomarev, 2010; Yan et al., 2024; Yan et al., 2020), along with activation of the UPR-PERK pathway, which coincided with an increase in the expression of ATF4 and CHOP (Yam et al., 2007a; Wang et al., 2007; Peters et al., 2015). Chronic levels of UPR activation occur because the ERAD pathway cannot effectively degrade MYOC variants (Qiu et al., 2014; Liu and Vollrath, 2004). Although the MYOC P370L and I477N variants are tagged for degradation through ubiquitination, their breakdown via the ERAD proteasome system fails due to mutant-specific prolonged interactions with GRP94 (Suntharalingam et al., 2012). Furthermore, the increase in ER stress and the activation of the PERK-ATF4-CHOP mediated UPR are correlated with the pathogenesis of glaucoma in multiple MYOC-dependent open-angle glaucoma mouse models expressing S341P, P370L, and Y437H variants. The elevated IOP, RGC death, and axon degeneration in these mouse models illustrate the molecular role of ER stress in glaucoma (Yan et al., 2024; Cheng et al., 2023; Kasetti et al., 2016; McDowell et al., 2012). Although the degree of UPR activation varied among the variants—from responses to oxidative stress to chronic activation of pro-apoptotic factors (Joe and Tomarev, 2010)—this finding aligns with previous studies indicating the crucial role of ATF4 expression results in dysfunction in TM cells, elevated IOP, and neurodegeneration (Peters et al., 2015; Kasetti et al., 2020).

Aggregation and autophagic degradation of MYOC variants

Defects in protein folding within the ER and failure of ERAD to degrade misfolded proteins can lead to protein aggregation. Accumulating evidence suggests that pathogenic E300K, E323K, G364V, Q368X, P370L, D380A, K423E, and Y437H MYOC variants are sequestered in detergent-insoluble fractions, indicating a propensity to form intracellular aggregates instead of being secreted (Zhou and Vollrath, 1999; Liu and Vollrath, 2004; Yam et al., 2007a; Kasetti et al., 2021; Scelsi et al., 2023). The pathogenic MYOC variants tend to heterodimerize or hetero oligomerize with WT MYOC, forming inclusion bodies that sequester WT MYOC from extracellular secretion and affect TM function (Gobeil et al., 2004; Yam et al., 2007a). Similarly, in various cells, the *in vitro* expression of E323K, G364V, P370L, D380A, and K423E MYOC variants demonstrated juxtanuclear aggregates (Liu and Vollrath, 2004). Similar findings were observed when the OLF domain-specific expression of P370L-OLF and Y437H-OLF variants as MBP fusion proteins in *E. coli* revealed their presence in the void volume, suggesting the formation of high molecular weight species (Burns et al., 2010; Orwig et al., 2012). These high-molecular-weight OLF domain aggregates exhibited morphological characteristics similar to protofibril oligomers and amyloid fibrils. When expressed in CHO cells, these amyloid-like aggregates were also noted in the context of full-length P370L MYOC protein (Orwig et al., 2012). Further, these aggregated variants (G364V, P370L, K423E, Y437H, I477N) that are retained in the ER cause cytotoxicity to the TM cells (Joe et al., 2003; Liu and Vollrath, 2004). These studies indicate that MYOC variants with folding defects that tend to aggregate are associated with a severe glaucoma phenotype. In contrast, variants displaying greater solubility are linked to a milder glaucoma phenotype (Scelsi et al., 2021).

The Ca^{2+} binding OLF domain of MYOC is responsible for pathogenic amyloid-like aggregation (Orwig et al., 2012). The WT MYOC also aggregates under ER stress conditions in a Ca^{2+}-dependent manner. Depleting cellular Ca^{2+} causes WT MYOC to accumulate inside the ER, becoming less soluble and aggregating like amyloid (Saccuzzo et al., 2022; Saccuzzo et al., 2024), suggesting that the aggregated WT MYOC may intensify ER stress (Saccuzzo et al., 2023). Although the WT OLF domain folds properly, conditions such as agitation, acidic pH, high temperature, or mutations encourage amyloid-like aggregation akin to disease-causing variants (Saccuzzo et al., 2024; Orwig et al., 2012). Mechanistically, the treatment of urea created a partially folded state of β-propeller, with the unfolding of WT OLF resulting from the central residues. At the same time, the exterior blades provide resistance to unfolding (Saccuzzo et al., 2024). The morphology of WT MYOC fibril formation varies between straight and circular fibrils based on the type of stress. Differences in fibril formation were also noted among the pathogenic variants. The highly pathogenic I499F variant displayed straight fibrils with an increase in aggregation rate, whereas the moderately pathogenic D380A variant showed circular fibrils (Hill et al., 2014; Saccuzzo et al., 2024; Burns et al., 2011). Compared to WT OLF, the variants D380A and I499F adopt unique partially folded structures, partly due to their differences in Ca^{2+} binding, accounting for the variations in fibril formation (Saccuzzo et al., 2024).

When the ER becomes overloaded with misfolded protein aggregates and the ERAD system fails, autophagy is triggered to serve a cytoprotective role mechanism. Some of the misfolded S341P, P370L, Y437H, N450Y, and I477N MYOC variants are reported to be degraded through the autophagy pathway (Yan et al., 2024; Qiu et al., 2014; Suntharalingam et al., 2012; Kasetti et al., 2021; Yan et al., 2022). However, whether these aggregated ER-retained MYOC variants are specifically degraded through ER-phagy remains unexplored. The induction of ER stress and UPR activation, combined with the extended interaction of misfolded variants with ER chaperones, indicates that the chaperones' attempts at refolding were unsuccessful. This failure, along with fibril formation, complicates the fate of these variants, leading to their degradation via the autophagy pathway and causing TM and RGC dysfunction. The interaction between MYOC amyloids and the GRP94 chaperone directs the aggregates

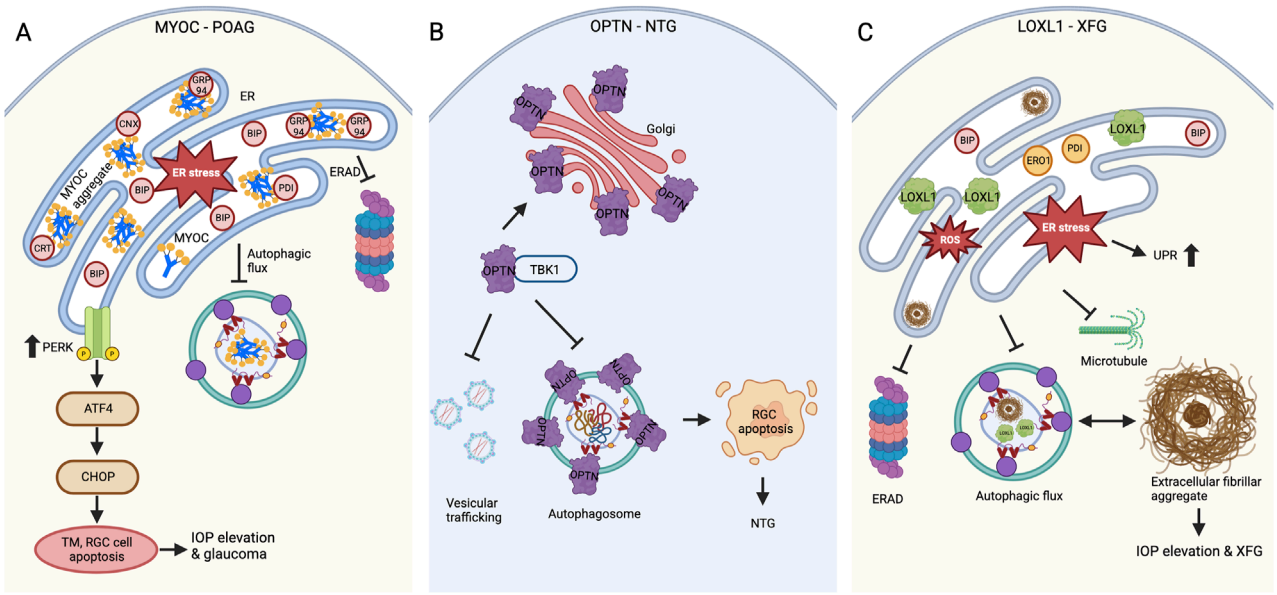

FIGURE 2
Defects in protein folding and proteostasis in glaucoma **(A)** MYOC variants causing POAG. MYOC mutations lead to amyloid-like protein aggregation, while insufficient secretion results in ER stress and activates the PERK-ATF4-CHOP UPR pathway. Further, the inadequate ERAD and defects in autophagic flux cause TM and RGC cell death through apoptosis, which leads to IOP elevation and glaucomatous neurodegeneration. **(B)** OPTN variants causing NTG. OPTN mutations cause altered localization with increased foci formation around the Golgi apparatus. The enhanced interaction of E50K OPTN with TBK1 affects RAB8-mediated vesicular trafficking and autophagosome formation, which ultimately contributes to RGC apoptosis and glaucomatous neurodegeneration. **(C)** LOXL1 polymorphisms contribute to the risk of XFG. In XFG, the exfoliative fibrillar aggregate material builds up because of the loss of cellular proteostasis, resulting in ER stress, UPR, defective ERAD, and autophagy. The pathogenic LOXL1 variant expression also caused aggregation, ER-oxidative stress, and defective autophagy.

toward ERAD while obstructing the ERAD pathway, resulting in inefficient degradation. Interestingly, preventing the GRP94 interaction allowed the MYOC amyloids (P370L, I477N) to degrade through autophagy efficiently (Suntharalingam et al., 2012). However, recent studies indicate that while misfolded variants are targeted for autophagy, the altered autophagic flux in S341P and Y437H variants has led to diminished autophagic clearance, which accounts for chronic ER stress (Yan et al., 2024; Kasetti et al., 2021). Crucially, reducing CHOP or enhancing autophagic flux facilitated the degradation of Y437H, promoted cellular homeostasis, and lowered IOP levels (Kasetti et al., 2021). Thus, MYOC variants cause a toxic gain-of-function due to misfolding, leading to the formation of amyloid fibrils that induce ER stress and activate the PERK-ATF4-CHOP pathway while disrupting autophagic flux (Figure 2A) and (Table 1).

Optineurin

Optic neuropathy-inducing protein (Optineurin, OPTN) is a cytoplasmic protein encoded by the *OPTN* gene. OPTN has several functional domains, including three CC domains, a LZD, an LIR motif, a ubiquitin-binding domain (UBD), and a C-terminal zinc finger domain. OPTN predominantly localizes in the cytoplasm and has multi-functional properties involved in vesicular trafficking, autophagic clearance of protein aggregates and defective mitochondria, and the inflammatory response. OPTN, as an adapter protein, executes its diverse function by interacting with its binding proteins, including RAB8, myosin VI, TFR, TBK1, huntingtin, transcription factor IIIA, and inflammatory and interferon signaling (Ying and Yue, 2012). The aggregation of OPTN protein has been implicated in ALS and other neurodegenerative diseases (Osawa et al., 2011).

OPTN plays a key role in Golgi-mediated vesicular trafficking. When overexpressed, the OPTN forms foci around the Golgi apparatus, leading to its fragmentation and apoptosis (Park et al., 2006). These OPTN foci are also induced in response to viral RNA, which leads to the dampening of pro-inflammatory immune responses (O'Loughlin et al., 2020). In its native form, OPTN appears as homo-hexamers. The homo-hexamerization seems to be the functional form, as indicated by the assembly of super-complexes with vesicular trafficking proteins like RAB8, myosin VI, and TFR (Ying et al., 2010). OPTN is a soluble macro autophagy receptor that binds ubiquitin and plays a crucial role in degrading protein aggregates, faulty mitochondria, and intracellular bacterial pathogens through autophagy. It has demonstrated its ability to facilitate the maturation of autophagosomes during the degradation process of various cargoes, including the degradation of α-synuclein in Parkinson's disease (Wise and Cannon, 2016). The mechanism by which OPTN regulates autophagy involves the critical binding of TBK1 to the N-terminal CC domain of OPTN, which is essential in controlling the latter's autophagy process. When OPTN identifies the ubiquitinated cargo, TBK1 phosphorylates the S177 residue of the OPTN LIR motif, enhancing its binding affinity for LC3. Additionally, phosphorylation of the S473 residue

TABLE 1 Pathogenic mechanism and potential drug target for glaucoma mutants.

Disease	Mutation	Model system	Pathogenic mechanism	Potential drug target	References
POAG	MYOC E300K	Cell lines	Impaired secretion, aggregation		Scelsi et al. (2023), Zadoo et al. (2016)
POAG	MYOC E323K	Cell lines	Impaired secretion, insoluble, aggregation		Aroca-Aguilar et al. (2008), Liu and Vollrath (2004), Zhou and Vollrath (1999)
POAG	MYOC S341P	TM cells, mouse model	ER stress, autophagy dysfunction, TM, RGC dysfunction	4-PBA	Yan et al. (2024)
POAG	MYOC G364V	Cell lines, TM cells	Impaired secretion, aggregation, TM cytotoxicity		Liu and Vollrath (2004), Joe et al. (2003), Kasetti et al. (2021)
POAG	MYOC Q368X	Cell lines, TM cells	Impaired secretion, heterooligomerize with WT, ER stress, UPR, defective proteasomal degradation, TM dysfunction		Aroca-Aguilar et al. (2008), Joe et al. (2003), Sohn et al. (2002), Zhou and Vollrath (1999), Gobeil et al. (2004), Qiu et al. (2014)
POAG	MYOC P370L	Cell lines, TM cells, mouse model	Impaired secretion, insoluble, amyloid-like aggregation, ER stress, UPR, impaired degradation, oxidative stress, mitochondrial dysfunction, TM and RGC dysfunction	Recombinant anti-OLF antibodies	Liu and Vollrath (2004), Aroca-Aguilar et al. (2008), Zhou et al. (2022a), Scelsi et al. (2023), Joe and Tomarev (2010), Yam et al. (2007a), Suntharalingam et al. (2012), Cheng et al. (2023), Orwig et al. (2012), Qiu et al. (2014), Wang et al. (2007), He et al. (2009), Ma et al. (2025)
POAG	MYOC D380A	Cell lines	Impaired secretion, insoluble, circular fibril aggregation		Liu and Vollrath (2004), Aroca-Aguilar et al. (2008), Zhou and Vollrath (1999), Saccuzzo et al. (2024)
POAG	MYOC K423E	Cell lines	Impaired secretion, insoluble, heterooligomerize with WT, aggregation, TM cytotoxicity		Liu and Vollrath (2004), Joe et al. (2003), Zhou et al. (2022a), Zhou and Vollrath (1999), Gobeil et al. (2004)
POAG	MYOC C433R	Cell lines	Impaired secretion, impaired disulfide bond formation		Zhou et al. (2022a), Donegan et al. (2015)
POAG	MYOC Y437H	Cell lines, mouse model	Impaired secretion, insoluble, aggregation, ER stress, oxidative stress, UPR, autophagy dysfunction, TM cytotoxicity, RGC death	4-PBA, Torin-2, Tat-Beclin-1, 4-Br-BnIm, CRISPR-Cas9-based genome editing, TM stem cell transplantation	Liu and Vollrath (2004), Joe et al. (2003), Zadoo et al. (2016), Zhou et al. (2022a), Joe and Tomarev (2010), Zhou and Vollrath (1999), Zode et al. (2011), Kasetti et al. (2021), Stothert et al. (2014), Kasetti et al. (2016), Jain et al. (2017), Patil et al. (2024), Xiong et al. (2021), Zhu et al. (2016)

(Continued on the following page)

TABLE 1 (*Continued*) Pathogenic mechanism and potential drug target for glaucoma mutants.

Disease	Mutation	Model system	Pathogenic mechanism	Potential drug target	References
POAG	MYOC N450Y	TM cells, mouse model	Impaired secretion, ER stress, autophagy, TM and RGC death	4-PBA	Yan et al. (2020), Yan et al. (2022)
POAG	MYOC I477N	Cell lines	Impaired secretion, insoluble, ER stress, oxidative stress, defective ERAD, TM cytotoxicity	4-Br-BnIm, Recombinant anti-OLF antibodies	Zadoo et al. (2016), Joe et al. (2003), Zhou et al. (2022a), Joe and Tomarev (2010), Zhou and Vollrath (1999), Suntharalingam et al. (2012), Stothert et al. (2014), Ma et al. (2025)
POAG	MYOC I499F	Purified protein	Partially insoluble, fibrillar aggregation		Burns et al. (2011), Scelsi et al. (2023)
NTG	OPTN E50K	Cell lines, hPSCs, mouse model	Insoluble, aggregation, defective autophagy, defective mitochondrial dynamics, increased ROS, RGC apoptosis	Amlexanox, BX795	Gao et al. (2014), Chalasani et al. (2014), VanderWall et al. (2020), Zhang et al. (2021a), Shim et al. (2016), Chalasani et al. (2007), Minegishi et al. (2013), Minegishi et al. (2016), Surma et al. (2023)
NTG	OPTN M98K	Cell lines	ER stress, UPR activation, increased autophagy, RGC cell death	BX795	Sayyad et al. (2023), Sirohi et al. (2013), Sirohi et al. (2015)
XFG	LOXL1 R141L, G153D	Cell lines	Charge alteration, aggregation, ER-oxidative stress, defective autophagy		Sharma et al. (2016), Bernstein et al. (2019), Bernstein et al. (2018), Venkatesan et al. (2023)

in the UBD domain further strengthens OPTN's connection to ubiquitinated cargoes. Consequently, TBK1's dual phosphorylation facilitates OPTN in sequestering cargoes into autophagosomes (Heo et al., 2015; Wild et al., 2011). Likewise, OPTN is recruited to the damaged, ubiquitinated mitochondria mediated by the PINK1-Parkin pathway and transports them to autophagosomes for degradation (Heo et al., 2015). Also, recent studies show that the C-terminal domain of OPTN regulates the axonal transport of mitochondria by interacting with microtubules (Liu et al., 2025). While OPTN resides in the cytosol, any issues with its expression can disrupt ER and mitochondrial homeostasis, likely by influencing autophagy regulation. The knockdown of OPTN led to heightened ER stress, activation of the PERK-ATF4 UPR pathway, increased reactive oxygen species (ROS) levels, enhanced chaperone-mediated autophagy, and impaired macro autophagy (Ali et al., 2019). Beyond its role in vesicular trafficking and autophagy, OPTN regulates inflammatory signaling pathways to prevent chronic inflammation. OPTN shares 53% sequence homology with NF-κB essential modulator and acts as a negative regulator of TNFα-induced NF-κB activation (Slowicka and van Loo, 2018). Therefore, mutations in OPTN disrupt its biological function and could ultimately result in disease.

Pathogenic OPTN variants in glaucoma

Mutations in OPTN are associated with NTG and ALS, a fatal motor neuron disease. Missense mutations in OPTN, such as H26D, E50K, and M98K, along with H486R and E322K, are associated with NTG, which leads to RGC damage without an increase in IOP.

The OPTN E50K (RGC) mutation is the most common mutation linked to NTG. While the WT OPTN is soluble and forms homo-oligomers to perform its function during normal physiological conditions, the overexpression of E50K OPTN causes the protein to misfold and accumulate more in the insoluble fraction, forming improper higher-order oligomeric complexes. Further studies revealed that the OPTN mutations induce a novel trimer and oligomers via the UBD, which resembles the complexes observed during oxidative stress in WT OPTN (Gao et al., 2014). This could be partly due to the change of amino acid charge in the mutant, which may have led to enhanced interaction of E50K OPTN oligomers with TBK1 (Ying et al., 2010). The insoluble higher-order complex formation of E50K OPTN caused its altered cellular localization and cell death. The foci formation is increased around the Golgi apparatus and ER organelles in the E50K over-expressing cells, patient-derived induced pluripotent cells, and mouse models

(Minegishi et al., 2013; Park et al., 2006). Furthermore, the modified localization also hindered its interaction with RAB8, a regulator of vesicular trafficking, and impacted TFR complex recycling (Vaibhava et al., 2012; Chalasani et al., 2014).

E50K OPTN overexpression causes defects in proteasomal and autophagy-mediated degradation, ultimately triggering apoptosis in RGCs. While both WT and E50K mutant overexpression reduce proteasomal activity, E50K overexpression uniquely affects autophagic flux, resulting in decreased autophagosome formation. This leads to the accumulation of misfolded proteins and organelles, causing toxicity (Chalasani et al., 2014; Shen et al., 2011). The expression of OPTN E50K in a human pluripotent stem cell model exhibited autophagy defects alongside neurodegenerative issues, including neurite retraction and hyperexcitability (VanderWall et al., 2020). In addition to impaired autophagic degradation, E50K OPTN overexpression also affected the degradation of TDP43, a protein involved in mRNA biogenesis with implications for ALS. E50K, but not WT OPTN interaction with TDP43, impairs its autophagic degradation, accumulating TDP43 in the cytosol of the retina and contributing to proteinopathy (Zhang et al., 2021a). Moreover, defective autophagy in E50K OPTN cells is causative for increased foci formation and apoptosis. However, these defects are reversed by inducing autophagy with rapamycin (Shen et al., 2011; Chalasani et al., 2014). The defects in mitochondrial dynamics also contribute to the degeneration of RGCs in E50K OPTN (Shim et al., 2016). The mitochondrial defects are thoroughly discussed in the later sections of this review. Thus, the E50K mutation in OPTN causes a toxic gain-of-function due to altered interactions, improper localization, and impaired autophagy, ultimately leading to the death of photoreceptor cells in NTG pathogenesis (Figure 2B).

Unlike E50K, the M98K OPTN polymorphism is associated with NTG at higher rates in Asian and African populations but not in Caucasian or Hispanic groups (Ayala-Lugo et al., 2007; Rezaie et al., 2002). This suggests that the M98K OPTN polymorphism alone is not a causative factor for glaucoma pathogenesis. Although research on the impact of the M98K OPTN mutation on solubility and oligomerization is limited, recent evidence suggests that this variant leads to the death of RGCs because of increased autophagy. The expression of M98K OPTN increases the number of autophagosomes due to the involvement of ATG5. Additionally, cells overexpressing M98K OPTN displayed enhanced UPR activations with increased IRE1α, PERK, and ATF6 expressions. Retinal cells with M98K OPTN become more sensitive to TNFα and tunicamycin, an ER stress agent. This is due to its modulation of ER stress response signaling pathways, potentially leading to increased autophagy and cell death through CHOP-mediated caspase activation (Sayyad et al., 2023). The mechanism of cell death is also reasoned by the stronger interaction of M98K with RAB12 than WT OPTN. RAB12, found in autophagosomes, plays a role in regulating vesicular trafficking. The enhanced activation of RAB12 by M98K OPTN causes abnormal lysosomal degradation of TFR and causes cell death (Sirohi et al., 2013). However, the degradation of TFR is also regulated by OPTN's binding partner, TBK1. While the association of TBK1 is reduced with M98K OPTN, the increase in autophagy was due to the prolonged phosphorylation of S177 of M98K OPTN by TBK1 (Sirohi et al., 2015). Thus, the M98K OPTN polymorphism causes disease through a gain-of-function mechanism that enhances autophagic flux, leading to inflammasome activation and cell death (Table 1).

Lysyl oxidase-like 1

Lysyl oxidase-like 1 (LOXL1) is part of the LOX family of enzymes (LOX, LOXL1-4). These enzymes are involved in the covalent cross-linking of lysine residues in elastin and collagen fibrils within the ECM, facilitating tissue integrity. While LOX and LOXL1 contribute to maintaining ECM integrity, LOXL2-4 are implicated in fibrosis and various cancers (Rodriguez-Pascual and Rosell-Garcia, 2018). The LOXL1 protein consists of two domains, with the C-terminal copper binding-dependent catalytic domain being highly conserved among the LOX protein family. The N-terminal domain varies within the lysyl oxidases, and the proline-rich N-terminal domain of LOXL1 is predicted to have an intrinsically disordered region (IDR) (Bernstein et al., 2019). While LOXL1 is encoded as an inactive pre-pro-enzyme, it becomes catalytically active after the N-terminal cleavage of its pro-region by BMP-1 protease in cell supernatants. This enables the catalytically active LOXL1 protein to cross-link its client proteins, such as tropoelastin monomers, through its oxidative deamination activity (Thomassin et al., 2005). Although the C-terminal domain is responsible for this cross-linking activity, the N-terminal IDR region plays a critical role in elastogenesis by interacting with fibulin-5 to promote efficient polymer formation (Liu et al., 2004).

Pathogenic LOXL1 variants in glaucoma

XFG is a systemic disease associated with aging, marked by abnormal ocular elastosis and the accumulation of extracellular fibrillar aggregates in the AH outflow pathway, resulting in elevated IOP. The glaucomatous degeneration resulting from exfoliation material includes elastic fiber components like elastin, fibrillin-1, fibulins, latent TGF-β binding proteins, and LOXL1 (De Maria et al., 2021; Zenkel and Schlotzer-Schrehardt, 2014), which is the recognized cause of secondary open-angle glaucoma, XFG. GWAS studies have identified polymorphisms in the *LOXL1* gene as the major risk factor for the development of XFG. The common nonsynonymous LOXL1 polymorphisms R141L and G153D reside in exon 1, which encodes the N-terminal IDR domain (Aung et al., 2017). Although these LOXL1 polymorphisms are reversed in some populations, they remain the primary XFG-associated risk factors reported across multiple populations worldwide (Li et al., 2021). While the LOXL1 crystal structure remains unresolved, *in silico* analyses have revealed that substitutions in LOXL1 from both R141L and G153D resulted in charge alterations. These changes may impact the local electrostatic potential of the protein, potentially affecting its interaction partners (Sharma et al., 2016). Expression of R141L and G153D LOXL1 variants do not impact cellular secretion and extracellular accumulation (Aung et al., 2017; Sharma et al., 2016). Moreover, the variants do not influence the amine oxidase activity of LOXL1 when using recombinant proteins (Kim and Kim, 2012). However, the BMP-1 protease processing of LOXL1 was altered when over-expressed as an L141_G153 variant, but its extracellular

accumulation was not altered (Sharma et al., 2016). Thus, LOXL1 variants in XFG do not primarily affect its localization and function.

Although knowledge about the cellular biological effects of LOXL1 variants on protein folding and aggregation is limited, over-expression of the N-terminal IDR domain alone has shown punctate aggregates. These aggregates seem more pronounced under serum-free conditions and stained positive for the protein aggregation dye Proteostat, indicating that LOXL1 may misfold during cellular stress. The aggregation might stem from the two IDR domain disordered peak residues 28 and 125 since their removals decreased the aggregation. Both high-risk LOXL1 variants coincide with the IDR peaks, indicating that LOXL1 has a higher potential for aggregation in XFG, aligning with its presence in the exfoliation material (Bernstein et al., 2019). Consistent with the aggregation, overexpression of LOXL1 in our lab induced ER stress, as evidenced by increased BIP expression. However, the ER stress did not activate the UPR; instead, it triggered the activation of the oxidative folding pathway, accompanied by increased expressions of PDI and ERO1α (Venkatesan et al., 2023). This signifies the increase of LOXL1 occurs during profibrotic growth factor TGF-β and under oxidative stress conditions.

XFG is an aging-related disease, and understanding its pathogenesis is hindered by the lack of an animal model (Anderson et al., 2018). Although *LOXL1* is a major risk variant in XFG, knocking down *Loxl1* in mouse models did not produce an XFG phenotype (Wareham et al., 2022; Wiggs et al., 2014). Lens tissue-specific overexpression of mouse *Loxl1* showed an increase in IOP at 1 month but no differences in 2-month-old transgenic animals. Intriguingly, overexpression enlarged rough ER cisterns filled with electron-dense Loxl1 aggregates measuring 20–30 nm in diameter, demonstrating that LOXL1 is an aggregation-prone protein influencing the fibrotic process (Zadravec et al., 2019). Emerging evidence also indicates that LOXL1 is degraded through the autophagy pathway, where the autophagic flux is altered in the primary Tenon fibroblast (TF) cells explanted from XFG patient Tenon tissues (Table 1) (Bernstein et al., 2018). Furthermore, these primary TF cells exhibited signs typically associated with protein misfolding, leading to neurodegenerative diseases. These signs include defects in autophagosome clearance rates, microtubule organization, and mitochondrial depolarization (Want et al., 2016; Wolosin et al., 2018). The decreased proteasome activity and impaired UPR in the lens capsule of XFG patients also contribute to the accumulation of misfolded proteins and impact autophagy (Hayat et al., 2019). Thus, available data supports that the XFG is an aggregopathy disease, where the proteostasis imbalance caused the accumulation of misfolded aggregates and contributed to the buildup of exfoliation material (Figure 2C). Future research will explore how these aggregates are formed and organized outside of cells and identify mechanisms to enhance proteostasis and prevent increases in IOP.

Mitochondrial dysfunction in glaucoma

Mitochondria are dynamic organelles with a double membrane that is a major source of cellular ATP. Although mitochondria possess their own genome (mtDNA) that encodes genes related to oxidative phosphorylation (OXPHOS), they largely depend on nuclear DNA for other mitochondrial proteins, which are imported by the translocase of the outer mitochondrial membrane (OMM) and inner mitochondrial membrane (IMM) TOM/TIM machinery. Mitochondria continually alter their shape through fission and fusion processes, crucial for sustaining mitochondrial function, energy generation, and cellular homeostasis. The dynamin-related super-family GTPase proteins regulate the fission-fusion events, with DRP1 controlling mitochondrial fission (Smirnova et al., 2001). Mitochondrial fusion is regulated by OPA1 in IMM and MFN1, and 2 in the OMM (Santel and Fuller, 2001) (Figure 3A). Mitochondrial ATP production occurs in the cristae of the IMM, controlled by the electron transport chain (ETC) complexes (I-IV) and ATP synthase (complex V) that shuttle electrons from the oxidation of nutrients in the form of NADH and $FADH_2$ to molecular oxygen, generating protonmotive force (Kuhlbrandt, 2015) (Figure 3B). During this process, ROS produced as a by-product in the IMM are effectively neutralized by an antioxidant defense system in healthy cells. However, the inability to remove the ROS directly impacts mtDNA and the, ETC, leading to the loss of membrane potential, a decrease in bioenergetic capacity, and apoptosis in age-related pathologies (Balaban et al., 2005). Mitochondrial calcium ($MitCa^{2+}$) homeostasis plays a crucial role in the above-mentioned processes, as it alters the organelle's functions and mitochondrial dynamics. The $MitCa^{2+}$ is received via the ER through the mitochondrial calcium uniporter (MCU) complex, and the excess Ca^{2+} influx is effectively removed through the permeability transition pore (PTP) to prevent ROS elevation, cytochrome c release, and apoptosis (Pinton et al., 2008). Mitochondria are constantly exposed to cellular stress and ROS. To maintain homeostasis, these organelles have developed a mechanism to eliminate dysfunctional mitochondria through mitophagy, a selective autophagic process. The most well-studied mechanism for mitophagy is the canonical PINK1/Parkin pathway. In the functional mitochondria, PINK1 in OMM is imported into the IMM, rapidly cleaved, and degraded by mitoprotease. However, PINK1 is stabilized by auto-phosphorylation at OMM in the damaged mitochondria. PINK1 recruits an E3 ubiquitin ligase, Parkin, to polyubiquitinate OMM proteins further recognized by the autophagy receptors and direct the mitochondria for autophagosome formation and degradation (Figure 3C) (Lazarou et al., 2015).

Emerging evidence indicates mitochondrial dysfunction in glaucoma patients and various animal models of glaucoma involving the TM in the anterior chamber and RGCs in the posterior eye segment. Initial studies showed that mitochondrial respiratory activity was reduced in the lymphocytes of POAG patients with mtDNA changes in complexes I, III, IV, and V (Abu-Amero et al., 2006). The mitochondrial bioenergetics, which is considered an important measure to assess pathogenicity in different mitochondrial diseases, is impaired in POAG patient-derived ocular TF cells and peripheral blood mononuclear cells (Vallabh et al., 2022; Petriti et al., 2024). Also, the TM cells from the outflow flow pathway of POAG patients showed increased ROS accumulation, decreased ATP levels, and lower mitochondrial membrane potential (MMPT). These defects are exacerbated when the mitochondria are inhibited with the complex I inhibitor Rotenone, leading to TM cell apoptosis (He et al., 2008b). The increased accumulation of ROS in primary cells is consistent with increased oxidative mtDNA damage in the TM cells from the POAG and XFG

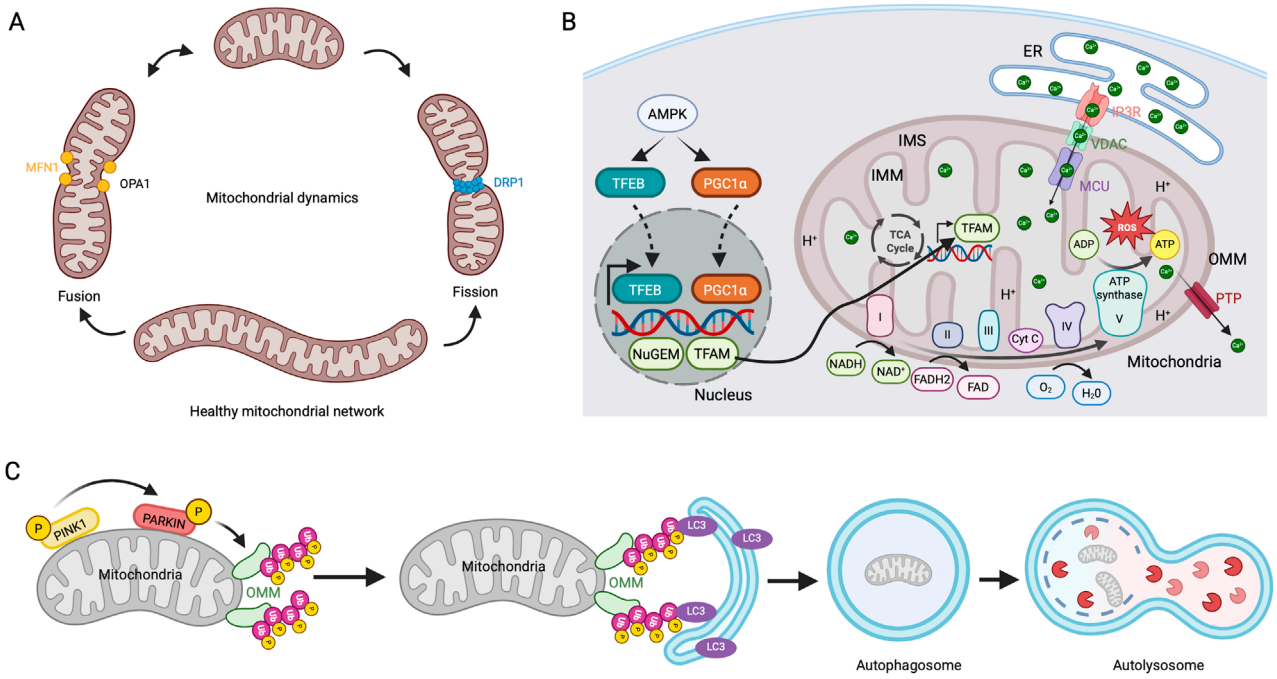

FIGURE 3
Mitochondrial dynamics, biogenesis, respiration, and mitophagy **(A)** Mitochondrial fission and fusion mechanisms. Mitochondria continuously undergo fission and fusion cycles. DRP1 regulates the fission process, while MFN1 and OPA1 drive its fusion. **(B)** Mitochondrial biogenesis and respiration. Involvement of, ETC, in ATP production. ER releases Ca^{2+} through the IP3R receptor, which is imported into the mitochondrial matrix via MCU and released through PTP. **(C)** PINK1/PARKIN mediated mitophagy pathway. In dysfunctional mitochondria, stabilizing PINK1 in the OMM leads to the activation and recruitment of PARKIN. This action initiates the polyubiquitination of OMM proteins, recruitment of LC3-coated autophagosomes, and degradation of mitochondria in autolysosomes.

glaucoma patients (Izzotti et al., 2003), highlighting the role of oxidative stress in glaucoma. Additionally, genetic studies reporting SNPs in nuclear and mtDNA genes that encode mitochondrial proteins explain the susceptibility to glaucoma associated with mitochondria (Lascaratos et al., 2012). Similar to mitochondrial dysfunction in the anterior eye chamber, RGCs from patients with POAG demonstrated degeneration due to programmed cell death (Kerrigan et al., 1997). Further studies involving glaucoma donors' lamina cribrosa cells revealed oxidative stress and mitochondrial dysfunction, as evidenced by impaired redox and Ca^{2+} homeostasis (McElnea et al., 2011). Recent studies also support these findings from POAG patients' ONH measuring flavoprotein fluorescence. They show that mitochondrial dysfunction is caused by the oxidation of mitochondrial flavoproteins at the ONH rim due to glaucomatous damage (Zhou et al., 2022b). Thus, oxidative stress occurs in glaucoma, and mitochondrial dysfunction may be a cause or consequence of TM and RGC cell apoptosis.

IOP and mitochondrial dysfunction in RGCs of glaucoma models

Several glaucomatous animal models have been studied, enhancing our understanding of mitochondrial dysfunction related to glaucoma pathophysiology. Mitochondria are essential to the ONH, and mitochondrial dysfunction and RGC apoptosis are key features of glaucomatous optic neuropathy. Due to their phototransduction function, retinal neurons have the highest energy demands, making them susceptible to oxidative stress and mechanical stretch injuries caused by elevated IOP. In glaucoma, RGC apoptosis occurs due to various factors, including aging, elevated IOP, oxidative stress, and mitochondrial dysfunction (Chrysostomou et al., 2010). Studies with glaucoma animal models have clearly shown this association. In the D2 secondary glaucoma mouse model, elevated IOP leads to oxidative stress and mitochondrial defects, including reduced OXPHOS and ATP production, altered morphology of mitochondria and cristae, and impaired mitophagy (Coughlin et al., 2015). Similarly, the IOP increase in Wister rats showed decreased ATP production with increased ROS and extensive mtDNA damage, contributing to RGC loss (Wu et al., 2015). The IOP increase in OHT mouse models also revealed an unusual accumulation of mitochondria in the Soma and axons (Maddineni et al., 2020; Kaipa et al., 2025). Additional research indicated hydrostatic pressure exposure in RGC cells influences mitochondrial fission-fusion processes, resulting in mitochondrial fragmentation and decreased ATP production (Ju et al., 2007). This indicates that diminished energy availability for RGCs makes them susceptible to apoptosis and glaucomatous damage. Recent research has shed light on how mitochondrial dysfunction occurs in glaucoma, highlighting the role of the mitochondrial fission-fusion cycle in safeguarding RGCs (Ju et al., 2010; Kim et al., 2015; Ju et al., 2008). Kim et al. proposed a vicious cycle in which elevated IOP in D2 glaucomatous mice leads to oxidative stress. This oxidative stress triggers enhanced

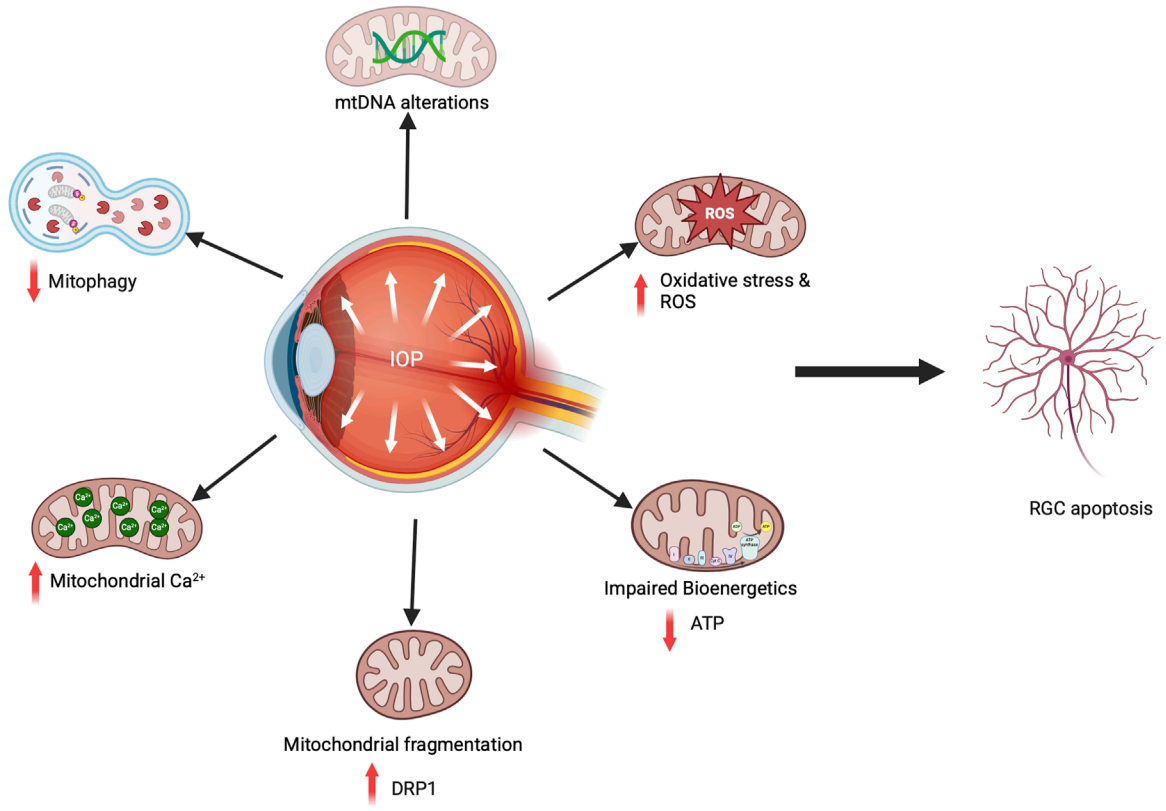

FIGURE 4
Mitochondrial dysfunction in glaucoma causes RGC death. In glaucomatous animal models, elevated IOP and oxidative stress result in mtDNA mutations, decreased ATP production, increased fission, enhanced mitochondrial Ca^{2+} transport from the ER, and reduced mitophagy flux, all contributing to RGC cell death.

mitochondrial fission through DRP1, leading to mitochondrial fragmentation in RGCs. Inhibiting DRP1 or over-expressing OPA1 safeguards RGCs, indicating a significant mitochondria-dependent pathophysiological mechanism in glaucomatous neurodegeneration (Kim et al., 2015; Ju et al., 2010). Additionally, these models revealed the presence of inflammatory signaling in RGCs linked to mitochondrial dysfunction (Jassim et al., 2021), signifying the complexity of the disease. Thus, increasing IOP directly affects mitochondrial health and causes RGC cell death (Figure 4).

Disease-causing mitochondrial variants in glaucoma

In addition to somatic and age-related mutations, mtDNA damage contributes to the development of various degenerative diseases, including glaucoma (Lascaratos et al., 2012). Twenty-two distinct transversion mutations in mitochondrial complex genes that impact mitochondrial bioenergetics were reported from peripheral blood leukocytes of POAG patients (Abu-Amero et al., 2006). Complex I mutations were also observed in the peripheral blood leukocytes of POAG patients from diverse ethnic backgrounds (Sundaresan et al., 2015), consistent with the impaired complex I-linked respiration (Lee et al., 2012). Studies from European populations have identified SNPs in the complex I genes, *MT-ND2*, *MT-ND4*, and the complex III gene, *MT-CYB* (Lo Faro et al., 2021; Singh et al., 2018). The common 4,977 bp mtDNA deletions were significantly elevated when analyzed in the POAG patients' ocular tissue, specifically the TM (Izzotti et al., 2010). The development of next-generation sequencing (NGS) technologies confirmed the heteroplasmy in the mitochondrial complex genes associated with POAG and highlighted the importance of using ocular tissues for genetic studies (Vallabh et al., 2024).

While large-scale mtDNA deletions were uncommon in NTG, SNPs in mitochondrial complex I genes were noted (Piotrowska-Nowak et al., 2019). NGS studies of mtDNA identified genetic variants across 21 genes, with polymorphisms in *MT-ND2*, *MT-COX3*, and *MT-CYTB* showing increased frequency in the peripheral blood of NTG patients (Jeoung et al., 2014). Various groups have identified polymorphisms in nuclear DNA-encoded mitochondrial genes, including *OPA1*, *MFN1*, and *MFN2*, indicating an imbalance between mitochondrial fission and fusion in NTG (Lascaratos et al., 2012). While genetic studies increasingly report mitochondrial gene variants in NTG, research is lacking to understand the mechanisms of mitochondrial dysfunction caused by these variants in NTG pathogenesis. In XFG, GWAS studies conducted across various ethnic populations did not identify SNPs

on mitochondrial genes. However, a 6.3-fold increased likelihood of mtDNA deletions was reported in the TM of XFG patients (Izzotti et al., 2011). Additionally, SNPs in complex I and II genes were observed in the Saudi Arabian population (Abu-Amero et al., 2008). The role of mitochondrial gene mutations in disease outcomes is a burgeoning field of study. Although expansive studies are not yet available, these studies collectively highlight the importance of mitochondrial genetic defects in POAG, NTG, and XFG pathogenesis.

In POAG, most reported mitochondrial gene polymorphisms occur in the mitochondrial complex I genes, directly impacting OXPHOS. The various IOP-inducing POAG glaucoma mouse models have also revealed diverse mitochondrial defects that contribute to RGC death. Although MYOC is not a mitochondrial protein, its mutations have been shown to affect mitochondrial function. The highly pathogenic MYOC P370L variant expression causes cellular apoptosis due to mutant MYOC aggregation in the ER, induces ER stress, and fails to clear via autophagy (Wang et al., 2007). In addition to protein folding defects, the P370L MYOC variant expression in human TM cells also caused mitochondrial dysfunction with decreased ATP production, lower MMPT, and higher ROS and cellular Ca^{2+} levels. Interestingly, while MYOC is a secreted protein, the overexpression of both WT and P370L MYOC variants led to the localization of MYOC in the mitochondria (He et al., 2009). This indicates that MYOC may have an unexplored role in regulating mitochondrial function.

While OPTN is not a mitochondrial protein, mutations in the *OPTN* gene in patients having NTG have been shown to cause mitochondrial dysfunction. OPTN is identified as one of the autophagy receptors and manages the PINK1/Parkin-mediated degradation of defective mitochondria through its UBD and LIR domains. After identifying its substrates, OPTN interacts with LC3 via the LIR domain to regulate autophagosome maturation. The mechanism of OPTN in regulating mitophagy has recently been clarified. OPTN is recruited to the OMM of depolarized mitochondria through a Parkin-dependent mechanism, with its UBN domain providing stabilization. The TBK1-dependent phosphorylation of OPTN also facilitates the recruitment of OPTN to the cargo site and boosts its binding to the ubiquitinated mitochondria (Heo et al., 2015; Richter et al., 2016). However, in ALS disease, the failure of ALS OPTN mutant recruitment impairs autophagosome maturation and disrupts mitophagy, accumulating misfolded mitochondrial proteins, ultimately contributing to disease pathogenesis (Wong and Holzbaur, 2014). Intriguingly, none of the OPTN glaucoma variants influenced OPTN recruitment for mitophagy, suggesting a distinct disease mechanism (Chernyshova et al., 2019).

The expression of E50K OPTN led to defective autophagy and RGC cell death. It also increased ROS levels through an unknown mechanism. Notably, antioxidant treatment prevented RGC death, indicating that oxidative stress plays a role in disease development (Chalasani et al., 2007). Nevertheless, the role of OPTN pathological variants in regulating mitochondrial biogenesis remained unclear. Recently, the RGC death in E50K OPTN NTG has been demonstrated due to mitochondrial-mediated oxidative stress-induced upregulation of ROS and the pro-apoptotic protein Bax. In contrast to the defective macro autophagy reported in the E50K OPTN over-expression cells, the transgenic animals showed increased mitophagosome formation. It is unclear whether the mitophagosome buildup is due to a defective mitophagic flux. However, the E50K OPTN expression in aged mice influenced the regulators of mitochondrial biogenesis with defects in mitochondrial fission/fusion cycles, causing fragmented mitochondria with higher cristae density and lower mitochondrial volume in RGC axons. These defects were replicated in RGC somas. Moreover, the mitochondrial transport and OXPHOS were not impaired in RGC axons. Therefore, the defects in mitochondrial biogenesis mediated by oxidative stress in E50K OPTN may also play a role in RGC death and the development of glaucoma (Shim et al., 2016).

In XFG, the accumulation of fibrillar ECM aggregates on the outflow pathway and proteostasis stress are more likely to induce mitochondrial dysfunction. Our lab has previously reported defective autophagy with reduced MMPT in the XFG patient-derived TFs (Want et al., 2016). Recently, we reported that the XFG TFs demonstrated mitochondrial dysfunction, characterized by impaired mitochondrial bioenergetics with decreased ATP, increased ROS, defective mitophagy flux, and altered mitochondrial ultrastructure with smaller mitochondria showing swollen cristae (Venkatesan et al., 2025). These defects are also observed in patients with other forms of glaucoma and animal models, indicating a common mechanism, such as IOP and oxidative stress involvement in glaucoma pathogenesis, as previously discussed. Interestingly, promoting mitophagy and enhancing mitochondrial biogenesis can reverse these mitochondrial defects in XFG TFs (Venkatesan et al., 2025). Future research will clarify the mechanism behind these mitochondrial defects in XFG disease.

ER-mitochondria crosstalk in glaucoma

Mitochondrial-associated membranes (MAMs) are structures derived from the ER that act as contact points between the ER and mitochondria, facilitating the transport of lipids and Ca^{2+} to mitochondria. These structures act as friend and foe and are often regulated by the ER-UPR response, particularly by PERK. They are also implicated in autophagy by regulating autophagosome formation and mitochondrial fission-fusion events through MAMs, suggesting that ER stress directly affects mitochondrial function (Senft and Ronai, 2015; Kasi et al., 2025). In glaucoma, protein misfolding causes ER stress, and UPR-PERK activation may be the primary cause of oxidative stress, mitochondrial dysfunction, and the apoptosis of TM or RGC. While research has not established direct mechanistic links between ER stress and mitochondrial dysfunction in glaucoma, emerging evidence suggests that elevated Ca^{2+} uptake by mitochondria due to ER stress leads to RGC apoptosis (Hurley et al., 2022). This hypothesis is further supported by the observed recovery of RGCs when UPR activations are inhibited in animal models of glaucoma (Kasetti et al., 2020). Additionally, TM cells from patients with POAG show impaired Ca^{2+} regulation, which leads to the opening of mitochondrial permeability transition pores (He et al., 2008a). Thus, future studies in glaucoma are required to evaluate the role of MAMs in RGC degeneration.

Biomarkers in glaucoma

The most effective treatment for glaucoma today is to reduce IOP (Wagner et al., 2022). However, glaucoma is often diagnosed late due to its slow progression, lack of warning signs, and asymptomatic early stages. Although IOP measurements and fundus photography are commonly used to identify glaucomatous damage, at least yearly visits to the Ophthalmologist are required to diagnose the condition before significant damage occurs (Schuster et al., 2020). This gap may be addressed using insights from GWAS studies, as genetic testing identified high-risk glaucoma variants (Ayala et al., 2023) in asymptomatic carriers who were at least 7 years younger than those diagnosed with clinical symptoms of glaucoma (Souzeau et al., 2017). Moreover, insights obtained from polygenic prediction (Craig et al., 2020) and genotype-phenotype studies offer prognostic value by enabling early diagnosis in individuals carrying certain high-risk genetic mutations associated with worse disease results.

Biomarkers in the AH that are associated with glaucoma have been heavily studied, including the identification of POAG-specific exosome characteristics. Glaucoma patients exhibited higher exosome particle counts and smaller sizes compared to controls, whereas higher exosome density was correlated with more severe visual field loss (Shin et al., 2024). In plasma, analysis of extracellular vesicle mRNAs in NTG patients revealed mitochondrial dysfunction and enrichment of central nervous system degenerative pathways relative to controls (Xu et al., 2024). Other cellular activities that correlate with disease progression include lipid peroxidation and total antioxidant activity (Hernandez-Martinez et al., 2016). Correspondingly, a recent review highlighted metabolic dysfunction in POAG. Key oxidative stress biomarkers were the enrichment of the arginine and proline metabolism pathway in both AH and plasma and the phenylalanine metabolism pathway in plasma (Golpour et al., 2025). Another metabolic study demonstrated that the concentration of small metabolites in the AH of glaucoma patients is altered. The imbalance affects membrane components, especially those of the mitochondria, suggesting that mitochondrial abnormalities either initiate or are a consequence of glaucoma (Lillo et al., 2022; Dammak et al., 2021). In addition to metabolic studies there are numerous other studies using AH and plasma from glaucoma patients. In XFG patients, the protein folding chaperone-clusterin was found to be significantly elevated in the AH compared to controls (Can Demirdogen et al., 2020). Another study demonstrated that IL-8 and Endothelin-1 are early biomarkers in the AH that are associated with XFS, prior to clinical manifestation of the disease, whereas Serum Amyloid A is associated with the later stage disease (Kadoh et al., 2025). Interestingly, another study supports the role of Endothelin-1 in glaucoma as AH from POAG and NTG patients relative to controls. These data suggest that dysregulation of vascular perfusion may have a role in the pathophysiology of POAG (Hedberg-Buenz et al., 2025). In a separate study that employed ELISA to measure inflammatory cytokines in the AH and compared POAG, XFG, and control groups, the researchers identified significant differences in several IL cytokines and growth factors across all groups. The key conclusion was that inflammation is closely linked to glaucoma, and specific cytokines may be associated with the severity of the condition (Gallardo Martin et al., 2025). Other studies have utilized glaucomatous primary cells for cell biological studies, leading to better characterization of the markers that define the glaucomatous outflow pathway (Yang et al., 2025). In-depth proteomic studies in cells have been used to understand the complex role of oxidative stress in age-related ocular disease. These data sets were compared to the AH from cataract and glaucoma patients, demonstrating RAD23B protein, involved in nuclear excision, repair, and proteasome regulation, as a potentially important glaucoma diagnostic marker (Rejas-Gonzalez et al., 2024). Overall, given the accessibility of AH and plasma for study, it is likely that diagnostic tools will become available to identify glaucoma patients prior to the onset of visual disability.

Therapeutics targeting protein misfolding

Different therapeutic strategies have been suggested to enhance protein folding, inhibit aberrant interaction, and alleviate the glaucoma phenotype. Mutations in *MYOC* lead to POAG, resulting in a toxic gain of function caused by MYOC misfolding and aggregation, leading to ER stress-induced TM cell death. In addition to surgical approaches, therapeutics improve the folding and clearance of mutant MYOC, alleviate ER stress, and restore proteostasis to improve TM function and lower IOP. On that note, over-expression of the HSP chaperone GRP94 facilitates the triaging of mutant I477N MYOC, thereby preventing its degradation (Suntharalingam et al., 2012). Treatment with the GRP94 inhibitor 4-Br-BnIm enhances MYOC solubility and decreases TM cell toxicity (Stothert et al., 2014). A similar approach using small molecule chaperones, such as sodium-4-Phenylbutyrate (4-PBA), enhances the folding of MYOC variants by reducing interaction with chaperones, leading to greater secretion, fewer insoluble aggregates, less ER stress, and reduced PERK-ATF4-CHOP activation (Kasetti et al., 2016; Yam et al., 2007b; Zode et al., 2011). The 4-PBA can also reduce abnormal ECM deposition in a glucocorticoid-induced OHT model (Maddineni et al., 2021). Moreover, in the Y437H MYOC mouse model, treatment of 4-PBA for 5 weeks prevented nocturnal IOP elevation, RGCs loss, and ON degeneration (Zode et al., 2011). Similarly, Valdecoxib or Bexarotene treatments also reduced RGC apoptosis by preventing ER stress in different glaucoma models (Gao et al., 2022; Dheer et al., 2019). Furthermore, an *in vitro* study demonstrates that the efficacy of epicatechin gallate in preventing the aggregation of the OLF domain of MYOC into amyloid fibrils shows promise for future drug discovery studies (Sharma et al., 2022). A novel antibody-based therapy that showed promise in clearing misfolded proteins associated with protein-folding diseases is being investigated for *MYOC* pathogenic variants. Anti-OLF antibodies effectively recognize and degrade intracellular insoluble aggregated mutant MYOC through autophagy in *in vitro* cell line models, indicating potential for future gene therapy (Ma et al., 2025). This aligns with the OHT model, which demonstrated a decrease in IOP in animal models after inducing autophagic flux to break down mutant MYOC (Kasetti et al., 2021). The CRISPR-Cas9-based genome editing of the *MYOC* OHT mouse model also showed promising therapeutic results, as it reduced ER stress and led to lower IOP in the animals, improving TM tissue homeostasis and preventing further glaucomatous damage (Jain et al., 2017; Patil et al., 2024).

Additionally, restoring TM cell function through stem cell-based transplantation approaches offers promising alternative therapies for glaucoma (Xiong et al., 2021; Zhu et al., 2016).

In OPTN-based NTG, drugs targeting TBK1 were effective in enhancing the solubility and neuroprotection of E50K OPTN. BX795, an aminopyrimidine chemical inhibitor, is known to inhibit the kinase activity of TBK1. Amlexanox is an anti-inflammatory, antiallergic immunomodulator that inhibits IKKε and TBK1 by competing for ATP binding to the enzyme. Since the TBK1 interaction is enhanced in E50K OPTN, treatment of both BX795 and Amlexanox in E50K OPTN cells increased the mutant solubility by limiting its interaction with TBK1. Additionally, a high dose of Amlexanox treatment in an E50K OPTN knock-in mouse model suppressed RGC layer thinning and improved neuroprotection without any adverse reactions in the animals (Minegishi et al., 2013; Minegishi et al., 2016). Although the TBK1 interaction is reduced in the case of M98K OPTN, the BX795 treatment rescued RGC-5 cell death by inhibiting S177 phosphorylation (Sirohi et al., 2015). Thus, the interaction of TBK1 with OPTN variants could serve as a potential treatment for OPTN-based NTG (Table 1). While strategies to properly fold pathogenic protein variants present promising options for treating POAG and NTG, such therapeutics have not been explored in XFG disease. Nevertheless, existing insights in XFG indicate that therapies designed to boost autophagy for better cellular proteostasis could represent a valuable approach. Nonetheless, a peptide-based method for the *ex vivo* extraction of fibrillar aggregates from human lens capsules demonstrates potential as a therapeutic approach (Ghaffari Sharaf et al., 2022).

Therapeutics improving mitochondrial function

Due to the high energy demands of retinal tissue, mitochondrial dysfunction in glaucoma leads to RGC death. Several blood and AH-based non-invasive and invasive biomarker approaches, which target DNA analysis for mtDNA mutations, copy number variations (Vallabh et al., 2024), and mitochondrial oxidative/redox stress biomarkers, show promising diagnostic and prognostic value for glaucoma patients (Sorkhabi et al., 2011; Hondur et al., 2017; Takayanagi et al., 2020). Subsequent research has indicated that racial differences in oxidative stress biomarkers and distinct pathological characteristics offer prognostic insights for the targeted populations (Wu et al., 2022). Thus, these approaches could help identify at-risk patients early, before disease progression.

While mechanistic insights into mitochondrial dysfunction in glaucomatous neurodegeneration are still being developed, various therapeutic approaches to enhancing mitochondrial function have been proposed for glaucoma. These interventions focus on improving RGCs and ONH health by decreasing oxidative stress and enhancing mitochondrial function in glaucoma models. Antioxidant supplementation is an emerging therapy to reduce oxidative stress and protect RGCs. Coenzyme Q10 is an antioxidant cofactor, and its administration in the rat IOP model promoted RGC survival by blocking the apoptotic pathway (Ju et al., 2018). As we age, NAD^+ levels decrease. However, using NAD^+ precursors like nicotinamide and nicotinamide ribose is gaining attention as promising complementary therapies, including glaucoma. In glaucomatous animal models, treatment with NAD^+ precursors demonstrated a protective effect on preserving RGCs and ONH by preventing mitochondrial damage (Williams et al., 2017; Zhang et al., 2021b). Strategies focusing on improving mitophagy to clear the damaged mitochondria are also explored in glaucoma. In a rat glaucoma model, the over-expression of the mitophagy modulator Parkin using adeno-associated virus 2 (AAV2) resulted in a notable reduction in RGC death, accompanied by a minor decrease in IOP (Dai et al., 2018). A similar approach, using AAV2-OPA1 overexpression in a rat glaucoma model, resulted in healthier mitochondria by promoting Parkin expression and protecting against RGC loss (Hu et al., 2018). Similarly, in E50K OPTN human stem cell-derived RGCs, inhibiting TBK1 with BX795 boosts mitochondrial biogenesis, enhances ATP production, and addresses various mitochondrial problems (Table 1) (Surma et al., 2023). In our lab, we recently demonstrated that treating XFG TFs with the mitophagy inducer Urolithin A and nicotinamide ribose enhanced mitochondrial bioenergetics and decreased ROS production (Venkatesan et al., 2025). Thus, improving mitochondrial health, which is often compromised by aging, genetic factors, and disease pathophysiology, may help slow the progression of glaucoma.

Discussion

Glaucoma is a multifaceted disease influenced by genetic, environmental, and lifestyle factors. While its severity varies across subtypes, emerging evidence indicates that protein misfolding is a common underlying factor in POAG, NTG, and XFG. Advances in identifying risk alleles and experimental studies focused on molecular mechanisms suggest that the misfolding of mutant proteins causes toxicity by triggering increased ER stress, activating the UPR, and disrupting protein degradation due to altered cellular localization and function. The expression of these variant proteins impacts mitochondrial function, leading to elevated ROS levels, altered mitochondrial morphology, reduced ATP production, and impaired mitophagy, which ultimately contribute to RGC degeneration. Therapeutic strategies using chemical chaperones to enhance protein folding and antioxidant supplementation to boost mitochondrial function demonstrate promising results in glaucoma models. These crucial findings arise from primary patient samples, glaucomatous animal models, and *in vitro* overexpression of genetic variants. Further exploring gene-gene and gene-environment interactions remains essential, extending beyond epidemiological studies to enhance personalized medicine and disease management. Despite the development of novel therapies in the pre-clinical stage, there remains a pressing need for further research into the molecular mechanisms linking ER stress and mitochondrial dysfunction to the onset and progression of glaucoma.

Author contributions

AV: Formal Analysis, Writing – original draft, Conceptualization, Writing – review and editing, Funding

acquisition. AB: Project administration, Funding acquisition, Writing – review and editing, Supervision, Conceptualization.

Funding

The author(s) declare that financial support was received for the research and/or publication of this article. This work was funded by the National Eye Institute NIH R01 EY030567, NIH R01 EY024942, NIH R44 EY035188, and Merit Review Award (I01 BX005360) from the United States Department of Veteran's Affairs to AB. The Glaucoma Foundation/Bright Focus Award to AB and AV. The Mayer Family Foundation to AB. Unrestricted grant from the Research to Prevent Blindness to the Department of Ophthalmology.

Acknowledgments

The figures are created with BioRender.com.

Conflict of interest

The authors declare that the research was conducted in the absence of any commercial or financial relationships that could be construed as a potential conflict of interest.

Generative AI statement

The author(s) declare that no Generative AI was used in the creation of this manuscript.

Publisher's note

References

Abu-Amero, K. K., Bosley, T. M., and Morales, J. (2008). Analysis of nuclear and mitochondrial genes in patients with pseudoexfoliation glaucoma. *Mol. Vis.* 14, 29–36.

Abu-Amero, K. K., Morales, J., and Bosley, T. M. (2006). Mitochondrial abnormalities in patients with primary open-angle glaucoma. *Invest. Ophthalmol. Vis. Sci.* 47, 2533–2541. doi:10.1167/iovs.05-1639

Adam, M. F., Belmouden, A., Binisti, P., Brezin, A. P., Valtot, F., Bechetoille, A., et al. (1997). Recurrent mutations in a single exon encoding the evolutionarily conserved olfactomedin-homology domain of TIGR in familial open-angle glaucoma. *Hum. Mol. Genet.* 6, 2091–2097. doi:10.1093/hmg/6.12.2091

Aldred, M. A., Baumber, L., Hill, A., Schwalbe, E. C., Goh, K., Karwatowski, W., et al. (2004). Low prevalence of MYOC mutations in UK primary open-angle glaucoma patients limits the utility of genetic testing. *Hum. Genet.* 115, 428–431. doi:10.1007/s00439-004-1171-1

Ali, D. M., Ansari, S. S., Zepp, M., Knapp-Mohammady, M., and Berger, M. R. (2019). Optineurin downregulation induces endoplasmic reticulum stress, chaperone-mediated autophagy, and apoptosis in pancreatic cancer cells. *Cell. Death Discov.* 5, 128. doi:10.1038/s41420-019-0206-2

Allingham, R. R., Liu, Y., and Rhee, D. J. (2009). The genetics of primary open-angle glaucoma: a review. *Exp. Eye Res.* 88, 837–844. doi:10.1016/j.exer.2008.11.003

Alvarado, J., Murphy, C., and Juster, R. (1984). Trabecular meshwork cellularity in primary open-angle glaucoma and nonglaucomatous normals. *Ophthalmology* 91, 564–579. doi:10.1016/s0161-6420(84)34248-8

Anderson, M. G., Meyer, K. J., Hedberg-Buenz, A., and Fingert, J. H. (2018). Update on animal models of exfoliation syndrome. *J. Glaucoma* 27 (Suppl. 1), S78-S82–S82. doi:10.1097/IJG.0000000000000911

Aroca-Aguilar, J. D., Sanchez-Sanchez, F., Martinez-Redondo, F., Coca-Prados, M., and Escribano, J. (2008). Heterozygous expression of myocilin glaucoma mutants increases secretion of the mutant forms and reduces extracellular processed myocilin. *Mol. Vis.* 14, 2097–2108.

Aung, T., Ozaki, M., Lee, M. C., Schlotzer-Schrehardt, U., Thorleifsson, G., Mizoguchi, T., et al. (2017). Genetic association study of exfoliation syndrome identifies a protective rare variant at LOXL1 and five new susceptibility loci. *Nat. Genet.* 49, 993–1004. doi:10.1038/ng.3875

Ayala-Lugo, R. M., Pawar, H., Reed, D. M., Lichter, P. R., Moroi, S. E., Page, M., et al. (2007). Variation in optineurin (OPTN) allele frequencies between and within populations. *Mol. Vis.* 13, 151–163.

Ayala, M., Zetterberg, M., and Zettergren, A. (2023). Single nucleotide polymorphisms in LOXL1 as biomarkers for progression of exfoliation glaucoma in Sweden. *Acta Ophthalmol.* 101, 521–529. doi:10.1111/aos.15630

Balaban, R. S., Nemoto, S., and Finkel, T. (2005). Mitochondria, oxidants, and aging. *Cell.* 120, 483–495. doi:10.1016/j.cell.2005.02.001

Balch, W. E., Morimoto, R. I., Dillin, A., and Kelly, J. W. (2008). Adapting proteostasis for disease intervention. *Science* 319, 916–919. doi:10.1126/science.1141448

Bernstein, A. M., Ritch, R., and Wolosin, J. M. (2018). Exfoliation syndrome: a disease of autophagy and LOXL1 proteopathy. *J. Glaucoma* 27 (Suppl. 1), S44-S53–S53. doi:10.1097/IJG.0000000000000919

Bernstein, A. M., Ritch, R., and Wolosin, J. M. (2019). LOXL1 folding in exfoliation glaucoma. *Adv. Protein Chem. Struct. Biol.* 118, 273–288. doi:10.1016/bs.apcsb.2019.09.005

Burns, J. N., Orwig, S. D., Harris, J. L., Watkins, J. D., Vollrath, D., and Lieberman, R. L. (2010). Rescue of glaucoma-causing mutant myocilin thermal stability by chemical chaperones. *ACS Chem. Biol.* 5, 477–487. doi:10.1021/cb900282e

Burns, J. N., Turnage, K. C., Walker, C. A., and Lieberman, R. L. (2011). The stability of myocilin olfactomedin domain variants provides new insight into glaucoma as a protein misfolding disorder. *Biochemistry* 50, 5824–5833. doi:10.1021/bi200231x

Caballero, M., and Borras, T. (2001). Inefficient processing of an olfactomedin-deficient myocilin mutant: potential physiological relevance to glaucoma. *Biochem. Biophys. Res. Commun.* 282, 662–670. doi:10.1006/bbrc.2001.4624

Can Demirdogen, B., Demirkaya-Budak, S., Ozge, G., and Mumcuoglu, T. (2020). Evaluation of tear fluid and aqueous humor concentration of clusterin as biomarkers for early diagnosis of pseudoexfoliation syndrome and pseudoexfoliative glaucoma. *Curr. Eye Res.* 45, 805–813. doi:10.1080/02713683.2019.1698055

Chalasani, M. L., Kumari, A., Radha, V., and Swarup, G. (2014). E50K-OPTN-induced retinal cell death involves the Rab GTPase-activating protein, TBC1D17 mediated block in autophagy. *PLoS One* 9, e95758. doi:10.1371/journal.pone.0095758

Chalasani, M. L., Radha, V., Gupta, V., Agarwal, N., Balasubramanian, D., and Swarup, G. (2007). A glaucoma-associated mutant of optineurin selectively induces death of retinal ganglion cells which is inhibited by antioxidants. *Invest. Ophthalmol. Vis. Sci.* 48, 1607–1614. doi:10.1167/iovs.06-0834

Cheng, Y., Wu, S., Yan, X., Liu, Q., Lin, D., Zhang, J., et al. (2023). Human Pro370Leu mutant myocilin induces the phenotype of open-angle glaucoma in transgenic mice. *Cell. Mol. Neurobiol.* 43, 2021–2033. doi:10.1007/s10571-022-01280-x

Chen, W., Zhao, H., and Li, Y. (2023). Mitochondrial dynamics in health and disease: mechanisms and potential targets. *Signal Transduct. Target Ther.* 8, 333. doi:10.1038/s41392-023-01547-9

Chernyshova, K., Inoue, K., Yamashita, S. I., Fukuchi, T., and Kanki, T. (2019). Glaucoma-associated mutations in the optineurin gene have limited impact on parkin-dependent mitophagy. *Invest. Ophthalmol. Vis. Sci.* 60, 3625–3635. doi:10.1167/iovs.19-27184

Christianson, J. C., and Carvalho, P. (2022). Order through destruction: how ER-associated protein degradation contributes to organelle homeostasis. *EMBO J.* 41, e109845. doi:10.15252/embj.2021109845

Chrysostomou, V., Trounce, I. A., and Crowston, J. G. (2010). Mechanisms of retinal ganglion cell injury in aging and glaucoma. *Ophthalmic Res.* 44, 173–178. doi:10.1159/000316478

Coughlin, L., Morrison, R. S., Horner, P. J., and Inman, D. M. (2015). Mitochondrial morphology differences and mitophagy deficit in murine glaucomatous optic nerve. *Invest. Ophthalmol. Vis. Sci.* 56, 1437–1446. doi:10.1167/iovs.14-16126

Craig, J. E., Han, X., Qassim, A., Hassall, M., Cooke Bailey, J. N., Kinzy, T. G., et al. (2020). Multitrait analysis of glaucoma identifies new risk loci and enables polygenic prediction of disease susceptibility and progression. *Nat. Genet.* 52, 160–166. doi:10.1038/s41588-019-0556-y

Dai, Y., Hu, X., and Sun, X. (2018). Overexpression of parkin protects retinal ganglion cells in experimental glaucoma. *Cell. Death Dis.* 9, 88. doi:10.1038/s41419-017-0146-9

Dammak, A., Huete-Toral, F., Carpena-Torres, C., Martin-Gil, A., Pastrana, C., and Carracedo, G. (2021). From oxidative stress to inflammation in the posterior ocular diseases: diagnosis and treatment. *Pharmaceutics* 13, 1376. doi:10.3390/pharmaceutics13091376

de Maria, A., Zientek, K. D., David, L. L., Wilmarth, P. A., Bhorade, A. M., Harocopos, G. J., et al. (2021). Compositional analysis of extracellular aggregates in the eyes of patients with exfoliation syndrome and exfoliation glaucoma. *Invest. Ophthalmol. Vis. Sci.* 62, 27. doi:10.1167/iovs.62.15.27

Dheer, Y., Chitranshi, N., Gupta, V., Sharma, S., Pushpitha, K., Abbasi, M., et al. (2019). Retinoid x receptor modulation protects against ER stress response and rescues glaucoma phenotypes in adult mice. *Exp. Neurol.* 314, 111–125. doi:10.1016/j.expneurol.2019.01.015

Dietze, J., Blair, K., Zeppieri, M., and Havens, S. J. (2024). *Glaucoma. StatPearls*. Treasure Island (FL).

Dismuke, W. M., Mckay, B. S., and Stamer, W. D. (2012). Myocilin, a component of a membrane-associated protein complex driven by a homologous Q-SNARE domain. *Biochemistry* 51, 3606–3613. doi:10.1021/bi300073r

Dixon, A., Shim, M. S., Nettesheim, A., Coyne, A., Su, C. C., Gong, H., et al. (2023). Autophagy deficiency protects against ocular hypertension and neurodegeneration in experimental and spontanous glaucoma mouse models. *Cell. Death Dis.* 14, 554. doi:10.1038/s41419-023-06086-3

Doh, S. H., Kim, J. H., Lee, K. M., Park, H. Y., and Park, C. K. (2010). Retinal ganglion cell death induced by endoplasmic reticulum stress in a chronic glaucoma model. *Brain Res.* 1308, 158–166. doi:10.1016/j.brainres.2009.10.025

Donegan, R. K., Hill, S. E., Freeman, D. M., Nguyen, E., Orwig, S. D., Turnage, K. C., et al. (2015). Structural basis for misfolding in myocilin-associated glaucoma. *Hum. Mol. Genet.* 24, 2111–2124. doi:10.1093/hmg/ddu730

Donegan, R. K., Hill, S. E., Turnage, K. C., Orwig, S. D., and Lieberman, R. L. (2012). The glaucoma-associated olfactomedin domain of myocilin is a novel calcium binding protein. *J. Biol. Chem.* 287, 43370–43377. doi:10.1074/jbc.M112.408906

Fautsch, M. P., and Johnson, D. H. (2001). Characterization of myocilin-myocilin interactions. *Invest. Ophthalmol. Vis. Sci.* 42, 2324–2331.

Fingert, J. H., Heon, E., Liebmann, J. M., Yamamoto, T., Craig, J. E., Rait, J., et al. (1999). Analysis of myocilin mutations in 1703 glaucoma patients from five different populations. *Hum. Mol. Genet.* 8, 899–905. doi:10.1093/hmg/8.5.899

Fingert, J. H., Stone, E. M., Sheffield, V. C., and Alward, W. L. (2002). Myocilin glaucoma. *Surv. Ophthalmol.* 47, 547–561. doi:10.1016/s0039-6257(02)00353-3

Gallardo Martin, L., Burgos-Blasco, B., Vidal-Villegas, B., Fernandez-Vigo, J. I., Garcia-Feijoo, J., and Martinez-de-la-Casa, J. M. (2025). Cytokine analysis to evaluate severity in primary open-angle glaucoma and exfoliative glaucoma. *Arch. Soc. Esp. Oftalmol.* doi:10.1016/j.oftale.2025.03.019

Ganguly, G., Chakrabarti, S., Chatterjee, U., and Saso, L. (2017). Proteinopathy, oxidative stress and mitochondrial dysfunction: cross talk in Alzheimer's disease and Parkinson's disease. *Drug Des. Devel Ther.* 11, 797–810. doi:10.2147/DDDT.S130514

Gao, J., Ohtsubo, M., Hotta, Y., and Minoshima, S. (2014). Oligomerization of optineurin and its oxidative stress- or E50K mutation-driven covalent cross-linking: possible relationship with glaucoma pathology. *PLoS One* 9, e101206. doi:10.1371/journal.pone.0101206

Gao, Z., Li, M., Yao, F., Xia, X., Duan, T., Meng, J., et al. (2022). Valdecoxib protects against cell apoptosis induced by endoplasmic reticulum stress via the inhibition of PERK-ATF4-CHOP pathway in experimental glaucoma. *Int. J. Mol. Sci.* 23, 12983. doi:10.3390/ijms232112983

Ghaffari Sharaf, M., Waduthanthri, K. D., Crichton, A., Damji, K. F., and Unsworth, L. D. (2022). Towards preventing exfoliation glaucoma by targeting and removing fibrillar aggregates associated with exfoliation syndrome. *J. Nanobiotechnology* 20, 459. doi:10.1186/s12951-022-01665-6

Gobeil, S., Rodrigue, M. A., Moisan, S., Nguyen, T. D., Polansky, J. R., Morissette, J., et al. (2004). Intracellular sequestration of hetero-oligomers formed by wild-type and glaucoma-causing myocilin mutants. *Invest. Ophthalmol. Vis. Sci.* 45, 3560–3567. doi:10.1167/iovs.04-0300

Golpour, N., Brautaset, R. L., Hui, F., Nilsson, M., Svensson, J. E., Williams, P. A., et al. (2025). Identifying potential key metabolic pathways and biomarkers in glaucoma: a systematic review and meta-analysis. *BMJ Open Ophthalmol.* 10, e002103. doi:10.1136/bmjophth-2024-002103

Gould, D. B., Miceli-Libby, L., Savinova, O. V., Torrado, M., Tomarev, S. I., Smith, R. S., et al. (2004). Genetically increasing Myoc expression supports a necessary pathologic role of abnormal proteins in glaucoma. *Mol. Cell. Biol.* 24, 9019–9025. doi:10.1128/MCB.24.20.9019-9025.2004

Gould, D. B., Reedy, M., Wilson, L. A., Smith, R. S., Johnson, R. L., and John, S. W. (2006). Mutant myocilin nonsecretion *in vivo* is not sufficient to cause glaucoma. *Mol. Cell. Biol.* 26, 8427–8436. doi:10.1128/MCB.01127-06

Hayat, B., Padhy, B., Mohanty, P. P., and Alone, D. P. (2019). Altered unfolded protein response and proteasome impairment in pseudoexfoliation pathogenesis. *Exp. Eye Res.* 181, 197–207. doi:10.1016/j.exer.2019.02.004

Hedberg-Buenz, A., Boese, E. A., Nyunt, A. W., Sears, N. C., Pouw, A. E., Wang, K., et al. (2025). Increased aqueous humor levels of endothelin-1 in patients with open angle glaucoma. *BMC Ophthalmol.* 25, 46. doi:10.1186/s12886-025-03861-y

Heo, J. M., Ordureau, A., Paulo, J. A., Rinehart, J., and Harper, J. W. (2015). The PINK1-PARKIN mitochondrial ubiquitylation pathway drives a program of OPTN/NDP52 recruitment and TBK1 activation to promote mitophagy. *Mol. Cell.* 60, 7–20. doi:10.1016/j.molcel.2015.08.016

Hernandez-Martinez, F. J., Pinas-Garcia, P., Lleo-Perez, A. V., Zanon-Moreno, V. C., Bendala-Tufanisco, E., Garcia-Medina, J. J., et al. (2016). Biomarkers of lipid peroxidation in the aqueous humor of primary open-angle glaucoma patients. *Arch. Soc. Esp. Oftalmol.* 91, 357–362. doi:10.1016/j.oftal.2016.01.031

He, Y., Ge, J., and Tombran-Tink, J. (2008a). Mitochondrial defects and dysfunction in calcium regulation in glaucomatous trabecular meshwork cells. *Invest. Ophthalmol. Vis. Sci.* 49, 4912–4922. doi:10.1167/iovs.08-2192

He, Y., Leung, K. W., Zhang, Y. H., Duan, S., Zhong, X. F., Jiang, R. Z., et al. (2008b). Mitochondrial complex I defect induces ROS release and degeneration in trabecular meshwork cells of POAG patients: protection by antioxidants. *Invest. Ophthalmol. Vis. Sci.* 49, 1447–1458. doi:10.1167/iovs.07-1361

He, Y., Leung, K. W., Zhuo, Y. H., and Ge, J. (2009). Pro370Leu mutant myocilin impairs mitochondrial functions in human trabecular meshwork cells. *Mol. Vis.* 15, 815–825.

Hill, S. E., Donegan, R. K., and Lieberman, R. L. (2014). The glaucoma-associated olfactomedin domain of myocilin forms polymorphic fibrils that are constrained by partial unfolding and peptide sequence. *J. Mol. Biol.* 426, 921–935. doi:10.1016/j.jmb.2013.12.002

Hill, S. E., Nguyen, E., Donegan, R. K., Patterson-Orazem, A. C., Hazel, A., Gumbart, J. C., et al. (2017). Structure and misfolding of the flexible tripartite coiled-coil domain of glaucoma-associated myocilin. *Structure* 25, 1697–1707. doi:10.1016/j.str.2017.09.008

Hirt, J., Porter, K., Dixon, A., Mckinnon, S., and Liton, P. B. (2018). Contribution of autophagy to ocular hypertension and neurodegeneration in the DBA/2J spontaneous glaucoma mouse model. *Cell. Death Discov.* 4, 14. doi:10.1038/s41420-018-0077-y

Hondur, G., Goktas, E., Yang, X., Al-Aswad, L., Auran, J. D., Blumberg, D. M., et al. (2017). Oxidative stress-related molecular biomarker candidates for glaucoma. *Invest. Ophthalmol. Vis. Sci.* 58, 4078–4088. doi:10.1167/iovs.17-22242

Huang, C., Xie, L., Wu, Z., Cao, Y., Zheng, Y., Pang, C. P., et al. (2018). Detection of mutations in MYOC, OPTN, NTF4, WDR36 and CYP1B1 in Chinese juvenile onset open-angle glaucoma using exome sequencing. *Sci. Rep.* 8, 4498. doi:10.1038/s41598-018-22337-2

Hurley, D. J., Normile, C., Irnaten, M., and O'Brien, C. (2022). The intertwined roles of oxidative stress and endoplasmic reticulum stress in glaucoma. *Antioxidants (Basel)* 11, 886. doi:10.3390/antiox11050886

Hu, X., Dai, Y., Zhang, R., Shang, K., and Sun, X. (2018). Overexpression of optic atrophy type 1 protects retinal ganglion cells and upregulates parkin expression in experimental glaucoma. *Front. Mol. Neurosci.* 11, 350. doi:10.3389/fnmol.2018.00350

Hu, Y., Park, K. K., Yang, L., Wei, X., Yang, Q., Cho, K. S., et al. (2012). Differential effects of unfolded protein response pathways on axon injury-induced death of retinal ganglion cells. *Neuron* 73, 445–452. doi:10.1016/j.neuron.2011.11.026

Izzotti, A., Longobardi, M., Cartiglia, C., and Sacca, S. C. (2011). Mitochondrial damage in the trabecular meshwork occurs only in primary open-angle glaucoma and in pseudoexfoliative glaucoma. *PLoS One* 6, e14567. doi:10.1371/journal.pone.0014567

Izzotti, A., Sacca, S. C., Cartiglia, C., and de Flora, S. (2003). Oxidative deoxyribonucleic acid damage in the eyes of glaucoma patients. *Am. J. Med.* 114, 638–646. doi:10.1016/s0002-9343(03)00114-1

Izzotti, A., Sacca, S. C., Longobardi, M., and Cartiglia, C. (2010). Mitochondrial damage in the trabecular meshwork of patients with glaucoma. *Arch. Ophthalmol.* 128, 724–730. doi:10.1001/archophthalmol.2010.87

Jacobson, N., Andrews, M., Shepard, A. R., Nishimura, D., Searby, C., Fingert, J. H., et al. (2001). Non-secretion of mutant proteins of the glaucoma gene myocilin in cultured trabecular meshwork cells and in aqueous humor. *Hum. Mol. Genet.* 10, 117–125. doi:10.1093/hmg/10.2.117

Jain, A., Zode, G., Kasetti, R. B., Ran, F. A., Yan, W., Sharma, T. P., et al. (2017). CRISPR-Cas9-based treatment of myocilin-associated glaucoma. *Proc. Natl. Acad. Sci. U. S. A.* 114, 11199–11204. doi:10.1073/pnas.1706193114

Jassim, A. H., Inman, D. M., and Mitchell, C. H. (2021). Crosstalk between dysfunctional mitochondria and inflammation in glaucomatous neurodegeneration. *Front. Pharmacol.* 12, 699623. doi:10.3389/fphar.2021.699623

Jeoung, J. W., Seong, M. W., Park, S. S., Kim, D. M., Kim, S. H., and Park, K. H. (2014). Mitochondrial DNA variant discovery in normal-tension glaucoma patients by next-generation sequencing. *Invest. Ophthalmol. Vis. Sci.* 55, 986–992. doi:10.1167/iovs.13-12968

Joe, M. K., Sohn, S., Hur, W., Moon, Y., Choi, Y. R., and Kee, C. (2003). Accumulation of mutant myocilins in ER leads to ER stress and potential cytotoxicity in human trabecular meshwork cells. *Biochem. Biophys. Res. Commun.* 312, 592–600. doi:10.1016/j.bbrc.2003.10.162

Joe, M. K., and Tomarev, S. I. (2010). Expression of myocilin mutants sensitizes cells to oxidative stress-induced apoptosis: implication for glaucoma pathogenesis. *Am. J. Pathol.* 176, 2880–2890. doi:10.2353/ajpath.2010.090853

Johri, A., and Beal, M. F. (2012). Mitochondrial dysfunction in neurodegenerative diseases. *J. Pharmacol. Exp. Ther.* 342, 619–630. doi:10.1124/jpet.112.192138

Ju, W. K., Kim, K. Y., Duong-Polk, K. X., Lindsey, J. D., Ellisman, M. H., and Weinreb, R. N. (2010). Increased optic atrophy type 1 expression protects retinal ganglion cells in a mouse model of glaucoma. *Mol. Vis.* 16, 1331–1342.

Ju, W. K., Kim, K. Y., Lindsey, J. D., Angert, M., Duong-Polk, K. X., Scott, R. T., et al. (2008). Intraocular pressure elevation induces mitochondrial fission and triggers OPA1 release in glaucomatous optic nerve. *Invest. Ophthalmol. Vis. Sci.* 49, 4903–4911. doi:10.1167/iovs.07-1661

Ju, W. K., Liu, Q., Kim, K. Y., Crowston, J. G., Lindsey, J. D., Agarwal, N., et al. (2007). Elevated hydrostatic pressure triggers mitochondrial fission and decreases cellular ATP in differentiated RGC-5 cells. *Invest. Ophthalmol. Vis. Sci.* 48, 2145–2151. doi:10.1167/iovs.06-0573

Ju, W. K., Shim, M. S., Kim, K. Y., Bu, J. H., Park, T. L., Ahn, S., et al. (2018). Ubiquinol promotes retinal ganglion cell survival and blocks the apoptotic pathway in ischemic retinal degeneration. *Biochem. Biophys. Res. Commun.* 503, 2639–2645. doi:10.1016/j.bbrc.2018.08.016

Kadoh, Y., Takayanagi, Y., Sugihara, K., Kaidzu, S., Takai, Y., and Tanito, M. (2025). Aqueous humor cytokine profiling reveals distinct roles for serum amyloid A, interleukin-8, and endothelin-1 in pseudoexfoliation syndrome and glaucoma. *Int. J. Mol. Sci.* 26, 1461. doi:10.3390/ijms26041461

Kaipa, B. R., Kasetti, R., Sundaresan, Y., Li, L., Yacoub, S., Millar, J. C., et al. (2025). Impaired axonal transport contributes to neurodegeneration in a Cre-inducible mouse model of myocilin-associated glaucoma. *JCI Insight* 10, e188710. doi:10.1172/jci.insight.188710

Kasetti, R. B., Maddineni, P., Kiehlbauch, C., Patil, S., Searby, C. C., Levine, B., et al. (2021). Autophagy stimulation reduces ocular hypertension in a murine glaucoma model via autophagic degradation of mutant myocilin. *JCI Insight* 6, e143359. doi:10.1172/jci.insight.143359

Kasetti, R. B., Patel, P. D., Maddineni, P., Patil, S., Kiehlbauch, C., Millar, J. C., et al. (2020). ATF4 leads to glaucoma by promoting protein synthesis and ER client protein load. *Nat. Commun.* 11, 5594. doi:10.1038/s41467-020-19352-1

Kasetti, R. B., Phan, T. N., Millar, J. C., and Zode, G. S. (2016). Expression of mutant myocilin induces abnormal intracellular accumulation of selected extracellular matrix proteins in the trabecular meshwork. *Invest. Ophthalmol. Vis. Sci.* 57, 6058–6069. doi:10.1167/iovs.16-19610

Kasi, A., Steidl, W., and Kumar, V. (2025). Endoplasmic reticulum-mitochondria crosstalk in fuchs endothelial corneal dystrophy: current status and future prospects. *Int. J. Mol. Sci.* 26, 894. doi:10.3390/ijms26030894

Kerrigan, L. A., Zack, D. J., Quigley, H. A., Smith, S. D., and Pease, M. E. (1997). TUNEL-positive ganglion cells in human primary open-angle glaucoma. *Arch. Ophthalmol.* 115, 1031–1035. doi:10.1001/archopht.1997.01100160201010

Kim, B. S., Savinova, O. V., Reedy, M. V., Martin, J., Lun, Y., Gan, L., et al. (2001). Targeted disruption of the myocilin gene (Myoc) suggests that human glaucoma-causing mutations are gain of function. *Mol. Cell. Biol.* 21, 7707–7713. doi:10.1128/MCB.21.22.7707-7713.2001

Kim, K. Y., Perkins, G. A., Shim, M. S., Bushong, E., Alcasid, N., Ju, S., et al. (2015). DRP1 inhibition rescues retinal ganglion cells and their axons by preserving mitochondrial integrity in a mouse model of glaucoma. *Cell. Death Dis.* 6, e1839. doi:10.1038/cddis.2015.180

Kim, S., and Kim, Y. (2012). Variations in LOXL1 associated with exfoliation glaucoma do not affect amine oxidase activity. *Mol. Vis.* 18, 265–270.

Klemmensen, M. M., Borrowman, S. H., Pearce, C., Pyles, B., and Chandra, B. (2024). Mitochondrial dysfunction in neurodegenerative disorders. *Neurotherapeutics* 21, e00292. doi:10.1016/j.neurot.2023.10.002

Kubota, R., Noda, S., Wang, Y., Minoshima, S., Asakawa, S., Kudoh, J., et al. (1997). A novel myosin-like protein (myocilin) expressed in the connecting cilium of the photoreceptor: molecular cloning, tissue expression, and chromosomal mapping. *Genomics* 41, 360–369. doi:10.1006/geno.1997.4682

Kuhlbrandt, W. (2015). Structure and function of mitochondrial membrane protein complexes. *BMC Biol.* 13, 89. doi:10.1186/s12915-015-0201-x

Kwon, Y. H., Fingert, J. H., Kuehn, M. H., and Alward, W. L. (2009). Primary open-angle glaucoma. *N. Engl. J. Med.* 360, 1113–1124. doi:10.1056/NEJMra0804630

Lam, D. S., Leung, Y. F., Chua, J. K., Baum, L., Fan, D. S., Choy, K. W., et al. (2000). Truncations in the TIGR gene in individuals with and without primary open-angle glaucoma. *Invest. Ophthalmol. Vis. Sci.* 41, 1386–1391.

Lascaratos, G., Garway-Heath, D. F., Willoughby, C. E., Chau, K. Y., and Schapira, A. H. (2012). Mitochondrial dysfunction in glaucoma: understanding genetic influences. *Mitochondrion* 12, 202–212. doi:10.1016/j.mito.2011.11.004

Lazarou, M., Sliter, D. A., Kane, L. A., Sarraf, S. A., Wang, C., Burman, J. L., et al. (2015). The ubiquitin kinase PINK1 recruits autophagy receptors to induce mitophagy. *Nature* 524, 309–314. doi:10.1038/nature14893

Lee, S., Sheck, L., Crowston, J. G., van Bergen, N. J., O'Neill, E. C., O'Hare, F., et al. (2012). Impaired complex-I-linked respiration and ATP synthesis in primary open-angle glaucoma patient lymphoblasts. *Invest. Ophthalmol. Vis. Sci.* 53, 2431–2437. doi:10.1167/iovs.12-9596

Lillo, A., Marin, S., Serrano-Marin, J., Binetti, N., Navarro, G., Cascante, M., et al. (2022). Targeted metabolomics shows that the level of glutamine, kynurenine, acyl-carnitines and lysophosphatidylcholines is significantly increased in the aqueous humor of glaucoma patients. *Front. Med. (Lausanne)* 9, 935084. doi:10.3389/fmed.2022.935084

Lin, M. T., and Beal, M. F. (2006). Mitochondrial dysfunction and oxidative stress in neurodegenerative diseases. *Nature* 443, 787–795. doi:10.1038/nature05292

Liu, D., Webber, H. C., Bian, F., Xu, Y., Prakash, M., Feng, X., et al. (2025). Optineurin-facilitated axonal mitochondria delivery promotes neuroprotection and axon regeneration. *Nat. Commun.* 16, 1789. doi:10.1038/s41467-025-57135-8

Liu, X., Zhao, Y., Gao, J., Pawlyk, B., Starcher, B., Spencer, J. A., et al. (2004). Elastic fiber homeostasis requires lysyl oxidase-like 1 protein. *Nat. Genet.* 36, 178–182. doi:10.1038/ng1297

Liu, Y., and Vollrath, D. (2004). Reversal of mutant myocilin non-secretion and cell killing: implications for glaucoma. *Hum. Mol. Genet.* 13, 1193–1204. doi:10.1093/hmg/ddh128

Li, X., He, J., and Sun, J. (2021). LOXL1 gene polymorphisms are associated with exfoliation syndrome/exfoliation glaucoma risk: an updated meta-analysis. *PLoS One* 16, e0250772. doi:10.1371/journal.pone.0250772

Lo Faro, V., Nolte, I. M., Ten Brink, J. B., Snieder, H., Jansonius, N. M., and Bergen, A. A. (2021). Mitochondrial genome study identifies association between primary open-angle glaucoma and variants in MT-CYB, MT-ND4 genes and haplogroups. *Front. Genet.* 12, 781189. doi:10.3389/fgene.2021.781189

Ma, M. T., Qerqez, A. N., Hill, K. R., Azouz, L. R., Youngblood, H. A., Hill, S. E., et al. (2025). Antibody-mediated clearance of an ER-resident aggregate that causes glaucoma. *PNAS Nexus* 4, pgae556. doi:10.1093/pnasnexus/pgae556

Maddineni, P., Kasetti, R. B., Kodati, B., Yacoub, S., and Zode, G. S. (2021). Sodium 4-phenylbutyrate reduces ocular hypertension by degrading extracellular matrix deposition via activation of MMP9. *Int. J. Mol. Sci.* 22, 10095. doi:10.3390/ijms221810095

Maddineni, P., Kasetti, R. B., Patel, P. D., Millar, J. C., Kiehlbauch, C., Clark, A. F., et al. (2020). CNS axonal degeneration and transport deficits at the optic nerve head precede structural and functional loss of retinal ganglion cells in a mouse model of glaucoma. *Mol. Neurodegener.* 15, 48. doi:10.1186/s13024-020-00400-9

Mcdowell, C. M., Luan, T., Zhang, Z., Putliwala, T., Wordinger, R. J., Millar, J. C., et al. (2012). Mutant human myocilin induces strain specific differences in ocular hypertension and optic nerve damage in mice. *Exp. Eye Res.* 100, 65–72. doi:10.1016/j.exer.2012.04.016

Mcelnea, E. M., Quill, B., Docherty, N. G., Irnaten, M., Siah, W. F., Clark, A. F., et al. (2011). Oxidative stress, mitochondrial dysfunction and calcium overload in human lamina cribrosa cells from glaucoma donors. *Mol. Vis.* 17, 1182–1191.

Minegishi, Y., Iejima, D., Kobayashi, H., Chi, Z. L., Kawase, K., Yamamoto, T., et al. (2013). Enhanced optineurin E50K-TBK1 interaction evokes protein insolubility and initiates familial primary open-angle glaucoma. *Hum. Mol. Genet.* 22, 3559–3567. doi:10.1093/hmg/ddt210

Minegishi, Y., Nakayama, M., Iejima, D., Kawase, K., and Iwata, T. (2016). Significance of optineurin mutations in glaucoma and other diseases. *Prog. Retin Eye Res.* 55, 149–181. doi:10.1016/j.preteyeres.2016.08.002

Mochida, K., and Nakatogawa, H. (2022). ER-phagy: selective autophagy of the endoplasmic reticulum. *EMBO Rep.* 23, e55192. doi:10.15252/embr.202255192

Nguyen, T. D., Chen, P., Huang, W. D., Chen, H., Johnson, D., and Polansky, J. R. (1998). Gene structure and properties of TIGR, an olfactomedin-related glycoprotein cloned from glucocorticoid-induced trabecular meshwork cells. *J. Biol. Chem.* 273, 6341–6350. doi:10.1074/jbc.273.11.6341

O'Loughlin, T., Kruppa, A. J., Ribeiro, A. L. R., Edgar, J. R., Ghannam, A., Smith, A. M., et al. (2020). OPTN recruitment to a Golgi-proximal compartment regulates immune signalling and cytokine secretion. *J. Cell. Sci.* 133, jcs239822. doi:10.1242/jcs.239822

Orwig, S. D., Perry, C. W., Kim, L. Y., Turnage, K. C., Zhang, R., Vollrath, D., et al. (2012). Amyloid fibril formation by the glaucoma-associated olfactomedin domain of myocilin. *J. Mol. Biol.* 421, 242–255. doi:10.1016/j.jmb.2011.12.016

Osawa, T., Mizuno, Y., Fujita, Y., Takatama, M., Nakazato, Y., and Okamoto, K. (2011). Optineurin in neurodegenerative diseases. *Neuropathology* 31, 569–574. doi:10.1111/j.1440-1789.2011.01199.x

Park, B. C., Shen, X., Samaraweera, M., and Yue, B. Y. (2006). Studies of optineurin, a glaucoma gene: Golgi fragmentation and cell death from overexpression of wild-type and mutant optineurin in two ocular cell types. *Am. J. Pathol.* 169, 1976–1989. doi:10.2353/ajpath.2006.060400

Patil, S. V., Kaipa, B. R., Ranshing, S., Sundaresan, Y., Millar, J. C., Nagarajan, B., et al. (2024). Lentiviral mediated delivery of CRISPR/Cas9 reduces intraocular pressure in a mouse model of myocilin glaucoma. *Sci. Rep.* 14, 6958. doi:10.1038/s41598-024-57286-6

Peters, J. C., Bhattacharya, S., Clark, A. F., and Zode, G. S. (2015). Increased endoplasmic reticulum stress in human glaucomatous trabecular meshwork cells and tissues. *Invest. Ophthalmol. Vis. Sci.* 56, 3860–3868. doi:10.1167/iovs.14-16220

Petriti, B., Rabiolo, A., Chau, K. Y., Williams, P. A., Montesano, G., Lascaratos, G., et al. (2024). Peripheral blood mononuclear cell respiratory function is associated with progressive glaucomatous vision loss. *Nat. Med.* 30, 2362–2370. doi:10.1038/s41591-024-03068-6

Pinton, P., Giorgi, C., Siviero, R., Zecchini, E., and Rizzuto, R. (2008). Calcium and apoptosis: ER-mitochondria Ca2+ transfer in the control of apoptosis. *Oncogene* 27, 6407–6418. doi:10.1038/onc.2008.308

Piotrowska-Nowak, A., Kosior-Jarecka, E., Schab, A., Wrobel-Dudzinska, D., Bartnik, E., Zarnowski, T., et al. (2019). Investigation of whole mitochondrial genome variation in normal tension glaucoma. *Exp. Eye Res.* 178, 186–197. doi:10.1016/j.exer.2018.10.004

Poothong, J., Jang, I., and Kaufman, R. J. (2021). Defects in protein folding and/or quality control cause protein aggregation in the endoplasmic reticulum. *Prog. Mol. Subcell. Biol.* 59, 115–143. doi:10.1007/978-3-030-67696-4_6

Porter, K., Hirt, J., Stamer, W. D., and Liton, P. B. (2015). Autophagic dysregulation in glaucomatous trabecular meshwork cells. *Biochim. Biophys. Acta* 1852, 379–385. doi:10.1016/j.bbadis.2014.11.021

Qiu, Y., Shen, X., Shyam, R., Yue, B. Y., and Ying, H. (2014). Cellular processing of myocilin. *PLoS One* 9, e92845. doi:10.1371/journal.pone.0092845

Quigley, H. A. (1999). Neuronal death in glaucoma. *Prog. Retin Eye Res.* 18, 39–57. doi:10.1016/s1350-9462(98)00014-7

Rejas-Gonzalez, R., Montero-Calle, A., Pastora Salvador, N., Crespo Carballes, M. J., Ausin-Gonzalez, E., Sanchez-Naves, J., et al. (2024). Unraveling the nexus of oxidative stress, ocular diseases, and small extracellular vesicles to identify novel glaucoma biomarkers through in-depth proteomics. *Redox Biol.* 77, 103368. doi:10.1016/j.redox.2024.103368

Rezaie, T., Child, A., Hitchings, R., Brice, G., Miller, L., Coca-Prados, M., et al. (2002). Adult-onset primary open-angle glaucoma caused by mutations in optineurin. *Science* 295, 1077–1079. doi:10.1126/science.1066901

Richter, B., Sliter, D. A., Herhaus, L., Stolz, A., Wang, C., Beli, P., et al. (2016). Phosphorylation of OPTN by TBK1 enhances its binding to Ub chains and promotes selective autophagy of damaged mitochondria. *Proc. Natl. Acad. Sci. U. S. A.* 113, 4039–4044. doi:10.1073/pnas.1523926113

Rodriguez-Pascual, F., and Rosell-Garcia, T. (2018). Lysyl oxidases: functions and disorders. *J. Glaucoma* 27 (Suppl. 1), S15-S19–S19. doi:10.1097/IJG.0000000000000910

Saccuzzo, E. G., Martin, M. D., Hill, K. R., Ma, M. T., Ku, Y., and Lieberman, R. L. (2022). Calcium dysregulation potentiates wild-type myocilin misfolding: implications for glaucoma pathogenesis. *J. Biol. Inorg. Chem.* 27, 553–564. doi:10.1007/s00775-022-01946-3

Saccuzzo, E. G., Mebrat, M. D., Scelsi, H. F., Kim, M., Ma, M. T., Su, X., et al. (2024). Competition between inside-out unfolding and pathogenic aggregation in an amyloid-forming beta-propeller. *Nat. Commun.* 15, 155. doi:10.1038/s41467-023-44479-2

Saccuzzo, E. G., Youngblood, H. A., and Lieberman, R. L. (2023). Myocilin misfolding and glaucoma: a 20-year update. *Prog. Retin Eye Res.* 95, 101188. doi:10.1016/j.preteyeres.2023.101188

Santel, A., and Fuller, M. T. (2001). Control of mitochondrial morphology by a human mitofusin. *J. Cell. Sci.* 114, 867–874. doi:10.1242/jcs.114.5.867

Sayyad, Z., Kaveti, S., Bhattacharjee, D., Vedagiri, D., Jain, N., and Swarup, G. (2023). A glaucoma-associated OPTN polymorphism, M98K sensitizes retinal cells to endoplasmic reticulum stress and tumour necrosis factor α. *FEBS J.* 290, 3110–3127. doi:10.1111/febs.16739

Sazhnyev, Y., Venkat, A., and Zheng, J. J. (2024). Somatic mutations within myocilin due to aging may Be a potential risk factor for glaucoma. *Genes. (Basel)* 15, 203. doi:10.3390/genes15020203

Scelsi, H. F., Barlow, B. M., Saccuzzo, E. G., and Lieberman, R. L. (2021). Common and rare myocilin variants: predicting glaucoma pathogenicity based on genetics, clinical, and laboratory misfolding data. *Hum. Mutat.* 42, 903–946. doi:10.1002/humu.24238

Scelsi, H. F., Hill, K. R., Barlow, B. M., Martin, M. D., and Lieberman, R. L. (2023). Quantitative differentiation of benign and misfolded glaucoma-causing myocilin variants on the basis of protein thermal stability. *Dis. Model. Mech.* 16, dmm049816. doi:10.1242/dmm.049816

Schuster, A. K., Erb, C., Hoffmann, E. M., Dietlein, T., and Pfeiffer, N. (2020). The diagnosis and treatment of glaucoma. *Dtsch. Arztebl Int.* 117, 225–234. doi:10.3238/arztebl.2020.0225

Senft, D., and Ronai, Z. A. (2015). UPR, autophagy, and mitochondria crosstalk underlies the ER stress response. *Trends Biochem. Sci.* 40, 141–148. doi:10.1016/j.tibs.2015.01.002

Sharma, R., Kumari, A., Kundu, B., and Grover, A. (2022). Amyloid fibrillation of the glaucoma associated myocilin protein is inhibited by epicatechin gallate (ECG). *RSC Adv.* 12, 29469–29481. doi:10.1039/d2ra05061g

Sharma, S., Martin, S., Sykes, M. J., Dave, A., Hewitt, A. W., Burdon, K. P., et al. (2016). Biological effect of LOXL1 coding variants associated with pseudoexfoliation syndrome. *Exp. Eye Res.* 146, 212–223. doi:10.1016/j.exer.2016.03.013

Shen, X. A., Ying, H. Y., Qiu, Y., Park, J. S., Shyam, R., Chi, Z. L., et al. (2011). Processing of optineurin in neuronal cells. *J. Biol. Chem.* 286, 3618–3629. doi:10.1074/jbc.M110.175810

Shepard, A. R., Jacobson, N., Sui, R., Steely, H. T., Lotery, A. J., Stone, E. M., et al. (2003). Characterization of rabbit myocilin: implications for human myocilin glycosylation and signal peptide usage. *BMC Genet.* 4, 5. doi:10.1186/1471-2156-4-5

Shim, M. S., Takihara, Y., Kim, K. Y., Iwata, T., Yue, B. Y., Inatani, M., et al. (2016). Mitochondrial pathogenic mechanism and degradation in optineurin E50K mutation-mediated retinal ganglion cell degeneration. *Sci. Rep.* 6, 33830. doi:10.1038/srep33830

Shin, D. Y., Han, J. S., Park, C. K., Lee, N. Y., and Jung, K. I. (2024). Parallel analysis of exosomes and cytokines in aqueous humor samples to evaluate biomarkers for glaucoma. *Cells* 13, 1030. doi:10.3390/cells13121030

Singh, L. N., Crowston, J. G., Lopez Sanchez, M. I. G., van Bergen, N. J., Kearns, L. S., Hewitt, A. W., et al. (2018). Mitochondrial DNA variation and disease susceptibility in primary open-angle glaucoma. *Invest. Ophthalmol. Vis. Sci.* 59, 4598–4602. doi:10.1167/iovs.18-25085

Sirohi, K., Chalasani, M. L., Sudhakar, C., Kumari, A., Radha, V., and Swarup, G. (2013). M98K-OPTN induces transferrin receptor degradation and RAB12-mediated autophagic death in retinal ganglion cells. *Autophagy* 9, 510–527. doi:10.4161/auto.23458

Sirohi, K., Kumari, A., Radha, V., and Swarup, G. (2015). A glaucoma-associated variant of optineurin, M98K, activates Tbk1 to enhance autophagosome formation and retinal cell death dependent on Ser177 phosphorylation of optineurin. *PLoS One* 10, e0138289. doi:10.1371/journal.pone.0138289

Slowicka, K., and van Loo, G. (2018). Optineurin functions for optimal immunity. *Front. Immunol.* 9, 769. doi:10.3389/fimmu.2018.00769

Smirnova, E., Griparic, L., Shurland, D. L., and van der Bliek, A. M. (2001). Dynamin-related protein Drp1 is required for mitochondrial division in mammalian cells. *Mol. Biol. Cell.* 12, 2245–2256. doi:10.1091/mbc.12.8.2245

Sohn, S., Hur, W., Joe, M. K., Kim, J. H., Lee, Z. W., Ha, K. S., et al. (2002). Expression of wild-type and truncated myocilins in trabecular meshwork cells: their subcellular localizations and cytotoxicities. *Invest. Ophthalmol. Vis. Sci.* 43, 3680–3685.

Sorkhabi, R., Ghorbanihaghjo, A., Javadzadeh, A., Rashtchizadeh, N., and Moharrery, M. (2011). Oxidative DNA damage and total antioxidant status in glaucoma patients. *Mol. Vis.* 17, 41–46.

Souzeau, E., Tram, K. H., Witney, M., Ruddle, J. B., Graham, S. L., Healey, P. R., et al. (2017). Myocilin predictive genetic testing for primary open-angle glaucoma leads to early identification of at-risk individuals. *Ophthalmology* 124, 303–309. doi:10.1016/j.ophtha.2016.11.011

Stamer, W. D., Perkumas, K. M., Hoffman, E. A., Roberts, B. C., Epstein, D. L., and Mckay, B. S. (2006). Coiled-coil targeting of myocilin to intracellular membranes. *Exp. Eye Res.* 83, 1386–1395. doi:10.1016/j.exer.2006.07.018

Stothert, A. R., Suntharalingam, A., Huard, D. J., Fontaine, S. N., Crowley, V. M., Mishra, S., et al. (2014). Exploiting the interaction between Grp94 and aggregated myocilin to treat glaucoma. *Hum. Mol. Genet.* 23, 6470–6480. doi:10.1093/hmg/ddu367

Sundaresan, P., Simpson, D. A., Sambare, C., Duffy, S., Lechner, J., Dastane, A., et al. (2015). Whole-mitochondrial genome sequencing in primary open-angle glaucoma using massively parallel sequencing identifies novel and known pathogenic variants. *Genet. Med.* 17, 279–284. doi:10.1038/gim.2014.121

Suntharalingam, A., Abisambra, J. F., O'Leary, J. C., 3Rd, Koren, J., 3Rd, Zhang, B., Joe, M. K., et al. (2012). Glucose-regulated protein 94 triage of mutant myocilin through

endoplasmic reticulum-associated degradation subverts a more efficient autophagic clearance mechanism. *J. Biol. Chem.* 287, 40661–40669. doi:10.1074/jbc.M112.384800

Surma, M., Anbarasu, K., Dutta, S., Olivera Perez, L. J., Huang, K. C., Meyer, J. S., et al. (2023). Enhanced mitochondrial biogenesis promotes neuroprotection in human pluripotent stem cell derived retinal ganglion cells. *Commun. Biol.* 6, 218. doi:10.1038/s42003-023-04576-w

Takayanagi, Y., Takai, Y., Kaidzu, S., and Tanito, M. (2020). Evaluation of redox profiles of the serum and aqueous humor in patients with primary open-angle glaucoma and exfoliation glaucoma. *Antioxidants (Basel)* 9, 1305. doi:10.3390/antiox9121305

Tamm, E. R., Russell, P., Epstein, D. L., Johnson, D. H., and Piatigorsky, J. (1999). Modulation of myocilin/TIGR expression in human trabecular meshwork. *Invest. Ophthalmol. Vis. Sci.* 40, 2577–2582.

Tham, Y. C., Li, X., Wong, T. Y., Quigley, H. A., Aung, T., and Cheng, C. Y. (2014). Global prevalence of glaucoma and projections of glaucoma burden through 2040: a systematic review and meta-analysis. *Ophthalmology* 121, 2081–2090. doi:10.1016/j.ophtha.2014.05.013

Thomassin, L., Werneck, C. C., Broekelmann, T. J., Gleyzal, C., Hornstra, I. K., Mecham, R. P., et al. (2005). The Pro-regions of lysyl oxidase and lysyl oxidase-like 1 are required for deposition onto elastic fibers. *J. Biol. Chem.* 280, 42848–42855. doi:10.1074/jbc.M506832200

Tirendi, S., Domenicotti, C., Bassi, A. M., and Vernazza, S. (2023). Genetics and Glaucoma: the state of the art. *Front. Med. (Lausanne)* 10, 1289952. doi:10.3389/fmed.2023.1289952

Vaibhava, V., Nagabhushana, A., Chalasani, M. L., Sudhakar, C., Kumari, A., and Swarup, G. (2012). Optineurin mediates a negative regulation of Rab8 by the GTPase-activating protein TBC1D17. *J. Cell. Sci.* 125, 5026–5039. doi:10.1242/jcs.102327

Vallabh, N. A., Armstrong, J., Czanner, G., Mcdonagh, B., Choudhary, A., Criddle, D. N., et al. (2022). Evidence of impaired mitochondrial cellular bioenergetics in ocular fibroblasts derived from glaucoma patients. *Free Radic. Biol. Med.* 189, 102–110. doi:10.1016/j.freeradbiomed.2022.07.009

Vallabh, N. A., Lane, B., Simpson, D., Fuchs, M., Choudhary, A., Criddle, D., et al. (2024). Massively parallel sequencing of mitochondrial genome in primary open angle glaucoma identifies somatically acquired mitochondrial mutations in ocular tissue. *Sci. Rep.* 14, 26324. doi:10.1038/s41598-024-72684-6

Vanderwall, K. B., Huang, K. C., Pan, Y., Lavekar, S. S., Fligor, C. M., Allsop, A. R., et al. (2020). Retinal ganglion cells with a glaucoma OPTN(E50K) mutation exhibit neurodegenerative phenotypes when derived from three-dimensional retinal organoids. *Stem Cell. Rep.* 15, 52–66. doi:10.1016/j.stemcr.2020.05.009

Venkatesan, A., Castro, N., Wolosin, J. M., and Bernstein, A. M. (2023). Loxl1 protein aggregation and impaired mitochondrial bioenergetics in exfoliation glaucoma. *Investigative Ophthalmol. and Vis. Sci.* 64.

Venkatesan, A., Ridilla, M., Castro, N., Wolosin, J. M., Henty-Ridilla, J. L., Knox, B. E., et al. (2025). Mitochondrial and microtubule defects in exfoliation glaucoma. *Free Radic. Biol. Med.* 233, 226–239. doi:10.1016/j.freeradbiomed.2025.03.046

Venkatesan, A., Satin, L. S., and Raghavan, M. (2021). Roles of calreticulin in protein folding, immunity, calcium signaling and cell transformation. *Prog. Mol. Subcell. Biol.* 59, 145–162. doi:10.1007/978-3-030-67696-4_7

Wagner, I. V., Stewart, M. W., and Dorairaj, S. K. (2022). Updates on the diagnosis and management of glaucoma. *Mayo Clin. Proc. Innov. Qual. Outcomes* 6, 618–635. doi:10.1016/j.mayocpiqo.2022.09.007

Walter, P., and Ron, D. (2011). The unfolded protein response: from stress pathway to homeostatic regulation. *Science* 334, 1081–1086. doi:10.1126/science.1209038

Wang, L., Zhuo, Y., Liu, B., Huang, S., Hou, F., and Ge, J. (2007). Pro370Leu mutant myocilin disturbs the endoplasm reticulum stress response and mitochondrial membrane potential in human trabecular meshwork cells. *Mol. Vis.* 13, 618–625.

Want, A., Gillespie, S. R., Wang, Z., Gordon, R., Iomini, C., Ritch, R., et al. (2016). Autophagy and mitochondrial dysfunction in Tenon fibroblasts from exfoliation glaucoma patients. *PLoS One* 11, e0157404. doi:10.1371/journal.pone.0157404

Wareham, L. K., Kuchtey, J., Wu, H. J., Krystofiak, E., Wu, Y., Reinhart-King, C. A., et al. (2022). Lysyl oxidase-like 1 deficiency alters ultrastructural and biomechanical properties of the peripapillary sclera in mice. *Matrix Biol. Plus* 16, 100120. doi:10.1016/j.mbplus.2022.100120

Wentz-Hunter, K., Ueda, J., and Yue, B. Y. (2002). Protein interactions with myocilin. *Invest. Ophthalmol. Vis. Sci.* 43, 176–182.

Wiggs, J. L. (2007). Genetic etiologies of glaucoma. *Arch. Ophthalmol.* 125 1, 30–37. doi:10.1001/archopht.125.1.30

Wiggs, J. L., and Pasquale, L. R. (2017). Genetics of glaucoma. *Hum. Mol. Genet.* 26, R21–R27. doi:10.1093/hmg/ddx184

Wiggs, J. L., Pawlyk, B., Connolly, E., Adamian, M., Miller, J. W., Pasquale, L. R., et al. (2014). Disruption of the blood-aqueous barrier and lens abnormalities in mice lacking lysyl oxidase-like 1 (LOXL1). *Invest. Ophthalmol. Vis. Sci.* 55, 856–864. doi:10.1167/iovs.13-13033

Wiggs, J. L., and Vollrath, D. (2001). Molecular and clinical evaluation of a patient hemizygous for TIGR/MYOC. *Arch. Ophthalmol.* 119, 1674–1678. doi:10.1001/archopht.119.11.1674

Wild, P., Farhan, H., Mcewan, D. G., Wagner, S., Rogov, V. V., Brady, N. R., et al. (2011). Phosphorylation of the autophagy receptor optineurin restricts Salmonella growth. *Science* 333, 228–233. doi:10.1126/science.1205405

Williams, P. A., Harder, J. M., Foxworth, N. E., Cardozo, B. H., Cochran, K. E., and John, S. W. M. (2017). Nicotinamide and WLD(S) act together to prevent neurodegeneration in glaucoma. *Front. Neurosci.* 11, 232. doi:10.3389/fnins.2017.00232

Wise, J. P., JR., and Cannon, J. (2016). From the cover: alterations in optineurin expression and localization in pre-clinical Parkinson's disease models. *Toxicol. Sci.* 153, 372–381. doi:10.1093/toxsci/kfw133

Wolosin, J. M., Ritch, R., and Bernstein, A. M. (2018). Is autophagy dysfunction a key to exfoliation glaucoma? *J. Glaucoma* 27, 197–201. doi:10.1097/IJG.0000000000000606

Wong, Y. C., and Holzbaur, E. L. (2014). Optineurin is an autophagy receptor for damaged mitochondria in parkin-mediated mitophagy that is disrupted by an ALS-linked mutation. *Proc. Natl. Acad. Sci. U. S. A.* 111, E4439–E4448. doi:10.1073/pnas.1405752111

Wu, J. H., Zhang, S. H., Nickerson, J. M., Gao, F. J., Sun, Z., Chen, X. Y., et al. (2015). Cumulative mtDNA damage and mutations contribute to the progressive loss of RGCs in a rat model of glaucoma. *Neurobiol. Dis.* 74, 167–179. doi:10.1016/j.nbd.2014.11.014

Wu, H., Shui, Y. B., Liu, Y., Liu, X., and Siegfried, C. J. (2022). Trabecular meshwork mitochondrial function and oxidative stress: clues to racial disparities of glaucoma. *Ophthalmol. Sci.* 2, 100107. doi:10.1016/j.xops.2021.100107

Xiong, S., Kumar, A., Tian, S., Taher, E. E., Yang, E., Kinchington, P. R., et al. (2021). Stem cell transplantation rescued a primary open-angle glaucoma mouse model. *Elife* 10, e63677. doi:10.7554/eLife.63677

Xu, S. L., Li, J. H., Zhang, W. M., Fu, M. J., Xing, H. M., Ma, H., et al. (2024). Transcriptomic analysis of plasma-derived small extracellular vesicles reveals the pathological characteristics of normal tension glaucoma. *Extracell. Vesicles Circ. Nucl. Acids* 5, 438–454. doi:10.20517/evcna.2024.45

Yam, G. H., Gaplovska-Kysela, K., Zuber, C., and Roth, J. (2007a). Aggregated myocilin induces russell bodies and causes apoptosis: implications for the pathogenesis of myocilin-caused primary open-angle glaucoma. *Am. J. Pathol.* 170, 100–109. doi:10.2353/ajpath.2007.060806

Yam, G. H., Gaplovska-Kysela, K., Zuber, C., and Roth, J. (2007b). Sodium 4-phenylbutyrate acts as a chemical chaperone on misfolded myocilin to rescue cells from endoplasmic reticulum stress and apoptosis. *Invest. Ophthalmol. Vis. Sci.* 48, 1683–1690. doi:10.1167/iovs.06-0943

Yang, Y. F., Holden, P., Sun, Y. Y., Faralli, J. A., Peters, D. M., and Keller, K. E. (2025). Fibrosis-related gene and protein expression in normal and glaucomatous trabecular meshwork cells. *Invest. Ophthalmol. Vis. Sci.* 66, 48. doi:10.1167/iovs.66.3.48

Yan, X., Wu, S., Liu, Q., Cheng, Y., Teng, Y., Ren, T., et al. (2024). Serine to proline mutation at position 341 of MYOC impairs trabecular meshwork function by causing autophagy deregulation. *Cell. Death Discov.* 10, 21. doi:10.1038/s41420-024-01801-1

Yan, X., Wu, S., Liu, Q., Cheng, Y., Zhang, J., and Wang, N. (2022). Myocilin gene mutation induced autophagy activation causes dysfunction of trabecular meshwork cells. *Front. Cell. Dev. Biol.* 10, 900777. doi:10.3389/fcell.2022.900777

Yan, X., Wu, S., Liu, Q., Li, Y., Zhu, W., and Zhang, J. (2020). Accumulation of Asn450Tyr mutant myocilin in ER promotes apoptosis of human trabecular meshwork cells. *Mol. Vis.* 26, 563–573.

Ying, H., Shen, X., Park, B., and Yue, B. Y. (2010). Posttranslational modifications, localization, and protein interactions of optineurin, the product of a glaucoma gene. *PLoS One* 5, e9168. doi:10.1371/journal.pone.0009168

Ying, H., and Yue, B. Y. (2012). Cellular and molecular biology of optineurin. *Int. Rev. Cell. Mol. Biol.* 294, 223–258. doi:10.1016/B978-0-12-394305-7.00005-7

Ying, Y., Xue, R., Yang, Y., Zhang, S. X., Xiao, H., Zhu, H., et al. (2021). Activation of ATF4 triggers trabecular meshwork cell dysfunction and apoptosis in POAG. *Aging (Albany NY)* 13, 8628–8642. doi:10.18632/aging.202677

Zadoo, S., Nguyen, A., Zode, G., and Hulleman, J. D. (2016). A novel luciferase assay for sensitively monitoring myocilin variants in cell culture. *Invest. Ophthalmol. Vis. Sci.* 57, 1939–1950. doi:10.1167/iovs.15-18789

Zadravec, P., Braunger, B. M., Melzer, B., Kroeber, M., Bosl, M. R., Jagle, H., et al. (2019). Transgenic lysyl oxidase homolog 1 overexpression in the mouse eye results in the formation and release of protein aggregates. *Exp. Eye Res.* 179, 115–124. doi:10.1016/j.exer.2018.11.001

Zenkel, M., and Schlotzer-Schrehardt, U. (2014). The composition of exfoliation material and the cells involved in its production. *J. Glaucoma* 23, S12–S14. doi:10.1097/IJG.0000000000000123

Zhang, S., Shao, Z., Liu, X., Hou, M., Cheng, F., Lei, D., et al. (2021a). The E50K optineurin mutation impacts autophagy-mediated degradation of TDP-43 and leads to RGC apoptosis *in vivo* and *in vitro*. *Cell. Death Discov.* 7, 49. doi:10.1038/s41420-021-00432-0

Zhang, X., Zhang, N., Chrenek, M. A., Girardot, P. E., Wang, J., Sellers, J. T., et al. (2021b). Systemic treatment with nicotinamide riboside is protective

in two mouse models of retinal ganglion cell damage. *Pharmaceutics* 13, 893. doi:10.3390/pharmaceutics13060893

Zhou, D. B., Castanos, M. V., Geyman, L., Rich, C. A., Tantraworasin, A., Ritch, R., et al. (2022b). Mitochondrial dysfunction in primary open-angle glaucoma characterized by flavoprotein fluorescence at the optic nerve head. *Ophthalmol. Glaucoma* 5, 413–420. doi:10.1016/j.ogla.2021.12.006

Zhou, B., Lin, X., Li, Z., Yao, Y., Yang, J., and Zhu, Y. (2022a). Structure-function-pathogenicity analysis of C-terminal myocilin missense variants based on experiments and 3D models. *Front. Genet.* 13, 1019208. doi:10.3389/fgene.2022.1019208

Zhou, Z., and Vollrath, D. (1999). A cellular assay distinguishes normal and mutant TIGR/myocilin protein. *Hum. Mol. Genet.* 8, 2221–2228. doi:10.1093/hmg/8.12.2221

Zhu, W., Gramlich, O. W., Laboissonniere, L., Jain, A., Sheffield, V. C., Trimarchi, J. M., et al. (2016). Transplantation of iPSC-derived TM cells rescues glaucoma phenotypes *in vivo*. *Proc. Natl. Acad. Sci. U. S. A.* 113, E3492–E3500. doi:10.1073/pnas.1604153113

Zode, G. S., Kuehn, M. H., Nishimura, D. Y., Searby, C. C., Mohan, K., Grozdanic, S. D., et al. (2011). Reduction of ER stress via a chemical chaperone prevents disease phenotypes in a mouse model of primary open angle glaucoma. *J. Clin. Invest.* 121, 3542–3553. doi:10.1172/JCI58183

Glossary

4-PBA	Sodium-4-Phenylbutyrate
AAV2	Adeno-associated virus 2
AH	Aqueous humor
ALS	Amyotrophic lateral sclerosis
CC	Coiled-coil domain
CNX	Calnexin
CRT	Calreticulin
D2	DBA/2J
ECM	Extracellular matrix
ER	Endoplasmic reticulum
ERAD	ER-associated degradation
ERCa^{2+}	Endoplasmic reticulum calcium
ERQC	ER protein quality control
ETC	Electron transport chain
GWAS	Genome-wide association studies
IDR	Intrinsically disordered region
IMM	Inner mitochondrial membrane
IOP	Intraocular pressure
JOAG	Juvenile open-angle glaucoma
LOXL1	Lysyl oxidase-like one
LZ	Leucine Zipper
MAM	Mitochondrial-associated membrane
MCU	Mitochondrial calcium uniporter
MitCa^{2+}	Mitochondrial calcium
MMPT	Mitochondrial membrane potential
mtDNA	Mitochondrial DNA
MYOC	Myocilin
NGS	Next-generation sequencing
NTG	Normal tension glaucoma
OHT	Ocular hypertension
OLF	Olfactomedin
OMM	Outer mitochondrial membrane
ON	Optic nerve
ONH	Optic nerve head
OPTN	Optineurin
OXPHOS	Oxidative phosphorylation
POAG	Primary open-angle glaucoma
PTM	Post-translational modification
PTP	Permeability transition pore
RGCs	Retinal ganglion cells
ROS	Reactive oxygen species
SC	Schlemm's canal
TF	Tenon fibroblast
TM	Trabecular meshwork
UBD	Ubiquitin-binding domain
UPR	Unfolded protein response
WT	Wild-type
XFG	Exfoliation glaucoma

frontiers | Frontiers in Molecular Biosciences

TYPE Methods
PUBLISHED 13 May 2025
DOI 10.3389/fmolb.2025.1505250

OPEN ACCESS

EDITED BY
Anoop Arunagiri,
East Tennessee State University, United States

REVIEWED BY
Rakesh Kumar,
Karolinska Institutet (KI), Sweden
Maria Del Carmen Fernandez-Ramirez,
University of Texas Southwestern Medical Center, United States

*CORRESPONDENCE
Giulio Agnetti,
giulio.agnetti@unibo.it

RECEIVED 02 October 2024
ACCEPTED 14 April 2025
PUBLISHED 13 May 2025

CITATION
Oldam J, Tchernyshyov I, Van Eyk J, Troncoso J, Glabe CG and Agnetti G (2025) Thioflavin T in-gel staining for *ex vivo* analysis of cardiac amyloid .
Front. Mol. Biosci. 12:1505250.
doi: 10.3389/fmolb.2025.1505250

Thioflavin T in-gel staining for *ex vivo* analysis of cardiac amyloid

Joseph Oldam[1], Irina Tchernyshyov[2], Jennifer Van Eyk[2], Juan Troncoso[1], Charles G. Glabe[3] and Giulio Agnetti[1,4]*

[1]Johns Hopkins University School of Medicine, Baltimore, MD, United States, [2]Advanced Clinical Biosystems Institute, Cedars-Sinai Hospital, Beverly Hills, CA, United States, [3]University of California Irvine School of Biological Sciences, Irvine, CA, United States, [4]Department of Biomedical and Neuromotor Sciences (DIBINEM), University of Bologna, Bologna, Italy

There are limited options to quantify and characterize amyloid species from biological samples in a simple manner. Thioflavin T (ThT) has been used for decades to stain amyloid fibrils, but to our knowledge, we were the first to use it in-gel. Thioflavin T in-gel staining is convenient as it is fast, inexpensive, accessible to most laboratories, and compatible with other fluorescent stains and downstream analyses such as mass spectrometry (MS).

KEYWORDS

amyloid, mass spectrometry, proteinopathies, desmin, heart failure

Introduction

Organ and systemic proteinopathies represent one of the main areas of public health concern in Westernized society in this century (Chiti and Dobson, 2009). The toxic nature of pre-fibrillar and fibrillar amyloid is well-established in neurocognitive disease (Mullapudi et al., 2023); however, their role and prevalence are also emerging in cardiovascular diseases (Del Monte and Agnetti, 2014). Most amyloid species are quantified using either fluorescent, radiolabeled, or immunological probes, as well as mass spectrometry (MS) (Seino et al., 2021; Wall et al., 2013; Ruiz-Arias et al., 2022; Iino et al., 2021). From the technological standpoint, MS is arguably one of the techniques with the highest impact on biomedical sciences in this century (Agnetti et al., 2016). Cutting-edge MS-based approaches such as isotope incorporation are currently being used in the study of protein misfolding, but their application is still confined to a few laboratories worldwide (Mackmull et al., 2022). It is our opinion that a simple way to detect and quickly isolate amyloid species *ex vivo*, which is compatible with "classic" MS, would greatly benefit the study of an increasing number of organ-based proteinopathies.

We optimized a straightforward, affordable method to stain amyloid species in-gel and tested it on a well-established model of murine cardiac amyloidosis (Sanbe et al., 2004), a kind gift from Dr. Jeffrey Robbins and others. The idea of an in-gel fluorescent staining for amyloids was inspired by an ingenious study by Hervé et al. (2009) who used thioflavin T (ThT) in combination with a general fluorescent protein stain (SYPRO Ruby) to assess cross-contamination of surgical tools with prions. As SYPRO Ruby is typically used to stain proteins separated by gel electrophoresis, we hypothesized that ThT would also work in-gel. We combined the staining with both a modified version of blue native gels in the presence of SDS—referred to as not-so-native (NSN) gels—and regular SDS-PAGE. These approaches have the advantage of separating oligomers and fibrils while enabling easy quantification of these species in a simple gel format across a wide range of molecular sizes. ThT and other related compounds have an affinity for both fibrils and pre-fibrillar oligomers

(Maezawa et al., 2008; Khurana et al., 2005) (named pre-amyloid oligomers, or PAOs henceforth), and its fluorescence increases when ThT is bound to these species (Biancalana and Koide, 2010).

Thioflavin T's signal can be conveniently acquired using a laser scanner equipped with a Cy2 filter ($\lambda_{ex/em}$ = 488/520). A Cy5 ($\lambda_{ex/em}$ = 633/670) filter can be used as a reference filter and for total protein quantification based on Coomassie staining. In short, these aspects, combined with the low cost of the dye, make the described method accessible to a variety of laboratories. The additional optimization of a classical reducing method also allows us to compare the results using ThT with those obtained using more classical approaches [e.g., the A11 antibody (Kayed et al., 2003)]. For these reasons, we believe that this new approach will enable the expeditious quantification, purification, and characterization of amyloid species in different proteinopathies (e.g., cardiac amyloidosis, Alzheimer's disease (AD), and Parkinson's disease).

We first used the ThT in-gel stain to validate the amyloid properties of desmin oligomers in a canine model of dyssynchronous heart failure (HF) (Agnetti et al., 2014). In the study, we separated the oligomers under non-reducing conditions and in the presence of sodium dodecyl sulfate (SDS), using a blue native gel format, which we nicknamed NSN.

More recently, we tested the performance of the staining and optimized the protocol for classical (reducing) SDS-PAGE using the most established model of cardiac proteotoxicity (Sanbe et al., 2004; Rainer et al., 2018). The transgenic mice used in this study express a mutated form (R120G) of the most abundant small heat shock protein in the heart: α-B-crystallin (cryAB). The cardiac-specific expression of this mutated chaperone in transgenic mice induces the formation of desmin PAOs and fibrils.

In the optimized protocol outlined in Figure 1, cardiac extracts are prepared according to our optimized protocol to separate myofilament and cytosolic-enriched fractions (Rainer et al., 2018). This separation consists of a homogenization step in the absence of detergents (cytosolic-enriched, soluble fraction), followed by centrifugation and re-suspension in the presence of detergents (SDS for the myofilament-enriched, insoluble fraction), similar to the protocols used in neuroscience to enrich for fibrils (Wirths, 2017) (Figure 1A). After protein quantification (Figure 1B), samples are diluted in the proper sample buffer for either NSN-PAGE or classical SDS-PAGE, boiled in the latter case, and separated using a standard 1D-PAGE apparatus (Figure 1C). After separation, the gel, which is already blue in the case of NSN and clear in the case of regular denaturing gels, is fixed, rinsed thoroughly in water, and stained with Coomassie for the reducing gels, and its images are digitized before staining with ThT to ensure that potential protein auto-fluorescence in the ThT (Cy2) channel is accounted for (Figure 1D). The gel is then incubated with 50 μM ThT in acidified water and rinsed several times in acidified water to reduce the background and remove ThT speckles before final image acquisition (Figure 1D, see *Methods* for details). Following image acquisition, the gel can be stored in bi-distilled water or dried. The ThT-positive gel bands can be located using the Coomassie image as a reference and excised for downstream in-gel digestion and MS analysis (Figures 1E, F).

When this procedure was used to analyze short cardiac amyloid fibrils using NSN-PAGE, we could detect a ~5-fold increase in a sharp ThT-positive band in R120G cryAB (R120G) mice vs. non-transgenic (NTG) controls (P = 0.0002). Signals for both ThT and Coomassie were digitized and contrast-enhanced (Figure 2A) to enable improved visualization and quantification (Figure 2B). Interestingly, the ThT-positive band was detected at an apparent molecular weight of ~600 kDa. Although NSN separation does not allow for proper molecular weight calibration, we reported a similar electrophoretic mobility of ThT-positive bands in canine failing hearts (Agnetti et al., 2014), suggesting a mechanism of fibrillization that is conserved across species and independent of genetic mutations. This is relevant as many organ proteinopathies (e.g., Parkinson) are sporadic in nature (Del Monte and Agnetti, 2014).

To broaden the applicability of the protocol, we adapted it for use with reducing (classical) SDS-PAGE. We tested the method using both R120G cryAB samples vs. NTG controls and clinical brain specimens from AD patients vs. healthy individuals (CTRL) (Figure 2C). In agreement with our previously published results and the NSN protocol, we detected a ~5-fold significant increase in a ThT-positive band at ~200 kDa under reducing conditions in cryAB R120G cardiac extracts vs. NTG controls (P = 0.0003; Figures 2D, E). We also detected a ~1.5-fold increase in a ~200-kDa ThT-positive band compatible with fibrils in brain extracts from Alzheimer's patients compared to healthy controls (P = 0.176; Figure 2E). We attribute the lack of significance with the latter comparison to the limited number of samples used in this study and the larger variability in patients' cohorts compared to mice with homogeneous genetic backgrounds. As mentioned, Coomassie post-stain allowed us to cross-reference, excise the ThT-positive bands with the naked eye (Figure 2C, mid panel), and confirm equal loading. Under these settings, we were able to confirm the specificity of the stain using a standardized and more robust separation method (classical SDS-PAGE).

Finally, we used the ThT in-gel protocol to measure the accumulation of desmin-positive amyloid fibrils in an established murine model of HF based on transverse aortic constriction (TAC) vs. sham-operated controls (Rainer et al., 2018). We detected a ~2-fold increase in a ~200-kDa ThT-positive band in extracts from TAC mouse samples vs. controls (P = 0.0169; Figure 2G).

To further validate the specificity of ThT staining for amyloid aggregates, we exploited the ability of the small-molecule epigallocatechin gallate (EGCG) to reduce or reverse fibrillization in prion strains (Roberts et al., 2009). Notably, treating cardiac extracts with 100 μM EGCG for 30 min at room temperature (RT) reversed the increase in ThT observed in TAC samples to control levels (P = 0.0039) (Figure 2G). This observation supports the specificity of ThT staining for amyloid species. These combined data suggest that ThT in-gel staining could be applied to a wide number of proteinopathies, including those afflicting organs other than the heart (e.g., the brain).

Methods

Tissue procurement

Eight- to twelve-week-old C57BL/6 mice were subjected to TAC or sham surgery through the Cardiac Physiology Core at Johns Hopkins, as previously described (Rainer et al., 2018; Oeing et al.,

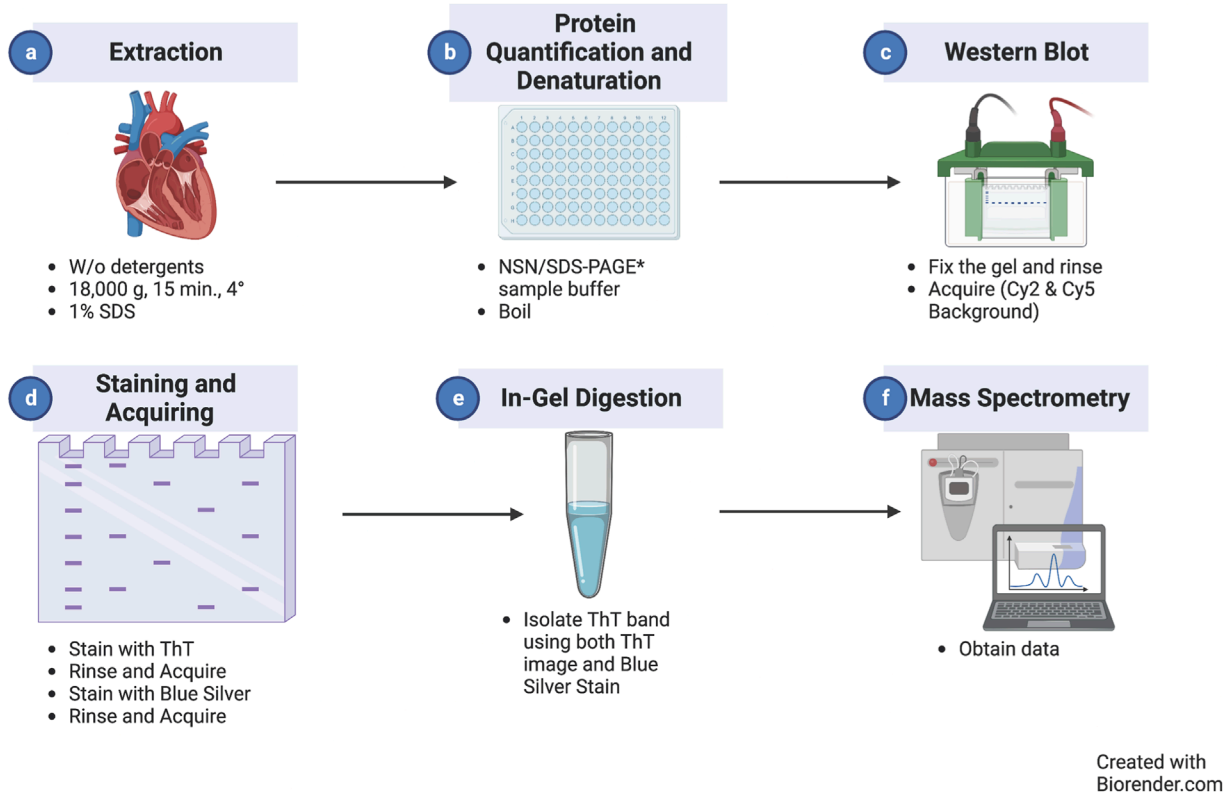

FIGURE 1
Thioflavin T staining/MS workflow. Diagram representing the workflow of the experimental method introduced in this study starting with protein extraction **(a)** followed by protein quantification/detection **(b)**, western blot to fix the gel **(c)**, staining and acquisition **(d)**, in-gel digestion **(e)**, and mass spectrometry for analysis **(f)**.

2021). Four weeks after surgery, TAC mice developed overt HF, as indicated by a decrease in fractional shortening (≤40%) measured by echocardiography. At that time point, mice were anesthetized, and the heart was harvested and snap-frozen according to the protocol approved by the local IACUC. In brief, mice were anesthetized using isoflurane. Upon reaching deep anesthesia with isoflurane (absence of the toe pinch reflex), cervical vertebrae were dislocated, and the heart was quickly extracted through thoracotomy. Freshly explanted hearts were quickly rinsed in ice-cold PBS containing protease (cOmplete Mini, Roche) and phosphatase inhibitors (PhosSTOP, Sigma) to remove excess blood, gently blotted on the clean filter paper to remove excess liquid, snap-frozen in liquid nitrogen, and stored at −80C until further processing. Frozen ventricles from R120G cryAB mice were kindly provided by Dr. Jeff Robbins at the Cincinnati Children's Hospital. Frozen brain tissue from Alzheimer's patients and healthy controls was kindly provided by DR. Juan Troncoso as part of the Baltimore Longitudinal Study on Aging at Johns Hopkins University School of Medicine. All frozen tissue samples were stored at −80 °C until ready for protein extraction.

Protein extraction

Thirty to fifty milligrams of frozen tissue were homogenized in cold PBS (Gibco), supplemented with protease (cOmplete Mini, Roche) and phosphatase (PhosSTOP, Sigma) inhibitors and 25 mM HEPES (AMRESCO). Pre-weighed 2-mL vials were used to obtain the tissue weight. A dry ice-cooled metal bead (Retsch) was placed in each vial, along with five volumes (V/W) of homogenization buffer. Samples were then homogenized for 2 min at 28 Hz using a bead mill (MM400, Retsch) and cooled racks. After milling, samples were pulse-centrifuged and placed in a magnetic rack (Invitrogen) to ensure that the metal bead remained on the side of the vial, and the homogenate was transferred to a new clean vial on ice. The beads were rinsed with three volumes of ice-cold homogenization buffer (V/W) under vortexing, and the resulting solution was combined with the respective homogenate. The resulting tissue homogenates were centrifuged for 15 min (18,000 rcf, 4°C) to obtain soluble and insoluble fractions, which were separated, snap-frozen, and stored at −80°C until further use.

Soluble and insoluble fractions were denatured in LDS buffer (Thermo) within the homogenization buffer, supplemented with 1% DTT (V/V), followed by heat denaturation at 95°C for 10 min. Protein concentration in the denatured samples was measured using the EZQ Protein Quantification Kit (Thermo).

Electrophoresis

For NSN gels, protein extracts from the insoluble fraction were diluted in blue native sample buffer (25 mM Bis-Tris, Bio-Rad; 0.015

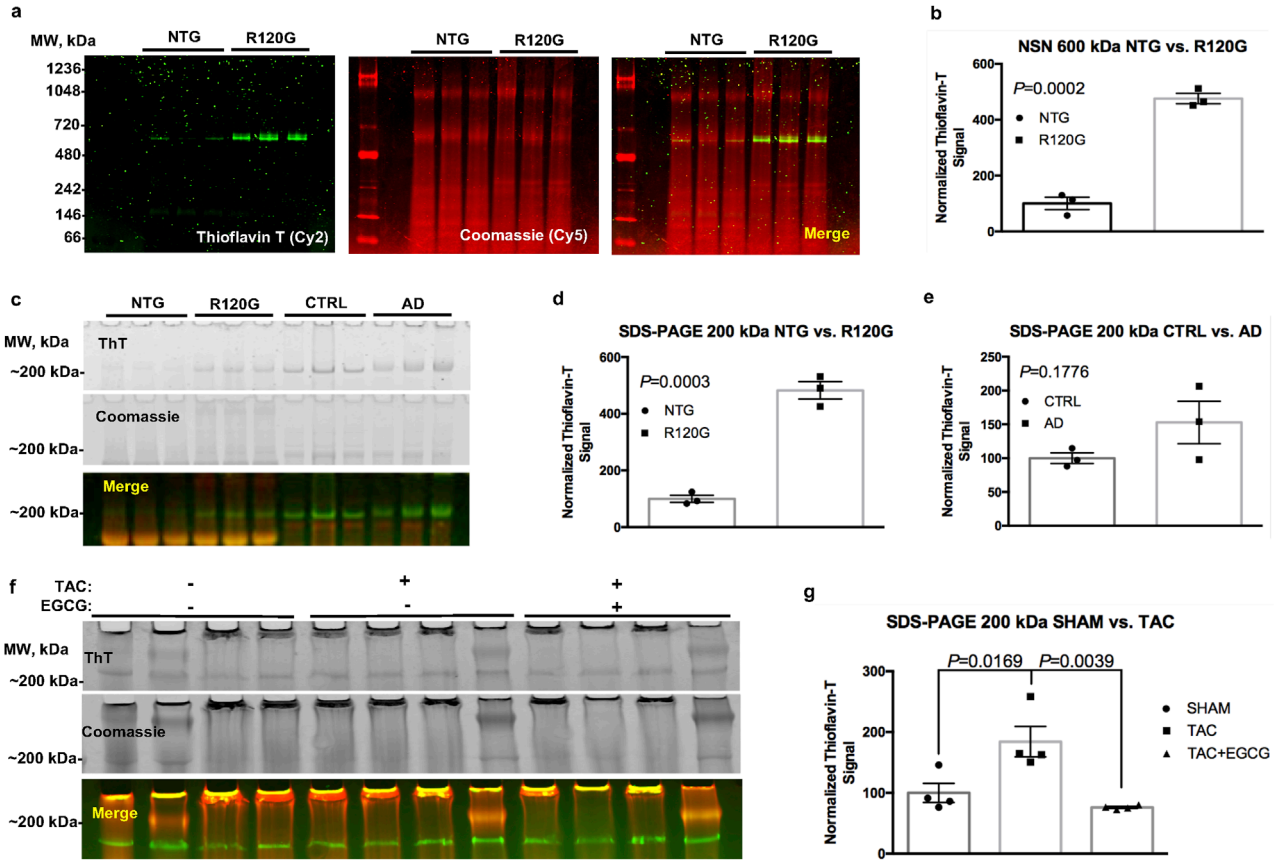

FIGURE 2
ThT stain in cardiac and brain tissue extracts. Representative image of an NSN gel used to separate fibrillar aggregates from NTG and R120G cryAB mice **(a)**, ThT in green and Coomassie in red; corresponding densitometric analysis of the ThT signal at ~ 600 kDA is also provided **(b)**. Representative image of a classical SDS-PAGE gel showing a ThT signal at ~200 kDa in NTG and R120G cryAB mouse cardiac extracts and extracts from healthy human brain (CTRL) and AD human brain tissues from the Baltimore Longitudinal Study on Aging (BLSA) **(c)**. Densitometric analysis of the ThT signal at ~200 kDA is also provided **(d, e)**, respectively). A representative image of the effects of EGCG on extracts from TAC and sham-operated mouse hearts is also provided **(f)**, along with the respective densitometric analysis **(g)**. NTG, non-transgenic; R120G, R120G cryAB mouse heart extracts; CTRL, healthy human brain tissue; AD, Alzheimer's disease; EGCG, epigallocatechin gallate; ThT, Thioflavin T. Mean ± SD is plotted in all graphs. *P*-values were obtained using a student's *t*-test **(b, d–e)** or one-way ANOVA, followed by Sidak's multiple comparison tests **(g)**. Please refer to the text for the abbreviations.

ml of 1 N hydrochloric acid, Fisher Scientific; 10% glycerol, Sigma Aldrich; 25 mM NaCl, Sigma Aldrich; 0.001% Ponceau S, Fisher Scientific; 2% SDS, Fisher Scientific). After incubating samples at RT for 30 min, they were clarified by centrifugation (18,000 rcf, 30 min, 4°C) to remove the insoluble material, and the resulting supernatant was supplemented with 0.25% Coomassie Blue G-250 (Fisher Scientific). A measure of 40 µg of protein per sample was then separated using NuPAGE pre-cast native gels (Thermo) for NSN, while 20 µg of protein were used for classic SDS-PAGE using 3%–12% NuPAGE gels (Thermo). Both types of electrophoreses were performed at 150 V for approximately 1 h. After separation, gels were fixed in 10% acetic acid (Fisher Chemical), 40% methanol (Fisher Chemical), and bi-distilled water overnight to remove excess SDS for downstream excess analysis.

Gel staining and acquisition

The following day, gels were rinsed several times in bi-distilled water to remove excess methanol, and the background fluorescent signal for ThT and Coomassie (Cy2 and Cy5 filters, respectively) was acquired using a Typhoon laser scanner (GE). Gels were subsequently stained with 0.1% (W/V) ThT in acidified water [13.8 µL of 1 N hydrochloric acid (Fisher Scientific) per 50 mL of bi-distilled water] for 1 h in the dark. The ThT working solution was prepared at least 1 hour in advance to maximize solubilization and was kept in the dark. After ThT staining, gels were rinsed extensively in acidified water to remove speckles, followed by a new acquisition of the Cy2 and Cy5 signals using the Typhoon. Following ThT signal acquisition, gels were stained with blue silver

(Candiano et al., 2004) for ≥20 min at RT, rinsed extensively in acidified water, and imaged again to acquire the fluorescent signal for Coomassie (Cy5 filter). The resulting merged images of Coomassie and ThT signals (Figure 2) were used for quantitative analysis and to locate the ThT-positive bands with the naked eye using Coomassie as a reference.

Mass spectrometry

Please refer to the online Methods and Results for LC-MS analysis (Supplementary Figures 1, 2).

Data availability statement

The original contributions presented in the study are included in the article/Supplementary Material; further inquiries can be directed to the corresponding author.

Ethics statement

The studies involving humans were approved by NIH and Johns Hopkins University IRBs. The studies were conducted in accordance with the local legislation and institutional requirements. The participants provided their written informed consent to participate in this study. The animal study was approved by the Johns Hopkins University Institutional Review Board. The study was conducted in accordance with the local legislation and institutional requirements.

Author contributions

JO: writing – review and editing. IT: resources and writing – review and editing. JV: writing – review and editing. JT: resources and writing – review and editing. CG: resources and writing – review and editing. GA: writing – original draft and writing – review and editing.

Funding

The author(s) declare that financial support was received for the research and/or publication of this article. The study was supported by the 18TPA34170382 from the American Heart Association, the RFO from the Italian Ministry of Research and Education, and the Leducq Foundation (20CVD01) to GA.

Conflict of interest

The authors declare that the research was conducted in the absence of any commercial or financial relationships that could be construed as a potential conflict of interest.

Generative AI statement

The author(s) declare that no Generative AI was used in the creation of this manuscript.

Publisher's note

All claims expressed in this article are solely those of the authors and do not necessarily represent those of their affiliated organizations, or those of the publisher, the editors and the reviewers. Any product that may be evaluated in this article, or claim that may be made by its manufacturer, is not guaranteed or endorsed by the publisher.

Supplementary material

The Supplementary Material for this article can be found online at: https://www.frontiersin.org/articles/10.3389/fmolb.2025.1505250/full#supplementary-material

References

Agnetti, G., Halperin, V. L., Kirk, J. A., Chakir, K., Guo, Y., Lund, L., et al. (2014). Desmin modifications associate with amyloid-like oligomers deposition in heart failure. *Cardiovasc. Res.* 102, 24–34. doi:10.1093/cvr/cvu003

Agnetti, G., Lindsey, M. L., and Foster, D. B. (2016). *SpringerLink. Manual of cardiovascular proteomics. 1st 2016*. edn, Germany, (Springer International Publishing : Imprint: Springer.

Biancalana, M., and Koide, S. (2010). Molecular mechanism of Thioflavin-T binding to amyloid fibrils. *Biochimica Biophysica Acta (BBA) - Proteins Proteomics* 1804, 1405–1412. doi:10.1016/j.bbapap.2010.04.001

Candiano, G., Bruschi, M., Musante, L., Santucci, L., Ghiggeri, G. M., Carnemolla, B., et al. (2004). Blue silver: a very sensitive colloidal Coomassie G-250 staining for proteome analysis. *ELECTROPHORESIS* 25, 1327–1333. doi:10.1002/elps.200305844

Chiti, F., and Dobson, C. M. (2009). Amyloid formation by globular proteins under native conditions. *Nat. Chem. Biol.* 5, 15–22. doi:10.1038/nchembio.131

Del Monte, F., and Agnetti, G. (2014). Protein post-translational modifications and misfolding: new concepts in heart failure. *Proteomics Clin. Appl.* 8, 534–542. doi:10.1002/prca.201400037

Hervé, R., Collin, R., Pinchin, H. E., Secker, T., and Keevil, C. W. (2009). A rapid dual staining procedure for the quantitative discrimination of prion amyloid from tissues reveals how interactions between amyloid and lipids in tissue homogenates may hinder the detection of prions. *J. Microbiol. Methods* 77, 90–97. doi:10.1016/j.mimet.2009.01.017

Iino, T., Watanabe, S., Yamashita, K., Tamada, E., Hasegawa, T., Irino, Y., et al. (2021). Quantification of amyloid-β in plasma by simple and highly sensitive immunoaffinity enrichment and LC-MS/MS assay. *J. Appl. Laboratory Med.* 6, 834–845. doi:10.1093/jalm/jfaa225

Kayed, R., Head, E., Thompson, J. L., McIntire, T. M., Milton, S. C., Cotman, C. W., et al. (2003). Common structure of soluble amyloid oligomers implies common mechanism of pathogenesis. *Science* 300, 486–489. doi:10.1126/science.1079469

Khurana, R., Coleman, C., Ionescu-Zanetti, C., Carter, S. A., Krishna, V., Grover, R. K., et al. (2005). Mechanism of thioflavin T binding to amyloid fibrils. *J. Struct. Biol.* 151, 229–238. doi:10.1016/j.jsb.2005.06.006

Mackmull, M. T., Nagel, L., Sesterhenn, F., Muntel, J., Grossbach, J., Stalder, P., et al. (2022). Global, *in situ* analysis of the structural proteome in individuals with Parkinson's disease to identify a new class of biomarker. *Nat. Struct. Mol. Biol.* 29, 978–989. doi:10.1038/s41594-022-00837-0

Maezawa, I., Hong, H. S., Liu, R., Wu, C. Y., Cheng, R. H., Kung, M. P., et al. (2008). Congo red and thioflavin-T analogs detect Aβ oligomers. *J. Neurochem.* 104 (2). 457–468. doi:10.1111/j.1471-4159.2007.04972.x

Mullapudi, V., Vaquer-Alicea, J., Bommareddy, V., Vega, A. R., Ryder, B. D., White, C. L., 3rd, et al. (2023). Network of hotspot interactions cluster tau amyloid folds. *Nat. Commun.* 14, 895. doi:10.1038/s41467-023-36572-3

Oeing, C. U., Jun, S., Mishra, S., Dunkerly-Eyring, B. L., Chen, A., Grajeda, M. I., et al. (2021). MTORC1-Regulated metabolism controlled by TSC2 limits cardiac reperfusion injury. *Circ. Res.* 128, 639–651. doi:10.1161/CIRCRESAHA.120.317710

Rainer, P. P., Dong, P., Sorge, M., Fert-Bober, J., Holewinski, R. J., Wang, Y., et al. (2018). Desmin phosphorylation triggers preamyloid oligomers formation and myocyte dysfunction in acquired heart failure. *Circ. Res.* 122, e75–e83. doi:10.1161/CIRCRESAHA.117.312082

Roberts, B. E., Duennwald, M. L., Wang, H., Chung, C., Lopreiato, N. P., Sweeny, E. A., et al. (2009). A synergistic small-molecule combination directly eradicates diverse prion strain structures. *Nat. Chem. Biol.* 5, 936–946. doi:10.1038/nchembio.246

Ruiz-Arias, Á., Jurado, R., Fueyo-González, F., Herranz, R., Gálvez, N., González-Vera, J. A., et al. (2022). A FRET pair for quantitative and superresolution imaging of amyloid fibril formation. *Sensors Actuators B Chem.* 350, 130882. doi:10.1016/j.snb.2021.130882

Sanbe, A., Osinska, H., Saffitz, J. E., Glabe, C. G., Kayed, R., Maloyan, A., et al. (2004). Desmin-related cardiomyopathy in transgenic mice: a cardiac amyloidosis. *Proc. Natl. Acad. Sci. U. S. A.* 101, 10132–10136. doi:10.1073/pnas.0401900101

Seino, Y., Nakamura, T., Harada, T., Nakahata, N., Kawarabayashi, T., Ueda, T., et al. (2021). Quantitative measurement of cerebrospinal fluid amyloid-β species by mass spectrometry. *J. Alzheimer's Dis.* 79, 573–584. doi:10.3233/JAD-200987

Wall, J. S., Richey, T., Macy, S., Heidel, E., Wooliver, C., and Kennel, S. J. (2013). A novel method for quantifying peripheral tissue amyloid load by using the radiolabeled amyloidophilic peptide, p5. *Amyloid* 20, 21–26. doi:10.3109/13506129.2012.757216

Wirths, O. (2017). Extraction of soluble and insoluble protein fractions from mouse brains and spinal cords. *Bio Protoc.* 7, e2422. doi:10.21769/BioProtoc.2422

frontiers | Frontiers in Molecular Biosciences

TYPE Review
PUBLISHED 02 December 2025
DOI 10.3389/fmolb.2025.1719678

OPEN ACCESS

EDITED BY
Maurizio Renna,
University of Naples Federico II, Italy

REVIEWED BY
Katja Venko,
National Institute of Chemistry, Slovenia
Miha Lukšič,
University of Ljubljana, Slovenia

*CORRESPONDENCE
Ambuja Navalkar,
ambuja@nccs.res.in
Anoop Arunagiri,
arunagiri@etsu.edu

RECEIVED 06 October 2025
REVISED 11 November 2025
ACCEPTED 12 November 2025
PUBLISHED 02 December 2025

CITATION
Navalkar A, Arunagiri A, Kee T, Panchal K and Dick K (2025) Protein aggregates and biomolecular condensates: implications for human health and disease.
Front. Mol. Biosci. 12:1719678.
doi: 10.3389/fmolb.2025.1719678

Protein aggregates and biomolecular condensates: implications for human health and disease

Ambuja Navalkar[1]*, Anoop Arunagiri[2]*, Tovaria Kee[2], Kathigna Panchal[2] and Kathryn Dick[2]

[1]National Centre for Cell Science, Savitribai Phule Pune University Campus, Pune, Maharashtra, India, [2]Department of Biological Sciences, East Tennessee State University, Johnson City, TN, United States

Biomolecular condensates are at the forefront of understanding biological concepts, representing one of the most revolutionary areas in cell biology over the last decade. Numerous proteins, peptides, and nucleic acids have been shown to form membrane-less organelles, also known as condensates, in cells, demonstrating their functional relevance. Multiple research approaches in the fields of physics, chemistry, and biophysics investigate the underlying multivalent interactions that influence the phase separation of biomolecules. As failure to regulate condensate properties, such as formation and/or dissolution has been postulated as a driver of the misfolding and aggregation of proteins in stress, aging, and neurodegeneration disorders, understanding the fundamentals of condensate assembly has been considered of utmost importance. In this review, we will focus on the key regulators and biophysical drivers of phase separation and protein aggregation, evidenced in the literature. We will elaborate on the dynamic interplay between phase separated and aggregated state, highlighting the emergent properties of condensates that can contribute to the misfolding of proteins in the context of physiology and diseases. An in-depth understanding of condensate pathology can reveal novel avenues for targeting proteinopathies linked to misfolding.

KEYWORDS

protein aggregates, biomolecular condensates, protein misfolding, proteinopathies, amyloid

1 Introduction

A plethora of proteins maintain cell homeostasis, which is facilitated by protein conformations often associated with specific functions. In recent years, research has focused on understanding the biophysical properties associated with protein assemblies and how they relate to function and diseases (Jucker and Walker, 2018; Kroschwald et al., 2022). Amino acid sequence and the environment (solvent milieu) in which the protein is present can dictate the protein folding landscape (Rumbley et al., 2001), in which a vast array of possible conformations a protein can adopt. Within this landscape, the protein structure assumes a specific three-dimensional arrangement by which it can perform its biological function. This structure typically includes primary, secondary, tertiary, and at times quaternary levels of organization (Englander and Mayne, 2014). Protein structural elucidation is important for understanding how proteins fold, function, and interact

(Chiesa et al., 2020). Researchers have adopted a range of methods, such as Nuclear Magnetic Resonance (NMR) spectroscopy, X-ray crystallography, and, more recently, AlphaFold, aimed at accurately experimentally determining protein states and predicting structures, respectively (Jumper et al., 2021; Kuh et al., 2019). Proteins achieve their specific native structure through a precise and complex folding process. The formation of partially folded intermediates and the crucial involvement of various cellular components, including molecular chaperones, various ions, and inorganic molecules, can influence protein stability and interactions. In some cases, cellular membranes can provide a scaffold or environment for folding (Saibil, 2013). When one or more of these factors fail to exist or function, the protein folding process can go awry, leading to misfolded structures that deviate from their native conformation (Kha et al., 2022). One such outcome is the formation of amyloids—insoluble fibrillar aggregates characterized by a cross-β-sheet structure. Amyloid formation is often associated with a shift in the protein energy landscape, where misfolded intermediates become trapped in energetically stable states (Kha et al., 2022; Eisenberg and Jucker, 2012). While the amyloid state is not completely understood, the formation of protein aggregates is implicated in a variety of neurodegenerative diseases, including Alzheimer's, Parkinson's, and Huntington's disease (Eisenberg and Jucker, 2012). A subset of protein aggregation, however, is reversible and has been evidenced to be associated with function (Hammer et al., 2008; Iconomidou and Hamodrakas, 2008). Functional amyloids are fascinating examples of how proteins can self-assemble to benefit cells across all life forms (Gebbink et al., 2005; Badtke et al., 2009; Maury, 2009). Unlike the pathological amyloids associated with diseases, these evolved structures perform native-like functions, acting as crucial components in various biological processes (Gebbink et al., 2005; Badtke et al., 2009; Maury, 2009). The precise self-assembly allows them to carry out vital roles within the cell without the cellular toxicity, which is often associated with the pathological amyloids (Iconomidou and Hamodrakas, 2008; Wang and Chapman, 2008). Studying how the protein landscape contributes to both proper functions associated with folding and pathological misfolding provides critical insights into disease mechanisms and opens potential avenues for therapeutic intervention.

In the recent decade, an interesting paradigm shift has been observed in the field of protein assemblies due to the observation of organizational assemblies called biomolecular condensates (Banani et al., 2017; Lyon et al., 2021; Li et al., 2022). With the emerging evidence of biomolecular condensates, the process of phase separation has been extensively recalled as an underlying driving force. In cells, phase separation has been predicted to organize specific biomolecules like proteins, RNA, and DNA into dynamic, membrane-less compartments (Fare et al., 2021). This organization has been speculated to be associated with diverse but targeted cellular roles by proteins (Fare et al., 2021). Phase separation has been postulated to facilitate the formation of various membraneless organelles or compartments within the cytoplasm and nucleus. Few extensively studied examples of biomolecular condensates include: processing bodies (P bodies), stress granules (SGs), Balbiani bodies, germ granules, promyelocytic leukemia (PML) bodies, Cajal bodies, nuclear speckles, and nucleoli, among others (Banani et al., 2017; Fare et al., 2021; Alberti and Hyman, 2021; Li et al., 2022).

Biomolecules within these condensates are shown to be highly dynamic, and the dynamicity has been measured using fluorescence-based techniques like FRAP. However, in the recent decade, several studies have focused on the alternation of this dynamic nature of condensates over time or under specific cellular contexts (Lyon et al., 2021). For example, during pathological aggregation or stress conditions, these molecules are shown to lose their dynamicity to form immobile states. Often these arrested assemblies have been termed gel- or solid-like, a rheological phenomenon which needs to be explored further (Alberti and Hyman, 2021; Visser et al., 2024). Abnormal phase separation has been speculated to be involved in protein condensation and aggregation, as well as in the development and progression of numerous diseases. Over the past decade, research from various groups has attempted to establish a link between protein phase separation and aggregation, which is relevant in understanding the mechanism of pathogenesis of neurodegenerative disorders (Han et al., 2024; Mathieu et al., 2020; Vendruscolo and Fuxreiter, 2022). While these findings have deepened our mechanistic understanding of such diseases, they also highlight the need to explore the complex nature of protein assemblies for appropriate therapeutic intervention. The current experimental efforts in the fields of phase separation and aggregation are extensively reviewed in the literature (Visser et al., 2024; Hribar-Lee and Luksic, 2024; Chakraborty and Zweckstetter, 2023).

Here, we first sought to define the biophysical characterization and the underlying principles of the protein assemblies. We further highlight the studies that demonstrate the functional relevance of different protein assemblies that have been under study for their condensate-forming and aggregation potential. In this review, we aim to enhance the current understanding of the connection between protein phase separation, aggregation, and major aggregation-linked diseases, and predict future advancements needed for establishing a mechanistic foundation across cellular pathways governed by condensates and protein aggregates.

2 Assembly of biomolecules in cells

Biomolecules form hierarchies of assemblies depending on the governing interactions and the underlying grammar of amino acid sequences (Figure 1). Biophysical properties of the protein assemblies can contribute to the formation, stability, and ultimately functional relevance in the context of a cell. We further describe some of these assemblies based on their measurable and predictable properties.

2.1 Condensates

Biological systems have recently garnered attention for their ability to form dynamic liquid-like compartments through the multivalent interactions of proteins and/or nucleic acids, which allows them to organize cellular biochemistry without membranes (Banani et al., 2017). Weak, multivalent, and reversible interactions among intrinsically disordered regions (IDRs), low-complexity domains, and folded domains of the proteins have been speculated to be involved in the formation of these dynamic, membrane-less organelles (Figure 1, Types of multivalent assemblies). The

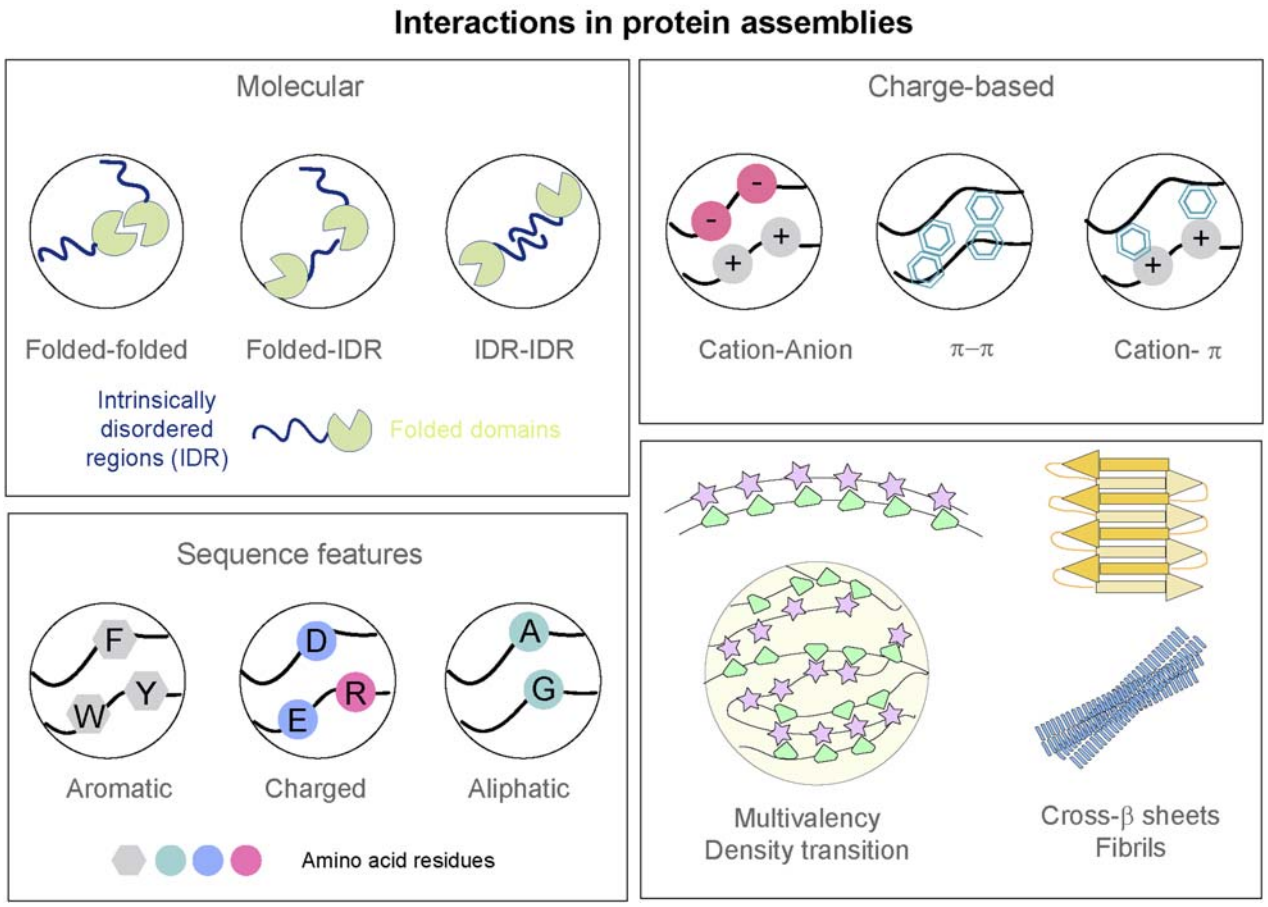

FIGURE 1
Interactions governing formation of protein assemblies. *Top left:* Interactions between folded domains and intrinsically disordered regions (IDR) of protein polypeptides. *Top right:* Schematic representation of the multivalent interactions—including electrostatic, π–π stacking, cation-π, that can possibly drive the assembly of proteins. *Bottom left:* Amino acid residues with aromatic, charged, and aliphatic natures can dictate the sequence features of the protein polypeptides. *Bottom right:* Multivalency in biomolecules can lead to condensate formation. Cross-β architecture and ordering can lead to more rigid and irreversible amyloid states.

classification of these assemblies, the nomenclature (called as dynamic droplets/condensates/hubs/puncta) and the underlying principles have been a topic of debate. The nomenclature is ambiguous due to lack of concrete biophysical characterization of these membraneless assemblies but for simplicity and clarity, we will use the term "condensates" throughout the review. These condensates are shown to undergo coalescence with high internal molecular mobility in several cases (Choi et al., 2020; Feng et al., 2019). The functional role of condensates in organizing biochemical reactions has been elucidated in biological processes linked to nucleoli, stress granules, and P bodies (Boeynaems et al., 2018). Additionally, cellular processes, like transcription (Pei et al., 2025), translation (Ramat and Simonelig, 2022), and DNA damage repair (Kilic et al., 2019; Pessina et al., 2019), are under scrutiny for studying the regulatory control of biomolecular condensates.

Various groups have investigated the dynamics, as well as the viscoelasticity and surface tension, of condensates involved in different cellular processes. The condensate assemblies are highly responsive to environmental changes like concentration of salt, pH, temperature, crowding, and stress. Aberrant formation of condensates due to the deregulation of cellular processes has been hypothesized (Alberti and Hyman, 2021; Mathieu et al., 2020). Aging and maturation of condensates leading to loss of dynamicity have been linked to neurodegenerative diseases such as Alzheimer's disease and Parkinson's disease (Alberti and Hyman, 2021; Visser et al., 2024; Han et al., 2024; Mathieu et al., 2020; Ray et al., 2020).

Furthermore, percolated networks can arise with a mixture of individual biomolecules, typically proteins or nucleic acids. In a percolated network, the multivalent biomolecules behave like associative polymers that form reversible, noncovalent cross-links. When the number of cross-links crosses a threshold known as the percolation threshold, the molecules are incorporated into a system-spanning (percolated) network. The cross-linking in such percolation networks is formed via transient or stable non-covalent interactions, often driven by multivalent domains (e.g., repeats of SH3, PRM, or intrinsically disordered regions). Mittag and Pappu (2022) offer a comprehensive "phase separation coupled to percolation" (PSCP) framework that unifies phase separation and network formation in biomolecular condensates

(Mittag and Pappu, 2022). The cellular condensates are dense liquid droplets with a viscoelastic network whose properties derive from the interplay between polymer-like networking (percolation) and density-driven phase separation. This coupling can lead to sequence- and topology-specific internal structures and allows the formation of protein clusters even below phase separation thresholds (Mittag and Pappu, 2022). Further, Das and Deniz (2023) focus on how topological characteristics, particularly percolation and polymer entanglement, shape condensate architecture and material behaviours. The network topology provides a mechanistic basis for condensates' connectivity, while entanglement influences their dynamics and viscoelasticity, highlighting open questions for future research (Das and Deniz, 2023). Deniz (2022) extends the conceptual discussion by linking percolation theories from polymer physics to biomolecular condensation phenomena observed experimentally and computationally (Deniz, 2022). This supports the prediction that pre-percolation clusters can form well below saturation concentrations, challenging classical nucleation models and implying a role for percolation in diseases like neurodegeneration. This line of thought supports the integrated perspective that condensate behaviours emerge from a balance of density transitions and network connectivity. The percolated networks may form within biomolecular condensates and can impart biophysical features to the assemblies. These networks may be subjected to changes depending on the proteins involved and environmental factors. Hence, these biophysical features have to be thoroughly investigated to understand and predict the protein behaviour in cells.

2.2 Reversible fibrils

Reversible fibrils are filamentous assemblies that can dynamically assemble and disassemble under physiological conditions, often serving as regulatory or storage structures (Saad et al., 2017). The fibrils are ordered and β–sheet–rich but may not be tightly packed as amyloid fibrils. The reversibility of the fibrils is attributed to the changes in conditions such as pH or phosphorylation. Several of these reversible amyloids have been demonstrated to work in signaling, scaffolding, or reversible sequestration in the cellular *milieu* (Saad et al., 2017; Gui et al., 2019; Lacroix et al., 2021). Proteins like hnRNPA1 have been predicted to contain low-complexity domains that facilitate reversible fibril formation (Gui et al., 2019). These domains can form labile, reversible fibrils that are sensitive to environmental conditions, aiding in dynamic cellular processes. Several peptide hormones, including insulin, somatostatin, growth hormone, and β-endorphin, are known to adopt reversible amyloid-like states as part of their normal physiological packaging and storage (Horváth et al., 2023; Maji et al., 2009; Anoop et al., 2014; Jacob et al., 2016). In the secretory granules of endocrine and neuroendocrine cells, these hormones form dense, amyloid-like aggregates that serve to concentrate and stabilize hormones for regulated secretion. Unlike disease-associated amyloids, these aggregates are dynamically reversible: they disassemble upon exocytosis to release active, functional monomers in response to stimuli (Maji et al., 2009). This paradigm of reversible amyloid formation illustrates how nature harnesses protein assemblies and conformations with amyloid-like structures for beneficial roles, distinguishing them from pathogenic aggregates in neurodegenerative diseases.

2.3 Amyloid fibrils

Amyloid fibrils are highly ordered, β–sheet–rich polypeptide aggregates characterized by a cross-β spine architecture, where β-strands are stacked perpendicularly to the fibril axis (Maji et al., 2009; Toyama and Weissman, 2011). These structures are extremely stable, resistant to proteolysis, detergents, and heat, and exhibit very low molecular mobility in cells. Amyloid fibrils grow by recruiting monomeric proteins, and can seed the formation of new fibrils in a prion-like manner. The nucleation step is crucial to the assembly of amyloid aggregates and is often thought to be the rate-limiting step in the assembly process (Rambaran and Serpell, 2008). Pathological amyloids, such as Aβ in Alzheimer's (Selkoe, 1991), α-synuclein in Parkinson's (Goedert et al., 2001), and TDP-43 (Prasad et al., 2019) or FUS in ALS are implicated in neurodegenerative diseases (Takanashi and Yamaguchi, 2014).

A critical determinant of function *versus* pathological state of proteins may be their way of assembly into higher-order assemblies and, therefore, the emergent properties of these assemblies. Together, the elucidation of molecular aspects of protein assemblies marks an important paradigm shift in viewing protein assemblies through the dual lenses of biological assemblies and network physics, and calls for further exploration of their topology-function relationships in health and disease.

The above classified assemblies and their properties have been explored in detail cellular processes and in the context of disease. Hereafter, we will delve into the studies that highlight the interplay between protein phase separation and aggregation as observed in various proteins to date (Table 1).

3 Implications of condensate formation and aggregation in physiology and disease

3.1 Stress granules

Stress granules (SGs) are membrane-less cytoplasmic assemblies of mRNA and proteins that form in response to cellular stress (e.g., oxidative stress, heat shock, viral infection) (Alberti and Hyman, 2021). They are known to sequester stalled translation initiation complexes, helping to reprogram gene expression and protect mRNA until stress resolves (Ramaswami et al., 2013). Recent evidence indicates that the formation of stress-granules is attributed to multivalent interactions between involved proteins (Riback et al., 2017). Furthermore, SGs have been increasingly linked to neurodegenerative diseases because alteration of their phase-behaviour of the proteins can lead to persistent, aggregation-prone assemblies. We summarize below the key reports on proteins involved in the formation of stress granule assemblies.

3.1.1 G3BP1

G3BP1 and G3BP2 proteins are shown to assemble stress granules (SGs) through multivalent crosslinking of

TABLE 1 Protein aggregation and condensation in physiological contexts.

	Observations		Key references
Protein	Aggregation	Phase separation	
Stress granules			
G3BP1	G3BP1 drives the nucleation stress of granule formation, aiding in the formation and dynamics of protein-RNA aggregates	G3BP1 undergoes phase separation with RNA to form condensates (possibly leading to stress granule formation) in response to cellular stress G3BP1 condensation is regulated by protein concentration, RNA binding, and interactions with partners like Caprin-1 and USP10	Matsuki et al. (2013), Guillén-Boixet et al. (2020), Yang et al. (2020), Parker et al. (2025), Schulte et al. (2023)
hnRNPA1	Mutations in hnRNPA1 promote irreversible amyloid formation and impair droplet dynamics, potentially leading to pathological protein aggregation Dysregulated PARylation contributes to hnRNPA1 aggregation and neurodegenerative disease	hnRNPA1 undergoes phase separation via its low-complexity domain, which aids in stress granule assembly during cellular stress	Molliex et al. (2015), McGurk et al. (2018), Linsenmeier et al. (2023), Das et al. (2025)
TDP-43	When TDP-43 exceeds a threshold and RNA recognition motif 1 (RRM1) unfolds, exposed hydrophobic regions and cysteines form disulfide bonds, leading to amyloid-like aggregates in stress granules Mutations that prevent TDP-43 demixing block pathological aggregation, showing that stress granules can become pathological when intra-condensate organization seeds facilitate the aggregation process	TDP-43 forms condensate within stress granules under cellular stress, with intra-condensate demixing modulated by its multidomain structure and RNA interactions YAP directly binds to TDP-43 and regulates the dynamic behavior of stress granules and condensates by promoting TDP-43 homotypic multimerization and phase separation This interaction helps maintain the number and fluidity of TDP-43 condensates while preventing their pathological solidification under stress conditions	de Boer et al. (2020), Yan et al. (2024), Scherer et al. (2024), Matsushita et al. (2025)
Secretory granules			
Insulin	At insulin injection sites, insulin can aggregate into amyloid fibrils, leading to localized amyloidosis; these fibrils are stabilized by hydrophobic interactions and disulfide bonds Insulin aggregation is influenced by pH, temperature, and reducing agents, while macrocyclic compounds like pentaphenarene (PPAS) can inhibit and reverse fibrillation	Insulin undergoes phase separation and forms condensates for efficient storage in pancreatic β-cell secretory granules, a process facilitated by chromogranin proteins Insulin can assemble into metastable nano-condensates that serve as precursors to aggregation and fibrillation	Parchure et al. (2022), Vorontsova et al. (2015), Toledo et al. (2023), Suladze et al. (2024), Karmakar et al. (2022), Wang et al. (2014)
Chromogranin	Chromogranin condensates transition from a liquid-like to a solid aggregate state, hindering the protein's ability to recruit hormones, disrupting proper packaging Premature aggregation in the TGN hinders hormone storage and secretion	Chromogranin A and B undergo phase separation in the trans-Golgi network, forming condensates that act as scaffolds for hormone packaging into secretory granules	Parchure et al. (2022), Campelo et al. (2024)
Protein assemblies in diabetes			
IAPP	In type 2 diabetes, IAPP aggregates into highly stable, β-sheet-rich amyloid fibrils within the islets, contributing to β-cell dysfunction and death	IAPP is stored in pancreatic β-cell secretory granules in a soluble or reversible condensate state It prevents premature aggregation and allows for regulated hormone secretion	Westermark and Westermark (2011), Akter et al. (2016), Mukherjee et al. (2017), Wang et al. (2014), Hassan et al. (2022)
Proinsulin	Misfolded proinsulin forms insoluble aggregates in the ER, leading to β-cell dysfunction and diabetes Genetic mutations or ER stress can increase proinsulin aggregation, as in MIDY, where mutant proinsulin traps wild-type proinsulin and reduces insulin production	Proinsulin forms dynamic, reversible condensates during maturation, essential for proper insulin sorting and secretion ER chaperones prevent unwanted condensation, but in the Golgi, condensation enables efficient hormone storage; disruption can cause harmful aggregation and β-cell failure	Parchure et al. (2022), Toledo et al. (2023), Arunagiri et al. (2019), Parashar et al. (2021), Arunagiri et al. (2024)

(Continued on the following page)

TABLE 1 (*Continued*) Protein aggregation and condensation in physiological contexts.

	Observations		Key references
Protein	Aggregation	Phase separation	
Neurodegeneration-associated proteins			
Tau	Tau droplets serve as intermediates in forming Tau aggregates by spatial organization within the cytoplasm Also, it helps in forming amyloid aggregates by being involved in the formation of toxic oligomers that develop into amyloid aggregates	Tau undergoes phase separation to form Tau condensates in cells Tau condensates regulate microtubule assembly but have been involved in the formation of toxic oligomers that develop into amyloid aggregates	Wegmann et al. (2018), Ambadipudi et al. (2017), Hernández-Vega et al. (2017), Tsoi et al. (2025)
Amyloid-β (Aβ)	The condensates mature into aggregates via the biomolecular condensate phase of the peptide, which increases the fundamental nucleation step in Aβ42 aggregation These aggregates are involved in neurodegenerative diseases such as Alzheimer's disease and other amyloid diseases	Amyloid-β also forms condensates primarily of Aβ42 with the help of lipids as a cofactor. Thus, it is present near or on the cell surface Also, it needs a cell to grow into aggregates, supporting the role of the cell membrane in the development of the condensates	Chen et al. (2017), Yang et al. (2019), Morris et al. (2024), Šneiderienė et al. (2025)
α-Synuclein (αSYN)	The condensates formed help in an increased rate of amyloid aggregates The fibril aggregates formed from the condensates are seen in neurodegenerative diseases like Parkinson's disease	α-Synuclein also forms condensates by phase separation These condensates help in fibril aggregation through C-terminal domains and electrostatic forces α-Synuclein condensate formation may be implicated in driving disease associated aggregation of the protein	Luk et al. (2009), Sacino et al. (2014), Ray et al. (2020), Chandran et al. (2025), Hardenberg et al. (2021)

This table summarizes the aggregation and condensation behaviours of various proteins, highlighting how these behaviours are influenced by different physiological conditions.

ribonucleoprotein particles (RNPs) (Matsuki et al., 2013; Guillén-Boixet et al., 2020). The protein G3BP1 serves as a central molecular switch controlling stress granule formation via phase separation (Yang et al., 2020). G3BP1 promotes interaction with RNA at the intermolecular level (Parker et al., 2025) to initiate RNA-dependent condensate formation, potentially driving stress granule assembly. It is speculated that extrinsic binding factors/proteins can modulate this process, either promoting or inhibiting stress granule assembly by interacting with the G3BP1-driven core network. G3BP proteins, thus, act as a central node and molecular switch in SG assembly (Guillén-Boixet et al., 2020). The G3BP1 homodimer undertakes both distinct expanded and compact conformations in solution, with transitions modulated little by physiological changes in ionic strength and pH, as G3BP1 can undergo RNA-independent phase separation at pH 6. G3BP1's function is modulated by interactions with proteins such as Caprin-1 and USP10. Caprin-1 promotes SG formation, while USP10 inhibits it. Interestingly, the C-terminal domain of Caprin-1 can undergo spontaneous phase separation, facilitating SG assembly, whereas its N-terminal domain suppresses G3BP1's phase separation, highlighting a regulatory mechanism (Schulte et al., 2023; Han et al., 2025).

More importantly, reconstituted stress granules from cell lysates show that G3BP1 concentration and RNA availability determine whether assemblies remain liquid-like or undergo aggregation-prone maturation (Freibaum et al., 2021). It was demonstrated that G3BP1 also has "condensate chaperone" functions, which enhance the assembly of SGs but get dispersed after the initial condensation. After the granule formation, G3BP1 is used for the RNA component of granules to continue *in vitro* and in cells when RNA decondensers are inactivated. These findings demonstrate that G3BP1 functions as an "RNA condenser" (Parker et al., 2025). The evidence also showcases the role of G3BP1 conformational plasticity in condensate assembly and aggregation. Thus, the evidences suggest that the critical interplay of interactions in proteins and RNA can dictate the properties and the fate of the assemblies formed. The role of RNA (its sequence and/or its length in affecting the network formation and maturation of protein assemblies. Hence, a detailed study of this relationship is essential to distinguish properties of reversible condensate formation of G3BP1 from pathological aggregation and to understand their impact on cellular stress responses.

3.1.2 hnRNPA1

Heterogeneous nuclear ribonucleoprotein A1 (hnRNPA1) is one of the most abundant proteins expressed in eukaryotic cells and is a pivotal RNA-binding protein involved in RNA metabolism processes such as pre-mRNA splicing, transcriptional regulation, localization, and transport (Guil et al., 2006). Under cellular stress, hnRNPA1 contributes to the formation of stress granules and phase separation, a process driven primarily by its intrinsically disordered low-complexity domain (LCD) (Molliex et al., 2015; Wang et al., 2021). Reversible interactions within hnRNPA1 droplets decrease their dynamicity, reinforcing phase separation and possibly facilitating stress granule assembly (Molliex et al., 2015; Wang et al., 2021). Mutations promoting irreversible

amyloid formation impair droplet dynamics, potentially leading to pathological aggregates (Molliex et al., 2015). Poly (ADP-ribosyl)ation (PARylation) of hnRNPA1 enhances its phase separation and promotes co-phase separation with other RNA-binding proteins like TDP-43 (McGurk et al., 2018). Additionally, increasing cellular PARylation levels by knocking down PARG delays the disassembly of stress granules, which contain components like hnRNPA1 and FUS (Liu et al., 2025). This modification regulates stress granule dynamics and, when dysregulated, may contribute to neurodegenerative disease pathogenesis. For establishing a link between phase separation and aggregation of hnRNPA1, Linsenmeier et al. showed that the hnRNPA1 low-complexity domain forms amyloid fibrils predominantly at the condensate interface, suggesting that molecular orientation and conformation at the boundary actively promote fibrillation (Linsenmeier et al., 2023). In contrast, Das et al. reported that condensates formed by prion-like domains, while also nucleating fibrils at their interfaces, inhibit fibril growth within and act as protein sinks, sequestering soluble proteins and releasing them slowly, thereby restricting fibril development in the surrounding phase (Das et al., 2025). These reports underline the importance of understanding the emergent properties of condensates and their interfaces. The systems used to study the biophysical properties can also influence the pathogenic aggregation pathways and therefore have to be systematically characterized with caution.

3.1.3 TDP-43

TDP-43, a nuclear RNA-binding protein linked to amyotrophic lateral sclerosis (ALS) and frontotemporal dementia (FTD), is known to mislocalize and accumulate in cytoplasmic stress granules under cellular stress (de Boer et al., 2020). Under oxidative conditions, TDP-43 undergoes intra-condensate demixing (Yan et al., 2024). TDP-43 forms a sub-phase inside the granule that acts as a seed for pathological amyloid-like aggregates (Yan et al., 2024). TDP-43-polyA interactions are formed when TDP-43 binds with RNA (Scherer et al., 2024), which further can alter the viscoelastic properties of the condensates. The presence of polyA increases elasticity, making viscosity and elasticity comparable in magnitude. These findings suggest that the multidomain structure of TDP-43 and its RNA interactions orchestrates condensate organization and modulates their viscoelastic properties (Matsushita et al., 2025). The study highlights how stress granules, normally protective, can become pathological environments when intra-condensate organization facilitates protein aggregation (Matsushita et al., 2025). Fernandes et al. also demonstrate that while stress granules can facilitate TDP-43 aggregation, they are not strictly required for its cytoplasmic assembly (Fernandes et al., 2020). In yeast, most TDP-43 foci initially co-localize with SG-like structures, but many later dissociate and associate with P-bodies or exist independently. Similarly, in mammalian cells, disrupting SG formation reduces but does not abolish TDP-43 foci, highlighting a modulatory rather than essential role for SGs (Fernandes et al., 2020). These observations reflect how sequence composition, RNA concentration, and composition of biomolecules can tune the internal dynamics and material states of condensates. Therefore, such emergent viscoelastic behaviour can help understand the underlying transition from functional RNA–protein assemblies to aberrant, aggregation-prone states linked to disease.

Overall, the examples of proteins from stress granule assemblies demonstrate that the state and composition of protein assemblies can be influenced by intrinsically disordered regions, post-translational modifications, and environmental cues. The formation and maintenance of SGs is a vital phenomenon to demonstrate the complex balance between condensate formation and amyloid aggregation of proteins. Understanding the inherent tug-of-war identifies molecular targets to restore stress granule dynamics and design therapeutics for neurodegeneration and stress-related diseases. Future research in this area can be directed at understanding the changes associated with the dynamicity of molecules, material properties, and rheology of heterogeneous systems.

3.2 Secretory granules

3.2.1 Insulin

Insulin, a peptide hormone vital for glucose regulation, has a notable tendency to undergo aggregation under specific conditions (Mori et al., 2022). This behaviour holds both physiological importance, as seen in insulin's storage within pancreatic β-cell secretory granules, and pathological relevance, such as the formation of amyloid deposits at injection sites for diabetic patients. In pancreatic β-cells, insulin is stored in secretory granules, with studies suggesting that chromogranin proteins facilitate this by undergoing condensate formation in the trans-Golgi network, recruiting insulin for packaging without needing specific cargo receptors (Parchure et al., 2022). Insulin can also form metastable nano-condensates, or "mesoscopic clusters", which are precursors to fibrillation (Vorontsova et al., 2015; Toledo et al., 2023). Pathologically, at frequent insulin injection sites, insulin can aggregate into amyloid fibrils, leading to localized amyloidosis, where the fibrils arestabilized by hydrophobic interactions and disulfide bonds, forming the amyloid core (Suladze et al., 2024). Factors like pH, temperature, and reducing agents significantly influence the aggregation; for instance, protein disulfide isomerase can catalyse disulfide bond reduction, promoting structures rich in antiparallel β-sheets (Suladze et al., 2024). Understanding these mechanisms and the connection between phase separation and aggregation is crucial for improving insulin storage and delivery as well as for mitigating amyloid-related complications in diabetic patients.

Recent research has significantly advanced our understanding of the intricate processes governing insulin aggregation and condensation *in vitro*, revealing diverse pathways, intermediate states, and potential applications. Across separate investigations, scientists have illuminated how molecular design, environmental factors, and specific interacting agents influence the formation and characteristics of insulin aggregates, from amyloid fibrils to reversible condensates. A recent study showed that the length of an oligolysine segment (Kn) from insulin-derived peptides (ACC1-13Kn) determines their ATP-driven aggregation (Dec et al., 2023). The shorter Kn variants (n = 8, 16) formed amyloid fibrils directly, whereas longer ones (n = 24, 32, 40) first underwent phase separation before forming insulin fibrils. ATP acted as a key counterion, likely engaging the cationic oligolysine via Coulombic attraction, thereby directing these transitions. Given ATP's role in secretory granules,

this mechanism may underlie its influence on insulin storage and aggregation. Environmental factors such as ionic strength and pressure further modulated these phase-to-fibril conversions (Dec et al., 2023). Expanding on the concept of varied aggregation pathways, another study meticulously differentiated two distinct types of human insulin amyloids: (i)-amyloid and (r)-amyloid. The (i)-amyloid, formed without a reducing agent, characteristically exhibited a transient phase separation phase, manifesting as fluid, hydrophobic droplets that subsequently matured into fibrils. Its formation was notably inhibited by 1,6-hexanediol, which dissolved these droplets and, importantly, preserved cytotoxic soluble oligomers. This pathway was also accelerated by chaotropic anions. In stark contrast, the (r)-amyloid, formed in the presence of a reducing agent, directly generated amorphous aggregates without any observable phase separation intermediate. These aggregates displayed lower fluidity, stronger hydrophobic interactions, and were promoted by kosmotropic ions, underscoring fundamental differences in their formation mechanisms and potential for toxicity (Mori et al., 2022). Further demonstrating the versatility of insulin's self-assembly, Karmakar et al. (2022) explored zinc-induced insulin condensation (Karmakar et al., 2022). This research identified an optimal equimolar ratio of zinc to insulin combined with thermal stress that promoted robust insulin aggregation into a unique protein condensate. This process involved a shift in insulin's isoelectric point and the formation of specific conformational variants (Karmakar et al., 2022). The resulting condensates exhibited hallmark properties of protein condensates: a porous, amorphous, and macromolecular structure, viscoelastic behavior, and remarkable reversibility, capable of dissolution upon pH reduction.

Collectively, these studies underscore the complex and tunable nature of insulin aggregation, ranging from ATP- and oligo-lysine-driven phase separation intermediates to distinct amyloid polymorphs and zinc-induced condensates with engineered functionalities. This body of work aligns with the broader understanding that functional amyloids can serve as natural storage mechanisms for peptide hormones (Maji et al., 2009), extending this concept to the intricate behaviors of insulin in physiological contexts.

3.2.2 Chromogranin

Chromogranin proteins, particularly chromogranin A (CgA) and chromogranin B (CgB), are integral to the formation of secretory granules in endocrine and neuroendocrine cells (Feldman and Eiden, 2003). Recent studies have elucidated that these proteins undergo phase separation within the trans-Golgi network (TGN), facilitating the packaging of hormones like insulin into secretory granules (Parchure et al., 2022).

In vitro studies have shown that CgA aggregation can be influenced by divalent cations such as zinc and magnesium, as well as an aggregation chaperone [hexahistidine-epitope-tagged secreted alkaline phosphatase (SEAP-His)] (Jain et al., 2002). The presence of calcium ions has also been shown to significantly affect the secondary structure of CgA and to promote an increased rate of CgA aggregation at pH 5.5 compared to pH 7.5. This suggests that granin aggregation depends on conditions relevant to the TGN, namely, a mildly acidic pH (~5.5–6.1) and millimolar calcium concentrations. Inside neuroendocrine cells, chromogranins themselves aggregate and are packaged within secretory granules through a process of selective aggregation (Jain et al., 2002). Furthermore, they promote the sorting of associated hormones into the regulated secretory pathway by co-packaging them inside dense-core secretory granules. CgA has been demonstrated to play an important catalytic role in secretory granule biogenesis and can act as a modulator for endocrine cell secretory activity (Feldman and Eiden, 2003). Therefore, chromogranin aggregation is a vital step governing the packaging and storage of hormones, neuropeptides, and neurotransmitters within granules in these cells. While the expression of CgA itself is sufficient for secretory granule formation, the precise role of CgA aggregation in secretory granule biogenesis is understudied. Characterizing the nature of CgA aggregates within secretory granules and their role in granule formation and the regulated secretory pathway is essential for a clearer understanding of secretory granulogenesis. This understanding has been advanced by the proposal that phase separation may be the key mechanism for secretory protein sorting (Parchure et al., 2022). Unlike often irreversible and pathological protein aggregation, phase-separated condensates are shown to form dynamic compartments, offering a flexible sorting mechanism that is relevant for the regulation of cellular processes. This study demonstrated that CgB, and to a lesser extent CgA, undergo phase separation *in vitro* at a mildly acidic pH (6.1), mimicking the TGN environment (Parchure et al., 2022). These formed droplets displayed classic liquid-like properties, such as fusion and rapid recovery after photobleaching. Crucially, the acidic pH of the TGN was identified as the primary trigger for CgB phase separation, with high calcium concentrations being dispensable at physiological TGN levels. In contrast, high zinc concentrations led to non-dynamic, solid CgB aggregates, highlighting the distinct nature of phase separation *versus* irreversible aggregation. Within living cells (INS1 832/13 beta-cells and HeLa cells), both proinsulin and CgB formed dynamic, punctate, condensate-like structures at the Golgi apparatus, confirming their liquid-like behavior *in vivo*. Furthermore, CgB condensates effectively recruited proinsulin *in vitro*, and remarkably, also recruited other constitutively secreted proteins like LyzC and Cathepsin D, suggesting that client recruitment is largely non-specific and depends on the cargo's abundance (Parchure et al., 2022). A critical insight was that only the liquid-like condensates of CgB could recruit clients; solid, zinc-induced CgB aggregates failed to do so, underscoring the paramount importance of the material properties of the assembly for proper sorting (Parchure et al., 2022). The intrinsically disordered N-terminal domain of CgB was identified as the primary driver of its phase separation capability and its ability to induce ectopic granule formation in non-secretory cells. Functionally, CgB-driven phase separation was found to be vital for accurate cargo sorting (e.g., PC2 localization) and the efficient secretion of mature insulin, facilitating granule biogenesis and hormone release (Parchure et al., 2022). In conclusion, this research establishes phase separation of Chromogranin B (CgB) at the trans-Golgi network as a fundamental molecular mechanism for sorting proinsulin and other proteins into secretory granules. CgB condensates act as a dynamic "client sponge," recruiting proteins based on abundance rather than specific sequences. This dynamic, liquid-like state is essential for precise protein sorting, efficient granule formation, and robust insulin secretion, thereby resolving a long-standing question in pancreatic

beta-cell biology regarding proinsulin sorting. Granins, as helper proteins, are themselves able to form aggregates and are stored along with proteins to be secreted within electron-dense core granules inside the cells. The storage and release of peptides/proteins inside the secretory granules thus depend on the kind of aggregates the granins form (Sobota et al., 2006). Therefore, characterizing the nature of chromogranin aggregates within secretory granules remains a crucial area of investigation. Research on secretory granule proteins provides critical insights into the fundamental mechanisms of protein self-assembly and paves the way for future therapeutic strategies.

4 Protein aggregation in human diseases

4.1 Protein misfolding and aggregation in diabetes

4.1.1 Islet amyloid polypeptide (IAPP)

Islet amyloid polypeptide (IAPP, or amylin) is a major secretory product of the pancreatic β-cells, co-secreted and co-stored with insulin, and plays a physiological role in the regulation of satiety, inhibition of gastric emptying, and suppression of glucagon secretion (Westermark and Westermark, 2011; Alrouji et al., 2023). Under normal conditions, IAPP is stored in secretory granules in a soluble or reversible amyloid-like condensate state, which allows for functional biomolecular dense hormone packing and regulated secretion. This reversible condensate state helps preserve IAPP's functional structure and prevents premature aggregation (Westermark and Westermark, 2011). At the molecular level, IAPP contains a disulfide bond between residues 2 and 7, which is critical to its correct folding, stability, and function. Disruption of this bond alters IAPP's aggregation properties, initiating amyloid formation and β-cell death (Akter et al., 2016). In type 2 diabetes, IAPP has a strong tendency to pathologically aggregate into highly stable, β-sheet-rich amyloid fibrils within the islets of Langerhans, a process observed in over 90% of patients with the disease (Westermark and Westermark, 2011; Mukherjee et al., 2017). These amyloid deposits are characterized by a cross-β spine architecture, which can be formed from extended β-strands or, in some cases, β-hairpin motifs. This structure makes them extremely resistant to degradation and effectively irreversible under physiological conditions. The aggregation of IAPP is a nucleation-dependent process, in which monomeric IAPP is recruited to growing fibrils, and can be seeded in a prion-like manner by preformed aggregates (Westermark and Westermark, 2011; Mukherjee et al., 2017). Cross-seeding is a process in which amyloid fibrils of one protein act as a seed for the aggregation of another protein. This phenomenon is implicated in the pathology of several diseases, including Alzheimer's, Parkinson's, and type 2 diabetes. This is due to amyloid fibrils sharing significant similarity in both sequence and structure, which enables their β-sheet regions to effectively cross-seed each other's aggregation (Subedi et al., 2022). Experiments have shown that individuals with type 2 diabetes and Alzheimer's often exhibit co-localized deposits of IAPP and amyloid-β (Aβ), providing strong evidence of cross-seeding between these amyloid proteins (Subedi et al., 2022). Importantly, cross-seeding can either accelerate or inhibit aggregation depending on the similarity of sequence and structural compatibility (Subedi et al., 2022). Therefore, the accumulation of IAPP aggregates is closely linked to β-cell dysfunction and loss, contributing to the progression of type 2 diabetes by overwhelming the cells' protein degradation systems, inducing oxidative stress, and ultimately triggering apoptosis (Akter et al., 2016; Miraee-Nedjad et al., 2018).

Insulin normally acts as a potent inhibitor of IAPP aggregation, so insulin resistance leads to increased IAPP production and promotes amyloid formation (Wang et al., 2014). While not all IAPP aggregates are toxic, the formation of specific toxic oligomers and insoluble fibrils is believed to be a critical factor in β-cell death and islet failure. The formation of harmful IAPP aggregates can be further driven by factors such as environmental stressors, genetic mutations, and abnormal post-translational processing (Alrouji et al., 2023). In summary, these findings indicate that the dysfunction of biomolecular condensates initiates IAPP aggregation, which acts as a central mechanism in type 2 diabetes by linking oxidative stress, increased β-cell stress and apoptosis, toxic oligomer formation, proteasome dysfunction, and the promotion of chronic inflammation (Moya-Gudiño et al., 2025).

4.1.2 Proinsulin

Proinsulin is the precursor of insulin synthesized and folded in the endoplasmic reticulum (ER) in pancreatic β-cells. Structurally, proinsulin consists of the A chain, B chain, and C-peptide, which are linked together by disulfide bonds, enabling proper folding and structural stability (Liu et al., 2018). In type 2 diabetes (T2D), pathological aggregation of proinsulin results from disruptions in its trafficking and folding. These disruptions can be triggered by genetic, environmental, or proteostatic stress, forming aggregates (Arunagiri et al., 2019). Proinsulin aggregates can be differentiated from condensates by their stable disulfide complexes, which are slowly cleared by normal cellular mechanisms such as proteasomal degradation (ERAD) or autophagy (ER-phagy) (Cunningham et al., 2019). Notably, the FKBP2, IRE1–XBP1, and PERK/EIF2AK3 pathways in β-cells play crucial roles in regulating chaperone expression and oxidative folding, and their dysfunction is linked to increased proinsulin aggregation (Sowers et al., 2018; Hoefner et al., 2023; Tsuchiya et al., 2018). The impact of these mechanisms is highlighted in monogenic conditions like Mutant INS-gene induced Diabetes of Youth (MIDY), where specific mutations in proinsulin greatly enhance its tendency to form insoluble aggregates. MIDY can be characterized by the accumulation of misfolded mutant proinsulin in the ER of pancreatic β-cells, leading to β-cell failure (Liu et al., 2010). These misfolded mutants lead to the formation of aberrant disulfide-linked aggregates. Moreover, MIDY exerts a dominant-negative effect by isolating wild-type proinsulin within the ER, thereby impairing its export and further diminishing insulin production (Sun et al., 2020).

Besides abnormal disulfide-linked aggregation, proinsulin has a natural tendency to form condensates (Toledo et al., 2023; Campelo et al., 2024). The ER relies on specialized chaperones to suppress unwanted intermolecular condensation, thus facilitating proper intramolecular folding. When proinsulin exits the ER and enters the cis-Golgi, where chaperone activity diminishes and the pH drops slightly below 7.0, its condensation tendency prevails, enabling it to form dimers, hexamers, and higher-order assemblies,

a process further facilitated by zinc ions (Toledo et al., 2023). This regulation ensures proinsulin does not prematurely assemble into higher-order structures such as nanocondensates that would disrupt maturation and export through the secretory pathway. The process is further orchestrated by co-condensation with proteins such as RESP18Hh and chromogranin B, which drives the transition of proinsulin from nanocondensates to microcondensates while undergoing phase separation (Toledo et al., 2023). These biomolecular condensates are highly dynamic in contrast to irreversible secretory granules and play an essential role in the sorting, packaging, and budding of immature secretory granules, thereby ensuring efficient insulin storage and secretion (Toledo et al., 2023; Parashar et al., 2021). Studies of the disease-relevant *Akita* mutant proinsulin showed that a dynamic liquid-like condensate accumulates in the ER (Parashar et al., 2021), instead of forming an irreversible aggregate. These condensates can be distinguished from aggregates by their high mobility and the rapid exchange of their contents with the surrounding ER environment. When the ER-phagy receptor pathway is disrupted, *Akita* condensates enlarge and accumulate, especially when the COPII coat subunit SEC24C and the tubular ER-phagy receptor RTN3 are involved. In instances where enlargement is not prevented, condensates can transition into irreversible aggregates, ultimately contributing to β-cell dysfunction and progression of diabetes (Parashar et al., 2021).

It should be noted that proinsulin aggregation (Arunagiri et al., 2019; Westermark and Wilander, 1983) or IAPP aggregation/amyloid formation (Westermark and Wilander, 1983; Hassan et al., 2022) are implicated in the development and progression of the disease itself, directly contributing to β-cell pathology. Insulin aggregation, on the other hand, is primarily an iatrogenic (treatment-induced) or pharmaceutical problem that impacts the effectiveness and safety of insulin therapy, but it is not a part of the underlying biological mechanisms that cause diabetes in the first place. Therefore, while understanding condensate formation and aggregation of these proteins, it is apt to consider the cellular consequences and pathological outcomes.

4.2 Neurodegeneration-associated protein aggregation

Neurodegenerative diseases like ALS, FTD, Alzheimer's, and Parkinson's have been studied to demonstrate disordered proteins that undergo phase separation to form dynamic biomolecular condensates (Mathieu et al., 2020). The condensates have been postulated to transition into solid, aggregation-prone states, which are linked to disease pathology. This pathological shift, often triggered by mutations, chronic stress, or impaired clearance, leads to amyloid-like inclusions, disrupts cellular homeostasis, and promotes neuronal death. We next discuss the key proteins reported in this context.

4.2.1 Tau

Tau is an intrinsically disordered protein that undergoes condensate formation under physiological conditions, primarily through interactions between its proline-rich and microtubule-binding repeat domains. These interactions are driven by electrostatic forces and π–π stacking, especially in the presence of cofactors such as RNA, heparin, or molecular crowding agents like PEG (Wegmann et al., 2018). Recent reviews in the literature discuss the association of phase separation of Tau with aggregation thereby linking physiology and disease (Li et al., 2023; Rai et al., 2021; Boyko and Surewicz, 2022; Islam et al., 2024).

Tau has been studied extensively to understand the driving forces of condensate formation. One such study focuses on characterizing two mechanistically distinct modes, self-coacervation (SC; Tau–Tau) and complex coacervation (CC; Tau with polyanions such as RNA). The *invitro* experiments complemented with coarse-grained computational modeling show that electrostatics (charge interactions) is the primary driving force for both CC and SC: Tau–RNA and Tau–Tauassociations (Najafi et al., 2021). Droplets formed by complex coacervation (Tau and RNA) are measurably more viscous (higher micro-viscosity) and show greater thermal stability than droplets from Tau self-coacervation (Najafi et al., 2021). These rheological differences imply that distinct internal dynamics and molecular packing in the two types of assemblies, influencing Tau's conformational ensemble and its subsequent aggregation behaviour.

The formation of dynamic Tau condensates is shown to facilitate spatial organization within the cytoplasm but also predisposes Tau to gelation and amyloid aggregation (Ambadipudi et al., 2017). Over time, these condensates mature into less dynamic, solid-like assemblies, providing nucleation centres for β–sheet–rich amyloid fibrils (Ambadipudi et al., 2017). Also, Tau condensates regulate microtubule assembly but have also been involved in the formation of toxic oligomers that develop into amyloid aggregates implicated in neurodegenerative diseases. Tau condensates can also recruit kinases and RNA, enhancing pathogenic modification and mislocalization, forming a direct bridge from functional phase behaviour to pathological aggregation (Hernández-Vega et al., 2017). Tau showcased condensate formation under cellular conditions, which was predicted to serve as an intermediate on pathway to Tau aggregate formation (Wegmann et al., 2018). Another study, focused on condensate formation and dissolution of wild-type and disease-linked (hyperphosphorylated and missense mutated) Tau variants. All Tau variants [wild-type (WT), hyperphosphorylated (pTau), and missense familial mutation (P301S)] can exist as monomers, nanocondensates, and microcondensates, or a combination of these states (Tsoi et al., 2025). All three forms of Tau exhibited similar condensation formation properties in the presence of increased salt concentration, which showcases that at the nano-condensate level, the forces driving Tau condensation were not significantly affected by changes in charge distribution caused by phosphorylation (Tsoi et al., 2025). A complementary work shows that as Tau oligomerizes the condensate formation propensity declines. The early oligomers can be recruited into condensates where they promote maturation whereas mature fibrils cannot be recruited, implying a temporal window linking condensates to Tau aggregation (Lucas et al., 2025). Thus, these studies highlight the need for exploring types of Tau assemblies and their fate over different time-scales. A recent work by Wen et al. shows that condensate formation and conformational opening are mechanistically coupled, arising from and enforcing a shift to extended Tau conformers that expose the microtubule-binding region, creating locally concentrated, interaction-rich environments that lower nucleation barriers and

accelerate amyloid formation of Tau (Wen et al., 2025). Disease-associated mutations (P301L, P301S) further promote conversion from dynamic condensates into irreversible amyloids. Interestingly, in another work, by increasing the fibril nucleation barrier, peptide L-arginine counteracts the age-dependent decline of the Tau condensates by selectively impeding condensate-to-fibril transition without perturbing phase separation in a valence and chemistry-specific manner (Mahendran et al., 2025). This showcases that the small molecule metabolites can enhance the metastability of protein condensates against a condensate-to-amyloid transition, thereby preserving condensate state and function.

Despite strong *invitro* and cellular evidence for the connect between condensates and fibrils, the pathophysiological relevance, precise temporal order of events, and structural transitions within condensates in living neurons remain major gaps in current understanding of Tau pathology.

4.2.2 Amyloid-β (Aβ)

Amyloid-β (Aβ) protein peptides, especially the 42-residue isoform $A\beta_{42}$, are central to Alzheimer's disease pathology (Finder and Glockshuber, 2007). The peptides are known to accumulate in the brains of diseased patients. Accumulation of Aβ in the brain is considered an early toxic event in Alzheimer's disease, characterized by the formation of amyloid plaques and neurofibrillary tangles (Chen et al., 2017). The accumulated Aβ fibrils adopt highly ordered, β-sheet-rich structures, with individual peptides stacking into cross-β spines that stabilize the fibril core. Structural studies reveal polymorphic fibril forms, where variations in β-strand arrangement and inter-peptide interactions contribute to morphological diversity and disease-specific aggregation properties (Yang et al., 2019; Kollmer et al., 2021). These Aβ species disrupt cellular homeostasis through oxidative stress, membrane perturbation, and synaptic dysfunction (Musa et al., 2023).

Aβ40 itself can undergo phase separation, forming condensates under physiological-like conditions. Within these condensates, Aβ40 aggregation is accelerated compared to dilute solution, and nucleation occurs preferentially inside the dense phase (Morris et al., 2024). A detailed review which highlights the mechanisms underlying Aβ aggregation and the regulatory role of condensate formation has been published (Niu et al., 2024). Further, Gui, et al. have demonstrated that soluble Aβ oligomers are capable of undergoing phase separation, forming micron-scale, dynamic droplets. Condensate formation accelerates downstream amyloidogenesis, supporting a condensate-mediated microreactor model for primary nucleation (Gui et al., 2023). Further, Aβ peptides can form condensate-like clusters under specific conditions such as acidic pH, metal ion presence (Zn^{2+}, Cu^{2+}), or membrane interfaces (Šneiderienė et al., 2025). The condensate phase can increase the rate of nucleation for Aβ42 aggregation. The fundamental nucleation step in Aβ42 aggregation can be increased in rate by a biomolecular condensate phase of the peptide. This type of two-stage nucleation process could be a general pathway for neurodegenerative disease-related phase-separating proteins, as seen in other systems such as FUS, TDP-43, α-synuclein, hnRNPA1, and Tau. This evidence suggests that the mechanism of phase separation can govern the pathology of amyloid diseases (Šneiderienė et al., 2025). *In vitro* studies suggest that phase-separated Aβ states can form dynamic oligomeric condensates, especially when combined with polyanions or lipid membranes. These intermediate states lower the energetic barrier for fibril nucleation, potentially representing early-stage pathogenesis in Alzheimer's disease (Šneiderienė et al., 2025). Although the reversibility of these condensates is limited, their formation and maturation can be influenced by environmental factors such as ionic strength, glycosaminoglycans, and redox states. These findings align with the hypothesis that non-canonical phase separation may serve as a pre-fibrillar organizational mechanism for Aβ. Cumulatively, Aβ condensate formation and associated environmental conditions have key roles in dictating the nucleation, scaffolding and fate of higher order aggregated species implicated in disease pathology.

4.2.3 α-Synuclein (αSYN)

α-Synuclein (αSYN) aggregation is a hallmark of Parkinson's disease and involves the transition of soluble protein monomers into oligomers, protofibrils, and mature amyloid fibrils (Vidović and Rikalovic, 2022). The aggregation process is driven by misfolding and self-association, often influenced by mutations, post-translational modifications, and/or interactions with membranes (Luk et al., 2009). The resulting amyloid fibrils and oligomeric species are neurotoxic, disrupting cellular homeostasis, impairing synaptic function, and contributing to Lewy body formation in affected neurons (Sacino et al., 2014). αSYN protein contains an amphipathic N-terminal domain, a hydrophobic NAC region (critical for aggregation), and a negatively charged C-terminal tail, which collectively have been speculated to govern its phase separation behavior. *In vitro*, αSYN undergoes phase separation in the presence of molecular crowding agents, RNA, liposomes, or polyphosphates, forming spherical, fusion-capable droplets (Hardenberg et al., 2021). These liquid droplets mature over time into gel-like or solid fibrillar states, especially under stress conditions (e.g., metal ions, low pH, or oxidative stress). Parkinson's disease mutations (A30P, E46K, A53T) enhance the propensity for condensate formation and show rapid droplet aging, accelerating the transition to fibrils (Ray et al., 2020). Truncation of the acidic C-terminal region, which normally imparts solubility, also promotes phase separation and subsequent aggregation (Ray et al., 2020). These findings suggest that αSYN droplets serve as nucleation-enhancing condensates, linking biophysical phase transitions to disease pathology. The role of electrostatic forces in driving αSYN phase separation is shown by phase diagrams in presence of NaCl (Cui et al., 2025).

A study using cellular models and *in vitro* reconstitution shows that αSYN condensates concentrate monomers and exogenous fibrillar seeds, accelerating seed-dependent fibril elongation and promoting maturation into needle-like, Amytracker-positive aggregates. This study directly correlates condensate formation with propagation of fibrils (Piroska et al., 2023). Surprisingly, another study showcased that αSYN binding with lipids enhances their phase separation, correlating with the Aβ42's phase separation process (Chandran et al., 2025). Ziaunys et al. show that phase separation of αSYN promotes the formation of structurally diverse fibrils. The presence of condensates accelerates aggregation and produces fibrils with increased morphological variability compared to those formed in bulk solution (Ziaunys et al., 2024). These findings showcase that αSYN exhibits dichotomy associated with the dysregulation of aSYN phase separation, which may directly

affect disease pathogenesis. Recent studies also showed that αSYN proceeds through phase separation to increase the rate of amyloid aggregation, β-Synuclein (βSYN), a part of the synuclein family, co-condenses with αSYN and affects its aggregation by negatively regulating the phase separation of αSYN (Xu et al., 2025). βSYN also decreases the mobility of αSYN in αSYN/βSYN coacervates, leading to diminished condensate fusion, growth, and maturation (Xu et al., 2025). These evidences cumulatively suggest the role of βSYN in the neuroprotection of β-Syn and the targeting of α-Syn phase separation in disease treatments (Xu et al., 2025). Hence, this alludes to how heterotypic condensate formation can regulate the fate of complex assemblies and dictate both the nature and extent of aggregation.

The studies highlighted above, using different protein systems and physiological assemblies indicate a complex tug-of-war between the formation of condensates and aggregated fibrils.

5 Emergent properties of protein self-assemblies influencing function and disease

The emergent properties that are elucidated from the above studies can assist in guiding future studies in the fields of protein aggregation. For instance, biomolecular condensates display emergent properties that may not be achieved from the sum of their individual molecular components (Visser et al., 2024). Through multivalent interactions, often between intrinsically disordered regions (IDRs) and folded domains, these assemblies undergo phase separation to form dense, droplet-like compartments that concentrate specific biomolecules, creating unique microenvironments where reaction rates, specificity, and selectivity can be dramatically enhanced (Banani et al., 2017; Alberti and Hyman, 2021). These condensates exhibit dynamic behavior, the ability to fuse, deform, and exchange molecules. The assemblies can also mature into viscoelastic or gel-like networks, reflecting material states that are emergent from collective interactions (Elbaum-Garfinkle et al., 2015; Brangwynne et al., 2009; Wang et al., 2022). Crucially, their capacity to tune material properties (viscosity, diffusion barriers) via sequence features, post-translational modifications, and partner interactions enables responsive cellular regulation and biochemical compartmentalization (Wang et al., 2022; Sanfeliu-Cerdán and Krieg, 2025). Such tunability underpins their roles in signalling cascades, stress responses, and metabolic integration. Conversely, dysregulated transitions can drive pathological aggregation linked to neurodegeneration and other diseases (Tejedor et al., 2023). Thus, we highlight the emergent features of protein assemblies (Figure 2) that can link and deconvolute the relation between condensate formation and amyloid aggregation.

5.1 Energy landscape in protein assemblies

The energy landscape is a conceptual model that maps the free energy of a system as a function of its conformational states. In the context of proteins and their higher-order assemblies, it illustrates the possible assembly forms and their associated stabilities (Figure 3). Condensates formed via phase separation can be driven by multivalent weak interactions (e.g., π-π stacking, cation-π, hydrogen bonding) (Banani et al., 2017). The energy landscape for condensate assemblies has been predicted to dictate dynamic rearrangements of molecules (Biswas and Potoyan, 2025). The assemblies may attain multiple low-energy states, contributing to fluidity and adaptability in the system, and facilitating fast exchange with the surrounding environment (Espinosa et al., 2020). In contrast, amyloid fibrils arise from ordered aggregation, typically involving β-sheet-rich structures (Adamcik and Mezzenga, 2018). The energy landscape here is deep and narrow, featuring high energy barriers between states. The energy landscape also has stable "traps" representing fibril structures (Adamcik and Mezzenga, 2018; Almeida and Brito, 2020). These states may have irreversibility or very slow reversibility with kinetically trapped states.

Due to increasing local concentrations, condensates can lower the effective free-energy barrier for nucleation, biasing ensembles toward aggregation-competent conformers and possibly enabling structural transitions that are improbable in dilute solution. Over time, droplet aging or intra-condensate reorganization can steer the system to thermodynamically favored amyloid minima. A liquid→ gel → solid trajectory driven by accumulation of β-sheet contacts, cross-β spine formation, and stabilizing inter-molecular bonds can be achieved in a temporal manner. Additionally, heterogeneous environments within droplets (interfaces, cofactors, membranes, RNA, post-translational modifications) can create local sub-states and kinetic pathways that favor particular fibril polymorphs, accounting for the structural diversity observed experimentally in case of proteins associated with neurodegeneration. Conversely, chaperones and small molecules can reshape the landscape by stabilizing liquid basins or raising barriers to amyloid basins, thereby decoupling benign condensation from pathological fibrillization. Viewing condensates and fibrils on the energy landscape, thus, can aid to reconcile their dual roles. Hence, understanding the relation of condensates and higher-order assemblies like fibrils in the context of energetics is crucial to map out the processes that are involved in processes like stress granule formation and neurodegenerative diseases.

5.2 Viscoelasticity in condensate assembly

Viscoelasticity is the material property describing both viscous (fluid-like) and elastic (solid-like) responses to deformation. Condensates have been shown to exhibit tunable viscoelasticity depending on protein sequence, interactions, and conditions (e.g., salt, pH) (Tejedor et al., 2023). Such assemblies can also behave as viscous liquids or soft solids, characterized by low elastic modulus (G') and higher loss modulus (G'') in liquid-like states. Percolation within a condensate with the progressive formation of an interconnected molecular network that spans the entire droplet is speculated. As this network strengthens or develops over time, molecular mobility can decrease. The internal rearrangements can slow down leading to increased viscosity and reduced dynamics, attributed to be hallmarks of condensate ageing or maturation. Alshareedah et al. show that condensates of prion-like low-complexity domains of hnRNPA1 behave as

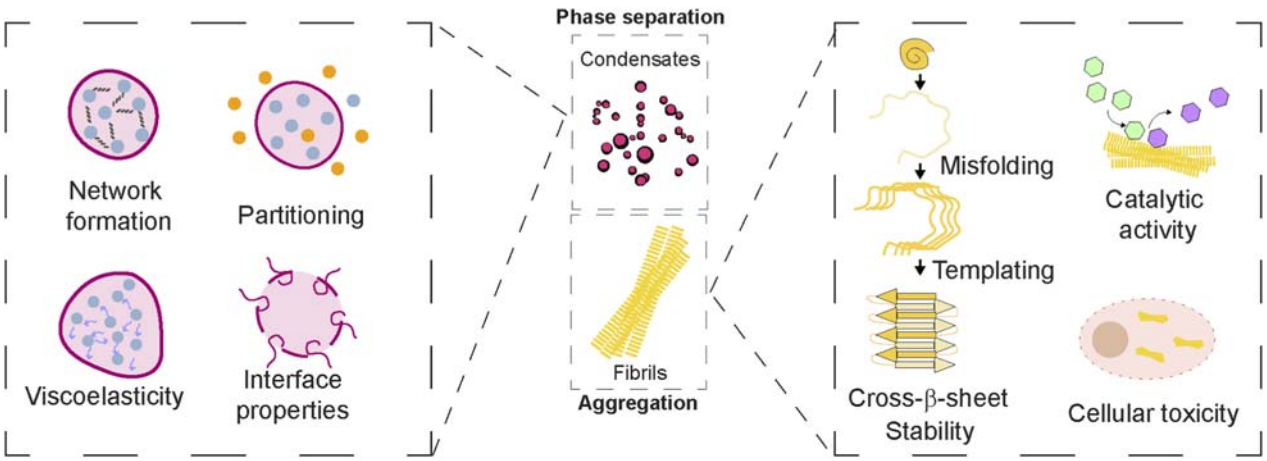

FIGURE 2
Emergent Properties of Protein Assemblies. *Middle panel:* Protein assemblies such as biomolecular condensates and amyloid fibrils display emergent properties that arise from collective organization beyond individual protein behaviour. *Left panel:* Condensates exhibit dynamic features like network formation, selective compartmentalization/partitioning properties. They can possess material properties in the form of viscoelasticity and contribute to interfacial properties. *Right panel:* Amyloid fibrils are known to acquire structural rigidity via cross-β sheet assemblies as well as templating capacity. While the surface of fibrils can catalyse cellular reactions, the toxic gain-of-function can contribute to cellular toxicity. Together, these emergent properties of protein assemblies underlie both functional roles in physiology and pathogenic outcomes in disease.

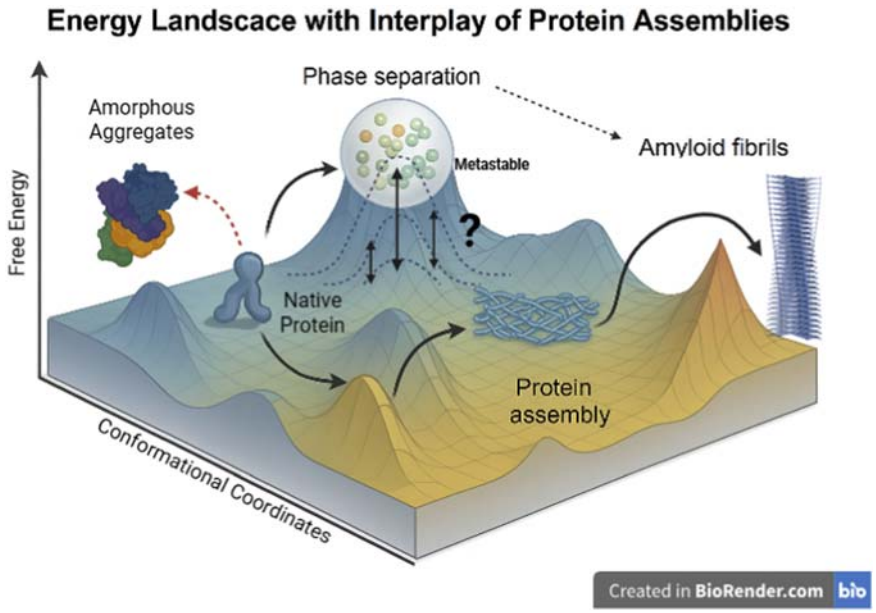

FIGURE 3
Energy Landscape Depicting the Interplay of Protein Conformational States and Assemblies. This three-dimensional energy landscape illustrates the possible conformational transitions of a protein. The y-axis represents Free Energy, indicating the thermodynamic favourability of each state, with lower energy corresponding to more stable structures. The x- and z-axes collectively represent Conformational Coordinates, which trace the structural transitions influenced by factors such as the protein's sequence, multivalency, and the cellular environment. The protein starts in a low-energy well as the native protein, from which it can transition along several pathways: It may form ordered protein assemblies in an intermediate energy minimum, or undergo phase separation into dense, droplet-like compartments, which is depicted as a "metastable" state. Alternatively, the native protein can transition to unstructured amorphous aggregates via a high-energy route. The assembled states show potential routes toward the formation of highly stable, misfolded amyloid fibrils, which represent the deepest thermodynamic sink on the landscape. The various connections shown, including the dynamic equilibrium of the phase-separated state and the link between amorphous aggregates and phase separation, highlight the complex interconversion and interplay among these assembly states.

aging viscoelastic (Maxwell-like) fluids whose elastic and viscous moduli, and the timescales over which elasticity dominates, are encoded by sequence-specific sticker–sticker interactions (especially aromatic contacts). Aging is shown to be accompanied by disorder-to-order transitions in some protein sequences, producing non-fibrillar, β-sheet–containing semi-crystalline solids (Kelvin–Voigt–like-behavior) (Alshareedah et al., 2024).

The condensates have been claimed to undergo time-dependent aging or hardening into more solid-like states (e.g., gelation or maturation) (Dabbaghi et al., 2021). The molecules in the dense phase can undergo dynamic internal rearrangement, which can influence networking properties while leading to recovery after stress. Fibrils form rigid, elastic structures that exhibit strongly elastic mechanical behavior, characterized by a high storage modulus (G') and negligible loss modulus (G''), indicating minimal energy dissipation (Dabbaghi et al., 2021). This mechanical profile confers significant resilience and resistance to deformation, allowing fibrils to act as durable structural scaffolds. In pathological contexts, such as Alzheimer's disease, amyloid fibrils provide a stable yet detrimental framework that contributes to neurodegeneration. Conversely, in functional contexts like spider silk or certain microbial matrices, fibrils perform essential mechanical roles, demonstrating how similar structural properties can underpin both disease and physiological utility (Qi et al., 2023). Thus, percolation can provide the physical basis for the transition from a liquid-like, reversible condensate to a more gel-like or solidified state associated with functional stabilization or pathological aggregation. Taken together, these directions emphasize moving from descriptive accounts of condensate ageing to mechanistic, quantitative maps that connect sequence and composition → percolation/network topology → viscoelastic spectra → functional or pathological outcomes.

5.3 Distinct chemical microenvironment

Condensates and fibrils create distinct chemical microenvironments that critically influence the behavior of associated molecules. In condensates, the microenvironment is highly dynamic and selectively permeable, enriched with co-aggregators, RNA, intrinsically disordered proteins (IDPs), and molecular chaperones that modulate assembly and disassembly (Niu et al., 2023). These environments favor weak, multivalent interactions, allowing for rapid exchange with the surrounding cytoplasm and facilitating regulated biochemical reactions. Chaperones, such as HSP70 or HSP40, often localize to condensates to prevent aberrant aggregation, maintaining their liquid-like properties (Li et al., 2022). In contrast, fibrils form a rigid, dehydrated, and sterically constrained microenvironment, often excluding dynamic co-factors and entrapping proteins in kinetically trapped, β-sheet-rich aggregates (Jia et al., 2020; Akaree et al., 2025). Chaperones are generally less effective once fibrils are fully formed, but may engage early oligomeric intermediates to prevent fibrillization. Thus, the transition from condensate to fibril potentially reflects not only a shift in the material state but also a profound remodelling of the molecular milieu and regulatory potential of the assembly.

5.4 Network formation of protein assemblies

In biomolecular condensates, the network formation of protein and/or nucleic acid polymers plays a pivotal role in modulating protein aggregation dynamics. These networks, formed through multivalent interactions, can create a dense, highly interactive environment that can either accelerate or decelerate aggregation depending on the molecular context (Fare et al., 2021). Network formation, therefore, can modulate partitioning and viscoelastic behavior in a temporal manner. On one hand, condensates can concentrate aggregation-prone proteins, increase local concentrations, and promote nucleation events that lead to fibrillization. RNA and other scaffolding molecules can also act as structural templates or seeds that stabilize aggregation-prone conformers (Fare et al., 2021; Li et al., 2022). On the other hand, the same networks can buffer aggregation by maintaining proteins in a dynamic, reversible interaction network, especially in the presence of regulatory factors like chaperones or RNA-binding proteins that disrupt pathological contacts (Akaree et al., 2025). Thus, the polymeric network within condensates could function as a double-edged sword, capable of either fostering or restraining protein aggregation based on the balance of intermolecular interactions and regulatory components.

5.5 Interface properties

As evidenced by the studied discussed earlier, phase separation not only serves to compartmentalize constituents but also gives rise to constituent emergent properties by the formation of multivalent interaction networks. The emergent properties of biomolecular condensates are speculated to contribute to specific functions like diffusivity and interfacial tension, and have been studied using interdisciplinary approaches in pan-cellular biomolecular condensates (Jeon et al., 2025). While several lines of evidence suggest that condensates have emergent properties, a concrete extrapolation to in-cell systems has not been achieved. One aspect of condensates that is absent from other higher-order assemblies is the interface. Interface serves as a bridge between the coexisting dense phase and the dilute phase in the two-phase regime. The properties of the interface with respect to the mesoscale organization of molecules have been studied (Farag et al., 2022).

In the context of protein aggregation, contrasting observations have been made for interfacial contributions to fibril formation. Linsenmeier et al. investigate how the low-complexity domain (LCD) of the hnRNPA1 protein, associated with amyotrophic lateral sclerosis (ALS), transitions from liquid-like condensates to amyloid fibrils (Linsenmeier et al., 2023). The research demonstrates that amyloid fibril formation predominantly occurs at the interface of the condensates rather than uniformly throughout. This work predicts that the interface plays a crucial role in promoting fibril formation, possibly due to the orientation and conformation of molecules at the boundary (Linsenmeier et al., 2023). As an example of contrasting behaviours, Das et al. recently demonstrated that condensates formed by prion-like domains prone to fibril formation can facilitate nucleation of fibrils at their interfaces while inhibiting fibril growth within their interiors (Das et al., 2025). The

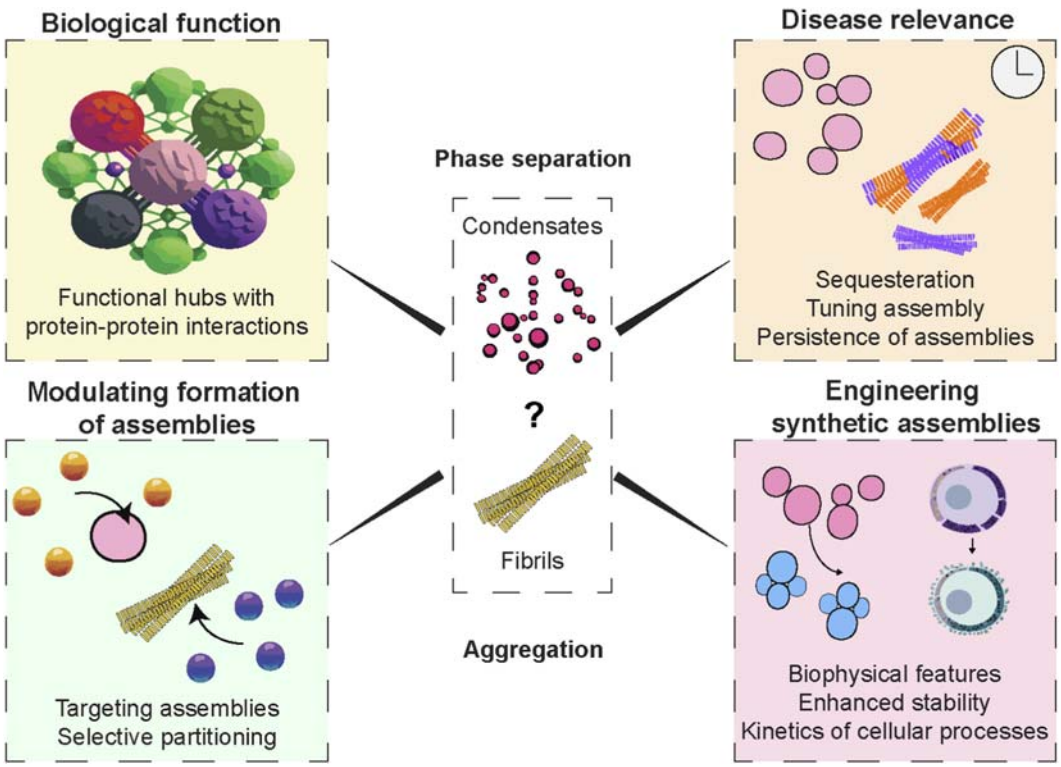

FIGURE 4
Protein Assemblies in Biology, Disease, and Therapy. Schematic overview of protein assemblies such as condensates and amyloid fibrils, highlighting their dual nature. In physiology, they enable biological functions including compartmentalization, signalling, and structural support. In pathology, aberrant assemblies contribute to diseases such as neurodegeneration and cancer by sequestration and persistence of insoluble aggregates. Therapeutic approaches target their formation, dynamics, or clearance to restore cellular balance. Advances in synthetic biology can harness these principles to engineer programmable assemblies with applications in diagnostics, drug delivery, and biomaterials.

fibrils develop in the surrounding dilute phase, and the metastable condensates hinder their growth by sequestering soluble proteins and releasing them slowly, thereby acting as protein sinks.

The emergent properties studied so far have illuminated the intricate interplay between protein phase separation and the aggregation of biomolecular condensates. We further provide a comprehensive overview of conclusions across the various systems studied to provide new directions in the mechanistic understanding of fundamentals of human diseases and potentially the development of targeted therapeutic interventions.

6 Conclusion

The interplay between reversible phase separation and irreversible aggregation of proteins is central to understanding both normal cell physiology and disease pathology (Vendruscolo and Fuxreiter, 2022). While phase-separated condensates can organize biochemical reactions and promote adaptability, their transition into aggregates under stress or mutation is linked to neurodegeneration, cancer, and aging (Visser et al., 2024).

Biomolecular condensates form through interactions that often involve IDRs or modular interaction domains that enable flexible and reversible binding. IDRs facilitate π–π stacking, cation-π interactions, electrostatic complementarity, and transient hydrogen bonding, enabling dynamic assembly of biomolecular condensates (Banani et al., 2017). Proteins such as FUS, TDP-43, hnRNPA1, and Tau exemplify this, forming condensates in response to changes in concentration, ionic strength, or temperature. Importantly, RNA molecules can act as scaffolds or regulators of phase separation by stabilizing or disrupting condensates depending on their concentration and sequence specificity (Boeynaems et al., 2018; Boeynaems et al., 2019; Maharana et al., 2018).

While condensates are initially dynamic, exhibiting fusion, internal mobility, and fluorescence recovery after photobleaching (FRAP), many proteins have been reported to undergo aging or maturation over time with loss of dynamicity. This process has been predicted by increased cross-linking, β-sheet formation, and the eventual development of amyloid fibrils, often pertinent in neurodegenerative diseases (Han et al., 2024; Mathieu et al., 2020). Proteins like Tau, α-Synuclein, and FUS exhibit liquid-to-solid transitions influenced by post-translational modifications, mutations, and environmental stressors (Farina et al., 2021). These matured condensates show reduced dynamics and increased structural order, resembling pathological aggregates such as those in Alzheimer's, Parkinson's, and ALS. The transition is driven by nucleation-limited kinetics, where the condensate environment accelerates monomer recruitment and fibrillization. On the other hand, ATP-dependent chaperones and RNA helicases modulate condensate dynamics, preventing unwanted aggregation and

maintaining cellular proteostasis (Patel et al., 2015; Patel et al., 2017). The transitions of material properties of secretory granules proteins are unexplored in detail. Hence, the need of the hour is to critically evaluate the changes in the material properties of protein assemblies during the cellular processes to assess their importance. While in several studies, FRAP is widely used to probe condensate dynamics, it has major limitations in reporting material properties of the assemblies. FRAP recovery curves are highly model-dependent and conflate diffusion with binding kinetics, making them unreliable as sole evidence for "liquid" behaviour. Partitioning at condensate interfaces, photobleaching artifacts, and fluorescent tags can distort results, while spatial averaging hides heterogeneity and material transitions (Taylor et al., 2019). Thus, FRAP should be combined with orthogonal methods like single-particle tracking, FCS, and micro-rheology for robust interpretation of material properties.

We predict that the study of protein assemblies will have a deep impact on several avenues in the upcoming future (Figure 4). The future research in the arena of linking condensate formation to aggregation will need to focus on the following key aspects of protein assemblies:

1. Molecular Determinants: Defining the precise sequence features, post-translational modifications, and RNA interactions that control whether proteins remain in a dynamic state or lead to the formation of aggregates. The material properties like viscoelasticity have to be understood at the basal level and across the temporal scales to connect the maturation process of assemblies to pathology.
2. Interface Biology: Investigating condensate interfaces as critical sites where amyloid formation is postulated to initiate, and exploring strategies to modulate these boundaries to prevent pathological aggregation.
3. Cellular Stress and Environment: Understanding how pH, ionic strength, crowding, or oxidative stress tips the balance from phase separation to aggregation, especially in aging cells.
4. Therapeutic Modulation: Therapeutic intervention possibilities for biomolecular condensates are an emerging and rapidly expanding area of biomedical research, with several promising strategies under investigation. Developing small molecules, peptides, or nucleic acids that stabilize physiologically functional condensates or dissolve/prevent pathological ones, creating new treatments for diseases like ALS, Alzheimer's, and cancer. This also enables identifying early condensate-to-aggregate transitions as diagnostic markers, enabling intervention before irreversible damage occurs. A step into precision biology would involve engineering condensates with built-in safeguards against aggregation, and tailoring interventions based on individual genetic mutations that affect protein phase behavior.

Linking the biophysical principles of condensate formation and protein aggregation to therapeutic approaches opens new avenues for treating neurodegenerative and proteinopathies-related diseases. Understanding how biomolecular condensates form, mature, and convert into pathological aggregates offers actionable targets for drug design, molecular chaperone modulation, and phase behavior tuning. Hence, the future research focus would aid in decoding the molecular "switches" that decide between functional condensates and toxic aggregates, and in harnessing this knowledge for therapeutic benefit.

Author contributions

AN: Writing – review and editing, Writing – original draft, Conceptualization, Visualization. AA: Visualization, Writing – original draft, Conceptualization, Writing – review and editing, Supervision. TK: Writing – review and editing, Writing – original draft. KP: Writing – review and editing, Writing – original draft. KD: Writing – review and editing, Writing – original draft.

Funding

The authors declare that financial support was received for the research and/or publication of this article. Department of Science and Technology (DST), Government of India through DSTINSPIRE faculty funding (AN) Grant number IFA-23-LSMB-276, and East Tennessee State University funds (AA).

Conflict of interest

The authors declare that the research was conducted in the absence of any commercial or financial relationships that could be construed as a potential conflict of interest.

The author(s) declared that they were an editorial board member of Frontiers, at the time of submission. This had no impact on the peer review process and the final decision.

Generative AI statement

The authors declare that no Generative AI was used in the creation of this manuscript.

Any alternative text (alt text) provided alongside figures in this article has been generated by Frontiers with the support of artificial intelligence and reasonable efforts have been made to ensure accuracy, including review by the authors wherever possible. If you identify any issues, please contact us.

Publisher's note

References

Adamcik, J., and Mezzenga, R. (2018). Amyloid polymorphism in the protein folding and aggregation energy landscape. *Angew. Chem. Int. Ed.* 57, 8370–8382. doi:10.1002/anie.201713416

Akaree, N., Secco, V., Levy-Adam, F., Younis, A., Carra, S., and Shalgi, R. (2025). Regulation of physiological and pathological condensates by molecular chaperones. *FEBS J.* 292, 3271–3297. doi:10.1111/febs.17390

Akter, R., Cao, P., Noor, H., Ridgway, Z., Tu, L. H., Wang, H., et al. (2016). Islet amyloid polypeptide: structure, function, and pathophysiology. *J. Diabetes Res.* 2016, 2798269. doi:10.1155/2016/2798269

Alberti, S., and Hyman, A. A. (2021). Biomolecular condensates at the nexus of cellular stress, protein aggregation disease and ageing. *Nat. Rev. Mol. Cell Biol.* 22, 196–213. doi:10.1038/s41580-020-00326-6

Almeida, Z. L., and Brito, R. M. M. (2020). Structure and aggregation mechanisms in amyloids. *Mol. (Basel, Switzerland)*. 25, 1195. doi:10.3390/molecules25051195

Alrouji, M., Al-Kuraishy, H. M., Al-Gareeb, A. I., Alexiou, A., Papadakis, M., Saad, H. M., et al. (2023). The potential role of human islet amyloid polypeptide in type 2 diabetes mellitus and Alzheimer's diseases. *Diabetology and Metabolic Syndrome* 15, 101. doi:10.1186/s13098-023-01082-1

Alshareedah, I., Borcherds, W. M., Cohen, S. R., Singh, A., Posey, A. E., Farag, M., et al. (2024). Sequence-specific interactions determine viscoelasticity and aging dynamics of protein condensates. *Nat. Phys.* 20, 1482–1491. doi:10.1038/s41567-024-02558-1

Ambadipudi, S., Biernat, J., Riedel, D., Mandelkow, E., and Zweckstetter, M. (2017). Liquid–liquid phase separation of the microtubule-binding repeats of the Alzheimer-related protein Tau. *Nat. Commun.* 8, 275. doi:10.1038/s41467-017-00480-0

Anoop, A., Ranganathan, S., Das Dhaked, B., Jha, N. N., Pratihar, S., Ghosh, S., et al. (2014). Elucidating the role of disulfide bond on amyloid formation and fibril reversibility of somatostatin-14: relevance to its storage and secretion. *J. Biol. Chem.* 289, 16884–16903. doi:10.1074/jbc.M114.548354

Arunagiri, A., Haataja, L., Pottekat, A., Pamenan, F., Kim, S., Zeltser, L. M., et al. (2019). Proinsulin misfolding is an early event in the progression to type 2 diabetes. *Elife* 8, e44532. doi:10.7554/eLife.44532

Arunagiri, A., Alam, M., Haataja, L., Draz, H., Alasad, B., Samy, P., et al. (2024). Proinsulin folding and trafficking defects trigger a common pathological disturbance of endoplasmic reticulum homeostasis. *Protein Sci.* 33, e4949. doi:10.1002/pro.4949

Badtke, M. P., Hammer, N. D., and Chapman, M. R. (2009). Functional amyloids signal their arrival. *Sci. Signal* 2, pe43. doi:10.1126/scisignal.280pe43

Banani, S. F., Lee, H. O., Hyman, A. A., and Rosen, M. K. (2017). Biomolecular condensates: organizers of cellular biochemistry. *Nat. Rev. Mol. Cell Biol.* 18, 285–298. doi:10.1038/nrm.2017.7

Biswas, S., and Potoyan, D. A. (2025). Decoding biomolecular condensate dynamics: an energy landscape approach. *PLoS Comput. Biol.* 21, e1012826. doi:10.1371/journal.pcbi.1012826

Boeynaems, S., Alberti, S., Fawzi, N. L., Mittag, T., Polymenidou, M., Rousseau, F., et al. (2018). Protein phase separation: a new phase in cell biology. *Trends Cell Biol.* 28, 420–435. doi:10.1016/j.tcb.2018.02.004

Boeynaems, S., Holehouse, A. S., Weinhardt, V., Kovacs, D., Van Lindt, J., Larabell, C., et al. (2019). Spontaneous driving forces give rise to protein-RNA condensates with coexisting phases and complex material properties, *Proc. Natl. Acad. Sci. U. S. A.* 116, 7889–7898. doi:10.1073/pnas.1821038116

Boyko, S., and Surewicz, W. K. (2022). Tau liquid-liquid phase separation in neurodegenerative diseases. *Trends Cell Biol.* 32, 611–623. doi:10.1016/j.tcb.2022.01.011

Brangwynne, C. P., Eckmann, C. R., Courson, D. S., Rybarska, A., Hoege, C., Gharakhani, J., et al. (2009). Germline P granules are liquid droplets that localize by controlled dissolution/condensation. *Science* 324, 1729–1732. doi:10.1126/science.1172046

Campelo, F., Lillo, J. V., and von Blume, J. (2024). Protein condensates in the the secretory pathway: unraveling biophysical interactions and function. *Biophysical J.* 123, 1531–1541. doi:10.1016/j.bpj.2024.04.031

Chakraborty, P., and Zweckstetter, M. (2023). Role of aberrant phase separation in pathological protein aggregation. *Curr. Opin. Struct. Biol.* 82, 102678. doi:10.1016/j.sbi.2023.102678

Chandran, A., Agarwal, A., Wang, T., Amaral, L., Chaves, S. R., Outeiro, T. F., et al. (2025). Dual effect of α-synuclein disease variants on condensate formation. *bioRxiv* 2006, 2025-06.

Chen, G.-f., Xu, T. H., Yan, Y., Zhou, Y. R., Jiang, Y., Melcher, K., et al. (2017). Amyloid beta: structure, biology and structure-based therapeutic development. *Acta Pharmacol. Sin.* 38, 1205–1235. doi:10.1038/aps.2017.28

Chiesa, G., Kiriakov, S., and Khalil, A. S. (2020). Protein assembly systems in natural and synthetic biology. *BMC Biol.* 18, 35. doi:10.1186/s12915-020-0751-4

Choi, J. M., Holehouse, A. S., and Pappu, R. V. (2020). Physical principles underlying the complex biology of intracellular phase transitions. *Annu. Rev. Biophys.* 49, 107–133. doi:10.1146/annurev-biophys-121219-081629

Cui, Z., Wang, X., Zhang, Q., Li, L., and Liu, F. (2025). Liquid–liquid phase separation technologies of α-synuclein governed by its C-terminus via electrostatic interactions: unveiling potential therapeutic targets for Parkinson's disease. *Adv. Technol. Neurosci.* 2, 1–8. doi:10.4103/atn.atn-d-24-00027

Cunningham, C. N., Williams, J. M., Knupp, J., Arunagiri, A., Arvan, P., and Tsai, B. (2019). Cells deploy a two-pronged strategy to rectify misfolded proinsulin aggregates. *Mol. Cell* 75, 442–456.e4. doi:10.1016/j.molcel.2019.05.011

Dabbaghi, M., Namjoshi, S., Panchal, B., Grice, J. E., Prakash, S., Roberts, M. S., et al. (2021). Viscoelastic and deformation characteristics of structurally different commercial topical systems. *Pharmaceutics* 13, 1351. doi:10.3390/pharmaceutics13091351

Das, D., and Deniz, A. A. (2023). Topological considerations in biomolecular condensation. *Biomolecules* 13, 151. doi:10.3390/biom13010151

Das, T., Zaidi, F. K., Farag, M., Ruff, K. M., Mahendran, T. S., Singh, A., et al. (2025). Tunable metastability of condensates reconciles their dual roles in amyloid fibril formation. *Mol. Cell* 85, 2230–2245.e7. doi:10.1016/j.molcel.2025.05.011

de Boer, E. M. J., Orie, V. K., Williams, T., Baker, M. R., De Oliveira, H. M., Polvikoski, T., et al. (2020). TDP-43 proteinopathies: a new wave of neurodegenerative diseases. *J. Neurol. Neurosurg. Psychiatry* 92, 86–95. doi:10.1136/jnnp-2020-322983

Dec, R., Jaworek, M. W., Dzwolak, W., and Winter, R. (2023). Liquid-droplet-mediated ATP-triggered amyloidogenic pathway of insulin-derived chimeric peptides: unraveling the microscopic and molecular processes. *J. Am. Chem. Soc.* 145, 4177–4186. doi:10.1021/jacs.2c12611

Deniz, A. A. (2022). Percolation physics and density transition frameworks converge in biomolecular condensation. *Proc. Natl. Acad. Sci. U. S. A.* 119, e2210177119. doi:10.1073/pnas.2210177119

Duan, Y., Du, A., Gu, J., Duan, G., Wang, C., Gui, X., et al. (2019). Poly(ADP-Ribose) regulates stress granule dynamics and neurotoxicity of disease-related RNA-binding proteins. *Cell res.* 29, 233–247. doi:10.1038/s41422-019-0141-z

Eisenberg, D., and Jucker, M. (2012). The amyloid state of proteins in human diseases. *Cell* 148, 1188–1203. doi:10.1016/j.cell.2012.02.022

Elbaum-Garfinkle, S., Kim, Y., Szczepaniak, K., Chen, C. C. H., Eckmann, C. R., Myong, S., et al. (2015). The disordered P granule protein LAF-1 drives phase separation into droplets with tunable viscosity and dynamics, *Proc. Natl. Acad. Sci. U. S. A.* 112, 7189–7194. doi:10.1073/pnas.1504822112

Englander, S. W., and Mayne, L. (2014). The nature of protein folding pathways. *Proc. Natl. Acad. Sci. U. S. A.* 111, 15873–15880. doi:10.1073/pnas.1411798111

Espinosa, J. R., Joseph, J. A., Sanchez-Burgos, I., Garaizar, A., Frenkel, D., and Collepardo-Guevara, R. (2020). Liquid network connectivity regulates the stability and composition of biomolecular condensates with many components, *Proc. Natl. Acad. Sci. U. S. A.* 117, 13238–13247. doi:10.1073/pnas.1917569117

Farag, M., Cohen, S. R., Borcherds, W. M., Bremer, A., Mittag, T., and Pappu, R. V. (2022). Condensates formed by prion-like low-complexity domains have small-world network structures and interfaces defined by expanded conformations. *Nat. Commun.* 13, 7722. doi:10.1038/s41467-022-35370-7

Fare, C. M., Villani, A., Drake, L. E., and Shorter, J. (2021). Higher-order organization of biomolecular condensates. *Open Biol.* 11, 210137. doi:10.1098/rsob.210137

Farina, S., Esposito, F., Battistoni, M., Biamonti, G., and Francia, S. (2021). Post-translational modifications modulate proteinopathies of TDP-43, FUS and hnRNP-A/B in amyotrophic lateral sclerosis. *Front. Mol. Biosci.* 8, 693325. doi:10.3389/fmolb.2021.693325

Feldman, S. A., and Eiden, L. E. (2003). The chromogranins: their roles in secretion from neuroendocrine cells and as markers for neuroendocrine neoplasia. *Endocr. Pathol.* 14, 3–23. doi:10.1385/ep:14:1:3

Feng, Z., Chen, X., Wu, X., and Zhang, M. (2019). Formation of biological condensates via phase separation: characteristics, analytical methods, and physiological implications. *J. Biol. Chem.* 294, 14823–14835. doi:10.1074/jbc.REV119.007895

Fernandes, N., Nero, L., Lyons, S. M., Ivanov, P., Mittelmeier, T. M., Bolger, T. A., et al. (2020). Stress granule assembly can facilitate but is not required for TDP-43 cytoplasmic aggregation. *Biomolecules* 10, 1367. doi:10.3390/biom10101367

Finder, V. H., and Glockshuber, R. (2007). Amyloid-beta aggregation. *Neurodegenerative Dis.* 4, 13–27. doi:10.1159/000100355

Freibaum, B. D., Messing, J., Yang, P., Kim, H. J., and Taylor, J. P. (2021). High-fidelity reconstitution of stress granules and nucleoli in Mammalian cellular lysate. *J. Cell Biol.* 220, e202009079. doi:10.1083/jcb.202009079

Gebbink, M. F., Claessen, D., Bouma, B., Dijkhuizen, L., and Wosten, H. A. (2005). Amyloids–a functional coat for microorganisms. *Nat. Rev. Microbiol.* 3, 333–341. doi:10.1038/nrmicro1127

Goedert, M., Jakes, R., Anthony Crowther, R., and Grazia Spillantini, M. (2001). Parkinson's disease, dementia with lewy bodies, and multiple system atrophy as alpha-synucleinopathies. *Methods Mol Med* 62, 33–59. doi:10.1385/1-59259-142-6:33

Gui, X., Luo, F., Li, Y., Zhou, H., Qin, Z., Liu, Z., et al. (2019). Structural basis for reversible amyloids of hnRNPA1 elucidates their role in stress granule assembly. *Nat. Commun.* 10, 2006. doi:10.1038/s41467-019-09902-7

Gui, X., Feng, S., Li, Z., Li, Y., Reif, B., Shi, B., et al. (2023). Liquid-liquid phase separation of amyloid-beta oligomers modulates amyloid fibrils formation. *J. Biol. Chem.* 299, 102926. doi:10.1016/j.jbc.2023.102926

Guil, S., Long, J. C., and Caceres, J. F. (2006). hnRNP A1 relocalization to the stress granules reflects a role in the stress response. *Mol. Cell Biol.* 26, 5744–5758. doi:10.1128/MCB.00224-06

Guillén-Boixet, J., Kopach, A., Holehouse, A. S., Wittmann, S., Caceres, J. F., Jahnel, M., Kim, K., et al. (2020). RNA-induced conformational switching and clustering of G3BP drive stress granule assembly by condensation. *Cell* 181, 346–361.e317. doi:10.1016/j.cell.2020.03.049

Hammer, N. D., Wang, X., McGuffie, B. A., and Chapman, M. R. (2008). Amyloids: friend or foe? *J. Alzheimers Dis.* 13, 407–419. doi:10.3233/jad-2008-13406

Han, T. W., Portz, B., Young, R. A., Boija, A., and Klein, I. A. (2024). RNA and condensates: disease implications and therapeutic opportunities. *Cell Chem. Biol.* 31, 1593–1609. doi:10.1016/j.chembiol.2024.08.009

Han, X., Sun, R., Graewert, M. A., Zhou, Q., Resink, T., Blanchet, C. E., et al. (2025). SAXS reveals the molecular basis underlying pH-driven G3BP1 conformational dynamics: implications for stress granule formation. *bioRxiv* 03, 645651. doi:10.1101/2025.03.27.645651

Hardenberg, M. C., Sinnige, T., Casford, S., Dada, S. T., Poudel, C., Robinson, E. A., et al. (2021). Observation of an α-synuclein liquid droplet state and its maturation into lewy body-like assemblies. *J. Mol. cell Biol.* 13, 282–294. doi:10.1093/jmcb/mjaa075

Hassan, S., White, K., and Terry, C. (2022). Linking hIAPP misfolding and aggregation with type 2 diabetes mellitus: a structural perspective. *Biosci. Rep.* 42, BSR20211297. doi:10.1042/BSR20211297

Hernández-Vega, A., Braun, M., Scharrel, L., Jahnel, M., Wegmann, S., Hyman, B. T., et al. (2017). Local nucleation of microtubule bundles through tubulin concentration into a condensed tau phase. *Cell Rep.* 20, 2304–2312. doi:10.1016/j.celrep.2017.08.042

Hoefner, C., Bryde, T. H., Pihl, C., Tiedemann, S. N., Bresson, S. E., Hotiana, H. A., et al. (2023). FK506-Binding protein 2 participates in proinsulin folding. *Biomolecules* 13, 152. doi:10.3390/biom13010152

Horváth, D.A.-O., Dürvanger, Z., K Menyhárd, D., Sulyok-Eiler, M., Bencs, F., Gyulai, G., et al. (2023). Polymorphic amyloid nanostructures of hormone peptides involved in glucose homeostasis display reversible amyloid formation. *Nat. Commun.* 14, 4621. doi:10.1038/s41467-023-40294-x

Hribar-Lee, B., and Luksic, M. (2024). Biophysical principles emerging from experiments on protein-protein association and aggregation. *Annu. Rev. Biophys.* 53, 1–18. doi:10.1146/annurev-biophys-030722-111729

Iconomidou, V. A., and Hamodrakas, S. J. (2008). Natural protective amyloids. *Curr. Protein Pept. Sci.* 9, 291–309. doi:10.2174/138920308784534041

Islam, M., Shen, F., Regmi, D., Petersen, K., Karim, M. R. U., and Du, D. (2024). Tau liquid-liquid phase separation: at the crossroads of tau physiology and tauopathy. *J. Cell Physiol.* 239, e30853. doi:10.1002/jcp.30853

Jacob, R. S., Das, S., Ghosh, S., Anoop, A., Jha, N. N., Khan, T., et al. (2016). Amyloid formation of growth hormone in presence of zinc: relevance to its storage in secretory granules. *Sci. Rep.* 6, 23370. doi:10.1038/srep23370

Jain, R. K., Chang, W. T., Geetha, C., Joyce, P. B., and Gorr, S. U. (2002). *In vitro* aggregation of the regulated secretory protein chromogranin A. *Biochem. J.* 368, 605–610. doi:10.1042/BJ20021195

Jeon, S., Jeon, Y., Lim, J. Y., Kim, Y., Cha, B., and Kim, W. (2025). Emerging regulatory mechanisms and functions of biomolecular condensates: implications for therapeutic targets. *Signal Transduct. Target. Ther.* 10, 4. doi:10.1038/s41392-024-02070-1

Jia, Z., Schmit, J. D., and Chen, J. (2020). Amyloid assembly is dominated by misregistered kinetic traps on an unbiased energy landscape. *Proc. Natl. Acad. Sci. U. S. A.* 117, 10322–10328. doi:10.1073/pnas.1911153117

Jucker, M., and Walker, L. C. (2018). Propagation and spread of pathogenic protein assemblies in neurodegenerative diseases. *Nat. Neurosci.* 21, 1341–1349. doi:10.1038/s41593-018-0238-6

Jumper, J., Evans, R., Pritzel, A., Green, T., Figurnov, M., Ronneberger, O., et al. (2021). Highly accurate protein structure prediction with AlphaFold. *Nature* 596, 583–589. doi:10.1038/s41586-021-03819-2

Karmakar, S., Sankhla, A., and Katiyar, V. (2022). Reversible and biocompatible AuNP-decorated [Zn2+]:[Insulin] condensed assembly for potential therapeutic applications. *Eur. J. Pharm. Sci.* 173, 106168. doi:10.1016/j.ejps.2022.106168

Khan, A. N., and Khan, R. H. (2022). Protein misfolding and related human diseases: a comprehensive review of toxicity, proteins involved, and current therapeutic strategies. *Int. J. Biol. Macromol.* 223, 143–160. doi:10.1016/j.ijbiomac.2022.11.031

Kilic, S., Lezaja, A., Gatti, M., Bianco, E., Michelena, J., Imhof, R., et al. (2019). Phase separation of 53BP1 determines liquid-like behavior of DNA repair compartments. *EMBO J.* 38, e101379. doi:10.15252/embj.2018101379

Kollmer, M., Thurber, K. R., Yau, W. M., and Tycko, R. (2021). Molecular structure of a prevalent amyloid-β fibril polymorph from Alzheimer's disease brain tissue. *Proc. Natl. Acad. Sci.* 118, e2023089118. doi:10.1073/pnas.2023089118

Kroschwald, S., Arunagiri, A., Ventura, S., Ranganathan, S., and Kohler, V. (2022). Editorial: molecular determinants of protein assemblies in health and disease. *Front. Mol. Biosci.* 9, 1107686. doi:10.3389/fmolb.2022.1107686

Kuhlman, B., and Bradley, P. (2019). Advances in protein structure prediction and design. *Nat. Rev. Mol. Cell Biol.* 20, 681–697. doi:10.1038/s41580-019-0163-x

Lacroix, E., Pereira, L., Yoo, B., Coyle, K. M., Chandhok, S., Zapf, R., et al. (2021). Evolutionary conservation of systemic and reversible amyloid aggregation. *J. Cell Sci.* 134, jcs258907. doi:10.1242/jcs.258907

Li, Y., Gu, J., Wang, C., Hu, J., Zhang, S., Liu, C., et al. (2022). Hsp70 exhibits a liquid-liquid phase separation ability and chaperones condensed FUS against amyloid aggregation. *iScience* 25, 104356. doi:10.1016/j.isci.2022.104356

Li, P., Chen, J., Wang, X., Su, Z., Gao, M., and Huang, Y. (2023). Liquid - liquid phase separation of tau: driving forces, regulation, and biological implications. *Neurobiol. Dis.* 183, 106167. doi:10.1016/j.nbd.2023.106167

Linsenmeier, M., Faltova, L., Morelli, C., Capasso Palmiero, U., Seiffert, C., Küffner, A. M., et al. (2023). The interface of condensates of the hnRNPA1 low-complexity domain promotes formation of amyloid fibrils. *Nat. Chem.* 15, 1340–1349. doi:10.1038/s41557-023-01289-9

Liu, M., Haataja, L., Wright, J., Wickramasinghe, N. P., Hua, Q. X., Phillips, N. F., et al. (2010). Mutant INS-gene induced diabetes of youth: proinsulin cysteine residues impose dominant-negative inhibition on wild-type proinsulin transport. *PLoS One* 5, e13333. doi:10.1371/journal.pone.0013333

Liu, M., Weiss, M. A., Arunagiri, A., Yong, J., Rege, N., Sun, J., et al. (2018). Biosynthesis, structure, and folding of the insulin precursor protein. *Diabetes Obes. Metab.* 20 (Suppl. 2), 28–50. doi:10.1111/dom.13378

Liu, H., Pillai, M., and Leung, A. K. L. (2025). PARPs and ADP-ribosylation-mediated biomolecular condensates: determinants, dynamics, and disease implications. *Trends Biochem. Sci.* 50, 224–241. doi:10.1016/j.tibs.2024.12.013

Lucas, L., Tsoi, P. S., Ferreon, J. C., and Ferreon, A. C. M. (2025). Tau oligomers resist phase separation. *Biomolecules* 15, 336. doi:10.3390/biom15030336

Luk, K. C., Song, C., O'Brien, P., Stieber, A., Branch, J. R., Brunden, K. R., et al. (2009). Exogenous alpha-synuclein fibrils seed the formation of lewy body-like intracellular inclusions in cultured cells, *Proc. Natl. Acad. Sci. U. S. A.* 106, 20051–20056. doi:10.1073/pnas.0908005106

Lyon, A. S., Peeples, W. B., and Rosen, M. K. (2021). A framework for understanding the functions of biomolecular condensates across scales. *Nat. Rev. Mol. Cell Biol.* 22, 215–235. doi:10.1038/s41580-020-00303-z

Maharana, S., Wang, J., Papadopoulos, D. K., Richter, D., Pozniakovsky, A., Poser, I., et al. (2018). RNA buffers the phase separation behavior of prion-like RNA binding proteins. *Science* 360, 918–921. doi:10.1126/science.aar7366

Mahendran, T. S., Singh, A., Srinivasan, S., Jennings, C. M., Neureuter, C., Gindra, B. H., et al. (2025). Decoupling phase separation and fibrillization preserves activity of biomolecular condensates. *bioRxiv*. 2025.03.18.643977. doi:10.1101/2025.03.18.643977

Maji, S. K., Perrin, M. H., Sawaya, M. R., Jessberger, S., Vadodaria, K., Rissman, R. A., et al. (2009). Functional amyloids as natural storage of peptide hormones in pituitary secretory granules. *Science* 325, 328–332. doi:10.1126/science.1173155

Mathieu, C., Pappu, R. V., and Taylor, J. P. (2020). Beyond aggregation: pathological phase transitions in neurodegenerative disease. *Science* 370, 56–60. doi:10.1126/science.abb8032

Matsuki, H., Takahashi, M., Higuchi, M., Makokha, G. N., Oie, M., and Fujii, M. (2013). Both G3BP1 and G3BP2 contribute to stress granule formation. *Genes. cells.* 18, 135–146. doi:10.1111/gtc.12023

Matsushita, Y., Yasuda, I., Watanabe, F., and Yamamoto, E. (2025). *arXiv:2504*, 19790.

Maury, C. P. (2009). The emerging concept of functional amyloid. *J. Intern Med.* 265, 329–334. doi:10.1111/j.1365-2796.2008.02068.x

Miraee-Nedjad, S., Sims, P. F. G., Schwartz, J.-M., and Doig, A. J. (2018). Effect of IAPP on the proteome of cultured Rin-5F cells. *BMC Biochem.* 19, 9. doi:10.1186/s12858-018-0099-3

Mittag, T., and Pappu, R. V. (2022). A conceptual framework for understanding phase separation and addressing open questions and challenges. *Mol. Cell* 82, 2201–2214. doi:10.1016/j.molcel.2022.05.018

Molliex, A., Temirov, J., Lee, J., Coughlin, M., Kanagaraj, A. P., Kim, H. J., et al. (2015). Phase separation by low complexity domains promotes stress granule assembly and drives pathological fibrillization. *Cell* 163, 123–133. doi:10.1016/j.cell.2015.09.015

Mori, W., Kawakami, R., Niko, Y., Haruta, T., Imamura, T., Shiraki, K., et al. (2022). Differences in interaction lead to the formation of different types of insulin amyloid. *Sci. Rep.* 12, 8556. doi:10.1038/s41598-022-12212-6

Morris, O. M., Toprakcioglu, Z., Röntgen, A., Cali, M., Knowles, T. P. J., and Vendruscolo, M. (2024). Aggregation of the amyloid-β peptide (Aβ40) within condensates generated through liquid-liquid phase separation. *Sci. Rep.* 14, 22633. doi:10.1038/s41598-024-72265-7

Moya-Gudiño, V., Altamirano-Bustamante, N. F., Revilla-Monsalve, C., and Altamirano-Bustamante, M. M. (2025). Decoding the contribution of IAPP Amyloid aggregation to beta cell dysfunction: a systematic review and epistemic meta-analysis of type 1 diabetes. *Int J Mol Sci.* 26, 767. doi:10.3390/ijms26020767

Mukherjee, A., Morales-Scheihing, D., Salvadores, N., Moreno-Gonzalez, I., Gonzalez, C., Taylor-Presse, K., et al. (2017). Induction of IAPP amyloid deposition and associated diabetic abnormalities by a prion-like mechanism. *J. Exp. Med.* 214, 2591–2610. doi:10.1084/jem.20161134

Musa, O., Iliyasu, I., Musa, S., Oladele, S. B., and Iliya, A. I. (2023). Amyloid-β aggregation implicates multiple pathways in Alzheimer's disease: understanding the mechanisms. *Front. Neurosci.* 17, 1081938. doi:10.3389/fnins.2023.1081938

Najafi, S., Lin, Y., Longhini, A. P., Zhang, X., Delaney, K. T., Kosik, K. S., et al. (2021). Liquid-liquid phase separation of tau by self and complex coacervation. *Protein Sci.* 30, 1393–1407. doi:10.1002/pro.4101

Niu, X., Zhang, L., Wu, Y., Zong, Z., Wang, B., Liu, J., et al. (2023). Biomolecular condensates: formation mechanisms, biological functions, and therapeutic targets. *MedComm* 4, e223. doi:10.1002/mco2.223

Niu, Z., Gui, X., Feng, S., and Reif, B. (2024). Aggregation mechanisms and molecular structures of amyloid-beta in Alzheimer's disease. *Chemistry* 30, e202400277. doi:10.1002/chem.202400277

Parashar, S., Chidambaram, R., Chen, S., Liem, C. R., Griffis, E., Lambert, G. G., et al. (2021). Endoplasmic reticulum tubules limit the size of misfolded protein condensates. *eLife* 10, e71642. doi:10.7554/eLife.71642

Parchure, A., Tian, M., Stalder, D., Boyer, C. K., Bearrows, S. C., Rohli, K. E., et al. (2022). Liquid-liquid phase separation facilitates the biogenesis of secretory storage granules. *J. Cell Biol.* 221, e202206132. doi:10.1083/jcb.202206132

Parker, D. M., Tauber, D., and Parker, R. (2025). G3BP1 promotes intermolecular RNA-RNA interactions during RNA condensation. *Mol. Cell.* 85, 571–584.e7. doi:10.1016/j.molcel.2024.11.012

Patel, A., Lee, H. O., Jawerth, L., Maharana, S., Jahnel, M., Hein, M. Y., et al. (2015). A liquid-to-solid phase transition of the ALS protein FUS accelerated by disease mutation. *Cell* 162, 1066–1077. doi:10.1016/j.cell.2015.07.047

Patel, A., Malinovska, L., Saha, S., Wang, J., Alberti, S., Krishnan, Y., et al. (2017). ATP as a biological hydrotrope. *Science* 356, 753–756. doi:10.1126/science.aaf6846

Pei, G., Lyons, H., Li, P., and Sabari, B. R. (2025). Transcription regulation by biomolecular condensates. *Nat. Rev. Mol. Cell Biol.* 26, 213–236. doi:10.1038/s41580-024-00789-x

Pessina, F., Giavazzi, F., Yin, Y., Gioia, U., Vitelli, V., Galbiati, A., et al. (2019). Functional transcription promoters at DNA double-strand breaks mediate RNA-driven phase separation of damage-response factors. *Nat. Cell Biol.* 21, 1286–1299. doi:10.1038/s41556-019-0392-4

Piroska, L., Fenyi, A., Thomas, S., Plamont, M. A., Redeker, V., Melki, R., et al. (2023). α-Synuclein liquid condensates fuel fibrillar α-synuclein growth. *Sci. Adv.* 9, eadg5663. doi:10.1126/sciadv.adg5663

Prasad, A., Bharathi, V., Sivalingam, V., Girdhar, A., and Patel, B. K. (2019). Molecular mechanisms of TDP-43 misfolding and pathology in amyotrophic lateral sclerosis. *Front. Mol. Neurosci.* 12, 25. doi:10.3389/fnmol.2019.00025

Qi, X., Wang, Y., Yu, H., Liu, R., Leppert, A., Zheng, Z., et al. (2023). Spider silk protein forms amyloid-like nanofibrils through a non-nucleation-dependent polymerization mechanism. *Small (Weinheim der Bergstrasse, Germany)* 19, e2304031. doi:10.1002/smll.202304031

Rai, S. K., Savastano, A., Singh, P., Mukhopadhyay, S., and Zweckstetter, M. (2021). Liquid-liquid phase separation of tau: from molecular biophysics to physiology and disease. *Protein Sci.* 30, 1294–1314. doi:10.1002/pro.4093

Ramaswami, M., Taylor, J. P., and Parker, R. (2013). Altered ribostasis: RNA–protein granules in degenerative disorders. *Cell* 154, 727–736. doi:10.1016/j.cell.2013.07.038

Ramat, A., and Simonelig, M. (2022). Activating translation with phase separation. *Science* 377, 712–713. doi:10.1126/science.add6323

Rambaran, R. N., and Serpell, L. C. (2008). Amyloid fibrils: abnormal protein assembly. *Prion* 2, 112–117. doi:10.4161/pri.2.3.7488

Ray, S., Singh, N., Kumar, R., Patel, K., Pandey, S., Datta, D., et al. (2020). α-Synuclein aggregation nucleates through liquid-liquid phase separation. *Nat. Chem.* 12, 705–716. doi:10.1038/s41557-020-0465-9

Riback, J. A., Katanski, C. D., Kear-Scott, J. L., Pilipenko, E. V., Rojek, A. E., Sosnick, T. R., et al. (2017). Stress-triggered phase separation is an adaptive, evolutionarily tuned response. *Cell* 168, 1028–1040.e19. doi:10.1016/j.cell.2017.02.027

Rumbley, J., Hoang, L., Mayne, L., and Englander, S. W. (2001). An amino acid code for protein folding. *Proc. Natl. Acad. Sci. U. S. A.* 98, 105–112. doi:10.1073/pnas.98.1.105

Saad, S., Cereghetti, G., Feng, Y., Picotti, P., Peter, M., and Dechant, R. (2017). Reversible protein aggregation is a protective mechanism to ensure cell cycle restart after stress. *Nat. Cell Biol.* 19, 1202–1213. doi:10.1038/ncb3600

Sacino, A. N., Brooks, M., McKinney, A. B., Thomas, M. A., Shaw, G., Golde, T. E., et al. (2014). Brain injection of α-synuclein induces multiple proteinopathies, gliosis, and a neuronal injury marker. *J. Neurosci.* 34, 12368–12378. doi:10.1523/JNEUROSCI.2102-14.2014

Saibil, H. (2013). Chaperone machines for protein folding, unfolding and disaggregation. *Nat. Rev. Mol. Cell Biol.* 14, 630–642. doi:10.1038/nrm3658

Sanfeliu-Cerdán, N., and Krieg, M. (2025). The mechanobiology of biomolecular condensates. *Biophys. Rev.* 6, 011310. doi:10.1063/5.0236610

Scherer, N., Maurel, C., Graus, M. S., McAlary, L., Richter, G., Radford, R. A. W., et al. (2024). RNA-binding properties orchestrate TDP-43 homeostasis through condensate formation *in vivo*. *Nucleic Acids Res.* 52, 5301–5319. doi:10.1093/nar/gkae112

Schulte, T., Panas, M. D., Han, X., Williams, L., Kedersha, N., Fleck, J. S., et al. (2023). Caprin-1 binding to the critical stress granule protein G3BP1 is influenced by pH. *Open Biol.* 13, 220369. doi:10.1098/rsob.220369

Selkoe, D. J. (1991). The molecular pathology of Alzheimer's disease. *Neuron* 6, 487–498. doi:10.1016/0896-6273(91)90052-2

Šneiderienė, G., González Díaz, A., Adhikari, S. D., Wei, J., Michaels, T., Šneideris, T., et al. (2025). Lipid-induced condensate formation from the Alzheimer's Aβ peptide triggers amyloid aggregation. *Proc. Natl. Acad. Sci. U. S. A.* 122, e2401307122. doi:10.1073/pnas.2401307122

Sobota, J. A. F. F., Bäck, N., Eipper, B. A., and Mains, R. E. (2006). Not all secretory granules are created equal: partitioning of soluble content proteins. *Mol. Biol. Cell* 17, 5038–5052. doi:10.1091/mbc.e06-07-0626

Sowers, C. R., Wang, R., Bourne, R. A., McGrath, B. C., Hu, J., Bevilacqua, S. C., et al. (2018). The protein kinase PERK/EIF2AK3 regulates proinsulin processing not via protein synthesis but by controlling endoplasmic reticulum chaperones. *J. Biol. Chem.* 293, 5134–5149. doi:10.1074/jbc.M117.813790

Subedi, S., Sasidharan, S., Nag, N., Saudagar, P., and Tripathi, T. (2022). Amyloid cross-seeding: mechanism, implication, and inhibition. *Mol. (Basel, Switzerland)* 27, 1776. doi:10.3390/molecules27061776

Suladze, S., Sarkar, R., Rodina, N., Bokvist, K., Krewinkel, M., Scheps, D., et al. (2024). Atomic resolution structure of full-length human insulin fibrils. *Proc. Natl. Acad. Sci. U. S. A.* 121, e2401458121. doi:10.1073/pnas.2401458121

Sun, J., Xiong, Y., Li, X., Haataja, L., Chen, W., Mir, S. A., et al. (2020). Role of proinsulin self-association in mutant INS gene-induced diabetes of youth. *Diabetes* 69, 954–964. doi:10.2337/db19-1106

Takanashi, K., and Yamaguchi, A. (2014). Aggregation of ALS-linked FUS mutant sequesters RNA binding proteins and impairs RNA granules formation. *Biochem. Biophys. Res. Commun.* 452, 600–607. doi:10.1016/j.bbrc.2014.08.115

Taylor, N. O., Wei, M. T., Stone, H. A., and Brangwynne, C. P. (2019). Quantifying dynamics in phase-separated condensates using fluorescence recovery after photobleaching. *Biophysical J.* 117, 1285–1300. doi:10.1016/j.bpj.2019.08.030

Tejedor, A. R., Collepardo-Guevara, R., Ramírez, J., and Espinosa, J. R. (2023). Time-dependent material properties of aging biomolecular condensates from different viscoelasticity measurements in molecular dynamics simulations. *J. Phys. Chem. B* 127, 4441–4459. doi:10.1021/acs.jpcb.3c01292

Toledo, P. L., Vazquez, D. S., Gianotti, A. R., Abate, M. B., Wegbrod, C., Torkko, J. M., et al. (2023). Condensation of the beta-cell secretory granule luminal cargoes pro/insulin and ICA512 RESP18 homology domain. *Protein Sci.* 32, e4649. doi:10.1002/pro.4649

Toyama, B. H., and Weissman, J. S. (2011). Amyloid structure: conformational diversity and consequences. *Annu. Rev. Biochem.* 80, 557–585. doi:10.1146/annurev-biochem-090908-120656

Tsoi, P. S., Lucas, L., Rhoades, D., Ferreon, J. C., and Ferreon, A. C. M. (2025). Electrostatic effects on tau nanocondensates. *Biomolecules* 15, 406. doi:10.3390/biom15030406

Tsuchiya, Y., Saito, M., Kadokura, H., Miyazaki, J. I., Tashiro, F., Imagawa, Y., et al. (2018). IRE1-XBP1 pathway regulates oxidative proinsulin folding in pancreatic beta cells. *J. Cell Biol.* 217, 1287–1301. doi:10.1083/jcb.201707143

Vendruscolo, M., and Fuxreiter, M. (2022). Protein condensation diseases: therapeutic opportunities. *Nat. Commun.* 13, 5550. doi:10.1038/s41467-022-32940-7

Vidović, M., and Rikalovic, M. G. (2022). Alpha-synuclein aggregation pathway in parkinson's disease: current status and novel therapeutic approaches. *Cells* 11, 1732. doi:10.3390/cells11111732

Visser, B. S., Lipinski, W. P., and Spruijt, E. (2024). The role of biomolecular condensates in protein aggregation. *Nat. Rev. Chem.* 8, 686–700. doi:10.1038/s41570-024-00635-w

Vorontsova, M. A., Chan, Ho Y., Lubchenko, V., and Vekilov, P. G. (2015). Lack of dependence of the sizes of the mesoscopic protein clusters on electrostatics. *Biophysical J.* 109, 1959–1968. doi:10.1016/j.bpj.2015.09.025

Wang, X., and Chapman, M. R. (2008). Curli provide the template for understanding controlled amyloid propagation. *Prion* 2, 57–60. doi:10.4161/pri.2.2.6746

Wang, H., and Raleigh, D. P. (2014). The ability of insulin to inhibit the formation of amyloid by pro-islet amyloid polypeptide processing intermediates is significantly reduced in the presence of sulfated glycosaminoglycans. *Biochemistry* 53, 2605–2614. doi:10.1021/bi4015488

Maharana, S., Wang, J., Papadopoulos, D. K., Richter, D., Pozniakovsky, A., Poser, I., et al. (2021). RNA binding and phase separation by a naturally prion-like protein. *Science*. 360, 918–921. doi:10.1126/science.aar7366

Wang, Z., Lou, J., and Zhang, H. (2022). Essence determines phenomenon: assaying the material properties of biological condensates. *J. Biol. Chem.* 298, 101782. doi:10.1016/j.jbc.2022.101782

Wegmann, S., Eftekharzadeh, B., Tepper, K., Zoltowska, K. M., Bennett, R. E., Dujardin, S., et al. (2018). Tau protein liquid–liquid phase separation can initiate tau aggregation. *EMBO J.* 37, e98049. doi:10.15252/embj.201798049

Wen, J., Tang, Y., Sneideris, T., Ausserwöger, H., Hong, L., Knowles, T. P. J., et al. (2025). Direct observation of the conformational transitions in tau and their correlation with phase behavior. *JACS Au* 5, 4268–4280. doi:10.1021/jacsau.5c00625

Westermark, P., and Westermark, G. T. (2011). Islet amyloid polypeptide, islet amyloid, and diabetes mellitus. *Physiol. Rev.* 91, 795–826. doi:10.1152/physrev.00042.2009

Westermark, P., and Wilander, E. (1983). Islet amyloid in type 2 (non-insulin-dependent) diabetes is related to insulin. *Diabetologia* 24, 342–346. doi:10.1007/BF00251821

Xu, B., He, W., Fan, F., Chen, S., Zhu, M., Hou, Y., et al. (2025). β-synuclein blocks α-synuclein condensate fusion to disrupt the maturation of phase separation. *Cell Rep.* 44, 115761. doi:10.1016/j.celrep.2025.115761

Yan, X., Kuster, D., Mohanty, P., Nijssen, J., Pombo-García, K., Rizuan, A., et al. (2024). Intra-condensate demixing of TDP-43 inside stress granules generates pathological aggregates. *bioRxiv*, 2024.01.23.576837. [Preprint]. doi:10.1101/2024.01.23.576837

Yang, Y., Close, W., Funk, L., Rasmussen, J., Bsoul, A., Schierhorn, A., et al. (2019). Cryo-EM structure and polymorphism of Aβ amyloid fibrils purified from Alzheimer's brain tissue. *Nat. Commun.* 10, 4760. doi:10.1038/s41467-019-12683-8

Yang, P., Mathieu, C., Kolaitis, R. M., Zhang, P., Messing, J., Yurtsever, U., et al. (2020). G3BP1 is a tunable switch that triggers phase separation to assemble stress granules. *Cell* 181, 325–345.e28. doi:10.1016/j.cell.2020.03.046

Ziaunys, M., Sulskis, D., Veiveris, D., Kopustas, A., Snieckute, R., Mikalauskaite, K., et al. (2024). Liquid-liquid phase separation of alpha-synuclein increases the structural variability of fibrils formed during amyloid aggregation. *FEBS J.* 291, 4522–4538. doi:10.1111/febs.17244

Frontiers in
Molecular Biosciences

Explores biological processes in living organisms on a molecular scale

Focuses on the molecular mechanisms underpinning and regulating biological processes in organisms across all branches of life.

Discover the latest Research Topics

See more →

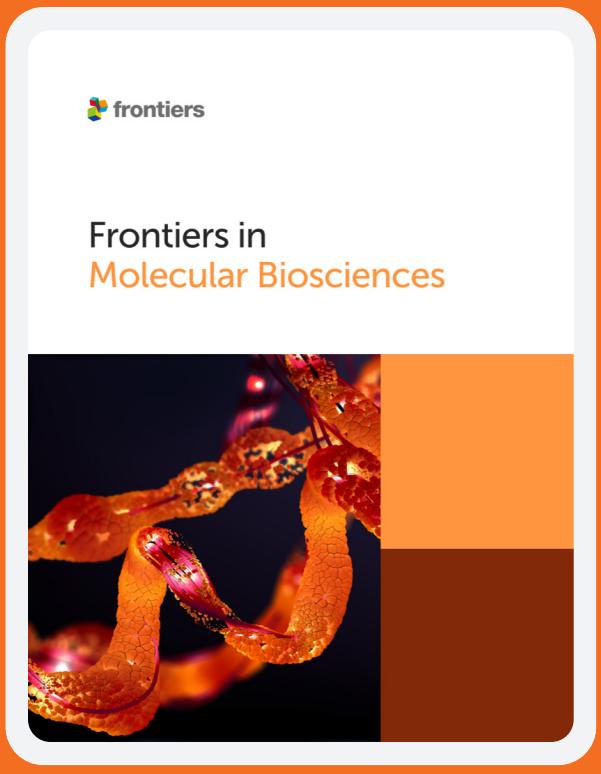

Frontiers

Avenue du Tribunal-Fédéral 34
1005 Lausanne, Switzerland
frontiersin.org

Contact us

+41 (0)21 510 17 00
frontiersin.org/about/contact